UNIVERSITÉ PARIS DIDEROT – PARIS 7
UNIVERSIDAD DE CANTABRIA – SANTANDER

THÈSE

présentée et soutenue publiquement le 31 mai 2010 pour l'obtention du

DOCTORAT DE L'UNIVERSITÉ PARIS DIDEROT – PARIS 7

(spécialité Informatique)

Multitriangulations, pseudotriangulations et quelques problèmes de réalisation de polytopes

Vincent PILAUD

Membres du jury :

Mireille BOUSQUET-MELOU (CNRS, Univ. Bordeaux 1)	*Examinatrice*
Christian CHOFFRUT (Univ. Paris 7)	*Examinateur*
Jakob JONSSON (KTH Stockholm)	*Rapporteur*
Marc NOY (UPC Barcelona)	*Examinateur*
Michel POCCHIOLA (Univ. Paris 6)	*Directeur de thèse*
Jorge RAMIREZ ALFONSIN (Univ. Montpellier 2)	*Examinateur*
Francisco SANTOS LEAL (Univ. Cantabria)	*Directeur de thèse*

Autre rapporteur :

Stefan FELSNER (TU Berlin)	*Rapporteur*

Laboratoire d'Informatique de l'École Normale Supérieure

Équipe Combinatoire et Optimisation de Paris 6

Departamento de Matemáticas, Estadística y Computación, Universidad de Cantabria

Multitriangulations, pseudotriangulations et quelques problèmes de réalisation de polytopes

Multitriangulaciones, pseudotriangulaciones y algunos problemas de realización de politopos

Multitriangulations, pseudotriangulations and some problems of realization of polytopes

---

VINCENT PILAUD

sous la direction de
bajo la dirección de
under the supervision of

MICHEL POCCHIOLA
École Normale Supérieure, Paris
Université Pierre et Marie Curie, Paris

FRANCISCO SANTOS LEAL
Universidad de Cantabria, Santander

À Claude et Bernard

Remerciements

Je tiens à remercier en premier lieu mes deux directeurs de thèse, qui m'ont guidé chacun à leur manière pour mes premiers pas dans le monde de la recherche. Qu'ils sachent tous les deux ma reconnaissance et mon admiration.

À Paris, *Michel Pocchiola* m'a orienté et conseillé à bien des égards depuis mon master. Sur le plan scientifique, il m'a fait découvrir ses thèmes de recherche avec patience et m'a proposé des sujets riches et stimulants. Il m'a transmis une noble vision de la recherche, que j'espère pouvoir un jour défendre aussi bien que lui. Sur le plan personnel, il a fait preuve d'attention et d'amitié tout au long de cette thèse, et a toujours su m'encourager dans les moments compliqués.

À Santander, *Francisco Santos* m'a accueilli chaleureusement au sein de l'Université de Cantabrie. Toujours entrain à me faire partager avec beaucoup de pédagogie et d'enthousiasme ses connaissances intarissables et ses idées originales, il a aussi su m'écouter et rendre intéressantes les fantaisies que je lui exposais. Je veux en particulier le remercier pour l'attention qu'il a portée à la rédaction de ce manuscrit. Par ailleurs, j'ai eu l'occasion de découvrir et d'apprécier ses qualités humaines, son altruisme, ainsi que son hospitalité lors de mes séjours à Santander.

J'adresse mes sincères remerciements à *Stefan Felsner* et *Jakob Jonsson* pour avoir accepté d'être rapporteurs de cette thèse. Je suis très honoré de l'intérêt qu'ils portent à mon travail, au regard de leurs diverses compétences. Merci également aux examinateurs qui ont accepté de siéger dans le jury de ma soutenance, malgré les emplois du temps chargés des uns et l'éloignement géographique des autres.

Au cours de cette thèse, j'ai eu l'occasion de faire la connaissance de nombreuses personnes passionnantes et bienveillantes. En particulier, j'ai beaucoup apprécié les relations scientifiques et personnelles que j'ai eues avec mes coauteurs. Outre mes directeurs de thèse, je pense particulièrement à *Julian Pfeifle* dont la passion pour la géométrie est communicative et contagieuse, et qui m'a accueilli à plusieurs reprises chez lui (j'ai ainsi pu constater que ses enfants ont su construire des polytopes avant d'apprendre à faire du vélo). Un grand merci aussi à *Benjamin Matschke* pour un séjour à Berlin aussi agréable que productif, et pour ses nombreuses idées lancées entre deux balles de baby-foot. Je suis par ailleurs très reconnaissant à *Jürgen Bokowski* pour notre travail commun qui a beaucoup alimenté ma réflexion.

Je tiens à remercier les membres des laboratoires qui m'ont accueilli durant ma thèse. À l'ÉNS, merci à *Éric Colin de Verdière* pour son soutien et ses conseils, mais aussi à l'équipe administrative pour son efficacité et sa disponibilité. À Paris 6, j'ai apprécié la bonne humeur des membres de l'équipe C&O, et les échanges que j'ai eus avec les uns et les autres. À Santander, je remercie les thésards avec qui j'ai partagé un bureau et mes premiers mots en espagnol.

Je veux aussi exprimer ma gratitude envers les organisateurs et les participants du *DocCourse Combinatorics and Geometry 2009* de Barcelone, qu'ils ont su rendre aussi intéressant que convivial. Je n'oublierai pas le soutien qu'ils m'ont apporté dans un moment personnel difficile.

J'aimerais pouvoir dire tout ce que je dois à mes amis, en qui je puise chaque jour l'énergie de mener à bien mes projets. En premier lieu, *Lionel* et *Anthony* que je tiens à remercier (le mot est faible) pour leurs conseils, leur soutien et leurs sourires. Je veux aussi faire un clin d'oeil à mes amis HX2 de Rhône-Alpes et d'ailleurs, qu'aucune distance ne semble pouvoir séparer. Merci encore à *Pascal* et *Pierre*, mes deux compères de la prépa agreg, qui m'ont toujours tiré vers le haut, et dont l'amitié me touche. Enfin, je ne sais pas dans quelle langue remercier *Cassandra* : en français parce que c'est sa langue de coeur, in English for all that she taught me, o en espagnol por todo lo que compartimos.

Je souhaite exprimer toute mon affection à ma famille. Même si tous connaissent les sentiments que j'ai pour eux, il y a des évidences qui sont parfois bonnes à dire. Merci donc tout d'abord à *Claude* pour son soutien indéfectible et ses attentions permanentes. Qu'elle trouve dans cette thèse les échos de tout ce qu'elle m'a appris, et dans ces mots le témoignage de ma gratitude. Merci à *Christophe* et *Thomas* : ils sont comme les deux autres côtés d'un triangle que chaque épreuve rend plus solide, et il faudrait une thèse entière pour en étudier les propriétés. Je pense aussi à *DD* et *Tatou* et je suis touché de lire dans leurs yeux l'admiration objective des grands-parents. Enfin, je n'oublie pas *Christiane*, *Yvette*, *Daniel* et *Gérard* qui m'ont toujours traité plus comme un fils que comme un neveu, et dont j'ai su apprécier la présence dans les jours sombres.

En terminant cette thèse, j'ai une pensée pour *Bernard*, pour notre complicité, pour tout ce qu'il était pour moi. Je me souviens avec beaucoup d'émotion de nos *Saturday Maths fever*, durant lesquels il m'a transmis sa passion pour les mathématiques, son goût de l'esthétique et de la simplicité des démonstrations. J'aurais aimé qu'il puisse feuilleter cette thèse comme il aurait déambulé dans les dédales d'un musée, en s'émerveillant devant chaque figure comme face à un tableau de Rothko.

CONTENTS

List of Figures

RÉSUMÉ

1 INTRODUCTION

Les thèmes abordés dans cette thèse s'inscrivent dans le champ de la *géométrie discrète et algorithmique* [GO04] : les problèmes rencontrés font en général intervenir des ensembles finis d'objets géométriques élémentaires (points, droites, demi-espaces, etc.), et les questions portent sur la manière dont ils sont reliés, arrangés, placés les uns par rapport aux autres (comment s'intersectent-ils ? comment se voient-ils ? que délimitent-ils ? etc.). Cette thèse traite de deux sujets particuliers : les *multitriangulations* et les *réalisations polytopales de produits*. Leurs diverses connexions avec la géométrie discrète nous en ont fait découvrir de nombreuses facettes, dont nous donnons quelques exemples dans cette introduction. Nous commençons par présenter leur problématique commune, la recherche d'une réalisation polytopale d'une structure donnée, qui a orienté nos recherches sur ces deux sujets.

Un polytope (convexe) est l'enveloppe convexe d'un ensemble fini de points d'un espace euclidien. Si l'intérêt porté à certains polytopes remonte à l'Antiquité (solides de Platon), leur étude systématique est relativement récente et les principaux résultats datent du XX$^{\text{e}}$ siècle (voir [Grü03, Zie95] et leurs références). L'étude des polytopes porte non seulement sur leurs propriétés géométriques mais surtout sur leurs aspects plus combinatoires. Il s'agit notamment de comprendre leurs faces (leurs intersections avec un hyperplan support) et le treillis qu'elles composent (c'est-à-dire les relations d'inclusion entre ces faces).

Les questions de *réalisation polytopale* forment en quelque sorte le problème inverse : elles portent sur l'existence et la construction de polytopes à partir d'une structure combinatoire donnée. Par exemple, étant donné un graphe, on voudrait déterminer s'il s'agit du graphe d'un polytope : on dira alors que le graphe est polytopal. Le résultat fondateur dans ce domaine est le Théorème de Steinitz [Ste22] qui caractérise les graphes des 3-polytopes. Dès la dimension 4, la situation est nettement moins satisfaisante : malgré certaines conditions nécessaires [Bal61, Kle64, Bar67], les graphes de polytopes n'admettent pas de caractérisation locale en dimension générale [RG96]. Lorsqu'un graphe est polytopal, on s'interroge sur les propriétés des éventuelles réalisations, par exemple leur nombre de faces, leur dimension, etc. On cherche à construire des exemples qui optimisent certaines de ces propriétés : typiquement, on veut construire un polytope de dimension minimale ayant un graphe donné [Gal63, JZ00, SZ10]. Ces questions de réalisations polytopales sont intéressantes pour des graphes qui proviennent soit de graphes de transformation sur des ensembles combinatoires ou géométriques (graphe des transpositions adjacentes sur les permutations, graphe des flips sur les triangulations, etc.), soit d'opérations sur des graphes (qui peuvent être locales comme la transformation ΔY, ou globales comme le produit cartésien). Ces questions ne se posent pas uniquement pour un graphe, mais plus généralement pour n'importe quel sous-ensemble de treillis.

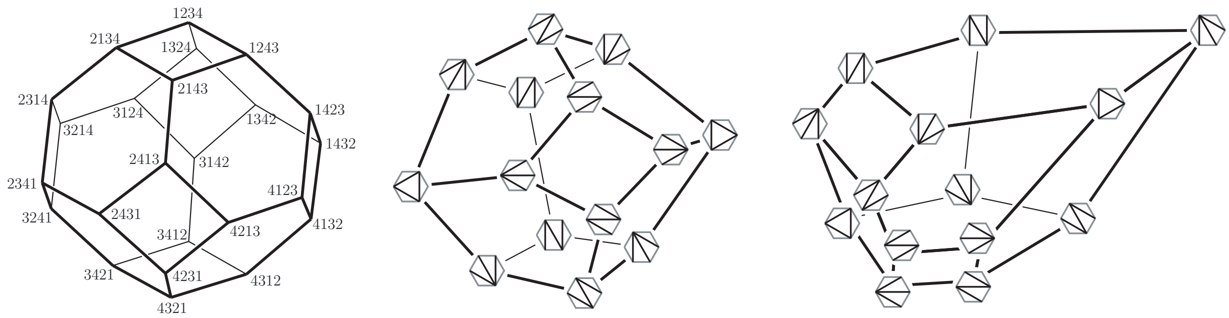

Figure 1 : Le permutoèdre et deux réalisations de l'associaèdre.

Polytopalité de graphes de flips. L'existence de réalisations polytopales est d'abord étudiée pour des graphes de transformation sur des structures combinatoires ou géométriques. Citons ici le permutoèdre dont les sommets correspondent aux permutations de $[n]$ et dans lequel deux sommets sont reliés par une arête si les permutations correspondantes diffèrent d'une transposition de deux positions adjacentes. D'autres exemples, ainsi que des classes de polytopes permettant de réaliser certaines structures sont exposés dans [Zie95, Lecture 9]. D'une manière générale, les questions de polytopalité de structures combinatoires sont intéressantes non seulement pour leurs résultats, mais aussi parce que leur étude force à comprendre la combinatoire des objets et amène à développer des méthodes nouvelles.

Deux exemples particuliers de structures combinatoires polytopales ont un rôle important dans le cadre de cette thèse. Nous rencontrons d'abord l'associaèdre, dont le bord réalise le dual du complexe simplicial formé par tous les ensembles de cordes du n-gone qui ne se croisent pas. Le graphe de l'associaèdre correspond au graphe des flips sur les triangulations du n-gone. L'associaèdre apparaît dans divers contextes et plusieurs réalisations polytopales ont été proposées [Lee89, BFS90, GKZ94, Lod04, HL07]. Nous rencontrons ensuite le polytope des pseudotriangulations d'un ensemble de points du plan euclidien [RSS03]. Introduites pour l'étude du complexe de visibilité d'obstacles convexes disjoints du plan [PV96b, PV96c], les pseudotriangulations ont été utilisées dans divers contextes géométriques [RSS08]. Leurs propriétés de rigidité [Str05] ont permis d'établir la polytopalité de leur graphe de flips [RSS03].

Dans la première partie de cette thèse, nous nous intéressons à la polytopalité du graphe des flips sur les multitriangulations. Ces objets, apparus de manière relativement contingente [CP92, DKM02, DKKM01], possèdent une riche structure combinatoire [Nak00, Jon03, Jon05]. Une *k-triangulation* est un ensemble maximal de cordes du n-gone ne contenant pas de sous-ensemble de $k+1$ cordes qui se croisent deux à deux. Nous considérons le graphe des flips dans lequel deux multitriangulations sont reliées si elles diffèrent d'une corde. Comme pour les triangulations que l'on retrouve lorsque $k = 1$, ce graphe est régulier et connexe, et nous nous interrogeons sur sa polytopalité. Jakob Jonsson [Jon03] a fait un premier pas dans cette direction en montrant que le complexe simplicial des ensembles de cordes ne contenant pas de sous-ensemble de $k+1$ cordes qui se croisent deux à deux est une sphère topologique. Bien que nous n'ayons que des réponses partielles à cette question, elle a entraîné des résultats inattendus que nous exposons dans cette thèse.

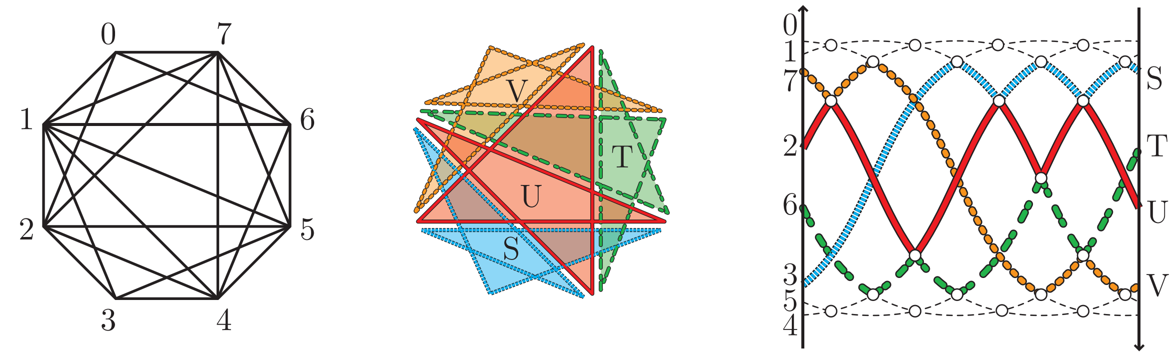

Figure 2 : Une 2-triangulation, sa décomposition en étoiles, et son arrangement dual.

Plusieurs constructions de l'associaèdre [BFS90, Lod04] sont basées, directement ou indirectement, sur les triangles des triangulations. Pour les multitriangulations, aucun objet élémentaire similaire n'apparaît dans les travaux antérieurs. Nous avons donc cherché dans un premier temps à comprendre ce que deviennent les triangles dans les multitriangulations. Les *étoiles* que nous introduisons au Chapitre 2 répondent à cette question. Au même titre que les triangles dans les triangulations, nous estimons que ces étoiles donnent le bon point de vue pour comprendre les multitriangulations. Pour preuve, nous commençons par retrouver à l'aide de ces étoiles toutes les propriétés combinatoires de base connues jusqu'alors sur les multitriangulations. D'abord, nous étudions les relations d'incidence entre les étoiles et les cordes (chaque corde interne est contenue dans deux étoiles) qui nous permettent de retrouver que toutes les k-triangulations du n-gone ont même cardinal. Ensuite, en considérant les bissectrices des étoiles, nous donnons une interprétation locale de l'opération de flip (une corde interne est remplacée par l'unique bissectrice commune des deux étoiles qui lui sont adjacentes), ce qui éclaire l'étude du graphe des flips et de son diamètre. Nous redéfinissons par ailleurs en termes d'étoiles des opérations inductives sur les multitriangulations qui permettent d'ajouter ou de supprimer un sommet au n-gone. Enfin, nous utilisons la décomposition d'une multitriangulation en étoiles pour l'interpréter comme une décomposition polygonale d'une surface, et nous appliquons cette interprétation à la construction de décompositions régulières de surfaces.

Dans un deuxième temps, nous avons cherché à comprendre les multitriangulations par dualité. L'espace des droites du plan est un ruban de Möbius ; l'ensemble des droites qui passent par un point du plan est une pseudodroite du ruban de Möbius ; et les pseudodroites duales d'une configuration de points forment un arrangement de pseudodroites [Goo97].

Notre point de départ est la dualité entre les pseudotriangulations d'un ensemble P de points et les arrangements de pseudodroites dont le support est l'arrangement dual de P privé de son premier niveau [PV94, PV96a]. Nous établissons une dualité similaire pour les multitriangulations. D'une part, l'ensemble des bissectrices d'une étoile est une pseudodroite du ruban de Möbius. D'autre part, les pseudodroites duales aux étoiles d'une k-triangulation du n-gone forment un arrangement de pseudodroites avec points de contact, supporté par l'arrangement dual des sommets du n-gone privé de ses k premiers niveaux. Nous montrons que tout arrangement avec points de contact ayant ce support est bien l'arrangement dual d'une multitriangulation. Cette dualité fait le lien entre les pseudotriangulations et les multitriangulations et explique ainsi leurs propriétés communes (nombre de cordes, flip, etc.).

Plus généralement, nous étudions au Chapitre 3 les *arrangements de pseudodroites avec points de contact* qui partagent un même support. Nous définissons une opération de flip qui correspond au flip des multitriangulations et des pseudotriangulations, et nous étudions le graphe des flips. Les propriétés de certains arrangements gloutons, définis comme les sources de certaines orientations acycliques de ce graphe, nous permettent en particulier d'énumérer ce graphe de flips en gardant un espace polynomial. Notre travail éclaire ainsi l'algorithme existant d'énumération des pseudotriangulations [BKPS06] et en donne une preuve complémentaire.

Pour finir, nous donnons au Chapitre 4 des pistes pour l'étude de trois problèmes ouverts qui reflètent la richesse combinatoire et géométrique des multitriangulations.

Le premier concerne le comptage des multitriangulations. Jakob Jonsson [Jon05] a prouvé (grâce à des considérations sur des $0/1$-remplissages de polyominos qui évitent certains motifs) que les multitriangulations sont comptées par un certain déterminant de Hankel de nombres de Catalan, qui compte aussi certaines familles de k-uplets de chemins de Dyck. Cependant, mis à part des résultats partiels [Eli07, Nic09], on ne connaît pas de preuve bijective de ce résultat. On entre ici dans le domaine de la *combinatoire bijective* dont le but est de construire des bijections entre des familles combinatoires qui conservent des paramètres caractéristiques : on voudrait ici exhiber une bijection qui permette de lire les étoiles sur les k-uplets de chemins de Dyck.

Le second problème est celui de la *rigidité*. Alors que la rigidité des graphes est bien comprise en dimension 2 [Lam70, Gra01, GSS93], aucune caractérisation satisfaisante n'est connue à partir de la dimension 3. Nous montrons que certaines propriétés typiques des graphes rigides en dimension $2k$ sont vérifiées par les k-triangulations. Ceci amène naturellement à conjecturer que les k-triangulations sont rigides en dimension $2k$, ce que nous prouvons lorsque $k = 2$. Une réponse positive à cette conjecture permettrait de se rapprocher de la polytopalité du graphes des flips sur les multitriangulations, de la même façon que le polytope des pseudotriangulations [RSS03] a pu être construit en s'appuyant sur leurs propriétés de rigidité.

Enfin, nous revenons sur la *réalisation polytopale du graphe des flips* sur les multitriangulations. Dans un premier temps, nous étudions le premier exemple non trivial : nous montrons que le graphe des flips sur les 2-triangulations de l'octogone est bien le graphe d'un polytope de dimension 6. Pour trouver un tel polytope, nous décrivons complètement l'espace des réalisations polytopales symétriques de ce graphe en dimension 6, en étudiant d'abord tous les matroides orientés [BVS+99, Bok06] symétriques qui peuvent le réaliser. Dans un deuxième temps, en généralisant une construction de l'associaèdre due à Jean-Louis Loday [Lod04], nous construisons un polytope qui réalise le graphe des flips restreint aux multitriangulations dont le graphe dual orienté est acyclique.

Par ailleurs, nous présentons dans l'Annexe A les résultats d'un algorithme d'énumération des petits arrangements de pseudodroites et de *double pseudodroites*. À l'instar des arrangements de pseudodroites qui offrent un modèle combinatoire des configurations de points, les arrangements de double pseudodroites ont été introduits comme modèles de configurations de convexes disjoints [HP09]. Notre travail d'implémentation nous a permis de manipuler ces objets et de nous familiariser avec leurs propriétés, ce qui s'est révélé utile lors de notre étude de la dualité.

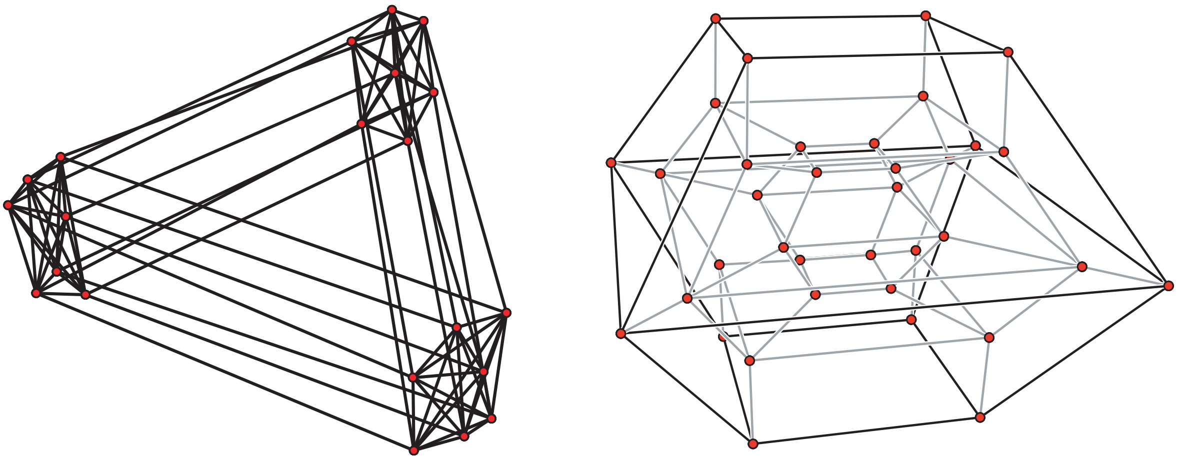

Figure 3 : (Gauche) Un produit de graphes complets. Ce graphe est celui d'un produit de simplexes, mais aussi celui de polytopes de dimensions inférieures. (Droite) Un produit polytopal de graphes non-polytopaux.

Polytopalité de produits cartésiens. Le *produit cartésien* de graphes est défini de sorte que le graphe d'un produit de polytopes est le produit des graphes de ses facteurs. Ainsi, un produit de graphes polytopaux est automatiquement polytopal. Nous étudions dans un premier temps la réciproque : la polytopalité d'un produit de graphes implique-t-elle celle de ses facteurs ? Le Chapitre 6 apporte des éléments de réponse en prêtant une attention particulière aux graphes réguliers et à leur réalisation comme polytopes simples (les polytopes simples ont des propriétés très particulières : entre autres, ils sont déterminés par leur graphe [BML87, Kal88]). Nous discutons en particulier la question de la polytopalité du produit de deux graphes de Petersen, qui a été soulevée par Günter Ziegler [CRM09]. Ce travail sur la polytopalité des produits nous a conduit à étudier des exemples de graphes qui se révèlent non-polytopaux bien qu'ils satisfassent les conditions nécessaires connues pour être polytopaux [Bal61, Kle64, Bar67].

Nous recherchons ensuite la dimension minimale d'un polytope dont le graphe est isomorphe à celui d'un produit fixé de polytopes. Cette question s'inscrit dans la recherche systématique de polytopes de dimension extrémale ayant des propriétés fixées : par exemple, les d-polytopes *neighborly* [Gal63] sont ceux dont le $\left\lfloor \frac{d}{2} \right\rfloor$-squelette est complet (et qui atteignent le maximum de faces autorisé par le Théorème de la Borne Supérieure [McM70]) ; les d-polytopes *neighborly* cubiques [JZ00, Zie04, JR07] sont ceux dont le $\left\lfloor \frac{d}{2} \right\rfloor$-squelette est celui d'un n-cube, etc. Pour construire des polytopes de petite dimension ayant une propriété fixée, il est naturel et souvent efficace de partir d'une dimension suffisante pour s'assurer de l'existence de tels polytopes, et de projeter ces polytopes sur des sous-espaces de dimension inférieure en conservant la propriété recherchée. Ces techniques et leurs limites ont été largement étudiées dans la littérature [AZ99, Zie04, SZ10, San09, San08]. Nous les appliquons au Chapitre 7 pour construire des polytopes *$(k, \underline{n})$-neighborly prodsimpliciaux*, qui ont le même k-squelette qu'un certain produit de simplexes $\triangle_{\underline{n}} := \triangle_{n_1} \times \cdots \times \triangle_{n_r}$. Dans ce chapitre, nous donnons aussi des coordonnées entières pour de tels polytopes à l'aide de sommes de Minkowski explicites de polytopes cycliques.

2 MULTITRIANGULATIONS

Fixons n sommets sur le cercle unité et considérons les cordes entre ces sommets. On dit que deux cordes se croisent lorsque les segments ouverts s'intersectent. Un *ℓ-croisement* est un ensemble de ℓ cordes qui se croisent deux à deux. À l'instar des triangulations, nous nous intéressons aux ensembles maximaux qui évitent ces motifs :

Définition 1. *Une* k-triangulation *du n-gone est un ensemble maximal de cordes du n-gone sans $(k+1)$-croisement.*

Par définition, une corde ne peut apparaître dans un $(k+1)$-croisement que si elle a au moins k sommets de chaque côté. Nous disons qu'une telle corde est *k-pertinente*. Par maximalité, toute k-triangulation contient toutes les cordes qui ne sont pas k-pertinentes. Parmi ces cordes, celles qui séparent $k-1$ sommets de tous les autres sommets jouent un rôle particulier : nous les appelons *cordes du k-bord*.

Exemple 2. Pour certaines valeurs de k et n, il est facile de décrire les k-triangulations du n-gone :

- $\boxed{k=1}$ Les 1-triangulations sont juste les triangulations du n-gone.
- $\boxed{n=2k+1}$ Le graphe complet K_{2k+1} est l'unique k-triangulation du $(2k+1)$-gone car aucune de ses cordes n'est k-pertinente.
- $\boxed{n=2k+2}$ L'ensemble des cordes du $(2k+2)$-gone contient exactement un $(k+1)$-croisement formé par les $k+1$ diagonales du $(2k+2)$-gone reliant deux points antipodaux. Il y a donc $k+1$ k-triangulations du $(2k+2)$-gone, obtenues en retirant au graphe complet l'une de ses longues diagonales.
- $\boxed{n=2k+3}$ Les cordes k-pertinentes du $(2k+3)$-gone forment un cycle polygonal dans lequel deux cordes se croisent toujours sauf si elles sont consécutives. Par conséquent, les k-triangulations du $(2k+3)$-gone sont les unions disjointes de k paires de cordes k-pertinentes consécutives (auxquelles on ajoute toutes les cordes qui ne sont pas k-pertinentes).

Résultats antérieurs

Les ensembles de cordes du n-gone sans $(k+1)$-croisement apparaissent dans le cadre de la théorie extrémale des graphes géométriques (voir [PA95, Chapitre 14], [Fel04, Chapitre 1] et la discussion dans [CP92]). Dans le graphe d'intersection des cordes du n-gone, ces ensembles induisent en effet des sous-graphes sans k-clique, et sont donc à rapprocher du résultat classique de Turán qui borne le nombre d'arêtes d'un graphe sans k-clique. Vasilis Capoyleas et Janos Pach [CP92] ont montré que ces ensembles ne peuvent pas avoir plus de $k(2n-2k-1)$ cordes. Tomoki Nakamigawa [Nak00], et indépendamment Andreas Dress, Jacobus Koolen et Vincent Moulton [DKM02], ont prouvé que toutes les k-triangulations atteignent cette borne. Ces deux preuves sont basées sur l'opération de flip qui transforme une k-triangulation en une autre en changeant la position d'une seule corde. Tomoki Nakamigawa [Nak00] a montré que toute corde k-pertinente dans une k-triangulation peut être flippée, et que le graphe des flips est connexe. Nous tenons à observer que dans tous ces travaux antérieurs, les résultats sont obtenus de “manière indirecte” : d’abord, ils introduisent une opération de contraction (similaire à la contraction d’une arête du bord dans une triangulation), puis ils l’utilisent pour démontrer l’existence du flip (en toute généralité [Nak00], ou seulement dans des cas particuliers [DKM02]) et la connexité du graphe des flips, dont découle la formule sur le nombre de cordes. Pour résumer :

Théorème 3 ([CP92, Nak00, DKM02]). *(i) Il existe une opération inductive qui transforme les k-triangulations du $(n+1)$-gone en k-triangulations du n-gone et vice versa [Nak00].*

(ii) Toute corde k-pertinente d’une k-triangulation du n-gone peut être flippée et le graphe des flips est régulier et connexe [Nak00, DKM02].

(iii) Toute k-triangulation du n-gone a $k(2n-2k-1)$ cordes [CP92, Nak00, DKM02]. □

Jakob Jonsson [Jon03, Jon05] a complété ces résultats dans deux directions. D’une part, il a étudié les propriétés énumératives des multitriangulations :

Théorème 4 ([Jon05]). *Le nombre de k-triangulations du n-gone est donné par :*

$$\det(C_{n-i-j})_{1\le i,j\le k} = \det\begin{pmatrix} C_{n-2} & C_{n-3} & \cdots & C_{n-k-1} \\ C_{n-3} & \cdots & \cdots & \cdots \\ \cdots & \cdots & \cdots & C_{n-2k+1} \\ C_{n-k-1} & \cdots & C_{n-2k+1} & C_{n-2k} \end{pmatrix},$$

où $C_p := \frac{1}{p+1}\binom{2p}{p}$ dénote le p-ième nombre de Catalan. □

La preuve de ce théorème repose sur des résultats plus généraux concernant les $0/1$-remplissages de polyominos maximaux pour certaines restrictions sur leurs suites diagonales de 1.

Lorsque $k=1$, on retrouve simplement les nombres de Catalan qui comptent non seulement les triangulations, mais aussi les chemins de Dyck. Il se trouve que le déterminant de Hankel qui apparaît dans le théorème précédent compte aussi certaines familles de k-uplets de chemins de Dyck qui ne se croisent pas [GV85]. L’égalité des cardinaux de ces deux familles combinatoires motive la recherche d’une preuve bijective qui pourrait éclairer le résultat du Théorème 4. Même si Sergi Elizalde [Eli07] et Carlos Nicolas [Nic09] ont proposé deux bijections différentes dans le cas $k=2$, cette question reste ouverte dans le cas général. Nous discutons ce problème au Chapitre 4.

D’autre part, Jakob Jonsson [Jon03] a étudié le complexe simplicial $\Delta_{n,k}$ formé par les ensembles de cordes k-pertinentes du n-gone sans $(k+1)$-croisement. Comme tous les éléments maximaux de ce complexe ont $k(n-2k-1)$ éléments, il est pur de dimension $k(n-2k-1)-1$. Jakob Jonsson a en fait démontré le théorème suivant :

Théorème 5 ([Jon03]). *Le complexe simplicial $\Delta_{n,k}$ est une sphère épluchable de dimension $k(n-2k-1)-1$.* □

Volkmar Welker a conjecturé que ce complexe simplicial est même polytopal. Cette conjecture est vraie lorsque $k=1$ (le complexe simplicial des ensembles sans croisement de cordes internes du n-gone est isomorphe au complexe de bord du dual de l’associaèdre) et dans les cas de l’Exemple 2 (où l’on obtient respectivement un point, un simplexe et un polytope cyclique). Nous discutons cette question au Chapitre 4.

Décompositions des multitriangulations en étoiles

Notre contribution à l'étude des k-triangulations est basée sur leurs étoiles, qui généralisent les triangles des triangulations :

Définition 6. *Une k-étoile est un polygone (non-simple) avec $2k+1$ sommets $s_0, \dots, s_{2k}$ circulairement ordonnés sur le cercle unité, et $2k+1$ cordes $[s_0, s_k], [s_1, s_{k+1}], \dots, [s_{2k}, s_{k-1}]$.*

Les étoiles jouent pour les multitriangulations exactement le même rôle que les triangles pour les triangulations : elles les décomposent en entités géométriques plus simples et permettent d'en comprendre la combinatoire. Pour preuve, l'étude des propriétés d'incidence des étoiles dans les multitriangulations nous amène à retrouver au Chapitre 2 toutes les propriétés combinatoires des multitriangulations connues jusqu'alors. Notre premier résultat structurel est le suivant :

Théorème 7. *Soit T une k-triangulation du n-gone (avec $n \geq 2k+1$).*

(i) Une corde k-pertinente est contenue dans deux k-étoiles de T, une de chaque côté ; une corde du k-bord est contenue dans une k-étoile de T ; une corde qui n'est ni k-pertinente ni du k-bord n'est contenue dans aucune k-étoile de T.

(ii) T a exactement $n-2k$ k-étoiles et $k(2n-2k-1)$ cordes. □

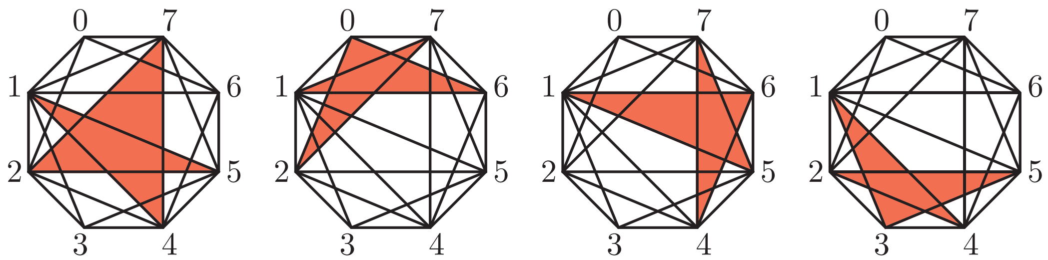

Figure 4 : Les 2-étoiles de la 2-triangulation de l'octogone de la Figure 2.

Nous prouvons le point (ii) de ce théorème par un argument direct de double comptage, en exhibant deux relations indépendantes entre le nombre de cordes et le nombre de k-étoiles d'une k-triangulation. Notre première relation provient du point (i) du théorème, tandis que la seconde repose sur les propriétés des bissectrices des k-étoiles. Une *bissectrice* d'une k-étoile est une bissectrice de l'un de ses angles, c'est-à-dire, une droite qui passe par l'un de ses sommets et sépare ses autres sommets en deux ensembles de cardinal k. Notre seconde relation est une conséquence directe de la correspondance entre les paires de k-étoiles de T et les cordes du n-gone qui ne sont pas dans T :

Théorème 8. *Soit T une k-triangulation du n-gone.*

(i) Toute paire de k-étoiles de T a une unique bissectrice commune, qui n'est pas dans T.

(ii) Réciproquement, toute corde qui n'est pas dans T est la bissectrice commune d'une unique paire de k-étoiles de T. □

Nous utilisons par ailleurs les étoiles et leurs bissectrices pour éclairer l'*opération de flip* et pour en donner une interprétation locale. De la même façon qu'un flip dans une triangulation remplace une diagonale par une autre dans un quadrangle formé par deux triangles adjacents, un flip dans une multitriangulation s'interprète comme une transformation ne faisant intervenir que deux étoiles adjacentes :

Théorème 9. *Soit T une k-triangulation du n-gone, soit e une corde k-pertinente de T et soit f la bissectrice commune aux deux k-étoiles de T qui contiennent e. Alors $T \triangle \{e, f\}$ est une k-triangulation du n-gone et c'est la seule, avec T, qui contienne $T \smallsetminus \{e\}$.* □

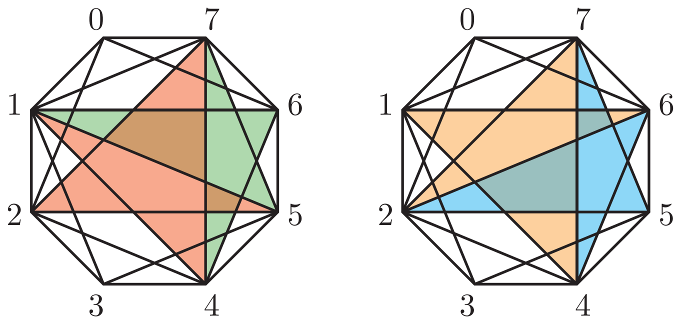

Figure 5 : Un flip dans la 2-triangulation de l'octogone de la Figure 2.

Cette interprétation simplifie l'étude du graphe des flips (dont les sommets sont les k-triangulations du n-gone et dont les arêtes sont les flips entre elles) et fournit de nouvelles preuves et des extensions partielles des résultats de [Nak00] :

Théorème 10. *Le graphe des flips sur les k-triangulations du n-gone est $k(n-2k-1)$-régulier, connexe, et pour tout $n > 4k^2(2k+1)$, son diamètre $\delta_{n,k}$ est borné par*

$$2\left\lfloor \frac{n}{2} \right\rfloor \left(k + \frac{1}{2}\right) - k(2k+3) \leq \delta_{n,k} \leq 2k(n-4k-1). \qquad \square$$

Nous utilisons aussi les étoiles pour étudier les *k-oreilles* dans les multitriangulations, c'est-à-dire les cordes qui séparent k sommets des autres sommets. Nous proposons une preuve simple du fait que toute k-triangulation a au moins $2k$ k-oreilles [Nak00], puis nous donnons plusieurs caractérisations des k-triangulations qui atteignent cette borne :

Théorème 11. *Le nombre de k-oreilles d'une k-triangulation est égal à $2k$ plus le nombre de* k-étoiles internes*, i.e. qui ne contiennent pas de cordes du k-bord.*

Si $k > 1$ et T est une k-triangulation, les assertions suivantes sont équivalentes :

(i) T a exactement $2k$ k-oreilles ;

(ii) T n'a aucune k-étoile interne ;

(iii) T est k-coloriable*, i.e. il existe une k-coloration de ses cordes k-pertinentes telle qu'aucun croisement n'est monochromatique ;*

(iv) l'ensemble des cordes k-pertinentes de T est l'union disjointe de k accordéons (un accordéon est une suite de cordes $[a_i, b_i]$ telle que pour tout i, soit $a_{i+1} = a_i$ et $b_{i+1} = b_i + 1$ soit $a_{i+1} = a_i - 1$ et $b_{i+1} = b_i$). □

Ensuite, nous réinterprétons en termes d'étoiles l'*opération inductive* du Théorème 3(i) qui transforme les k-triangulations du $(n+1)$-gone en k-triangulations du n-gone et *vice versa*. Dans un sens on écrase une k-étoile (contenant une corde du k-bord) en un k-croisement, et dans l'autre sens on enfle un k-croisement en une k-étoile. Volontairement, nous ne présentons cette opération qu'à la fin du Chapitre 2 pour souligner qu'aucune de nos preuves précédentes n'utilise cette transformation inductive.

Pour finir le Chapitre 2, nous utilisons le résultat du Théorème 7 pour interpréter une k-triangulation comme une *décomposition de surface* en $n - 2k$ k-gones. Des exemples sont présentés sur la Figure 6. Nous exploitons cette interprétation pour construire, à l'aide de multitriangulations, des décompositions très régulières d'une famille infinie de surfaces.

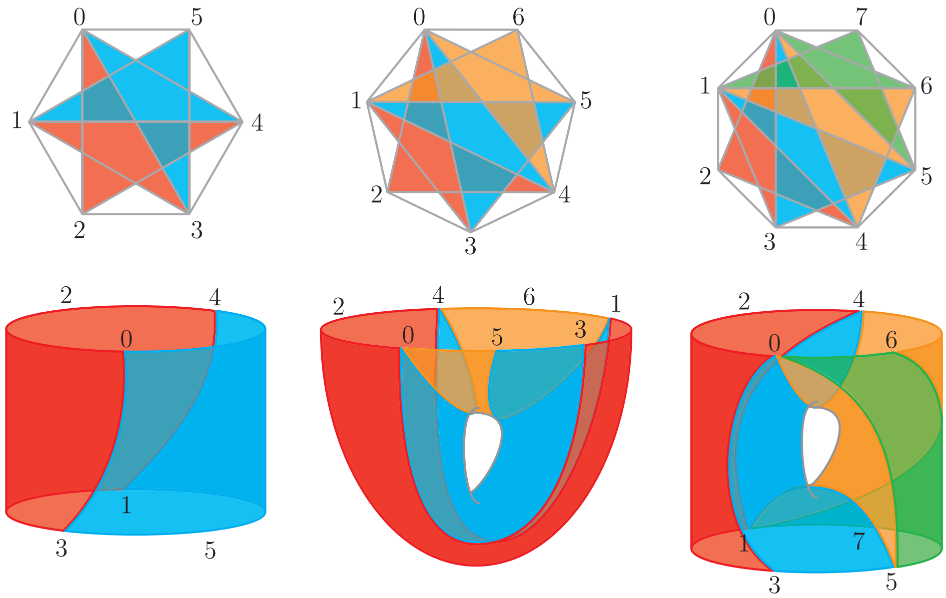

Figure 6 : Décompositions de surfaces associées aux multitriangulations.

Multitriangulations, pseudotriangulations et dualité

Dans le Chapitre 3, nous nous intéressons à l'interprétation des multitriangulations dans l'espace des droites du plan, c'est-à-dire dans le ruban de Möbius. Le cadre est celui de la dualité classique (voir [Fel04, Chapitres 5,6] et [Goo97]) entre configurations de points et arrangements de pseudodroites : l'ensemble p^* des droites qui passent par un point p du plan est une *pseudodroite* de l'espace des droites (une courbe fermée simple non-séparatrice), et l'ensemble $P^* := \{p^* \mid p \in P\}$ des pseudodroites duales à un ensemble fini P de points est un *arrangement de pseudodroites* (deux pseudodroites s'intersectent exactement une fois).

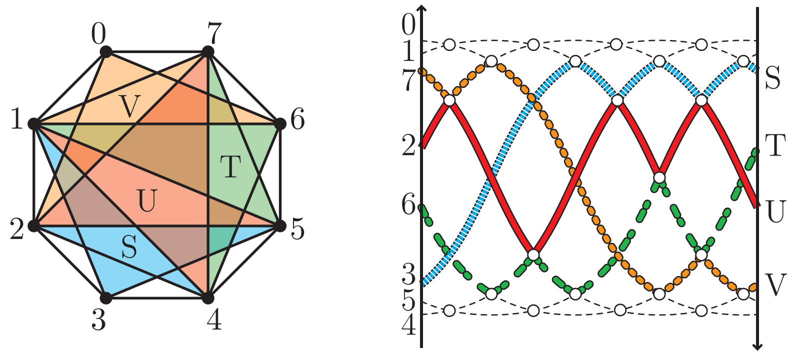

Figure 7 : Une 2-triangulation de l'octogone et son arrangement dual.

Le point de départ du Chapitre 3 est l'observation suivante (voir Figure 7) :

Observation 12. Soit T une k-triangulation du n-gone. Alors :

(i) l'ensemble S^* des bissectrices d'une k-étoile S de T est une pseudodroite ;

(ii) la bissectrice commune à deux k-étoiles R et S est un point de croisement des pseudodroites R^* et S^*, tandis qu'une corde commune à R et S est un point de contact entre R^* et S^* ;

(iii) l'ensemble $T^* := \{S^* \mid S\ k\text{-étoile de } T\}$ de toutes les pseudodroites duales aux k-étoiles de T est un *arrangement de pseudodroites avec points de contact* (deux pseudodroites se croisent exactement une fois, mais peuvent se toucher en un nombre fini de contacts) ;

(iv) le support de cet arrangement couvre exactement le support de l'arrangement dual V_n^* des sommets du n-gone privé de ses k premiers niveaux.

Nous montrons la réciproque de cette observation :

Théorème 13. *Tout arrangement de pseudodroites avec points de contact dont le support couvre exactement le support de l'arrangement dual V_n^* des sommets du n-gone privé de ses k premiers niveaux est l'arrangement dual d'une k-triangulation du n-gone.* □

Dans [PV94, PV96a], une observation similaire avait été faite pour les pseudotriangulations pointées d'un ensemble de points en position générale. Introduites pour l'étude du complexe de visibilité d'obstacles convexes disjoints du plan [PV96b, PV96c], les pseudotriangulations ont été utilisées dans divers contextes géométriques (tels que la planification de mouvements et la rigidité [Str05, HOR+05]) et leurs propriétés ont été largement étudiées (nombre de pseudotriangulations [AAKS04, AOSS08], polytope des pseudotriangulations [RSS03], considérations algorithmiques [Ber05, BKPS06, HP], etc.). Nous renvoyons à [RSS08] pour plus de détails.

Définition 14. *Un* pseudotriangle *est un polygone Δ avec exactement trois angles convexes reliés par trois chaînes polygonales concaves. Une droite est* tangente *à Δ si elle passe par un angle convexe de Δ et sépare ses deux arêtes adjacentes, ou si elle passe par un angle concave de Δ et ne sépare pas ses deux arêtes adjacentes. Une* pseudotriangulation *d'un ensemble P de points en position générale est un ensemble d'arêtes qui décompose l'enveloppe convexe de P en pseudotriangles.*

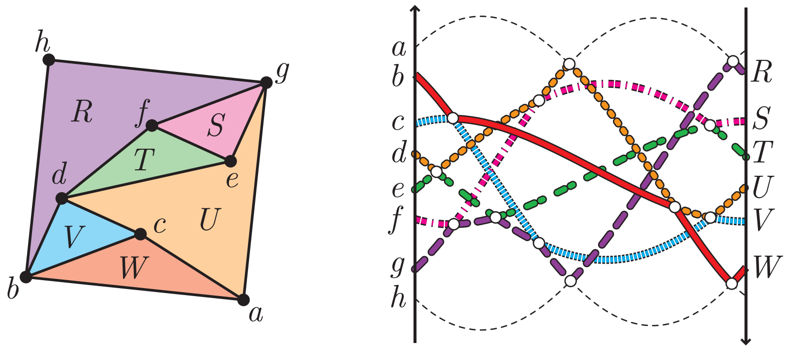

Figure 8 : Une pseudotriangulation et son arrangement dual.

Dans cette thèse, nous ne considérons que des pseudotriangulations *pointées*, c'est-à-dire les pseudotriangulations telles que par chaque point $p \in P$ passe une droite qui définit un demi-plan fermé ne contenant aucune des arêtes issues de p. Pour une pseudotriangulation pointée T de P, il a été observé [PV94, PV96a] que :

(i) l'ensemble Δ^* des droites tangentes à un pseudotriangle Δ est une pseudodroite ; et

(ii) l'ensemble $T^* := \{\Delta^* \mid \Delta \text{ pseudotriangle de } T\}$ est un arrangement de pseudodroites avec points de contact supporté par l'arrangement P^* dual de P privé de son premier niveau.

Nous donnons différentes preuves de la réciproque :

Théorème 15. *Soit P un ensemble de points en position générale et P^* son arrangement dual. Tout arrangement de pseudodroites avec points de contact dont le support couvre précisément le support de l'arrangement P^* privé de son premier niveau est l'arrangement dual d'une pseudotriangulation de P.* □

Motivés par ces deux théorèmes, nous considérons alors les arrangements de pseudodroites qui partagent un même support. Nous définissons une opération de flip qui correspond au flip dans les multitriangulations et les pseudotriangulations :

Définition 16. *Deux arrangements de pseudodroites avec le même support sont reliés par un flip si la différence symétrique de leurs ensembles de points de contact est réduite à une paire $\{u, v\}$. Dans ce cas, dans l'un des arrangements, u est un point de contact de deux pseudodroites qui se croisent en v, tandis que dans l'autre arrangement, v est un point de contact de deux pseudodroites qui se croisent en u.*

Nous étudions le graphe $G(\mathcal{S})$ des flips sur les arrangements supportés par $\mathcal{S}$. Par exemple, lorsque $\mathcal{S}$ est le support d'un arrangement de deux pseudodroites avec p points de contact, le graphe $G(\mathcal{S})$ est le graphe complet à $p + 1$ sommets. Nous nous intéressons à certaines orientations acycliques du graphe $G(\mathcal{S})$, données par des coupes verticales du support $\mathcal{S}$. Une telle orientation a une unique source que nous appelons *arrangement glouton* et que nous caractérisons en terme de réseaux de tri. L'étude de ces arrangements gloutons et de leur transformation lorsque l'orientation de $G(\mathcal{S})$ évolue fournit un algorithme d'énumération des arrangements de pseudodroites avec points de contact partageant un même support, dont l'espace de travail reste polynomial. Ainsi, nous éclairons et donnons une preuve complémentaire de l'algorithme similaire existant pour énumérer les pseudotriangulations d'un ensemble de points [BKPS06].

Nous revenons ensuite dans un cadre plus particulier. Au regard de la dualité entre les multitriangulations (resp. les pseudotriangulations) et les arrangements de pseudodroites avec points de contact, nous proposons la généralisation suivante des multitriangulations lorsque les points ne sont pas en position convexe :

Définition 17. *Une* k-pseudotriangulation *d'un arrangement de pseudodroites L est un arrangement de pseudodroites avec points de contact dont le support est l'arrangement L privé de ses k premiers niveaux. Une k-pseudotriangulation d'un ensemble de points P en position générale est un ensemble d'arêtes T qui correspond par dualité aux points de contact d'une k-pseudotriangulation T^* de P^*.*

Nous montrons que toutes les k-pseudotriangulations d'un ensemble de points P ont exactement $k(2|P| - 2k - 1)$ arêtes et ne peuvent pas contenir de configuration de $2k + 1$ arêtes alternantes, mais qu'elles peuvent en revanche éventuellement contenir un $(k + 1)$-croisement. Nous étudions ensuite leurs étoiles : une étoile d'une k-pseudotriangulation T de P est un polygone formé par l'ensemble des arêtes correspondantes aux points de contact sur une pseudodroite fixée de T^*. Nous discutons leur nombre possible de coins, et nous montrons que pour tout point q du plan, la somme des indices des étoiles de T autour de q est indépendante de T.

Nous terminons le Chapitre 3 avec trois questions reliées aux multipseudotriangulations :

(i) Nous étudions d'abord les *multipseudotriangulations itérées* : une k-pseudotriangulation d'une m-pseudotriangulation d'un arrangement de pseudodroites L est une $(k + m)$-pseudotriangulation de L. Nous donnons cependant un exemple de 2-triangulation qui ne contient pas de triangulation. Nous montrons en revanche que les multipseudotriangulations gloutonnes d'un arrangement sont des itérées de la pseudotriangulation gloutonne.

(ii) Nous donnons ensuite une caractérisation des arêtes de la k-pseudotriangulation gloutonne d'un ensemble de points P en terme de *k-arbres d'horizon* de P. Cette caractérisation généralise une observation de Michel Pocchiola [Poc97] pour les pseudotriangulations.

(iii) Finalement, nous définissons les multipseudotriangulations de configurations de convexes disjoints du plan et étudions leurs propriétés élémentaires. Les arrangements duaux des configurations de convexes sont les *arrangements de double pseudodroites*, introduits par Luc Habert et Michel Pocchiola [HP09]. Dans l'Appendice A, nous énumérons à isomorphisme près les arrangements d'au plus 5 double pseudodroites.

Trois problèmes ouverts

Finalement, nous discutons au Chapitre 4 trois problèmes ouverts qui illustrent la richesse combinatoire et géométrique des multitriangulations. Notre but est de présenter des idées naturelles basées sur les étoiles qui peuvent être fertiles bien qu'elles n'apportent pour l'heure que des réponses partielles à ces problèmes.

Le premier problème que nous discutons est celui de trouver une *bijection explicite* entre l'ensemble des multitriangulations et l'ensemble des k-uplets de chemins de Dyck sans croisement, qui sont tous deux comptés par le déterminant de Hankel du Théorème 4. Si dans une triangulation T, on note $\delta_i(T)$ le nombre de triangles de T dont le premier sommet est i, alors l'application $T \mapsto N^{\delta_0(T)}EN^{\delta_1(T)}E \dots N^{\delta_{n-3}(T)}E$ est une bijection des triangulations du n-gone dans les chemins de Dyck de demi-longueur $n-2$ (où N et E désignent les pas nord et est). Jakob Jonsson [Jon03] a généralisé cette remarque en comparant la répartition des séquences de degrés entrants des k-triangulations avec les signatures des k-uplets de chemins de Dyck (sans donner les définitions précises, signalons que ces deux k-uplets de séquences généralisent la séquence $(\delta_i(T))$ d'une triangulation T et la séquence des puissances de N dans un chemin de Dyck). Motivés par ce résultat, nous avons cherché à définir des k-colorations des cordes k-pertinentes d'une k-triangulation de sorte que les séquences respectives de degrés entrant de chaque couleur définissent des k-uplets de chemins de Dyck qui ne se croisent pas. Nous présentons une coloration basée sur les étoiles, qui vérifie cette propriété, mais pour laquelle l'application des multitriangulations dans les k-uplets de chemins de Dyck n'est malheureusement pas bijective.

Notre second problème concerne les propriétés de *rigidité* des multitriangulations. Une triangulation est *minimalement rigide* dans le plan : les seuls mouvements de ses sommets qui préservent les longueurs de ses arêtes sont des isométries du plan, et retirer n'importe quelle arête rend la structure flexible. De manière équivalente, une triangulation vérifie la condition de Laman : elle a $2n-3$ arêtes et tout sous-graphe à m sommets a au plus $2m-3$ arêtes. Nous observons deux connexions intéressantes entre les multitriangulations et la théorie de la rigidité :

(i) Tout d'abord, une k-triangulation est $\left(2k, \binom{2k+1}{2}\right)$-*raide* : elle contient $2kn - \binom{2k+1}{2}$ arêtes et tout sous-graphe à m sommets a au plus $2km - \binom{2k+1}{2}$ arêtes. Cette propriété combinatoire fait d'une k-triangulation un candidat raisonnable pour être un graphe génériquement minimalement rigide en dimension $2k$. Nous prouvons cette conjecture lorsque $k=2$.

(ii) Ensuite, nous montrons que le graphe dual d'une k-triangulation est (k,k)-raide. En particulier, il peut être décomposé en k arbres couvrants arêtes-disjoints, ce qui doit être rapproché du fait que le dual d'une triangulation est un arbre.

Finalement, nous revenons à la question de la *réalisation polytopale* du complexe simplicial $\Delta_{n,k}$ formé par les ensembles de cordes k-pertinentes du n-gone sans $(k+1)$-croisement. Nous présentons deux contributions modestes à cette question :

(i) Nous répondons d'une part au premier cas non-trivial en décrivant l'espace des réalisations symétriques de $\Delta_{8,2}$. Ce résultat est obtenu en deux étapes : d'abord nous énumérons par ordinateur tous les matroides orientés symétriques qui réalisent notre complexe simplicial ; ensuite nous étudions les réalisations polytopales symétriques de ces matroides orientés.

(ii) Nous nous intéressons d'autre part à une construction de l'associaèdre due à Jean-Louis Loday [Lod04]. Nous proposons une interprétation de sa construction en termes d'arrangements duaux des triangulations, qui se généralise naturellement aux multitriangulations. Nous obtenons un polytope dont les facettes sont définies par des inégalités simples et qui réalise le graphe des flips restreint à certaines multitriangulations (celles dont le graphe dual est acyclique). Ce polytope aurait pu être *a priori* une projection d'un polytope réalisant $\Delta_{n,k}$, mais nous montrons toutefois qu'une telle projection est impossible.

3 POLYTOPALITÉ DE PRODUITS

Dans la deuxième partie de cette thèse, nous nous intéressons à des questions de réalisation polytopale de graphes (ou de squelettes) obtenus par produits cartésiens d'autres graphes (ou squelettes).

Le *produit cartésien* de deux polytopes P, Q est le polytope $P \times Q := \{(p,q) \mid p \in P, q \in Q\}$. Sa structure combinatoire ne dépend que de celle de ses facteurs : la dimension de $P \times Q$ est la somme des dimensions de P et Q et les faces non-vides de $P \times Q$ sont précisément les produits d'une face non-vide de P par une face non-vide de Q.

Polytopalité de produits de graphes non-polytopaux

Dans le Chapitre 6, nous nous intéressons au produit de graphes. Le *produit cartésien* de deux graphes G et H est le graphe $G \times H$ dont les sommets sont $V(G \times H) := V(G) \times V(H)$ et dont les arêtes sont $E(G \times H) := \big(E(G) \times V(H)\big) \cup \big(V(G) \times E(H)\big)$. Autrement dit, pour tous sommets $a, c \in V(G)$ et $b, d \in V(H)$, les sommets (a, b) et (c, d) de $G \times H$ sont adjacents si $a = c$ et $\{b, d\} \in E(H)$, ou $b = d$ et $\{a, c\} \in E(G)$. Ce produit est en accord avec le produit de polytopes : le graphe d'un produit de polytopes est le produit de leurs graphes. En particulier, le produit de deux graphes polytopaux est automatiquement polytopal. Dans ce chapitre, nous étudions la question réciproque : étant donnés deux graphes G et H, la polytopalité du produit $G \times H$ implique-t-elle celle de ses facteurs G et H ?

Le produit d'un triangle par un chemin de longueur 2 est un contre-exemple simple à cette question : bien que le chemin ne soit pas polytopal, le produit est le graphe d'un 3-polytope obtenu en collant deux prismes triangulaires par une face triangulaire. Nous éliminons de tels exemples en exigeant que chaque facteur soit un graphe régulier. Si G et H sont réguliers de degré respectifs d et e, alors le produit $G \times H$ est $(d+e)$-régulier et il est naturel de se demander s'il est le graphe d'un $(d + e)$-polytope simple. La réponse est donnée par le théorème suivant :

Théorème 18. *Un produit $G \times H$ est le graphe d'un polytope simple si et seulement si ses deux facteurs G et H sont des graphes de polytopes simples. Dans ce cas, il existe un unique polytope simple dont le graphe est $G \times H$: c'est précisément le produit des uniques polytopes simples dont les graphes respectifs sont G et H.* □

Dans ce théorème, l'unicité du polytope simple réalisant $G \times H$ découle du fait qu'un polytope simple est complètement déterminé par son graphe [BML87, Kal88]. Ces résultats reposent sur la propriété suivante : tout ensemble de $k + 1$ arêtes adjacentes à un même sommet d'un polytope simple P définit une k-face de P.

En application du Théorème 18 nous obtenons une famille infinie de graphes 4-réguliers non-polytopaux : le produit d'un graphe 3-régulier non-polytopal par un segment est non-polytopal et 4-régulier.

Nous cherchons ensuite à savoir si un produit de graphes réguliers non-polytopaux peut être polytopal dans une dimension plus petite que son degré. Les exemples suivants répondent à cette question :

Théorème 19. *(i) Lorsque $n \geq 3$, le produit $K_{n,n} \times K_2$ d'un graphe complet bipartite par un segment n'est pas polytopal.*

(ii) Le produit d'un graphe d-polytopal par le graphe d'une subdivision régulière d'un e-polytope est $(d+e)$-polytopal. Ceci fournit des produits polytopaux de graphes réguliers non-polytopaux (par exemple le produit de deux dominos de la Figure 3 et le graphe de la Figure 9). □

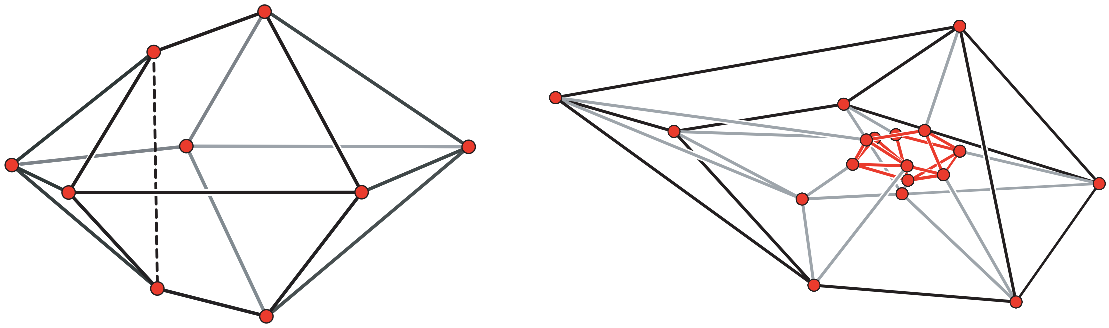

Figure 9 : Un graphe H 4-régulier et non-polytopal qui est le graphe d'une subdivision régulière d'un 3-polytope (gauche) et le diagramme de Schlegel d'un 4-polytope dont le graphe est le produit de H par un segment (droite).

Polytopes *neighborly* prodsimpliciaux

Au Chapitre 7, nous considérons des polytopes dont les squelettes sont ceux d'un produit de simplexes :

Définition 20. *Soient $k \geq 0$ et $\underline{n} := (n_1, \ldots, n_r)$, avec $r \geq 1$ et $n_i \geq 1$ pour tout i. Un polytope est* $(k, \underline{n})$-neighborly prodsimplicial *— ou en abrégé* $(k, \underline{n})$-PSN *— si son k-squelette est combinatoirement équivalent à celui du produit de simplexes $\triangle_{\underline{n}} := \triangle_{n_1} \times \cdots \times \triangle_{n_r}$.*

Cette définition généralise deux classes particulières de polytopes :

(i) On retrouve les polytopes *neighborly* lorsque $r = 1$. Dans la littérature, un polytope est *k-neighborly* si tout sous-ensemble de k de ses sommets forme une face. Avec notre définition, un tel polytope est $(k-1, n)$-PSN.

(ii) On retrouve les polytopes *neighborly cubiques* [JZ00, JR07, SZ10] lorsque $\underline{n} = (1, 1, \ldots, 1)$.

Le produit $\triangle_{\underline{n}}$ est un polytope $(k, \underline{n})$-PSN de dimension $\sum n_i$. Nous cherchons naturellement des polytopes $(k, \underline{n})$-PSN en dimension inférieure. Par exemple, le polytope cyclique $C_{2k+2}(n+1)$ est un polytope (k, n)-PSN en dimension $2k+2$. Nous notons $\delta(k, \underline{n})$ la dimension minimale que peut avoir un polytope $(k, \underline{n})$-PSN.

Certains polytopes PSN s'obtiennent en projetant le produit $\triangle_{\underline{n}}$, ou tout polytope combinatoirement équivalent, sur un sous-espace de dimension inférieure. Par exemple, le polytope cyclique $C_{2k+2}(n+1)$, comme n'importe quel polytope avec $n+1$ sommets, est une projection du simplexe $\triangle_n$ sur $\mathbb{R}^{2k+2}$.

Définition 21. *Un polytope* $(k, \underline{n})$-PSN *est* $(k, \underline{n})$-neighborly prodsimplicial projeté *— ou en abrégé* $(k, \underline{n})$-PPSN *— si c'est une projection d'un polytope combinatoirement équivalent à* $\triangle_{\underline{n}}$.

Nous notons $\delta_{pr}(k, \underline{n})$ la dimension minimale d'un polytope $(k, \underline{n})$-PPSN.

Notre Chapitre 7 se divise en deux parties. Dans la première, nous présentons trois méthodes pour construire des polytopes PPSN en petite dimension :
(i) par des réflexions de polytopes cycliques ;
(ii) par des sommes de Minkowski de polytopes cycliques ;
(iii) par des "projections de produits déformés", dans l'esprit des constructions de Raman Sanyal et Günter Ziegler [Zie04, SZ10].
Dans la seconde partie, nous obtenons des obstructions topologiques à l'existence de tels objets, en utilisant des techniques développées par Raman Sanyal [San09] pour borner le nombre de sommets d'une somme de Minkowski. Au regard de ces obstructions, nos constructions de la première partie se révèlent optimales pour un large spectre de paramètres.

Constructions. Notre premier exemple non-trivial est un polytope $(k, (1, n))$-PSN en dimension $2k + 2$, obtenu par réflexion du polytope cyclique $C_{2k+2}(n + 1)$ par rapport à un hyperplan bien choisi :

Proposition 22. *Pour tous* $k \geq 0$, $n \geq 2k + 2$ *et* $\lambda \in \mathbb{R}$ *suffisamment grand, le polytope*

$$\mathrm{conv}\left(\left\{(t_i, \dots, t_i^{2k+2})^T \mid i \in [n+1]\right\} \cup \left\{(t_i, \dots, t_i^{2k+1}, \lambda - t_i^{2k+2})^T \mid i \in [n+1]\right\}\right)$$

est un polytope $(k, (1, n))$-PSN *de dimension* $2k + 2$. $\square$

Par exemple, cette construction fournit un 4-polytope dont le graphe est $K_2 \times K_n$ $(n \geq 3)$.

Ensuite, à l'aide de sommes de Minkowski bien choisies de polytopes cycliques, nous obtenons des coordonnées explicites de polytopes $(k, \underline{n})$-PPSN :

Théorème 23. *Soient* $k \geq 0$ *et* $\underline{n} := (n_1, \dots, n_r)$ *avec* $r \geq 1$ *et* $n_i \geq 1$ *pour tout* i. *Il existe des ensembles* $I_1, \dots, I_r \subset \mathbb{R}$, *avec* $|I_i| = n_i$ *pour tout* i, *tels que le polytope*

$$\mathrm{conv}\left\{w_{a_1,\dots,a_r} \mid (a_1, \dots, a_r) \in I_1 \times \dots \times I_r\right\} \subset \mathbb{R}^{2k+r+1}$$

soit $(k, \underline{n})$-PPSN, *où* $w_{a_1,\dots,a_r} := \left(a_1, \dots, a_r, \sum_{i \in [r]} a_i^2, \dots, \sum_{i \in [r]} a_i^{2k+2}\right)^T$. *Par conséquent,*

$$\delta(k, \underline{n}) \leq \delta_{pr}(k, \underline{n}) \leq 2k + r + 1. \qquad \square$$

Lorsque $r = 1$ nous retrouvons les polytopes *neighborly*.

Finalement, nous étendons la technique de "projection de produits déformés de polygones" de Raman Sanyal et Günter Ziegler [Zie04, SZ10] aux produits de polytopes simples arbitraires : nous projetons un polytope bien choisi, combinatoirement équivalent à un produit de polytopes simples, de sorte à préserver son k-squelette complet. Plus concrètement, nous décrivons comment utiliser des colorations des graphes des polytopes polaires des facteurs du produit pour augmenter la dimension du squelette préservé. La version basique de cette technique fournit le résultat suivant :

Proposition 24. *Soient $P_1, \dots, P_r$ des polytopes simples. Pour chaque polytope P_i, on note n_i sa dimension, m_i son nombre de facettes, et $\chi_i := \chi(\mathrm{gr}(P_i^\diamond))$ le nombre chromatique du graphe du polytope polaire $P_i^\diamond$. Pour un entier fixé $d \le n$, soit t l'entier maximal tel que $\sum_{i=1}^t n_i \le d$. Alors il existe un d-polytope dont le k-squelette est combinatoirement équivalent à celui du produit $P_1 \times \cdots \times P_r$ dès lors que*

$$0 \le k \le \sum_{i=1}^{r}(n_i - m_i) + \sum_{i=1}^{t}(m_i - \chi_i) + \left\lfloor \frac{1}{2}\left(d - 1 + \sum_{i=1}^{t}(\chi_i - n_i)\right)\right\rfloor. \qquad \square$$

En spécialisant cette proposition à un produit de simplexes, nous obtenons une autre construction de polytopes PPSN. Lorsque certains des simplexes sont petits comparés à k, cette technique produit en fait nos meilleurs exemples de polytopes PPSN :

Théorème 25. *Pour tous $k \ge 0$ et $\underline{n} := (n_1, \dots, n_r)$ avec $1 = n_1 = \cdots = n_s < n_{s+1} \le \cdots \le n_r$,*

$$\delta_{pr}(k, \underline{n}) \le \begin{cases} 2(k+r) - s - t & \text{si } 3s \le 2k + 2r, \\ 2(k+r-s)+1 & \text{si } 3s = 2k+2r+1, \\ 2(k+r-s+1) & \text{si } 3s \ge 2k+2r+2, \end{cases}$$

où $t \in \{s, \dots, r\}$ est maximal tel que $3s + \sum_{i=s+1}^{t}(n_i + 1) \le 2k + 2r$. $\square$

Si $n_i = 1$ pour tout i, nous retrouvons les polytopes *neighborly* cubiques de [SZ10].

Obstructions. Pour obtenir des bornes inférieures sur la dimension minimale $\delta_{pr}(k, \underline{n})$ que peut avoir un polytope $(k, \underline{n})$-PPSN, nous appliquons une méthode due à Raman Sanyal [San09]. À toute projection qui préserve le k-squelette de $\triangle_{\underline{n}}$, nous associons par dualité de Gale un complexe simplicial qui doit être plongeable dans un espace d'une certaine dimension. L'argument repose ensuite sur une obstruction topologique dérivée du critère de Sarkaria pour le plongement d'un complexe simplicial en termes de colorations de graphes de Kneser [Mat03]. Nous obtenons le résultat suivant :

Théorème 26. *Soit $\underline{n} := (n_1, \dots, n_r)$ avec $1 = n_1 = \cdots = n_s < n_{s+1} \le \cdots \le n_r$.*

(i) Si

$$0 \le k \le \sum_{i=s+1}^{r} \left\lfloor \frac{n_i - 2}{2} \right\rfloor + \max\left\{0, \left\lfloor \frac{s-1}{2} \right\rfloor\right\},$$

alors $\delta_{pr}(k, \underline{n}) \ge 2k + r - s + 1$.

(ii) Si $k \ge \left\lfloor \frac{1}{2}\sum_i n_i \right\rfloor$ alors $\delta_{pr}(k, \underline{n}) \ge \sum_i n_i$. $\square$

En particulier, les bornes inférieure et supérieure des Théorèmes 23 et 26 se rejoignent sur un large champ de paramètres :

Théorème 27. *Pour tout* $\underline{n} := (n_1, \dots, n_r)$ *avec* $r \geq 1$ *et* $n_i \geq 2$ *pour tout* i*, et pour tout* k *tel que* $0 \leq k \leq \sum_{i\in[r]} \left\lfloor \frac{n_i-2}{2} \right\rfloor$*, le plus petit polytope* $(k, \underline{n})$*-PPSN est de dimension exactement* $2k + r + 1$*. Autrement dit :*

$$\delta_{pr}(k, \underline{n}) = 2k + r + 1. \qquad \square$$

Remarque 28. Les techniques de projection de polytopes et les obstructions que nous utilisons ont été développées par Raman Sanyal et Günter Ziegler [Zie04, SZ10, San09]. Nous avons décidé de les présenter dans cette thèse parce que leur application aux produits de simplexes fournit des résultats nouveaux qui complètent notre étude sur la polytopalité des produits. Par ailleurs, après avoir appliqué ces méthodes aux produits de simplexes, nous avons découvert que Thilo Rörig et Raman Sanyal avaient un travail similaire en cours sur le même sujet [RS09] (voir aussi [San08, Rör08]).

RESUMEN

1 INTRODUCCIÓN

Los temas tratados en esta memoria se insertan en el campo de la *geometría discreta y algorítmica* [GO04]: los problemas encontrados en general involucran conjuntos finitos de objetos geométricos elementales (como puntos, rectas, semi-espacios, etc.), y las preguntas tratan de la manera como están relacionados, colocados, situados unos respecto a otros (cómo se intersecan, cómo se ven, qué delimitan, etc.). Esta memoria versa sobre dos sujetos particulares: las *multitriangulaciones* y las *realizaciones politopales de productos*. Sus varias conexiones con la geometría discreta nos permitirán descubrir algunas de sus numerosas facetas. Presentamos algunos ejemplos en esta introducción. Empezamos por presentar su problemática común, la búsqueda de una realización politopal de una estructura, que ha dirigido nuestra investigación sobre estos sujetos.

Un politopo (convexo) es la envoltura convexa de un conjunto finito de puntos de un espacio euclidiano. Aunque el interés despertado por ciertos politopos se remonta a la Antigüedad (sólidos Platónicos), su estudio sistemático es relativamente reciente y los principales resultados datan del siglo XX (ver [Grü03, Zie95] y sus referencias). El estudio de los politopos versa no solamente sobre sus propiedades geométricas pero también sobre sus aspectos más combinatorios. Se trata especialmente de comprender sus caras (sus intersecciones con un hiperplano soporte) y el retículo que componen (es decir las relaciones de inclusión entre estas caras).

Las preguntas de *realización politopal* forman en cierto modo el problema recíproco: versan sobre la existencia y la construcción de politopos a partir de una estructura combinatoria dada. Por ejemplo, dado un grafo, querríamos determinar si es el grafo de un politopo: diremos entonces que el grafo es politopal. El resultado fundador en este campo es el Teorema de Steinitz [Ste22] que caracteriza los grafos de 3-politopos. En cuanto pasamos a dimensión 4, la situación es mucho menos satisfactoria: a pesar de ciertas condiciones necesarias [Bal61, Kle64, Bar67], los grafos de politopos no admiten ninguna caracterización local en dimensión general [RG96]. Cuando un grafo es politopal, nos preguntamos por las propiedades de sus realizaciones, por ejemplo su número de caras, su dimensión, etc. Intentamos construir ejemplos que optimizan ciertas de estas propiedades: típicamente, un politopo de dimensión mínima con un grafo dado [Gal63, JZ00, SZ10]. Estas preguntas de realizaciones politopales son interesantes para grafos que provienen bien de grafos de transformación sobre conjuntos combinatorios o geométricos (grafo de transposiciones adyacentes sobre las permutaciones, grafo de flips sobre las triangulaciones, etc.), bien de operaciones sobre otros grafos (que pueden ser locales como la transformación ΔY, o globales como el producto cartesiano). Estas preguntas son interesantes no solamente para un grafo, sino más generalmente para cualquier subconjunto de un retículo.

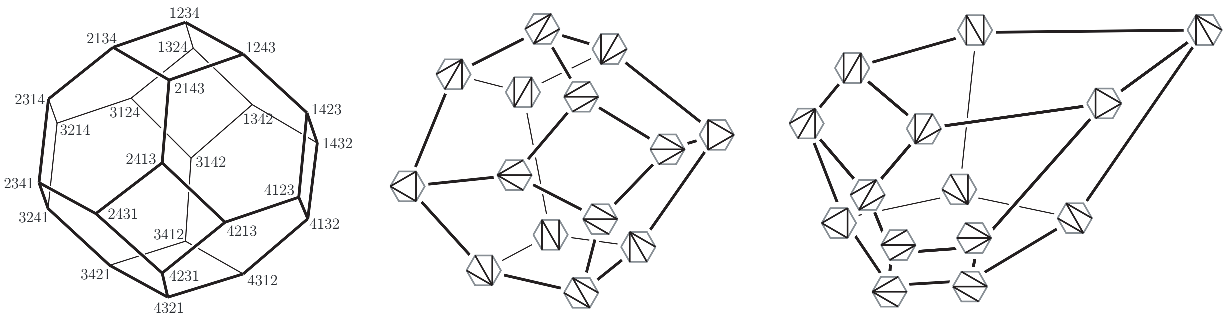

Figura 1: El permutoedro y dos realizaciones del asociaedro.

Politopalidad de grafos de flips. La existencia de realizaciones politopales es primero estudiada para grafos de transformación sobre estructuras combinatorias o geométricas. Podemos mencionar aquí el permutoedro cuyos vértices corresponden a las permutaciones de $[n]$ y donde dos vértices están relacionados por una arista si las permutaciones correspondientes difieren por una transposición de dos posiciones adyacentes. Otros ejemplos, así como clases de politopos que permitan realizar ciertas estructuras combinatorias están expuestos en [Zie95, Lectura 9]. De manera general, las preguntas de politopalidad de estructuras combinatorias son interesantes no solamente por sus resultados, sino también porque su estudio obliga a entender la combinatoria de los objetos y a desarrollar nuevas métodos.

Dos ejemplos particulares de estructuras combinatorias politopales desempeñan un papel importante en esta memoria. Encontramos primero el asociaedro cuyo borde realiza el dual del complejo simplicial formado por todos los conjuntos sin cruce de cuerdas del n-gono. El grafo del asociaedro corresponde al grafo de flips de las triangulaciones del n-gono. El asociaedro aparece en diversos contextos y varias realizaciones politopales han sido propuestas [Lee89, BFS90, GKZ94, Lod04, HL07]. Encontramos después el politopo de las pseudotriangulaciones de un conjunto de puntos del plano euclideano [RSS03]. Introducidas para el estudio del complejo de visibilidad de obstáculos convexos disjuntos del plano [PV96b, PV96c], las pseudotriangulaciones han sido utilizadas en diversos contextos geométricos [RSS08]. Sus propiedades de rigidez [Str05] permitían establecer la politopalidad de su grafo de flips [RSS03].

En la primera parte de esta memoria, nos interesamos por la politopalidad del grafo de flips de las multitriangulaciones. Estos objetos, aparecidos de manera relativamente contingente [CP92, DKM02, DKKM01], tienen una rica estructura combinatoria [Nak00, Jon03, Jon05]. Una *k-triangulación* es un conjunto maximal de cuerdas del n-gono que no contiene ningún subconjunto de $k+1$ cuerdas que se cruzan mutuamente. Consideramos el grafo de flips en el cual dos multitriangulaciones están relacionadas si difieren por una cuerda. Como para las triangulaciones, que ocurren cuando $k = 1$, este grafo es regular y conexo, y nos preguntamos por su politopalidad. Jakob Jonsson [Jon03] hizo un primer paso en esta dirección demostrando que el complejo simplicial formado por los conjuntos de cuerdas que no contienen ningún subconjunto de $k+1$ cuerdas que se cruzan mutuamente es una esfera topológica. Aunque solo tenemos respuestas parciales, esta pregunta reveló resultados interesantes que exponemos en esta memoria.

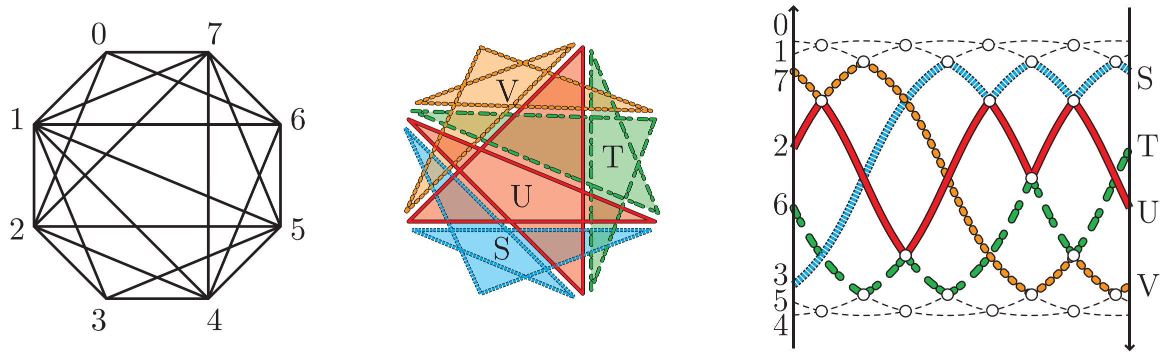

Figura 2: Una 2-triangulación, su descomposición en estrellas, y su arreglo dual.

Algunas construcciones del asociaedro [BFS90, Lod04] están basadas, directamente o indirectamente, en los triángulos de las triangulaciones. Para las multitriangulaciones, ningún objeto elemental similar aparece en los trabajos anteriores. En primer lugar, hemos intentado entender qué ha sido de los triángulos en las multitriangulaciones. Las *estrellas* que introducimos en el Capítulo 2 responden a esta pregunta. Tal como los triángulos en las triangulaciones, estimamos que estas estrellas dan el punto de vista pertinente para entender las multitriangulaciones. Como prueba, empezamos por recobrar con ayuda de estas estrellas todas las propiedades combinatorias elementales conocidas hasta entonces sobre las multitriangulaciones. Primero, estudiamos las relaciones de incidencia entre las estrellas y las cuerdas (cada cuerda interna está contenida en dos estrellas) que nos permiten recobrar que todas las k-triangulaciones del n-gono tienen el mismo cardinal. Después, considerando las bisectrices de las estrellas, damos una interpretación local de la operación de flip (una cuerda interna es substituida por la única bisectriz común de las dos estrellas que la contienen), lo que aclara el estudio del grafo de flips y de su diámetro. Redefinimos además en términos de estrellas operaciones inductivas sobre multitriangulaciones que permiten añadir o suprimir un vértice al n-gono. En fin, utilizamos la descomposición de una multitriangulación en estrellas para interpretarla como una descomposición poligonal de superficie, y aplicamos esta interpretación a la construcción de descomposiciones regulares de superficies.

En segundo lugar, hemos intentado entender las multitriangulaciones por dualidad. El espacio de las rectas del plano es una banda de Möbius; el conjunto de las rectas que pasan por un punto del plano es una pseudorecta de la banda de Möbius; y las pseudorectas duales de una configuración de puntos forman un arreglo de pseudorectas [Goo97].

Nuestro punto de partida es la dualidad entre las pseudotriangulaciones de un conjunto P de puntos y los arreglos de pseudorectas cuyo soporte es el arreglo dual de P salvo su primer nivel. Establecemos una dualidad similar para multitriangulaciones. Por una parte, el conjunto de las bisectrices de una estrella es una pseudorecta de la banda de Möbius. Por otra parte, las pseudorectas duales de las estrellas de una k-triangulación del n-gono forman un arreglo de pseudorectas con puntos de contacto, cuyo soporte es exactamente el soporte del arreglo dual de los vértices del n-gono salvo sus k primeros niveles. Mostramos que cualquier arreglo con puntos de contacto que tiene este soporte es efectivamente el arreglo dual de una multitriangulación.

Esta dualidad relaciona las pseudotriangulaciones y las multitriangulaciones y explica así sus propiedades comunes (número de cuerdas, flip, etc.).

Más generalmente, estudiamos en el Capítulo 3 los *arreglos de pseudorectas con puntos de contacto* que comparten el mismo soporte. Definimos una operación de flip que corresponde al flip en las multitriangulaciones, y estudiamos el grafo de flips. Las propiedades de ciertos arreglos "glotones", definidos como las fuentes de ciertas orientaciones acíclicas de este grafo, nos permiten en particular enumerar este grafo de flips manteniendo un espacio polinomial. Nuestro trabajo aclara así el algoritmo existente para enumerar las pseudotriangulaciones [BKPS06] y ofrece una prueba complementaria.

Por último, discutimos en el Capítulo 4 tres problemas abiertos que reflejan la riqueza combinatoria y geométrica de las multitriangulaciones.

El primero concierne el conteo de las multitriangulaciones. Jakob Jonsson [Jon05] probó (considerando $0/1$-rellenos de poliominos que evitan ciertos patrones) que las multitriangulaciones están contadas por un cierto determinante de Hankel de números de Catalan, que cuentan también ciertas familias de k-tuplas de caminos de Dyck. Sin embargo, excepto dos resultados parciales [Eli07, Nic09], no existe ninguna prueba biyectiva de este resultado. Entramos aquí el dominio de la *combinatoria biyectiva* cuyo objetivo es construir biyecciones entre familias combinatorias que conserven parámetros característicos: nos gustaría aquí una biyección que permitiera leer las estrellas sobre las k-tuplas de caminos de Dyck.

Nuestro segundo problema es el de la *rigidez*. Aunque la rigidez de grafos es bien entendida en dimensión 2 [Lam70, Gra01, GSS93], ninguna caracterización satisfactoria es conocida a partir de dimensión 3. Mostramos que las k-triangulaciones satisfacen las propiedades típicas de los grafos rígidos de dimensión $2k$. Esto incita naturalmente a conjeturar que las k-triangulaciones son rígidas en dimensión $2k$, lo que demostramos cuando $k = 2$. Una respuesta positiva a esta conjetura permitiría acercarse de la politopalidad del grafos de flips de las multitriangulaciones, tal como el politopo de las pseudotriangulaciones [RSS03] ha sido construido apoyándose en sus propiedades de rigidez.

Por fin, volvemos sobre la *realización politopal del grafo de flips* de las multitriangulaciones. En primer lugar, estudiamos el primer ejemplo no-trivial: mostramos que el grafo de flips sobre las 2-triangulacións del octógono es efectivamente el grafo de un politopo de dimensión 6. Para encontrar un tal politopo, describimos completamente el espacio de las realizaciones politopales simétricas de este grafo en dimensión 6, estudiando primero todos los matroides orientados [BVS$^+$99, Bok06] simétricos que pueden realizarlo. En segundo lugar, generalizando la construcción del asociaedro de Jean-Louis Loday [Lod04], construimos un politopo que realiza el grafo de los flips restringido a las multitriangulaciones cuyo grafo dual es acíclico.

Además, presentamos en el Apéndice A los resultados de un algoritmo de enumeración de pequeños arreglos de pseudorectas y de *doble pseudorectas*. A semejanza de los arreglos de pseudorectas que ofrecen un modelo combinatorio de las configuraciones de puntos, los arreglos de doble pseudorectas han sido introducidos como modelos de configuraciones de convexos disjuntos [HP09]. Nuestro trabajo de implementación nos permitía manipular estos objetos y familiarizarnos con sus propiedades, lo que resultó útil para nuestro estudio de la dualidad.

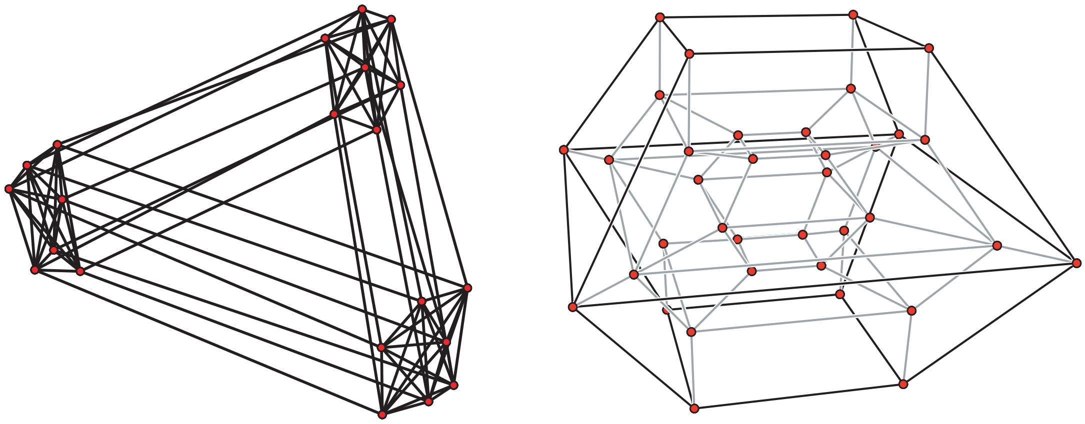

Figura 3: (Izquierda) Un producto de grafos completos. Este grafo es el de un producto de símplices, pero también el de politopos de dimensiónes inferiores. (Derecha) Un producto politopal de grafos no-politopales.

Politopalidad de productos cartesianos. El *producto cartesiano* de grafos está definido de tal manera que el grafo de un producto de politopos es el producto de los grafos de sus factores. Así, un producto de grafos politopales es automáticamente politopal. Estudiamos en primer lugar la recíproca: ¿Son los factores de un producto politopal necesariamente politopales? El Capítulo 6 responde a esta pregunta con una atención particular a los grafos regulares y a sus realizaciones como politopos simples (los politopos simples tienen propiedades muy particulares: entre otras, están determinados por sus grafos [BML87, Kal88]). Discutimos en particular la pregunta de la politopalidad del producto de dos grafos de Petersen, planteada por Günter Ziegler [CRM09]. Este trabajo sobre la politopalidad de productos nos llevaba además a estudiar ejemplos de grafos no-politopales aunque satisfagan las condiciones necesarias conocidas para ser politopales [Bal61, Kle64, Bar67].

Buscamos después la dimensión mínima de un politopo cuyo grafo es isomorfo al grafo de un producto dado de politopos. Esta pregunta se inserta en la búsqueda sistemática de politopos de dimensión extrema con propiedades fijadas: por ejemplo, los d-politopos *neighborly* [Gal63] son aquéllos cuyo $\lfloor \frac{d}{2} \rfloor$-esqueleto es completo (y consiguen el máximo número de caras permitido por el Teorema de la Cota Superior [McM70]); los d-politopos cúbicos *neighborly* [JZ00, Zie04, JR07] son aquéllos cuyo $\lfloor \frac{d}{2} \rfloor$-esqueleto es el del n-cubo, etc. Para construir politopos de pequeña dimensión con una propiedad dada, es natural y a menudo eficaz empezar en una dimensión suficiente para asegurarse de la existencia de tales politopos, y proyectar estos politopos sobre subespacios de dimensión inferior conservando la propiedad buscada. Estas técnicas y sus límites han sido ampliamente estudiadas en la literatura [AZ99, Zie04, SZ10, San09, San08]. Las aplicamos en el Capítulo 7 para construir politopos *$(k, \underline{n})$-neighborly prodsimpliciales*, que tienen el mismo k-esqueleto que cierto producto de símplices $\triangle_{\underline{n}} := \triangle_{n_1} \times \cdots \times \triangle_{n_r}$. En este capítulo, también damos coordenadas enteras para tales politopos utilizando sumas de Minkowski explícitas de politopos cíclicos.

2 MULTITRIANGULACIONES

Fijamos n vértices sobre un círculo y consideramos las cuerdas entre ellos. Dos cuerdas se cruzan cuando los segmentos abiertos se intersecan. Un *ℓ-cruce* es un conjunto de ℓ cuerdas que se cruzan mutuamente. A semejanza de las triangulaciones, nos interesamos por los conjuntos maximales que evitan estas configuraciones:

Definición 1. *Una k-triangulación del n-gono es un conjunto maximal de cuerdas del n-gono sin $(k+1)$-cruces.*

Por definición, una cuerda puede aparecer en un $(k+1)$-cruce solamente si deja al menos k vértices de cada lado. Decimos que una tal cuerda es *k-relevante*. Por maximalidad, cualquier k-triangulación contiene todas las cuerdas que no son k-relevantes. Entre estas cuerdas, llamamos *cuerdas del k-borde* a las que separan $k-1$ vértices de todos los otros vértices.

Ejemplo 2. Para ciertas valores de k y n, se describen fácilmente las k-triangulaciones del n-gono:

$\boxed{k=1}$ Las 1-triangulaciones son las triangulaciones del n-gono.

$\boxed{n=2k+1}$ El grafo completo K_{2k+1} es la única k-triangulación del $(2k+1)$-gono porque ningúna de sus cuerdas es k-relevante.

$\boxed{n=2k+2}$ El conjunto de las cuerdas del $(2k+2)$-gono contiene un $(k+1)$-cruce formado por las $k+1$ diagonales largas del $(2k+2)$-gono. Así existen $k+1$ k-triangulaciones del $(2k+2)$-gono, obtenidas retirando del grafo completo una de sus diagonales largas.

$\boxed{n=2k+3}$ Las cuerdas k-relevantes del $(2k+3)$-gono forman un ciclo poligonal en el cual dos cuerdas se cruzan siempre salvo si son consecutivas. Por consiguiente, las k-triangulaciones del $(2k+3)$-gono son las uniones disjuntas de k pares de cuerdas k-relevantes consecutivas (además de todas las cuerdas que no son k-relevantes).

Resultados anteriores

Los conjuntos de cuerdas del n-gono sin $(k+1)$-cruces aparecen en el contexto de la teoría extrema de los grafos geométricos (ver [PA95, Capítulo 14], [Fel04, Capítulo 1] y la discusión en [CP92]). En el grafo de intersección de las cuerdas del n-gono, estos conjuntos inducen en efecto subgrafos sin k-clan, y se pueden así acertar del resultado clásico de Turán (que acota el número de aristas de un grafo sin k-clan). Vasilis Capoyleas y Janos Pach [CP92] demostraron que estos conjuntos no pueden tener más que $k(2n-2k-1)$ cuerdas. Después, Tomoki Nakamigawa [Nak00], e independientemente Andreas Dress, Jacobus Koolen y Vincent Moulton [DKM02], probaron que todas las k-triangulaciones alcanzan este cota. Estas dos pruebas están basadas en la operación de flip que transforma una k-triangulación en otra cambiando la posición de una sola cuerda. Tomoki Nakamigawa [Nak00] demostró que cualquiera cuerda k-relevante de una k-triangulación puede ser flipada, y que el grafo de flips es conexo. Queremos observar que en todos estos trabajos anteriores, los resultados están obtenidos de “manera indirecta”: primero, una operación de contracción (similar a la contracción de una arista del borde de una triangulación) es introducida y utilizada para demostrar la existencia del flip (en toda generalidad [Nak00], o solamente en casos particulares [DKM02]) y la conexidad del grafo de flips, de la cual es deducida la formula del número de cuerdas. Para resumir:

Teorema 3 ([CP92, Nak00, DKM02]). *(i) Existe una operación inductiva que transforma las k-triangulaciones del $(n+1)$-gono en k-triangulaciones del n-gono y vice versa [Nak00].*

(ii) Cualquiera cuerda k-relevante de una k-triangulación del n-gono puede ser flipada y el grafo de flips es regular y conexo [Nak00, DKM02].

(iii) Todas las k-triangulaciones del n-gono tienen exactamente $k(2n-2k-1)$ cuerdas [CP92, Nak00, DKM02]. □

Jakob Jonsson [Jon03, Jon05] completó estos resultados en dos direcciones. Por una parte, estudió las propiedades enumerativas de las multitriangulaciones:

Teorema 4 ([Jon05]). *El número de k-triangulaciones del n-gono esta dado por:*

$$\det(C_{n-i-j})_{1\le i,j\le k} = \det \begin{pmatrix} C_{n-2} & C_{n-3} & \cdots & C_{n-k-1} \\ C_{n-3} & \cdots & \cdots & \cdots \\ \cdots & \cdots & \cdots & C_{n-2k+1} \\ C_{n-k-1} & \cdots & C_{n-2k+1} & C_{n-2k} \end{pmatrix},$$

donde $C_p := \frac{1}{p+1}\binom{2p}{p}$ denota el p-ésimo número de Catalan. □

La prueba de este teorema se apoya en resultados más generales concerniendo a los $0/1$-rellenos de poliominos maximales para ciertas restricciones sobre sus secuencias diagonales de 1.

Cuando $k=1$, encontramos simplemente los números de Catalan que cuentan no solamente las triangulaciones, sino también los caminos de Dyck. El determinante de Hankel que aparece en el teorema precedente también cuenta ciertas familias de k-tuplas de caminos de Dyck sin cruce [GV85]. La igualdad de los cardinales de estas dos familias combinatorias motiva la búsqueda de una prueba biyectiva que podría aclarar el resultado del Teorema 4. Aunque Sergi Elizalde [Eli07] y Carlos Nicolas [Nic09] propusieran dos biyeccciónes diferentes en el caso $k=2$, esta pregunta queda abierta en el caso general. Discutimos este problema en el Capítulo 4.

Por otra parte, Jakob Jonsson [Jon03] estudió el complejo simplicial $\Delta_{n,k}$ formado por los conjuntos de cuerdas k-relevantes del n-gono sin $(k+1)$-cruces. Como todos sus elementos maximales tienen $k(n-2k-1)$ cuerdas, este complejo es puro de dimensión $k(n-2k-1)-1$. Jakob Jonsson demostró el teorema siguiente:

Teorema 5 ([Jon03]). *El complejo simplicial $\Delta_{n,k}$ es una esfera de dimensión $k(n-2k-1)-1$.* □

Volkmar Welker conjeturó de que este complejo simplicial es además politopal. Esta conjetura es cierta cuando $k=1$ (el complejo simplicial de los conjuntos sin cruce de cuerdas internas del n-gono es isomorfo al complejo de borde del dual del asociaedro) y en los casos del Ejemplo 2 (donde obtenemos respectivamente un punto, un símplex y un politopo cíclico). Discutimos esta pregunta en el Capítulo 4.

Descomposicones de multitriangulaciones en estrellas

Nuestra contribución al estudio de las k-triangulaciones está basada en las estrellas, que generalizan los triángulos de las triangulaciones:

Definición 6. *Una* k-estrella *es un polígono (no-simple) con* $2k+1$ *vértices* $s_0, \dots, s_{2k}$ *en orden sobre el círculo, y* $2k+1$ *cuerdas* $[s_0, s_k], [s_1, s_{k+1}], \dots, [s_{2k}, s_{k-1}]$.

Las estrellas desempeñan para las multitriangulaciones exactamente el mismo papel que los triángulos por las triangulaciones: las descomponen en entidades geométricas más simples y permiten entender su combinatoria. Como prueba, el estudio de las propiedades de incidencia de las estrellas en las multitriangulaciones lleva a nuevas pruebas de todas las propiedades combinatorias de las multitriangulaciones conocidas, que presentamos en el Capítulo 2. Nuestro primer resultado estructural es el siguiente:

Teorema 7. *Sea T una k-triangulación del n-gono (con $n \geq 2k+1$).*
- *(i) Una cuerda k-relevante está contenida en dos k-estrellas de T, una de cada lado; una cuerda del k-borde está contenida en una k-estrella de T; una cuerda que no es k-relevante ni del k-borde no está contenida en ninguna k-estrella de T.*
- *(ii) T tiene exactamente $n-2k$ k-estrellas y $k(2n-2k-1)$ cuerdas.* □

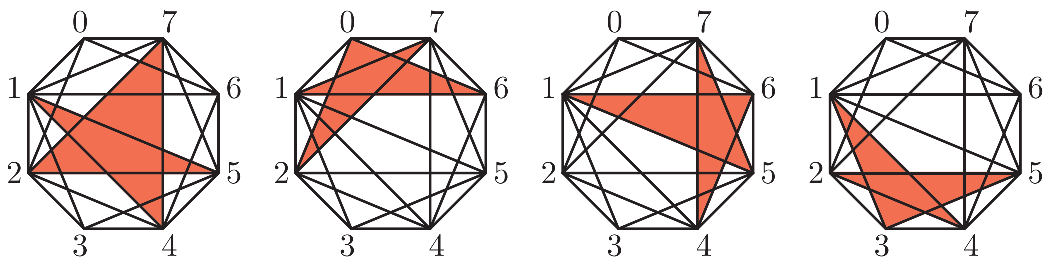

Figura 4: Las 2-estrellas de la 2-triangulación del octógono de la Figura 2.

Probamos el punto (ii) de este teorema con un argumento directo de doble cuenta, exhibiendo dos relaciones independientes entre el número de cuerdas y el número de k-estrellas de una k-triangulación. Nuestra primera relación proviene del punto (i) del teorema, mientras que la segunda se apoya en las propiedades de las bisectrices de las k-estrellas. Una *bisectriz* de una k-estrella es una bisectriz de uno de sus ángulos, es decir, una recta que pasa por uno de sus vértices y que separa sus otros vértices en dos conjuntos de cardinal k. Nuestra segunda relación es una consecuencia directa de la correspondencia entre los pares de k-estrellas de T y las cuerdas del n-gono que no están en T:

Teorema 8. *Sea T una k-triangulación del n-gono.*
- *(i) Cada par de k-estrellas de T tiene una única bisectriz común, que no está en T.*
- *(ii) Recíprocamente, cada cuerda que no está en T es la bisectriz común de un único par de k-estrellas de T.* □

Utilizamos además las estrellas y sus bisectrices para aclarar la *operación de flip* y para proponer una interpretación local. De la misma manera que un flip en una triangulación substituye una diagonal por la otra en un cuadrángulo formado por dos triángulos adyacentes, un flip en una multitriangulación se interpreta como una transformación donde solo intervienen dos estrellas adyacentes:

Teorema 9. *Sea T una k-triangulación del n-gono, sea e una cuerda k-relevante de T y sea f la bisectriz común a las k-estrellas de T que contienen e. Entonces $T \triangle \{e, f\}$ es una k-triangulación del n-gono y es la única, salvo T misma, que contiene $T \smallsetminus \{e\}$.* □

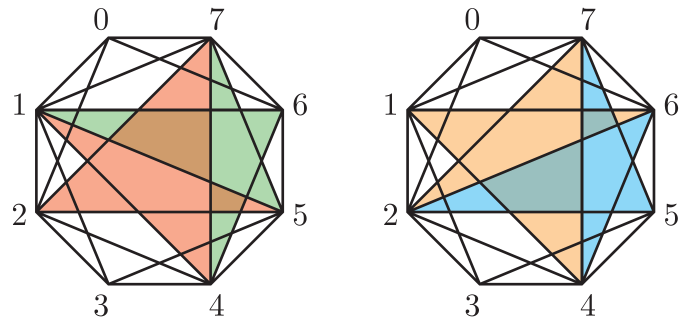

Figura 5: Un flip en la 2-triangulación del octógono de la Figura 2.

Esta interpretación simplifica el estudio del grafo de flips (cuyos vértices son las k-triangulaciones del n-gono y cuyas aristas son los flips entre ellas) y proporciona nuevas pruebas y extensiones parciales de los resultados de [Nak00]:

Teorema 10. *El grafo de flips de las k-triangulaciones del n-gono es $k(n-2k-1)$-regular, conexo, y por todo $n > 4k^2(2k+1)$, su diámetro $\delta_{n,k}$ está acotado por*

$$2\left\lfloor\frac{n}{2}\right\rfloor\left(k+\frac{1}{2}\right) - k(2k+3) \leq \delta_{n,k} \leq 2k(n-4k-1).$$ □

Utilizamos también las estrellas para estudiar las *k-orejas* de las multitriangulaciones, es decir las cuerdas que separan k vértices de los otros vértices. Proponemos una prueba simple del hecho que cada k-triangulación tiene al menos $2k$ k-orejas [Nak00], y damos luego varias caracterizaciones de las k-triangulaciones que alcanzan esta cota:

Teorema 11. *El número de k-orejas de una k-triangulación es igual a $2k$ más el número de* k-estrellas internas*, i.e. las que no contienen ninguna cuerdas del k-borde.*

Si $k > 1$ y T es una k-triangulación, las afirmaciones siguientes son equivalentes:

(i) *T tiene exactamente $2k$ k-orejas;*

(ii) *T no tiene ninguna k-estrella interna;*

(iii) *T es* k-colorable*, i.e. existe una k-coloración de sus cuerdas k-relevantes tal que ningun cruce es monocromático;*

(iv) *el conjunto de cuerdas k-relevantes de T es la unión disjunta de k acordeones (un* acordeón *es una secuencia de cuerdas $[a_i, b_i]$ tal que para todo i, o bien $a_{i+1} = a_i$ y $b_{i+1} = b_i + 1$ o bien $a_{i+1} = a_i - 1$ y $b_{i+1} = b_i$).* □

Después, reinterpretamos en términos de estrellas la *operación inductiva* del Teorema 3(i) que transforma las k-triangulaciones del $(n+1)$-gono en k-triangulaciones del n-gono y *vice versa*. En un sentido aplastamos una k-estrella (que contiene una cuerda del k-borde) hasta un k-cruce, y en el otro sentido inflamos un k-cruce para obtener una k-estrella. Intencionadamente, solo presentamos esta operación al final del Capítulo 2 para destacar que ninguna de nuestras pruebas precedentes usa este transformación inductiva.

Para acabar el Capítulo 2, utilizamos el resultado del Teorema 7 para interpretar una k-triangulación como una *descomposición de superficie* en $n - 2k$ k-gonos. Algunos ejemplos son presentados en la Figura 6. Explotamos esta interpretación para construir, con ayuda de multi-triangulaciones, unas descomposiciones muy regulares de una familia infinita de superficies.

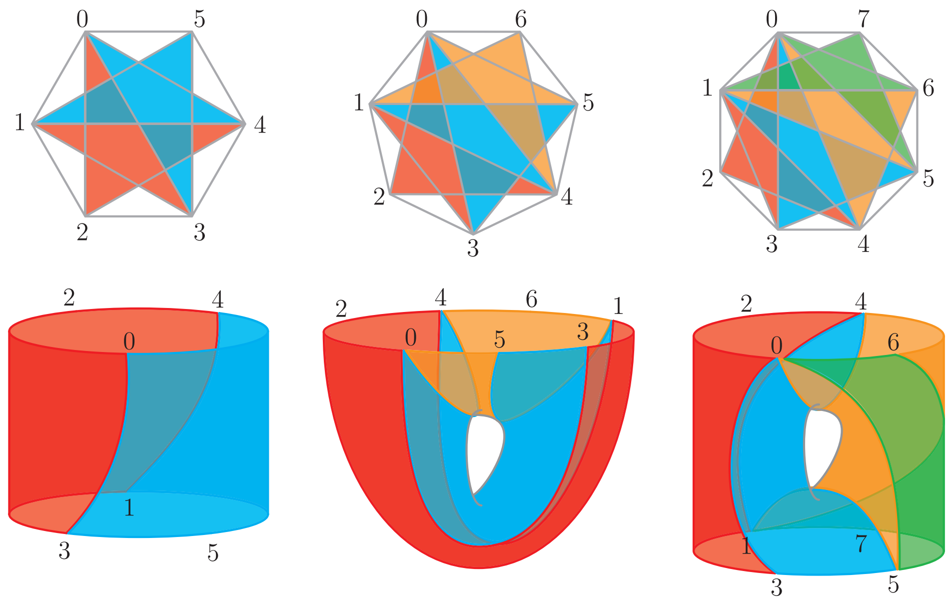

Figura 6: Descomposiciones de superficies associadas a multitriangulaciones.

Multitriangulaciones, pseudotriangulaciones y dualidad

En el Capítulo 3, nos interesamos por la interpretación de las multitriangulaciones en el espacio de rectas del plano, es decir en la banda de Möbius. Estamos en el contexto de la dualidad clásica (ver [Fel04, Capítulos 5,6] y [Goo97]) entre configuraciones de puntos y arreglos de pseudorectas: el conjunto p^* de las rectas que pasan por un punto p del plano es una *pseudorecta* del espacio de rectas (una curva cerrada simple no-separando), y el conjunto $P^* := \{p^* \mid p \in P\}$ de las pseudorectas duales de un conjunto finito P de puntos es un *arreglo de pseudorectas* (dos pseudorectas se intersecan exactamente una vez).

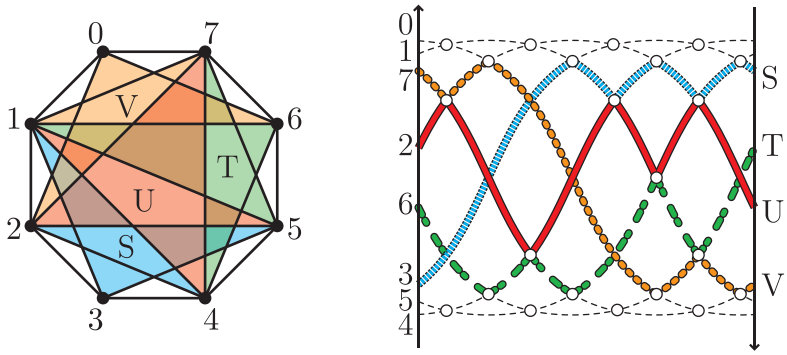

Figura 7: Una 2-triangulación del octógono y su arreglo dual.

El punto de partida del Capítulo 3 es la observación siguiente (ver Figura 7):

Observación 12. Sea T una k-triangulación del n-gono. Entonces:
(i) el conjunto S^* de las bisectrices de una k-estrella S de T es una pseudorecta;
(ii) la bisectriz común de dos k-estrellas R y S es un punto de cruce de las pseudorectas R^* y S^*, mientras que una cuerda común de R y S es un punto de contacto entre R^* et S^*;
(iii) el conjunto $T^* := \{S^* \mid S\ k\text{-estrella de } T\}$ de todas las pseudorectas duales de las k-estrellas de T es un *arreglo de pseudorectas con puntos de contacto* (dos pseudorectas se cruzan exactamente una vez, pero pueden tocarse en un número finito de puntos de contacto);
(iv) el soporte de este arreglo cubre exactamente el soporte del arreglo dual V_n^* de los vértices del n-gono salvo sus k primeros niveles.

Demostramos la recíproca de esta observación:

Teorema 13. *Cualquier arreglo de pseudorectas con puntos de contacto cuyo soporte cubre exactamente el soporte del arreglo dual V_n^* de los vértices del n-gono salvo sus k primeros niveles es el arreglo dual de una k-triangulación del n-gono.* □

En [PV94, PV96a], una observación similar ha sido hecha para las pseudotriangulaciones puntiagudas de un conjunto de puntos en posición general. Introducidas para el estudio del complejo de visibilidad de obstáculos convexos disjuntos del plano [PV96b, PV96c], las pseudotriangulaciones han sido utilizadas en varios contextos geométricos (como la planificación de movimiento y la rigidez [Str05, HOR$^+$05]) y sus propiedades han sido ampliamente estudiadas (número de pseudotriangulaciones [AAKS04, AOSS08], politopo de las pseudotriangulaciones [RSS03], consideraciones algorítmicas [Ber05, BKPS06, HP], etc.). Remitimos a [RSS08] para más detalles.

Definición 14. *Un* pseudotriángulo *es un polígono Δ con exactamente tres ángulos convexos, relacionados por tres cadenas poligonales cóncavas. Una recta es* tangente *a Δ si pasa por un ángulo convexo de Δ y separa sus dos aristas adyacentes, o si pasa por un ángulo cóncavo de Δ y no separa sus dos aristas adyacentes. Una* pseudotriangulación *de un conjunto P de puntos en posición general es un conjunto de aristas que descompone la envoltura convexa de P en pseudotriángulos.*

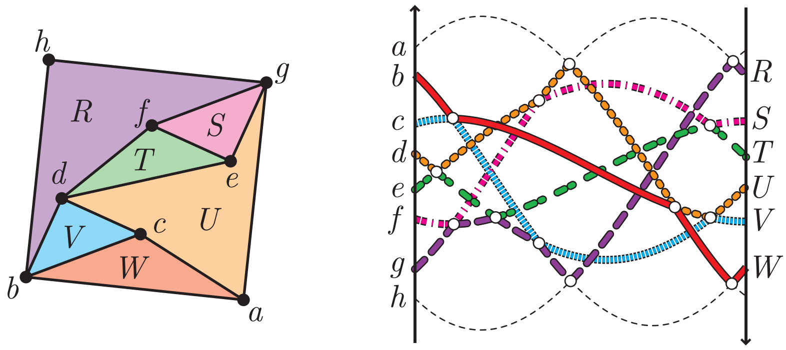

Figura 8: Una pseudotriangulación y su arreglo dual.

En esta memoria, consideramos sólo pseudotriangulaciones *puntiagudas*, es decir pseudotriangulaciones tales que por cada punto $p \in P$ pasa una recta que define un semi-plano cerrado que no contiene ninguna arista saliendo de p. Para una pseudotriangulación puntiaguda T de P, ha sido observado [PV94, PV96a] que:

(i) el conjunto Δ^* de las rectas tangentes a un pseudotriángulo Δ es una pseudorecta; y

(ii) el conjunto $T^* := \{\Delta^* \,|\, \Delta \text{ pseudotriángulo de } T\}$ es un arreglo de pseudorectas con puntos de contacto soportada por el arreglo P^* dual de P salvo su primer nivel.

Damos diferentes pruebas de la recíproca:

Teorema 15. *Sea P un conjunto de puntos en posición general y P^* su arreglo dual. Cualquier arreglo de pseudorectas con puntos de contacto cuyo soporte es precisamente el soporte del arreglo P^* salvo su primer nivel es el arreglo dual de una pseudotriangulación de P.* □

Motivados por estos dos teoremas, consideramos luego los arreglos de pseudorectas que comparten un mismo soporte. Definimos una operación de flip que corresponde al flip en las multitriangulaciones y las pseudotriangulaciones:

Definición 16. *Dos arreglos de pseudorectas con el mismo soporte están relacionados por un flip si la diferencia simétrica de sus conjuntos de puntos de contacto se reduce a un par $\{u, v\}$. En este caso, en uno de los arreglos, u es un punto de contacto de dos pseudorectas que se cruzan en v, mientras que en el otro arreglo, v es un punto de contacto de dos pseudorectas que se cruzan en u.*

Estudiamos el grafo $G(\mathcal{S})$ de flips de los arreglos soportados por $\mathcal{S}$. Por ejemplo, cuando $\mathcal{S}$ es el soporte de un arreglo de dos pseudorectas con p puntos de contacto, el grafo $G(\mathcal{S})$ es el grafo completo con $p+1$ vértices. Nos interesamos por ciertas orientaciones acíclicas del grafo $G(\mathcal{S})$, dadas por cortes verticales del soporte $\mathcal{S}$. Una tal orientación tiene una única fuente que llamamos *arreglo glotón* y que caracterizamos en términos de redes de selección. El estudio de estos arreglos glotones y de sus transformaciones cuando la orientación de $G(\mathcal{S})$ evoluciona proporciona un algoritmo de enumeración de los arreglos de pseudorectas con puntos de contacto que comparten un mismo soporte, cuyo espacio de trabajo queda polinomial. Así, aclaramos y damos una prueba complementaría del algoritmo similar que existía para la enumeración de las pseudotriangulaciones de un conjunto de puntos [BKPS06].

Volvemos después a un contexto más particular. A la luz de la dualidad entre las multitriangulaciones (resp. las pseudotriangulaciones) y los arreglos de pseudorectas con puntos de contacto, proponemos la generalización siguiente de las multitriangulaciones cuando los puntos no están en posición convexa:

Definición 17. *Una k-pseudotriangulación de un arreglo de pseudorectas L es un arreglo de pseudorectas con puntos de contacto cuyo soporte es el arreglo L salvo sus k primer niveles. Una k-pseudotriangulación de un conjunto de puntos P en posición general es un conjunto de aristas T que corresponden por dualidad a los puntos de contacto de una k-pseudotriangulación T^* de P^*.*

Mostramos que todas las k-pseudotriangulaciones de un conjunto de puntos P tienen exactamente $k(2|P| - 2k - 1)$ aristas, y que no pueden contener configuraciones de $2k + 1$ aristas alternativas, pero que pueden eventualmente contener un $(k + 1)$-cruce. Estudiamos después sus estrellas: una estrella de una k-pseudotriangulación T de P es un polígono formado por el conjunto de las aristas correspondientes a los puntos de contacto de una pseudorecta fijada de T^*. Discutimos su número possible de esquinas, y mostramos que para todo punto q del plano, la suma de los índices de las estrellas de T alrededor de q es independiente de T.

Acabamos el Capítulo 3 con tres preguntas relacionadas con las multipseudotriangulaciones:

(i) Estudiamos primero las *multipseudotriangulaciones iteradas*: una k-pseudotriangulación de una m-pseudotriangulación de un arreglo de pseudorectas L es un $(k + m)$-pseudotriangulación de L. Presentamos sin embargo un ejemplo de 2-triangulación que no contiene ninguna triangulación. Mostramos en cambio que las multipseudotriangulaciones glotonas de un arreglo son iteradas de la pseudotriangulación glotona.

(ii) Damos después una caracterización de las aristas de la k-pseudotriangulación glotona de un conjunto de puntos P en términos de *k-árboles de horizonte* de P. Esta caracterización generaliza una observación de Michel Pocchiola [Poc97] para las pseudotriangulaciones.

(iii) Finalmente, definimos las multipseudotriangulaciones de configuraciones de convexos disjuntos del plano y estudiamos sus propiedades elementales. Los arreglos duales de las configuraciones de convexos son los *arreglos de doble pseudorectas*, introducidos por Luc Habert y Michel Pocchiola [HP09]. En el Apéndice A, manipulamos estos arreglos para enumerar los arreglos con a lo más 5 doble pseudorectas.

Tres problemas abiertos

Finalmente, discutimos en el Capítulo 4 tres problemas abiertos que ilustran la riqueza combinatoria y geométrica de las multitriangulaciones. Nuestro objectivo no es únicamente presentar algunos resultados positivos parciales, sino también destacar ideas naturales basadas en las estrellas que pueden ser fértiles aunque suspendieran para resolver estos problemas.

El primer problema que discutimos es encontrar una *biyección explícita* entre el conjunto de las multitriangulaciones y el conjunto de las k-tuplas de caminos de Dyck sin cruce, que están ambos enumerados por el determinante de Hankel del Teorema 4. Si en una triangulación T, denotamos por $\delta_i(T)$ el número de triángulos de T cuyo primer vértice es i, entonces la aplicación $T \mapsto N^{\delta_0(T)}EN^{\delta_1(T)}E\dots N^{\delta_{n-3}(T)}E$ es una biyección de las triangulaciones del n-gono a los caminos de Dyck de semi-longitud $n-2$ (donde N y E denotan los pasos norte y este). Jakob Jonsson [Jon03] generalizó esta observación comparando la repartición de las secuencias de grados entrantes de las k-triangulaciones con las signaturas de las k-tuplas de caminos de Dyck (sin dar las definiciones concisas, señalamos que estas dos k-tuplas de secuencias generalizan la secuencia $(\delta_i(T))$ de una triangulación T y la secuencia de los potencias de N en un camino de Dyck). Motivados por este resultado, buscamos como definir k-coloraciones de las cuerdas k-relevantes de una k-triangulación de tal modo que las secuencias respectivas de grado entrante de cada color defina k-tuplas de caminos de Dyck sin cruces. Presentamos una coloración basada en las estrellas, que satisface esta propiedad, pero con la cual la función de las multitriangulaciones en las k-tuplas de caminos de Dyck no es desgraciadamente biyectiva.

Nuestro segundo problema concierne las propiedades de *rigidez* de las multitriangulaciones. Una triangulación es *mínimalmente rígida* en el plano: los únicos movimientos de sus vértices que preserven las longitudes de sus aristas son las isometrías del plano, y retirar cualquiera arista vuelve la estructura flexible. De manera equivalente, una triangulación satisface la condición de Laman: tiene $2n-3$ aristas y cada subgrafo con m vértices tiene a lo más $2m-3$ aristas. Observamos dos conexiones interesantes entre las multitriangulaciones y la teoría de la rigidez:

(i) Primero, una k-triangulación es $\left(2k, \binom{2k+1}{2}\right)$-*tenso*: contiene $2kn - \binom{2k+1}{2}$ aristas y cada subgrafo con m vértices tiene a lo más $2km - \binom{2k+1}{2}$ aristas. Esta propiedad combinatoria hace de una k-triangulación un candidato razonable para ser un grafo genéricamente mínimalmente rígido en dimensión $2k$. Probamos esta conjectura cuando $k=2$.

(ii) Después, mostramos que el grafo dual de una k-triangulación es (k,k)-tenso. En particular, puede ser descompuesto en k árboles de expansión con aristas disjuntas (en el dual de una triangulación, solo hay un árbol).

Finalmente, volvemos a la pregunta de la *realización politopal* del complejo simplicial $\Delta_{n,k}$ formado por los conjuntos de cuerdas k-relevantes del n-gono sin $(k+1)$-cruces. Presentamos dos contribuciones modestas a esta pregunta:

(i) Respondemos por una parte al caso no-trivial mínimo describiendo el espacio de las realizaciones simétricas de $\Delta_{8,2}$. Obtenemos este resultado en dos etapas: primero enumeramos por ordenador todos los matroides orientados simétricos que realizan nuestro complejo simplicial; después buscamos las realizaciones politopales simétricas de estos matroides orientados.

(ii) Consideramos por otra parte la construcción del asociaedro de Jean-Louis Loday [Lod04]. Interpretamos su construcción con los arreglos duales de las triangulaciones, lo que se generaliza naturalmente a las multitriangulaciones. Obtenemos un politopo cuyas facetas están definidas por desigualdades simples, y que realiza el grafo de flips restringido a ciertas multitriangulaciones (aquéllas con un grafo dual acíclico). Aunque este politopo habría podido ser *a priori* una proyección de una realización de $\Delta_{n,k}$, mostramos que no lo es.

3 POLITOPALIDAD DE PRODUCTOS

En la segunda parte de esta tesis, nos interesamos por preguntas de realización politopal de grafos (o de esqueletos) obtenidos como productos cartesianos de otros grafos (o esqueletos).

El *producto cartesiano* de dos politopos P, Q es el politopo $P \times Q := \{(p,q) \mid p \in P, q \in Q\}$. Su estructura combinatoria solo depende de la de sus factores: la dimensión de $P \times Q$ es la suma de las dimensiones de P y Q y las caras no-vacías de $P \times Q$ son precisamente los productos de una cara no-vacía de P por una cara no-vacía de Q.

Politopalidad de productos de grafos no-politopales

En el Capítulo 6, nos interesamos por el producto de grafos. El *producto cartesiano* de dos grafos G y H es el grafo $G \times H$ cuyos vértices son $V(G \times H) := V(G) \times V(H)$ y cuyas aristas son $E(G \times H) := \big(E(G) \times V(H)\big) \cup \big(V(G) \times E(H)\big)$. Dicho de otra manera, para todos vértices $a, c \in V(G)$ y $b, d \in V(H)$, los vértices (a, b) y (c, d) de $G \times H$ son adyacentes si $a = c$ y $\{b, d\} \in E(H)$, ó $b = d$ y $\{a, c\} \in E(G)$. Este producto es coherente con el producto de politopos: el grafo de un producto de politopos es el producto de sus grafos. En particular, el producto de dos grafos politopales es automáticamente politopal. En este capítulo, estudiamos la pregunta recíproca: ¿ Si un producto $G \times H$ es politopal, son necesariamente sus factores G y H politopales ?

El producto de un triángulo por un camino de longitud 2 es un contraejemplo simple a esta pregunta: aunque el camino no sea politopal, el producto es el grafo de un 3-politopo obtenido pegando dos prismos triangulares por una cara triangular. Eliminamos tales ejemplos exigiendo que cada factor sea un grafo regular. Si G y H son regulares de grado respectivos d y e, entonces el producto $G \times H$ es $(d + e)$-regular y es natural preguntarse si es el grafo de un $(d + e)$-politopo simple. El teorema siguiente responde a esta pregunta:

Teorema 18. *Un producto $G \times H$ es el grafo de un politopo simple si y solo si sus dos factores G y H son grafos de politopos simples. En este caso, existe un único politopo simple cuyo grafo es $G \times H$: es precisamente el producto de los únicos politopos simples cuyos grafos respectivos son G y H.* □

En este teorema, la unicidad del politopo simple realizando $G \times H$ es una aplicación directa del hecho de que un politopo simple es completamente determinado por su grafo [BML87, Kal88]. Estos resultados se apoyan en la propiedad siguiente de los politopos simples: cada conjunto de $k + 1$ aristas adyacentes a un mismo vértice de un politopo simple P define una k-cara de P.

Como aplicación del Teorema 18 obtenemos una familia infinita de grafos 4-regulares no-politopales: el producto de un grafo 3-regular no-politopal por un segmento es no-politopal y 4-regular.

Preguntamos después cuándo un producto de grafos regulares no-politopales puede ser politopal en una dimensión más pequeña que su grado. Los ejemplos siguientes responden parcialmente a esta pregunta:

Teorema 19. *(i) Cuando $n \geq 3$, el producto $K_{n,n} \times K_2$ de un grafo completo bipartito por un segmento no es politopal.*

(ii) El producto de un grafo d-politopal por el grafo de una subdivisión regular de un e-politopo es $(d+e)$-politopal. Esto proporciona productos politopales de grafos regulares no-politopales (por ejemplo el producto de dos dominós de la Figura 3 y el grafo de la Figura 9). □

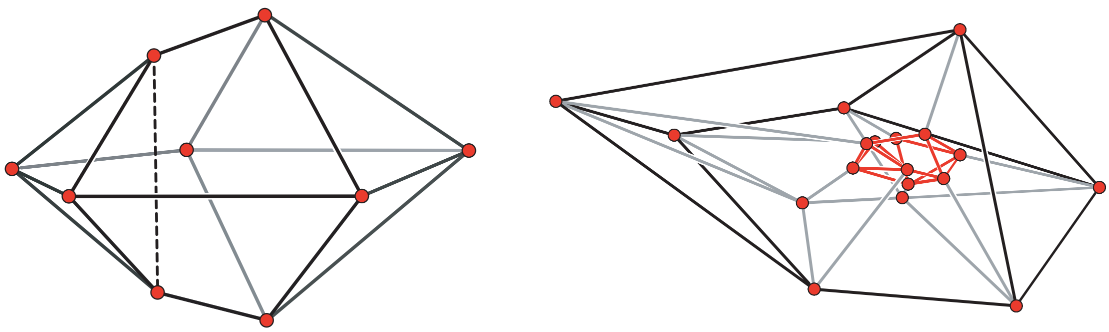

Figura 9: Un grafo H 4-regular y no-politopal que es el grafo de una subdivisión regular de un 3-politopo (izquierda) y el diagrama de Schlegel de un 4-politopo cuyo grafo es el producto de H por un segmento (derecha).

Politopos *neighborly* prodsimpliciales

En el Capítulo 7, consideramos politopos cuyos esqueletos son los de un producto de símplices:

Definición 20. *Sean $k \geq 0$ y $\underline{n} := (n_1, \ldots, n_r)$, con $r \geq 1$ y $n_i \geq 1$ por cada i. Un politopo es* $(k, \underline{n})$-neighborly prodsimplicial *— o para acotar* $(k, \underline{n})$-PSN *— si su k-esqueleto es combinatorialmente equivalente al del producto de símplices $\triangle_{\underline{n}} := \triangle_{n_1} \times \cdots \times \triangle_{n_r}$.*

Esta definición generaliza dos clases particulares de politopos:

(i) Encontramos los politopos *neighborly* cuando $r = 1$. En la literatura, un politopo es *k-neighborly* si cada subconjunto de k vértices forma una cara. Con nuestra definición, un tal politopo es $(k-1, n)$-PSN.

(ii) Encontramos los politopos *neighborly cúbicos* [JZ00, JR07, SZ10] cuando $\underline{n} = (1, \ldots, 1)$.

El producto $\triangle_{\underline{n}}$ es un politopo $(k, \underline{n})$-PSN de dimensión $\sum n_i$. Buscamos naturalmente politopos $(k, \underline{n})$-PSN en dimensión inferior. Por ejemplo, el politopo cíclico $C_{2k+2}(n+1)$ es un politopo (k, n)-PSN en dimensión $2k+2$. Denotamos $\delta(k, \underline{n})$ la dimensión mínima que puede tener un politopo $(k, \underline{n})$-PSN.

Ciertos politopos PSN se obtienen proyectando el producto $\triangle_{\underline{n}}$, o cualquier politopo combinatorialmente equivalente, sobre un subespacio de dimensión inferior. Por ejemplo, el politopo cíclico $C_{2k+2}(n+1)$, como cualquier politopo con $n+1$ vértices, es una proyección del símplice $\triangle_n$ sobre $\mathbb{R}^{2k+2}$.

Definición 21. *Un politopo* $(k, \underline{n})$-PSN *es* $(k, \underline{n})$-neighborly prodsimplicial proyectado *— o para acotar* $(k, \underline{n})$-PPSN *— si es una proyección de un politopo combinatorialmente equivalente a* $\triangle_{\underline{n}}$.

Denotamos $\delta_{pr}(k, \underline{n})$ la dimensión mínima de un politopo $(k, \underline{n})$-PPSN.

Nuestro Capítulo 7 se divide en dos partes. En la primera, presentamos tres métodos para construir politopos PPSN en pequeña dimensión:
(i) con reflexiones de politopos cíclicos;
(ii) con sumas de Minkowski de politopos cíclicos;
(iii) con "proyecciones de productos deformados", en el espíritu de las construcciones de Raman Sanyal y Günter Ziegler [Zie04, SZ10].

En la segunda parte, obtenemos obstrucciones topológicas a la existencia de tal objetos, utilizando técnicas desarrolladas por Raman Sanyal [San09] para acotar el número de vértices de una suma de Minkowski. A la luz de estas obstrucciones, nuestras construcciones de la primera parte se revelan optimas sobre un ancho espectro de parámetros.

Construcciones. Nuestro primer ejemplo no-trivial es un politopo $(k, (1, n))$-PSN en dimensión $2k + 2$, obtenido por reflexión del politopo cíclico $C_{2k+2}(n + 1)$ respecto a un hiperplano bien elegido:

Proposición 22. *Para todos* $k \geq 0$*,* $n \geq 2k + 2$ *y* $\lambda \in \mathbb{R}$ *suficientemente grande, el politopo*

$$\operatorname{conv}\left(\left\{(t_i, \dots, t_i^{2k+2})^T \,\middle|\, i \in [n+1]\right\} \cup \left\{(t_i, \dots, t_i^{2k+1}, \lambda - t_i^{2k+2})^T \,\middle|\, i \in [n+1]\right\}\right)$$

es un politopo $(k, (1, n))$-PSN *de dimensión* $2k + 2$. □

Por ejemplo, esta construcción produce un 4-politopo cuyo grafo es $K_2 \times K_n$ ($n \geq 3$).

Después, con ayuda de sumas de Minkowski bien elegidas de politopos cíclicos, obtenemos coordenadas explícitas de politopos $(k, \underline{n})$-PPSN:

Teorema 23. *Sean* $k \geq 0$ *y* $\underline{n} := (n_1, \dots, n_r)$ *con* $r \geq 1$ *y* $n_i \geq 1$ *para todo* i*. Existen conjuntos* $I_1, \dots, I_r \subset \mathbb{R}$*, con* $|I_i| = n_i$ *para todo* i*, tales que el politopo*

$$\operatorname{conv}\left\{w_{a_1,\dots,a_r} \,\middle|\, (a_1, \dots, a_r) \in I_1 \times \cdots \times I_r\right\} \subset \mathbb{R}^{2k+r+1}$$

sea $(k, \underline{n})$-PPSN*, donde* $w_{a_1,\dots,a_r} := \left(a_1, \dots, a_r, \sum_{i\in[r]} a_i^2, \dots, \sum_{i\in[r]} a_i^{2k+2}\right)^T$*. Por consiguiente,*

$$\delta(k, \underline{n}) \leq \delta_{pr}(k, \underline{n}) \leq 2k + r + 1. \qquad \square$$

Cuando $r = 1$ encontramos los politopos *neighborly*.

Finalmente, extendemos la técnica de "proyección de productos deformados de polígonos" de Raman Sanyal y Günter Ziegler [Zie04, SZ10] a productos de politopos simples arbitrarios: proyectamos un politopo bien elegido, combinatorialmente equivalente a un producto de politopos simples, de tal manera que preservamos su k-esqueleto completo. Más concretamente, describimos como usar coloraciones de los grafos de los politopos polares de los factores del producto para aumentar la dimensión del esqueleto preservado. La versión básica de esta técnica produce el resultado siguiente:

Proposición 24. *Sean $P_1, \dots, P_r$ unos politopos simples. Para cada politopo P_i, denotamos n_i su dimensión, m_i su número de facetas, y $\chi_i := \chi(\mathrm{gr}(P_i^\diamond))$ el número cromático del grafo del politopo polar $P_i^\diamond$. Para un entero fijo $d \le n$, sea t el entero máximo tal que $\sum_{i=1}^t n_i \le d$. Entonces existe un d-politopo cuyo k-esqueleto es combinatorialmente equivalente al del producto $P_1 \times \cdots \times P_r$ en cuanto*

$$0 \le k \le \sum_{i=1}^r (n_i - m_i) + \sum_{i=1}^t (m_i - \chi_i) + \left\lfloor \frac{1}{2}\left(d - 1 + \sum_{i=1}^t (\chi_i - n_i)\right)\right\rfloor. \qquad \square$$

Especializando esta proposición a un producto de símplices, obtenemos otra construcción de politopos PPSN. Cuando algunos de los símplices son pequeños respecto a k, esta técnica produce de hecho nuestro mejores ejemplos de politopos PPSN :

Teorema 25. *Para todos $k \ge 0$ y $\underline{n} := (n_1, \dots, n_r)$ con $1 = n_1 = \cdots = n_s < n_{s+1} \le \cdots \le n_r$,*

$$\delta_{pr}(k, \underline{n}) \le \begin{cases} 2(k+r) - s - t & \text{si } 3s \le 2k + 2r, \\ 2(k+r-s) + 1 & \text{si } 3s = 2k + 2r + 1, \\ 2(k+r-s+1) & \text{si } 3s \ge 2k + 2r + 2, \end{cases}$$

donde $t \in \{s, \dots, r\}$ es máximo tal que $3s + \sum_{i=s+1}^t (n_i + 1) \le 2k + 2r$. $\square$

Si $n_i = 1$ para todo i, encontramos los politopos *neighborly* cúbicos de [SZ10].

Obstrucciones. Para obtener cotas inferiores sobre la dimensión mínima $\delta_{pr}(k, \underline{n})$ que puede tener un politopo $(k, \underline{n})$-PPSN, aplicamos una método de Raman Sanyal [San09]. A cada proyección que preserve el k-esqueleto de $\triangle_{\underline{n}}$, asociamos por dualidad de Gale un complejo simplicial que debe ser encajable en un espacio de una cierta dimensión. El argumento se apoya después en una obstrucción topológica derivada del criterio de Sarkaria para el encaje de un complejo simplicial en términos de coloraciones de grafos de Kneser [Mat03]. Obtenemos el resultado siguiente:

Teorema 26. *Sea $\underline{n} := (n_1, \dots, n_r)$ con $1 = n_1 = \cdots = n_s < n_{s+1} \le \cdots \le n_r$.*

(i) Si

$$0 \le k \le \sum_{i=s+1}^r \left\lfloor \frac{n_i - 2}{2} \right\rfloor + \max\left\{0, \left\lfloor \frac{s-1}{2} \right\rfloor\right\},$$

entonces $\delta_{pr}(k, \underline{n}) \ge 2k + r - s + 1$.

(ii) Si $k \ge \left\lfloor \frac{1}{2} \sum_i n_i \right\rfloor$ entonces $\delta_{pr}(k, \underline{n}) \ge \sum_i n_i$. $\square$

En particular, las cotas inferior y superior de los Teoremas 23 y 26 se juntan sobre un largo campo de parámetros:

Teorema 27. *Para todos* $\underline{n} := (n_1, \ldots, n_r)$ *con* $r \geq 1$ *y* $n_i \geq 2$ *para cada* i*, y para cada* k *tal que* $0 \leq k \leq \sum_{i\in[r]} \left\lfloor \frac{n_i-2}{2} \right\rfloor$*, el politopo* $(k, \underline{n})$*-PPSN mínimo es de dimensión exactamente* $2k + r + 1$*. Dicho de otra manera:*

$$\delta_{pr}(k, \underline{n}) = 2k + r + 1. \qquad \square$$

Comentario 28. Las técnicas de proyección de politopos y las obstrucciones que utilizamos han sido desarrolladas por Raman Sanyal y Günter Ziegler [Zie04, SZ10, San09]. Decidimos presentarlas en esta memoria porque sus aplicaciones a productos de símplices producen resultados nuevos que completan nuestro estudio sobre la politopalidad de productos. Por otra parte, después de que acabamos de estudiar estos métodos a productos de símplices, descubrimos que Thilo Rörig y Raman Sanyal trabajaron sobre el mismo asunto [RS09] (ver también [San08, Rör08]).

MULTITRIANGULATIONS, PSEUDOTRIANGULATIONS AND SOME PROBLEMS OF REALIZATION OF POLYTOPES

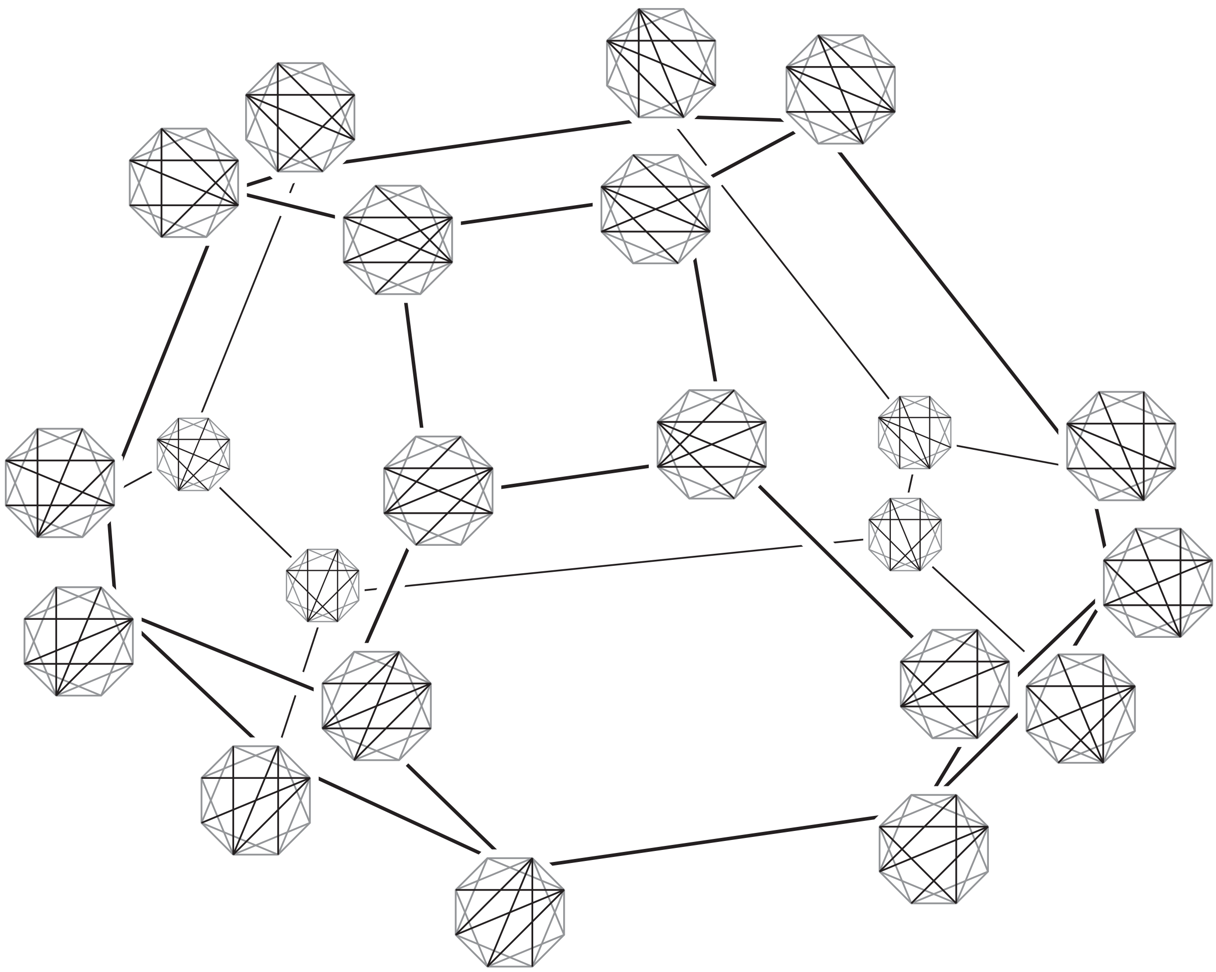

INTRODUCTION

This thesis explores subjects in the field of *discrete and computational geometry* [GO04]; it typically studies the ways in which simple geometric objects (such as points, lines, half-spaces, etc.) are related, arranged, or placed with respect to each other (whether they intersect, how they see each other, etc.). The two specific topics of *multitriangulations* and *polytopal realizations of products* are closely examined. Their various connections with discrete geometry enable us to uncover some of its multiple facets, examples of which are provided in this introduction. We studied these two topics with respect to a common problem, the study of the existence of a polytopal realization of a given structure.

A (convex) polytope is the convex hull of a finite point set of an Euclidean space. While interest in certain polytopes dates back to antiquity (Platonic solids), their systematic study is relatively recent and the main results only appeared last century (see [Grü03, Zie95] and the references therein). The study of polytopes deals not only with their geometric properties, but mainly with more combinatorial aspects. The goal is to understand their faces (their intersections with a supporting hyperplane) and the lattice they form (*i.e.* the inclusion relations between these faces).

The questions of *polytopal realization* are in a way the inverse problem: they deal with the existence and the construction of polytopes with a prescribed combinatorial structure. For example, given a graph, we would like to determine if it is the graph of a polytope: we then say that it is polytopal. Steinitz' Theorem [Ste22], which characterizes the graphs of 3-polytopes, provides the fundamental result on this question. Already in dimension 4, the situation is much less satisfactory: except certain necessary conditions [Bal61, Kle64, Bar67], polytopal graphs do not allow for local characterization in general dimension [RG96]. When a graph is polytopal, we are interested in the properties of its realizations, for example the number of faces, the dimension, etc. We often try to construct examples which optimize some of these properties; typically, we want to construct a polytope of minimal dimension for a given graph [Gal63, JZ00, SZ10]. These questions of polytopal realizations are interesting either for transformation graphs on combinatorial or geometric objects (for example, the graph of adjacent transpositions on permutations, or the graph of flips on triangulations, etc.) or for graphs derived from operations on other graphs (which may be local such as the ΔY transformation, or global such as the Cartesian product). These questions are not only interesting for a graph, but more generally for any subset of a lattice.

Polytopality of flip graphs. The existence of polytopal realizations is studied for transformation graphs on combinatorial or geometric structures. We can cite as an example the permutahedron, whose vertices correspond to permutations of $[n]$, and whose edges correspond to pairs of permutations which differ by an adjacent transposition. Other examples, as well as classes of

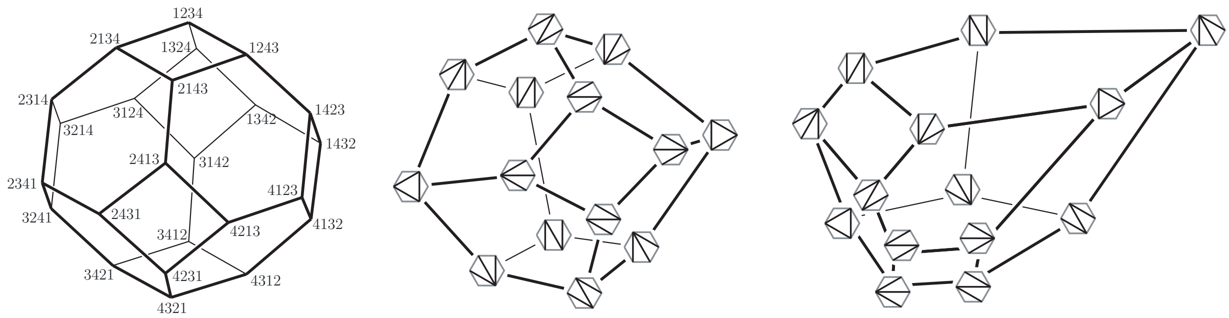

Figure 1: The permutahedron and two realizations of the associahedron.

polytopes providing realizations of certain general structures are presented in [Zie95, Lecture 9]. In general, polytopality questions on combinatorial structures are not only interesting in and of themself, but also because studying them forces us to understand the combinatorics of the objects and often leads to the development of new methods and results.

Two particular examples of polytopal combinatorial structures play an important role in this dissertation. We first encounter the associahedron whose boundary complex realizes the dual of the simplicial complex formed by all crossing-free sets of chords of the n-gon. The graph of the associahedron corresponds to the graph of flips on triangulations of the n-gon. The associahedron appears in several contexts, and various polytopal realizations have been developed [Lee89, BFS90, GKZ94, Lod04, HL07]. We then meet the polytope of pseudotriangulations of an Euclidean point set [RSS03]. Originally introduced in the study of the visibility complex of disjoint obstacles in the plane [PV96b, PV96c], pseudotriangulations have since been used in different geometric contexts [RSS08]. In particular, their interesting rigidity properties [Str05] yield the construction of a polytope which realizes their flip graph.

In the first part of this dissertation, we focus on the flip graph on multitriangulations. These objects appeared under different motivations [CP92, DKM02, DKKM01] and revealed a rich combinatorial structure [Nak00, Jon03, Jon05]. A *k-triangulation* is a maximal set of chords of the n-gon such that no $k + 1$ of them mutually cross. We consider the flip graph where two multitriangulations are related if they differ by one chord. As for triangulations which occur when $k = 1$, this graph is regular and connected, and we consider the question of its polytopality. Jakob Jonsson [Jon03] made an important step towards answering this question in proving that the simplicial complex formed by sets of chords with no $k + 1$ mutually crossing subsets is a topological sphere. Although we have only partial answers to this question, our study yields surprising results which we present in this dissertation.

Several constructions of the associahedron [BFS90, Lod04] are directly or indirectly based on the triangles of the triangulations. For multitriangulations, no similar elementary object has appeared in previous works. We thus started with the question: what are triangles for multitriangulations? The *stars* that we introduce in Chapter 2 address this question. We consider stars to be the right way of approaching multitriangulations, in much the same way that triangles, rather than chords, are the right way of approaching triangulations. As evidence for this, we use them

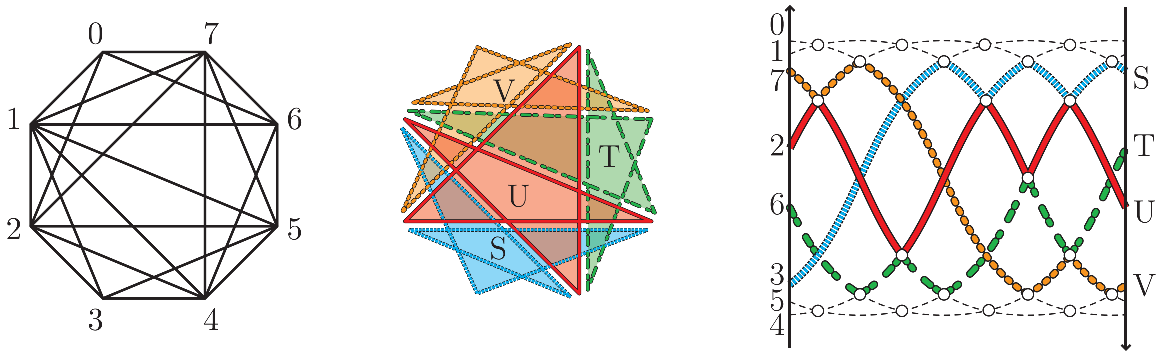

Figure 2: A 2-triangulation, its decomposition into stars, and its dual arrangement.

to arrive at new proofs of the basic properties of multitriangulations known to date. First, we study the incidence relations between stars and chords (each internal chord is contained in two stars) which provide a new proof showing that all k-triangulations of the n-gon have the same cardinality. Then, considering the bisectors of the stars, we provide a local interpretation of the flip operation (an internal chord is replaced by the unique bisector of the two stars adjacent to it), which sheds light upon the study of the flip graph and of its diameter. We also redefine inductive operations on multitriangulations which enable us to insert or suppress a vertex to the n-gon. Finally, we use the decomposition of a multitriangulation into stars to interpret it as a polyhedral decomposition of a surface, and we apply this interpretation to the construction of regular decompositions of surfaces.

In Chapter 3, we consider multitriangulations by duality. The line space of the plane is a Möbius strip; the set of lines passing through a point of the plane is a pseudoline of the Möbius strip; and the dual pseudolines to a point configuration form a pseudoline arrangement [Goo97].

Our starting point is the duality between the pseudotriangulations of a point set P and the pseudoline arrangements whose support is the dual arrangement of P minus its first level. We introduce a similar duality for multitriangulations. On the one hand, the set of bisectors of a star is a pseudoline of the Möbius strip. On the other hand, the dual pseudolines to the stars of a k-triangulation of the n-gon form a pseudoline arrangement with contact points supported by the dual arrangement of the vertex set of the n-gon minus its first k levels. We prove that any arrangement with contact points with this support is effectively the dual arrangement of a multitriangulation. This duality relates pseudotriangulations and multitriangulations and thus provides an explanation for their common properties (number of chords, flips, etc.).

More generally, we consider *pseudoline arrangements with contact points* which share a common support. We define a flip operation which corresponds to flips in multitriangulations and pseudotriangulations, and we study the flip graph. The properties of certain greedy arrangements, defined as sources of certain acyclic orientations on these graphs, enable us in particular to enumerate this flip graph with a polynomial working space. Our work elucidates the existing enumeration algorithm for pseudotriangulations [BKPS06] and provides a complementary proof for it.

To finish, we discuss in Chapter 4 three open problems which reflect the combinatorial and geometric richness of multitriangulations.

The first one looks at the enumeration of multitriangulations. Jakob Jonsson [Jon05] proved (considering $0/1$-fillings of polyominoes avoiding certain patterns) that the multitriangulations are counted by a Hankel deteminant of Catalan numbers, which also counts certain families of k-tuples of Dyck paths. However, apart from partial results [Eli07, Nic09], no bijective proof of this result is known. We enter here the field of *bijective combinatorics* which aims to construct bijections between combinatorial families which preserve characteristic parameters; here, we would like to find a bijection which would enable us to read the stars on the k-tuples of Dyck paths.

The second problem is that of *rigidity*. Although the rigidity of 2-dimensional graphs is well understood [Lam70, Gra01, GSS93], no satisfactory characterization is known in dimension 3 or higher. We prove that k-triangulations satisfy some typical properties of rigid graphs in dimension $2k$. This leads to conjecture that k-triangulations are rigid in dimension $2k$, which we prove when $k = 2$. A positive answer to this conjecture would provide insight to the polytopality question of the flip graph on multitriangulations, in much the same way as the polytope of pseudotriangulations [RSS03] relies on their rigidity properties.

Finally, we come back to the *polytopal realization of the flip graph* on multitriangulations. We study the first non-trivial example and we prove that the graph of flips on the 2-triangulations of the octagon is the graph of a 6-dimensional polytope. To find such a polytope, we completely describe its symmetric polytopal realizations in dimension 6, studying first all the symmetric oriented matroids [BVS+99, Bok06] which can realize it. Then generalizing Jean-Louis Loday's construction of the associahedron [Lod04], we construct a polytope which realizes the graph of flips restricted to multitriangulations whose oriented dual graph is acyclic.

In addition, we present in Appendix A the results of an enumeration algorithm for small arrangements of pseudolines and *double pseudolines*. Much like pseudoline arrangements which model point configurations, double pseudoline arrangements have been introduced as a combinatorial model of configurations of disjoint convex bodies [HP09]. Our work of implementation enabled us to manipulate these objects and to become familiar with their properties, which proved to be useful for our work on duality.

Polytopality of Cartesian products. The *Cartesian product* of graphs is defined in such a way to be coherent with products of polytopes: the graph of a product of polytopes is the product of their graphs. Thus, a product of polytopal graphs is automatically polytopal. We first study the reciprocal question: does the polytopality of a product of graphs imply the polytopality of its factors? Chapter 6 addresses this question, paying particular attention to regular graphs and their realization as simple polytopes (simple polytopes have special properties, including the fact that they are determined by their graph [BML87, Kal88]). We discuss in particular the polytopality of the product of two Petersen graphs, which was raised by Günter Ziegler [CRM09]. This work also led us to study examples of non-polytopal graphs which satisfy all known necessary conditions to be polytopal [Bal61, Kle64, Bar67].

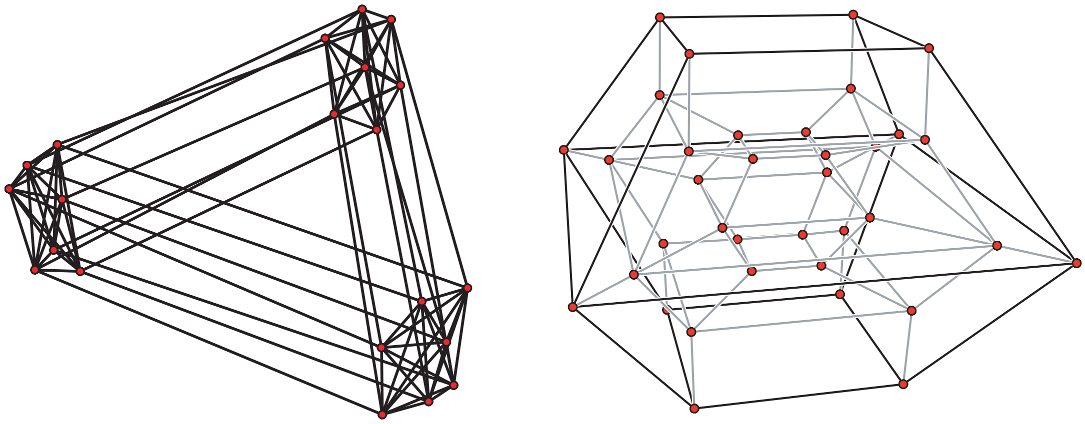

Figure 3: (Left) A product of complete graphs. This graph is that of a product of simplices, but also that of polytopes in smaller dimension. (Right) A polytopal product of non-polytopal graphs.

Second, we look for the minimal dimension of a polytope whose graph is isomorhpic to that of a fixed product of polytopes. This question is an example of the systematic research of extremal dimensions of polytopes with given properties. For example, neighborly polytopes [Gal63] are those whose $\left\lfloor \frac{d}{2} \right\rfloor$-skeleton is complete (and they reach the maximal number of faces allowed by the Upper Bound Theorem [McM70]); neighborly cubical polytopes [JZ00, Zie04, JR07] are those whose $\left\lfloor \frac{d}{2} \right\rfloor$-skeleton is that of the n-cube, etc. To construct polytopes in small dimension with a given property, it is natural and often efficient to start from a sufficiently large dimension to guarantee the existence of such polytopes, and to project these polytopes on low dimensional subspaces in such a way as to preserve the desired property. These techniques and their limits have been widely studied in the literature [AZ99, Zie04, SZ10, San09, San08]. We apply them in Chapter 7 to construct and study the minimal possible dimension of *$(k, \underline{n})$-prodsimplicial neighborly* polytopes whose k-skeleton is that of the product of simplices $\triangle_{\underline{n}} := \triangle_{n_1} \times \cdots \times \triangle_{n_r}$. In this chapter, we also provide explicit integer coordinates of such polytopes using suitable Minkowski sums of cyclic polytopes.

I

Part One

Multitriangulations

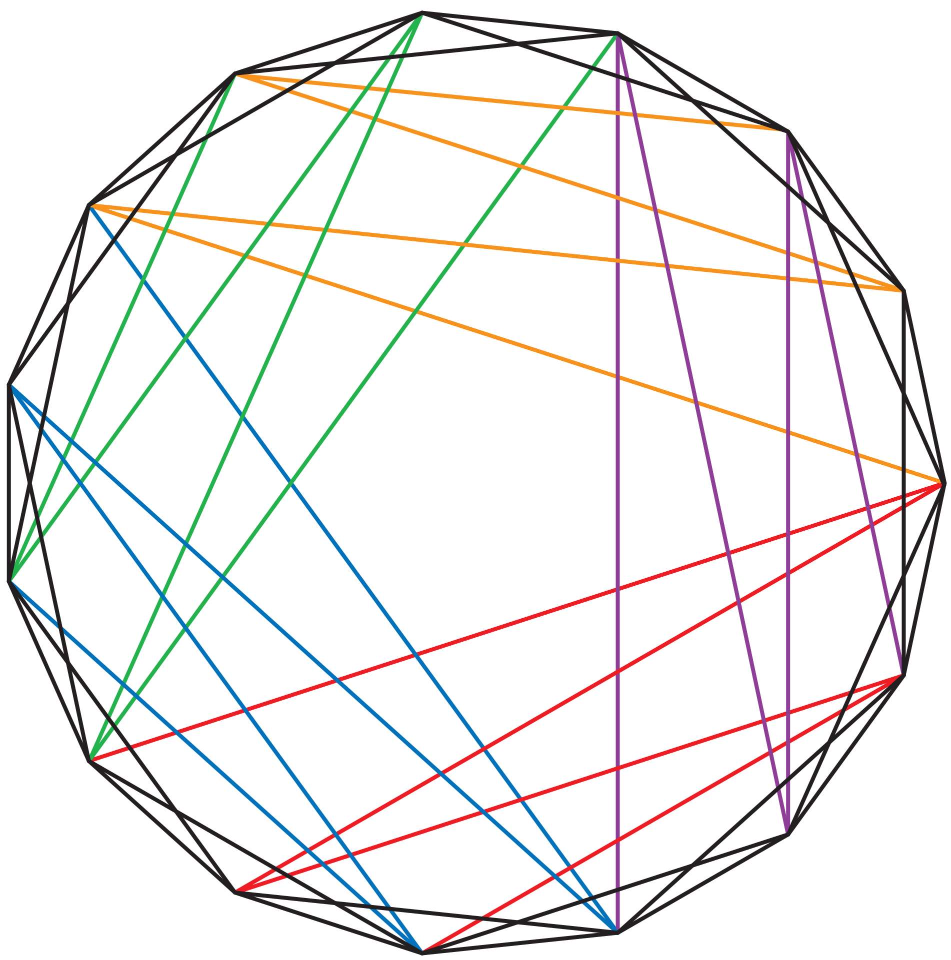

Chapter One

1

INTRODUCTION

1.1 ON TRIANGULATIONS... OF A CONVEX POLYGON

Fix n points on the unit circle (the vertices of a convex n-gon), and consider the set of $\binom{n}{2}$ straight chords between them. We say that two such chords *cross* if they have an intersection point which is not one of their vertices, and we consider sets of non-crossing chords of the n-gon. Among these sets, we focus on those that are maximal, which of course contain all the boundary edges of the n-gon and decompose it into triangles:

Definition 1.1. *A* triangulation *of the convex n-gon is:*
 (i) a maximal crossing-free subset of edges of the n-gon; or (equivalently)
 (ii) a set of non-overlapping triangles covering the n-gon.

For example, Figure 1.1 represents some triangulations of a convex hexagon (in fact, all of them modulo rotations and reflections). Observe that they all have the same number of triangles (namely 4) and of edges (namely 9), which can be generalized for any n:

Lemma 1.2. *A triangulation of the n-gon has exactly $n-2$ triangles and $2n-3$ edges.*

This simple fact can be proved with many different approaches: we use it as an excuse to briefly recall some of the multiple facets of triangulations and to give some flavor of the surprisingly rich combinatorial structure of these elementary objects.

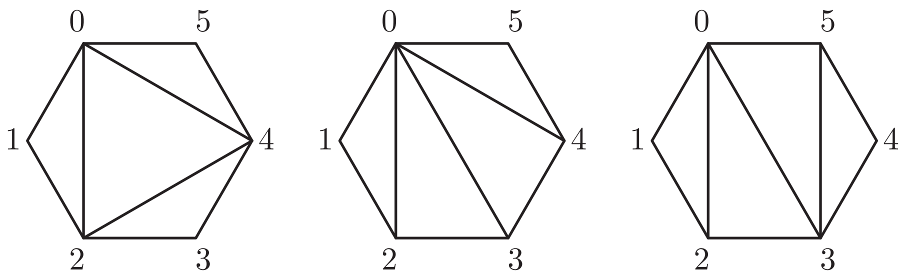

Figure 1.1: Three triangulations of the hexagon.

Double counting. Our first proof is probably the most direct one since it only involves a single triangulation. Indeed, Lemma 1.2 is easily derived from any two of the three following equalities between the number e of edges and the number t of triangles of a triangulation T of the n-gon:

(i) The first relation is derived from a *double count* of the number of incidences between edges and triangles: a triangle contains three edges and an edge is contained in two triangles (except for boundary edges), which yields the equality $3t = 2e - n$.

(ii) The second one is an application of *Euler's formula* (which relates the number of faces, edges and vertices of a polygonal decomposition of the sphere): $(t + 1) - e + n = 2$.

(iii) The last one is based on bisectors: a *bisector* of a triangle is any edge which bisects one of its angles. Any two triangles of T have a unique common bisector, while any edge not in T is the common bisector of a unique pair of triangles of T. This provides a bijection between pairs of distinct triangles of T and edges not in T and yields $\binom{t}{2} = \binom{n}{2} - e$.

Induction. Our second proof is a simple recurrence on the number n of vertices: in a triangulation T of the $(n + 1)$-gon, when we flatten a triangle which contains a boundary edge, we obtain a triangulation of the n-gon with one less triangle (the flattened one) and two less edges (in the flattened triangle, the boundary edge is contracted and the two other ones are merged). Lemma 1.2 immediately follows.

This flattening operation can also be used to compute the number $\theta(n)$ of triangulations of the n-gon, where the vertices of the n-gon are labeled, say from 0 to $n - 1$. Indeed, the contraction of a distinguished boundary edge, say $[0, n]$, defines a surjective map from triangulations of the $(n + 1)$-gon to triangulations of the n-gon, and the number of preimages of a triangulation of the n-gon is simply the degree of its merged vertex (call it $\bar{0}$). Thus, the quotient of $\theta(n+1)$ by $\theta(n)$ equals the average degree of vertex $\bar{0}$, which yields the formula $n\theta(n + 1) = (4n - 6)\theta(n)$.

There is another way to understand triangulations inductively: any triangulation of the n-gon can be decomposed into its root triangle $\{0, m, n - 1\}$ (with $1 \le m \le n - 2$) together with one triangulation of the $(m + 1)$-gon, formed by all the edges on the left of $[0, m]$, and one triangulation of the $(n - m)$-gon, formed by all the edges on the right of $[m, n - 1]$. Since the left and the right triangulations are independent, the number of triangulations of the n-gon can also be computed by the induction formula $\theta(n) = \sum_{m=1}^{n-2} \theta(m + 1)\theta(n - m)$.

From any of these two inductions, one can deduce the following closed formula:

Proposition 1.3. *The number $\theta(n)$ of triangulations of a convex n-gon is the* Catalan number*:*

$$\theta(n) = C_{n-2} := \frac{1}{n-1}\binom{2n-4}{n-2}. \qquad \square$$

Catalan numbers count several combinatorial "Catalan families" such as triangulations, *rooted binary trees* (trees whose $n-2$ nodes have either two or no children), or *Dyck paths* (lattice paths which use north steps $N := (0, 1)$ and east steps $E := (1, 0)$, start from $(0, 0)$, end at $(n-2, n-2)$ and never go below the diagonal $x = y$) — see [Sta99] for many other examples. Of course there are bijections from triangulations to any of these families; these bijections can be made explicit either by the inductive decomposition described above, or even directly. For example, if T is a triangulation of the n-gon, then:

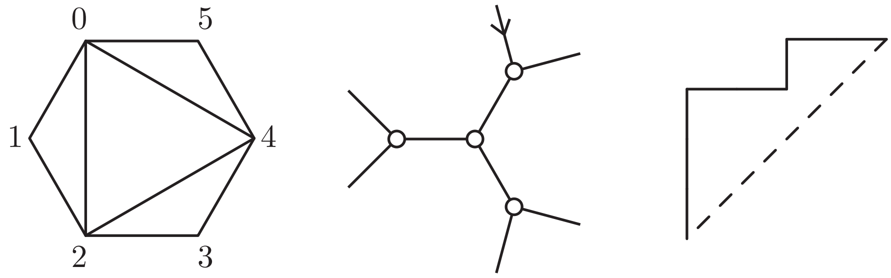

Figure 1.2: Three catalan families: a triangulation, its dual rooted binary tree, and the associated Dyck path.

(i) the dual graph of T (with one vertex for each triangle and one edge between two adjacent triangles) is a binary tree with $n-2$ nodes, rooted at the triangle containing the boundary edge $[0, n-1]$; and
(ii) the lattice path $N^{\delta_0(T)}EN^{\delta_1(T)}E \dots N^{\delta_{n-3}(T)}E$, where $\delta_i(T)$ is the number of triangles of T whose first vertex is i, is a Dyck path (of semilength $n-2$).

These two maps, from triangulations to rooted binary trees and to Dyck paths are bijective.

Flips. Our last proof of Lemma 1.2 illustrates flips in triangulations. A *flip* is a local operation which transforms a triangulation of the n-gon into another one: in any quadrangle formed by two adjacent triangles, we can replace one diagonal by the other one. Since a flip does not change neither the number of triangles, nor the number of edges, Lemma 1.2 is a consequence of:

Proposition 1.4. *The graph of flips, whose vertices are triangulations of the n-gon and whose edges are flips between them, is connected.* □

This proposition is proved by observing that any triangulation can be transformed into the "fan triangulation" with apex 0 (*i.e.* the triangulation obtained by relating vertex 0 to all the others): indeed, in any other triangulation, there is a flip which increases the degree of vertex 0. Observe that this even implies that we can reach the fan triangulation from any other triangulation with $n-1-\deg_0(T) \leq n-3$ flips, and therefore, that the diameter of this graph is at most $2n-6$.

This bound on the diameter can be slightly improved: we can relate any two triangulations of the n-gon through a fan triangulation whose apex maximizes the sum of the degrees (in our two triangulations). Since the average sum of degree is $4(2n-3)/n$, this bounds the diameter by $2n-10-12/n$, and thus, by $2n-10$ as soon as $n > 12$.

It is much less elementary to prove that this is in fact the exact diameter of the graph of flips:

Theorem 1.5 ([STT88]). *The graph of flips on triangulations of the n-gon has diameter $2n-10$ for sufficiently large values of n.* □

We finish this section with a last important property of the graph of flips (see Section 4.3.1):

Theorem 1.6 ([Lee89, BFS90, GKZ94, Lod04, HL07]). *The graph of flips on triangulations of the n-gon is the graph of a convex polytope of dimension $n-3$, called the* associahedron. □

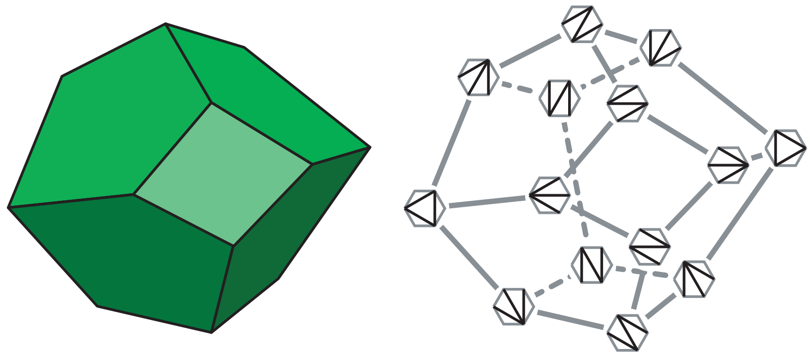

Figure 1.3: The 3-dimensional associahedron, with its vertices corresponding to the 14 triangulations of the hexagon, and its edges corresponding to flips between them.

1.2 Multitriangulations

The first topic of this dissertation is a generalization of triangulations, in which some chords are allowed to cross as long as the cardinality of the maximal set of mutually crossing chords remains sufficiently small. To be more precise, for $\ell \geq 2$, we call *ℓ-crossing* any set of ℓ mutually intersecting edges of the n-gon. As well as we were interested in non-crossing sets of edges, we now consider sets of edges which avoid $(k+1)$-crossings. Among them, maximal such sets play a special role:

Definition 1.7. *A k-triangulation is a maximal set of edges of the n-gon such that no $k+1$ of them are mutually crossing.*

All throughout our presentation, we will use the 2-triangulation of the following picture to illustrate results on multitriangulations:

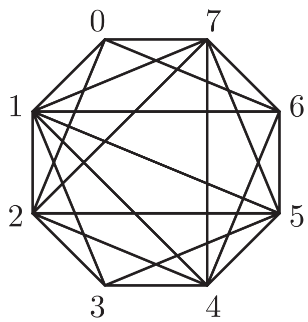

Figure 1.4: A 2-triangulation of the octagon.

Let us insist on the fact that triangulations occur when the parameter k equals 1. Surprisingly, multitriangulations share many combinatorial and structural properties with triangulations. Before reviewing the existing results and summarizing those of this dissertation, we present several interpretations under which multitriangulations have been motivated and studied.

1.2.1 Four different interpretations

Clique-free subgraphs of the intersection graph [CP92]. Consider the *intersection graph* of the complete geometric graph with vertices in convex position, that is, the graph whose vertices are the straight chords of the n-gon and whose edges relate any pair of crossing chords. By definition, an ℓ-crossing of the n-gon translates into an ℓ-clique in the intersection graph. Consequently, k-triangulations are those sets of chords which induce a subgraph of the intersection graph with no $(k+1)$-cliques (see Figure 1.5(a)).

With this formulation [CP92], multitriangulations are thought of as optimal graphs for a Turán-type Theorem on chords of the n-gon. Remember indeed Turán's famous Theorem:

Theorem 1.8 (Turán [Tur54]). *A graph on n vertices with no p-clique cannot have more than $\frac{n^2}{2}(1-\frac{1}{p-1})$ edges.* □

Line arrangements in the hyperbolic plane [DKM02]. Consider a finite set $\mathcal{L}$ of lines in a (Euclidean or hyperbolic) plane. Denote by $\kappa(\mathcal{L})$ the maximal number of mutually crossing lines of $\mathcal{L}$ and by $\nu(\mathcal{L})$ the number of points at infinity that coincide with at least one line in $\mathcal{L}$. For the Euclidean plane these numbers satisfy $1 \leq \kappa(\mathcal{L}) = \nu(\mathcal{L}) \leq |\mathcal{L}|$, since two non-crossing lines have the same point at infinity. Moreover, there is no further restriction: a line arrangement in general position satisfies $\kappa(\mathcal{L}) = \nu(\mathcal{L}) = |\mathcal{L}|$ and adding any line parallel to an existing line does not change $\kappa(\mathcal{L})$ or $\nu(\mathcal{L})$.

The situation for the hyperbolic plane is quite different: the number of lines cannot be arbitrarily large compared to the number of points at infinity. By definition, k-triangulations of the n-gon are exactly the representations in the Klein model of the hyperbolic plane of the maximal (for inclusion) hyperbolic line arrangements whose number of mutually crossing lines does not exceed k and whose number of points at infinity is n. In other words, while understanding the relations between k, n and the number of edges in k-triangulations of the n-gon, we will equivalently be dealing with $\kappa(\mathcal{L})$ and $\nu(\mathcal{L})$ in a hyperbolic line arrangement (see Figure 1.5(b)).

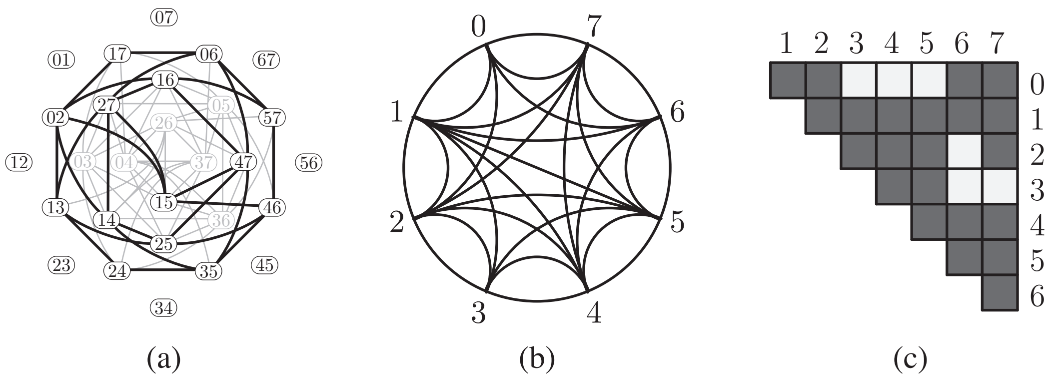

Figure 1.5: Three interpretations of the 2-triangulation of Figure 1.4: (a) A maximal triangle-free induced subgraph of the intersection graph; (b) A line arrangement in the hyperbolic plane (represented on the Poincaré Disk model); (c) A 3-diagonal-free $0/1$-filling of a triangular polyomino.

Diagonal-free fillings of polyominoes [Jon05]. Given a subset E of edges of the n-gon, consider the upper triangular part of its adjacency matrix (whose coefficient in the ith row and jth column is 1 if the edge $[i, j]$ is in T and 0 otherwise, for all $0 \le i < j \le n-1$). Two edges $[a, b]$ and $[c, d]$ of E cross whenever the two corresponding 1's in the adjacency matrix form a strictly decreasing diagonal (one 1 is below and to the right of the other) whose enclosing rectangle is contained in the upper triangular part of the adjacency matrix. Similarly, an ℓ-crossing in E translates in the adjacency matrix into a strictly decreasing ℓ-diagonal whose enclosing rectangle is contained in the upper part of the adjacency matrix (see Figure 1.5(c)).

This replaces multitriangulations in the broader context of the study of $0/1$-fillings of polyominoes (*i.e.* connected subsets of the integer lattice $\mathbb{Z}^2$) with restrictions on the length on their longest increasing and decreasing diagonals. This interpretation provides in particular interesting enumeration results on multitriangulations (see the discussion in Section 4.1).

Split systems [DKM04, DKKM01]. A *split* of a finite set X is a bipartition $A \sqcup B = X$, and a *split system* on X is a set of splits of X. Call two splits $A \sqcup B$ and $A' \sqcup B'$ *compatible* if at least one of the intersections $A \cap A'$, $A \cap B'$, $B \cap A'$, $B \cap B'$ is empty. Finally a split system is *k-compatible* if it does not contain a subset of $k+1$ pairwise incompatible splits.

Multitriangulations correspond to the very special "k-compatible and cyclic" split systems: a split system S on X is *cyclic* if there exists a bijection $\phi : \{0, \dots, |X|-1\} \to X$ such that any split of S is of the form $\phi([i, j)) \sqcup \phi([i, j)^C)$ for some $0 \le i < j \le n-1$. In this case, there is an obvious correspondence between a split $\phi([i, j)) \sqcup \phi([i, j)^C)$ and the chord $[i, j]$ of the $|X|$-gon, in which incompatible splits correspond to crossings. Thus, k-compatible cyclic split systems on X are nothing else but k-triangulations of the $|X|$-gon.

In fact, when $k \le 2$, the only k-compatible split systems with maximal cardinality are cyclic split systems [DKKM01]. This is not true anymore as soon as $k = 3$ (for example the split system $\big\{([i, j), [i, j)^C) \,\big|\, 0 \le i < j \le 3\big\} \cup \{(\{0, 2\}, \{1, 3\})\}$ is 3-compatible).

1.2.2 Previous related results

As far as we know, multitriangulations first appeared in the work of Vasilis Capoyleas and János Pach in the context of extremal theory for geometric graphs (see [PA95, Chapter 14], [Fel04, Chapter 1] and the discussion in [CP92]). They proved that a $(k+1)$-crossing-free subset of edges of the n-gon cannot have more than $k(2n-2k-1)$ edges. Tomoki Nakamigawa [Nak00], and independently Andreas Dress, Jacobus Koolen and Vincent Moulton [DKM02], then proved that all k-triangulations of the n-gon reach this bound. Both proofs rely on the concept of flips in multitriangulations: as for triangulations, a flip creates a k-triangulation from another one, removing and inserting a single edge. Tomoki Nakamigawa [Nak00] proved that every (sufficiently long) edge of a k-triangulation can be flipped, and that the graph of flips is connected. Let us observe that in these previous works, the results are obtained in an "indirect way": first, a flattening operation, similar to the contraction of a boundary edge in triangulations, is introduced and used to prove the existence of flips in multitriangulations (either in full generality, like in [Nak00], or only for partial cases, like in [DKM02]); then, the number of edges is deduced from the connectedness of the graph of flips. To summarize:

Theorem 1.9 ([CP92, Nak00, DKM02]). *(i) There is an inductive operation which transforms the k-triangulations of the $(n+1)$-gon into those of the n-gon and vice versa [Nak00].*

(ii) Any edge of length at least $k+1$ in a k-triangulation of the n-gon can be flipped and the graph of flips is regular and connected [Nak00, DKM02].

(iii) All k-triangulations of the n-gon have $k(2n-2k-1)$ edges [CP92, Nak00, DKM02]. □

In statement (ii), the *length* of an edge e of the n-gon is defined as the minimum between the numbers of remaining vertices of the n-gon located on each side of e, augmented by 1 (boundary edges have length 1). Only edges of length greater than k are *relevant* since the other ones cannot be part of a $(k+1)$-crossing (hence they appear in all k-triangulations).

Jakob Jonsson [Jon03, Jon05] then completed these fundamental structural results in two directions. On the one hand, he studied enumerative properties of multitriangulations, generalizing in particular Proposition 1.3 as follows:

Theorem 1.10 ([Jon05]). *The number $\theta(n,k)$ of k-triangulations of the n-gon equals:*

$$\theta(n,k) = \det(C_{n-i-j})_{1\le i,j\le k} = \det \begin{pmatrix} C_{n-2} & C_{n-3} & \cdot^{\cdot^{\cdot}} & \cdot^{\cdot^{\cdot}} & C_{n-k-1} \\ C_{n-3} & \cdot^{\cdot^{\cdot}} & \cdot^{\cdot^{\cdot}} & C_{n-k-1} & \cdot^{\cdot^{\cdot}} \\ \cdot^{\cdot^{\cdot}} & \cdot^{\cdot^{\cdot}} & \cdot^{\cdot^{\cdot}} & \cdot^{\cdot^{\cdot}} & \cdot^{\cdot^{\cdot}} \\ \cdot^{\cdot^{\cdot}} & C_{n-k-1} & \cdot^{\cdot^{\cdot}} & \cdot^{\cdot^{\cdot}} & C_{n-2k+1} \\ C_{n-k-1} & \cdot^{\cdot^{\cdot}} & \cdot^{\cdot^{\cdot}} & C_{n-2k+1} & C_{n-2k} \end{pmatrix}.$$ □

The proof of this theorem relies on a more general enumeration result concerning k-diagonal-free $0/1$-fillings of polyominoes. Interestingly, the Hankel determinant in this statement is also known to count a certain family of non-intersecting k-tuples of Dyck paths [GV85]. The equality of the cardinalities of these two combinatorial families raises the question to find an explicit bijection (generalizing the bijection in Figure 1.2). Even if Sergi Elizalde [Eli07] and Carlos Nicolas [Nic09] exhibit two different bijections for the case when $k=2$, this question remains open for general k. We discuss this problem in Section 4.1.

On the other hand, Jakob Jonsson studied in [Jon03] the simplicial complex $\Delta_{n,k}$ formed by all $(k+1)$-crossing-free subsets of relevant edges of the n-gon. Since all its maximal elements have cardinality $k(n-2k-1)$, this complex is pure of dimension $k(n-2k-1)-1$. Jakob Jonsson proved that this complex is even a topological sphere:

Theorem 1.11 ([Jon03]). *The simplicial complex $\Delta_{n,k}$ is a vertex-decomposable piece-wise linear sphere of dimension $k(n-2k-1)-1$.* □

This theorem, together with small cases examples, leads to conjecture that this complex is even polytopal (*i.e.* the boundary complex of a convex polytope) as happens when $k=1$ (see Theorem 1.6). We discuss this open question in Section 4.3.

1.2.3 Overview of our results

Our contribution to the study of multitriangulations is based on their stars, which generalize triangles for triangulations:

Definition 1.12. *A k-star is the subset of edges of length k of a complete geometric graph on $2k+1$ vertices in convex position. In other words, it is a (non-simple) polygon with $2k+1$ vertices $s_0, \dots, s_{2k}$ cyclically ordered, and $2k+1$ edges $[s_0, s_k], [s_1, s_{k+1}], \dots, [s_{2k}, s_{k-1}]$.*

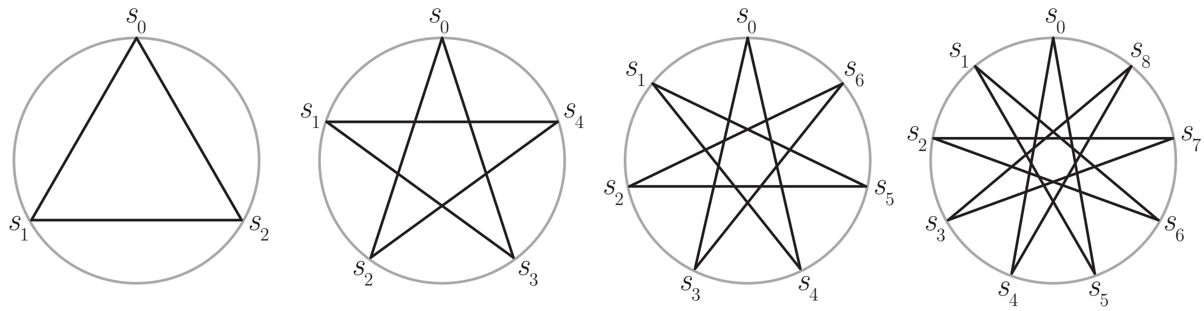

Figure 1.6: Examples of k-stars, for $k \in [4]$.

Stars in multitriangulations play exactly the same role as triangles for triangulations: they decompose multitriangulations into simpler pieces and provide a useful tool to study their combinatorial properties. As evidence for this, we give in Chapter 2 direct and simple proofs of the fundamental properties of multitriangulations of Theorem 1.9 (number of edges, definition and properties of the flip operation, etc.). Afterwards, we use stars in Chapter 3 to relate multitriangulations with pseudotriangulations and pseudoline arrangements. This new interpretation provides a natural generalization of multitriangulations to any point set in general position in the plane, which keeps the rich combinatorial properties of multitriangulations (in particular the flip operation). Finally, in Chapter 4, we discuss in terms of stars the open questions presented above, and present some partial solutions as well as some natural failed attempts based on properties of stars. In the end of this section, we present in more details our contribution, summarizing and underlying our main results.

1.2.3.1 Stars in multitriangulations

In Chapter 2, we study elementary properties of multitriangulations in terms of stars. In Section 2.2, we prove our main structural result concerning the incidence relations between the k-stars of a k-triangulation:

Theorem 1.13. *Let T be a k-triangulation of the n-gon (with $n \geq 2k+1$).*

(i) Each edge belongs to zero, one or two k-stars of T, depending on whether its length is smaller, equal or greater than k.

(ii) T has exactly $n-2k$ k-stars and $k(2n-2k-1)$ edges. □

Let us mention that we obtain Part (ii) of Theorem 1.13 by a direct double counting argument similar to our first proof of Lemma 1.2: we use two simple independent relations between the number of edges and the number of k-stars in a k-triangulation. The first relation is of course derived from Part (i) of Theorem 1.13, while the second one relies on the properties of the bisectors of k-stars. A *bisector* of a k-star is a bisector of one of its angles, that is, a line which passes through one of its vertices and separates its remaining vertices into two equal parts of cardinality k. As for triangulations, the second relation is derived from the following identification between the pairs of k-stars of a k-triangulation T and the edges of the n-gon which are not in T:

Theorem 1.14. *Let T be a k-triangulation of the n-gon.*

(i) Any pair of k-stars of T has a unique common bisector, which is not in T.

(ii) Reciprocally, any edge not in T is the common bisector of a unique pair of k-stars of T. □

We also use stars and their common bisectors in Section 2.3 to understand the flip operation as a local transformation. In much the same way than a flip in a triangulation consists in replacing one diagonal by the other in a quadrangle formed by two adjacent triangles, flips in multitriangulations can be interpreted as a transformation involving only two adjacent stars:

Theorem 1.15. *Let T be a k-triangulation of the n-gon, e be an edge of length greater than k, and f be the common bisector of the two k-stars of T containing e. Then $T \triangle \{e, f\}$ is a k-triangulation of the n-gon and it is the only one, except T itself, which contains $T \smallsetminus \{e\}$.* □

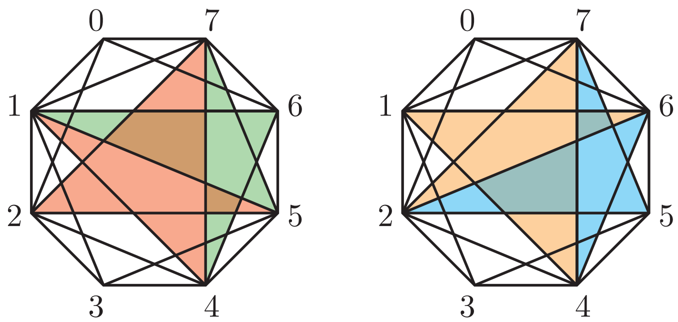

Figure 1.7: A flip in the 2-triangulation of the octagon of Figure 1.4.

This interpretation simplifies the study of the graph of flips (whose vertices are the k-triangulations of the n-gon and whose edges are the flips between them) and yields to new proofs of the results in [Nak00] as well as partial extensions of them:

Theorem 1.16. *The graph of flips on k-triangulations of the n-gon is $k(n-2k-1)$-regular and connected, and for all $n > 4k^2(2k+1)$, its diameter $\delta_{n,k}$ is bounded by*

$$2\left\lfloor\frac{n}{2}\right\rfloor\left(k+\frac{1}{2}\right) - k(2k+3) \leq \delta_{n,k} \leq 2k(n-4k-1).$$ □

The upper bound on the diameter in this theorem was already proved in [Nak00] (and has to be compared with the exact value $2n-10$ of the diameter of the graph of flips on triangulations of the n-gon mentioned in Theorem 1.5). The lower bound is new, but only slightly improves the trivial bound $\delta_{n,k} \geq k(n-2k-1)$.

We also use stars in Section 2.4 to study the *k-ears* (*i.e.* the edges of length $k+1$) of a k-triangulation. We present a simple proof that any k-triangulation contains at least $2k$ k-ears [Nak00], and we provide several characterizations of the k-triangulations which attain this bound:

Theorem 1.17. *The number of k-ears in a k-triangulation equals $2k$ plus its number of internal k-stars, i.e. those that do not contain an edge of length k.*

Furthermore, when $k > 1$ and T is a k-triangulation, the following conditions are equivalent:

(i) T contains exactly $2k$ k-ears;

(ii) T has no internal k-star;

(iii) T is k-colorable*, i.e. it is possible to color its relevant edges with k colors such that no crossing is monochromatic;*

(iv) the set of relevant edges of T is the union of k disjoint accordions (an accordion *is a sequence of edges $[a_i, b_i]$ such that for all i, either $a_{i+1} = a_i$ and $b_{i+1} = b_i+1$ or $a_{i+1} = a_i - 1$ and $b_{i+1} = b_i$).* □

In Section 2.5, we reinterpret in terms of stars the inductive operation of Theorem 1.9(i) which transforms the k-triangulations of the $(n+1)$-gon into those of the n-gon and *vice versa*. It consists in *flattening* (or *inflating*) a single k-star adjacent to an edge of length k. We voluntarily only introduce this operation at the end of Chapter 2 to emphasize that none of our proofs so far make use of induction.

Finally, Section 2.6 completes our study of the structural properties of multitriangulations in terms of stars. According to Theorem 1.13, we see k-triangulations of the n-gon as polygonal decompositions of a certain surface into $n-2k$ k-gons. We exploit this interpretation to construct, via multitriangulations, very regular decompositions of an infinite family of surfaces.

1.2.3.2 Multitriangulations, pseudotriangulations, and duality

Chapter 3 is devoted to the interpretation of multitriangulations in the line space of the plane, *i.e.* in the Möbius strip. We consider the usual duality between configurations of points and pseudoline arrangements (see [Fel04, Chapters 5,6] and [Goo97]): the set p^* of all lines passing through a point p of the plane is a *pseudoline* (a non-separating simple closed curve) of the Möbius strip, and the set $P^* := \{p^* \mid p \in P\}$ of all pseudolines dual to the points of a finite set P is a *pseudoline arrangement* (any two pseudolines have exactly one crossing point). The starting point of Chapter 3 is the following observation:

Observation 1.18. Let T be k-triangulation of the n-gon. Then:

(i) the set S^* of all bisectors to a k-star S of T is a pseudoline;

(ii) the common bisector of two k-stars R and S is a crossing point of the two pseudolines R^* and S^*, while a common edge of R and S is a contact point between R^* and S^*;

(iii) the set $T^* := \{S^* \mid S\ k\text{-star of } T\}$ of all pseudolines dual to the k-stars of T is a *pseudoline arrangement with contact points* (two pseudolines cross exactly once, but can touch each other a finite number of times);
(iv) the support of this arrangement covers precisely the support of the dual arrangement V_n^* of the vertex set of the n-gon, except its first k levels.

We prove the reciprocal statement of this observation:

Theorem 1.19. *Any pseudoline arrangement with contact points whose support covers precisely the support of the dual arrangement V_n^* of the vertex set of the n-gon except its first k levels is the dual arrangement of a k-triangulation of the n-gon.* □

A similar observation was made in [PV94, PV96a] for pointed pseudotriangulations of a point set in general position. A *pseudotriangle* is a polygon with only three convex angles joined by three concave polygonal chains, and a *pseudotriangulation* of a point set P in general position is a set of edges which decomposes the convex hull of P into pseudotriangles. It is *pointed* if for any point $p \in P$, there is a line passing through p which defines a closed half-plane containing no edge incident to p. For a pointed pseudotriangulation T of P, it was observed that:
(i) the set Δ^* of internal tangents to a pseudotriangle Δ is a pseudoline of the Möbius strip;
(ii) the set $T^* := \{\Delta^* \mid \Delta \text{ pseudotriangle de } T\}$ is a pseudoline arrangement with contact points supported by the dual arrangement P^* minus its first level.

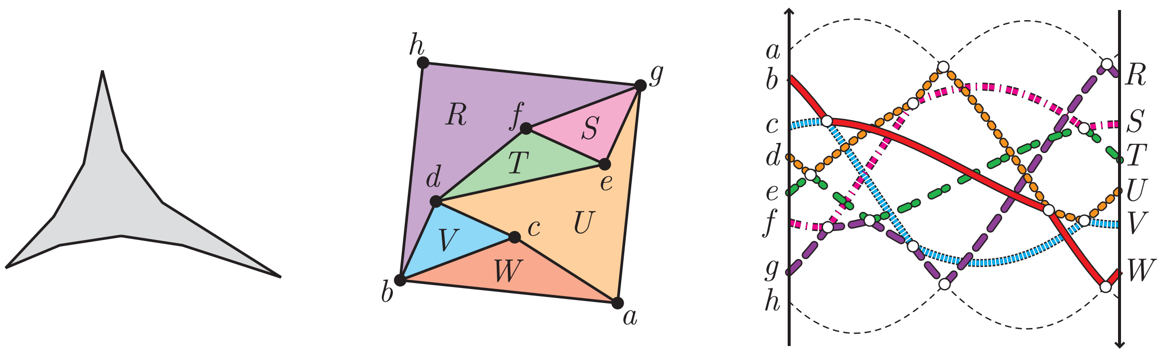

Figure 1.8: A pseudotriangle, a pseudotriangulation, and its dual pseudoline arrangement.

We provide again different proofs of the reciprocal statement:

Theorem 1.20. *Let P be a point set in general position and P^* denote its dual pseudoline arrangement. Then any pseudoline arrangement with contact points whose support covers precisely the support of P^* except its first level is the dual arrangement of a pseudotriangulation of P.* □

Motivated by these two theorems, we then consider *pseudoline arrangements with contact points* which share a common support. We define a flip operation corresponding to flips in multitriangulations and pseudotriangulations:

Definition 1.21. *Two pseudoline arrangements with the same support are related by a flip if the symmetric difference of their sets of contact points is only a pair $\{u, v\}$. In this case, in one of these arrangements u is a contact point of two pseudolines which cross at v, while in the other arrangement, v is a contact point of two pseudolines which cross at u.*

We study in Section 3.1 the graph $G(\mathcal{S})$ of flips on pseudoline arrangements with a common support $\mathcal{S}$. For example, when $\mathcal{S}$ is the support of an arrangement of two pseudolines with p contact points, $G(\mathcal{S})$ is the complete graph on $p+1$ vertices. We consider certain acyclic orientations of the graph $G(\mathcal{S})$, given by vertical cuts of the support $\mathcal{S}$. Each of these orientations has a unique source that we call the *greedy pseudoline arrangement*, and that we characterize in terms of sorting networks. The properties of these greedy pseudoline arrangements provide an enumeration algorithm for pseudoline arrangements with the same support, whose working space is polynomial. We thus sheds light upon a similar algorithm existing for the enumeration of pseudotriangulations of point sets [BKPS06], providing a complementary proof of it.

We then come back in Sections 3.2 and 3.3 to the specific cases of multitriangulations and pseudotriangulations. According to Theorems 1.19 and 1.20, we propose the following generalization of both multitriangulations and pseudotriangulations:

Definition 1.22. *A* k-pseudotriangulation *of a pseudoline arrangement L is a pseudoline arrangement whose support is L minus its first k levels. A* k-pseudotriangulation *of a point set P in general position in the plane is a set T of edges which correspond by duality to the contact points of a k-pseudotriangulation T^* of P^*.*

In contrast to other possible candidates for generalization of multitriangulations to non-convex position, this definition preserves the rich combinatorial structure of multitriangulations. For example, a k-pseudotriangulation of a point set P has automatically $k(2|P| - 2k - 1)$ edges, and any (sufficiently internal) edge can be flipped to create a new k-pseudotriangulation of P.

Following our directed line, we again focus on stars in multipseudotriangulations, which are now defined as follows: a *star* in a k-pseudotriangulation T is a set of edges corresponding to all the contact points of a single pseudoline of the dual pseudoline arrangement T^*. As immediate consequences of the definition, the stars of a multipseudotriangulation have analog properties to that of Theorems 1.13, 1.14 and 1.15.

We conclude Chapter 3 with three questions related to multipseudotriangulations:

1. We study *iterated multipseudotriangulations* in Section 3.4: a k-pseudotriangulation of an m-pseudotriangulation of a pseudoline arrangement L is a $(k+m)$-pseudotriangulation of L. We give an example of 2-triangulation not containing any triangulation. We prove though that greedy multipseudotriangulations are iterations of greedy pseudotriangulations.
2. In Section 3.5.1, we characterize the edges of the greedy k-pseudotriangulations of a point set P in terms of *k-horizon trees* of P. This characterization generalizes an observation of Michel Pocchiola [Poc97] in the context of pseudotriangulations.
3. Finally in Section 3.5.2, we study multipseudotriangulations of configurations of disjoint convex bodies of the plane. The dual arrangements of configurations of disjoint convex bodies are *double pseudoline arrangements*, introduced in [HP09] by Luc Habert and Michel Pocchiola. Let us mention that we manipulate these arrangements in Appendix A.1 to enumerate all arrangements of at most 5 double pseudolines up to isomorphism.

1.2.3.3 Further topics

Finally, we discuss in Chapter 4 three remaining open problems on multritriangulations which illustrate the rich combinatorial and geometric structure of multitriangulations. Our goal is to present natural ideas based on stars which could be fertile, although they provide at the present time only partial results to these problems.

Our first problem (Section 4.1) is that of finding an *explicit bijection* between the set of multitriangulations and the set of non-crossing k-tuples of Dyck paths, which are both counted by the Hankel determinant of Theorem 1.10. As mentioned in our introduction on triangulations, the indegree sequence of a triangulation defines a natural bijection to Dyck paths. Generalizing this simple remark, Jakob Jonsson compared in [Jon03] the repartition of indegree sequences of k-triangulations with that of signatures of non-crossing k-tuples of Dyck paths (see Definition 4.7 for the precise statement of the definition of these parameters). Following this result, we try to find a suitable way to decompose the relevant edges of a k-triangulation into k disjoint sets such that the respective indegree sequences of these sets define k non-crossing Dyck paths. We point out a simple such decomposition based on stars, for which the resulting map from k-triangulations to non-crossing k-tuples of Dyck paths is unfortunately not bijective.

Our second open problem (Section 4.2) concerns *rigidity* properties of multitriangulations. A triangulation is a *minimally rigid* object in the plane: the only continuous motions of its vertices which preserve its edges' lengths are the isometries of the plane, and removing any of its edges makes it flexible. Equivalently, a triangulation of the n-gon satisfies Laman's property: it has $2n-3$ edges and any subgraph on m vertices has at most $2m-3$ edges. We observe two interesting connections of multitriangulations to rigidity (and related topics):

(i) First, a k-triangulation of the n-gon is a $(2k, \binom{2k+1}{2})$-*tight graph*: it has $2kn - \binom{2k+1}{2}$ edges and any subgraph on m vertices has at most $2km - \binom{2k+1}{2}$ edges. This yields the conjecture that any k-triangulation is a (generically) minimally rigid graph in dimension $2k$. We prove this conjecture when $k = 2$.

(ii) We then show that the dual graph of a k-triangulation is (k, k)-tight: it can be decomposed into k edge-disjoint spanning trees. This has to be understood has a generalization of the dual tree of a triangulation.

We finally focus (in Section 4.3) on the *polytopality question* of the simplicial complex $\Delta_{n,k}$ formed by all $(k+1)$-crossing-free subsets of relevant edges of the n-gon. We propose two different contributions to this problem:

(i) On the one hand (Section 4.3.2), we answer the minimal non-trivial case: we describe the space of symmetric realizations of $\Delta_{8,2}$. This result is obtained in two steps: first, we enumerate by computer all symmetric oriented matroids realizing our simplicial complex; then, we study the possible geometric realizations of the resulting oriented matroids.

(ii) On the other hand (Section 4.3.3), we discuss a natural generalization of a construction of the associahedron due to Jean-Louis Loday [Lod04]. We obtain a polytope with a particularly simple facet description which realizes the flip graph restricted to certain multitriangulations (those whose dual graph is acyclic). This polytope could have been *a priori* a projection of a polytope realizing $\Delta_{n,k}$, but we show that such a projection is impossible.

1.3 Sources of material

The results presented in the first part of this dissertation have been partially published (or submitted) in the following papers:

1. Chapter 2 — where we introduce stars and use them to recover and simplify some structural properties of multitriangulations — is a joint work with Francisco Santos and appeared in [PS09]. Only few minor results, including those concerning the diameter of the graph of flips (Lemmas 2.35 and 2.39) and the construction of equivelar surfaces (Section 2.6.3), have been added since the publication of this article. This paper also contains a detailed discussion of various open questions related to multitriangulations, some of which are explored in Chapter 4.
2. All the content of Chapter 3 — the systematic study and enumeration of the graph of flips on pseudoline arrangements with the same support, the relationship between pseudotriangulations and multitriangulations, and the definition and properties of multipseudotriangulations — is the result of a joint work with Michel Pocchiola [PP09].
3. Chapter 4 is the concatenation of various discussions I had in particular with Francisco Santos, and a large part of this chapter is inspired from [PS09, Section 8]. As far as the two main contributions of this chapter are concerned:
   a) The description of the space of symmetric realizations of $\Delta_{8,2}$ is a joint work with Jürgen Bokowski [BP09]. Some HASKELL code developed to enumerate symmetric matroid realizations is presented and explained in Appendix A.2.
   b) The generalization of Loday's construction of the associahedron is a joint work with Francisco Santos [PS10].
4. Finally, Appendix A.1 — where we enumerate isomorphism classes of arrangements with few pseudolines and double pseudolines — is a joint work with Julien Ferté and Michel Pocchiola [FPP08].

Chapter Two

STARS IN MULTITRIANGULATIONS

In this chapter, we study structural properties of multitriangulations. Our approach is to decompose a multitriangulation into a complex of stars, which generalize triangles for triangulations. In much the same way as triangles are central objects in triangulations, stars are our main tool to understand multitriangulations. In this chapter, we use them to:

(i) Give a direct proof that the number of edges is the same in all multitriangulations.

(ii) Define locally the "flip operation" which transforms a multitriangulation into another one by exchanging a single edge. We study extensively the graph of flips, with a particular attention to its diameter.

(iii) Characterize a particularly nice and simple family of multitriangulations obtained as superpositions of triangulations.

(iv) Understand the "deletion operation" which transforms multitriangulations of an $(n+1)$-gon into multitriangulations of an n-gon, and *vice versa*. This transformation allows recursive proofs for some properties of multitriangulations.

(v) Interpret multitriangulations as decompositions of a certain surface. As an application of multitriangulaitons, we obtain examples of very regular decompositions of surfaces.

2.1 NOTATIONS AND EXAMPLES

2.1.1 Multicrossings, multitriangulations, and relevant edges

Let k and n be two integers such that $k \geq 1$ and $n \geq 2k+1$.

Let V_n be the *set of vertices* of a convex n-gon, *i.e.* any set of points on the unit circle, labeled counterclockwise by the cyclic set $\mathbb{Z}_n$. We always refer to the points in V_n by their labels to simplify notation. For $u, v, w \in V_n$, we write $u \prec v \prec w$ meaning that u, v and w are in counterclockwise order on the circle. For any $u, v \in V_n$, let $[\![u, v]\!]$ denote the *cyclic interval* $\{w \in V_n \,|\, u \preccurlyeq w \preccurlyeq v\}$. The intervals $]\!]u, v[\![$, $[\![u, v[\![$ and $]\!]u, v]\!]$ are defined similarly. Let $|u - v| := \min(|[\![u, v[\![|, |[\![v, u[\![|)$ be the *cyclic distance* between u and v.

For $u \neq v \in V_n$, let $[u, v]$ denote the straight *edge* connecting the vertices u and v. We say that $[u, v]$ is of *length* $|u - v|$. By definition, an edge of length ℓ passes through two points of V_n and separates $\ell - 1$ points from the other $n - \ell - 1$. Let $E_n := \binom{V_n}{2}$ be the *set of edges* of the

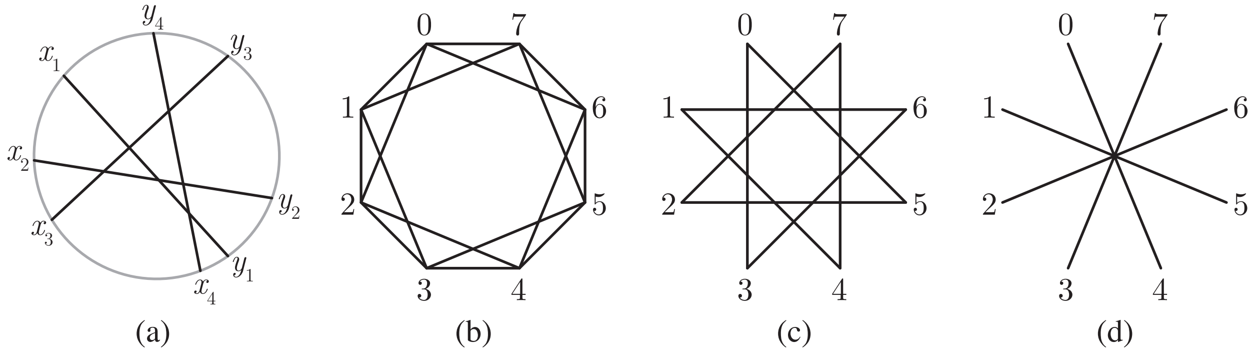

Figure 2.1: A 4-crossing (a) and the sets of 3-irrelevant (b), 3-boundary (c), and 3-relevant (d) edges of an octagon.

complete graph on V_n. Two edges $[u, v]$ and $[u', v']$ are said to *cross* when u and v lie one in each of the open cyclic intervals $]\!]u', v'[\![$ and $]\!]v', u'[\![$. In other words, the edges $[u, v]$ and $[u', v']$ cross when $u \prec u' \prec v \prec v' \prec u$ or $u' \prec u \prec v' \prec v \prec u'$. Observe that this definition is symmetric in the two edges involved and that it corresponds to an intersection of the straight open segments (u, v) and (u', v'). Similarly to our discussion on triangulations in Section 1.1, where we considered subsets of E_n avoiding crossings, we are now interested in subsets of E_n avoiding the following configuration:

Definition 2.1. *For $\ell \in \mathbb{N}$, an ℓ-crossing is a set of ℓ mutually intersecting edges.*

We will always order the edges of an ℓ-crossing $F := \{f_i \,|\, i \in [\ell]\}$ cyclically such that the endpoints x_i and y_i of f_i satisfy $x_1 \prec x_2 \prec \cdots \prec x_\ell \prec y_1 \prec y_2 \prec \cdots \prec y_\ell \prec x_1$ (see Figure 2.1).

As for triangulations, we have a particular attention to maximal sets of edges avoiding these forbidden configurations:

Definition 2.2. *A k-triangulation of the n-gon is a maximal $(k+1)$-crossing-free subset of E_n.*

Obviously, an edge $[u, v]$ of E_n can appear in a $(k+1)$-crossing only if it has at least k vertices on each side, *i.e.* if $|u - v| > k$. We distinguish three types of edges, according on whether their length is lower, equal or greater than k (see Figure 2.1):

Definition 2.3. *An edge $[u, v]$ of E_n is:*
(i) a k-relevant edge if $|u - v| > k$;
(ii) a k-boundary edge if $|u - v| = k$; and
(iii) a k-irrelevant edge if $|u - v| < k$.

By maximality, every k-triangulation of the n-gon consists of all the kn k-irrelevant plus k-boundary edges of E_n and some k-relevant edges.

2.1.2 Examples

Before going further, we consider small values of k and n (namely $k = 1$ or n close to $2k + 1$), for which we can easily describe all k-triangulations of the n-gon.

Example 2.4 ($k = 1$)**.** Since a 2-crossing is just a crossing, the 1-triangulations are just triangulations of the n-gon. All internal diagonals of the n-gon are 1-relevant, while the boundary edges of the n-gon are 1-boundary (and there is no 1-irrelevant edges). See Section 1.1 for a discussion on structural properties of triangulations of the n-gon.

Example 2.5 ($n = 2k+1$)**.** The complete graph K_{2k+1} on $2k+1$ vertices does not contain $k+1$ mutually intersecting edges, and thus it is the unique k-triangulation of the $(2k+1)$-gon. The longest diagonals $[i, i+k]$ are k-boundary, while all the other edges are k-irrelevant.

Example 2.6 ($n = 2k+2$)**.** The set of edges E_{2k+2} contains exactly one $(k+1)$-crossing formed by the $k+1$ long diagonals $[i, i+k+1]$ of the $(2k+2)$-gon. Consequently, there are $k+1$ k-triangulations of the $(2k+2)$-gon, each of them obtained from the complete graph K_{2k+2} by deleting one of these long diagonals (see Figures 2.1(b-c-d) and 2.2).

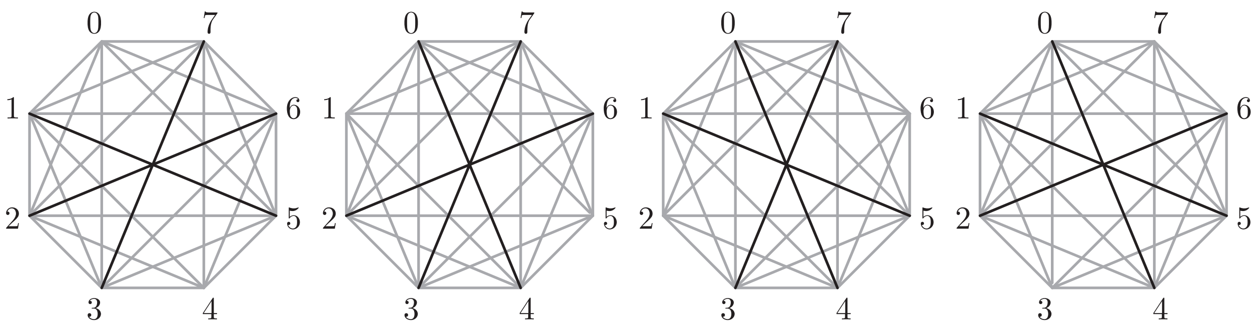

Figure 2.2: The four 3-triangulations of the octagon. 3-relevant edges are black, while 3-boundary and 3-irrelevant edges are gray.

Example 2.7 ($n = 2k+3$)**.** The k-relevant edges of E_{2k+3} are exactly the longest diagonals $e_i := [i, i+k+1]$. They form a polygonal cycle[1] $e_0, e_{k+1}, e_{2(k+1)}, \dots, e_{-(k+1)}, e_0$ in which any two diagonals cross except if they are consecutive (see for example Figure 2.3(a)). Consequently, if E is a $(k+1)$-crossing-free subset of E_{2k+3}, then:

(i) it cannot contain more than $k+1$ non-consecutive long diagonals; and

(ii) if E contains $2\ell+1$ consecutive long diagonals $e_i, e_{i+(k+1)}, \dots, e_{i+2\ell(k+1)}$, but neither the diagonal $e := e_{i+(2\ell+1)(k+1)}$ nor the diagonal $f := e_{i-(k+1)}$, then both sets $E \cup \{e\}$ and $E \cup \{f\}$ are still $(k+1)$-crossing-free.

We deduce from these two observations that the k-triangulations of the $(2k+3)$-gon are exactly the disjoint unions of k pairs of consecutive long diagonals of E_{2k+3} (plus of course the non-k-relevant edges). For example, there are fourteen 2-triangulations of the heptagon, all obtained by rotation of one of the two 2-triangulations of Figure 2.3(b-c).

[1]Remember that we have indexed the vertices of V_{2k+3} with the cyclic group $\mathbb{Z}_{2k+3}$, *i.e.* that the indices have to be understood modulo $2k+3$.

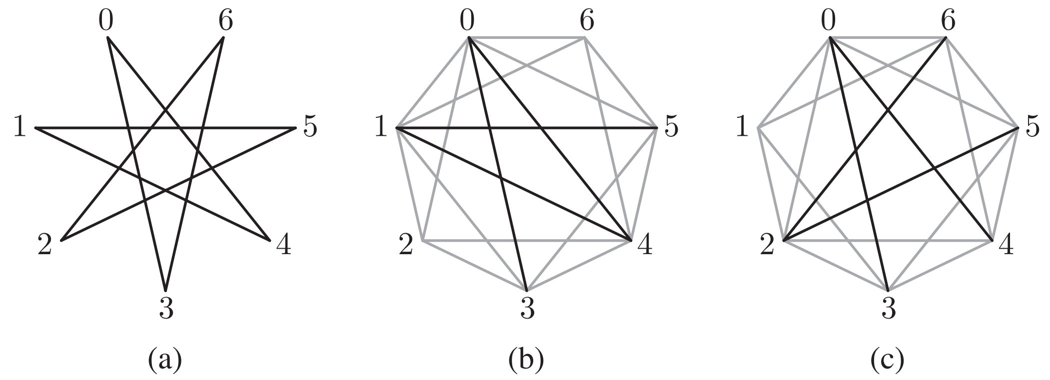

Figure 2.3: (a) The 2-relevant edges of the heptagon and (b-c) two 2-triangulations of the heptagon (representing all 2-triangulations of the heptagon up to rotation).

2.1.3 Stars

As mentioned in the introduction, our study of k-triangulations is based on a natural generalization of the triangles for triangulations. If p and q are two coprime integers, a *star polygon* of type $\{p/q\}$ is a polygon formed by connecting a set $V := \{s_j \mid j \in \mathbb{Z}_p\}$ of p points of the unit circle with the set $E := \{[s_j, s_{j+q}] \mid j \in \mathbb{Z}_p\}$ of edges (see [Cox69, Chapter 2.3, pp. 36-38], [Cox73, Chapter 6, pp. 93-95] and Figure 2.4). The role of triangles for k-triangulations is played by some special star polygons:

Definition 2.8. *A* k-star *is a star polygon of type* $\left\{\frac{2k+1}{k}\right\}$*: it is a (non-simple) polygon with* $2k+1$ *vertices* $s_0 \prec \cdots \prec s_{2k}$ *cyclically ordered and with* $2k+1$ *edges* $[s_0, s_k], [s_1, s_{k+1}], \ldots, [s_{2k}, s_{k-1}]$.

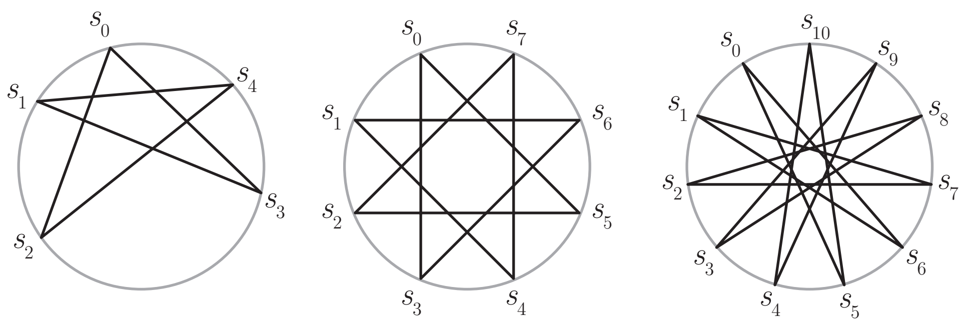

Figure 2.4: Star polygons of type $\{5/2\}$, $\{8/3\}$ and $\{11/5\}$. The left one is a 2-star and the right one is a 5-star.

Observe that there are two natural cyclic orders on the vertices of a k-star S: the *circle order*, defined as the cyclic order around the circle, and the *star order*, defined as the cyclic order tracing the edges of S. More precisely, if $s_0, \ldots, s_{2k}$ are the vertices of S cyclically ordered around the circle, we rename the vertices $r_i := s_{ik}$ to obtain the star order $r_0, \ldots, r_{2k}$.

2.2 ANGLES, BISECTORS, AND STAR DECOMPOSITION

In this section, we present our main tool to study structural properties of multitriangulations: we show that k-triangulations can be decomposed into k-stars in the same way that triangulations can be thought of as decompositions into triangles. This structural result is based on a careful comparison of the angles of a k-triangulation with the angles of its k-stars, where an angle is given by two edges adjacent to a common vertex and consecutive around it. More precisely:

Definition 2.9. *An angle $\angle(u, v, w)$ of a subset E of E_n is a pair $\{[u, v], [v, w]\}$ of edges of E such that $u \prec v \prec w$ and for all $t \in \rrbracket w, u \llbracket$, the edge $[v, t]$ is not in E.*

We call v the *vertex* of the angle $\angle(u, v, w)$. If $t \in \rrbracket w, u \llbracket$, we say that *$t$ is contained* in the angle $\angle(u, v, w)$. An angle is said to be *k-relevant* if both its edges are either k-relevant or k-boundary edges of E_n.

To illustrate these definitions, let us describe the angles of a k-star (see Figure 2.4(a-c)):

Lemma 2.10. *Let S be a k-star of E_n. Then:*

(i) the angles of S are the $2k + 1$ pairs of consecutive edges of S in star order;
(ii) all angles of S are k-relevant; and
(iii) any vertex t not in S is contained in a unique angle $\angle(u, v, w)$ of S.

Proof. Part (i) is nothing else but the definition of angle.

Since any edge of S separates the other vertices of S into two parts of size $k - 1$ and k respectively, it is at least a k-boundary edge, which implies Part (ii).

To prove Part (iii), denote by $\{s_i \mid i \in \mathbb{Z}_{2k+1}\}$ the vertices of S in cyclic order. Given a vertex t not in S, there exists a unique $i \in \mathbb{Z}_{2k+1}$ such that $s_i \prec t \prec s_{i+1}$. The angle $\angle(s_i, s_{i-k}, s_{i+1})$ is the unique angle containing t. □

2.2.1 Angles of k-stars *vs.* angles of k-triangulations

In order to compare the angles of a k-triangulation with the angles of its k-stars, we start with the following simple observation:

Lemma 2.11. *Let S be a k-star of a $(k + 1)$-crossing-free subset E of E_n. Then any angle of S is also a (k-relevant) angle of E.*

Proof. Let $\{s_j \mid j \in \mathbb{Z}_{2k+1}\}$ denote the vertices of S in star order. Suppose that E contains an edge $[s_j, t]$ where $j \in \mathbb{Z}_{2k+1}$ and $t \in \rrbracket s_{j+1}, s_{j-1} \llbracket$. Then the set of edges

$$\{[s_{j+1}, s_{j+2}], [s_{j+3}, s_{j+4}], \dots, [s_{j-2}, s_{j-1}], [s_j, t]\}$$

forms a $(k + 1)$-crossing. Consequently $\angle(s_{j-1}, s_j, s_{j+1})$ is an angle of E. □

It is interesting to observe that the reciprocal statement of this lemma is true for triangulations of the n-gon: any angle of a triangulation belongs to exactly one of its triangles. The similar statement for multitriangulations is much harder to prove, and is the basis of our study of the structural properties of multitriangulations:

Theorem 2.12. *Any k-relevant angle of a k-triangulation T belongs to a unique k-star of T.*

Proof. In this proof, we need the following definition (see Figure 2.5): let $\angle(u, v, w)$ be a k-relevant angle of T and let e and f be two edges of T that *intersect* $\angle(u, v, w)$ (*i.e.* that intersect both $[u, v]$ and $[v, w]$). If a, b, c and d denote their vertices such that $u \prec a \prec v \prec b \prec w$ and $u \prec c \prec v \prec d \prec w$, then we say that $e = [a, b]$ is *v-farther* than $f = [c, d]$ if $u \prec a \preccurlyeq c \prec v \prec d \preccurlyeq b \prec w$. Let E and F be two $(k-1)$-crossings that *intersect* $\angle(u, v, w)$. Let their edges be labeled $e_1 := [a_1, b_1], e_2 := [a_2, b_2], \ldots, e_{k-1} := [a_{k-1}, b_{k-1}]$ and $f_1 := [c_1, d_1]$, $f_2 := [c_2, d_2], \ldots, f_{k-1} := [c_{k-1}, d_{k-1}]$ such that $u \prec a_1 \prec a_2 \prec \cdots \prec a_{k-1} \prec v \prec b_1 \prec b_2 \prec \cdots \prec b_{k-1} \prec w$ and $u \prec c_1 \prec c_2 \prec \cdots \prec c_{k-1} \prec v \prec d_1 \prec d_2 \prec \cdots \prec d_{k-1} \prec w$. Then we say that E is *v-farther* than F if e_i is v-farther than f_i for every $i \in [k-1]$. We say that E is *v-maximal* if it does not exist any $(k-1)$-crossing intersecting $\angle(u, v, w)$ and v-farther than E.

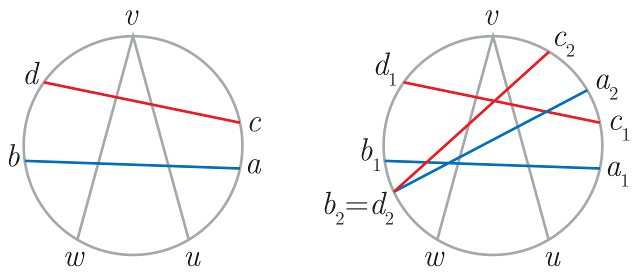

Figure 2.5: $[a, b]$ is v-farther than $[c, d]$ (left) and $\{[a_i, b_i]\}$ is v-farther than $\{[c_i, d_i]\}$ (right).

Let $\angle(u, v, w)$ be a k-relevant angle of T. If the edge $[u, v+1]$ is in T, then the angle $\angle(v+1, u, v)$ is a k-relevant angle of T and, if it is contained in a k-star S of T, then so is $\angle(u, v, w)$. Moreover, if $n > 2k+1$ ($n = 2k+1$ is a trivial case), T cannot contain all the edges $\{[u+i, v+i] \,|\, 0 \le i \le n-1\}$ and $\{[u+i, v+i+1] \,|\, 0 \le i \le n-1\}$. Consequently, we can assume that $[u, v+1]$ is not in T.

Thus we have a k-crossing E of the form $e_1 := [a_1, b_1], \ldots, e_k := [a_k, b_k]$ with $u \prec a_1 \prec \cdots \prec a_k \prec v+1$ and $v+1 \prec b_1 \prec \cdots \prec b_k \prec u$. Since $[u, v] \in T$, $a_k = v$ and since $\angle(u, v, w)$ is an angle, $v+1 \prec b_k \preccurlyeq w$. Consequently, $\{e_1, \ldots, e_{k-1}\}$ forms a $(k-1)$-crossing intersecting $\angle(u, v, w)$ and we can assume that it is v-maximal (see Figure 2.6(a)). We will prove that the edges $[u, b_1], [a_1, b_2], \ldots, [a_{k-2}, b_{k-1}], [a_{k-1}, w]$ are in T such that the points $u, a_1, \ldots, a_{k-1}$, v, $b_1, \ldots, b_{k-1}$, w are the vertices of a k-star of T containing the angle $\angle(u, v, w)$. To get this result, we use two steps: first we prove that $\angle(a_1, b_1, u)$ is an angle of T, and then we prove that the edges $e_2, \ldots, e_{k-1}, [v, w]$ form a $(k-1)$-crossing intersecting $\angle(a_1, b_1, u)$ and b_1-maximal (so that we can reiterate the argument).

First step. See Figure 2.6(b).
Suppose that $[u, b_1]$ is not in T. Thus we have a k-crossing F that prevents the edge $[u, b_1]$. Let $f_1 := [c_1, d_1], \ldots, f_k := [c_k, d_k]$ denote its edges with $u \prec c_1 \prec \cdots \prec c_k \prec b_1$ and $b_1 \prec d_1 \prec \cdots \prec d_k \prec u$.

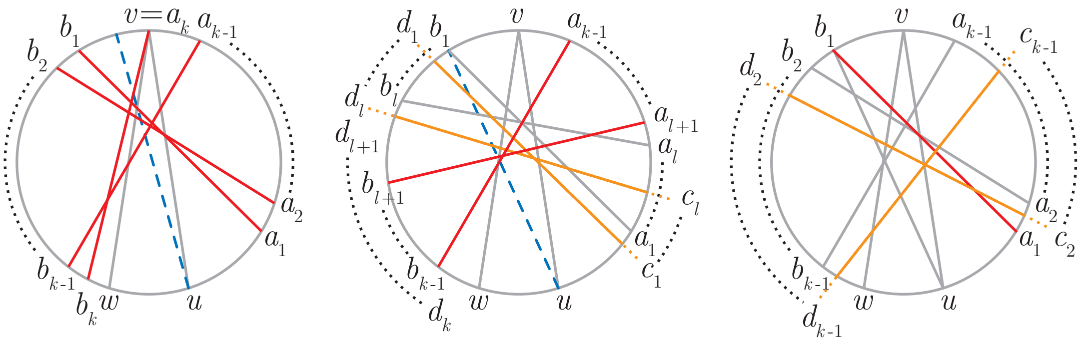

(a) (b) (c)

Figure 2.6: (a) The k-crossing E; (b) $[u, b_1] \in T$; (c) $\{e_2, \dots, e_{k-1}, [v, w]\}$ is b_1-maximal.

Note first that $v \prec d_k \preccurlyeq w$. Otherwise $d_k \in \rrbracket w, u \llbracket$ and $c_k \neq v$, because $\angle(u, v, w)$ is an angle. Thus either $c_k \in \rrbracket u, v \llbracket$ and then $F \cup \{[u, v]\}$ forms a $(k+1)$-crossing, or $c_k \in \rrbracket v, b_1 \llbracket$ and then $E \cup \{[c_k, d_k]\}$ forms a $(k+1)$-crossing. Consequently, we have $b_1 \prec d_1 \prec \cdots \prec d_{k-1} \prec w$.

Let $\ell := \max\{j \in [k-1] \mid b_i \prec d_i \prec w \text{ for any } i \text{ with } i \in [j]\}$. Then for any $i \in [\ell]$, since $\{e_1, \dots, e_i\} \cup \{f_i, \dots, f_k\}$ does not form a $(k+1)$-crossing, we have $u \prec c_i \preccurlyeq a_i$. Thus for any $i \in [\ell]$, $u \prec c_i \preccurlyeq a_i \prec v \prec b_i \prec d_i \prec w$, so that f_i is v-farther than e_i. Furthermore, we have $u \prec c_1 \prec \cdots \prec c_\ell \prec a_{\ell+1} \prec \cdots \prec a_{k-1} \prec v \prec d_1 \prec \cdots \prec d_\ell \prec b_{\ell+1} \prec \cdots \prec b_{k-1} \prec w$. Consequently, we get a $(k-1)$-crossing $\{f_1, \dots, f_\ell, e_{\ell+1}, \dots, e_{k-1}\}$ which is v-farther than $\{e_1, \dots, e_{k-1}\}$; this contradicts the definition of $\{e_1, \dots, e_{k-1}\}$. Thus we obtain that $[u, b_1] \in T$.

Suppose now that $\angle(a_1, b_1, u)$ is not an angle of T. Then there exists $a_0 \in \rrbracket u, a_1 \llbracket$ such that $[b_1, a_0] \in T$. But then the $(k-1)$-crossing $\{[a_0, b_1], e_2, \dots, e_{k-1}\}$ is v-farther than the $(k-1)$-crossing $\{e_1, \dots, e_{k-1}\}$. This implies that $\angle(a_1, b_1, u)$ is an angle of T.

Second step. See Figure 2.6(c).
Assume that there exists a $(k-1)$-crossing F intersecting $\angle(a_1, b_1, u)$ and b_1-farther than the $(k-1)$-crossing $\{e_2, \dots, e_{k-1}, [v, w]\}$. Let $f_2 := [c_2, d_2], \dots, f_k := [c_k, d_k]$ denote its edges, with $a_1 \prec c_2 \prec \cdots \prec c_k \prec b_1 \prec d_2 \prec \cdots \prec d_k \prec u$.

Note first that $b_k \preccurlyeq d_k \preccurlyeq w$. Otherwise $d_k \in \rrbracket w, u \llbracket$ and $c_k \neq v$, because $\angle(u, v, w)$ is an angle. Thus either $c_k \in \rrbracket a_1, v \llbracket$ and then $F \cup \{[u, v], e_1\}$ forms a $(k+1)$-crossing, or $c_k \in \rrbracket v, b_1 \llbracket$ and then $E \cup \{[c_k, d_k]\}$ forms a $(k+1)$-crossing. Thus, we have $b_1 \prec d_2 \prec \ldots \prec d_{k-1} \prec w$.

Furthermore, for any $2 \leq i \leq k-1$, the edge f_i is $\angle(a_1, b_1, u)$-farther than e_i, so that $a_1 \prec c_i \preccurlyeq a_i \prec b_1 \prec b_i \preccurlyeq d_i \prec u$. In particular, $a_1 \prec c_{k-1} \preccurlyeq a_{k-1} \prec v$ and we obtain that $u \prec a_1 \prec c_2 \prec \cdots \prec c_{k-1} \prec v \prec b_1 \prec d_2 \prec \cdots \prec d_{k-1} \prec w$. Consequently, the $(k-1)$-crossing $\{e_1, f_2, \dots, f_{k-1}\}$ is v-farther than $\{e_1, \dots, e_{k-1}\}$, which is a contradiction. $\square$

As an immediate corollary of Theorem 2.12, we obtain the incidence relations between the k-stars and the edges of a k-triangulation:

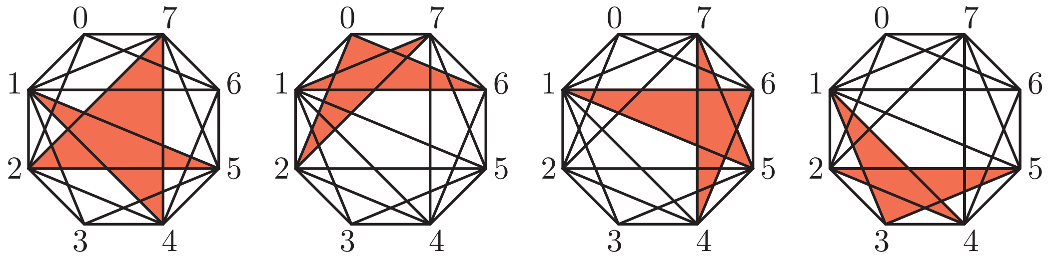

Figure 2.7: The four 2-stars in the 2-triangulation of the octagon of Figure 1.4.

Corollary 2.13. *Let e be an edge of a k-triangulation T.*

(i) If e is a k-relevant edge, then it belongs to exactly two k-stars of T (one on each side).

(ii) If e is a k-boundary edge, then it belongs to exactly one k-star of T (on its "inner" side).

(iii) If e is a k-irrelevant edge, then it does not belong to any k-star of T. □

We will see many repercussions of Corollary 2.13 throughout this chapter: in Corollary 2.21, we use it to obtain by double counting both the number of k-stars and of edges in a k-triangulation of the n-gon; in Section 2.3, it takes part in the definition of flips for k-triangulations; and in Section 2.6, we reinterpret it as a polygonal decomposition on a surface. Using tools developed in Section 3.2.3, we will also prove its reciprocal statement (see Theorem 3.19):

Theorem 2.14. *Let Σ be a set of k-stars of the n-gon such that:*

(i) any k-relevant edge of E_n is contained in zero or two k-stars of Σ, one on each side; and

(ii) any k-boundary edge of E_n is contained in exactly one k-star of Σ.

Then Σ is the set of k-stars of a k-triangulation of the n-gon. □

Example 2.15. To illustrate these results, Figure 2.7 shows the 2-stars contained in the 2-triangulation T of the octagon of Figure 1.4. Each of the twenty 2-relevant angles of T is contained in exactly one 2-star of T (Theorem 2.12) and every 2-relevant edge is contained in two 2-stars of T (Corollary 2.13).

To conclude, let us insist on the fact that the results of this section interpret k-triangulations as *complexes of k-stars*: a k-triangulation is just a way to glue together k-stars along k-relevant edges. This motivates the title of [PS09].

2.2.2 Common bisectors and the number of stars

We now want to obtain both the numbers of k-stars and of edges of a k-triangulation of the n-gon. As in the case of triangulations (see the "Double counting" paragraph in Section 1.1), this requires two relations between k-stars and edges: one is given by Theorem 2.12 and we derive the other one from the study of common bisectors of k-stars.

Definition 2.16. *A* bisector *of an angle $\angle(u, v, w)$ is an edge $[v, t]$ where $w \prec t \prec u$. A* bisector *of a k-star is a bisector of one of its angles.*

Observe that the bisectors of a k-star are exactly the edges of E_n that pass through one of its vertices and split the other ones into two sets of size k.

The following theorem will be used extensively in our study of multitriangulations, in particular for our local definition of flips in Section 2.3.

Theorem 2.17. *Every pair of k-stars whose union is $(k+1)$-crossing-free have a unique common bisector.*

Using notions developed in Section 3.2, we will obtain a very short proof of the existence of a common bisector. However, we propose here an alternative proof using only our current tools. We need the following two lemmas, in which E denotes a $(k+1)$-crossing-free subset of edges of E_n, and S denotes a k-star of E.

Lemma 2.18. *The numbers of vertices of S on each side of an edge e of E are different.*

Proof. Suppose that S has the same number of vertices on both sides of an edge e. Since the number of vertices of S is $2k+1$, one of the two vertices of e is a vertex of S, and e is a bisector of S. Lemma 2.11 then ensures that e is not in E. □

Let V be the set of vertices of the k-star S. If $|[\![u,v]\!] \cap V| < |[\![v,u]\!] \cap V|$, then we say that S lies on the *positive side* of the edge $[u,v]$ oriented from u to v (otherwise we say that S lies on the *negative side* of the edge $[u,v]$ oriented from u to v). The k-star S is said to be *contained in an angle* $\angle(u,v,w)$ if it lies on the positive side of both the edges $[u,v]$ and $[v,w]$ oriented from u to v and from v to w respectively.

Lemma 2.19. *Let $\angle(u,v,w)$ be an angle of E containing the k-star S. Then:*

(i) either v is a vertex of S and $\angle(u,v,w)$ is an angle of S;

(ii) or v is not a vertex of S and $\angle(u,v,w)$ has a common bisector with an angle of S.

Proof. Suppose first that v is a vertex of S. Let $\angle(x,v,y)$ denote the angle of S at vertex v. Since $\angle(u,v,w)$ contains S, we have $w \preccurlyeq y \prec x \preccurlyeq u$. But since $\angle(u,v,w)$ is an angle of E, we have $x = u$ and $y = w$, so that $\angle(u,v,w)$ is an angle of S.

Suppose now that v is not a vertex of S. Then, by Lemma 2.10(iii) there exists a unique angle $\angle(x,y,z)$ of S containing v. If $y \in]\!]u,v[\![$, then $]\!]u,v[\![$ contains all the $k+1$ vertices of S between y and z, which is not possible (because S lies on the positive side of the edge $[u,v]$, oriented from u to v). For the same reason, $y \notin]\!]v,w[\![$. If $y = u$ or $y = w$, then $[u,v]$ or $[v,w]$ is a bisector of $\angle(x,y,z)$, which contradicts Lemma 2.11. Consequently, $\angle(u,v,w)$ contains y, so that $[v,y]$ is a common bisector of $\angle(u,v,w)$ and $\angle(x,y,z)$. □

Proof of Theorem 2.17. Let R and S be two k-stars whose union is $(k+1)$-crossing-free.

Let $\{r_j \mid j \in \mathbb{Z}_{2k+1}\}$ denote the vertices of R in star order. Note that for any $j \in \mathbb{Z}_{2k+1}$, if S lies on the negative side of the edge $[r_{j-1}, r_j]$ oriented from r_{j-1} to r_j, then it lies on the positive side of the edge $[r_j, r_{j+1}]$ oriented from r_j to r_{j+1}. Since $2k+1$ is odd, this implies that there exists $j \in \mathbb{Z}_{2k+1}$ such that S lies on the positive side of both the edges $[r_{j-1}, r_j]$ and $[r_j, r_{j+1}]$

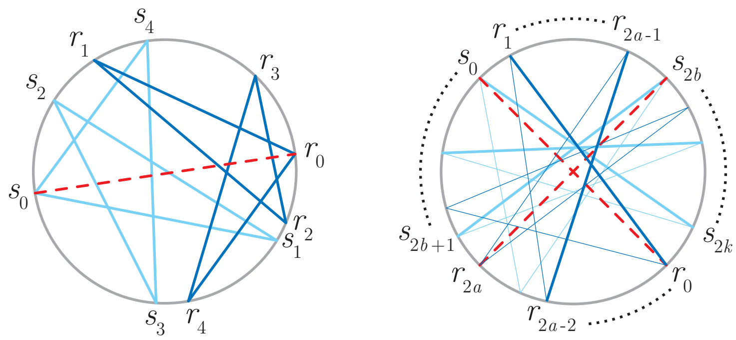

Figure 2.8: The unique common bisector of a 3-crossing-free pair of 2-stars (left) and a $(k+1)$-crossing in a pair of k-stars with two common bisectors (right).

oriented from r_{j-1} to r_j and from r_j to r_{j+1}, respectively. That is, in the angle $\angle(r_{j-1}, r_j, r_{j+1})$. The previous lemma thus ensures the existence of a common bisector.

Suppose now that the two k-stars R and S have two different common bisectors e and f, and let $\{r_j \mid j \in \mathbb{Z}_{2k+1}\}$ and $\{s_j \mid j \in \mathbb{Z}_{2k+1}\}$ denote the vertices of R and S in star order and labeled such that $e = [r_0, s_0]$. Let $\alpha, \beta \in \mathbb{Z}_{2k+1}$ be such that $f = [r_\alpha, s_\beta]$. Note that certainly, $\alpha \neq 0$, $\beta \neq 0$, and α and β have the same parity. By symmetry, we can assume that $\alpha = 2a$, $\beta = 2b$ with $1 \leq b \leq a \leq k$. But then the set

$$\{[r_{2i}, r_{2i+1}] \mid 0 \leq i \leq a-1\} \cup \{[s_{2j}, s_{2j+1}] \mid b \leq j \leq k\}$$

forms a $(k+1+a-b)$-crossing, and $k+1+a-b \geq k+1$. This proves uniqueness. □

Proposition 2.20. *Let T be a k-triangulation.*

(i) For any k-star S in T and for any vertex r not in S there is a unique k-star R in T such that r is a vertex of the common bisector of R and S.

(ii) Any k-relevant edge not in T is the common bisector of a unique pair of k-stars of T.

Proof. Let $\angle(u, s, v)$ be the unique angle of S which contains r (Lemma 2.10(iii)). Let $\angle(x, r, y)$ be the unique angle of T of vertex r which contains s. According to Theorem 2.12, the angle $\angle(x, r, y)$ belongs to a unique k-star R. The common bisector of R and S is $[r, s]$ and R is the only such k-star of T.

Let $e := [r, s]$ be a k-relevant edge, not in T. Let $\angle(x, r, y)$ (resp. $\angle(u, s, v)$) denote the unique angle of T of vertex r (resp. s) which contains s (resp. r). According to Theorem 2.12, the angle $\angle(x, r, y)$ (resp. $\angle(u, s, v)$) belongs to a unique k-star R (resp. S) of T. The common bisector of R and S is $[r, s]$ and (R, S) is the only such couple of k-stars of T. □

Observe that Parts (i) and (ii) of this proposition give bijections between:

(i) "vertices not used in the k-star S of T" and "k-stars of T different from S";

(ii) "k-relevant edges not used in T" and "pairs of k-stars of T".

From any of these two bijections, and using Corollary 2.13 for double counting, it is easy to derive the number of k-stars and of edges in T:

Corollary 2.21. *(i) Any k-triangulation of the n-gon contains $n-2k$ k-stars, $k(n-2k-1)$ k-relevant edges and $k(2n-2k-1)$ edges.*
(ii) k-triangulations are exactly $(k+1)$-crossing-free subsets of $k(2n-2k-1)$ edges of E_n.

Proof. Let T be a k-triangulation of the n-gon. Let σ denote the number of k-stars of T and ρ denote its number of k-relevant edges. Corollary 2.13 (or equivalently Theorem 2.12) ensures that $(2k+1)\sigma = 2\rho + n$ and Proposition 2.20(ii) affirms that $nk + \rho = \binom{n}{2} - \binom{\sigma}{2}$. Thus σ satisfies $\sigma^2 + 2k\sigma - n(n-2k) = 0$, which has $\sigma = n-2k$ as unique (positive) solution. Hence, $\rho = k(n-2k-1)$. Finally, the total number of edges of T is $nk + \rho = k(2n-2k-1)$. □

2.3 FLIPS

In this section, we introduce flips for multitriangulations: we transform a k-triangulation into another one by just exchanging one k-relevant edge. Even if this transformation was already known and used in [Nak00, DKM02, Jon03], we provide a new definition based on k-stars, which involves only a substructure of the k-triangulation during the transformation. In the second part of this section, we study the graph of flips and discuss upper and lower bounds on its diameter.

2.3.1 Mutual position of two k-stars and the local definition of flips

To start this section, we consider two k-stars R and S of a $(k+1)$-crossing-free subset E of E_n and we study their mutual position.

Lemma 2.22. *R and S cannot share any angle.*

Proof. By Lemma 2.11, the knowledge of one angle $\angle(s_{j-1}, s_j, s_{j+1})$ of S enables us to recover all the k-star S: the vertex s_{j+2} is the unique vertex such that $\angle(s_j, s_{j+1}, s_{j+2})$ is an angle of E (*i.e.* the first neighbour of s_{j+1} after s_j when moving clockwise), and so on. □

Corollary 2.23. *R and S cannot share more than k edges.* □

Observe that, for example, the two k-stars of any k-triangulation of a $(2k+2)$-gon share exactly k edges (see Figure 2.2).

By Theorem 2.17, we know that R and S have a unique common bisector e. In the following lemmas, we are interested in the position of their vertices relatively to this bisector. We denote by $\{r_j \mid j \in \mathbb{Z}_{2k+1}\}$ and $\{s_j \mid j \in \mathbb{Z}_{2k+1}\}$ the vertices of R and S, in star order, and such that the edge $e := [r_0, s_0]$ is the common bisector of R and S.

Lemma 2.24. *For every $i \in [k]$, we have $r_{2i-1} \in \rrbracket r_0, s_{2i} \rrbracket$ and $s_{2i-1} \in \rrbracket s_0, r_{2i} \rrbracket$. In particular, for every $i \in \mathbb{Z}_{2k+1}$ the edges $[r_i, r_{i+1}]$ and $[s_i, s_{i+1}]$ do not cross.*

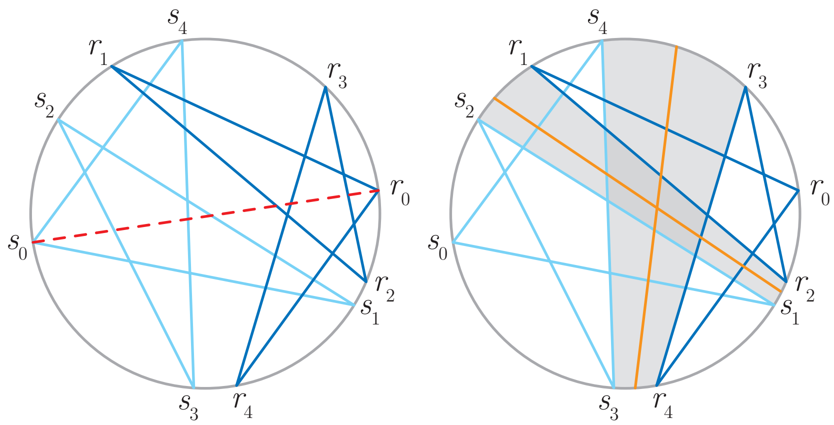

Figure 2.9: The common bisector of two 2-stars (left) and a 2-crossing that crosses it (right).

Proof. Suppose that there exists $i \in [k]$ such that $r_{2i-1} \in \rrbracket s_{2i}, s_0 \llbracket$ or $s_{2i-1} \in \rrbracket r_{2i}, r_0 \llbracket$. Let γ be the highest such integer, and assume for example that $r_{2\gamma-1} \in \rrbracket s_{2\gamma}, s_0 \llbracket$. Then the definition of γ ensures that $s_0 \prec s_{2\gamma+1} \preccurlyeq r_{2\gamma+2} \prec r_{2\gamma-2} \prec r_0 \prec s_{2k} \prec s_{2\gamma} \prec r_{2\gamma-1} \prec r_1 \prec s_0$ so that the set

$$\{[r_{2i}, r_{2i+1}] \,|\, 0 \leq i \leq \gamma - 1\} \cup \{[s_{2j}, s_{2j+1}] \,|\, \gamma \leq j \leq k\}$$

forms a $(k+1)$-crossing. $\square$

The previous lemma can be read as saying that corresponding edges of R and S are parallel. In fact, k of these $2k+1$ pairs of parallel edges, the ones of the form $([r_{2i-1}, r_{2i}], [s_{2i-1}, s_{2i}])$, with $i \in [k]$, separate R from S, meaning that R and S lie on opposite sides of both. The next lemma says that any k-crossing that, in turn, crosses the common bisector $e = [r_0, s_0]$, has one edge parallel to and between each such pair (see Figure 2.9).

Lemma 2.25. *Let F be a k-crossing of E such that all its edges cross $e = [r_0, s_0]$. Denote by $f_1 := [x_1, y_1], \dots, f_k := [x_k, y_k]$ the edges of F, such that $r_0 \prec x_1 \prec \cdots \prec x_k \prec s_0 \prec y_1 \prec \cdots \prec y_k \prec r_0$. Then $x_i \in \llbracket r_{2k-2i+1}, s_{2k-2i+2} \rrbracket$ and $y_i \in \llbracket s_{2k-2i+1}, r_{2k-2i+2} \rrbracket$, for any $i \in [k]$.*

Proof. Suppose that there exists $i \in [k]$ such that $r_0 \prec x_i \prec r_{2k-2i+1}$ and let

$$\ell := \max \{i \in [k] \,|\, r_0 \prec x_i \prec r_{2k-2i+1}\}.$$

If $\ell = k$, then the set $\{f_1, \dots, f_k, [r_0, r_1]\}$ is a $(k+1)$-crossing of E, thus we assume that $\ell < k$. In order for the set

$$\{f_1, \dots, f_\ell\} \cup \{[r_0, r_1], \dots, [r_{2k-2\ell}, r_{2k-2\ell+1}]\}$$

not to be a $(k+1)$-crossing, we have $r_{2k-2\ell} \preccurlyeq y_\ell \prec r_0$, so that $r_{2k-2\ell} \prec y_{\ell+1} \prec r_0$. But the definition of ℓ implies that $r_{2k-2\ell+1} \prec r_{2k-2\ell-1} \preccurlyeq x_{\ell+1} \prec s_0$, so that the set

$$\{[r_{2k-2\ell}, r_{2k-2\ell+1}], \dots, [r_{2k-2}, r_{2k-1}], [r_{2k}, r_0]\} \cup \{f_{\ell+1}, \dots, f_k\}$$

is a $(k+1)$-crossing of E. By symmetry, the lemma is proved. $\square$

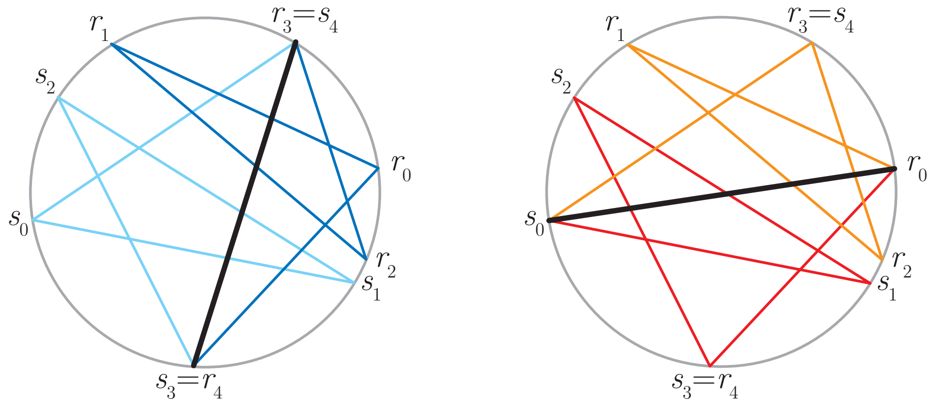

Figure 2.10: The flip of an edge.

In the following lemma, the symbol $\triangle$ denotes the symmetric difference between two sets: $X\triangle Y := (X \smallsetminus Y) \cup (Y \smallsetminus X)$. We refer to Figure 2.10 for an illustration of this lemma.

Lemma 2.26. *Let f be a common edge of R and S. Then:*

(i) there exists $i \in [k]$ such that $f = [r_{2i-1}, r_{2i}] = [s_{2i}, s_{2i-1}]$;

(ii) $E\triangle\{e, f\}$ is a $(k+1)$-crossing-free subset of E_n;

(iii) the vertices $s_0, \dots, s_{2i-2}, s_{2i-1} = r_{2i}, r_{2i+1}, \dots, r_{2k}, r_0$ (resp. $r_0, \dots, r_{2i-2}, r_{2i-1} = s_{2i}$, $s_{2i+1}, \dots, s_{2k}, s_0$) are the vertices of a k-star X (resp. Y) of $E\triangle\{e, f\}$, in star order;

(iv) X and Y share the edge e and their common bisector is f.

Proof. Let u and v denote the vertices of f. Lemma 2.24 ensures that $\{r_0, s_0\} \cap \{u, v\} = \emptyset$ so that we can assume $r_0 \prec u \prec s_0 \prec v \prec r_0$. Consequently, there exists $i, j \in [k]$ such that $u = r_{2i-1} = s_{2j}$ and $v = r_{2i} = s_{2j-1}$. Suppose that $i > j$. Then according to Lemma 2.24, we have $r_0 \prec r_{2i-1} \preccurlyeq s_{2i} \prec s_{2j} = r_{2i-1}$ which is impossible. By symmetry, we obtain that $i = j$ and $f = [r_{2i-1}, r_{2i}] = [s_{2i}, s_{2i-1}]$.

Lemma 2.25 then proves that any k-crossing of E that prevents e being in E contains f, so that $E\triangle\{e, f\}$ is $(k+1)$-crossing-free.

Let L be the list of vertices $(s_0, \dots, s_{2i-2}, r_{2i}, \dots, r_{2k}, r_0)$. Between two consecutive elements of L lie exactly $k-1$ others points of L (for the circle order). This implies that L is in star order. Part (iii) thus follows from the fact that any edge connecting two consecutive points of L is in $E\triangle\{e, f\}$.

Finally, the edge e is clearly common to X and Y. The edge f is a bisector of both angles $\angle(r_{2i-2}, r_{2i-1}, s_{2i+1})$ and $\angle(s_{2i-2}, s_{2i-1}, r_{2i+1})$, so that it is the common bisector of X and Y. $\square$

This lemma is at the heart of the concept of flips between k-triangulations. Assume that T is a k-triangulation of the n-gon, and let f be a k-relevant edge of T. Let R and S be the two k-stars of T containing f (Corollary 2.13), and let e be the common bisector of R and S (Theorem 2.17). Lemma 2.26 affirms that $T\triangle\{e, f\}$ is a $(k+1)$-crossing-free subset of E_n. Observe moreover that $T \triangle \{e, f\}$ is maximal: this follows from Corollary 2.21, but also from the fact that if $T \triangle \{e, f\}$ is properly contained in a k-triangulation $\widetilde{T}$, then $\widetilde{T} \triangle \{e, f\}$ is $(k+1)$-crossing-free and properly contains T. Thus, $T \triangle \{e, f\}$ is a k-triangulation of the n-gon.

Lemma 2.27. *T and $T \triangle \{e, f\}$ are the only k-triangulations of the n-gon containing $T \smallsetminus \{f\}$.*

Proof. Let e' be any edge of $E_n \smallsetminus T$ distinct from e. Let R' and S' be the two k-stars with common bisector e' (Proposition 2.20(ii)). Either R' or S' (or both) does not contain f, say R'. Then $R' \cup \{e'\}$ is contained in $T \triangle \{e', f\}$ and forms a $(k+1)$-crossing. □

We say that we obtain the k-triangulation $T \triangle \{e, f\}$ from the k-triangulation T by *flipping* the edge f. We insist on the definition using the common bisector of R and S (see Figure 2.10):

Definition 2.28. *The* flip *of a k-relevant edge f in a k-triangulation T of the n-gon is the transformation which replaces the edge f by the common bisector of the two k-stars of T containing f.*

Observe that Lemma 2.27 could be an alternative definition of flips (and it is the definition in all previous works involving flips in multitriangulations; see [Nak00, DKM02, Jon03, Jon05]). However, our definition is interesting theoretically as well as practically because it is a local definition: it only involves a subconfiguration formed by two adjacent k-stars. Given a k-relevant edge f of a k-triangulation T, we need a constant time to flip f in T:

(i) first, we compute the two k-stars of T containing f rotating around their angles (remember the proof of Lemma 2.22);

(ii) then we compute the common bisector of these two k-stars and substitute it to f.

Observe the difference with the method consisting in testing, among all edges not in T, which edge could be added to $T \smallsetminus \{f\}$ without creating a $(k+1)$-crossing.

2.3.2 The graph of flips

Let $G_{n,k}$ be the *graph of flips* on the set of k-triangulations of the n-gon, *i.e.* the graph whose vertices are the k-triangulations of the n-gon and whose edges are the pairs of k-triangulations related by a flip. It follows from Corollary 2.21 and Lemma 2.27 that $G_{n,k}$ is regular of degree $k(n-2k-1)$: every k-relevant edge of a k-triangulation can be flipped, in a unique way. In this section, we prove the connectedness of this graph and bound its diameter $\delta_{n,k}$.

Let T be a k-triangulation of the n-gon, f be a k-relevant edge of T and e be the common bisector of the two k-stars of T containing f. Then the edges e and f necessarily cross. In particular, if $e := [\alpha, \beta]$ and $f := [\gamma, \delta]$, with $0 \preccurlyeq \alpha \prec \beta \preccurlyeq n-1$ and $0 \preccurlyeq \gamma \prec \delta \preccurlyeq n-1$, then

(i) either $0 \preccurlyeq \alpha \prec \gamma \prec \beta \prec \delta \preccurlyeq n-1$ and the flip is said to be *slope-decreasing*,

(ii) or $0 \preccurlyeq \gamma \prec \alpha \prec \delta \prec \beta \preccurlyeq n-1$ and the flip is said to be *slope-increasing*.

We define a partial order on the set of k-triangulations of the n-gon as follows: for two k-triangulations T and T', we write $T < T'$ if and only if there exists a sequence of slope-increasing flips from T to T'. That this is indeed a partial order follows from the fact that each slope increasing flip increases the *total slope* of a k-triangulation, where the slope of an edge $[u, v]$ is defined as $u + v$ (with the sum taken in $\mathbb{N}$, not in $\mathbb{Z}_n$) and the total slope of a k-triangulation is the sum

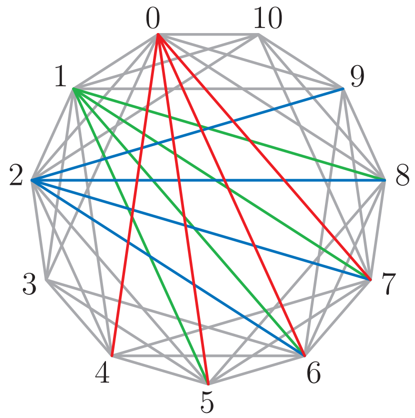

Figure 2.11: The minimal triangulation $T^{\min}_{11,3}$.

of slopes of its edges. The following k-triangulation of the n-gon (see Figure 2.11) is a minimal element for this order, and we will see that it is even the least element.

Lemma 2.29. *The set* $F := \{[i,j] \mid i \in [\![0,k-1]\!] \text{ and } j \in [\![i+k+1, i-k-1]\!]\}$ *is the set of* k*-relevant edges of a* k*-triangulation* $T^{\min}_{n,k}$ *of the* n*-gon which is minimal for the partial order* $<$.

Proof. Since F is the union of k disjoint crossing-free fans $\{[i,j] \mid j \in [\![i+k+1, i-k-1]\!]\}$, it is $(k+1)$-crossing-free and has $k(n-2k-1)$ edges. Thus, it is the set of k-relevant edges of a k-triangulation by Corollary 2.21. Furthermore, since the slope of any k-relevant edge e not in F is larger than the slope of any edge in F crossing e, any flip of $T^{\min}_{n,k}$ is increasing, and $T^{\min}_{n,k}$ is minimal. □

Lemma 2.30. *For any* k*-triangulation of the* n*-gon* T *different from* $T^{\min}_{n,k}$*, there exists a* k*-relevant edge* $f \in T \smallsetminus T^{\min}_{n,k}$ *such that the edge added by the flip of* f *is in* $T^{\min}_{n,k}$.

Proof. Let T be a k-triangulation of the n-gon distinct from $T^{min}_{n,k}$. Let

$$\ell := \max\{k+1 \le i \le n-k-1 \mid \{[0,i],[1,i+1],\dots,[k-1,i+k-1]\} \not\subseteq T\},$$

which exists because $T \ne T^{min}_{n,k}$.

Let $0 \le j \le k-1$ such that the edge $[j, \ell+j]$ is not in T. Let $\{[x_1,y_1],\dots,[x_k,y_k]\}$ denote a k-crossing which prevents $[j,\ell+j]$ to be in T, with the convention that:

(i) $x_1 \prec \ldots \prec x_k \prec y_1 \prec \ldots \prec y_k$;

(ii) if $j > 0$, then $j \in \,]\!]x_j, x_{j+1}[\![$ and $\ell+j \in \,]\!]y_j, y_{j+1}[\![$; and

(iii) if $j = 0$, then $0 \in \,]\!]y_k, x_1[\![$ and $\ell \in \,]\!]x_k, y_1[\![$.

With this convention, we are sure that $x_k \in [\![k, \ell-1]\!]$ and $y_k \in [\![\ell+k, n-1]\!]$. If $y_k \in \,]\!]\ell+k, n-1]\!]$, then the set $\{[0,\ell+1],\dots,[k-1,\ell+k],[x_k,y_k]\}$ is a $(k+1)$-crossing of T. Thus $y_k = \ell+k$, and there exists an edge $[x_k, \ell+k]$ with $x_k \in [\![k, \ell-1]\!]$.

Now let $m := \min\{k \leq i \leq \ell - 1 \mid [i, \ell + k] \in T\}$. Let f be the edge $[m, \ell + k]$, let S be the k-star containing the angle $\angle(m, \ell + k, k - 1)$ and let R be the other k-star containing f. Let $s_0, \dots, s_{k-2}, s_{k-1} = k - 1, s_k = m, s_{k+1}, \dots, s_{2k-1}, s_{2k} = \ell + k$ denote the vertices of the k-star S in circle order. Then $s_0 \in [\![\ell + k + 1, 0]\!]$, and the only way not to get a $(k+1)$-crossing is to have $s_0 = 0$. This implies that $s_j = j$ for all $0 \leq j \leq k - 1$.

Let e denote the common bisector of R and S and let s denote its vertex in S. Since $f = [m, \ell + k] = [s_k, s_{2k}]$ is a common edge of R and S, it is sure that $s \notin \{s_k, s_{2k}\}$. Moreover, since for any $0 \leq j \leq k - 2$ the interval $]\!]s_j, s_{j+1}[\![$ is empty, $s \notin \{s_{k+1}, s_{k+2}, \dots, s_{2k-1}\}$. Consequently, $s \in \{s_0, \dots, s_{k-1}\} = [\![0, k - 1]\!]$ and $e \in T^{\min}_{n,k} \smallsetminus T$. □

Corollary 2.31. *(i) The k-triangulation $T^{\min}_{n,k}$ is the unique least element of the set of k-triangulations of the n-gon, partially ordered by $<$.*

(ii) Any k-triangulation T of the n-gon can be transformed into the minimal k-triangulation $T^{\min}_{n,k}$ by a sequence of $|T \smallsetminus T^{\min}_{n,k}|$ flips.

(iii) The graph $G_{n,k}$ is connected, regular of degree $k(n - 2k - 1)$, and its diameter $\delta_{n,k}$ is at most $2k(n - 2k - 1)$.

Proof. Parts (i) and (ii) are immediate corollaries of the previous lemma: there is a sequence of $|T \smallsetminus T^{\min}_{n,k}|$ slope-decreasing flips from T to $T^{\min}_{n,k}$. As far as Part (iii) is concerned, the regularity follows from the fact that any of the $k(n - 2k - 1)$ k-relevant edges of T can be flipped. Finally, the connectedness as well as the bound on the diameter are obtained by joining any two k-triangulations T and T' of the n-gon by a path of flips passing through $T^{\min}_{n,k}$. □

Example 2.32. Figure 2.12 shows a path of slope-decreasing flips from the 2-triangulation of Figure 1.4 to $T^{\min}_{8,2}$.

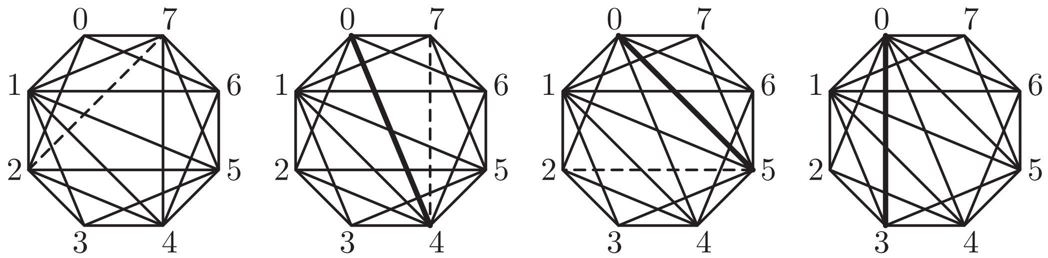

Figure 2.12: A path of slope-decreasing flips from the 2-triangulation of Figure 1.4 to $T^{\min}_{8,2}$. In each of the four pictures, the new edge is in bold and the dashed edge will be flipped.

Remark 2.33. We want to observe that Corollary 2.31(iii) is the way how [Nak00] and [DKM02] proved that the number of edges in all k-triangulations of the n-gon is the same: indeed, any two k-triangulations are related by a sequence of flips which preserves the number of edges. Compare it to our direct proof in Corollary 2.21.

Obviously, we would get symmetric results with the maximal k-triangulation $T_{n,k}^{\max}$ whose set of k-relevant edges is $\{[i,j] \mid i \in [\![n-k, n-1]\!] \text{ and } j \in [\![i+k+1, i-k-1]\!]\}$. Observe also that we would obtain the same results with any rotation of the labeling of V_n. Following [Nak00], this leads to the following improved bound for the diameter of the graph of flips:

Corollary 2.34. *When $n > 4k^2(2k+1)$, the diameter $\delta_{n,k}$ of $G_{n,k}$ is at most $2k(n-4k-1)$.*

Proof. Let ρ be the rotation $t \mapsto t+1$. For any $i \in \mathbb{Z}_n$, denote by T_i the k-triangulation $\rho^i(T_{n,k}^{\min})$. Using the same argument as before, any two k-triangulations T and T' of the n-gon are linked by a sequence of at most $|T \smallsetminus T_i| + |T' \smallsetminus T_i|$ flips, for any $i \in \mathbb{Z}_n$. In particular, there exists a path linking T and T' of length smaller than the average over i of $|T \smallsetminus T_i| + |T' \smallsetminus T_i|$. Thus, if $\deg_k(i,T)$ denotes the number of k-relevant edges of T adjacent to the vertex i, then the diameter of $G_{n,k}$ is bounded by

$$\begin{aligned}\delta_{n,k} &\le \frac{1}{n}\sum_{i\in\mathbb{Z}_n}\big(|T \smallsetminus T_i| + |T' \smallsetminus T_i|\big) = 2k(n-2k-1) - \frac{2}{n}\sum_{i\in\mathbb{Z}_n}\sum_{j\in[k]}\deg_k(i+j,T) \\ &= 2k(n-2k-1) - \frac{4k^2(n-2k-1)}{n} = 2k(n-4k-1) + \frac{4k^2(2k+1)}{n}.\end{aligned}$$

Thus, if $n > 4k^2(2k+1)$, we obtain that $\delta_{n,k} \le 2k(n-4k-1)$. □

The following related result uses the same argument based on the average degree of the k-triangulations of the n-gon:

Lemma 2.35. *The diameter $\delta_{n,k}$ of the graph of flips satisfies $\delta_{n+1,k} \le \delta_{n,k} + 4k - 1$.*

Proof. Let T and T' be two k-triangulations of the $(n+1)$-gon, and i be a distinguished vertex of V_{n+1}. Let T_i and T'_i denote the k-triangulations of the $(n+1)$-gon obtained from T and T' respectively by flipping all the k-relevant edges adjacent to the vertex i. Let τ and τ' denote the graphs obtained by forgetting from T_i and T'_i respectively the vertex i as well as the $2k$ edges adjacent to it. Observe that Corollary 2.21 implies that τ and τ' are k-triangulations of the n-gon. Consequently, there exists a path $\tau = \tau_0, \tau_1, \dots, \tau_p = \tau'$ of at most $\delta_{n,k}$ flips which transform τ into τ'. Remembering the vertex i and the $2k$ edges adjacent to it, this translates into a path of at most $\delta_{n,k}$ flips joining T_i to T'_i. We deduce from this that there exists a path in $G_{n+1,k}$ from T to T' with at most $\deg_k(i,T) + \delta_{n,k} + \deg_k(i,T')$ flips (where $\deg_k(i,T)$ denotes the number of k-relevant edges of T adjacent to the vertex i). Since the same argument works for any choice of the vertex $i \in \mathbb{Z}_{n+1}$, we can again use the average degree argument: the diameter of $G_{n+1,k}$ is bounded by

$$\begin{aligned}\delta_{n+1,k} &\le \frac{1}{n+1}\sum_{i\in\mathbb{Z}_{n+1}}\left(\deg_k(i,T) + \delta_{n,k} + \deg_k(i,T')\right) = \delta_{n,k} + \frac{2}{n+1}\sum_{i\in\mathbb{Z}_{n+1}}\deg_k(i,T) \\ &= \delta_{n,k} + \frac{4k(n+1-2k-1)}{n+1} = \delta_{n,k} + 4k - \frac{4k(2k-1)}{n+1}.\end{aligned}$$

We finally obtain the result since $\delta_{n+1,k}$ is an integer. □

Note that even if the improvement provided by Corollary 2.34 is asymptotically not relevant, for the case $k = 1$, the improved bound of $2n - 10$ is actually the exact diameter of the associahedron for large values of n [STT88]. The proof in [STT88] is based on the interpretation of a sequence of flips relating two triangulations T and T' of the n-gon as a triangulation of a 3-dimensional simplicial polytope whose boundary is made glueing T and T' along their boundary edges. Finding such a polytope with no small triangulation is achieved using 3-dimensional hyperbolic polytopes of large volume: indeed, since the volume of an hyperbolic tetrahedron is bounded by a constant, hyperbolic polytopes with large volume only admit triangulations with many tetrahedra.

When $k \neq 1$, the exact asymptotic value of the diameter $\delta_{n,k}$ is unknown. As far as lower bounds are concerned, the following simple argument shows a lower bound of order kn:

Lemma 2.36. *If $n \geq 4k$, then the diameter $\delta_{n,k}$ of $G_{n,k}$ is at least $k(n - 2k - 1)$.*

Proof. The proof consists in displaying two k-triangulations with no k-relevant edges in common. We call *k-zigzag* the following subset of k-relevant edges of E_n (see Figure 2.13):

$$Z := \left\{ [q-1, -q-k] \,\middle|\, 1 \leq q \leq \left\lfloor \frac{n-2k}{2} \right\rfloor \right\} \cup \left\{ [q, -q-k] \,\middle|\, 1 \leq q \leq \left\lfloor \frac{n-2k-1}{2} \right\rfloor \right\}.$$

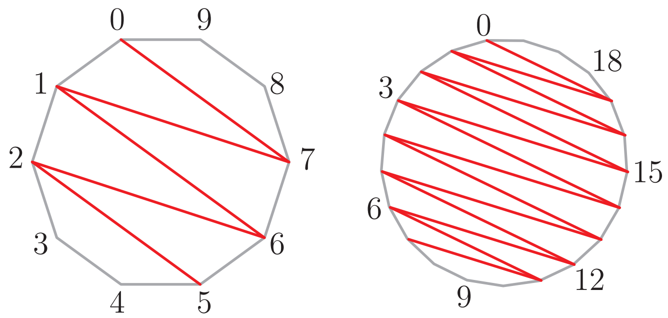

Figure 2.13: Examples of k-zigzags of E_n for $(n, k) = (10, 2)$ and $(21, 3)$.

Let ρ be the rotation $t \mapsto t + 1$. Observe that the $2k$ k-zigzags $Z, \rho(Z), \dots, \rho^{2k-1}(Z)$ are disjoint since $n \geq 4k$. Moreover,

(i) there is no 2-crossing in a zigzag, thus there is no $(k+1)$-crossing in the union of k of them;

(ii) a k-zigzag contains $n - 2k - 1$ k-relevant edges, so that the union of k disjoint k-zigzags contains $k(n - 2k - 1)$ k-relevant edges.

According to Corollary 2.21, this proves that the union of k disjoint k-zigzags is the set of k-relevant edges of a k-triangulation. Thus, we obtain the two k-triangulations we were looking for with the sets of k-relevant edges $\bigcup_{i=0}^{k-1} \rho^i(Z)$ and $\bigcup_{i=k}^{2k-1} \rho^i(Z)$. □

Another way to obtain Lemma 2.36 would be to prove the following conjecture:

Conjecture 2.37. *The diameter $\delta_{n,k}$ of the graph of flips $G_{n,k}$ satisfies $\delta_{n+1,k} \geq \delta_{n,k} + k$.*

This conjecture is easy to prove when $k = 1$ (see [dLRS10, Chapter 1]). The proof uses an operation on triangulations generalized to k-triangulations in Section 2.5, where we will discuss the reason why the natural generalization of this proof fails (see Remark 2.59). Embarrassingly, we even have no proof that the diameter $\delta_{n,k}$ of the graph of flips $G_{n,k}$ is an increasing function of n when k is fixed. This is closely related to the following conjecture (which is known to be true for triangulations [STT88, Lemma 3]):

Conjecture 2.38. *(i) The shortest path in the flip graph $G_{n,k}$ between two k-triangulations T and T' of the n-gon never flips a common edge of T and T'.*

(ii) Let T and T' be two k-triangulations of the n-gon, f be a k-relevant edge of T and e be the unique bisector of the two k-stars of T containing f. If e is an edge of T', then there exists a shortest path in the graph of flips $G_{n,k}$ from T to T' which first flips f.

The lower bound of Lemma 2.36 can be slightly improved by a more careful choice of two disjoint k-triangulations. Our best lower bound is the following:

Lemma 2.39. *If $m \geq 2k+1$, then both $\delta_{2m,k}$ and $\delta_{2m+1,k}$ are at least $2m\left(k+\frac{1}{2}\right) - k(2k+3)$.*

Proof. We first prove the result for the $(2m)$-gon. Choose an arbitrary k-triangulation τ of the m-gon, and define the following three subsets of E_{2m}:

$$\begin{aligned} A &:= \{[2i+1, 2i+1+j] \mid i \in \mathbb{Z}_m \text{ and } j \in [k]\}, \\ B &:= \{[2i, 2(i+j)-1] \mid i \in \mathbb{Z}_m \text{ and } j \in [k]\}, \quad \text{and} \\ C &:= \{[2i, 2j] \mid i, j \in \mathbb{Z}_m,\ [i,j] \text{ edge of } \tau\}. \end{aligned}$$

We consider the union $T := A \cup B \cup C$ of these three subsets of E_{2m} and we denote by $T' := \rho(T)$ its image under the rotation $\rho : t \mapsto t+1$ of the $(2m)$-gon. In a first step, we prove that T (and thus, T' as well) is a k-triangulation of the $(2m)$-gon, and in a second step, we prove that the number of flips needed to join T to T' is at least $2m\left(k+\frac{1}{2}\right) - k(2k+3)$.

To visualize an example, Figure 2.14 shows the two 2-triangulations T and T' of the 16-gon obtained from the 2-triangulation τ of the 8-gon represented in Figure 1.4.

First step. We prove first that the union $T = A \cup B \cup C$ is disjoint and $(k+1)$-crossing-free. Since $|A| + |B| + |C| = mk + mk + k(2m-2k-1) = k(4m-2k-1)$, Corollary 2.21 then ensures that T is a k-triangulation of the $(2m)$-gon.

To see that A, B and C are disjoint, orient all their edges in such a way that each edge has less vertices of V_{2m} on its right than on its left. With this orientation an edge $[2i+1, 2i+1+j] \in A$ has an odd tail, an edge $[2i, 2(i+j)-1] \in B$ has an even tail and on odd head, while both tail and head of any edge $[2i, 2j] \in C$ are even. This separates the three sets A, B and C.

Assume now that T contains a $(k+1)$-crossing F. Since the edges of A are k-irrelevant, F is included in $B \sqcup C$. We derive from F a subset F' of C as follows:

(i) we replace each edge $[2i, 2j+1] \in F \cap B$ by the edge $[2i, 2j+2] \in C$;
(ii) we replace each edge $[2i, 2j] \in F \cap C$, with $|i-j| < k$, by the edge $[2i, 2j+2]$; and
(iii) we keep all other edges of F (that is, the edges $[2i, 2j] \in F \cap C$ with $|i-j| \geq k$).

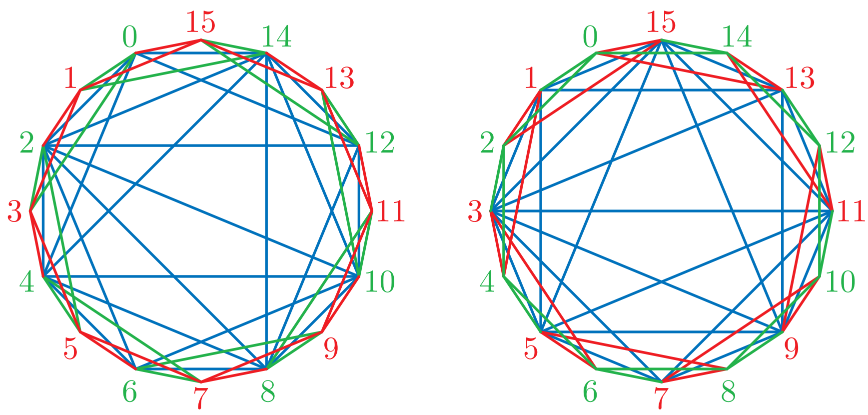

Figure 2.14: The two 2-triangulations T and T' of the 16-gon obtained from the 2-triangulation τ of the 8-gon represented in Figure 1.4.

In other words, we shift to the next even vertex the head of all the edges of F with length strictly smaller than $2k$. Observe that F' is indeed a subset of C since we only introduce edges of the form $[2i, 2j+2]$ where $|i-j| < k$ which are necessarily in C (because τ, as any k-triangulation of the m-gon, contains all non-k-relevant edges). Also F' has still $k+1$ different edges since we only modified the head of some edges which keep all the tails different. Finally, we claim that F' is still a $(k+1)$-crossing. Indeed, choose any two edges in F, and denote them $e := [a, b]$ and $f := [c, d]$ such that e (resp. f) is oriented from a to b (resp. c to d) and $a \prec c \prec b$. The only possible way to uncross e and f would be that $d = b + \varepsilon$, with $\varepsilon \in \{1, 2\}$ and that our transformation shifts the head of e by ε, keeping the head of f at d. But this would imply that e has length smaller than $2k - \varepsilon$ while f has length greater or equal $2k$, which is impossible if $a \prec c \prec b$ and $d = b + \varepsilon$. We obtain a contradiction with the $(k+1)$-crossing-freeness of τ; thus, T is $(k+1)$-crossing-free, and consequently is a k-triangulation.

Second step. We shall now study the number of flips needed to transform T into $T' = \rho(T)$. Observe first that T and T' have no k-relevant edges in common, again because all the tails of the k-relevant edges of T are even, while all the tails of the k-relevant edges of T' are odd. Thus, as in the proof of the previous lemma, we need at least $k(2m - 2k - 1)$ flips to destroy all the edges of T. Now consider a k-star S of T with only even vertices. At the moment when we first destroy an edge of this star, we necessarily construct an edge of length at least $2k+1$ and with one even endpoint (a vertex of S). Such an edge does not exist in the k-triangulation T' (the only edges of T' with an even endpoint have length strictly smaller than $2k$) so that we will have to destroy it again. Since T contains $m - 2k$ k-stars with all vertices even (the images of the k-stars of T under the map $t \mapsto 2t$), the number of flips needed to join the k-triangulations T and T' is at least

$$k(2m - 2k - 1) + m - 2k = 2m\left(k + \frac{1}{2}\right) - k(2k + 3).$$

Finally, the proof for the $(2m+1)$-gon is obtained similarly. We use our two k-triangulations T and T' of the $(2m)$-gon to which we add a vertex $2m$ (between vertices $2m-1$ and 0), connected only with the vertices of $\{2m-k,\dots,2m-1\}\cup\{0,\dots,k-1\}$. The analysis of the distance between the two resulting k-triangulations of the $(2m+1)$-gon is then exactly the same as in the case of even polygons. □

Observe that Conjecture 2.37 would prove that:

$$\delta_{2m+1,k} \geq \delta_{2m,k} + k \geq \left(k+\frac{1}{2}\right)2m - k(2k+3) + k,$$

and consequently that, for any $n \geq 2(2k+1)$,

$$\delta_{n,k} \geq \left\lfloor \left(k+\frac{1}{2}\right)n - k(2k+3)\right\rfloor.$$

To summarize our results on the diameter of the graph of flips $G_{n,k}$, we have proved that when $n > 4k^2(2k+1)$,

$$2\left\lfloor\frac{n}{2}\right\rfloor\left(k+\frac{1}{2}\right) - k(2k+3) \leq \delta_{n,k} \leq 2k(n-4k-1).$$

Furthermore, we know that the difference $\delta_{n+1,k} - \delta_{n,k}$ between two consecutive values of this diameter is at most $4k-1$, and we conjecture that it is at least k (for n sufficiently large).

For completeness, we collect the couples (n,k) for which the exact value of $\delta_{n,k}$ is known:

1. When $k=1$, the exact value of the diameter of the associahedron is known [STT88] for the following little values of n:

n	3	4	5	6	7	8	9	10	11	12	13	14	15	16	17	18
$\delta_{n,1}$	0	1	2	4	5	7	9	11	12	15	16	18	20	22	24	26

   Furthermore, there exists an integer N such that for any n larger than N, the diameter of the associahedron is exactly $2n-10$ [STT88]. The minimal value of N remains unknown (according to the previous table, it is conjectured to be 13).
2. When $k=2$ and $k=3$, a computer search provides the following tables:

n	5	6	7	8	9	10	11
$\delta_{n,2}$	0	1	3	6	8	11	14

n	7	8	9	10	11
$\delta_{n,3}$	0	1	3	6	10

3. When $n=2k+1$ (see Example 2.5), there exist only one k-triangulation and $\delta_{2k+1,k}=0$.
4. When $n=2k+2$ (see Example 2.6), the graph of flips $G_{2k+2,k}$ is complete and $\delta_{2k+2,k}=1$.
5. When $n=2k+3$ (see Example 2.7), the graph of flips $G_{2k+3,k}$ is the ridge graph of the $2k$-dimensional cyclic polytope with $2k+3$ vertices (see Lemma 4.26), and its diameter is $\delta_{2k+3,k}=3$ as soon as $k\geq 2$ (we refer to [Mak09] for the diameter of the ridge graph of the cyclic polytope).

2.4 k-EARS AND k-COLORABLE k-TRIANGULATIONS

Throughout this section, we assume that $n \geq 2k+3$. Generalizing similar notions for triangulations, we define:

Definition 2.40. *A k-ear of a k-triangulation is any edge of length $k+1$. A k-star of a k-triangulation is external if it contains at least one k-boundary edge, and internal otherwise.*

It is well known and easy to prove that the number of ears in any triangulation equals its number of internal triangles plus 2. In this section, we prove that the number of k-ears in any k-triangulation equals its number of internal k-stars plus $2k$. Then we characterize the triangulations that have no internal k-star in terms of colorability of their intersection complex.

2.4.1 The maximal number of k-ears

Let S be a k-star and $[u, v]$ be an edge of S such that S lies on the positive side of the oriented edge from u to v. We say that $[u, v]$ is a *positive ear* of S if $|[\![v, u]\!]| = k+1$. Said differently, $[u, v]$ is an ear, and S is the unique (by Corollary 2.13) k-star on the "outer" side of it.

Lemma 2.41. *Let $b \geq 1$ be the number of k-boundary edges of an external k-star S. Then, S has exactly $b-1$ positive ears. Moreover, k-boundary edges and positive ears of S form an alternating path in the k-star.*

Proof. Observe first that if $[x, x+k]$ is a k-boundary edge of S, then all $k+1$ vertices of $[\![x, x+k]\!]$ are vertices of S. Since S has $2k+1$ vertices, this implies that if $[x, x+k]$ and $[y, y+k]$ are two k-boundary edges of S, then $[\![x, x+k]\!]$ and $[\![y, y+k]\!]$ intersect; that is, for example, $y \in [\![x, x+k]\!]$. But then, all edges $[i, i+k]$ with $x \preccurlyeq i \preccurlyeq y$ are k-boundary edges of S, and all edges $[i, i+k+1]$ with $x \preccurlyeq i \prec y$ are positive ears of S. Thus, k-boundary edges and positive ears of S form an alternating path in the k-star, beginning and ending by a k-boundary edge. In particular, S has exactly $b-1$ positive ears. $\square$

Corollary 2.42. *(i) A k-star cannot have more than $k+1$ k-boundary edges.*
(ii) The k-boundary edges of a k-star are always consecutive around the circle. $\square$

Observe that any k-star with all vertices consecutive has $k+1$ k-boundary edges (*i.e.* attains the bound (i) in the previous corollary). Such a k-star is an alternating path of $k+1$ k-boundary edges and k k-ears.

Lemma 2.41 has also the following consequence:

Corollary 2.43. *The number of k-ears in a k-triangulation T equals the number of internal k-stars of T plus $2k$. In particular, T contains at least $2k$ k-ears.*

Proof. For any $0 \leq i \leq 2k+1$, let μ_i denote the number of k-stars of T with exactly i k-boundary edges. Let ν denote the number of k-ears of T. Then

$$\sum_{i=0}^{2k+1} \mu_i = n - 2k \quad \text{and} \quad \sum_{i=1}^{2k+1} i\mu_i = n.$$

Since any k-ear is a positive ear of exactly one k-star, Lemma 2.41 ensures moreover that

$$\sum_{i=1}^{2k+1} (i-1)\mu_i = \nu.$$

Thus, we obtain $\nu = n - (n-2k) + \mu_0 = 2k + \mu_0$. □

Example 2.44. The 2-triangulation in Figure 1.4 has five 2-ears and one internal 2-star.

2.4.2 k-colorable k-triangulations

We are now interested in a characterization of the k-triangulations that have exactly $2k$ k-ears, or equivalently that have no internal k-star. We need two additional definitions.

Definition 2.45. *We say that a k-triangulation is k-colorable if it is possible to color its k-relevant edges with k colors such that there is no monochromatic 2-crossing. Observe that, if this happens, then every k-crossing uses an edge of each color.*

Definition 2.46. *A k-accordion of E_n is a set $Z := \{[a_i, b_i] \mid i \in [n-2k-1]\}$ of $n-2k-1$ edges such that $b_1 = a_1 + k + 1$ and for any $2 \le i \le n-2k-1$, the edge $[a_i, b_i]$ is either $[a_{i-1}, b_{i-1}+1]$ or $[a_{i-1}-1, b_{i-1}]$.*

Note that, in this definition, $b_i = a_i + k + i$ for any $i \in [n-2k-1]$. When $k \ge 2$, observe that the definition is equivalent to being a set of $n-2k-1$ k-relevant edges of E_n without 2-crossing.

Lemma 2.47. *The union of k disjoint k-accordions of E_n is the set of k-relevant edges of a k-triangulation of the n-gon.*

Proof. Observe that:
(i) A k-accordion has no 2-crossing, so the union of k of them has no $(k+1)$-crossing.
(ii) A k-accordion contains $n-2k-1$ k-relevant edges; thus, the union of k disjoint k-accordions contains $k(n-2k-1)$ k-relevant edges.

This lemma thus follows from Corollary 2.21. □

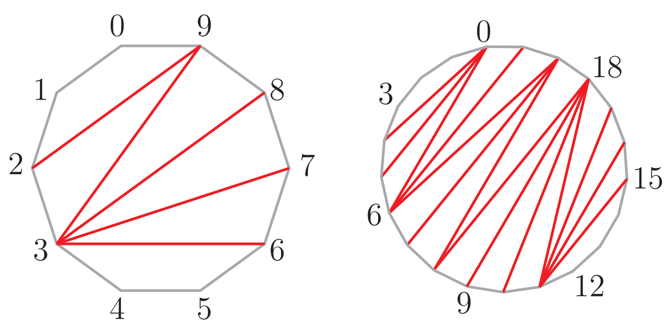

Figure 2.15: Examples of k-accordions of E_n for $(n, k) = (10, 2)$ and $(21, 3)$.

We have already met some particular k-accordions both when we constructed the triangulation $T_{n,k}^{\min}$ and in the proof of Lemma 2.36. The two types of k-accordions in these examples (the "fan" and the "zigzag") are somehow the two extremal examples of them: one has only alternating angles when the other has no of them.

The following theorem relates the two Definitions 2.45 and 2.46 and characterizes k-triangulations with exactly $2k$ k-ears:

Theorem 2.48. *Let T be a k-triangulation, with $k > 1$. The following properties are equivalent:*

(i) T is k-colorable.

(ii) There exists a k-coloring of the k-relevant edges of T such that no k-star of T contains three edges of the same color.

(iii) T has no internal k-star.

(iv) T contains exactly $2k$ k-ears.

(v) T contains exactly $2k$ edges of each length $k+1, \dots, \left\lfloor \frac{n-1}{2} \right\rfloor$ (and k of length $\frac{n}{2}$ if n is even).

(vi) The set of k-relevant edges of T is the union of k disjoint k-accordions.

Note that for $k = 1$, only (ii), (iii), (iv), (v) and (vi) are equivalent, while (i) always holds.

Proof of Theorem 2.48. When $k > 1$, any three edges of a k-star form at least one 2-crossing. Thus, any k-coloring of T without monochromatic 2-crossing is such that no k-star of T contains three edges of the same color, and (i)⇒(ii).

Let S be a k-star of a k-triangulation whose k-relevant edges are colored with k colors. If all edges of S are k-relevant, then, by the pigeon-hole principle, there is a color that colors three edges of S. Thus (ii)⇒(iii).

Corollary 2.43 ensures that (iii)⇔(iv). Thus, since (vi)⇒(v)⇒(iv) and (vi)⇒(i) are trivial, it only remains to prove that (iv)⇒(vi).

For this, we give an algorithm that finds the k disjoint k-accordions in a k-triangulation T with $2k$ k-ears. Recall that if S is an external k-star with b k-boundary edges, then S has $b-1$ positive ears, and moreover k-boundary edges and positive ears of S form an alternating path in the k-star. Thus, the edges of S which are neither k-boundary nor positive ears of S form a path of even length. This defines naturally a "pairing" of them: we say that the first and the second (resp. the third and the fourth, etc.) edges of this path form a *pair* of edges in S. Observe that such a pair of edges forms an angle containing no vertex.

Consider now a k-ear e_1 of T. Let S_0 be the k-star of T for which e_1 is a positive ear. Let S_1 be the other k-star of T containing e_1. Let e_2 be the pair of e_1 in S_1. Let S_2 be the other k-star of T containing e_2 and let e_3 be the pair of e_2 in S_2. Let continue so until we reach a k-ear. It is obvious that we get a k-accordion of E_n. To get another k-accordion, we do the same with a k-ear which is neither e_1 nor e_{n-2k-1}.

To prove the correctness of this algorithm, we only have to prove that the k-accordions we construct are disjoint. Suppose that two of them $\{e_1, \dots, e_{n-2k-1}\}$ and $\{f_1, \dots, f_{n-2k-1}\}$ intersect. Let i, j be such that $e_i = f_j$. Let S be a k-star containing e_i. Then by construction, either e_{i+1} or e_{i-1} (resp. either f_{j+1} or f_{j-1}) is the pair of e_i in S. Thus, either $e_{i+1} = f_{j+1}$, or $e_{i+1} = f_{j-1}$. By propagation, we get that $\{e_1, \dots, e_{n-2k-1}\} = \{f_1, \dots, f_{n-2k-1}\}$. □

Observe that the above proof of (iv)⇒(vi) also gives uniqueness (up to permutation of colors) of the k-coloring (decomposition into accordions) of a k-colorable k-triangulation T. Indeed, any k-coloring has to respect the pairing of edges in all k-stars of T.

Let us also remark that Part (v) implies that every k-colorable k-triangulation contains exactly $k(n-2p-1)$ p-relevant edges, for any $k \leq p \leq \left\lfloor \frac{n-1}{2} \right\rfloor$. It is proved by a flip method in [Nak00] that any k-triangulation of the n-gon contains at most this same number of p-relevant edges. We will prove this result in the next section, as an application of the flattening of k-stars in k-triangulations.

Let us conclude this section with the following remark. An easy "intuitive model" for a k-triangulation is just a superposition of k triangulations. Even if this model is sometimes useful, the results in this section say that it is also misleading:

- Theorem 2.48 says that the structure of k-triangulations obtained in this way is really particular: it is uniquely k-colorable, the number of edges of each length is $2k$, all k-stars are external, etc.

- The number of k-accordions of E_n containing a given k-ear of E_n is 2^{n-2k-2}. In particular, the number of k-colorable k-triangulations of E_n is at most $\binom{n}{k} 2^{k(n-2k-2)} \leq 2^{(k+1)n}$. This is much smaller than the total number of k-triangulations, which for constant k equals 4^{nk} modulo a polynomial factor in n (see Remark 4.2).

- Let T be any triangulation with only two ears. Then it is easy to see that there exists a 2-accordion Z disjoint from it, so that Z completes T to give the set of 2-relevant edges of a 2-colorable 2-triangulation. Surprisingly, this property fails when $k \geq 3$: even if a k-triangulation T is k-colorable, it is not always possible to find a $(k+1)$-accordion disjoint from T (see Figure 2.16).

- There even exist k-triangulations of the n-gon which do not contain a single triangulation of the n-gon. See Example 3.31 and Figure 3.18.

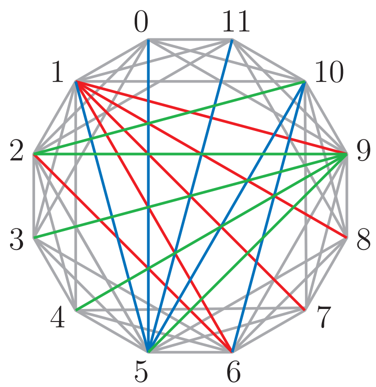

Figure 2.16: A 3-colorable 3-triangulation of the 12-gon with no 4-accordion disjoint from it.

2.5 Flattening a k-star, inflating a k-crossing

The goal of this section is to describe in terms of k-stars an operation that connects k-triangulations of n and of $n+1$ vertices. This operation, already present in [Nak00, Jon03], and when $k = 2$ in [Eli07, Nic09], is useful for recursive arguments and it was a step in all previous proofs of the flipability of k-relevant edges (Lemma 2.27). We only present this operation here to emphasize that none of our proofs so far make use of induction. In the end of this section, we discuss the properties of this operation with respect to flips (namely, how does this property commutes with flips), and we present some applications.

Before giving the precise definitions, let us present a simplified picture of this operation:

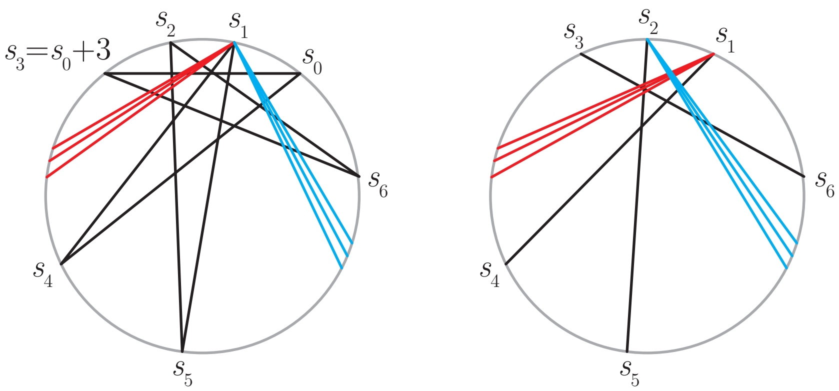

Figure 2.17: Flattening a 3-boundary edge, inflating a 3-crossing.

2.5.1 Flattening a k-star

Definition 2.49. *Let T be a k-triangulation of the $(n+1)$-gon, and $b := [s_0, s_0+k]$ be a k-boundary edge of T. Let $s_0, s_1 = s_0+1, \dots, s_k = s_0+k, s_{k+1}, \dots, s_{2k}$ be the vertices of the unique k-star S of T containing b, in their circle order.*

We call flattening of b in T the set of edges $T \curlyvee b$ whose underlying set of points is $V_{n+1} \smallsetminus \{s_0\}$ and which is constructed from T as follows (see Figure 2.17):

(i) for any edge of T whose vertices are not in $\{s_0, \dots, s_k\}$ just copy the edge;

(ii) forget all the edges $[s_0, s_i]$, for $i \in [k]$;

(iii) replace any edge of the form $[s_i, t]$ with $0 \le i \le k$, and $s_k \prec t \preccurlyeq s_{k+i}$ (resp. $s_{k+i+1} \preccurlyeq t \prec s_0$) by the edge $[s_i, t]$ (resp. $[s_{i+1}, t]$).

Remark 2.50. We sometimes call this operation "flattening of the k-star S". This is a more graphical description of the operation, but it is also a slight abuse of language: if S has more than one k-boundary edge, the result of the flattening depends on the k-boundary edge we flatten, and not only on its adjacent k-star.

We want to prove that $T \curlyvee b$ is a k-triangulation of the n-gon. Observe first that:

(1) If e is a k-relevant edge of $T \curlyvee b$, then:
   (i) either e is of the form $[s_i, s_{k+i}]$, for some $i \in [k]$, and then it arises as the gluing of two edges $e' = [s_{i-1}, s_{k+i}]$ and $e'' = [s_i, s_{k+i}]$ of the initial k-triangulation T;
   (ii) otherwise, e arises from a unique k-relevant edge e' of T.
(2) If e and f are two k-relevant edges of $T \curlyvee b$ arising from e' and f' respectively, then:
   (i) either e and f do not cross, and then e' and f' do not cross;
   (ii) or e and f do cross, and then e' and f' do cross, unless the following happens: there exists $i \in [k]$, and u, v two vertices such that $s_k \prec u \preccurlyeq s_{i+k} \prec s_{i+k+1} \preccurlyeq v \prec s_0$ and $e = [s_i, u]$, $f = [s_{i+1}, v]$, $e' = [s_i, u]$ and $f' = [s_i, v]$. Such a configuration is said to be a *hidden configuration* (see Figure 2.17).

It is easy to derive from this that $|T \curlyvee b| = |T| - 2k = k(2n - 2k - 1)$ and that any subset of E_n that properly contains $T \curlyvee b$ contains a $(k+1)$-crossing. However, this is not sufficient to conclude that $T \curlyvee b$ is a k-triangulation. Thus we have to prove that $T \curlyvee b$ is $(k+1)$-crossing-free. Note that this provides a third proof (which this time is recursive on n) of the formula for the number of edges of a k-triangulation of the n-gon.

Lemma 2.51. *The set $T \curlyvee b$ is $(k+1)$-crossing-free. Hence, it is a k-triangulation of the n-gon.*

Proof. Suppose that $T \curlyvee b$ contains a $(k+1)$-crossing E, and let $e_0 := [x_0, y_0], \dots, e_k := [x_k, y_k]$ denote the edges of E ordered such that $x_0 \prec x_1 \prec \cdots \prec x_k \prec y_0 \prec y_1 \prec \cdots \prec y_k$. Let $e'_0 := [x'_0, y'_0], \dots, e'_k := [x'_k, y'_k]$ be $k+1$ edges of T that give (when we flatten b) the edges $e_0, \dots, e_k$ respectively.

It is clear that if there exists no $0 \le i \le k$ such that the four edges $(e_i, e_{i+1}, e'_i, e'_{i+1})$ form a hidden configuration, then the edges $e'_0, \dots, e'_k$ form a $(k+1)$-crossing of T, which is impossible. Thus we can suppose that the number of hidden configurations in $\{(e_i, e_{i+1}, e'_i, e'_{i+1}) \,|\, 0 \le i \le k\}$ is at least 1. We can also assume that this number is minimal, that is that we cannot find a $(k+1)$-crossing F of $T \curlyvee b$ arising from a set F' of edges of T such that there are strictly less hidden configurations in $\{(f_i, f_{i+1}, f'_i, f'_{i+1}) \,|\, 0 \le i \le k\}$ than in $\{(e_i, e_{i+1}, e'_i, e'_{i+1}) \,|\, 0 \le i \le k\}$. Here, we raise an absurdity by finding such sets F and F'.

Let $0 \le i \le k$ be such that $(e_i, e_{i+1}, e'_i, e'_{i+1})$ is a hidden configuration. We can assume that $x_i = s_i$ and $x_{i+1} = s_{i+1}$ (if this is not the case, we renumber the edges of E such that this be true). Thus we know that $y_i \preccurlyeq s_{i+k} \prec s_{i+k+1} \preccurlyeq y_{i+1}$. Let

$$p := \min\{0 \le j < i \,|\, \text{for any } j < \ell \le i,\ x_\ell = s_\ell \text{ and } y_\ell \preccurlyeq s_{\ell+k}\}, \quad \text{and}$$
$$q := \max\{i+1 < j \le k+1 \,|\, \text{for any } i+1 \le \ell < j,\ x_\ell = s_\ell \text{ and } s_{\ell+k} \preccurlyeq y_\ell\}.$$

Let F be the set of $k+1$ edges of $T \curlyvee b$ deduced from E as follows:
- for all i with $p < i < q$, let f_i be $[s_i, s_{i+k}]$,
- for all i with $0 \le i \le p$ and $q \le i \le k$, let f_i be e_i.

Let F' be the set of $k+1$ edges of T constructed as follows:
- for all i with $p < i < q$, let f'_i be $[s_i, s_{i+k}]$,
- for all i with $0 \le i \le p$ or $q \le i \le k$, let f'_i be e'_i.

It is quite clear that F is a $(k+1)$-crossing of $T \curlyvee b$ arising from F'. We just have to verify that the number of hidden configurations in the set $\{(f_i, f_{i+1}, f'_i, f'_{i+1}) \,|\, 0 \le i \le k\}$ is less than in the set $\{(e_i, e_{i+1}, e'_i, e'_{i+1}) \,|\, 0 \le i \le k\}$. But:

(i) the number of hidden configurations in $\{(f_i, f_{i+1}, f'_i, f'_{i+1}) \,|\, i < p \text{ or } q \le i\}$ is exactly the same as in $\{(e_i, e_{i+1}, e'_i, e'_{i+1}) \,|\, i < p \text{ or } q \le i\}$;

(ii) there is no hidden configuration in $\{(f_i, f_{i+1}, f'_i, f'_{i+1}) \,|\, p < i < q-1\}$, whereas there is one in $\{(e_i, e_{i+1}, e'_i, e'_{i+1}) \,|\, p < i < q-1\}$; and

(iii) the edges $(f_p, f_{p+1}, f'_p, f'_{p+1})$ (resp. $(f_{q-1}, f_q, f'_{q-1}, f'_q)$) do not form a hidden configuration.

$\square$

Example 2.52. Figure 2.18 shows the flattening of the 2-relevant edge $[5, 7]$ in the 2-triangulation of Figure 1.4. The flattened 2-star is colored, as well as the resulting 2-crossing.

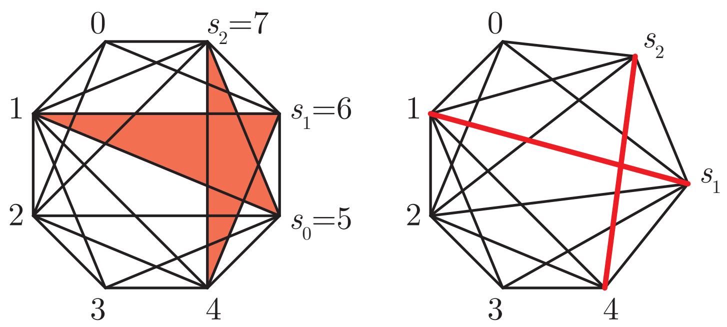

Figure 2.18: Flattening the 2-relevant edge $[5, 7]$ in the 2-triangulation of Figure 1.4.

2.5.2 Inflating a k-crossing

Definition 2.53. *Let T be a k-triangulation of the n-gon and X be a k-crossing. Denote by $[s_1, s_{1+k}], \dots, [s_k, s_{2k}]$ its edges, with $s_1 \prec s_2 \prec \dots \prec s_{2k}$. Assume further that $s_1, \dots, s_k$ are consecutive in the cyclic order of the n-gon (that is $s_k = s_1 + k - 1$). We call X an external k-crossing. Let s_0 be a new vertex on the circle, between $s_1 - 1$ and s_1.*

We call inflating of X at $[\![s_1, s_k]\!]$ in T the set of edges $T \curlywedge X$ whose underlying set of points is the set $V_n \cup \{s_0\}$ and which is constructed from T as follows (see Figure 2.17):

(i) for any edge of T whose vertices are not in $\{s_1, \dots, s_k\}$ just copy the edge;

(ii) add all the edges $[s_0, s_i]$, for $i \in [k]$; and

(iii) replace any edge of the form $[s_i, t]$ with $i \in [k]$, and $s_k \prec t \preccurlyeq s_{k+i}$ (resp. $s_{k+i} \preccurlyeq t \prec s_1$) by the edge $[s_i, t]$ (resp. $[s_{i-1}, t]$).

Remark 2.54. We are abusing notation: if X contains more than k consecutive vertices, then the result of the inflating of X depends on the k consecutive points we choose. It would also be an abuse of language to say that we inflate the cyclic interval $[\![s_1, s_k]\!]$ since several k-crossings may be adjacent to these k points. For example, when $k = 1$, we have to specify both an edge and a vertex of this edge to define an inflating.

Observe that:

(1) Any k-relevant edge e of $T \Lsh X$ arises from a unique edge e' of T.

(2) If e and f are two k-relevant edges of $T \Lsh X$ that cross, and e' and f' are the two edges of T that give e and f respectively, then e' and f' cross as well.

Point (2) ensures that $T \Lsh X$ is $(k+1)$-crossing-free. Moreover, it is easy to see that its cardinality is $|T \Lsh X| = |T| + 2k = k(2(n+1) - 2k - 1)$. Thus, by Corollary 2.21, we get:

Lemma 2.55. *$T \Lsh X$ is a k-triangulation of the $(n+1)$-gon.* □

Example 2.56. Figure 2.19 shows the inflating of the 2-crossing $\{[1,4],[2,7]\}$ at $[\![1,2]\!]$ in the 2-triangulation of Figure 1.4. The inflated 2-crossing is colored, as well as the new 2-star.

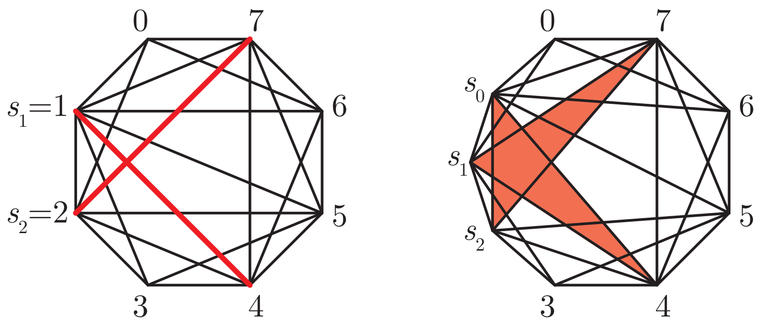

Figure 2.19: Inflating the 2-crossing $\{[1,4],[2,7]\}$ at $[\![1,2]\!]$ in the 2-triangulation of Figure 1.4.

2.5.3 Properties of the flattening & inflating operations

First of all, the following theorem is an immediate consequence of the definitions:

Theorem 2.57. *Flattening and inflating are inverse operations. More precisely:*

(i) if b is a k-boundary edge of a k-triangulation T, and X denotes the k-crossing of $T \curlyvee b$ consisting of edges that arise by gluing two edges of T, then $(T \curlyvee b) \Lsh X = T$; and

(ii) if X is a k-crossing with k consecutive vertices $s_1, \dots, s_k$, and b denotes the edge $[s_0, s_k]$ of $T \Lsh X$, then $(T \Lsh X) \curlyvee b = T$. □

Another interesting property is the behavior of the flattening and inflating operations with respect to flips:

Lemma 2.58. *Let T be a k-triangulation of the $(n+1)$-gon, f be a k-relevant edge of T and e be the common bisector of the two k-stars of T containing f. Let b be a k-boundary edge of the $(n+1)$-gon, and f' (resp. e') be the image of the edge f (resp. e) in $T \curlyvee b$ (resp. $(T \triangle \{e,f\}) \curlyvee b$) after flattening. If f is not an edge of the k-star of T containing b (or equivalently, if e is not an edge of the k-star of $T \triangle \{e,f\}$ containing b), then flip and flattening commute:*

$$(T \curlyvee b) \triangle \{e', f'\} = (T \triangle \{e,f\}) \curlyvee b.$$

Proof. The k-triangulations T and $T \triangle \{e, f\}$ have the same k-star containing b (since f is not an edge of this k-star). Consequently, the image of any edge of $T \cup \{e\}$ is the same in $T \curlyvee b$ and $(T \triangle \{e, f\}) \curlyvee b$. $\square$

Remark 2.59. In the previous lemma, it is interesting (and surprising) to observe that if f is an edge of the k-star of T containing b, then the two k-triangulations of the n-gon $T \curlyvee b$ and $(T \triangle \{e, f\}) \curlyvee b$ are not necessarily the same. Even worst, these two k-triangulations can be relatively far appart in the flip graph $G_{n,k}$. For example, let T_n be the 2-triangulation of the n-gon formed by all the edges adjacent to vertices 0 or 2, plus all the non-2-relevant edges (T_n is indeed a 2-triangulation since its set of 2-relevant edges is the union of two disjoint fans of edges). Then the 2-triangulation $T_{n+1} \curlyvee [1, n]$ equals the minimal 2-triangulation $T_{n,2}^{\min}$ while the 2-triangulation $(T_{n+1} \triangle \{[1, n-1], [2, n]\}) \curlyvee [1, n]$ is nothing else than T_n (see Figure 2.20). These two 2-triangulations have only $(n-5)$ 2-relevant edges in common.

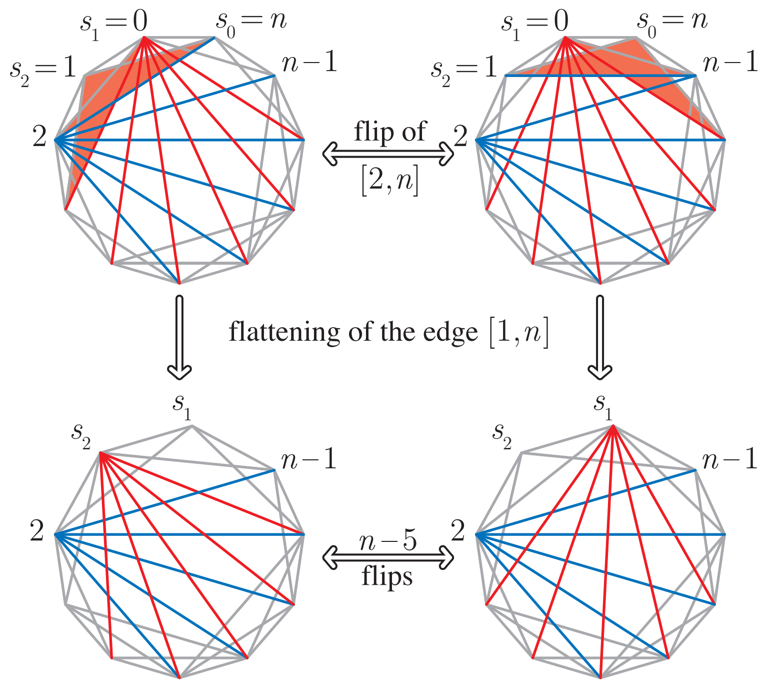

Figure 2.20: When the flattening of a 2-star takes away neighbors in the graph of flips.

Let us insist however on the fact that this property holds when $k = 1$: if T is a triangulation of the $(n+1)$-gon, with a distinguished boundary edge b, if f is a 1-relevant edge of the triangle of T adjacent to b, and if e is the common bisector of the two triangles of T adjacent to f, then $T \curlyvee b = (T \triangle \{e, f\}) \curlyvee b$. A proof is sketched on Figure 2.21. This property is interesting since it provides a simple proof of the fact that $\delta_{n+1,1} \geq \delta_{n,1} + 1$. If this property were also valid for k-triangulations, this proof would extend easily to the corresponding Conjecture 2.37 stated in Section 2.3.2.

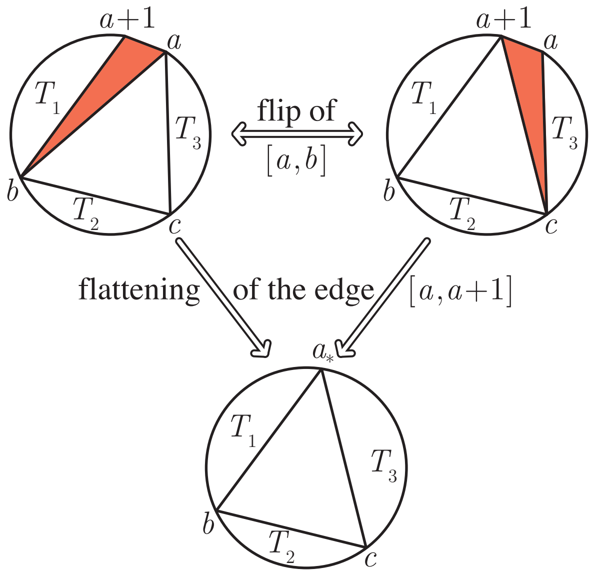

Figure 2.21: Flip and flattening for a triangulation.

Corollary 2.60. *Let T be a k-triangulation of the n-gon, let f be a k-relevant edge of T and let e be the common bisector of the two k-stars of T containing f. Let X be an external k-crossing of $T \smallsetminus \{f\}$, and let f' (resp. e') be the image of the edge f (resp. e) in $T \Wedge X$ (resp. $(T \triangle \{e, f\}) \Wedge X$) after inflating. Then flip and inflating commute:*

$$(T \Wedge X) \triangle \{e', f'\} = (T \triangle \{e, f\}) \Wedge X.$$

To close this section, we want to observe that the result of flattening several k-boundary edges of a k-triangulation is independent of the order:

Lemma 2.61. *Let b_1 and b_2 be two distinct k-boundary edges of a k-triangulation T. Let b_1' (resp. b_2') denote the edge of $T \Vee b_2$ (resp. $T \Vee b_1$) arising from b_1 (resp. b_2). Then b_1' (resp. b_2') is a k-boundary edge of $T \Vee b_2$ (resp. $T \Vee b_1$) and*

$$(T \Vee b_2) \Vee b_1' = (T \Vee b_1) \Vee b_2'. \qquad \square$$

In particular, one can define the flattening of a set of k-boundary edges. Similarly, it is possible to define the inflating of a set of edges-disjoint external k-crossings of a k-triangulation.

2.5.4 Examples of application

We now present some applications using these inverse transformations to prove results on k-triangulations by induction.

Corollary 2.62. *Let $\theta(n, k)$ denote the number of k-triangulations of an n-gon. Then the quotient $\theta(n + 1, k)/\theta(n, k)$ equals the average number, among all k-triangulations of the n-gon, of k-crossings adjacent to the first k points.*

Proof. Consider the set $\mathcal{X}$ of all couples (T, X) where T is a k-triangulation of the n-gon and X is a k-crossing of T on the first k points, and the set $\mathcal{Y}$ of all couples $(T, [0, k])$ where T is a k-triangulation of the $(n+1)$-gon where the k-boundary edge $[0, k]$ is distinguished. Then the inflating & flattening operations define opposite bijections between $\mathcal{X}$ and $\mathcal{Y}$, which proves that:

$$\theta(n+1, k) = |\mathcal{Y}| = |\mathcal{X}| = \sum_T |\{X \text{ } k\text{-crossing of } T \text{ on the first } k \text{ points}\}|,$$

and we derive the result dividing by $\theta(n, k)$. $\square$

For example:

(i) For $k = 1$, we get that $\theta(n+1, 1)/\theta(n, 1)$ equals the average degree of vertex 0 in triangulations of the n-gon, and we recover the well-known recursion for Catalan numbers:

$$C_{n-1} = \frac{4n-6}{n} C_{n-2}.$$

(Remember the proof of Proposition 1.3.)

(ii) For $n = 2k+1$ we have that $\theta(2k+1, k) = 1$ (the unique k-triangulation is the complete graph) and the number of k-crossings using the first k vertices in this k-triangulation is $k+1$ (any choice of k of the last $k+1$ vertices gives one k-crossing). In particular, we recover the fact that $\theta(2k+2, k) = k+1$ (see Example 2.6).

(iii) Unfortunately, for $n > 2k+1$, the number of k-crossings using k consecutive vertices is not independent of the k-triangulation. Otherwise the quotient $n\theta(n+1, k)/\theta(n, k)$ would be an integer, equal to that number (as happens in the case of triangulations).

The following lemma is another example of the use of a recursive argument. It is equivalent to Theorem 10 in [Nak00], where the proof uses flips. It is interesting to observe that k-colorable k-triangulations attain the following inequality (see Theorem 2.48).

Lemma 2.63. *Any k-triangulation of the n-gon contains at most $k(n-2p-1)$ p-relevant edges, for any $k \leq p \leq \frac{n-1}{2}$.*

Proof. When $n = 2p+1$, it is true since there are no p-relevant edges.

Suppose now that $n > 2p+1$. Let T be a k-triangulation of the n-gon. Let $b := [u, u+k]$ be a k-boundary edge of T. It is easy to check that if g is a k-relevant edge of T of length ℓ, then the corresponding edge g' in $T \curlyvee b$ has length ℓ or $\ell - 1$, and the latter is possible only if $g = [v, v+\ell]$ with $v \preccurlyeq u \prec u+k \preccurlyeq v+\ell$.

Let E be the k-crossing of $T \curlyvee b$ that arises from the edges of the k-star of T containing b. Let F be the set of edges of E of length at least p. Let G denote the set of edges of length p of $(T \curlyvee b) \smallsetminus E$ arising from an edge of length $p+1$ of T.

Any non-p-relevant edge of $(T \curlyvee b) \smallsetminus (E \cup G)$ (resp. of $E \smallsetminus F$) arises from one (resp. two) non-p-relevant edge of T. Thus we obtain by induction that the number of p-relevant edges is at most $k(n-1-2p-1) + |F| + |G|$.

To conclude, we only have to observe that any two edges of $F \cup G$ are crossing, which implies that $|F| + |G| = |F \cup G| \leq k$. $\square$

We finish this section by reinterpreting a construction we have done in Section 2.3:

Remark 2.64. Remember the construction in the proof of Lemma 2.39: we started from a k-triangulation τ of the m-gon and constructed a k-triangulation T of the $(2m)$-gon as the union of the sets $A = \{[2i, 2(i+j)-1] \,|\, i \in \mathbb{Z}_m \text{ and } j \in [k]\}$, $B = \{[2i+1, 2i+1+j] \,|\, i \in \mathbb{Z}_m \text{ and } j \in [k]\}$ and $C = \{[2i, 2j] \,|\, [i, j] \text{ edge of } \tau\}$ (see Figure 2.14).

For all $i \in \mathbb{Z}_n$, define the k-crossing $X_i = \{[i, i-k], [i-1, i-k-1], \dots, [i-k+1, i-2k+1]\}$ of τ. We just want to observe that the k-triangulation T can be seen as the k-triangulation obtained from τ by sequentially inflating the k-crossings $X_{m-1}, X_{m-2}, \dots, X_0$:

$$T = ((\tau \Uparrow X_{m-1}) \Uparrow X_{m-2}) \dots) \Uparrow X_0.$$

The inflated k-stars in the resulting k-triangulation T of the $2n$-gon are the k-stars with at least one odd vertex.

2.6 Decompositions of surfaces

Regarding a k-triangulation T of the n-gon as a complex of k-stars naturally defines a polygonal complex $\mathcal{C}(T)$ as follows:

(i) the vertices of $\mathcal{C}(T)$ are the vertices of the n-gon;
(ii) the edges of $\mathcal{C}(T)$ are the k-boundary edges and k-relevant edges of T;
(iii) the facets of $\mathcal{C}(T)$ are the k-stars of T, considered as $(2k+1)$-gons.

Since every k-relevant edge belongs to two k-stars and every k-boundary edge belongs to one, this complex is a surface with boundary, with $\gcd(n, k)$ boundary components. Also, it is orientable since the natural orientation of each k-star can be inherited on each polygon. Hence, from its Euler characteristic, we derive its genus:

$$g_{n,k} := \frac{1}{2}(2 - f + e - v - b) = \frac{1}{2}(2 - n + k + kn - 2k^2 - \gcd(n, k)).$$

That is, the surface does not depend on the k-triangulation T but only on n and k. We denote by $\mathcal{S}_{n,k}$ this surface. The polygonal complex $\mathcal{C}(T)$ of each k-triangulation T provides a polygonal decomposition of $\mathcal{S}_{n,k}$. In other words [MT01, Chapter 3.1, p. 78], we consider a *2-cell embedding* of the k-relevant plus k-boundary edges of T in the surface $\mathcal{S}_{n,k}$, where each cell is a $(2k+1)$-gon.

Example 2.65. When $k = 2$, the genus of the surface $\mathcal{S}_{n,2}$ is $g_{n,2} = \left\lfloor \frac{n-5}{2} \right\rfloor$. In Figure 2.22, we have represented the polygonal decompositions $\mathcal{C}(T^{\min}_{n,2})$ for $n = 6, 7$ and 8.

Remark 2.66. Observe that two polygons in $\mathcal{C}(T)$ can intersect improperly, sharing for example two opposite edges (see for example Figure 2.22), but that each connected component of the intersection of any two polygons $P, Q \in \mathcal{C}(T)$ is either a common vertex, or a common edge of P and Q.

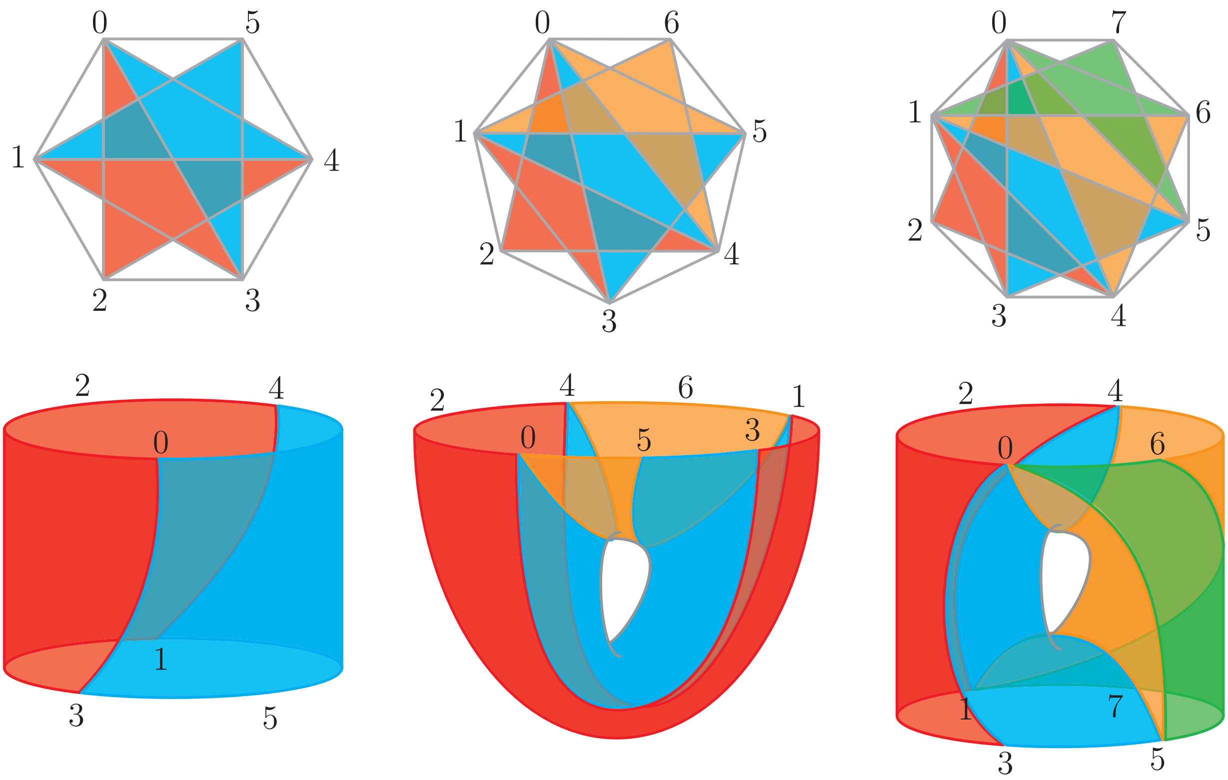

Figure 2.22: Examples of decompositions of surfaces associated to the 2-triangulations $T^{\min}_{6,2}$, $T^{\min}_{7,2}$ and $T^{\min}_{8,2}$.

2.6.1 Flips and twists

We can now interpret the operation of flip in this new setting.

Let T be a k-triangulation of the n-gon, and let f be a k-relevant edge of T. Let R and S be the two k-stars of T containing f, and let e be the common bisector of R and S. Let X and Y be the two k-stars of $T\triangle\{e,f\}$ containing e.

Then $T \smallsetminus \{f\}$ can be viewed as a decomposition of $\mathcal{S}_{n,k}$ into $n-2k-2$ $(2k+1)$-gons and one $4k$-gon, obtained from $\mathcal{C}(T)$ by gluing the two $(2k+1)$-gons corresponding to R and S along the edge f. And then $T\triangle\{e,f\}$ is obtained from $T \smallsetminus \{f\}$ by splitting the $4k$-gon into the two $(2k+1)$-gons corresponding to X and Y.

Example 2.67. In Figure 2.23, we have drawn the decomposition of the cylinder corresponding to the 2-triangulation $T^{\min}_{6,2}$. The second 2-triangulation is obtained from $T^{\min}_{6,2}$ by flipping the edge $[1,4]$, and we have represented the decomposition of the cylinder obtained by flipping the edge on the surface. If we now flip $[0,3]$ and then $[2,5]$, we obtain again the triangulation $T^{\min}_{6,2}$.

Observe that although the corresponding decomposition is combinatorially the same as in the first picture, it has been "twisted" on the surface. This phenomenon can be generalized to the following proposition:

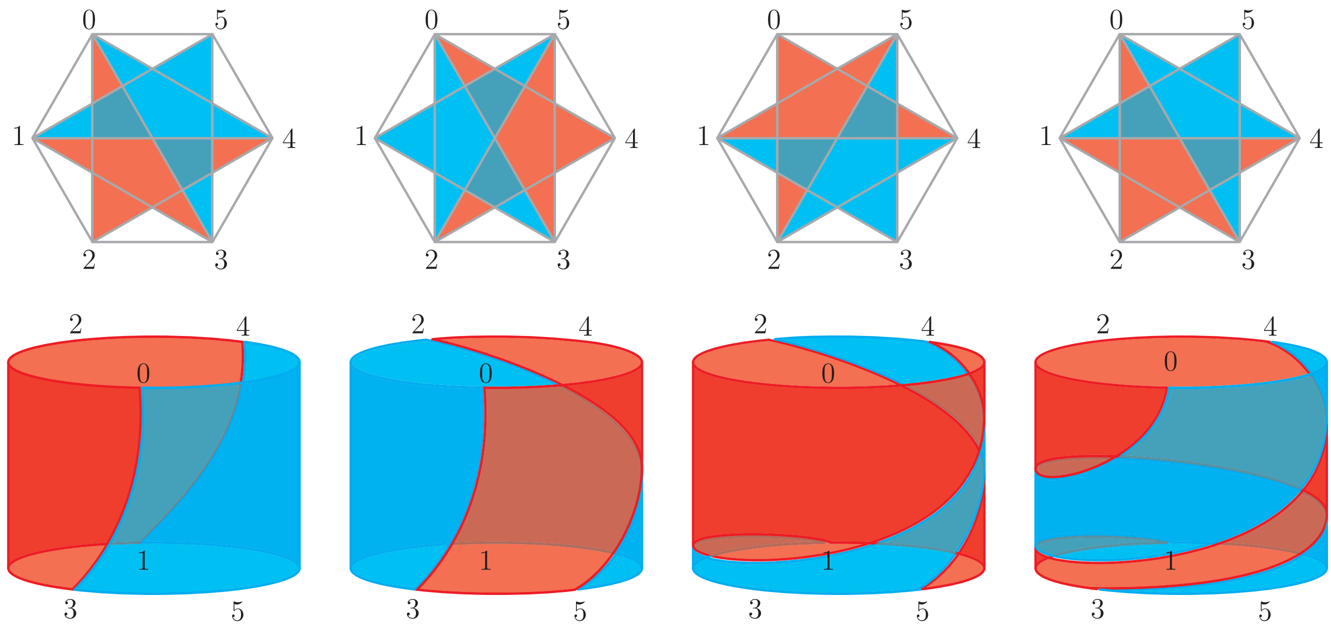

Figure 2.23: A cycle of flips gives raise to a twist.

Proposition 2.68. *There is a homomorphism between:*

(i) the fundamental group $\pi_{n,k}$ *of the graph of flips* $G_{n,k}$*, i.e. the set of closed walks in* $G_{n,k}$*, based at an initial* k*-triangulation, considered up to homotopy, and*

(ii) the mapping class group $\mathcal{M}_{n,k}$ *of the surface* $\mathcal{S}_{n,k}$*, i.e. the set of diffeomorphisms of the surface* $\mathcal{S}_{n,k}$ *into itself that preserve the orientation and that fix the boundary of* $\mathcal{S}_{n,k}$*, considered up to isotopy [Bir74, Iva02].* □

Observe that we know the structure of the fundamental group $\pi_{n,k}$: it is a free group, and its number of generators is the number of edges in $G_{n,k}$ minus the number of vertices in $G_{n,k}$ plus 1. This number grows as 4^{nk} modulo a rational function of degree $O(k^2)$ in n (see Remark 4.2). In contrast, the mapping class group $\mathcal{M}_{n,k}$ is generated by $2g+1$ Dehn twists (see [Iva02] for the definition). It may be interesting to understand the image and the kernel of this homomorphism. In particular, if this homomorphism is surjective, this interpretation provides a new combinatorial description of the mapping class group of $\mathcal{S}_{n,k}$.

2.6.2 The dual graph

We now consider the dual map of the 2-cell-embedding $\mathcal{C}(T)$ on the surface $\mathcal{S}_{n,k}$: we denote $T^\#$ the graph whose vertices are the k-stars of T and with an edge between two k-stars for each of their common k-relevant edge. Remember that two k-stars can have until k common edges, which means that $T^\#$ is a multigraph. Observe also that it is naturally embedded on the surface $\mathcal{S}_{n,k}$ as the dual map of $\mathcal{C}(T)$ (see Figure 2.24). Again, this embedding is "naturally" defined up to a boundary preserving diffeomorphism of $\mathcal{S}_{n,k}$.

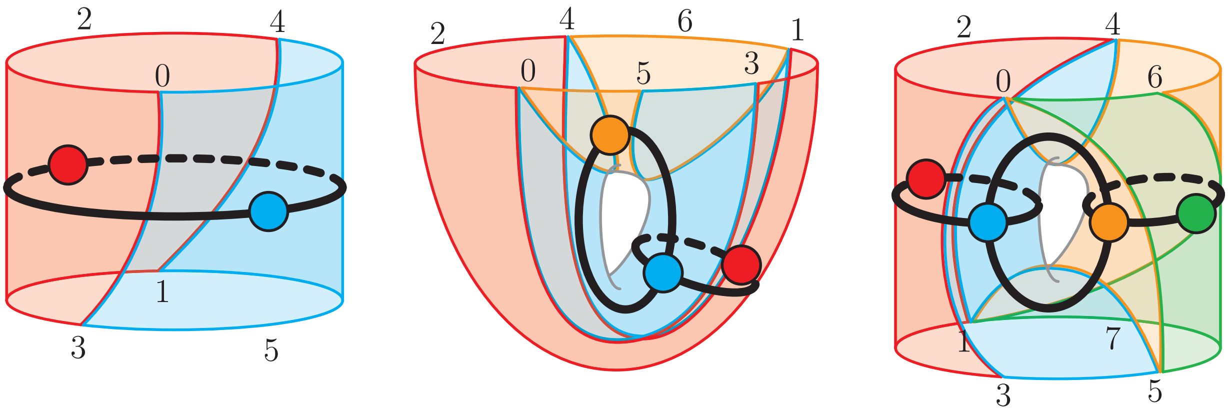

Figure 2.24: The dual maps of the surface decompositions of Figure 2.22.

By definition, this dual graph $T^{\#}$ has $n-2k$ vertices and $k(n-2k-1)$ edges. The degree of each vertex is between k and $2k+1$. It is also interesting to observe what happens when we cut the surface $\mathcal{S}_{n,k}$ along $T^{\#}$:

Lemma 2.69. *Cutting along the dual map $T^{\#}$ decomposes the surface $\mathcal{S}_{n,k}$ into $\gcd(n,k)$ cylinders. In each of these cylinders, one boundary is a boundary of $\mathcal{S}_{n,k}$ and the other one is formed only by edges of $T^{\#}$.*

Proof. When we have cut along all edges of $T^{\#}$, the polygons adjacent to a given boundary component B of $\mathcal{S}_{n,k}$ form a cycle of polygons, glued along edges. Since the surface is orientable, we obtain a cylinder, with B as one boundary, and a sequence of edges of $T^{\#}$ as the other boundary. Since all the vertices of $\mathcal{C}(T)$ are on the boundary of $\mathcal{S}_{n,k}$ there is no other pieces. $\square$

For example, when $k=1$, cutting along a tree included into a disk gives raise to a cylinder. It is intereseting to observe that duals of triangulations produce in fact all graphs which decompose the disk into a cylinder and whose vertices have degree between 1 and 3.

2.6.3 Equivelar polygonal decompositions

A polygonal decomposition of a surface is *(p,q)-equivelar* if all its faces are p-gons and all its vertices have degree q. Equivelarity is a local regularity condition: any regular polygonal decomposition (*i.e.* for which the automorphism group acts transitively on the flags), is clearly equivelar. For example, the boundary complexes of the Platonic solids define equivelar polygonal decompositions of the 2-sphere. Because of their symmetry, regular and equivelar decompositions of surfaces have received particular attention (see [BS97] and the references therein).

In this section, we use multitriangulations to derive equivelar polygonal decompositions of an infinite family of surfaces of high genus. The result is the following:

Theorem 2.70. *For any integers $\ell \geq 2$ and $m \geq 1$, there exists a $\big(2\ell m + 1, 2(\ell m - m + 1)\big)$-equivelar polygonal decomposition of the closed surface of genus*

$$g := (\ell - 1)\left(\ell^2 m^2 - \frac{\ell m}{2} - 1\right),$$

in which no two polygons share an edge. More precisely, we construct a proper polygonal decomposition of this surface with:

- $\ell(2\ell m + 1)$ *vertices, each of degree* $2(\ell m - m + 1)$*;*
- $\ell(\ell m - m + 1)(2\ell m + 1)$ *edges; and*
- $2\ell(\ell m - m + 1)$ *polygons, each of valence* $(2\ell m + 1)$*, and no two of which share two edges.*

We prove this theorem by constructing a multitriangulation T whose associated polygonal decomposition $\mathcal{C}(T)$ is equivelar. Choose $\ell \geq 2$ and $m \geq 1$. Let $k := \ell m$ and $n := \ell(2\ell m + 1)$. Since $\gcd(n, k) = \ell$, the surface $\mathcal{S}_{n,k}$ has ℓ boundary components, each of length $2\ell m + 1$, and has genus g. Thus, we obtain a closed surface $\hat{\mathcal{S}}_{n,k}$ of genus g by gluing a $(2\ell m + 1)$-gon on each boundary component of $\mathcal{S}_{n,k}$. Any k-triangulation of the n-gon defines a decomposition of $\hat{\mathcal{S}}_{n,k}$ into $2\ell(\ell m - m + 1)$ polygons of valence $(2\ell m + 1)$, with $\ell(\ell m - m + 1)(2\ell m + 1)$ edges and $\ell(2\ell m + 1)$ vertices. The end of this section is devoted to the construction of such a k-triangulation T with the property that:

(i) the degree of any vertex in T is $2m(2\ell - 1)$ (thus, the degree in $\mathcal{C}(T)$ is $2(\ell m - m + 1)$); and
(ii) any k-star of T shares at most one edge with each boundary component and with each other k-star of T.

We consider again (see Figure 2.13) the k-zigzag Z of E_n defined by:

$$Z := \left\{ [q-1, -q-k] \;\middle|\; 1 \leq q \leq \left\lfloor \frac{n-2k}{2} \right\rfloor \right\} \cup \left\{ [q, -q-k] \;\middle|\; 1 \leq q \leq \left\lfloor \frac{n-2k-1}{2} \right\rfloor \right\}.$$

Let ρ be the rotation $\rho : t \mapsto t + 2k + 1$, let θ be the rotation $\theta : t \mapsto t + 2$ and let σ be the reflection $\sigma : t \mapsto -t$. Let Γ denote the dihedral group of order 2ℓ generated by ρ and σ.

Lemma 2.71. *The set*

$$\bigcup_{i=0}^{m-1} \theta^i \left(\bigcup_{\gamma \in \Gamma} \gamma(Z) \right)$$

is the subset of the k-relevant edges of a k-triangulation $T_{l,m}$ of the n-gon.

Proof. Observe that Z has a stabilizer of cardinality 2 in Γ, so that $\bigcup_{\gamma \in \Gamma} \gamma(Z)$ consists of ℓ (and not 2ℓ) k-zigzags of E_n. Indeed,

(i) if ℓ is odd, then $\sigma(Z) = Z$, and $\bigcup_{\gamma \in \Gamma} \gamma(Z)$ is the disjoint union of the ℓ k-zigzags $\rho^i(Z)$, for $0 \leq i \leq \ell - 1$;
(ii) if ℓ is even, then $\rho^{\ell/2}(Z) = Z$, and $\bigcup_{\gamma \in \Gamma} \gamma(Z)$ is the disjoint union of the $\ell/2$ zigzags $\rho^i(Z)$, for $0 \leq i \leq \ell/2 - 1$, and the $\ell/2$ zigzags $\rho^i \circ \sigma(Z)$, for $0 \leq i \leq \ell/2 - 1$.

Consequently, the set $\bigcup_{i=0}^{m-1} \theta^i \left(\bigcup_{\gamma\in\Gamma} \gamma(Z)\right)$ is the union of $\ell m = k$ disjoint k-zigzags, which proves the result by Lemma 2.47. $\square$

In the end of this section, we always denote by $\bar{\Gamma}$ the quotient of Γ by the stabilizer of Z, so that each k-zigzag of $T_{l,m}$ is uniquely represented as the image of Z under a transformation of $\bar{\Gamma}$.

Example 2.72. Figure 2.25 shows these multitriangulations for the parameters

$$(\ell, m, n, k) \in \{(2, 1, 10, 2), (2, 2, 18, 4), (2, 3, 26, 6), (3, 1, 21, 3)\}.$$

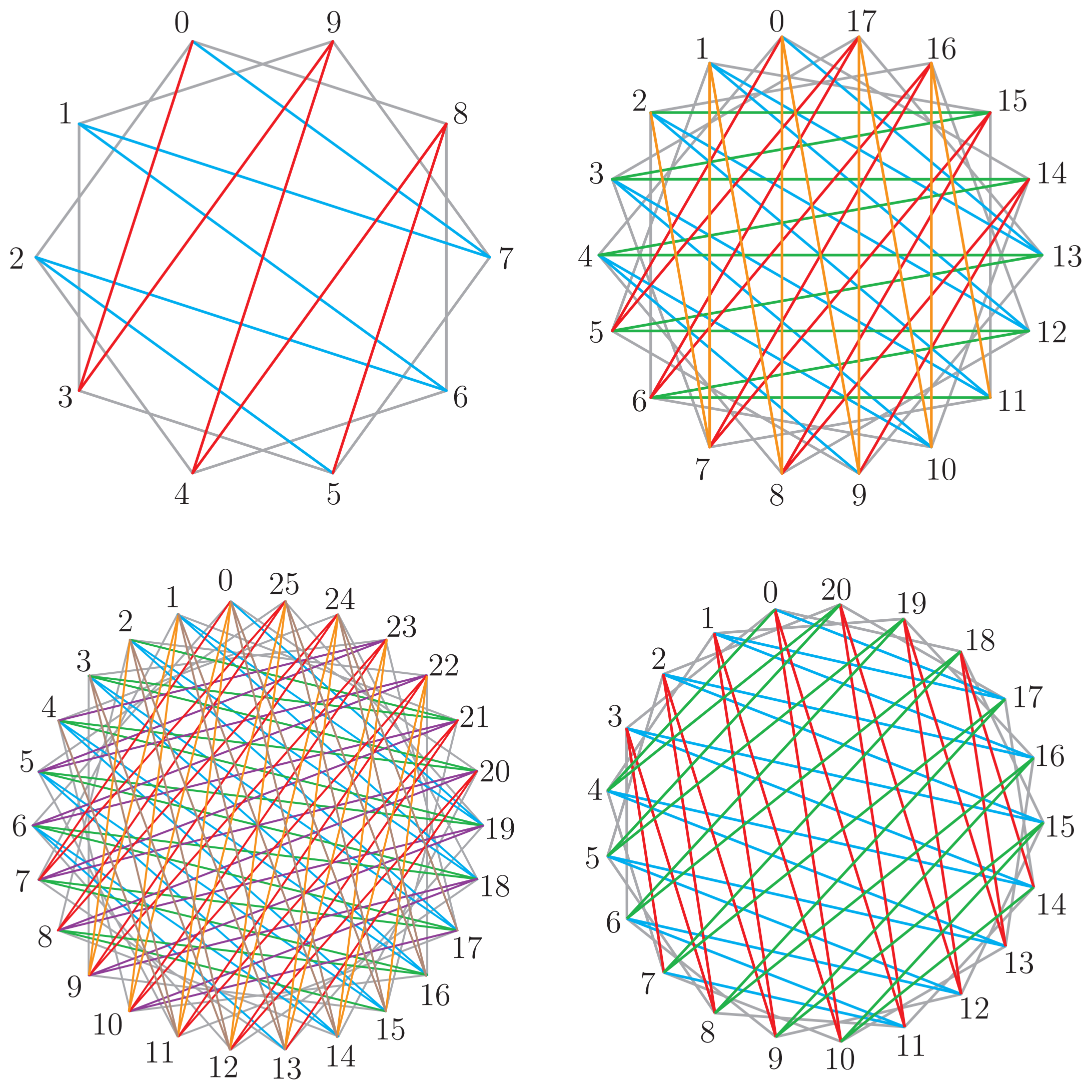

Figure 2.25: The very regular multitriangulation $T_{l,m}$ for $(\ell, m, n, k) = (2, 1, 10, 2)$ (top left), $(2, 2, 18, 4)$ (top right), $(2, 3, 26, 6)$ (bottom left), and $(3, 1, 21, 3)$ (bottom right).

Lemma 2.73. *The degree of any vertex in $T_{l,m}$ is $2m(2\ell - 1)$.*

Proof. Any vertex v of V_n is contained in $2(\ell - 1)$ edges of $\bigcup_{\gamma \in \Gamma} \gamma(Z)$. Consequently, v is contained in $2m(l - 1)$ k-relevant edges of $T_{l,m}$. Since it is contained in $2k$ k-irrelevant or k-boundary edges, the degree of v is $2m(\ell - 1) + 2m\ell = 2m(2\ell - 1)$. □

Lemma 2.74. *Any k-star of $T_{l,m}$ contains at most one edge on each boundary component of $\mathcal{S}_{n,k}$.*

Proof. Since $T_{l,m}$ does not contain any pair of consecutive k-ears, any k-star of $T_{l,m}$ contains at most two k-boundary edges (Lemma 2.41). These k-boundary edges are consecutive (for the cyclic order), and therefore they are not in the same boundary component of $\mathcal{S}_{n,k}$. □

It only remains to show that two k-stars of $T_{l,m}$ cannot share more than one edge. For this, we need to understand how k-stars and k-zigzags of $T_{l,m}$ are arranged together. Let $\bar{Z}$ be the unique $(k - 1)$-zigzag obtained by extending Z with to k-boundary edges.

Lemma 2.75. *Any k-star of $T_{l,m}$ contains exactly one k-boundary edge of $T_{l,m} \smallsetminus \cup_{\gamma \in \bar{\Gamma}} \gamma(\bar{Z})$ and exactly one angle of the zigzag $\gamma(\bar{Z})$ for each $\gamma \in \bar{\Gamma}$. Furthermore, the star order of these angles is given by the order of the set $\{\gamma(0) \mid \gamma \in \bar{\Gamma}\}$ around the circle.*

Proof. Since any two angles of a k-star define a crossing, a k-star can contain at most one angle of each zigzag. Since each zigzag $\gamma(\bar{Z})$ has $n - 2k$ angles, each k-star of $T_{l,m}$ has to contain exactly one angle of each zigzag. The last edge of each k-star is in no zigzags. Finally, the star order of the angles is given by the slope of the zigzags, which can be read on the positions of $\gamma(0)$. □

Lemma 2.76. *Any two k-stars of $T_{l,m}$ share at most one edge.*

Proof. Assume that two k-stars R and S share two edges. By symmetry, we can assume that these edges belong to the k-zigzags Z and $\gamma(Z)$, for a certain $\gamma \in \bar{\Gamma}$. Let $[r, r + k]$ denote the unique edge of R not contained in $\lambda(\bar{Z})$, for any $\lambda \in \bar{\Gamma}$. Define similarly the edge $[s, s + k]$ of S. Denote by $[a, b]$ and $[c, d]$ the common edges of R and S with $r \preccurlyeq a \prec b \preccurlyeq r + k$ and $s \preccurlyeq c \prec d \preccurlyeq s + k$. The previous lemma ensures that $|b - a| = |d - c|$ is the number of angles appearing between Z and $\gamma(Z)$ in star order around R and S. We deduce from this that all the edges $\{[a + i, c + i] \mid i < |b - a|\}$ are common to R and S. This finally implies that the transformation γ satisfies $\gamma(0) = 1$ which is absurd. □

Remark 2.77. Observe however that two k-stars of $T_{l,m}$ can share one edge plus some other vertices.

Finally, we want to observe the following properties of this polygonal decomposition:

1. When ℓ (or m) is big, the number of edges is equivalent to twice the genus, which is optimal.

2. When $m = 1$ (see Figure 2.25), the degree of the vertices and the number of edges of the polygons differ just by 1.
3. When $\ell = 2$ (see Figure 2.25), we have an equivelar decomposition of a surface of genus g with $4\sqrt{g}$ vertices of degree $\sqrt{g}$, with $2g$ edges, and with $2\sqrt{g}$ polygons of degree $2\sqrt{g}$.

Observe furthermore that the multitriangulation $T_{l,m}$, and thus the corresponding surface decomposition, is invariant by the dihedral group Γ.

Chapter Three

MULTIPSEUDOTRIANGULATIONS

In this chapter, we interpret multitriangulations in the line space of the plane. The set of all bisectors of a star is a pseudoline. Moreover, all pseudolines dual to the k-stars of a k-triangulation of the n-gon form a *pseudoline arrangement with contact points* whose support covers precisely the dual pseudoline arrangement of the vertex set of the n-gon except its first k levels. It relates multitriangulations with *pseudotriangulations*, for which a similar interpretation is known, and thus provides an explanation to their common properties.

Motivated by these two examples, we investigate in Section 3.1 the set of all pseudoline arrangements with contact points which cover a given support. We define a notion of *flip* between them, which extends the flip for multitriangulations and pseudotriangulations, and we study the graph of these flips. In particular, we provide an enumeration algorithm for pseudoline arrangements with a given support (similar to the enumeration algorithm of [BKPS06] for pseudotriangulations), based on certain *greedy pseudoline arrangements*. We define these greedy pseudoline arrangements as sources for certain orientations on the flip graph and we use extensively their relationship with *primitive sorting networks* [Knu73, Section 5.3.4]. Our algorithm requires a polynomial running time per multipseudotriangulation and its working space is polynomial.

The duality between pseudoline arrangements with contact points and multitriangulations (or pseudotriangulations) is only presented in Section 3.2. This duality leads to a natural definition of *multipseudotriangulations*, of which we study the elementary properties (number of edges, pointedness and crossings, stars, etc.) in Section 3.3.

3.1 PSEUDOLINE ARRANGEMENTS WITH THE SAME SUPPORT

3.1.1 Pseudoline arrangements in the Möbius strip

Let $\mathcal{M}$ denote the *Möbius strip* (without boundary), defined as the quotient set of the plane $\mathbb{R}^2$ under the map $\tau : \mathbb{R}^2 \to \mathbb{R}^2,\ (x, y) \mapsto (x + \pi, -y)$. The induced canonical projection will be denoted by $\pi : \mathbb{R}^2 \to \mathcal{M}$.

A *pseudoline* is the image under the canonical projection π of the graph $\{(x, f(x)) \mid x \in \mathbb{R}\}$ of a continuous and *π-antiperiodic* function $f : \mathbb{R} \to \mathbb{R}$ (that is, which satisfies $f(x+\pi) = -f(x)$ for all $x \in \mathbb{R}$). We say that f represents the pseudoline.

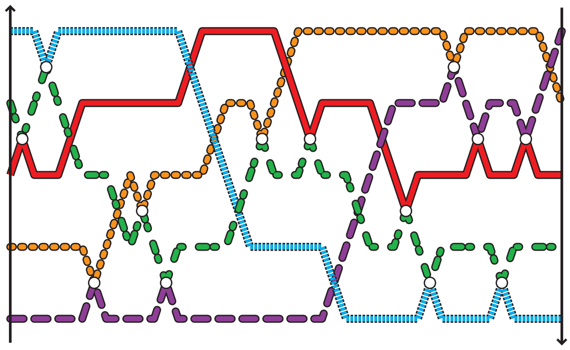

Figure 3.1: A pseudoline arrangement in the Möbius strip. Its contact points are represented by white circles.

When we consider two pseudolines, we always assume that they have a finite number of *intersection points*. Thus, these intersection points can only be either *crossing points* or *contact points* (see Figure 3.2(a)). Any two pseudolines always have an odd number of crossing points (in particular, at least one). When λ and μ have exactly one crossing point, we denote it by $\lambda \wedge \mu$.

A *pseudoline arrangement* is a finite set of pseudolines such that any two of them have exactly one crossing point and possibly some contact points (see Figure 3.1). In this chapter, we are only interested in *simple* arrangements, that is, where no three pseudolines meet in a common point. The *support* of a pseudoline arrangement is the union of its pseudolines. Observe that an arrangement is completely determined by its support together with its set of contact points.

Remark 3.1. Usually, the definition of pseudoline arrangements does not allow contact points. In this chapter, they play a crucial role since we are interested in all pseudoline arrangements which share a common support, and which only differ by their sets of contact points.

Pseudoline arrangements are also classically defined on the projective plane rather than the Möbius strip. The projective plane is obtained from the Möbius strip by adding a point at infinity.

For more details on pseudoline arrangements, we refer to the broad literature on the topic [Grü72, BVS+99, Knu92] and in particular the survey paper [Goo97]. In Appendix A.1, we discuss some classical features of arrangements (of pseudolines and double pseudolines) in the presentation of an enumeration algorithm for arrangements.

3.1.2 The flip graph and the greedy pseudoline arrangements

3.1.2.1 Flips

The following lemma defines the notion of flips (see Figure 3.2), to be studied in this chapter. As usual, we use the symbol $\triangle$ for the symmetric difference: $X \triangle Y := (X \smallsetminus Y) \cup (Y \smallsetminus X)$.

Lemma 3.2. *Let Λ be a pseudoline arrangement, S be its support, and V be the set of its contact points. Let $v \in V$ be a contact point of two pseudolines of Λ, and w denote their crossing point. Then $V \triangle \{v, w\}$ is also the set of contact points of a pseudoline arrangement Λ' supported by S.*

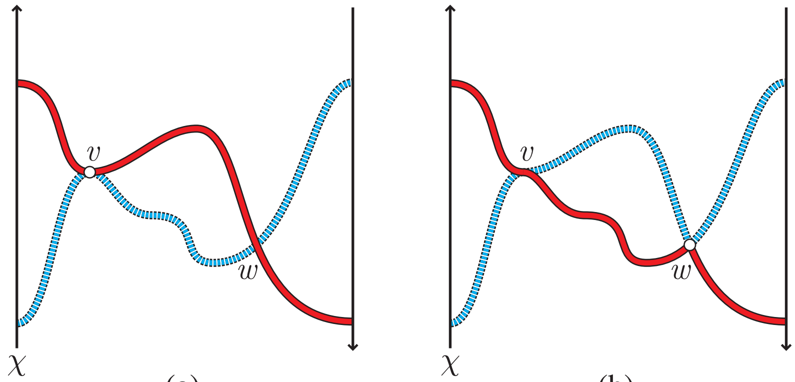

(a) (b)

Figure 3.2: (a) A pseudoline arrangement with one contact point v and one crossing point w; (b) Flipping v in the pseudoline arrangement of (a).

Proof. Let f and g represent the two pseudolines λ and μ of Λ in contact at v. Let x and y be such that $v = \pi(x, f(x))$, $w = \pi(y, f(y))$ and $x < y < x + \pi$. We define two functions f' and g' by:

$$f' := \begin{cases} f & \text{on } [x, y] + \mathbb{Z}\pi, \\ g & \text{otherwise,} \end{cases} \qquad \text{and} \qquad g' := \begin{cases} g & \text{on } [x, y] + \mathbb{Z}\pi, \\ f & \text{otherwise.} \end{cases}$$

These two functions are continuous and π-antiperiodic, and thus define two pseudolines λ' and μ'. These two pseudolines have a contact point at w and a unique crossing point at v, and they cross any pseudoline ν of $\Lambda \smallsetminus \{\lambda, \mu\}$ exactly once (since ν either crosses both λ and μ between v and w, or crosses both λ and μ between w and v). Consequently, $\Lambda' := \Lambda \triangle \{\lambda, \mu, \lambda', \mu'\}$ is a pseudoline arrangement, with support $\mathcal{S}$, and contact points $V \triangle \{v, w\}$. $\square$

The pseudoline arrangements Λ and Λ' are the only two pseudoline arrangements supported by $\mathcal{S}$ whose sets of contact points contain $V \smallsetminus \{v\}$. We call *flip* the transformation from Λ to Λ', interchanging the roles of v and w. The central object in this chapter is the flip graph:

Definition 3.3. *Let $\mathcal{S}$ be the support of a pseudoline arrangement. The* flip graph *of $\mathcal{S}$, denoted by $G(\mathcal{S})$, is the graph whose vertices are all the pseudoline arrangements supported by $\mathcal{S}$, and whose edges are flips between them.*

In other words, there is an edge in the graph $G(\mathcal{S})$ between two pseudoline arrangements if and only if their sets of contact points differ by exactly two points. Observe that the graph $G(\mathcal{S})$ is regular: there is one edge adjacent to a pseudoline arrangement Λ supported by $\mathcal{S}$ for each contact point of Λ, and two pseudoline arrangements with the same support have the same number of contact points.

Example 3.4. The flip graph of the support of an arrangement of two pseudolines with p contact points is the complete graph on $p + 1$ vertices.

3.1.2.2 Unique source orientations

Let $\mathcal{S}$ be the support of a pseudoline arrangement and $\bar{\mathcal{S}}$ denote its preimage under the projection π. We orient the graph $\bar{\mathcal{S}}$ along the abscissa increasing direction, and the graph $\mathcal{S}$ by projecting the orientations of the edges of $\bar{\mathcal{S}}$. We denote by $\preccurlyeq$ the induced partial order on the vertex set of $\bar{\mathcal{S}}$ (defined by $z \preccurlyeq z'$ if there exists an oriented path on $\bar{\mathcal{S}}$ from z to z').

A *filter* of $\bar{\mathcal{S}}$ is a proper set F of vertices of $\bar{\mathcal{S}}$ such that $z \in F$ and $z \preccurlyeq z'$ implies $z' \in F$. The corresponding *antichain* is the set of all edges and faces of $\bar{\mathcal{S}}$ with one vertex in F and one vertex not in F. This antichain has a linear structure, and thus, can be seen as the set of edges and faces that cross a vertical curve $\bar{\chi}$ of $\mathbb{R}^2$. The projection $\chi := \pi(\bar{\chi})$ of such a curve is called a *cut* of $\mathcal{S}$. We see the fundamental domain located between the two curves $\bar{\chi}$ and $\tau(\bar{\chi})$ as the result of cutting the Möbius strip along the cut χ. For example, we use such a cut to represent pseudoline arrangements in all figures of this chapter. See for example Figure 3.2.

The cut χ defines a partial order $\preccurlyeq_\chi$ on the vertex set of $\mathcal{S}$: for all vertices v and w of $\mathcal{S}$, we write $v \preccurlyeq_\chi w$ if there is an oriented path in $\mathcal{S}$ which does not cross χ. In other words, $v \preccurlyeq_\chi w$ if $\bar{v} \preccurlyeq \bar{w}$, where $\bar{v}$ (resp. $\bar{w}$) denotes the unique preimage of v (resp. w) between $\bar{\chi}$ and $\tau(\bar{\chi})$. For example, in the arrangements of Figure 3.2, we have $v \prec_\chi w$.

Let Λ be a pseudoline arrangement supported by $\mathcal{S}$, v be a contact point between two pseudolines of Λ and w denote their crossing point. Since v and w lie on a same pseudoline on $\mathcal{S}$, they are comparable for $\preccurlyeq_\chi$. We say that the flip of v is *χ-increasing* if $v \prec_\chi w$ and *χ-decreasing* otherwise. For example, the flip from (a) to (b) in Figure 3.2 is χ-increasing. We denote by $G_\chi(\mathcal{S})$ the directed graph of χ-increasing flips on pseudoline arrangements supported by $\mathcal{S}$.

Theorem 3.5. *The directed graph $G_\chi(\mathcal{S})$ is an acyclic connected graph with a unique source.*

Definition 3.6. *This unique source is denoted by $\Gamma_\chi(\mathcal{S})$ and called the* χ-greedy pseudoline arrangement *on $\mathcal{S}$.*

Proof of Theorem 3.5. If Λ and Λ' are two pseudoline arrangements supported by $\mathcal{S}$, we write $\Lambda \trianglelefteq_\chi \Lambda'$ if there exists a bijection ϕ between their sets of contact points such that $v \preccurlyeq_\chi \phi(v)$ for any contact point v of Λ. It is easy to see that this relation is a partial order on the vertices of $G_\chi(\mathcal{S})$. Since the edges of $G_\chi(\mathcal{S})$ are oriented according to $\trianglelefteq_\chi$, the graph $G_\chi(\mathcal{S})$ is acyclic. (In fact, $G_\chi(\mathcal{S})$ is even the Hasse diagram of the partial order $\trianglelefteq_\chi$.)

That $G_\chi(\mathcal{S})$ has a unique source will be proved next in Theorem 3.7, where we will provide a characterization of $\Gamma_\chi(\mathcal{S})$ in terms of sorting networks.

Finally, an acyclic directed graph with only one source is necessarily connected. $\square$

3.1.2.3 Sorting networks

Let n denote the number of pseudolines of the arrangements supported by $\mathcal{S}$ and $m \geq \binom{n}{2}$ their number of intersection points (crossing points plus contact points). We consider a chain $F = F_m \supset F_{m-1} \supset \cdots \supset F_1 \supset F_0 = \tau(F)$ of filters of $\bar{\mathcal{S}}$ such that two consecutive of them F_i and F_{i+1} only differ by a single element: $\{\bar{v}_i\} := F_{i+1} \setminus F_i$. This corresponds to a (backward) *sweep* $\chi = \chi_0, \chi_1, \dots, \chi_m = \chi$ of the Möbius strip, where each cut χ_{i+1} is obtained

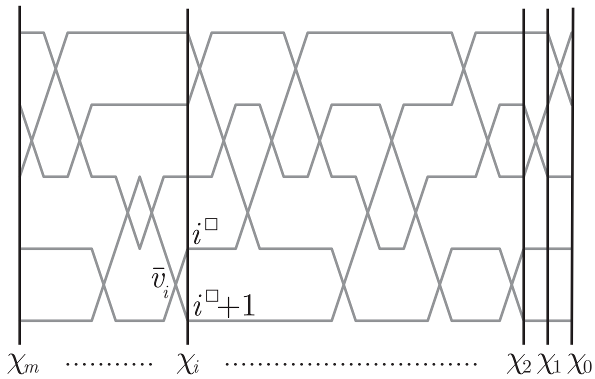

Figure 3.3: A (backward) sweep of the support of the pseudoline arrangement of Figure 3.1.

from the cut χ_i by sweeping a maximal vertex $v_i := \pi(\bar{v}_i)$ of $\mathcal{S}$ (for the partial order $\preccurlyeq_\chi$). For all i, let $e_i^1, e_i^2, \dots, e_i^n$ denote the sequence of edges of $\bar{\mathcal{S}}$ with exactly one vertex in F_i, ordered from top to bottom, and let $i^\square$ be the index such that $\bar{v}_i$ is the common point of edges $e_i^{i^\square}$ and $e_i^{i^\square+1}$ (see Figure 3.3).

Let $\Lambda := (\lambda_1, \dots, \lambda_n)$ be a pseudoline arrangement supported by $\mathcal{S}$. For all i, we denote by σ_i^Λ the permutation of $\{1, \dots, n\}$ whose jth entry $\sigma_i^\Lambda(j)$ is the index of the pseudoline supporting e_i^j, *i.e.* such that $\pi(e_i^j) \subset \lambda_{\sigma_i^\Lambda(j)}$. Up to reindexing the pseudolines of Λ, we can assume that σ_0^Λ is the inverted permutation $\sigma_0^\Lambda := (n, n-1, \dots, 2, 1)$, and consequently that σ_m^Λ is the identity permutation. Observe that for all i:

(i) if v_i is a contact point of Λ, then $\sigma_i^\Lambda = \sigma_{i+1}^\Lambda$;

(ii) otherwise, σ_{i+1}^Λ is obtained from σ_i^Λ by inverting its $i^\square$th and $(i^\square + 1)$th entries.

These permutations provide a characterization of the source of $G_\chi(\mathcal{S})$ (see Figure 3.4):

Theorem 3.7. *The unique source $\Gamma_\chi(\mathcal{S})$ of the directed graph $G_\chi(\mathcal{S})$ is characterized by the property that for all i, the permutation σ_{i+1}^Γ is obtained from σ_i^Γ by sorting its $i^\square$th and $(i^\square+1)$th entries.*

Proof. If Γ satisfies the above property, then it is obviously a source of the directed graph $G_\chi(\mathcal{S})$: any flip of Γ is χ-increasing since two of its pseudolines cannot touch before they cross.

Assume reciprocally that Γ is a source of $G_\chi(\mathcal{S})$. Let $a := \sigma_i^\Gamma(i^\square)$ and $b := \sigma_i^\Gamma(i^\square + 1)$. We have two possible situations:

(i) If $a < b$, then the two pseudolines λ_a and λ_b of Γ already cross before v_i. Consequently, v_i is necessarily a contact point of Γ, which implies that $\sigma_{i+1}^\Gamma(i^\square) = a$ and $\sigma_{i+1}^\Gamma(i^\square + 1) = b$.

(ii) If $a > b$, then the two pseudolines λ_a and λ_b of Γ do not cross before v_i. Since Γ is a source of $G_\chi(\mathcal{S})$, v_i is necessarily a crossing point of Γ. Thus $\sigma_{i+1}^\Gamma(i^\square) = b$ and $\sigma_{i+1}^\Gamma(i^\square + 1) = a$.

In both cases, σ_{i+1}^Γ is obtained from σ_i^Γ by sorting its $i^\square$th and $(i^\square + 1)$th entries. $\square$

Let us reformulate Theorem 3.7 in terms of sorting networks (see [Knu73, Section 5.3.4] for a detailed presentation; see also [dB74]). Let $i < j$ be two integers. A *comparator* $[i : j]$ transforms a sequence of numbers $(a_1, \dots, a_n)$ by sorting (a_i, a_j), *i.e.* replacing a_i by $\min(a_i, a_j)$

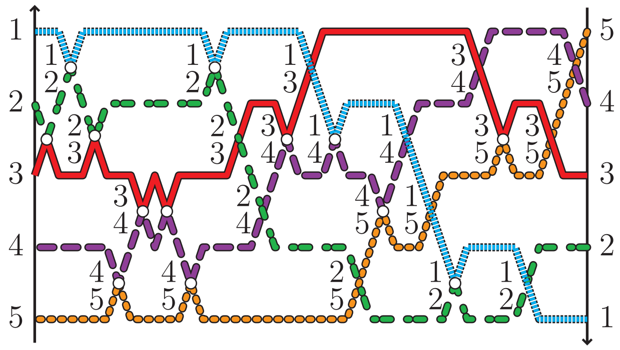

Figure 3.4: The greedy pseudoline arrangement on the support of Figure 3.1, obtained by sorting permutation $(5, 4, 3, 2, 1)$ on the corresponding network. The result of each comparator is written after it (*i.e.* to its left since we sweep backwards).

and a_j by $\max(a_i, a_j)$. A comparator $[i : j]$ is *primitive* if $j = i + 1$. A *sorting network* is a sequence of comparators that sorts any sequence $(a_1, \ldots, a_n)$.

The support $\mathcal{S}$ of an arrangement of n pseudolines together with a sweep $F_m \supset \cdots \supset F_0$ defines a primitive sorting network $[1^\square : 1^\square + 1], \ldots, [m^\square : m^\square + 1]$ (see [Knu92, Section 8]). Theorem 3.7 affirms that sorting the permutation $(n, n-1, \ldots, 2, 1)$ according to this sorting network provides a pseudoline arrangement supported by $\mathcal{S}$, which depends only upon the support $\mathcal{S}$ and the filter F_0 (not on the total order given by the sweep).

3.1.2.4 Greedy set of contact points

In this paragraph, we give another construction of the greedy pseudoline arrangement.

Let $\mathcal{S}$ be the support of a pseudoline arrangement, and χ be a cut of S. We construct recursively a sequence $v_1, \ldots, v_q$ of vertices of $\mathcal{S}$ where for all i, the vertex v_i is a minimal (for the partial order $\preccurlyeq_\chi$) remaining vertex of $\mathcal{S}$ such that $\{v_1, \ldots, v_i\}$ is a subset of the set of contact points of a pseudoline arrangement supported by $\mathcal{S}$. This procedure obviously finishes and provides a set $V := \{v_1, \ldots, v_q\}$ of vertices of $\mathcal{S}$, which turns out to be the set of contact points of the χ-greedy pseudoline arrangement:

Proposition 3.8. *The set V is exactly the set of contact points of $\Gamma_\chi(\mathcal{S})$.*

Proof. First of all, V is by construction the set of contact points of a pseudoline arrangement Λ supported by $\mathcal{S}$. If Λ is not the (unique) source $\Gamma_\chi(\mathcal{S})$ of the oriented graph $G_\chi(\mathcal{S})$, then there is a contact point v_i of Λ whose flip is χ-decreasing. Let w denote the corresponding crossing point, and Λ' the pseudoline arrangement obtained from Λ by flipping v_i. This implies that $\{v_1, \ldots, v_{i-1}, w\}$ is a subset of the set of contact points of Λ' and that $w \prec_\chi v_i$, which contradicts the minimality of v_i. $\square$

Essentially, this proposition affirms that we obtain the same pseudoline arrangement when:

(i) sweeping $\mathcal{S}$ increasingly and place crossing points as long as possible; or

(ii) sweeping $\mathcal{S}$ decreasingly and place contact points as long as possible.

3.1.2.5 Constrained flip graph

Let $\mathcal{S}$ be the support of a pseudoline arrangement, V be a subset of vertices of $\mathcal{S}$, and χ be a cut of $\mathcal{S}$. We denote by $G(\mathcal{S}\,|\,V)$ (resp. $G_\chi(\mathcal{S}\,|\,V)$) the subgraph of $G(\mathcal{S})$ (resp. $G_\chi(\mathcal{S})$) induced by the pseudoline arrangements with support $\mathcal{S}$ and whose set of contact points contains V.

Theorem 3.9. *The directed graph $G_\chi(\mathcal{S}\,|\,V)$ either is empty or is an acyclic connected graph with a unique source $\Gamma_\chi(\mathcal{S}\,|\,V)$ characterized by the property that for all i:*
(i) if $v_i \in V$, then $\sigma^\Gamma_{i+1} = \sigma^\Gamma_i$;
(ii) if $v_i \notin V$, then σ^Γ_{i+1} is obtained from σ^Γ_i by sorting its $i^\square$th and $(i^\square + 1)$th entries.

Proof. We transform our support $\mathcal{S}$ into another one $\mathcal{S}'$ by opening all intersection points of V (the local picture of this transformation is $\times \to \asymp$). If $\mathcal{S}'$ supports at least one pseudoline arrangement, we apply the result of Theorem 3.7: a pseudoline arrangement supported by $\mathcal{S}'$ corresponds to a pseudoline arrangement with support $\mathcal{S}$ whose set of contact points contains V. $\square$

In terms of sorting networks, $\Gamma_\chi(\mathcal{S}\,|\,V)$ is the result of the sorting of the inverted permutation $(n, n-1, \ldots, 2, 1)$ by the restricted primitive network $([i^\square : i^\square + 1])_{i\in I}$, where $I := \{i \,|\, v_i \notin V\}$.

Observe also that we can obtain, like in the previous subsection, the contact points of $\Gamma_\chi(\mathcal{S}\,|\,V)$ by an iterative procedure: we start from the set V and add recursively a minimal (for the partial order $\preccurlyeq_\chi$) remaining vertex v_i of $\mathcal{S}$ such that $V \cup \{v_1, \ldots, v_i\}$ is a subset of the set of contact points of a pseudoline arrangement supported by $\mathcal{S}$. The vertex set produced by this procedure is the set of contact points of the χ-greedy constrained pseudoline arrangement $\Gamma_\chi(\mathcal{S}\,|\,V)$.

3.1.3 Greedy flip property and enumeration

3.1.3.1 The greedy flip property

We are now ready to state the *greedy flip property* (see Figure 3.5) that says how to update the greedy pseudoline arrangement $\Gamma_\chi(\mathcal{S}\,|\,V)$ when either χ or V are slightly perturbed.

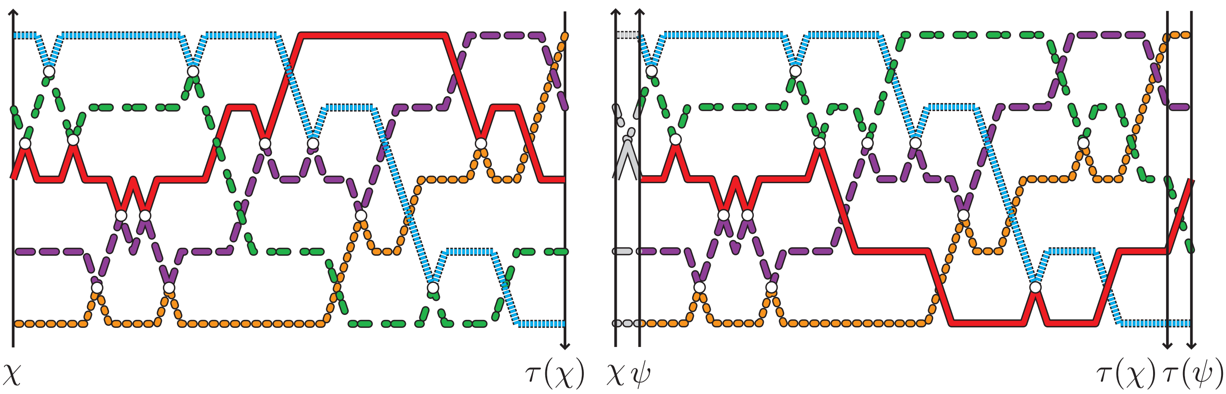

Figure 3.5: The greedy flip property.

Theorem 3.10 (Greedy flip property)**.** *Let $\mathcal{S}$ be the support of a pseudoline arrangement. Let χ be a cut of $\mathcal{S}$, v be a minimal (for the order $\preccurlyeq_\chi$) vertex of $\mathcal{S}$, and ψ denote the cut obtained from χ by sweeping v. Let V be a set of vertices of $\mathcal{S}$ (such that $G(\mathcal{S}\,|\,V)$ is not empty), and $W := V \cup \{v\}$. Then:*

1. *If v is a contact point of $\Gamma_\chi(\mathcal{S}\,|\,V)$ which is not in V, then $\Gamma_\psi(\mathcal{S}\,|\,V)$ is obtained from $\Gamma_\chi(\mathcal{S}\,|\,V)$ by flipping v. Otherwise, $\Gamma_\psi(\mathcal{S}\,|\,V) = \Gamma_\chi(\mathcal{S}\,|\,V)$.*
2. *If v is a contact point of $\Gamma_\chi(\mathcal{S}\,|\,V)$, then $\Gamma_\psi(\mathcal{S}\,|\,W) = \Gamma_\chi(\mathcal{S}\,|\,V)$. Otherwise, $G(\mathcal{S}\,|\,W)$ is empty.*

Proof. We consider a sweep

$$F_{m+1} = F \supset F_m = F' \supset F_{m-1} \supset \cdots \supset F_2 \supset F_1 = \tau(F) \supset F_0 = \tau(F')$$

such that F (resp. F') is a filter corresponding to the cut χ (resp. ψ). Define $\bar{v}_i := F_{i+1} \smallsetminus F_i$, $v_i := \pi(\bar{v}_i)$, and $i^\square$ as previously. Let $\sigma_1, \dots, \sigma_{m+1}$ denote the sequence of permutations corresponding to $\Gamma_\chi(\mathcal{S}\,|\,V)$ on the sweep $F_1 \subset \cdots \subset F_{m+1}$. In other words:

(i) σ_1 is the inverted permutation $(n, n-1, \dots, 2, 1)$;
(ii) if $v_i \in V$, then $\sigma_{i+1} = \sigma_i$;
(iii) otherwise, σ_{i+1} is obtained from σ_i by sorting its $i^\square$th and $(i^\square + 1)$th entries.

Similarly, let $\rho_0, \dots, \rho_m$ and $\omega_0, \dots, \omega_m$ denote the sequences of permutations corresponding to $\Gamma_\psi(\mathcal{S}\,|\,V)$ and $\Gamma_\psi(\mathcal{S}\,|\,W)$ respectively on the sweep $F_0 \subset \cdots \subset F_m$.

Assume first that v is a contact point of $\Gamma_\chi(\mathcal{S}\,|\,V)$, but is not in V. Let j denote the integer such that v_j is the crossing point of the two pseudolines of $\Gamma_\chi(\mathcal{S}\,|\,V)$ that are in contact at v. We claim that in this case $\Gamma_\psi(\mathcal{S}\,|\,V)$ is obtained from $\Gamma_\chi(\mathcal{S}\,|\,V)$ by flipping v, *i.e.* that:

(i) for all $1 \le i \le j$, ρ_i is obtained from σ_i by exchanging $m^\square$ and $m^\square + 1$;
(ii) for all $j < i \le m$, $\rho_i = \sigma_i$.

Indeed, ρ_1 is obtained by exchanging $m^\square$ and $m^\square + 1$ in $\rho_0 = (n, n-1, \dots, 2, 1) = \sigma_1$ (since $m^\square$ and $m^\square + 1$ are the $(0^\square + 1)$th and $0^\square$th entries of ρ_0 respectively). Then, any comparison between two consecutive entries give the same result in ρ_i and in σ_i, until $m^\square$ and $m^\square + 1$ are compared again, *i.e.* until $i = j$. At this stage, $m^\square$ and $m^\square + 1$ are already sorted in ρ_j but not in σ_j. Consequently, we have to exchange $m^\square$ and $m^\square + 1$ in σ_j and not in ρ_j, and we obtain $\sigma_{j+1} = \rho_{j+1}$. After this, all the comparisons give the same result in ρ_i and σ_i, and $\rho_i = \sigma_i$ for all $j < i \le m$.

We prove similarly that:

- When v is not a crossing point of $\Gamma_\chi(\mathcal{S}\,|\,V)$, or is in V, $\rho_i = \sigma_i$ for all $i \in [m]$, and $\Gamma_\psi(\mathcal{S}\,|\,V) = \Gamma_\chi(\mathcal{S}\,|\,V)$.
- When v is a contact point of $\Gamma_\chi(\mathcal{S}\,|\,V)$, $\omega_i = \sigma_i$ for all $i \in [m]$, and $\Gamma_\psi(\mathcal{S}\,|\,W) = \Gamma_\chi(\mathcal{S}\,|\,V)$.

Finally, we prove that $G(\mathcal{S}\,|\,W)$ is empty when v is not a contact point of $\Gamma_\chi(\mathcal{S}\,|\,V)$. For this, assume that $G(\mathcal{S}\,|\,W)$ is not empty, and consider the greedy arrangement $\Gamma = \Gamma_\chi(\mathcal{S}\,|\,W)$. The flip of any contact point of Γ not in W is χ-increasing. Furthermore, since v is a minimal element for $\preccurlyeq_\chi$, the flip of v is also χ-increasing. Consequently, Γ is a source in the graph $G_\chi(\mathcal{S}\,|\,V)$, which implies that $\Gamma_\chi(\mathcal{S}\,|\,V) = \Gamma$, and thus, v is a contact point of $\Gamma_\chi(\mathcal{S}\,|\,V)$. $\square$

3.1.3.2 Enumeration

From this greedy flip property, we derive an algorithm to enumerate all pseudoline arrangements with a given support. In the next section, we will see the relation between this algorithm and the enumeration algorithm of [BKPS06] for pseudotriangulations of a point set.

Let $\mathcal{S}$ be the support of a pseudoline arrangement with a cut χ. We say that a pseudoline arrangement is *colored* if its contact points are colored in blue, green or red. A green or red contact point is fixed for the end of the algorithm, while a blue one can be flipped. In the algorithm, we construct a binary tree $\mathcal{T}$, whose nodes are colored pseudoline arrangements supported by $\mathcal{S}$, as follows:

(i) The root of the tree is the χ-greedy pseudoline arrangement on $\mathcal{S}$, entirely colored in blue.

(ii) Any node Λ of $\mathcal{T}$ is a leaf of $\mathcal{T}$ if either it contains a green contact point or it only contains red contact points.

(iii) Otherwise, we choose a minimal blue point v of Λ. The right child of Λ is obtained by flipping v and coloring it in blue if the flip is χ-increasing and in green if the flip is χ-decreasing. The left child of Λ is obtained by changing the color of v into red.

This algorithm depends upon what minimal blue point v we choose at each step. However, no matter what this choice is, we obtain all pseudoline arrangements supported by $\mathcal{S}$:

Theorem 3.11. *The set of pseudoline arrangements supported by $\mathcal{S}$ is exactly the set of red-colored leafs of $\mathcal{T}$.*

Proof. The proof is similar to that of Theorem 9 in [BKPS06].

We define inductively a cut $\chi(\Lambda)$ for each node Λ of $\mathcal{T}$: the cut of the root is χ, and for each node Λ the cut of its children is obtained from χ by sweeping the contact point v. We also denote $V(\Lambda)$ the set of red contact points of Λ. With these notations, the greedy flip property (Theorem 3.10) ensures that $\Lambda = \Gamma_{\chi(\Lambda)}(\mathcal{S} \,|\, V(\Lambda))$, for each node Λ of $\mathcal{T}$.

The fact that any red-colored leaf of $\mathcal{T}$ is a pseudoline arrangement supported by $\mathcal{S}$ is obvious. Reciprocally, let us prove that any pseudoline arrangement supported by $\mathcal{S}$ is a red leaf of $\mathcal{T}$. Let Λ be a pseudoline arrangement supported by $\mathcal{S}$. We define inductively a path $\Lambda_0, \dots, \Lambda_p$ in the tree $\mathcal{T}$ as follows: Λ_0 is the root of $\mathcal{T}$ and for all $i \geq 0$, Λ_{i+1} is the left child of Λ_i if the minimal blue contact point of Λ_i is a contact point of Λ, and its right child otherwise (we stop when we reach a leaf). We claim that for all $0 \leq i \leq p$:

- the set $V(\Lambda_i)$ is a subset of contact points of Λ;
- the contact points of Λ not in $V(\Lambda_i)$ are not located between $\chi(\Lambda)$ and χ;

from which we derive that $\Lambda = \Lambda_p$ is a red-colored leaf. □

Let us briefly discuss the complexity of this algorithm. We assume that the input of the algorithm is a pseudoline arrangement and we consider a flip as an elementary operation. Then, this algorithm requires a polynomial running time per pseudoline arrangement supported by $\mathcal{S}$. As for many enumeration algorithms, the crucial point of this algorithm is that its working space is also polynomial (while the number of pseudoline arrangements supported by $\mathcal{S}$ is exponential).

3.2 Dual pseudoline arrangements

In this section, we prove that both the graph of flips on "(pointed) pseudotriangulations of a point set" and the graph of flips on "multitriangulations of a convex polygon" can be interpreted as graphs of flips on "pseudoline arrangements with a given support". This interpretation is based on the classical duality that we briefly recall in the first subsection, and yields to a natural definition of "multipseudotriangulations of a pseudoline arrangement" that we present in Section 3.3.

3.2.1 The dual pseudoline arrangement of a point set

To a given oriented line in the Euclidean plane, we usually associate its angle $\theta \in \mathbb{R}/2\pi\mathbb{Z}$ with the horizontal axis and its algebraic distance $d \in \mathbb{R}$ to the origin (*i.e.* the value of $\langle(-u, v) \,|\, .\rangle$ on the line, where (u, v) is its unitary direction vector). Since the same line oriented in the other direction gives an angle $\theta + \pi$ and a distance $-d$, this parametrization naturally associates a point of the Möbius strip to each line of the Euclidean plane. In other words, the line space of the Euclidean plane is (isomorphic to) the Möbius strip.

Via this parametrization, the set of lines passing through a point p forms a pseudoline p^*. The pseudolines p^* and q^* dual to two distinct points p and q have a unique crossing point dual to the line (pq). Thus, for a finite point set P in the Euclidean plane, the set $P^* := \{p^* \,|\, p \in P\}$ is a pseudoline arrangement without contact points (see Figure 3.6). Again, we always assume that the point set P is in general position (no three points lie in a same line), so that the arrangement P^* is simple.

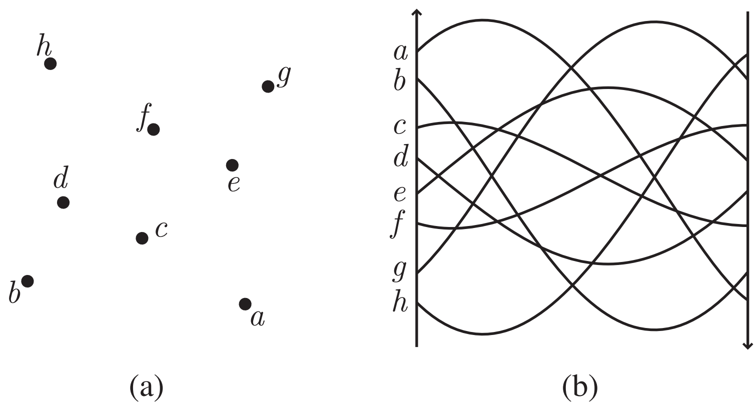

Figure 3.6: (a) A point set P in general position and (b) its dual pseudoline arrangement P^*.

This elementary duality also holds for any topological plane (or $\mathbb{R}^2$-plane, see [SBG+95] for a definition), not only for the real Euclidean plane $\mathbb{R}^2$. That is to say, the line space of a topological plane is (isomorphic to) the Möbius strip and the dual of a finite set of points in a topological plane is a pseudoline arrangement without contact points. Let us also recall that any pseudoline arrangement of the Möbius strip without contact points is the dual arrangement of a finite set of points in a certain topological plane [GPWZ94]. Thus, in the rest of this chapter, we deal with sets of points and their duals without restriction to the Euclidean plane.

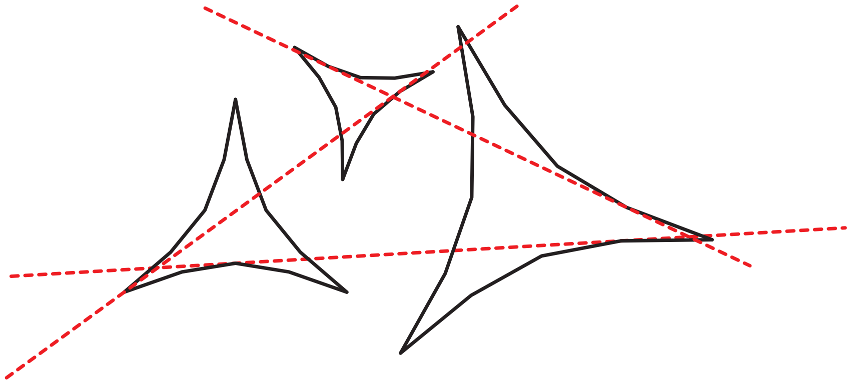

Figure 3.7: Three pseudotriangles and their common tangents.

3.2.2 The dual pseudoline arrangement of a pseudotriangulation

Introduced by Michel Pocchiola and Gert Vegter in their study of the visibility complex of a set of disjoint convex obstacles in the plane [PV96b, PV96c], pseudotriangulations were then used in different contexts such as motion planning and rigidity theory [Str05, HOR+05]. Their combinatorial and geometric structure has been extensively studied in the last decade (number of pseudotriangulations [AAKS04, AOSS08], polytope of pseudotriangulations [RSS03], algorithmic issues [Ber05, BKPS06, HP], etc.). We refer to [RSS08] for a detailed survey on the subject, and just recall here the elementary definitions we need:

Definition 3.12. *A pseudotriangle is a polygon Δ with only three convex vertices (the corners of Δ), joined by three concave polygonal chains (Figure 3.7). A line is said to be tangent to Δ if:*

(i) either it passes through a corner of Δ and separates the two edges incident to it;

(ii) or it passes through a concave vertex of Δ and does not separate the two edges incident to it.

A pseudotriangulation of a point set P in general position is a set of edges of P which decomposes the convex hull of P into pseudotriangles.

In this dissertation, we only deal with *pointed* pseudotriangulations, meaning that for any point $p \in P$, there exists a line which passes through p and defines a half-plane containing all the edges incident to p. Under this assumption, any two pseudotriangles of a pseudotriangulation have a unique common tangent. This leads to the following observation (first stated in [PV94, PV96a] in the context of pseudotriangulations of convex bodies):

Observation 3.13. Let T be a pseudotriangulation of a point set P in general position. Then:

(i) the set Δ^* of all tangents to a pseudotriangle Δ of T is a pseudoline in the Möbius strip;

(ii) the set $T^* := \{\Delta^* \mid \Delta \text{ pseudotriangle of } T\}$ of dual pseudolines of the pseudotriangles of T is a pseudoline arrangement (with contact points); and

(iii) T^* is supported by P^* minus its first level (see Figure 3.8(b)).

It turns out that this covering property characterizes pseudotriangulations:

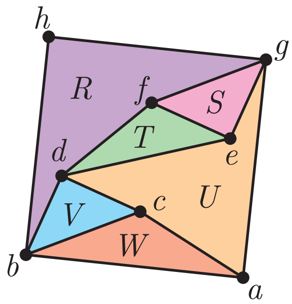

(a)

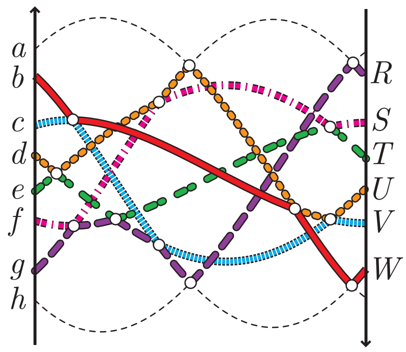

(b)

Figure 3.8: A pseudotriangulation (a) of the point set of Figure 3.6(a) and its dual arrangement (b). Each thick pseudoline in (b) corresponds to a pseudotriangle in (a); each contact point in (b) corresponds to an edge in (a); etc..

Theorem 3.14. *Let P be a finite point set (in general position), and P^{*1} denote the support of its dual pseudoline arrangement minus its first level. Then:*

(i) The dual pseudoline arrangement $T^* := \{\Delta^* \mid \Delta$ pseudotriangle of $T\}$ of a pseudotriangulation T of P is supported by P^{*1}.

(ii) The primal set of edges $E := \{[p,q] \mid p,q \in P,\ p^* \wedge q^*$ is not a crossing point of $\Lambda\}$ of a pseudoline arrangement Λ supported by P^{*1} is a pseudotriangulation of P.

In this section, we provide two proofs of Part (ii) of this result. The first one is based on flips. First, remember that there is also a simple flip operation on pseudotriangulations of P: replacing any internal edge e in a pseudotriangulation of P by the common tangent of the two pseudotriangles containing e produces a new pseudotriangulation of P. For example, Figure 3.9 shows two pseudotriangulations of the point set of Figure 3.6(a), related by a flip. We denote by $G(P)$ the graph of flips on pseudotriangulations of P, whose vertices are pseudotriangulations of P and whose edges are flips between them. In other words, there is an edge in $G(P)$ between two pseudotriangulations of P if and only if their symmetric difference is reduced to a pair.

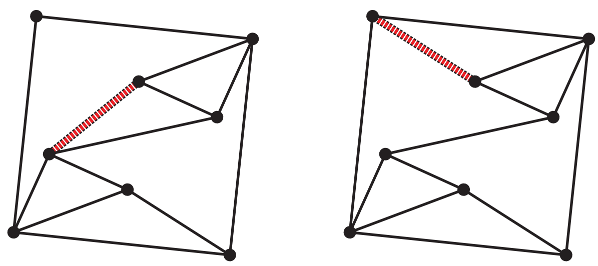

Figure 3.9: A flip in the pseudotriangulation of Figure 3.8(a).

Proof 1 *of Theorem 3.14(ii).* The two notions of flips (the primal notion on pseudotriangulations of P and the dual notion on pseudoline arrangements supported by P^{*1}) coincide via duality: an internal edge e of a pseudotriangulation T of P corresponds to a contact point e^* of the dual pseudoline arrangement T^*; the two pseudotriangles Δ and Δ' of T containing e correspond to the two pseudolines Δ^* and Δ'^* of T^* in contact at e^*; and the common tangent f of Δ and Δ' corresponds to the crossing point f^* of Δ^* and Δ'^*.

Thus, the graph $G(P)$ is a subgraph of $G(\mathcal{S})$. Since both are connected and regular of degree $|P|-3$, they coincide. In particular, any pseudoline arrangement supported by P^{*1} is the dual of a pseudotriangulation of P. □

Remark 3.15. Observe that this duality matches our greedy pseudoline arrangement supported by P^{*1} with the greedy pseudotriangulation of [BKPS06] (originally of [PV96b] for convex bodies). In particular, the greedy flip property and the enumeration algorithm of Subsection 3.1.3 are generalizations of results in [BKPS06, PV96b]. It is interesting to see however that our new proof of the greedy flip property (with the interpretation as sorting networks) does not use the notion of visibility complex, which is essential in [BKPS06, PV96b].

Our second proof of Theorem 3.14 is a bit more complicated, but is more direct and introduces a "witness method" that we will repeatedly use throughout this chapter. It is based on the following characterization of pseudotriangulations:

Lemma 3.16 ([Str05])**.** *A graph T on a point set P is a pseudotriangulation of P if and only if it is non-crossing, pointed and has $2|P|-3$ edges.* □

Proof 2 *of Theorem 3.14(ii).* We check that E is non-crossing, pointed and has $2|P|-3$ edges:

Cardinality. First, the number of edges of E equals the difference between the number of crossing points of P^* and of Λ:

$$|E| = \binom{|P^*|}{2} - \binom{|\Lambda|}{2} = \binom{|P|}{2} - \binom{|P|-2}{2} = 2|P|-3.$$

Crossing-free. Let p, q, r, s be four points of P in convex position. Let t be the intersection of $[p, r]$ and $[q, s]$ (see Figure 3.10(a)). We use the pseudoline t^* as a *witness* to prove that $[p, r]$ and $[q, s]$ cannot both be in E. For this, we count crossings of t^* with P^* and Λ respectively:

(i) Since P is in general position, t is not in P and $P^* \cup \{t^*\} = (P \cup \{t\})^*$ is a (non-simple) pseudoline arrangement. Thus, t^* crosses P^* exactly $|P|$ times.

(ii) Since t^* is a pseudoline, it crosses each pseudoline of Λ at least once. Thus, it crosses Λ at least $|\Lambda| = |P|-2$ times.

(iii) For each of the points $p^* \wedge r^*$ and $q^* \wedge s^*$, replacing the crossing point by a contact point removes two crossings with t^*.

Thus, $[p, r]$ and $[q, s]$ cannot both be in E, and E is crossing-free.

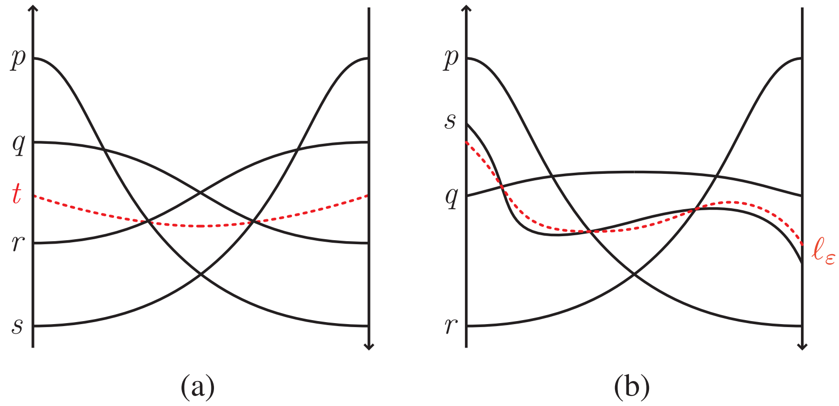

Figure 3.10: (a) Four points p, q, r, s in convex position with the intersection t of $[p, r]$ and $[q, s]$; (b) A point s inside a triangle pqr with the witness pseudoline ℓ_ε.

Pointed. Let p, q, r, s be four points of P such that s lies inside the triangle pqr. We first construct a witness pseudoline (see Figure 3.10(b)) that we use to prove that $[p, s]$, $[q, s]$ and $[r, s]$ cannot all be in E. Let f_p, f_q, f_r and f_s represent p^*, q^*, r^* and s^* respectively. Let $x, y, z \in \mathbb{R}$ be such that $f_p(x) = f_s(x)$, $f_q(y) = f_s(y)$ and $f_r(z) = f_s(z)$. Let g be a continuous and π-antiperiodic function vanishing exactly on $\{x, y, z\} + \mathbb{Z}\pi$ and changing sign each time it vanishes; say for example $g(t) := \sin(t - x)\sin(t - y)\sin(t - z)$. For all $\varepsilon > 0$, we define the function $h_\varepsilon : \mathbb{R} \to \mathbb{R}$ by $h_\varepsilon(t) = f_s(t) + \varepsilon g(t)$. The function h_ε is continuous and π-antiperiodic. The corresponding pseudoline ℓ_ε crosses s^* three times. It is also easy to see that if ε is sufficently small, then ℓ_ε crosses the pseudolines of $(P \smallsetminus \{s\})^*$ exactly as s^* does (see Figure 3.10(b)). For such a small ε, we count the crossings of ℓ_ε with P^* and Λ respectively:

(i) ℓ_ε crosses P^* exactly $|P|+2$ times (it crosses s^* three times and any other pseudoline of P^* exactly once).

(ii) Since ℓ_ε is a pseudoline, it crosses Λ at least $|\Lambda| = |P| - 2$ times.

(iii) For each of the points $p^* \wedge s^*$, $q^* \wedge s^*$ and $r^* \wedge s^*$, replacing the crossing point by a contact point removes two crossings with ℓ_ε.

Thus, $[p, r]$, $[q, s]$ and $[r, s]$ cannot all be in E, and E is pointed. $\square$

3.2.3 The dual pseudoline arrangement of a multitriangulation

Our study of stars (see Chapter 2) yields to a similar observation for multitriangulations:

Observation 3.17. Let T be a k-triangulation of a convex n-gon. Then:

(i) the set S^* of all bisectors of a k-star S of T is a pseudoline of the Möbius strip;

(ii) the set $T^* := \{S^* \mid S\ k\text{-star of } T\}$ of dual pseudolines of k-stars of T is a pseudoline arrangement (with contact points); and

(iii) T^* is supported by the dual pseudoline arrangement V_n^* of V_n minus its first k levels (see Figure 3.11(b)).

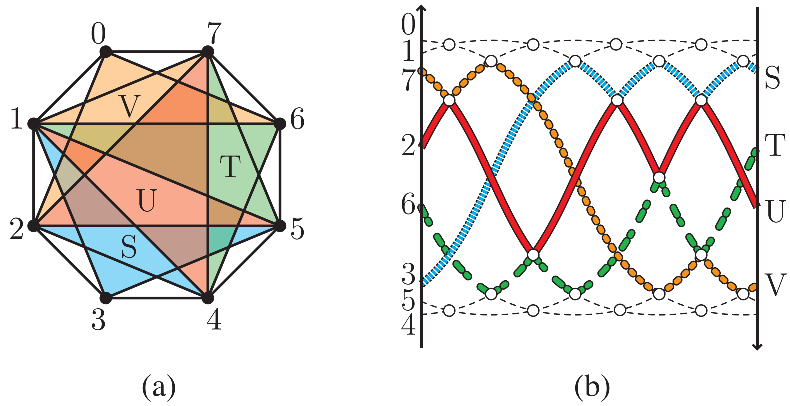

Figure 3.11: A 2-triangulation of the octagon (a) and its dual arrangement (b). Each thick pseudoline in (b) corresponds to a 2-star in (a); each contact point in (b) corresponds to an edge in (a); etc.

Again, it turns out that this observation provides a characterization of multitriangulations of a convex polygon (and we present again two different proofs of this result):

Theorem 3.18. *Let V_n denote the set of vertices of a convex n-gon, and V_n^{*k} denote the dual pseudoline arrangement of V_n minus its first k levels. Then:*

(i) The dual pseudoline arrangement $T^* := \{S^* \mid S\ k\text{-star of } T\}$ of a k-triangulation T of the n-gon is supported by V_n^{*k}.

(ii) The primal set of edges $E := \{[p,q] \mid p,q \in V_n,\ p^* \wedge q^* \text{ is not a crossing point of } \Lambda\}$ of a pseudoline arrangement Λ supported by V_n^{*k} is a k-triangulation of the n-gon.

Proof 1 *of Theorem 3.18(ii).* The two notions of flips (the primal notion on k-triangulations of the n-gon and the dual notion on pseudoline arrangements supported by V_n^{*k}) coincide. Thus, the flip graph $G_{n,k}$ on k-triangulations of the n-gon is a subgraph of $G(V_n^{*k})$. Since they are both connected and regular of degree $k(n-2k-1)$, these two graphs coincide. In particular, any pseudoline arrangement supported by V_n^{*k} is the dual of a k-triangulation of the n-gon. □

Proof 2 *of Theorem 3.18(ii).* We follow the method of our second proof of Theorem 3.14(ii). Since E has the right number of edges (namely $k(2n-2k-1)$), we only have to prove that it is $(k+1)$-crossing-free. We consider $2k+2$ points $p_0,\dots,p_k,q_0,\dots,q_k$ cyclically ordered around the unit circle. Since the definition of crossing (and thus, of ℓ-crossing) is purely combinatorial, *i.e.* depends only on the cyclic order of the points and not on their exact positions, we can move all the vertices of our n-gon on the unit circle while preserving their cyclic order. In particular, we can assume that the lines $(p_iq_i)_{i\in\{0,\dots,k\}}$ all contain a common point t. Its dual pseudoline t^* crosses V_n^* exactly n times and Λ at least $|\Lambda| = n-2k$ times. Furthermore, for any point $p_i^* \wedge q_i^*$, replacing the crossing point by a contact point removes two crossings with t^*. Thus, the pseudoline t^* provides a witness which proves that the edges $[p_i,q_i]$, $i \in \{0,\dots,k\}$, cannot be all in E, and thus ensures that E is $(k+1)$-crossing-free. □

As an application of Theorem 3.18, we provide the promised proof of the Characterization Theorem 2.14 mentioned in Chapter 2:

Theorem 3.19. *Let Σ be a set of k-stars of the n-gon such that:*
(i) any k-relevant edge of E_n is contained in zero or two k-stars of Σ, one on each side; and
(ii) any k-boundary edge of E_n is contained in exactly one k-star of Σ.
Then Σ is the set of k-stars of a k-triangulation of the n-gon.

Proof. By duality, Σ corresponds to a set of pseudolines Λ of the Möbius strip. We just have to prove that Λ forms a pseudoline arrangement supported by V_n^{*k} (the dual arrangement of n pseudolines in convex position, except its first k levels).

Observe first that the pseudolines of Λ partition V_n^{*k} (meaning that each edge of V_n^{*k} is contained in precisely one pseudoline of Λ). Indeed:

1. Consider the set A of all pseudosegments of a pseudoline $\ell \in L$, which are located in V_n^{*k}. The number of pseudolines of Λ containing a pseudosegment of A is constant on A. Otherwise, when this number changes, the contact point would not satisfy condition (i).
2. By condition (ii), this number is 1 for each pseudoline.

This immediately implies that $|\Sigma| = n - 2k$. Consequently (double counting) we know that we have kn non-k-relevant edges and $k(n-2k-1)$ k-relevant ones. This only leaves $\binom{n}{2} - nk - k(n-2k-1) = \binom{n-2k}{2}$ crossing points. Since two pseudolines of the Möbius strip cross at least once, this implies that Λ is a pseudoline arrangement, and finishes the proof. $\square$

3.3 MULTIPSEUDOTRIANGULATIONS

Motivated by Theorems 3.14 and 3.18, we define in terms of pseudoline arrangements a natural generalization of both pseudotriangulations and multitriangulations. We then study elementary properties of the corresponding set of edges in the primal space.

3.3.1 Definition

Let L be a pseudoline arrangement supported by $\mathcal{S}$. Define its *k-kernel* $\mathcal{S}^k$ to be its support minus its first k levels (which are the iterated external hulls of the support of the arrangement). Denote by V^k the set of contact points of L in $\mathcal{S}^k$.

Definition 3.20. *A* k-pseudotriangulation *of L is a pseudoline arrangement whose support is $\mathcal{S}^k$ and whose set of contact points contains V^k.*

Pseudotriangulations of a point set P correspond via duality to 1-pseudotriangulations of the dual pseudoline arrangement P^*. Similarly, k-triangulations of the n-gon correspond to k-pseudotriangulations of the pseudoline arrangement V_n^* in convex position. If L is a pseudoline arrangement with no contact point, then any pseudoline arrangement supported by $\mathcal{S}^k$ is a k-pseudotriangulation of L. In general, the condition that the contact points of L in its k-kernel should be contact points of any k-pseudotriangulation of L is a natural assumption for iterating multipseudotriangulations (see Section 3.4).

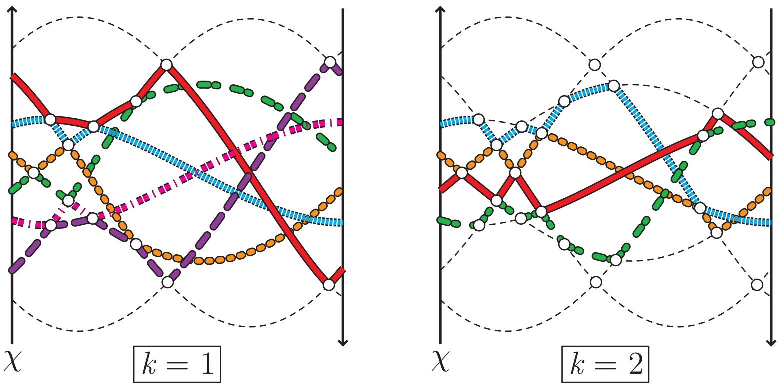

Figure 3.12: The χ-greedy 1-pseudotriangulation and the χ-greedy 2-pseudotriangulation of the pseudoline arrangement of Figure 3.6(b).

Let Λ be a k-pseudotriangulation of L. We denote by $V(\Lambda)$ the union of the set of contact points of Λ with the set of intersection points of the first k levels of L. In other words, $V(\Lambda)$ is the set of intersection points of L which are not crossing points of Λ. As for pseudoline arrangements, the set $V(\Lambda)$ completely determines Λ.

Flips for multipseudotriangulations are defined as in Lemma 3.2, with the restriction that the contact points in V^k cannot be flipped. In other words, the flip graph on k-pseudotriangulations of L is exactly the graph $G(\mathcal{S}^k \,|\, V^k)$. Section 3.1 asserts that the graph of flips is regular and connected, and provides an enumeration algorithm for multipseudotriangulations of L.

Let χ be a cut of (the support of) L. It is also a cut of the k-kernel $\mathcal{S}^k$ of L. A particularly interesting example of k-pseudotriangulation of L is the source of the graph of χ-increasing flips on k-pseudotriangulations of L (see Figure 3.12 for an illustration):

Definition 3.21. *The χ-greedy k-pseudotriangulation of L, denoted $\Gamma_\chi^k(L)$, is the greedy pseudoline arrangement $\Gamma_\chi(\mathcal{S}^k \,|\, V^k)$.*

3.3.2 Pointedness and crossings

Let P be a point set in general position. Let Λ be a k-pseudotriangulation of P^* and $V(\Lambda)$ be the set of crossing points of P^* which are not crossing points of Λ. We call *primal of Λ* the set $E := \{[p,q] \,|\, p,q \in P,\ p^* \wedge q^* \in V(\Lambda)\}$ of edges of P primal to $V(\Lambda)$ — see Figure 3.13. Here, we discuss general properties of primals of multipseudotriangulations. We start with elementary properties that we already observed for the special cases of pseudotriangulations and multitriangulations in the proofs of Theorems 3.14 and 3.18:

Lemma 3.22. *The set E has $k(2|P|-2k-1)$ edges.*

Proof. The number of edges of E is the difference between the number of crossing points in the pseudoline arrangements P^* and Λ:

$$|E| = \binom{|P^*|}{2} - \binom{|\Lambda|}{2} = \binom{|P|}{2} - \binom{|P|-2k}{2} = k(2|P|-2k-1). \qquad \square$$

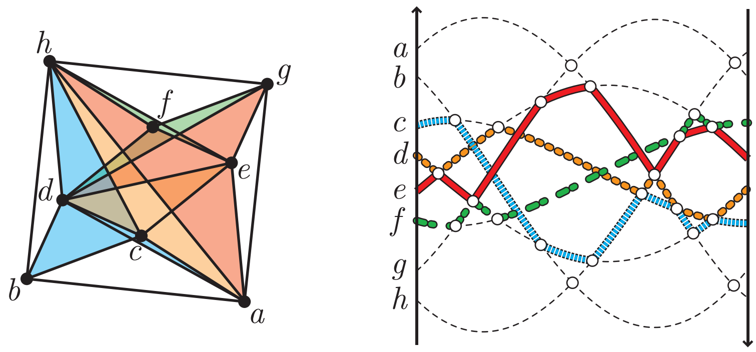

(a) (b)

Figure 3.13: The primal set of edges (a) of a 2-pseudotriangulation (b) of the dual pseudoline of the point set of Figure 3.6(a).

We now discuss pointedness of E. We call *k-alternation* any set $\{f_i \,|\, i \in \mathbb{Z}_{2k+1}\}$ of $2k+1$ edges all adjacent to a common vertex and whose cyclic order around it is given by $f_0 \prec \bar{f}_{1+k} \prec f_1 \prec \bar{f}_{2+k} \prec \ldots \prec f_{2k} \prec \bar{f}_k \prec f_0$, where $\bar{f}_i$ denotes the opposite direction of the edge f_i.

Lemma 3.23. *The set E cannot contain a k-alternation.*

Proof. We simply mimic the proof of pointedness in Theorem 3.14. Let $p_0, \ldots, p_{2k}$ and q be $2k+2$ points of P such that $F := \{[p_i, q] \,|\, i \in \mathbb{Z}_{2k+1}\}$ is a k-alternation. We prove that F cannot be a subset of E by constructing a witness pseudoline ℓ that separates all the crossing points $p_i^* \wedge q^*$ corresponding to F, while crossing q^* exactly $2k+1$ times and the other pseudolines of P^* exactly as q^* does. (We skip the precise construction, since it is exactly the same as in the proof of Theorem 3.14.) Counting the crossings of ℓ with P^* and Λ, we obtain:

(i) ℓ crosses P^* exactly $|P| + 2k$ times;
(ii) ℓ crosses Λ at least $|\Lambda| = |P| - 2k$ times;
(iii) for each of the points $p_i^* \wedge q^*$, replacing the crossing point by a contact point removes two crossings with ℓ. □

Remark 3.24. Observe that a set of edges is pointed if and only if it is 1-alternation-free. In contrast, we want to observe the difference between k-alternation-freeness and the following natural notion of k-pointedness: we say that a set F of edges with vertices in P is *k-pointed* if for all p in P, there exists a line which passes through p and defines a half-plane that contains at most $k-1$ segments of F adjacent to p. Observe that a k-pointed set is automatically k-alternation-free but that the reciprocal statement does not hold (see Figure 3.14(a)).

Finally, contrarily to pseudotriangulations ($k=1$) and multitriangulations (convex position), the condition of avoiding $(k+1)$-crossings does not hold for k-pseudotriangulations in general:

Remark 3.25. There exist k-pseudotriangulations with $(k+1)$-crossings (see Figure 3.14(b)) as well as $(k+1)$-crossing-free k-alternation-free sets of edges that are not subsets of k-pseudotriangulations (see Figure 3.14(c)).

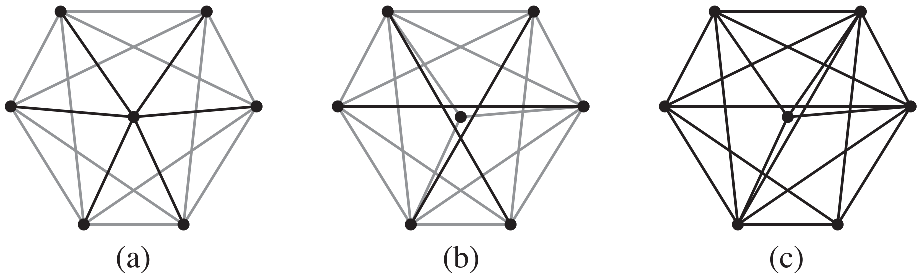

Figure 3.14: (a) A non-2-pointed (but 2-alternation-free) 2-pseudotriangulation; (b) A 2-pseudotriangulation containing a 3-crossing; (c) A 3-crossing-free 2-alternation-free set not contained in a 2-pseudotriangulation.

3.3.3 Stars in multipseudotriangulations

To complete our understanding of the primal of multipseudotriangulations, we need to generalize pseudotriangles of pseudotriangulations and k-stars of k-triangulations: both pseudotriangles and k-stars correspond to pseudolines of the covering pseudoline arrangement.

We keep the notations of the previous section: P is a point set in general position, Λ is a k-pseudotriangulation of P^* and E is the primal set of edges of Λ. Consider now a pseudoline λ of Λ. We call *star* the set of edges $S(\lambda) := \{[p,q] \mid p,q \in P,\ p^* \wedge q^* \text{ contact point of } \lambda\}$ primal to the contact points of λ.

Lemma 3.26. *For any $\lambda \in \Lambda$, the star $S(\lambda)$ is non-empty.*

Proof. We have to prove that any pseudoline λ of Λ supports at least one contact point. If it is not the case, then λ is also a pseudoline of P^*, and all the $|P|-1$ crossing points of λ with $P^* \smallsetminus \{\lambda\}$ should be crossing points of λ with $\Lambda \smallsetminus \{\lambda\}$. This is impossible since $|\Lambda \smallsetminus \{\lambda\}| = |P|-2k-1$. □

Similarly to the case of k-triangulations of the n-gon, we say that an edge $[p,q]$ of E is a *k-relevant* (resp. *k-boundary*, resp. *k-irrelevant*) edge if there remain strictly more than (resp. exactly, resp. strictly less than) $k-1$ points of P on each side (resp. one side) of the line (pq). In other words, $p^* \wedge q^*$ is located in the k-kernel (resp. in the intersection of the kth level and the k-kernel, resp. in the first k levels) of the pseudoline arrangement P^*. Thus, the edge $[p,q]$ is contained in 2 (resp. 1, resp. 0) stars of Λ.

The edges of a star $S(\lambda)$ are cyclically ordered by the order of their dual contact points on λ, and thus $S(\lambda)$ forms a (not-necessarily simple) polygonal cycle. For any point q in the plane, let $\sigma_\lambda(q)$ denote the *winding number* of $S(\lambda)$ around q, that is, the number of rounds made by $S(\lambda)$ around the point q (see Figure 3.15(a)). For example, the winding number of a point in the external face is 0.

We call *k-depth* of a point q the number $\delta^k(q)$ of k-boundary edges of P crossed by any (generic continuous) path from q to the external face, counted positively when passing from the "big" side (the one containing at least k vertices of P) to the "small side" (the one containing $k-1$ vertices of P), and negatively otherwise (see Figure 3.15(b)). That this number is independent

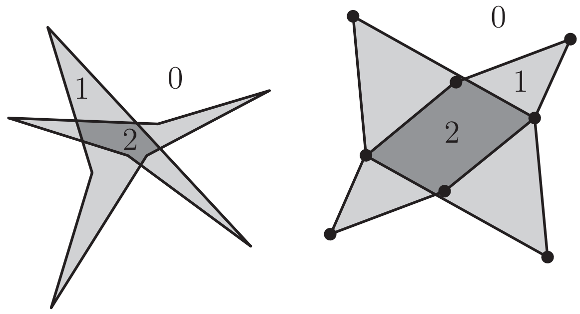

Figure 3.15: (a) Winding number of a star; (b) 2-depth in the point set of Figure 3.6(a).

from the path can be seen by mutation. For example, $\delta^1(q)$ is 1 if q is in the convex hull of P and 0 otherwise.

Proposition 3.27. *Any point q of the plane is covered $\delta^k(q)$ times by the stars $S(\lambda)$, $\lambda \in \Lambda$, of the k-pseudotriangulation Λ of P^*:*

$$\delta^k(q) = \sum_{\lambda\in\Lambda} \sigma_\ell(q).$$

The proposition is intuitively clear: let us walk on a continuous path from the external face to the point q. Initially, the winding numbers of all stars of Λ are zero (we start outside all stars of Λ). Then, each time we cross an edge e:

(i) If e is k-irrelevant, it is not contained in any star of Λ, and we do not change the winding numbers of the stars of Λ.

(ii) If e is a k-boundary edge, and if we cross it positively, we increase the winding number of the star S of Λ containing e; if we cross e negatively, we decrease the winding number of S.

(iii) If e is k-relevant, then we decrease the winding number of one star of Λ containing e and increase the winding number of the other star of Λ containing e.

Let us give a formal proof in the dual:

Proof of Proposition 3.27. Both $\sigma_\lambda(q)$ and $\delta^k(q)$ can be read on the pseudoline q^*:

(i) If $\tau_\lambda(q)$ denotes the number of intersection points between q^* and λ (that is, the number of tangents to $S(\lambda)$ passing through q), then $\sigma_\lambda(q) = (\tau_\lambda(q) - 1)/2$.

(ii) If $\gamma^k(q)$ denotes the number of intersection points between q^* and the first k levels of P^*, then $\delta^k(q) = k - \gamma^k(q)/2$.

The pseudoline q^* has exactly $|P|$ crossings with P^* (since $P^* \cup \{q^*\}$ is an arrangement), which are crossings either with the pseudolines of Λ or with the first k levels of P^*. Hence,

$$|P| = \gamma^k(q) + \sum_{\lambda\in\Lambda} \tau_\lambda(q) = 2k - 2\delta^k(q) + |\Lambda| + 2\sum_{\lambda\in\Lambda} \sigma_\lambda(q),$$

and we get the aforementioned result since $|\Lambda| = |P| - 2k$. $\square$

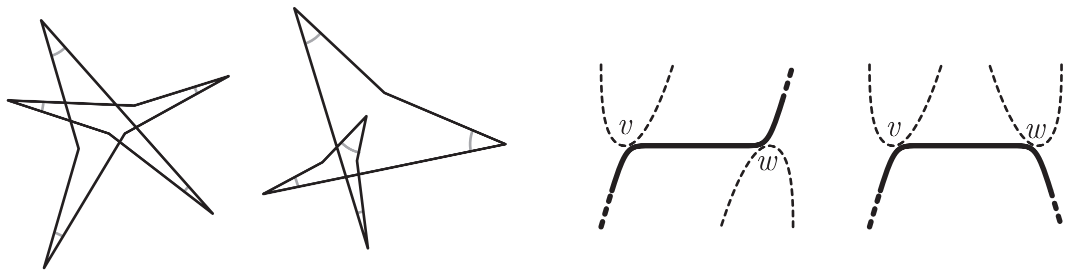

(a) (b)

Figure 3.16: (a) Two stars with 5 corners; (b) The two possible configurations of two consecutive contact points on λ: convex (left) and concave (right).

A *corner* of the star $S(\lambda)$ is an internal convex angle of it (see Figure 3.16(a)). In the following proposition, we are interested in the number of corners of $S(\lambda)$:

Proposition 3.28. *The number of corners of a star $S(\lambda)$ of a k-pseudotriangulation of P^* is odd and between $2k+1$ and $2(k-1)|P|+2k+1$.*

Proof. We read convexity of internal angles of $S(\lambda)$ on the preimage $\bar{\lambda}$ of the pseudoline λ under the projection π. Let pqr be an internal angle, let $v = p^* \wedge q^*$ and $w = q^* \wedge r^*$ denote the contact points corresponding to the two edges $[p,q]$ and $[q,r]$ of this angle, and let $\bar{v}$ and $\bar{w}$ denote two consecutive preimages of v and w on $\bar{\lambda}$ (meaning that $\bar{w}$ is located between $\bar{v}$ and $\tau(\bar{v})$). The angle pqr is a corner if and only if $\bar{v}$ and $\bar{w}$ lie on opposite sides of $\bar{\lambda}$, meaning that the other curves touching $\bar{\lambda}$ at $\bar{v}$ and $\bar{w}$ lie on opposite sides, one above and one below $\bar{\lambda}$ (see Figure 3.16(b)).

In particular, the number $c(\lambda) = c$ of corners of $S(\lambda)$ is the number of opposite consecutive contact points on $\bar{\lambda}$ between two versions $\bar{v}$ and $\tau(\bar{v})$ of a contact point v of λ. To see that c is odd, imagine that we are discovering the contact points of λ one by one. The first contact point v that we see corresponds to two opposite contact points $\bar{v}$ and $\tau(\bar{v})$ on $\bar{\lambda}$. Then, at each stage, we insert a new contact point $\bar{w}$ between two old contact points that can be:

(i) either on opposite sides and then we are not changing c;

(ii) or on the same side and we are adding to c either 0 (if $\bar{w}$ is also on the same side) or 2 (if $\bar{w}$ is on the opposite side).

Thus, c remains odd in any case.

To prove the lower bound, we use our witness method. We perturb a little bit λ to obtain a pseudoline μ that passes on the opposite side of each contact point (this is possible since c is odd). This pseudoline μ crosses λ between each pair of opposite contact points and crosses the other pseudolines of Λ exactly as λ does. Thus, μ crosses Λ exactly $|\Lambda| - 1 + c$ times. But since μ is a pseudoline, it has to cross all the pseudolines of P^* at least once. Thus, we get $|P| \leq |\Lambda| - 1 + c = |P| - 2k - 1 + c$ and $c \geq 2k+1$.

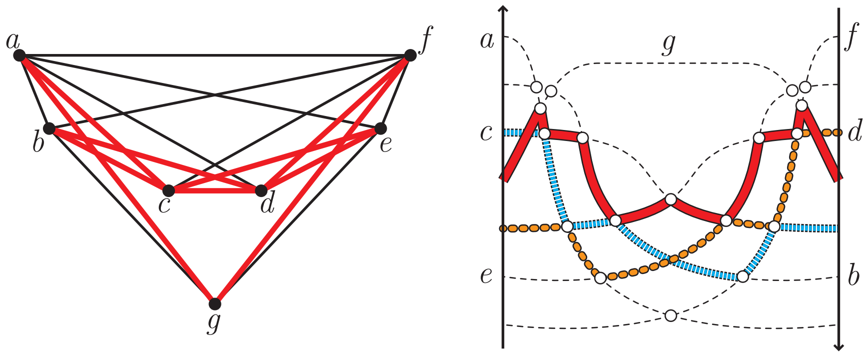

Figure 3.17: A star of a 2-pseudotriangulation with almost $2|P|$ corners.

From this lower bound, we derive automatically the upper bound. Indeed, we know that the number of corners around one point p is at most $\deg(p) - 1$. Consequently,

$$\sum_{p \in P} (\deg(p) - 1) \geq \sum_{\nu \in \Lambda} c(\nu) = c(\lambda) + \sum_{\substack{\nu \in \Lambda \\ \nu \neq \lambda}} c(\nu).$$

The left sum equals $2k(2|P| - 2k - 1) - |P|$ while, according to the previous lower bound, the right one is at least $c + (|P| - 2k - 1)(2k + 1)$. Thus we get $c \leq 2(k-1)|P| + 2k + 1$. $\square$

For general k, contrary to the case of convex position (Section 3.2.3), the number of corners of a star is not necessarily $2k + 1$ (Figure 3.17 presents a star of a 2-pseudotriangulation with almost $2|P|$ corners).

When $k = 1$ however, both bounds turn out to be 3 and this proposition affirms that the primal of a pseudoline of Λ is a pseudotriangle. Proposition 3.27 ensures that the convex hull of P is covered once by these $|P| - 2$ pseudotriangles, and hence provides another alternative proof of Theorem 3.14.

Finally, let us mention that the definitions developed in this section provide some alternative conditions in the Characterization Theorem 3.19:

Lemma 3.29. *Let Σ be a set of k-stars of the convex n-gon such that each k-relevant edge of E_n is contained either in zero or in two k-stars of Σ, one on each side. Then the following properties are equivalent:*

1. *Every k-boundary edge of the n-gon is contained in exactly one k-star of Σ.*
2. *On each of the $\gcd(n, k)$ cycles of k-boundary edges of the n-gon, there is one k-boundary edge which is contained in exactly one k-star of Σ.*
3. *The k-depth of every chamber of the n-gon equals the sum of the winding numbers of the k-stars of Σ around it.*
4. *For one chamber of the n-gon of k-depth k, the sum of the winding numbers of the k-stars of Σ around it equals k.*

5. *For every (generic) direction, each line parallel to this direction passing through one of the $n-2k$ central vertices of the n-gon (for this direction) is the bisector of a unique k-star of Σ.*
6. *There is one (generic) direction for which each line parallel to this direction passing through one of the $n-2k$ central vertices of the n-gon (for this direction) is the bisector of a unique k-star of Σ.* □

3.4 ITERATED MULTIPSEUDOTRIANGULATIONS

By definition, a k-pseudotriangulation of an m-pseudotriangulation of a pseudoline arrangement L is a $(k+m)$-pseudotriangulation of L. In this section, we study these iterated sequences of multipseudotriangulations. In particular, we compare multipseudotriangulations with iterated sequences of 1-pseudotriangulations.

3.4.1 Definition and examples

Let L be a pseudoline arrangement. An *iterated multipseudotriangulation* of L is a sequence $\Lambda_1, \dots, \Lambda_r$ of pseudoline arrangements such that Λ_i is a multipseudotriangulation of Λ_{i-1} for all i (by convention, $\Lambda_0 = L$). We call *signature* of $\Lambda_1, \dots, \Lambda_r$ the sequence $k_1 < \dots < k_r$ of integers such that Λ_i is a k_i-pseudotriangulation of L for all i. Observe that the assumption that contact points of a pseudoline arrangement L should be contact points of any multipseudotriangulation of L is natural in this setting: iterated multipseudotriangulations correspond to decreasing sequences of sets of crossing points.

A *decomposition* of a multipseudotriangulation Λ of a pseudoline arrangement L is an iterated multipseudotriangulation $\Lambda_1, \dots, \Lambda_r$ of L such that $\Lambda_r = \Lambda$ and $r > 1$. We say that Λ is *decomposable* if such a decomposition exists, and *irreducible* otherwise. The decomposition is *complete* if its signature is $1, 2, \dots, r$.

Example 3.30 (k-colorable k-triangulations of the convex n-gon)**.** Consider a k-colorable k-triangulation T of the n-gon (see Section 2.4). It is easy to construct from the k k-accordions of T a deomposition $\Lambda_1, \dots, \Lambda_k$ of T^* of V_n^*, where each multipseudotriangulation Λ_i is in convex position (*i.e.* the dual pseudoline arrangement of points in convex position). In particular, the set of decomposable k-triangulations of the convex n-gon is much bigger than the set of k-colorable k-triangulations. However, as the following example shows, there are still irreducible multitriangulations.

Example 3.31 (An irreducible 2-triangulation of the 15-gon)**.** We consider the geometric graph T of Figure 3.18. The edges are:

(i) all the 2-irrelevant and 2-boundary edges of the 15-gon, and
(ii) the five zigzags $Z_a = \{[3a, 3a+6], [3a+6, 3a+1], [3a+1, 3a+5], [3a+5, 3a+2]\}$, for $a \in \{0, 1, 2, 3, 4\}$.

Thus, T has 50 edges and is 3-crossing-free (since the only 2-relevant edges of T that cross a zigzag Z_a are edges of Z_{a-1} and Z_{a+1}). Consequently, T is a 2-triangulation of the 15-gon.

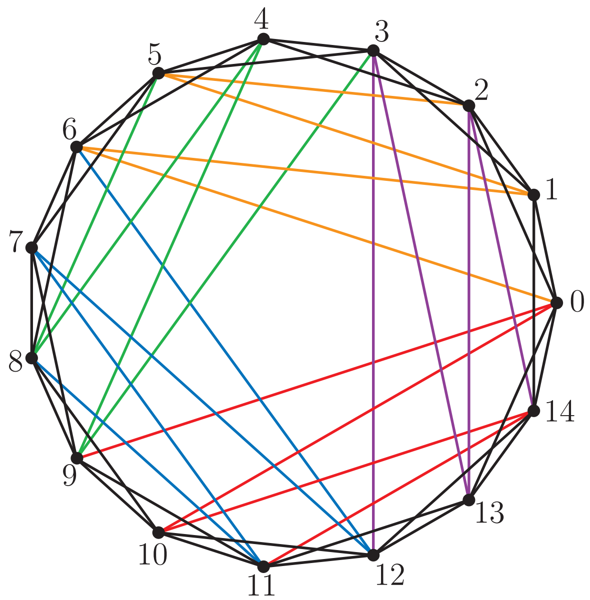

Figure 3.18: An irreducible 2-triangulation of the 15-gon: it contains no triangulation.

Let us now prove that T^* is irreducible, that is, that T contains no triangulation. Observe first that the edge $[0,6]$ cannot be an edge of a triangulation contained in T since none of the triangles $06i$, $i \in \{7,\dots,14\}$, is contained in T. Thus, we are looking for a triangulation contained in $T \smallsetminus \{[0,6]\}$. Repeating the argument successively for the edges $[1,6]$, $[1,5]$ and $[2,5]$, we prove that the zigzag Z_0 is disjoint from any triangulation contained in T. By symmetry, this prove the irreducibility of T^*.

3.4.2 Iterated greedy pseudotriangulations

Greedy multipseudotriangulations provide interesting examples of iteration of pseudotriangulations. Let L be a pseudoline arrangement, and χ be a cut of L.

Theorem 3.32. *For any positive integers a and b, $\Gamma_\chi^{a+b}(L) = \Gamma_\chi^b(\Gamma_\chi^a(L))$. Consequently, for any integer k, $\Gamma_\chi^k(L) = \Gamma_\chi^1 \circ \Gamma_\chi^1 \circ \cdots \circ \Gamma_\chi^1(L)$, where $\Gamma_\chi^1(.)$ is iterated k times.*

Proof. Since χ is a cut of L, it is also a cut of $\Gamma_\chi^a(L)$ and thus $\Gamma_\chi^b(\Gamma_\chi^a(L))$ is well-defined. Observe also that we can assume that L has no contact point (otherwise, we can open them). Let $n := |L|$ and $m := \binom{n}{2}$.

Let $\chi = \chi_0, \dots, \chi_m = \chi$ be a backward sweep of L. For all i, let v_i denote the vertex of L swept when passing from χ_i to χ_{i+1}, and $i^\square$ denote the integer such that the pseudolines that cross at v_i are the $i^\square$th and $(i^\square+1)$th pseudolines of L on χ_i.

Let $\sigma_0, \dots, \sigma_m$ denote the sequence of permutations corresponding to $\Gamma_\chi^a(L)$ on the sweep $\chi_0, \dots, \chi_m$. In other words, σ_0 is the permutation

$$(1, \dots, a, n-a, n-a-1, \dots, a+2, a+1, n-a+1, \dots, n),$$

whose first a and last a entries are preserved, while its $n-2a$ intermediate entries are inverted. Then, for all i, the permutation σ_{i+1} is obtained from σ_i by sorting its $i^\square$th and $(i^\square+1)$th entries.

Similarly, let $\rho_0, \dots, \rho_m$ and $\omega_0, \dots, \omega_m$ denote the sequences of permutations corresponding to $\Gamma_\chi^{a+b}(L)$ and $\Gamma_\chi^b(\Gamma_\chi^a(L))$ respectively: both ρ_0 and ω_0 equal the permutation whose first and last $a+b$ entries are preserved and whose $n-2a-2b$ intermediate entries are inverted, and for all i:

- ρ_{i+1} is obtained from ρ_i by sorting its $i^\square$th and $(i^\square+1)$th entries;
- if $v_i \notin \Gamma_\chi^a(L)$, then ω_{i+1} is obtained from ω_i by sorting its $i^\square$th and $(i^\square+1)$th entries; otherwise, $\omega_{i+1} = \omega_i$.

We claim that for all i,

(A) all the inversions of ρ_i are also inversions of σ_i: $\rho_i(p) > \rho_i(q)$ implies $\sigma_i(p) > \sigma_i(q)$ for all $1 \le p < q \le n$; and

(B) $\rho_i = \omega_i$.

We prove this claim by induction on i. It is clear for $i=0$. Assume that it is true for i and let us prove it for $i+1$. We have two possible situations:

1. **First case:** $\sigma_i(i^\square) < \sigma_i(i^\square+1)$. Then, $\sigma_{i+1} = \sigma_i$ and $v_i \in \Gamma_\chi^a(L)$. Thus, $\omega_{i+1} = \omega_i$. Furthermore, using Property (A) at rank i, we know that $\rho_i(i^\square) < \rho_i(i^\square+1)$, and thus $\rho_{i+1} = \rho_i$. To summarize, $\sigma_{i+1} = \sigma_i$, $\omega_{i+1} = \omega_i$, and $\rho_{i+1} = \rho_i$, which trivially implies that Properties (A) and (B) remain true.
2. **Second case:** $\sigma_i(i^\square) > \sigma_i(i^\square+1)$. Then, σ_{i+1} is obtained from σ_i by exchanging the $i^\square$th and $(i^\square+1)$th entries, and $v_i \notin \Gamma_\chi^a(L)$. Consequently, ρ_{i+1} and ω_{i+1} are both obtained from ρ_i and ω_i respectively by sorting their $i^\square$th and $(i^\square+1)$th entries. Thus, Property (B) obviously remains true. As far as Property (A) is concerned, the result is obvious if p and q are different from $i^\square$ and $i^\square+1$. By symmetry, it is enough to prove that for any $p < i^\square$, $\rho_{i+1}(p) > \rho_{i+1}(i^\square)$ implies $\sigma_{i+1}(p) > \sigma_{i+1}(i^\square)$. We have to consider two subcases:
   a) **First subcase:** $\rho_i(i^\square) < \rho_i(i^\square+1)$. Then $\rho_{i+1} = \rho_i$. Thus, if $p < i^\square$ is such that $\rho_{i+1}(p) > \rho_{i+1}(i^\square)$, then we have $\rho_i(p) > \rho_i(i^\square)$. Consequently, we obtain that $\sigma_{i+1}(p) = \sigma_i(p) > \sigma_i(i^\square) > \sigma_i(i^\square+1) = \sigma_{i+1}(i^\square)$.
   b) **Second subcase:** $\rho_i(i^\square) > \rho_i(i^\square+1)$. Then ρ_{i+1} is obtained from ρ_i by exchanging its $i^\square$th and $(i^\square+1)$th entries. If $p < i^\square$ is such that $\rho_{i+1}(p) > \rho_{i+1}(i^\square)$, then $\rho_i(p) > \rho_i(i^\square+1)$. Consequently, $\sigma_{i+1}(p) = \sigma_i(p) > \sigma_i(i^\square+1) = \sigma_{i+1}(i^\square)$.

Obviously, Property (B) of our claim proves the theorem. $\square$

3.4.3 Flips in iterated multipseudotriangulations

Let $\Lambda_1, \dots, \Lambda_r$ be an iterated multipseudotriangulation of a pseudoline arrangement L, with signature $k_1 < \dots < k_r$. Let v be a contact point of Λ_r (which is not a contact point of L), and let i denote the first integer for which v is a contact point of Λ_i (thus, v is a contact point of Λ_j if and only if $i \le j \le r$). For all $i \le j \le r$, let Λ'_j denote the pseudoline arrangement obtained from Λ_j by flipping v, and let w_j denote the new contact point of Λ'_j. Let j denote the biggest integer such that $w_j = w_i$. There are three possibilities:

(i) If $j = r$, then $\Lambda_1, \dots, \Lambda_{i-1}, \Lambda'_i, \dots, \Lambda'_r$ is an iterated multipseudotriangulation of L. We say that it is obtained from $\Lambda_1, \dots, \Lambda_r$ by a *complete flip* of v .

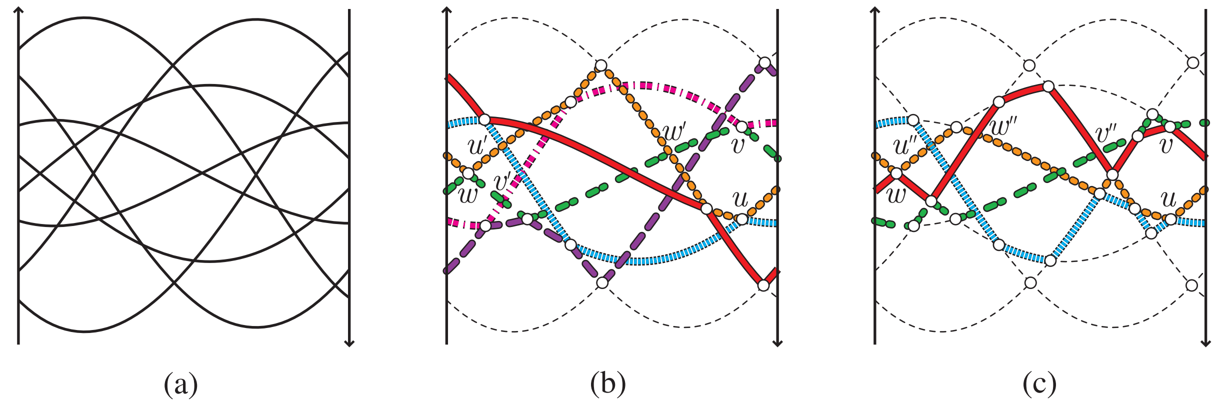

Figure 3.19: The three possible situations for flipping a contact point in an iterated multipseudotriangulation.

(ii) If $j < r$, and $w_i = w_j$ is a contact point of Λ_{j+1}, then $\Lambda_1, \dots, \Lambda_{i-1}, \Lambda'_i, \dots, \Lambda'_j, \Lambda_{j+1}, \dots, \Lambda_r$ is an iterated multipseudotriangulation of L. We say that it is obtained from $\Lambda_1, \dots, \Lambda_r$ by a *partial flip* of v.

(iii) If $j < r$, and $w_i = w_j$ is a crossing point in Λ_{j+1}, then we cannot flip v in Λ_i maintaining an iterated multipseudotriangulation of L.

To illustrate these three possible cases, we have labeled on Figure 3.19 some intersection points of an iterated pseudotriangulation. We have choosen three contact points u, v, w in (b). For $z \in \{u, v, w\}$, we label z' (resp. z'') the crossing point corresponding to z in (b) (resp. in (c)). Observe that:

(i) points u' and u'' coincide. Thus we can flip simultaneously point u in (b) and (c) (complete flip);

(ii) points v' is different from v'' but is a contact point in (c). Thus, we can just flip v in (b), without changing (c) and we preserve an iterated pseudotriangulation (partial flip);

(iii) point w' is a crossing point in (c), different from w''. Thus, we cannot flip w in (b) maintaining an iterated pseudotriangulation.

Let $G^{k_1,\dots,k_r}(L)$ be the graph whose vertices are the iterated multipseudotriangulations of L with signature $k_1 < \dots < k_r$, and whose edges are the pairs of iterated multipseudotriangulations linked by a (complete or partial) flip.

Theorem 3.33. *The graph of flips $G^{k_1,\dots,k_r}(L)$ is connected.*

To prove this proposition, we need the following lemma:

Lemma 3.34. *Any intersection point v in the k-kernel of a pseudoline arrangement is a contact point in a k-pseudotriangulation of it.*

Proof. The result holds when $k = 1$. We obtain the general case by iteration. □

Proof of Theorem 3.33. We prove the result by induction on r (L is fixed). When $r = 1$, we already know that the flip graph is connected. Now, let A_- and A_+ be two iterated multipseudotriangulations of L with signature $k_1 < \ldots < k_r$, that we want to join by flips. Let B_- and B_+ be iterated multipseudotriangulations of L with signature $k_1 < \ldots < k_{r-1}$, and Λ_- and Λ_+ be k_r-pseudotriangulations of L such that $A_- = B_-, \Lambda_-$ and $A_+ = B_+, \Lambda_+$.

By induction, $G^{k_1,\ldots,k_{r-1}}(L)$ is connected: let $B_- = B_1, B_2, \ldots, B_{p-1}, B_p = B_+$ be a path from B_- to B_+ in $G^{k_1,\ldots,k_{r-1}}(L)$. For all j, let v_j be such that B_{j+1} is obtained from B_j by flipping v_j and let w_j be such that B_j is obtained from B_{j+1} by flipping w_j. Let Λ_j be a k_r-pseudotriangulation of L containing the contact points of B_j plus w_j (it exists by Lemma 3.34), and let $C_j = B_j, \Lambda_j$. Let D_j be the iterated multipseudotriangulation of L obtained from the iterated pseudotriangulation C_j by a partial flip of v_j. Finally, since $G^{k_r}(B_j)$ is connected, there is a path of complete flips from D_{j-1} to C_j.

Merging all these paths, we obtain a global path from A_- to A_+: we transform A_- into C_1 via a path of complete flips; then C_1 into D_1 by the partial flip of v_1; then D_1 into C_2 via a path of complete flips; then C_2 into D_2 by the partial flip of v_2; and so on. □

3.5 Further topics on multipseudotriangulations

To finish this chapter, we discuss the extensions in the context of multipseudotriangulations of two known results on pseudotriangulations:

1. The first one concerns the relationship between the greedy pseudotriangulation of a point set and its horizon trees.
2. The second one extends to arrangements of double pseudolines the definition and properties of multipseudotriangulations.

3.5.1 Greedy multipseudotriangulations and horizon graphs

We have seen in previous sections that the greedy k-pseudotriangulation of a pseudoline arrangement L can be seen as:

1. the unique source of the graph of increasing flips on k-pseudotriangulations of L;
2. a greedy choice of crossing points given by a sorting network;
3. a greedy choice of contact points;
4. an iteration of greedy 1-pseudotriangulations.

In this section, we provide a "pattern avoiding" characterization of the crossing points of the greedy k-pseudotriangulation of L.

Let L be a pseudoline arrangement, and χ be a cut of L. We index by $\ell_1, \ldots, \ell_n$ the pseudolines of L in the order in which they cross χ (it is well defined, up to a complete inversion).

We define the *k-upper χ-horizon set* of L to be the set $\mathbb{U}_\chi^k(L)$ of crossing points $\ell_\alpha \wedge \ell_\beta$, with $1 \le \alpha < \beta \le n$, such that there is no $\gamma_1, \ldots, \gamma_k$ satisfying $\alpha < \gamma_1 < \ldots < \gamma_k$ and $\ell_\alpha \wedge \ell_{\gamma_i} \preccurlyeq_\chi \ell_\alpha \wedge \ell_\beta$ for all $i \in [k]$. In other words, on each pseudoline ℓ_α of L, the set $\mathbb{U}_\chi^k(L)$ consists of the smallest k crossing points of the form $\ell_\alpha \wedge \ell_\beta$, with $\alpha < \beta$.

Similarly, define the *k-lower χ-horizon set* of L to be the set $\mathbb{L}^k_\chi(L)$ of crossing points $\ell_\alpha \wedge \ell_\beta$, with $1 \le \alpha < \beta \le n$, such that there is no $\delta_1, \dots, \delta_k$ satisfying $\delta_1 < \dots < \delta_k < \beta$ and $\ell_\beta \wedge \ell_{\delta_i} \preccurlyeq_\chi \ell_\alpha \wedge \ell_\beta$ for all $i \in [k]$. On each pseudoline ℓ_β of L, the set $\mathbb{L}^k_\chi(L)$ consists of the smallest k crossing points of the form $\ell_\alpha \wedge \ell_\beta$, with $\alpha < \beta$.

Finally, we define the set $\mathbb{G}^k_\chi(L)$ to be the set of crossing points $\ell_\alpha \wedge \ell_\beta$, with $1 \le \alpha < \beta \le n$, such that there is no $\gamma_1, \dots, \gamma_k$ and $\delta_1, \dots, \delta_k$ satisfying:

(i) $\alpha < \gamma_1 < \dots < \gamma_k$, $\delta_1 < \dots < \delta_k < \beta$, and $\delta_k < \gamma_1$; and

(ii) $\ell_\alpha \wedge \ell_{\gamma_i} \preccurlyeq_\chi \ell_\alpha \wedge \ell_\beta$ and $\ell_\beta \wedge \ell_{\delta_i} \preccurlyeq_\chi \ell_\alpha \wedge \ell_\beta$ for all $i \in [k]$.

Obviously, the sets $\mathbb{U}^k_\chi(L)$ and $\mathbb{L}^k_\chi(L)$ are both contained in $\mathbb{G}^k_\chi(L)$.

Example 3.35. In Figure 3.20, we have labeled the vertices of the pseudoline arrangement L of Figure 3.6(b) with different geometric tags according to their status:

($\triangle$) crossing points of the k-upper χ-horizon set $\mathbb{U}^k_\chi(L)$ are represented by up triangles $\triangle$;

($\triangledown$) crossing points of the k-lower χ-horizon set $\mathbb{L}^k_\chi(L)$ are represented by down triangles $\triangledown$;

(✡) crossing points in both $\mathbb{U}^k_\chi(L)$ and $\mathbb{L}^k_\chi(L)$) are represented by up and down triangles ✡;

($\square$) crossing points of $\mathbb{G}^k_\chi(L)$ but neither in $\mathbb{U}^k_\chi(L)$, nor in $\mathbb{L}^k_\chi(L)$ are represented by squares $\square$.

Observe that the remaining vertices are exactly the crossing points of the χ-greedy k-pseudotriangulation of L.

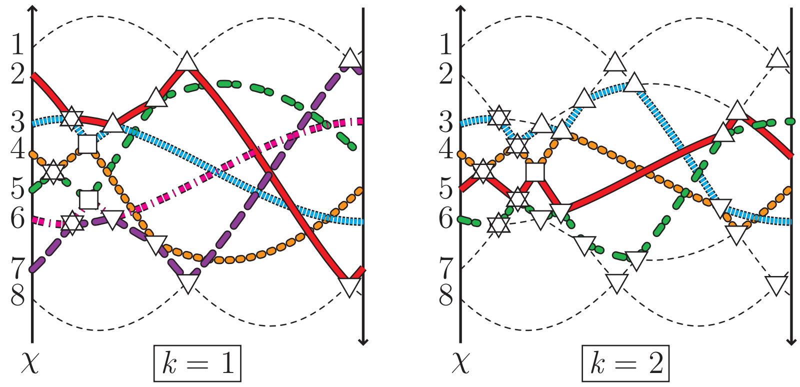

Figure 3.20: The sets $\mathbb{U}^k_\chi(L)$, $\mathbb{L}^k_\chi(L)$, and $\mathbb{G}^k_\chi(L)$ for the pseudoline arrangement of Figure 3.6(b) and $k \in \{1, 2\}$. The underlying k-pseudotriangulation is the greedy k-pseudotriangulation of L.

Example 3.36. We consider the arrangement V_n^* of n pseudolines in convex position. Let z be a vertex on the upper hull of its support, $F := \{z' \mid z \preccurlyeq z'\}$ denote the filter generated by z, and χ denote the corresponding cut (see Figure 3.21). It is easy to check that:

(i) $\mathbb{U}^k_\chi(V_n^*) = \{\ell_\alpha \wedge \ell_\beta \mid 1 \le \alpha \le n \text{ and } \alpha < \beta \le \alpha + k\}$;

(ii) $\mathbb{L}^k_\chi(V_n^*) = \{\ell_\alpha \wedge \ell_\beta \mid 1 \le \alpha \le k \text{ and } \alpha < j \le n\}$; and

(iii) $\mathbb{G}^k_\chi(V_n^*) = \mathbb{U}^k_\chi(\mathcal{C}_n) \cup \mathbb{L}^k_\chi(\mathcal{C}_n)$.

Observe again that the remaining vertices are exactly the crossing points of the χ-greedy k-pseudotriangulation of V_n^*.

Theorem 3.37 extends this observation to all pseudoline arrangements, using convex position as a starting point for a proof by mutation.

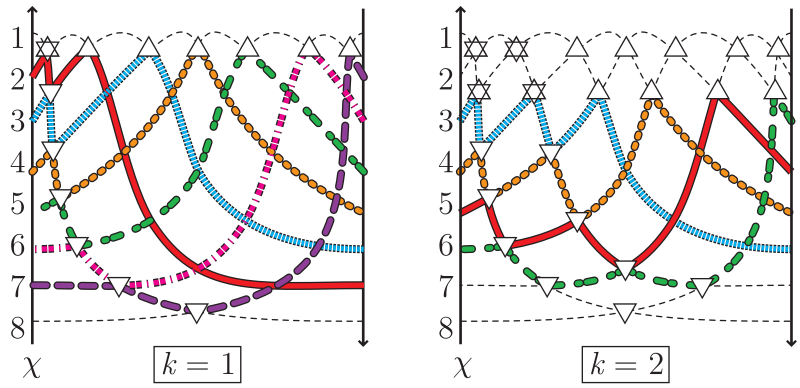

Figure 3.21: The sets $\mathbb{U}^k_\chi(V^*_8)$, $\mathbb{L}^k_\chi(V^*_8)$, and $\mathbb{G}^k_\chi(V^*_8)$ for the arrangement V^*_8 of 8 pseudolines in convex position, and $k \in \{1, 2\}$. The underlying k-pseudotriangulation is the greedy k-pseudotriangulation of V^*_8.

Theorem 3.37. *For any pseudoline arrangement L with no contact point, and any cut χ of L, the sets $V(\Gamma^k_\chi(L))$ and $\mathbb{G}^k_\chi(L)$ coincide.*

The proof of this theorem works by mutation. A *mutation* is a local transformation of an arrangement L that only inverts one triangular face of L. More precisely, it is a homotopy of arrangements during which only one curve $\ell \in L$ moves, sweeping a single vertex of the remaining arrangement $L \smallsetminus \{\ell\}$ (see Figure 3.22 and Appendix A.1 for more details).

If P is a point set of a topological plane, mutating an empty triangle $p^*q^*r^*$ of P^* by sweeping the vertex $q^* \wedge r^*$ with the pseudoline p^* corresponds in the primal to moving a little bit p such that only the orientation of the triangle pqr changes.

The graph of mutations on pseudoline arrangements is known to be connected: any two pseudoline arrangements (with no contact points and the same number of pseudolines) are homotopic via a finite sequence of mutations (followed by a homeomorphism). In fact, one can even avoid mutations of triangles that cross a given cut of L:

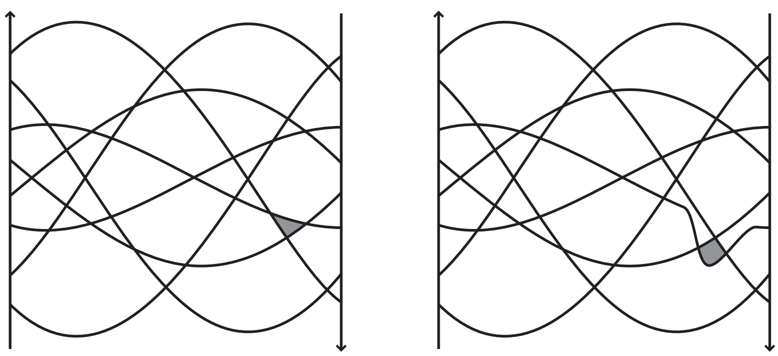

Figure 3.22: A mutation in the arrangement of Figure 3.6(b).

Proposition 3.38. *Let L and L' be two pseudoline arrangements of $\mathcal{M}$ (with no contact points and the same number of pseudolines) and χ be a cut of both of L and L'. There is a finite sequence of mutations of triangles disjoint from χ that transforms L into L'.*

Proof. We prove that any arrangement L of n pseudolines can be transformed into the arrangement V_n^* of n pseudolines in convex position (see Figure 3.21).

Let $\ell_1, \dots, \ell_n$ denote the pseudolines of L (ordered by their crossings with χ). Let Δ denote the triangle formed by χ, ℓ_1 and ℓ_2. If there is a vertex of the arrangement $L \smallsetminus \{\ell_1, \ell_2\}$ inside Δ, then there is a triangle of the arrangement L inside Δ and adjacent to ℓ_1 or ℓ_2. Mutating this triangle reduces the number of vertices of $L \smallsetminus \{\ell_1, \ell_2\}$ inside Δ such that after some mutations, there is no more vertex inside Δ. If Δ is intersected by pseudolines of $L \smallsetminus \{\ell_1, \ell_2\}$, then there is a triangle inside Δ formed by ℓ_1, ℓ_2 and one of these intersecting pseudolines (the one closest to $\ell_1 \wedge \ell_2$). Mutating this triangle reduces the number of pseudolines intersecting Δ. Thus, after some mutations, Δ is a triangle of the arrangement L.

Repeating these arguments, we can affirm that, for all $i \in \{2, \dots, n-1\}$ and after some mutations, ℓ_i, ℓ_1, ℓ_{i+1} and χ delimit a face of the arrangement L. Thus, one of the two topological disk delimited by χ and ℓ_1 contains no more vertex of L, and the proof is then straightforward by induction. $\square$

Let ∇ be a triangle of L not intersecting χ. Let L' denote the pseudoline arrangement obtained from L by mutating the triangle ∇ into the inverted triangle Δ. Let $a < b < c$ denote the indices of the pseudolines ℓ_a, ℓ_b and ℓ_c that form ∇ and Δ. In ∇, we denote $A = \ell_b \wedge \ell_c$, $B = \ell_a \wedge \ell_c$ and $C = \ell_a \wedge \ell_b$; similarily, in Δ, we denote $D = \ell_b \wedge \ell_c$, $E = \ell_a \wedge \ell_c$ and $F = \ell_a \wedge \ell_b$ (see Figure 3.23).

Lemma 3.39. *With these notations, the following properties hold:*

(i) $B \in \mathbb{U}_\chi^k(L) \Leftrightarrow C \in \mathbb{U}_\chi^{k-1}(L) \Leftrightarrow E \in \mathbb{U}_\chi^{k-1}(L') \Leftrightarrow F \in \mathbb{U}_\chi^k(L')$
$A \in \mathbb{U}_\chi^k(L) \Leftrightarrow D \in \mathbb{U}_\chi^k(L')$
$E \in \mathbb{L}_\chi^k(L') \Leftrightarrow D \in \mathbb{L}_\chi^{k-1}(L') \Leftrightarrow B \in \mathbb{L}_\chi^{k-1}(L) \Leftrightarrow A \in \mathbb{L}_\chi^k(L)$
$F \in \mathbb{L}_\chi^k(L') \Leftrightarrow C \in \mathbb{L}_\chi^k(L)$

(ii) $C \in \mathbb{U}_\chi^k(L) \Rightarrow A \in \mathbb{U}_\chi^k(L)$
$E \in \mathbb{U}_\chi^k(L') \Rightarrow D \in \mathbb{U}_\chi^k(L')$
$D \in \mathbb{L}_\chi^k(L') \Rightarrow F \in \mathbb{L}_\chi^k(L')$
$B \in \mathbb{L}_\chi^k(L) \Rightarrow C \in \mathbb{L}_\chi^k(L)$
$B \in \mathbb{G}_\chi^k(L) \Rightarrow C \in \mathbb{G}_\chi^k(L) \wedge D \in \mathbb{G}_\chi^k(L') \wedge F \in \mathbb{G}_\chi^k(L')$
$E \in \mathbb{G}_\chi^k(L') \Rightarrow D \in \mathbb{G}_\chi^k(L') \wedge C \in \mathbb{G}_\chi^k(L) \wedge A \in \mathbb{G}_\chi^k(L)$

(iii) $C \in \mathbb{G}_\chi^k(L) \Rightarrow A \in \mathbb{U}_\chi^k(L) \vee C \in \mathbb{L}_\chi^k(L)$
$D \in \mathbb{G}_\chi^k(L') \Rightarrow F \in \mathbb{L}_\chi^k(L') \vee D \in \mathbb{U}_\chi^k(L')$
$A \in \mathbb{G}_\chi^k(L) \Rightarrow A \in \mathbb{U}_\chi^k(L) \vee C \in \mathbb{L}_\chi^{k-1}(L)$
$F \in \mathbb{G}_\chi^k(L') \Rightarrow F \in \mathbb{L}_\chi^k(L') \vee D \in \mathbb{U}_\chi^{k-1}(L')$

(iv) $C \in \mathbb{G}_\chi^k(L) \wedge E \notin \mathbb{G}_\chi^k(L') \Rightarrow A \notin \mathbb{G}_\chi^k(L)$
$D \in \mathbb{G}_\chi^k(L') \wedge B \notin \mathbb{G}_\chi^k(L) \Rightarrow F \notin \mathbb{G}_\chi^k(L')$

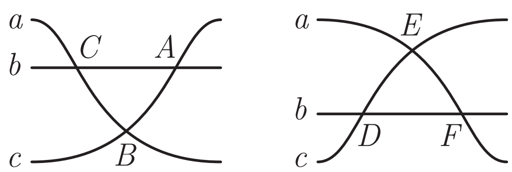

Figure 3.23: A local image of a mutation.

Proof. By symmetry, it is enough to prove the first line of each of the four points of the lemma.

Properties of point (i) directly come from the definitions. For example, all the assertions of the first line are false if and only if there exist $\gamma_1, \dots, \gamma_{k-1}$ with $a < \gamma_1 < \dots < \gamma_{k-1}$ and, for all $i \in [k-1]$, $\ell_a \wedge \ell_{\gamma_i} \preccurlyeq_\chi C$ (or equivalently $\ell_a \wedge \ell_{\gamma_i} \preccurlyeq_\chi E$).

We derive point (ii) from the following observation: if $\gamma > b$ and if $\ell_b \wedge \ell_\gamma \preccurlyeq_\chi C$, then $\gamma > a$ and $\ell_a \wedge \ell_\gamma \preccurlyeq_\chi B$.

For point (iii), assume that $A \notin \mathbb{U}^k_\chi(L)$ and $C \notin \mathbb{L}^k_\chi(L)$. Then there exist $\gamma_1, \dots, \gamma_k$ and $\delta_1, \dots, \delta_k$ such that $\delta_1 < \dots < \delta_k < b < \gamma_1 < \dots < \gamma_k$ and, for all $i \in [k]$, $\ell_b \wedge \ell_{\gamma_i} \preccurlyeq_\chi A$ (and therefore $\ell_a \wedge \ell_{\gamma_i} \preccurlyeq_\chi C$) and $\ell_b \wedge \ell_{\delta_i} \preccurlyeq_\chi C$. Thus $C \notin \mathbb{G}^k_\chi(L)$.

Finally, assume that $C \in \mathbb{G}^k_\chi(L)$ and $E \notin \mathbb{G}^k_\chi(L')$. Then, there exist $\gamma_1, \dots, \gamma_k$ and $\delta_1, \dots, \delta_k$ such that $a < \gamma_1 < \dots < \gamma_k$, $\delta_1 < \dots < \delta_k < c$, $\delta_k < \gamma_1$, and for all $i \in [k]$, $\ell_a \wedge \ell_{\gamma_i} \preccurlyeq_\chi E$ and $\ell_c \wedge \ell_{\delta_i} \preccurlyeq_\chi E$. Since $C \in \mathbb{G}^k_\chi(L)$, we have $\delta_k > b$. Thus $b < \gamma_1 < \dots < \gamma_k$ and for all $i \in [k]$, $\ell_b \wedge \ell_{\gamma_i} \preccurlyeq_\chi A$ and $\ell_c \wedge \ell_{\delta_i} \preccurlyeq_\chi A$. This implies that $A \notin \mathbb{G}^k_C(L)$. $\square$

We are now ready to establish the proof of Theorem 3.37:

Proof of Theorem 3.37. The proof works by mutation. We already observed the result when the pseudoline arrangement is in convex position (see Example 3.36 and Figure 3.21). Proposition 3.38 ensures that any pseudoline arrangement can be reached from this convex configuration by mutations of triangles not intersecting χ. Thus, it is sufficient to prove that such a mutation preserves the property.

Assume that L is a pseudoline arrangement and χ is a cut of L, for which the result holds. Let ∇ be a triangle of L not intersecting χ. Let L' denote the pseudoline arrangement obtained from L by mutating the triangle ∇ into the inverted triangle Δ. Let A, B, C and D, E, F denote the vertices of ∇ and Δ as indicated in Figure 3.23.

If v is a vertex of the arrangement L' different from D, E, F, then:

$$v \in V(\Gamma^k_\chi(L')) \Leftrightarrow v \in V(\Gamma^k_\chi(L)) \Leftrightarrow v \in \mathbb{G}^k_\chi(L) \Leftrightarrow v \in \mathbb{G}^k_\chi(L').$$

Thus, we only have to prove the equivalence when $v \in \{D, E, F\}$. The proof is a (computational) case analysis: using the properties of Lemma 3.39 as boolean equalities relating the boolean variables "$X \in \mathbb{Y}^p_\chi(L)$" (where $X \in \{A, B, C, D, E, F\}$, $\mathbb{Y} \in \{\mathbb{U}, \mathbb{L}, \mathbb{G}\}$, and $p \in \{k-1, k\}$), we have written a short boolean satisfiability program which affirms that:

(i) either $\{A, B, C\} \subset \mathbb{G}^k_\chi(L)$ and $\{D, E, F\} \subset \mathbb{G}^k_\chi(L')$;

(ii) or $\{A, B, C\} \cap \mathbb{G}^k_\chi(L) = \{A, C\}$ and $\{D, E, F\} \cap \mathbb{G}^k_\chi(L') = \{D, E\}$;

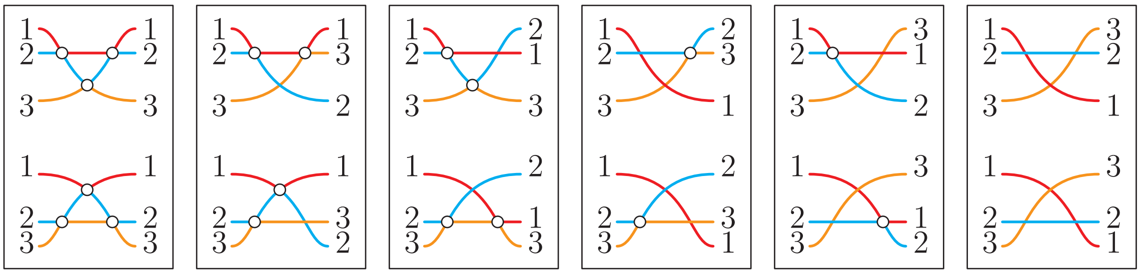

Figure 3.24: The six possible cases for the mutation of the greedy k-pseudotriangulation.

(iii) or $\{A, B, C\} \cap \mathbb{G}^k_\chi(L) = \{B, C\}$ and $\{D, E, F\} \cap \mathbb{G}^k_\chi(L') = \{D, F\}$;
(iv) or $\{A, B, C\} \cap \mathbb{G}^k_\chi(L) = \{A\}$ and $\{D, E, F\} \cap \mathbb{G}^k_\chi(L') = \{D\}$;
(v) or $\{A, B, C\} \cap \mathbb{G}^k_\chi(L) = \{C\}$ and $\{D, E, F\} \cap \mathbb{G}^k_\chi(L') = \{F\}$;
(vi) or $\{A, B, C\} \cap \mathbb{G}^k_\chi(L) = \emptyset$ and $\{D, E, F\} \cap \mathbb{G}^k_\chi(L') = \emptyset$.

It is easy to check that these six cases correspond to sorting the six possible permutations of $\{1, 2, 3\}$ on ∇ and Δ (see Figure 3.24). Thus, if $V(\Gamma^k_\chi(L)) \cap \{A, B, C\} = \mathbb{G}^k_\chi(L) \cap \{A, B, C\}$, then $V(\Gamma^k_\chi(L')) \cap \{D, E, F\} = \mathbb{G}^k_\chi(L') \cap \{D, E, F\}$, which finishes the proof. □

Let us finish this discussion by recalling the interpretation of the horizon sets when $k = 1$. Let P be a finite point set. For any $p \in P$, let $u(p)$ denote the point q that minimizes the angle (Ox, pq) among all points of P with $y_p < y_q$ (by convention, for the higher point p of P, $u(p) = p$). The *upper horizon tree* of P is the set $\mathbb{U}(P) = \{pu(p) \,|\, p \in P\}$. The *lower horizon tree* $\mathbb{L}(P)$ of P is defined symetrically. See Figure 3.25.

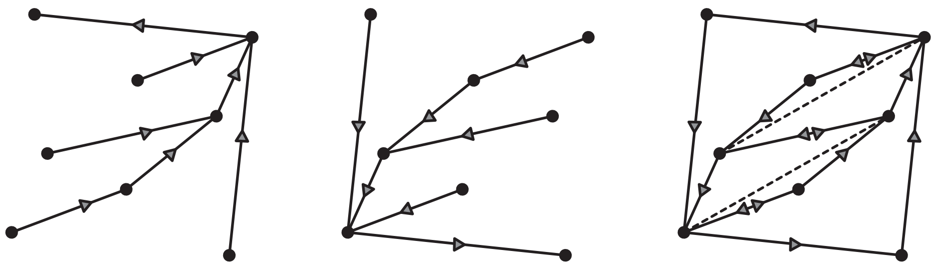

Figure 3.25: The upper horizon tree (left), the lower horizon tree (middle), and the greedy pseudotriangulation (right) of the point set of Figure 3.6(a). The dashed edges in the greedy pseudotriangulation are not in the horizon trees.

Choosing a cut χ of P^* corresponding to the point at infinity $(-\infty, 0)$ makes coincide primal and dual definitions of horizon sets: $\mathbb{U}^1_\chi(P^*) = \mathbb{U}(P)^*$ and $\mathbb{L}^1_\chi(P^*) = \mathbb{L}(P)^*$.

In [Poc97], Michel Pocchiola observed that the set $\mathbb{U}(P) \cup \mathbb{L}(P)$ of edges can be completed into a pseudotriangulation of P just by adding the sources of the faces of P^* intersected by the cut χ. The obtained pseudotriangulation is our χ-greedy 1-pseudotriangulation $\Gamma^1_\chi(P^*)$.

3.5.2 Multipseudotriangulations of double pseudoline arrangements

In this section, we deal with double pseudoline arrangements, *i.e.* duals of sets of disjoint convex bodies. Definitions and properties of multipseudotriangulations naturally extend to these objects.

3.5.2.1 Definitions

A simple closed curve in the Möbius strip can be:
(i) either contractible (homotopic to a point);
(ii) or non separating, or equivalently homotopic to a generator of the fundamental group of $\mathcal{M}$: it is a pseudoline;
(iii) or separating and non-contractible, or equivalently homotopic to the double of a generator of the fundamental group of $\mathcal{M}$: it is called a *double pseudoline* (see Figure 3.26(a)).

The complement of a double pseudoline ℓ has two connected components: the bounded one is a Möbius strip M_ℓ and the undounded one is an open cylinder C_ℓ (see Figure 3.26(a)).

The canonical example of a double pseudoline is the set C^* of tangents to a convex body C of the plane. Observe also that the pth level of a pseudoline arrangement is a double pseudoline. If C is a convex body of the plane, then the Möbius strip M_{C^*} corresponds to lines that pierce C, while C_{C^*} corresponds to lines disjoint from C. If C and C' are two disjoint convex bodies, the two corresponding double pseudolines C^* and C'^* cross four times (see Figure 3.27 and Figure 3.28). Each of these four crossings corresponds to one of the four *bitangents* (or *common tangents*) between C and C'.

Definition 3.40 ([HP09]). *A* double pseudoline arrangement *is a finite set of double pseudolines such that any two of them have exactly four intersection points, cross transversally at these points, and induce a cell decomposition of the Möbius strip (i.e. the complement of their union is a union of topological disks, together with the external cell).*

Given a set Q of disjoint convex bodies in the plane (or in any topological plane), its dual $Q^* := \{C^* \mid C \in Q\}$ is an arrangement of double pseudolines (see Figure 3.27 and Figure 3.28).

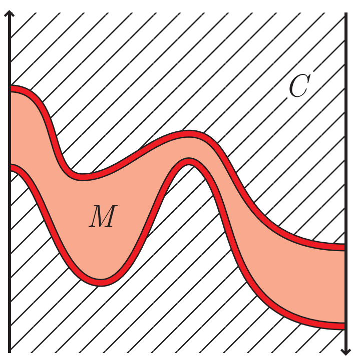

(a)

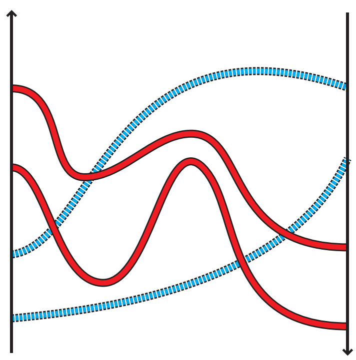

(b)

Figure 3.26: (a) A double pseudoline; (b) An arrangement of 2 double pseudolines.

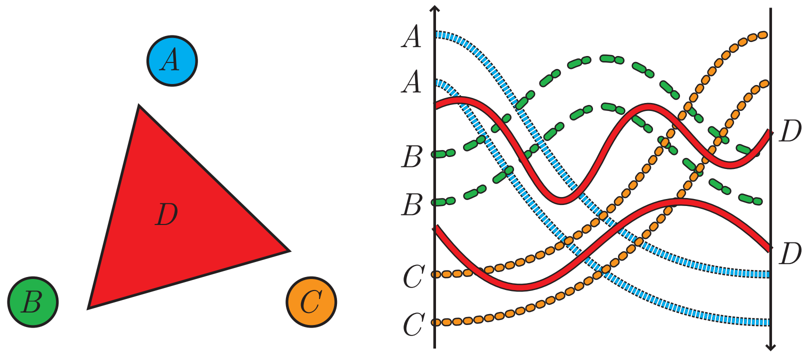

Figure 3.27: A configuration of four disjoint convex bodies and its dual double pseudoline arrangement.

Furthermore, as for pseudoline arrangements, any double pseudoline arrangement can be represented by (*i.e.* is the dual of) a set of disjoint convex bodies in a topological plane [HP09]. For more details on double pseudoline arrangements, we refer to our Appendix A.1, where we discuss an algorithm to enumerate all arrangements with few double pseudolines.

In this chapter, we only consider *simple* arrangements of double pseudolines. Defining the *support*, the *levels*, and the *kernels* of double pseudoline arrangements as for pseudoline arrangements, we can extend multipseudotriangulations to double pseudoline arrangements (see Figure 3.29):

Definition 3.41. *A k-pseudotriangulation of a double pseudoline arrangement L is a pseudoline arrangement supported by the k-kernel of L.*

All the properties related to flips developed in Section 3.1 apply in this context. In the end of this section, we only revisit the properties of the primal of a multipseudotriangulation of a double pseudoline arrangement.

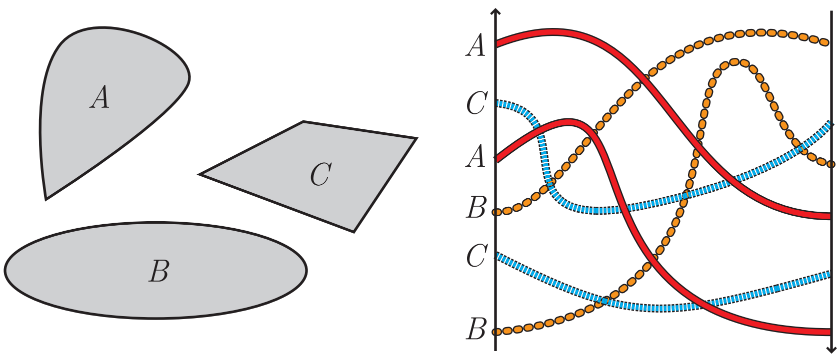

Figure 3.28: A configuration of three disjoint convex bodies and its dual double pseudoline arrangement.

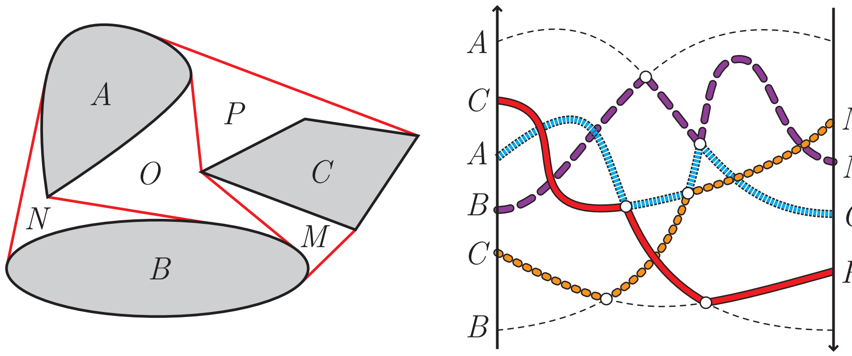

Figure 3.29: A pseudotriangulation of the set of disjoint convex bodies of Figure 3.28.

3.5.2.2 Elementary properties

Let Q be a set disjoint convex bodies in general position in the plane and Q^* be its dual arrangement. Let Λ be a k-pseudotriangulation of Q^*, $V(\Lambda)$ denote all crossing points of Q^* that are not crossing points of Λ, and E denote the corresponding set of bitangents of Q. As in Subsection 3.3.2, we discuss the properties of the primal configuration E:

Lemma 3.42. *The set E has $4|Q|k - |Q| - 2k^2 - k$ edges.*

Proof. The number of edges of E is the number of crossing points of Q^* minus the number of crossing points of Λ, *i.e.*

$$|E| = 4\binom{|Q^*|}{2} - \binom{|\Lambda|}{2} = 4\binom{|Q|}{2} - \binom{2|Q| - 2k}{2} = 4|Q|k - |Q| - 2k^2 - k. \qquad \square$$

We now discuss pointedness. For any convex body C of Q, we arbitrarily choose a point p_C in the interior of C, and we consider the set X_C of all segments between p_C and a sharp boundary point of C. We denote by $X := \bigcup_{C \in Q} X_C$ the set of all these segments.

Lemma 3.43. *The set $E \cup X$ cannot contain a k-alternation.*

Proof. Let C be a convex body of Q, q be a sharp point of C and $F := \{[p_i, q] \mid i \in [2k]\}$ be a set of edges incident to q such that $\{[p_C, q]\} \cup F$ is a k-alternation. We prove that F is not contained in E. Indeed, the dual pseudolines $\{p_i^* \mid i \in [2k]\}$ intersect alternately the double pseudoline C^* between the tangents to C at q (see Figure 3.30). This ensures the existence of a witness pseudoline ℓ that separates all the contact points $p_i^* \wedge C^*$, while crossing C^* exactly $2k$ times and the other double pseudolines of Q^* exactly has q^* does. (As usual, we obtain it by a perturbation of the pseudoline q^*.) Counting the crossings of ℓ with Q^* and Λ respectively, we obtain:

(i) ℓ crosses Q^* exactly $2|(Q \smallsetminus \{C\})^*| + 2k = 2|Q| + 2k - 2$ times;
(ii) ℓ crosses Λ at least $|\Lambda| = 2|Q| - 2k$ times;
(iii) for each of the points $p_i \wedge q^*$, replacing the crossing point by a contact point removes two crossings with ℓ. $\square$

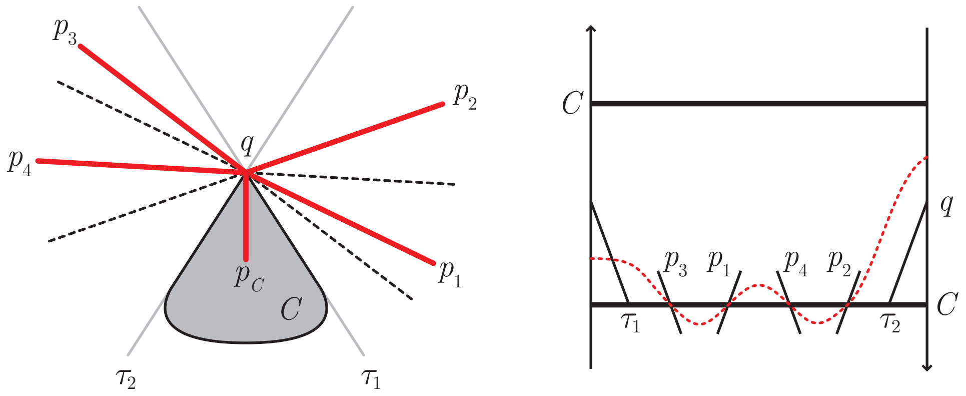

Figure 3.30: A k-alternation at a sharp point.

3.5.2.3 Stars

If λ is a pseudoline of Λ, we call *star* the envelope $S(\lambda)$ of the primal lines of the points of λ. The star $S(\lambda)$ contains:

(i) all bitangents τ between two convex bodies of Q such that τ is a contact point of λ; and

(ii) all convex arcs formed by the tangent points of the lines covered by λ with the convex bodies of Q.

This star is a (non-necessarily simple) closed curve. We again have bounds on the number of *corners* (*i.e.* convex internal angles) of $S(\lambda)$:

Proposition 3.44. *The number of corners of $S(\lambda)$ is odd and between $2k-1$ and $4k|Q|-2k-1$.*

Proof. In the case of double pseudoline arrangements, corners are even easier to characterize: a bitangent τ between two convex C and C' of Q always defines two corners, one at each extremity. These corners are contained in one of the two stars adjacent to τ. Let λ be a pseudoline with a contact point at τ. In a neighbourhood of τ, the pseudoline λ can be contained either in M_{C^*} or in C_{C^*}. In the first case, the star $S(\lambda)$ contains the corner formed by the bitangent τ and the convex C (or possibly, by the bitangent τ and another tangent to C); while in the second case, it does not. (The same observation holds for C'.)

In other words, if the double pseudoline C^* supports a pseudoline λ between two contact points v and w, then one of the three following situations occurs (see Figure 3.31):

(i) either v and w lie on opposite sides of λ; then exactly one of these contact points lies in M_{C^*}, and $S(\lambda)$ has one corner at C.

(ii) or v and w both lie on M_{C^*}, and $S(\lambda)$ has two corners at C.

(iii) or v and w both lie on C_{C^*}, and $S(\lambda)$ has no corners at C.

In particular, the number $c = c(\lambda)$ of corners of λ is the number of situations (i) plus twice the number of situations (ii). This proves that c is odd and (at least) bigger than the number of opposite consecutive contact points of the pseudoline λ.

In order to get a lower bound on this number, we construct (as in the proof of Proposition 3.28) a witness pseudoline μ that crosses λ between each pair of opposite contact points and passes on

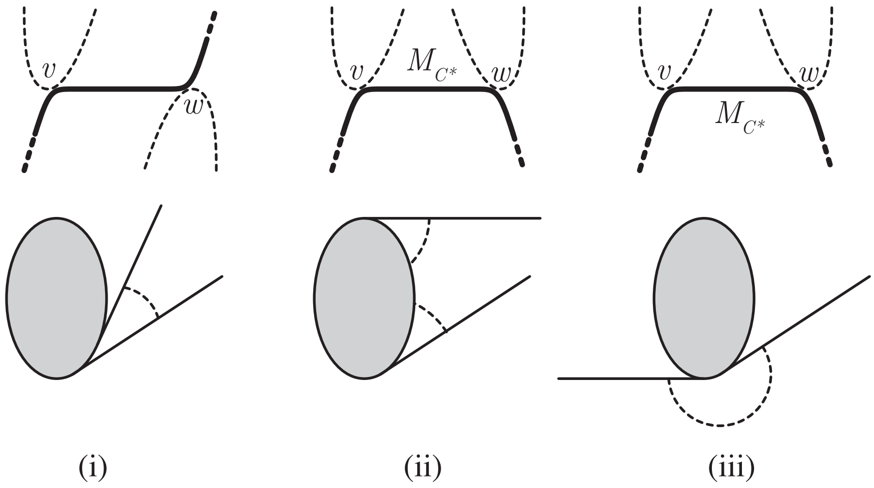

Figure 3.31: The three possible situations for two consecutive contact points on ℓ.

the opposite side of each contact point. It crosses λ at most c times and $\Lambda \smallsetminus \{\lambda\}$ exactly $|\Lambda| - 1$ times. Moreover, if α is a pseudoline and β is a double pseudoline of $\mathcal{M}$, then either α is contained in M_β and has no crossing with β, or α and β have an even number of crossings. Since μ is a pseudoline and can be contained in at most one Möbius strip M_C^* (for $C \in Q$), the number of crossings of μ with Q^* is at least $2(|Q| - 1)$. Thus, we obtain the lower bound $2(|Q| - 1) \leq 2|Q| - 2k - 1 + c$, *i.e.* $c \geq 2k - 1$.

From this lower bound, we obtain the upper bound: the total number of corners is at most twice the number of bitangents:

$$2(4k|Q| - |Q| - 2k^2 - k) \geq \sum_{\mu \in \Lambda} c(\mu) \geq c(\lambda) + (2|Q| - 2k - 1)(2k - 1),$$

and we get, $c \leq 4|Q|k - 2k - 1$. □

When $k = 1$, we can even prove that all stars are pseudotriangles. Indeed, since any star has at least 3 corners, the upper bound calculus gives $2(3|Q| - 3) \geq c + 3(2|Q| - 3)$, *i.e.* $c \leq 3$.

For general k, observe that contrary to the case of pseudoline arrangements, a star may have $2k - 1$ corners (see Figure 3.32).

Let us now give an analogue of Proposition 3.27. For any point q in the plane, we denote by $\eta^k(q)$ the number of crossings between q^* and the support of Q^* minus its first k levels. Let $\delta^k(q) := \eta^k(q)/2 - |Q| + k$. For any $\lambda \in \Lambda(U)$ and any point q in the plane, we still denote by $\sigma_\lambda(q)$ the *winding number* of $S(\lambda)$ around q.

Proposition 3.45. *For any point q of the plane $\delta^k(q) = \sum_{\lambda \in \Lambda} \sigma_\lambda(q)$.*

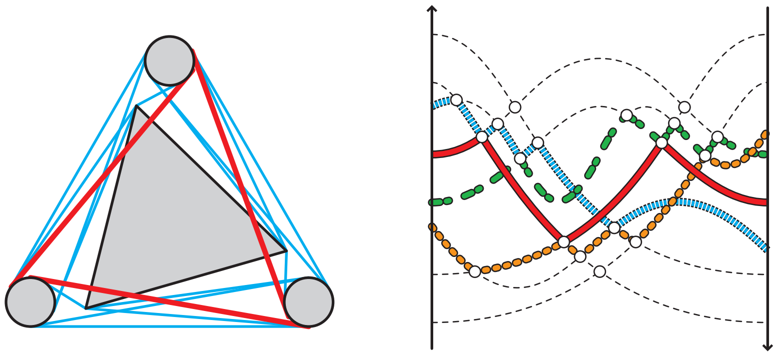

Figure 3.32: A 2-pseudotriangulation of the double pseudoline arrangement of Figure 3.27. Observe that the bolded red star has only 3 corners.

Proof. Remember that if $\tau_\lambda(q)$ denotes the number of intersection points between q^* and λ, then $\sigma_\lambda(q) = (\tau_\lambda(q) - 1)/2$. Thus, we have

$$\eta^k(q) = \sum_{\lambda\in\Lambda} \tau_\lambda(q) = |\Lambda| + 2\sum_{\lambda\in\Lambda} \sigma_\lambda(q),$$

and we get the result since $|\Lambda| = 2|Q| - 2k$. $\square$

When $k = 1$, it is easy to see that $\delta^1(q)$ is 1 if q is inside the *free space* of the convex hull of Q (*i.e.* in the convex hull of Q, but not in Q), and 0 otherwise. Remember that a *pseudotriangulation* of Q is a pointed set of bitangents that decomposes the free space of the convex hull of Q into pseudotriangles [PV96a]. Propositions 3.44 and 3.45 provide, when $k = 1$, the following analogue of Theorem 3.14:

Theorem 3.46. *Let Q be a set of disjoint convex bodies (in general position) and Q^* denote its dual arrangement. Then:*

(i) The dual pseudoline arrangement $T^* := \{\Delta^* \,|\, \Delta$ pseudotriangle of $T\}$ of a pseudotriangulation T of Q is a 1-pseudotriangulation of Q^*.

(ii) primal set of edges $E := \{[p, q] \,|\, p, q \in P,\ p^* \wedge q^*$ is not a crossing point of $\Lambda\}$ of a 1-pseudotriangulation Λ of Q^* is a pseudotriangulation of Q.

Observe that at least two other arguments are possible to prove (ii):

1. either comparing the degrees of the flip graphs as in our first proof of Theorem 3.14;
2. or checking that all forbidden configurations of the primal (two crossing bitangents, a non-pointed sharp vertex, a non-free bitangent) may not appear in the dual, as in our second proof of Theorem 3.14.

Let us finish this discussion about stars by interpreting the number $\delta^k(q)$ for general k and for “almost every” point q. For any convex body C of Q, let ∇C denote the intersection of all closed half-planes delimited by a bitangent between two convex bodies of Q, and containing C (see Figure 3.33). By definition, the bitangents between two convex bodies C and C' of Q coincide

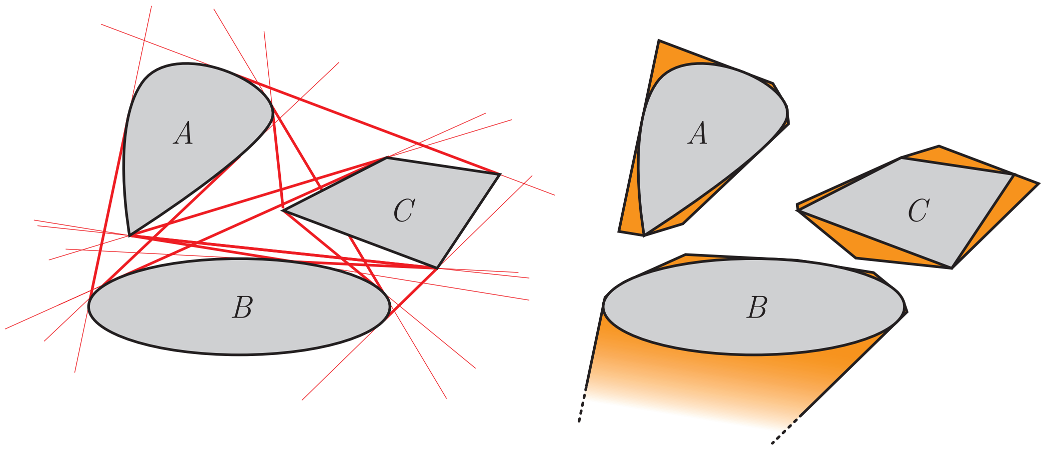

Figure 3.33: The set of all bitangents to the arrangement of convex bodies of Figure 3.28 and the corresponding maximal convex bodies.

with the bitangent of ∇C and $\nabla C'$. Furthermore, the convex bodies ∇C ($C \in Q$) are maximal for this property. We denote $\nabla Q := \{\nabla C \,|\, C \in Q\}$ the set of maximal convex bodies of Q.

For a point q outside ∇Q, the interpretation of $\delta^k(q)$ is similar to the case of points. We call *level* of a bitangent τ the level of the corresponding crossing point in Q^*. Given a point q outside ∇Q, the number $\delta^k(q)$ is the number of bitangents of level k crossed by any (generic continuous) path from q to the external face (in the complement of ∇Q), counted positively when passing from the "big" side to the "small side", and negatively otherwise.

Chapter Four

THREE OPEN PROBLEMS

In this chapter, we discuss three further topics on multitriangulations:

1. *Dyck multipaths*: k-triangulations of the n-gon are counted by the same Hankel determinant of Catalan numbers which counts certain families of non-crossing Dyck paths [Jon03, Jon05]. We investigate explicit bijections between these two combinatorial sets.
2. *Rigidity*: The number of edges in a k-triangulation is exactly that of a minimally generically rigid graph in a $2k$-dimensional space. We conjecture that k-triangulations are minimally rigid graphs in dimension $2k$, and prove it for $k = 2$.
3. *Multiassociahedron*: The simplicial complex of all $(k+1)$-crossing-free sets of k-relevant edges of the n-gon is known to be a combinatorial sphere [Jon03] and conjectured to be polytopal (as happens for $k = 1$ where it is the polar of the associahedron [Lee89, BFS90, GKZ94, Lod04, HL07]). We realize the first non-trivial case (namely, $k = 2$ and $n = 8$) and discuss possible generalizations of two constructions of the associahedron (the first one is the secondary polytope of the regular n-gon [GKZ94] and the second one is Loday's construction [Lod04]).

Throughout the chapter, the goal is to present natural and promising ideas based on stars in multitriangulations, although they provide at the present time only partial results to these problems.

4.1 CATALAN NUMBERS AND DYCK MULTIPATHS

Let $C_m := \frac{1}{m+1}\binom{2m}{m}$ denote the mth *Catalan number*. Catalan numbers count several combinatorial families (thus called *Catalan families*) such as triangulations, rooted binary trees, Dyck paths, etc. — see [Sta99, Sta09] for an exhaustive list. These families all share the same recursive structure: a Catalan object of size p can be decomposed into an object of size q and another one of size $p - q - 1$, for some $1 \leq q \leq p - 1$. This recursive structure is apparent in the equation $f(x) = 1 + xf(x)^2$ on the generating function $f(x) := \sum_{m\in\mathbb{N}} C_m x^m$ of a Catalan family, and it inductively defines natural bijections between Catalan families.

The goal of this section is to discuss enumerative and bijective combinatorics of multitriangulations. We give in particular a brief overview of the existing literature on this quesiton.

4.1.1 Enumeration of multitriangulations and Dyck multipaths

As mentioned in the introduction, Jakob Jonsson proved in [Jon03, Jon05] that:

Theorem 4.1 ([Jon03, Jon05]). *The number $\theta(n,k)$ of k-triangulations of the n-gon equals:*

$$\theta(n,k) = \det(C_{n-i-j})_{1\le i,j\le k} = \det \begin{pmatrix} C_{n-2} & C_{n-3} & \iddots & \iddots & C_{n-k-1} \\ C_{n-3} & \iddots & \iddots & C_{n-k-1} & \iddots \\ \iddots & \iddots & \iddots & \iddots & \iddots \\ \iddots & C_{n-k-1} & \iddots & \iddots & C_{n-2k+1} \\ C_{n-k-1} & \iddots & \iddots & C_{n-2k+1} & C_{n-2k} \end{pmatrix}. \qquad \square$$

Remark 4.2. This Hankel determinant can be expressed by the explicit product formula [Vie00]:

$$\theta(n,k) = \prod_{1\le i<j\le n-2k-1} \frac{i+j+2k}{i+j}.$$

For the asymptotics of it, observe that the recurrence $C_n = \frac{4n-2}{n+1}C_{n-1}$ makes each entry of the matrix equal to C_n times a rational function of degree at most $2k$ in n. Since $C_n \in \Theta(4^n n^{-3/2})$ we conclude that, for fixed k, the number of k-triangulations of an n-gon grows as 4^{nk}, modulo a rational function of degree $O(k^2)$ in n.

On the other hand, the determinant in Theorem 4.1 also counts another class of objects:

Definition 4.3. *A Dyck path of semilength ℓ is a lattice path using north steps $N := (0,1)$ and east steps $E := (1,0)$ starting from $(0,0)$ and ending at (ℓ,ℓ), and such that it never goes below the diagonal $y = x$ — see Figure 4.1(a). We call Dyck k-path of semilength ℓ any k-tuple $(D_1,\ldots,D_k)$ of Dyck paths of semilength ℓ such that each D_i never goes above D_{i-1}, for $2\le i\le k$ — see Figure 4.1(b).*

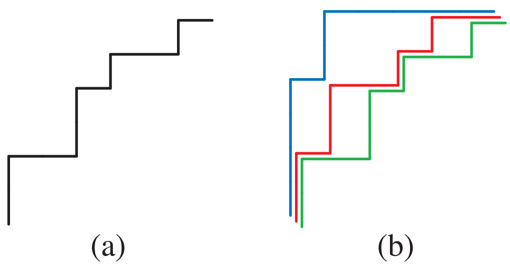

Figure 4.1: (a) A Dyck path $NNEENNENEENE$ and (b) a Dyck 3-path of semilength 6.

That the Catalan determinant of Theorem 4.1 also counts the number of Dyck k-paths of semilength $n-2k$ is an almost direct application of Lindström-Gessel-Viennot technique [Lin73, GV85, dSCV86] to count non-intersecting lattice paths. The equality of their cardinality raises the question to find an explicit bijection between the set $T_{n,k}$ of k-triangulations of the n-gon and the set $D_{n,k}$ of Dyck k-paths of semilength $n-2k$. This question was stated by Jakob Jonsson in [Jon03, Jon05] and studied in different articles [Eli07, Nic09, Kra06, Rub07]. Finding an explicit bijection between these two families would provide a simpler proof of the enumeration formula of Theorem 4.1, and may also reveal properties hidden on one family but apparent on the other one.

4.1.2 Overview of existing proofs

In this section, we give a short overview of different approaches to Theorem 4.1. This theorem, conjectured by Andreas Dress, Jacobus Koolen, Vincent Moulton and Volkmar Welker, was first proved by Jakob Jonsson in [Jon03] with a direct but "complicated" method (according to its author). This unpublished manuscript also contains a discussion on reasonable properties that should have an explicit bijection between $T_{n,k}$ and $D_{n,k}$ (we develop this discussion later in Section 4.1.3). Afterwards, the topic followed two different directions: on the one hand, it was replaced in the more general context of the study of fillings of polyominoes with restricted length of increasing and decreasing chains [Jon05, Kra06, Rub07]; on the other hand, two different bijections between 2-triangulations and 2-paths recently appeared [Eli07, Nic09].

4.1.2.1 Fillings of polyominoes

In [Jon05], Jakob Jonsson gave an alternative simpler (but this time indirect) proof of Theorem 4.1, using the following polyominoes (see Figure 4.2 and [Jon05, Kra06, Rub07] for details):

Definition 4.4. *A stack polyomino is a subset $\{(i,j) \,|\, 0 \le i \le s_j,\ j \in [r]\}$ of $\mathbb{Z}^2$, where there exists $t \in [r]$ such that $0 \le s_1 \le \cdots \le s_t$ and $s_t \ge \cdots \ge s_r \ge 0$. The r-tuple $(s_1, \dots, s_r)$ is the shape of the polyomino, while the multiset $\{s_1, \dots, s_r\}$ is its content. A filling of a polyomino is an assignment of 0 and 1 to its boxes. For $\ell \in \mathbb{N}$, an ℓ-diagonal of a filling of a polyomino Λ is a chain $(\alpha_1, \beta_1), \dots, (\alpha_\ell, \beta_\ell)$ of ℓ boxes of Λ filled with 1 and such that:*

- *$\alpha_1 < \alpha_2 < \dots < \alpha_\ell$ and $\beta_1 < \beta_2 < \dots < \beta_\ell$, and*
- *the rectangle $\{(\alpha,\beta) \,|\, \alpha_1 \le \alpha \le \alpha_\ell$ and $\beta_1 \le \beta \le \beta_\ell\}$ is a subset of Λ.*

Two special polyominoes are particularly interesting for us:

(i) It was proved in [HT92] that the Hankel determinant of Catalan numbers of Theorem 4.1 also counts the number of maximal $(k+1)$-diagonal-free fillings of the triangular polyomino $A_n := \{(i,j) \,|\, 0 \le i \le n-j-1,\ j \in [n-1]\}$ (see Figure 4.2(c)).

(ii) The adjacency matrix of any subset E of E_n defines a filling of the triangular polyomino $B_n := \{(i,j) \,|\, 0 \le i < j \le n-1\}$ (see Figure 4.2(d)) in which ℓ-diagonals correspond to ℓ-crossings of E. In particular, this gives a straightforward bijection between k-triangulations of an n-gon and maximal $(k+1)$-diagonal-free fillings of B_n.

According to these two examples, the proof of Theorem 4.1 is a direct consequence of:

Theorem 4.5 ([Jon05]). *The number of maximal $(k+1)$-diagonal-free fillings of a stack polyomino does not depend on its shape, but only on its content.* □

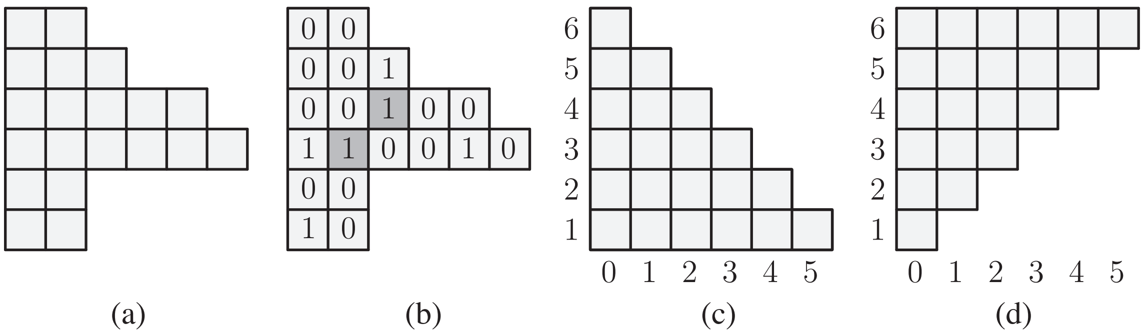

Figure 4.2: (a) A stack polyomino of shape $(2, 2, 6, 5, 3, 2)$; (b) a filling of this polyomino, with a shaded 2-diagonal; (c) the polyomino A_7; and (d) the polyomino B_7.

Enumeration properties of fillings of polyominoes with restrictions on the length of the longest increasing and decreasing chains have been studied in other related articles. In particular, Christian Krattenthaler [Kra06] used growth diagrams to study symmetries of crossings and nestings in fillings of Ferrers shapes (generalizing results of [CDD+07]). Following this method, Martin Rubey [Rub07] extended Theorem 4.5 to more general moon polyominoes (using a very different method from the original proof). He also emphasized that "the problem of finding a completely bijective proof [...] remains open. However, it appears that this problem is difficult".

4.1.2.2 Two inductive bijections when $k = 2$

In recent papers, Sergi Elizalde [Eli07] and Carlos Nicolas [Nic09, Nic08] both obtained explicit bijections between 2-triangulations and Dyck 2-paths. Although the details are quite different, these two papers are both based on induction. The idea is to construct two isomorphic generating trees for the sets $T_{n,2}$ and $D_{n,2}$, that is to say, two parallel constructions which generate on the one hand $T_{n+1,2}$ from $T_{n,2}$, and on the other hand $D_{n+1,2}$ from $D_{n,2}$. Of course, in both articles, the generating tree for 2-triangulations is based on the flattening & inflating operation developed in Section 2.5 (this operation is very implicit in [Eli07], but completely explicit in [Nic09, Nic08]). The two bijections essentially differ in the way they use this flattening & inflating operation:

1. In [Eli07], Sergi Elizalde starts from a 2-triangulation and inductively flattens the 2-star which contains the last 2-ear. During this inductive process, the 2-relevant edges of the 2-triangulation are colored with two different colors. Then, each color is used to define one of the Dyck paths (see Section 4.1.3).
2. In [Nic09, Nic08], Carlos Nicolas defines a generalized notion of *returns* in a Dyck multipath. There is a parallelism between returns in Dyck k-paths and k-crossings incident to $\{0, \dots, k-1\}$ in k-triangulations: similarly to the inflating operation of Section 2.5, a return in a Dyck k-path of semilength ℓ can be inflated to obtain a Dyck k-path of semilength $\ell + 1$. This parallelism is exploited to obtain two isomorphic generating trees for 2-triangulations and Dyck 2-paths. By construction, the resulting bijection has the nice property to identify returns with k-crossings incident to $\{0, \dots, k-1\}$.

Unfortunately, it seems that none of these two bijections can be directly extended to general k.

4.1.3 Edge colorings and indegree sequences

We now present a relevant attempt to define an explicit and direct (meaning non-inductive) bijection between k-triangulations and Dyck k-paths. The starting point of our definition is the following well-known bijection between triangulations and Dyck paths:

Proposition 4.6. *The application $d : T \mapsto d(T) := N^{\delta_0(T)}EN^{\delta_1(T)}E \dots N^{\delta_{n-3}(T)}E$, where $\delta_i(T)$ is the number of triangles of T whose first vertex is i, is a bijection between triangulations of the n-gon and Dyck paths of semilength $n-2$.* $\square$

In other words, the sequence of north powers of the Dyck path $d(T)$ is the sequence of indegrees of the vertices of the n-gon in the oriented graph whose edges are the interior edges of T together with the top edge $[0, n-1]$, all oriented towards their smallest vertex.

Observe that this bijection

(i) respects triangles: each triangle of T corresponds to a pair of NE steps in $d(T)$. Namely, the Dyck path $d(T)$ has a north step at the first vertex of each triangle and an east step at the second vertex of each triangle.

(ii) is compatible with the natural partial orders: if T and T' are two triangulations of the n-gon, with $T < T'$ (*i.e.* such that T' can be obtained from T by a sequence of slope-increasing flips — see Section 2.3), then $d(T)$ is above $d(T')$.

Generalizing this simple bijection, Jakob Jonsson studied in [Jon03] the repartition of indegree sequences in multitriangulations. He defined the two following parallel notions:

Definition 4.7. *Given a k-triangulation T of the n-gon, consider the oriented graph whose edges are the k-relevant edges of T together with the the top k-boundary edges of the n-gon $[0, n-k]$, $[1, n-k+1], \dots, [k-1, n-1]$, all oriented towards their smallest vertex. The indegree sequence of T is the sequence of indegrees of the first $n-k-1$ vertices of the n-gon in this oriented graph.*

The signature of a Dyck k-path $(N^{\nu_0^1}EN^{\nu_1^1}E \dots N^{\nu_{\ell-1}^1}E, \dots, N^{\nu_0^k}EN^{\nu_1^k}E \dots N^{\nu_{\ell-1}^k}E)$ of semilength ℓ is the sequence $(\sum_{i=1}^k \nu_{j-i}^i)_{j \in [\ell+k-1]}$ (with the convention $\nu_p^q := 0$ if $p < 0$ or $p \geq \ell$).

Example 4.8. In Figure 4.3, the indegree sequence of the 2-triangulation and the signature of the Dyck 2-path both equal $(1, 4, 2, 0, 1)$.

The following theorem refines Theorem 4.1, comparing indegree sequences in multitriangulations *vs.* signatures in Dyck multipaths:

Theorem 4.9 ([Jon03]). *For any $k \geq 1$, $n \geq 2k+1$ and any sequence $\delta := (\delta_1, \dots, \delta_{n-k-1})$, the number of k-triangulations of the n-gon with indegree sequence δ equals the number of Dyck k-paths of semilength $n-2k$ with signature δ.* $\square$

It is reasonable to look for a bijection between multitriangulations and Dyck multipaths which respects these parameters. In other words, the indegree sequence of a k-triangulation already tells us the signature that should have its associated Dyck k-path, and it "only remains" to separate this signature into k distinct north power sequences.

Using this heuristic, we attempt to generalize the function d of Proposition 4.6 in a seemingly natural fashion. Unfortunately, the generalized function D that we construct is not bijective; but

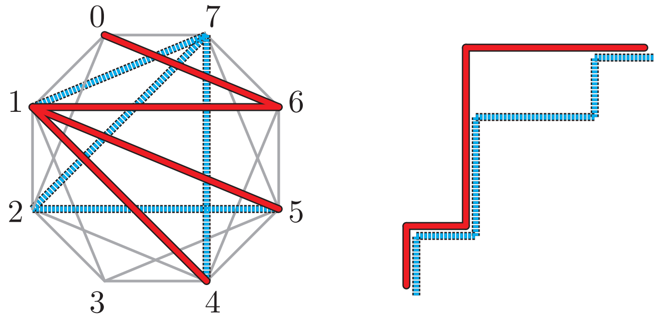

Figure 4.3: The Dyck 2-path $D(T)$ associated to the 2-triangulation T of Figure 1.4.

it is surprisingly close to a bijection for small cases (see Figure 4.5 and the discussion above), which makes it plausible that a clever modification of it makes it a bijection.

We consider the application D, which associates to a k-triangulation of the n-gon the k-tuple $D(T) := (D_1(T), \dots, D_k(T))$ of lattice paths defined by

$$D_j(T) := N^{\delta^j_{j-1}(T)} E N^{\delta^j_j(T)} E \dots N^{\delta^j_{j+n-2k-2}(T)} E,$$

where $\delta^j_i(T)$ denotes the number of k-stars of T whose jth vertex is the vertex i. See Figure 4.3 for an example.

This application can also be interpreted in terms of colored indegrees of the vertices of the n-gon. For $j \in [k]$, and for any k-star S of T, with vertices $0 \preccurlyeq s_1 \prec s_2 \prec \cdots \prec s_{2k+1} \preccurlyeq n-1$, color the edge $[s_j, s_{k+j+1}]$ with color j. This coloring decomposes the set of all k-relevant edges of T together with the top k-boundary edges $[0, n-k], \dots, [k-1, n-1]$ into k disjoint sets $\tau_1, \dots, \tau_k$ each containing $n-2k$ edges. The sequence of north powers of the jth Dyck path $D_j(T)$ is the sequence of indegrees of the vertices of the n-gon in the oriented graph τ_j (where each edge is oriented towards its smallest vertex), after $j-1$ shifts.

The two following lemmas tend to show that the application D is a reasonable approximation of the bijection we are looking for.

Lemma 4.10. *For any k-triangulation of the n-gon, the k-tuple of lattice paths $D(T)$ is a Dyck k-path of semilength $n-2k$.*

Proof. We first prove that each $D_j(T)$ is a Dyck path of semilength $n-2k$. Observe that for each $i \in [n-2k]$, there exists a unique k-star S_i whose $(k+1)$th vertex is $k-1+i$ (indeed, it is the unique k-star bisected by the line passing through the vertex $k-1+i$ and through the midpoint of $[0, n-1]$). The jth vertex of this k-star S_i is certainly smaller or equal $i+j-2$. Thus, the number of north steps in $D_j(T)$ before the ith east step (which is the number of k-stars of T whose jth vertex is smaller or equal $i+j-2$) is at least i. Since the total numbers of north steps and of east steps both equal the number $n-2k$ of k-stars of T, the lattice path $D_j(T)$ is indeed a Dyck path of semilength $n-2k$.

Finally, in each k-star of T, the $(j-1)$th vertex is certainly before the jth vertex, which implies that for all i, the number of k-stars of T whose $(j-1)$th vertex is smaller or equal $i+j-3$

is at least the number the number of k-stars of T whose jth vertex is smaller or equal $i + j - 2$. Consequently, the Dyck path $D_j(T)$ never goes above the Dyck path $D_{j-1}(T)$ for all j, and $D(T)$ is indeed a Dyck k-path. $\square$

By construction, the function D respects k-stars and preserves the parameters of Theorem 4.9. Furthermore, it is compatible with the following partial orders:

(i) For two k-triangulations T and T' we write $T < T'$ if T' can be obtained from T by a sequence of slope-increasing flips — see Section 2.3.

(ii) For two Dyck k-paths $D := (D_1, \dots, D_k)$ and $D' := (D'_1, \dots, D'_k)$ we write $D < D'$ if D_1 is above D'_1, or $D_1 = D'_1$ and D_2 is above D'_2, or etc. (lexicographic order for the "above" relation).

Lemma 4.11. *The application D is increasing with respect to these partial orders: for any two k-triangulations T and T' of the n-gon, $T < T'$ implies $D(T) < D(T')$.*

Proof. It is sufficient to prove that a single slope-increasing flip in a multitriangulation also increases the associated Dyck multipath (for the order $<$ on Dyck multipaths).

Consider a slope-increasing flip from a k-triangulation T to another one T'. Let $a < c$ denote the vertices of the edge in $T \smallsetminus T'$ and $b < d$ the vertices of the edge in $T' \smallsetminus T$. Since the flip is slope-increasing, we have $0 \preccurlyeq a \prec b \prec c \prec d \preccurlyeq n-1$. Let R (resp. S) be the k-star of T adjacent to $[a, c]$ and containing the vertex b (resp. d). Similarly, let X (resp. Y) be the k-star of T' adjacent to $[b, d]$ and containing the vertex a (resp. c). See Figure 4.4 for an example.

It is easy to check that, before vertex a, the vertices of X are exactly the vertices of R while the vertices of Y are exactly the vertices of S. Furthermore, we have more vertices of R than vertices of S before a. Consequently, if a is the jth vertex of S, then:

(i) for all $i < j$ we have $D_i(T) = D_i(T')$, since the ith vertex of R is also the ith vertex of X and the ith vertex of S is also the ith vertex of Y; and

(ii) $D_j(T)$ is strictly above $D_j(T')$, since the jth vertex of R is also the jth vertex of X, but the jth vertex of S (*i.e.* a) is strictly before the jth vertex of Y (because $a \notin Y$).

This proves that $D(T) < D(T')$, by definition of the lexicographic order. $\square$

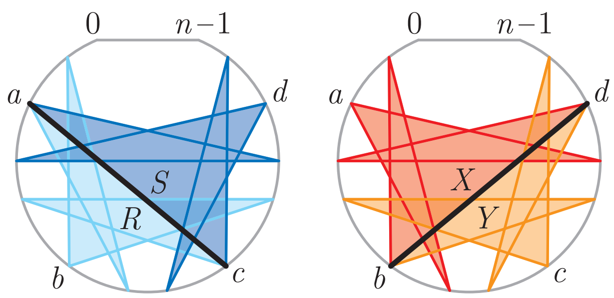

Figure 4.4: An increasing flip.

Despite these promising properties, it turns out that D is not a bijection between $T_{n,k}$ and $D_{n,k}$, but it is surprisingly close to be:

(i) For $k = 2$ and $n \leq 7$, the function D is a bijection.

(ii) For $k = 2$ and $n = 8$ it is not, but there is a unique pair of 2-triangulations producing the same Dyck 2-path. They are shown in Figure 4.5.

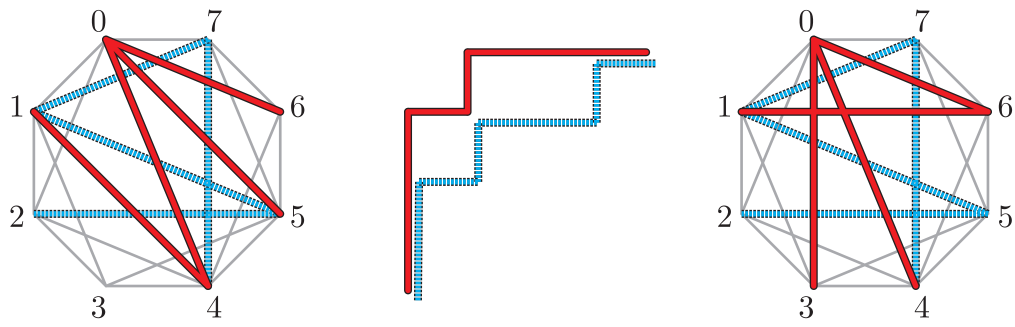

Figure 4.5: Two 2-triangulations of the octagon with the same associated Dyck 2-path.

We have tried other possible functions from $T_{n,k}$ to $D_{n,k}$, all obtained as a generalization of a well-known bijection between $T_{n,1}$ and $D_{n,1}$, and compatible with k-stars. It turns out that all of them are equivalent to D (in the sense that for $k = 2$ and $n = 8$, we always obtain twice the Dyck 2-path of Figure 4.5).

We hope however that k-stars will help to find a direct general bijection.

4.1.4 Beam arrangement

To finish this section, we construct another lattice path configuration associated to a multitriangulation, namely its dual pseudoline arrangement presented in Chapter 3 that we embed on the integer grid. For this, we exploit again the adjacency matrix of a multitriangulation, drawing lattice paths on its rows and columns according to its entries.

Let T be a k-triangulation of the n-gon. For each edge (u, v) of T (with $u < v$), we place a *mirror* at the grid point of coordinates (u, v). This mirror is a double faced mirror parallel to the diagonal $x = y$ so that it reflects a ray coming from $(-\infty, v)$ to a ray going to $(u, +\infty)$, and a ray coming from $(u, -\infty)$ to a ray going to $(+\infty, v)$. Furthermore, for $1 \leq i \leq n - 2k$, we place a *light beam* at $(-\infty, k - 1 + i)$ pointing horizontally. We obtain $n - 2k$ beams which reflect on the mirrors of T — see *e.g.* Figure 4.6. All throughout this chapter, we will call this ray configuration the *beam arrangement* associated to T.

Our study of pseudoline arrangements in Chapter 3 implies the following properties:

Proposition 4.12. *(i) All beams are x- and y-monotone lattice paths.*

(ii) The ith beam comes from $(-\infty, k - 1 + i)$ and goes to $(k - 1 + i, +\infty)$.

(iii) Each beam reflects exactly $2k+1$ times, and thus, has k vertical segments (plus one vertical half-line) and k horizontal segments (plus one horizontal half-line).

(iv) The beams form a pseudoline arrangement: any two of them cross exactly once. □

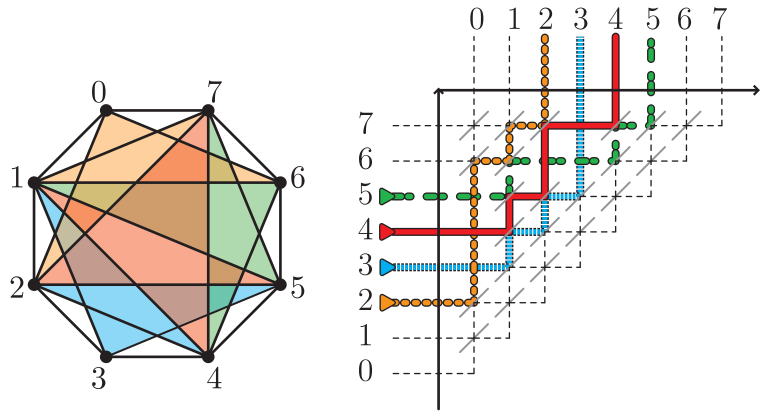

Figure 4.6: The beam arrangement of the triangulation of Figure 1.4.

Let us recall that the ith beam B_i "corresponds" via duality to the k-star S_i of T whose $(k+1)$th vertex is the vertex $k-1+i$ (in other words, the k-star bisected by the line passing through the vertex $k-1+i$ and through the midpoint of $[0, n-1]$). Indeed:

(i) the beam B_i is (by duality) the set of all bisectors of S_i;

(ii) the mirrors which reflect B_i are the edges of S_i; and

(iii) the intersection of two beams B_i and B_j is the common bisector of S_i and S_j.

Observe that instead of k Dyck paths of semi-length $n-2k$, the beam arrangement of a k-triangulation has $n-2k$ beams which all have k horizontal steps. Despite these similarities, we have not found any bijection between Dyck k-paths and beam arrangements.

4.2 RIGIDITY

Triangulations are rigid graphs in the plane: the only continuous motions of their vertices which preserve their edges' lengths are the isometries of the plane. In this section, we investigate rigidity properties of multitriangulations. We recall some rigidity notions, and refer to [Gra01, Fel04] for very nice introductions to combinatorial rigidity, and to [GSS93] for a more technical one.

4.2.1 Combinatorial rigidity, sparsity and arboricity

A d-dimensional *framework* is a finite graph together with an embedding of its vertices in $\mathbb{R}^d$. We think of the straight edges of a framework as rigid bars connected by flexible joints, and we want to distinguish *flexible* frameworks (those that can be deformed preserving their edges' lengths) from *rigid* ones.

To be more precise, define a *motion* of a framework to be a continuous motion of its vertices which preserves the lengths of all its edges (see Figure 4.7). Of course, any framework admits *rigid motions* which correspond to isometries of $\mathbb{R}^d$ (*i.e.* in which not only the edges' lengths are preserved, but also all distances between all pairs of vertices). *Rigid* frameworks are those that admit only rigid motions.

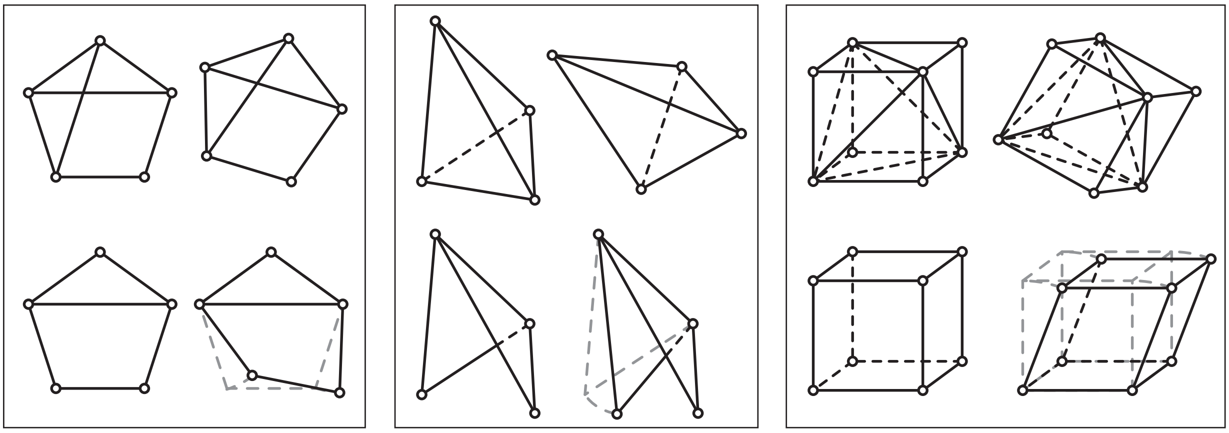

Figure 4.7: Motions of frameworks. Each of the three groups represents a rigid graph (top left) with a rigid motion (top right) and a flexible subgraph (bottom left) with a non-rigid motion (bottom right). The first group lies in the plane while the other two lie in 3-dimensional space.

In other words, a framework is rigid if the system of quadratic equations whose variables are the coordinates of its vertices and whose equations encode the lengths of its edges has locally no other non-congruent solution. Each edge of the graph is thus encoded by a quadratic equation which normally reduces the dimension of the solution by one (intuitively, one edge removes one "degree of freedom"). Since the space of geometric embeddings of a graph with n vertices in $\mathbb{R}^d$ has dimension dn while the space of congruent frameworks to a given framework has dimension $\binom{d+1}{2}$, it is reasonable to expect a framework to be rigid as soon as it has $dn - \binom{d+1}{2}$ edges "properly placed" (in the sense that no edge is redundant). The reality is a bit more complicated as the following examples show:

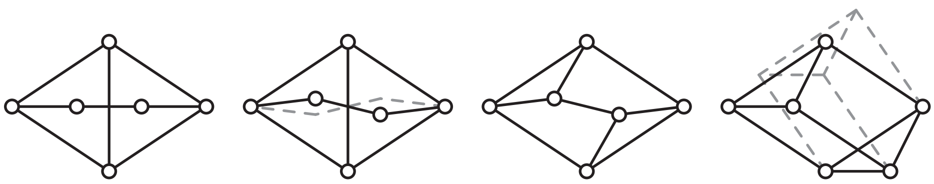

(a) (b) (c) (d)

Figure 4.8: Four 2-dimensional frameworks with 6 vertices.

We would expect 9 edges to be required to make a 2-dimensional framework with 6 vertices rigid. However, the behavior of (a) and (d) is not the one expected: (a) is rigid (because the middle horizontal chain is tight) although it has only 8 edges and (d) is flexible (because it has three parallel edges) although it has 9 edges. These frameworks (a) and (d) are *singular* in the sense that there exist arbitrarily close frameworks (for example (b) and (c)) which behave differently with respect to rigidity: just break the colinearity in (a) (like in (b)) or the parallelism in (d) (like in (c)). In fact, the d-dimensional embeddings of a given finite graph are either almost all rigid or almost all flexible. In the first case, the graph is said to be *generically rigid* in dimension d. Generic rigidity is a combinatorial property: it only depends on the graph and not of a specific embedding. In the plane, generic rigidity is completely characterized:

Theorem 4.13 ([Lam70, Hen11, Rec84]). *The following conditions on a graph $G := (V, E)$ are equivalent:*

1. *G is minimally generically rigid in the plane, i.e. G is generically rigid and removing any edge from G produces a generically flexible graph.*
2. *Laman's Condition [Lam70]: $|E| = 2|V| - 3$ and any subgraph of G on v vertices has at most $2v - 3$ edges.*
3. *Henneberg's Constructions [Hen11]: G can be constructed from a single edge by a sequence of Henneberg's additions: there exists a sequence $G_0 := (\{v, w\}, \{(v, w)\}), \dots, G_i := (V_i, E_i), \dots, G_p = G$ such that for any $i \in [p]$:*
   a) *either there exist three vertices $v \in V_i \smallsetminus V_{i-1}$ and $x, y \in V_{i-1}$ such that $V_i = V_{i-1} \cup \{v\}$ and $E_i = E_{i-1} \cup \{(v, x), (v, y)\}$;*
   b) *or there exist four vertices $v \in V_i \smallsetminus V_{i-1}$ and $x, y, z \in V_{i-1}$ with $(x, y) \in E_{i-1}$ such that $V_i = V_{i-1} \cup \{v\}$ and $E_i = E_{i-1} \triangle \{(v, x), (v, y), (v, z), (x, y)\}$.*
4. *Recski's Theorem [Rec84]: For any two distinct vertices $v, w \in V$, the (multi)graph $(V, E \cup \{(v, w)\})$ is the union of two spanning trees.* □

In dimension 3 and higher, combinatorial rigidity is far less understood. Generic rigid graphs still require sufficiently many non-redundant edges:

Proposition 4.14 (Laman's Condition). *A minimally generically rigid graph $G := (V, E)$ in dimension d is a d-Laman graph: $|E| = d|V| - \binom{d+1}{2}$ and any subgraph of G on v vertices has at most $dv - \binom{d+1}{2}$ edges.* □

However, this condition is not sufficient to be generically minimally rigid. The classical example is that of the *double banana* (see Figure 4.9) which is obtained by gluing two bananas (which are just two glued tetrahedra) at their endpoints. It has 8 vertices and 18 edges, and any induced subgraph on v vertices has less than $3v - 6$ edges. However, it is flexible since the bananas can rotate independently around the axis passing through their endpoints.

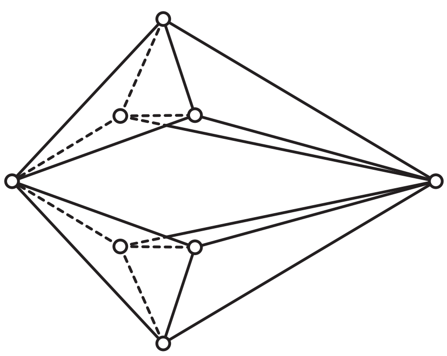

Figure 4.9: The double banana: a flexible but Laman 3-dimensional framework.

Laman graphs are particular examples of the following class of graphs:

Definition 4.15. *A (multi)graph $G := (V, E)$ is (p, q)-sparse if any subgraph of G on v vertices has at most $pv - q$ vertices. If furthermore $|E| = p|V| - q$, then G is said to be (p, q)-tight.*

Sparsity for several families of parameters (p, q) is relevant in rigidity theory, matroid theory and pebble games — see [LS08] and the references therein. The equivalence between properties (2), (3) and (4) of Theorem 4.13 is a specialization of the following theorem to the case $(p, q) = (2, 3)$.

Theorem 4.16 ([Haa02])**.** *Let p, q be to integers such that $0 \le p \le q < 2p$. The following conditions on a graph $G := (V, E)$ are equivalent:*

1. *G is (p, q)-tight: $|E| = p|V| - q$ and any subgraph of G on v vertices has at most $pv - q$ edges.*
2. *G is a $(p, q - p)$-arborescence: Adding any $q - p$ edges to G (including multiple edges) results in a (multi)graph decomposable into p edge-disjoint spanning trees.*

If furthermore $q \le 3p/2$, then these two conditions are equivalent to the following:

3. *G can be constructed by a Henneberg construction, starting from the graph with 2 vertices and $2p - q$ (multiple) edges, and repeating the following operation: remove a subset F of E with $0 \le |F| \le p$, and add a new vertex v to V adjacent to the $2|F|$ endpoints of F (with possibly multiple edges) and to $p - |F|$ additional arbitrary vertices of V, in such a way that no edge has multiplicity greater than $2p - q$.* □

Observe that (p, p)-tight graphs are exactly unions of p edge-disjoint spanning trees.

4.2.2 Sparsity in multitriangulations

The goal of this section is to present where rigidity, sparsity and arboricity show up in the context of multitriangulations. The motivation comes from the application of rigidity properties to the construction of the polytope of pseudotriangulations (see Remarks 4.81 and 4.82). The starting observation is the following consequence of Corollary 2.21:

Corollary 4.17. *k-triangulations are $\left(2k, \binom{2k+1}{2}\right)$-tight graphs.* □

As mentioned previously, being $\left(2k, \binom{2k+1}{2}\right)$-tight is a necessary, but not sufficient, condition for a graph to be minimally generically rigid in dimension $2k$. This suggests the conjecture:

Conjecture 4.18. *Every k-triangulation is minimally generically rigid in dimension $2k$.*

This conjecture is true when $k = 1$. More interestingly, we can prove it for $k = 2$:

Theorem 4.19. *Every 2-triangulation is a generically minimally rigid graph in dimension 4.*

Proof. We prove by induction on n that 2-triangulations of the n-gon are generically rigid in dimension 4. Minimality then follows from the fact that a generically rigid graph in dimension d needs to have at least $dn - \binom{d+1}{2}$ edges.

Induction begins with the unique 2-triangulation on five points, that is, the complete graph K_5, which is generically rigid in dimension 4.

For the inductive step, let us recall the following graph-theoretic construction called "vertex split" (see Figure 4.10 and [Whi90] for more details). Let $G := (V, E)$ be a graph, $u \in V$ be a vertex of G and $U := \{u' \in V \mid (u, u') \in E\}$ denote the vertices adjacent to u. Let $U = X \sqcup Y \sqcup Z$ be a partition of U. The *vertex split* of u on Y is the graph whose vertex set is $V \cup \{v\}$ (where v is a new vertex) and whose edge set is obtained from E by removing $\{[u, z] \mid z \in Z\}$ and adding $\{[u, v]\} \cup \{[v, y] \mid y \in Y\} \cup \{[v, z] \mid z \in Z\}$.

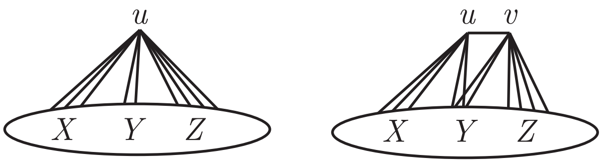

Figure 4.10: A vertex split on two edges.

The key result that we need is that a vertex split on $d - 1$ edges in a generically rigid graph in dimension d is also generically rigid in dimension d [Whi90].

So, let $n \geq 5$ and assume that we have already proved that every 2-triangulation of the n-gon is rigid. Let T be a 2-triangulation of the $(n + 1)$-gon. Let S be a 2-star of T with at least two 2-boundary edges (such a 2-star exists since it appears in the "outer" side of any 2-ear). It is easy to check that the inverse transformation of the flattening of S is exactly a vertex split on 3 edges. Thus, the result follows. □

Generalizing this proof, observe that if T is a k-triangulation and S a k-star of T with k k-boundary edges (or equivalently $k - 1$ consecutive k-ears), then the inverse transformation of the flattening of S is exactly a vertex split on $2k - 1$ edges. However, our proof of Theorem 4.19 cannot be directly applied since there exist k-triangulations with no k-star containing k k-boundary edges, or equivalently, without $k - 1$ consecutive k-ears, for $k \geq 3$ (see Figure 4.11).

Sparsity also shows up on dual graphs of multitriangulations. Remember from Section 2.6.2 that we defined the dual graph $T^{\#}$ of a k-triangulation T to be the multigraph whose vertices are

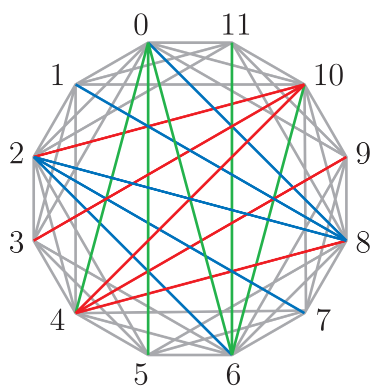

Figure 4.11: A 3-triangulation without 2 consecutives 3-ears.

the k-stars of T and with one edge between two k-stars for each of their common edges. As well as dual graphs of triangulations are trees, duals of multitriangulations are arborescences:

Proposition 4.20. *The dual graph of a k-triangulation is the union of k edge-disjoint spanning trees. In other words, dual graphs of k-triangulations are (k, k)-tight.*

Proof. The proof works again by induction on n. When $n = 2k + 1$, the dual graph is a single vertex and there is nothing to prove. For the inductive step, consider a k-triangulation T of the n-gon, and a k-crossing X of T which is external, *i.e.* adjacent to k consecutive vertices. We want to derive from a decomposition of the dual graph of T into k edge-disjoint spanning trees a similar decomposition of the dual graph of the inflating $T \Uparrow X$ of X in T.

Observe first that the graph $(T \Uparrow X)^\#$ can be easily described from $T^\#$: Let Y denote the multiset of vertices of $T^\#$ corresponding to all k-stars of T adjacent to an edge of X (a k-star appears in Y as many times as its number of edges in X) and let Z denote the set of edges of $T^\#$ corresponding to k-relevant edges of X. Then $(T \Uparrow X)^\#$ is obtained from $T^\#$ by removing the edges of Z and adding a new vertex v adjacent to all vertices of Y (with multiple edges if necessary). Observe that the vertex v has degree $|Y| = k + |Z|$.

Now consider a decomposition $\tau_1, \dots, \tau_k$ of $T^\#$ into k edge-disjoint spanning trees. For each $1 \le i \le k$, let $\alpha_i := |\tau_i \cap Z|$ be the number of edges of the k-crossing X whose dual edge is in τ_i. Then $\tau_i \smallsetminus Z$ is a forest with $1 + \alpha_i$ trees. For all i such that $\alpha_i \neq 0$, we transform this forest into a tree $\tilde{\tau}_i$ by choosing $1 + \alpha_i$ edges between v and the $2\alpha_i$ endpoints of $\tau_i \cap Z$. Then, the vertex v still has $k + |Z| - \sum_{i \,|\, \alpha_i \neq 0} (1 + \alpha_i) = |\{i \,|\, \alpha_i = 0\}|$ uncolored edges. We arbitrarily affect one such edge to connect v to each tree τ_i with $\alpha_i = 0$. The resulting trees $\tilde{\tau}_1, \dots, \tilde{\tau}_k$ form a decomposition of $(T \Uparrow X)^\#$. This finishes the proof since any k-triangulation of the $(n+1)$-gon can be obtained from a k-triangulation of the n-gon by inflating an external k-crossing. □

Example 4.21. k-colorable k-triangulations are exactly the k-triangulations whose dual graph is the union of k edge-disjoint paths. Indeed, we already implicitly proved in Section 2.4 that the dual graph of a k-colorable k-triangulation is a union of k disjoint paths (remember the algorithm which computes the k disjoint k-accordions of a k-colorable k-triangulation in the proof of Theorem 2.48). Reciprocally, if the dual graph of a k-triangulation can be decomposed into k paths, then no k-star of T can contain more than $2k$ k-relevant edges. Thus all k-stars of T are external, which characterizes k-colorable k-triangulations (Theorem 2.48).

Example 4.22. In Section 4.1.3, we have defined a k-coloring of the k-relevant edges of a k-triangulation T: for any k-star of T with vertices $0 \preccurlyeq s_1 \prec s_2 \prec \cdots \prec s_{2k+1} \preccurlyeq n-1$, color the first top edge $[s_1, s_{k+2}]$ with color 1, the second top edge $[s_2, s_{k+3}]$ with color 2, and so on until the kth top edge $[s_k, s_{2k+1}]$ with color k.

When $k = 2$, this 2-coloring of the 2-relevant edges of a 2-triangulation defines a decomposition of the dual graph $T^\#$ into two edge-disjoint spanning trees. Indeed, it is easy to check that if a 2-star S (with vertices $0 \preccurlyeq s_1 \prec \cdots \prec s_5 \preccurlyeq n-1$) shares its first top edge $[s_1, s_4]$ with another 2-star R (with vertices $0 \preccurlyeq r_1 \prec \cdots \prec r_5 \preccurlyeq n-1$), then the first top edge $[r_1, r_4]$ of R is smaller than that of S for the order defined by $[a, b] < [c, d] \Leftrightarrow (a < c)$ or $(a = c$ and $b > d)$. Thus, the subgraph of $T^\#$ corresponding to the edges colored with 1 has no cycle (its vertices are partially

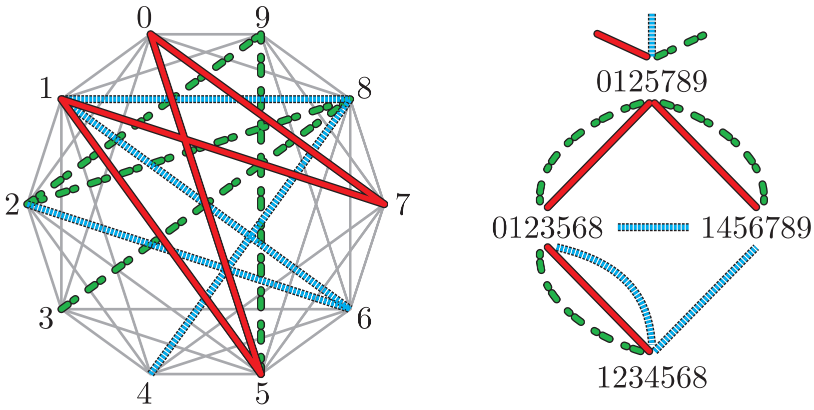

Figure 4.12: A 3-triangulation of the 10-gon in which coloring in each 3-star the first top edge in red, the second in blue and the third in green does not decompose the dual graph into three edge-disjoint spanning trees.

ordered). Since it has one edge less than the number of vertices, it is a spanning tree. The proof is symmetric for the graph produced by the edges colored with 2.

However, when $k > 2$, the resulting coloring is not necessarily a decomposition of $T^{\#}$ into edge-disjoint spanning trees. See for example Figure 4.12, where one color has a cycle.

4.3 Multiassociahedron

In this section, we consider the following complex:

Definition 4.23. *We denote by $\Delta_{n,k}$ the simplicial complex of all $(k+1)$-crossing-free subsets of k-relevant edges of E_n.*

It is indeed a simplicial complex since $(k+1)$-crossing-freeness is a hereditary condition: if a set of edges has no $(k+1)$-crossing, then any of its subsets is $(k+1)$-crossing-free.

Observe that we do not include the non-k-relevant edges of the n-gon in the sets of $\Delta_{n,k}$. Indeed, since it cannot appear in a $(k+1)$-crossing, a non-k-relevant edge would be a cone point of the complex: the simplicial complex of all $(k+1)$-crossing-free subsets of E_n is a kn-fold cone over $\Delta_{n,k}$. However, in order to keep notations and explanations simple, we sometimes implicitly include all the non-k-relevant edges of the n-gon in the elements of $\Delta_{n,k}$, as for example in the next paragraph.

Our study of k-triangulations of the n-gon already gave some combinatorial information about the simplicial complex $\Delta_{n,k}$:

(i) The maximal elements of $\Delta_{n,k}$ are the k-triangulations of the n-gon. Since all k-triangulations of the n-gon have $k(n-2k-1)$ k-relevant egdes (Corollary 2.21), the simplicial complex $\Delta_{n,k}$ is *pure* of dimension $k(n-2k-1)-1$.

(ii) The codimension 1 elements of $\Delta_{n,k}$ are flips between k-triangulations: they are obtained by removing one k-relevant edge from a k-triangulation, and we know that such a set of edges is contained in exactly two k-triangulations. Thus, every codimension 1 face of $\Delta_{n,k}$ is contained in exactly two facets of $\Delta_{n,k}$ (in other words, $\Delta_{n,k}$ is a pseudo-manifold). The graph of flips that we studied in Section 2.3 is the ridge-graph of $\Delta_{n,k}$.

(iii) Finally, a subset of at most k edges never contains a $(k+1)$-crossing. Thus, the simplicial complex $\Delta_{n,k}$ is *k-neighborly*: it contains all sets of at most k elements.

Before going further, we revisit the examples of Section 2.1.2:

Example 4.24 ($k = 1$)**.** The simplicial complex $\Delta_{n,1}$ of all crossing-free sets of internal diagonals of the n-gon is isomorphic to the boundary complex of the polar of the associahedron [Lee89, BFS90, GKZ94, Lod04, HL07]. We recall two constructions of this polytope in Section 4.3.1.

Example 4.25 ($n = 2k + \varepsilon$ with $\varepsilon \in [3]$)**.** Since the $(2k+1)$-gon has no k-relevant edge, and thus a unique k-triangulation, the simplicial complex $\Delta_{2k+1,k} = \{\emptyset\}$ is trivial.

More interestingly, the k-relevant edges of the $(2k+2)$-gon are its $k+1$ long diagonals, which form the unique $(k+1)$-crossing. Any set of at most k of them is $(k+1)$-crossing-free, and the simplicial complex $\Delta_{2k+2,k}$ is isomorphic to the boundary complex of the k-simplex $\triangle_k$ (see Figure 4.13).

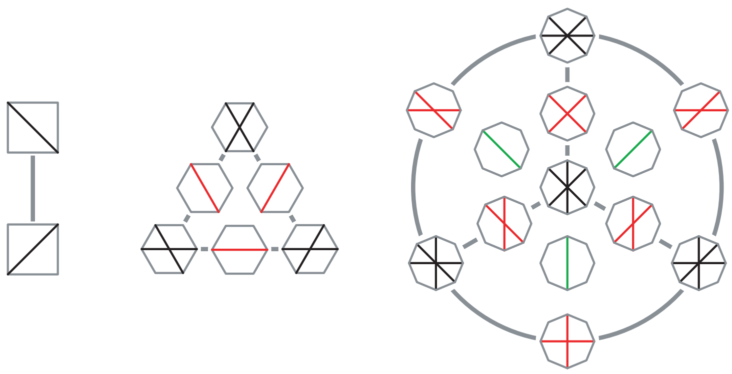

Figure 4.13: The simplicial complex $\Delta_{2k+2,k}$ for $k \in [3]$ (in the rightmost picture, the external face corresponds to the horizontal edge).

Finally, the last small case completely described in Section 2.1.2 is when $n = 2k+3$. The corresponding simplicial complex has also a very nice description:

Lemma 4.26. *The simplicial complex $\Delta_{2k+3,k}$ is the boundary complex of the cyclic polytope of dimension $2k$ with $2k+3$ vertices.*

Proof. Remember from Example 2.7 that the k-triangulations of the $(2k+3)$-gon are exactly the disjoint unions of k pairs of consecutive long diagonals of E_{2k+3}. This translates, by Gale's evenness criterion (see Proposition 5.6), into the facets of the cyclic polytope. $\square$

According to these examples, it is reasonable to wonder whether there exists a polytope generalizing the associahedron for all values of k:

Question 4.27. Is $\Delta_{n,k}$ the boundary complex of a polytope for any n and k?

If so, we will say that $\Delta_{n,k}$ is *realizable*. Observe that any *realization* would certainly be a simplicial $k(n-2k-1)$-polytope.

An important step towards the answer of this question is to know whether the simplicial complex $\Delta_{n,k}$ has the topology of a sphere. This was proved by Jakob Jonsson [Jon03, Theorem 1] in the following sense:

Theorem 4.28 ([Jon03])**.** *The simplicial complex $\Delta_{n,k}$ is a vertex-decomposable piece-wise linear sphere of dimension $k(n-2k-1)-1$.* □

Being a topological sphere is a necessary — but not sufficient — condition to be realizable.

Despite our efforts to solve it, Question 4.27 remains open in general. However, we present here two interesting steps in its direction:

1. In Section 4.3.2, we prove that the simplicial complex $\Delta_{8,2}$ is realizable, which solves the first non-trivial case (remember Examples 4.24 and 4.25). In fact, we do even more than just providing a single realization of $\Delta_{8,2}$, since we completely describe its space of symmetric realizations.
2. In Section 4.3.3, we propose a natural generalization of a construction of the associahedron due to Jean-Louis Loday [Lod04]. This results in the construction of a polytope with a rich combinatorial structure: its graph is the graph of flips restricted to certain k-triangulations, and it has a very simple facet description. *A priori* this polytope could have been a projection of a polytope realizing $\Delta_{n,k}$ (we will see why it cannot be such a projection).

4.3.1 Two constructions of the associahedron

In this section, we recall two constructions of the associahedron of which we will discuss the generalization later. In both constructions, a vector is associated to each triangulation of the n-gon, and the associahedron is obtained as the convex hull of the vectors associated to all triangulations of the n-gon. However, to associate a vector to a triangulation, the point of view is very different from one construction to the other: the first construction is based on the vertices of the n-gon (the vector has one coordinate for each vertex), while the second construction focusses on the triangles of a triangulation (the vector has one coordinate per triangle).

4.3.1.1 The secondary polytope of the n-gon

This first construction is due to Israel Gel'fand, Mikhail Kapranov and Andrei Zelevinski. In this construction, the vector associated to each triangulation is defined as follows:

Definition 4.29 ([GKZ94])**.** *The area vector of a triangulation T of the n-gon is the vector $\phi(T)$ of $\mathbb{R}^n$, whose vth coordinate (for $v \in V_n$) is the sum of the areas of the triangles of T containing the vertex v. The secondary polytope Σ_n is the convex hull of the area vectors of all triangulations of the n-gon.*

Remark 4.30. We obtain affine relations among the coordinates of the area vectors of the triangulations of the n-gon by using the triangles to decompose the total area and the center of mass of the n-gon. Indeed, the areas of all the triangles of a triangulation T sum to the area of the n-gon:

$$\mathcal{A}(\mathrm{conv}(V_n)) = \sum_{\triangle \in T} \mathcal{A}(\triangle) = \langle \mathbb{1} \,|\, \phi(T) \rangle.$$

Furthermore, the center of mass $\textsc{cm}(\mathrm{conv}(V_n))$ of the n-gon is the barycenter, with coefficients $\mathcal{A}(\triangle)$, of the centers of mass $\textsc{cm}(\triangle)$ of the triangles of T. Since the center of mass of a triangle is also its isobarycenter, we obtain:

$$\textsc{cm}(\mathrm{conv}(V_n)) = \sum_{\triangle \in T} \mathcal{A}(\triangle)\,\textsc{cm}(\triangle) = \sum_{\triangle \in T} \left(\mathcal{A}(\triangle) \sum_{v \in \triangle} \frac{v}{3} \right) = \frac{1}{3} \sum_{v \in V_n} \left(v \sum_{v \in \triangle \in T} \mathcal{A}(\triangle) \right).$$

Consequently, the secondary polytope Σ_n lies in an affine subspace of codimension 3.

Theorem 4.31 ([GKZ94])**.** *The boundary complex of the polar $\Sigma_n^\diamond$ of the secondary polytope is isomorphic to the simplicial complex $\Delta_{n,1}$ of crossing-free sets of diagonals of the n-gon.*

Proof. Consider a vector $\omega \in \mathbb{R}^n$. For any triangulation T of the n-gon,

$$\langle \omega \,|\, \phi(T) \rangle = \sum_{v \in V_n} \left(\omega_v \sum_{v \in \triangle \in T} \mathcal{A}(\triangle) \right) = \sum_{\triangle \in T} \left(\mathcal{A}(\triangle) \sum_{v \in \triangle} \omega_v \right) = 3 \sum_{\triangle \in T} \mathcal{V}(\mathrm{prism}(\triangle, \omega)),$$

where $\mathcal{V}(\mathrm{prism}(\triangle, \omega))$ denotes the volume of the prism with vertices $(v, 0)_{v \in \triangle}$ and $(v, \omega_v)_{v \in \triangle}$. The last sum equals the volume below the piecewise linear function $f(\omega, T) : \mathrm{conv}(V_n) \to \mathbb{R}$ which is linear on each triangle of T and which evaluates to ω on V_n (*i.e.* whose value at any vertex $v \in V_n$ is ω_v). Consequently, the scalar product $\langle \omega \,|\, \phi(T) \rangle$ is minimized precisely for the triangulations T for which $f(\omega, T)$ coincides with the lower envelope of the lifted point set $\{(v, \omega_v) \,|\, v \in V_n\} \subset \mathbb{R}^3$, that is, for the triangulations which refine the polygonal subdivision of the n-gon obtained as the projection of the lower envelope of this lifted point set.

Any crossing-free set S of diagonals of the n-gon is *regular*: there exists a lifting vector ω such that the projection of the lower envelope of the lifted point set coincides with the polygonal subdivision induced by S. According to the discussion above, ω is a normal vector of a face of Σ_n which contains exactly the area vectors of the triangulations of the n-gon containing S. □

For example, the secondary polytopes Σ_3 (of a triangle), Σ_4 (of a square), and Σ_5 (of a regular pentagon) are respectively a single point, a segment, and a regular pentagon. More interesting is the secondary polytope of an hexagon:

Example 4.32 (The 3-dimensional associahedron)**.** Figure 4.14 displays the secondary polytope Σ_6 of a regular hexagon and its polar polytope $\Sigma_6^\diamond$. As mentioned previously, a vertex (resp. an edge, resp. a facet) of Σ_6 corresponds to a triangulation (resp. a flip, resp. a diagonal) of the hexagon (and the reverse holds for the polar polytope).

It is easy to observe on the picture that the facets of the associahedron are products of two smaller associahedra. Here the facets of Σ_6 are either pentagons (*i.e.* $\Sigma_3 \times \Sigma_5$) or squares

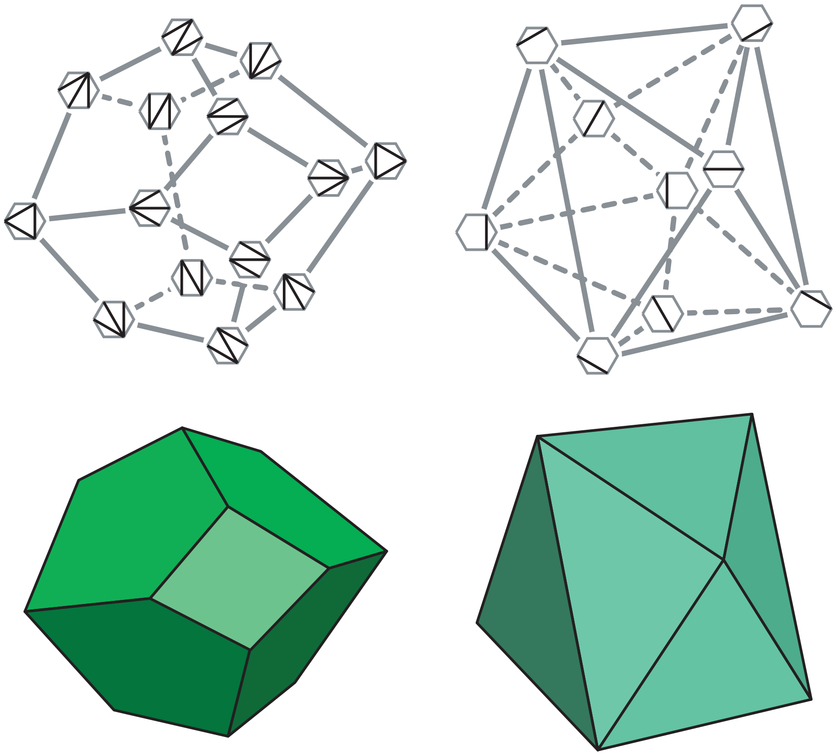

Figure 4.14: The 3-dimensional associahedron (left) and its polar (right).

(*i.e.* $\Sigma_4 \times \Sigma_4$). This is a general fact since an internal diagonal separates the n-gon into two smaller polygons, one of size $\ell + 1$ and the other one of size $n - \ell + 1$ (where ℓ is the length of the diagonal). More generally, all codimension p faces of a d-dimensional associahedron are products of $p + 1$ smaller associahedra whose dimensions sum to $d - p$.

It is interesting to observe that the full isometry group of the regular n-gon defines an isometry action on the secondary polytope:

Lemma 4.33. *The dihedral group $\mathbb{D}_n$ of isometries of the regular n-gon acts on its secondary polytope Σ_n by isometry.*

Proof. An isometry of the regular n-gon translates on the secondary polytope into a permutation of the coordinates. $\square$

Example 4.34 (The 3-dimensional associahedron continued)**.** Figure 4.15 displays the action of two isometries of the regular hexagon on the 3-dimensional associahedron Σ_6 and its dual $\Sigma_6^\diamond$. The first one is the reflection ρ_v of the hexagon with respect to the vertical axis, which translates on the secondary polytope Σ_6 into a rotation (whose axis contains the point corresponding to the horizontal edge of the hexagon). The second one is the reflection ρ_h of the hexagon with respect to the horizontal axis, which translates on the secondary polytope Σ_6 into a reflection (with respect to the plane containing the fixed triangulations). Even if our two isometries are

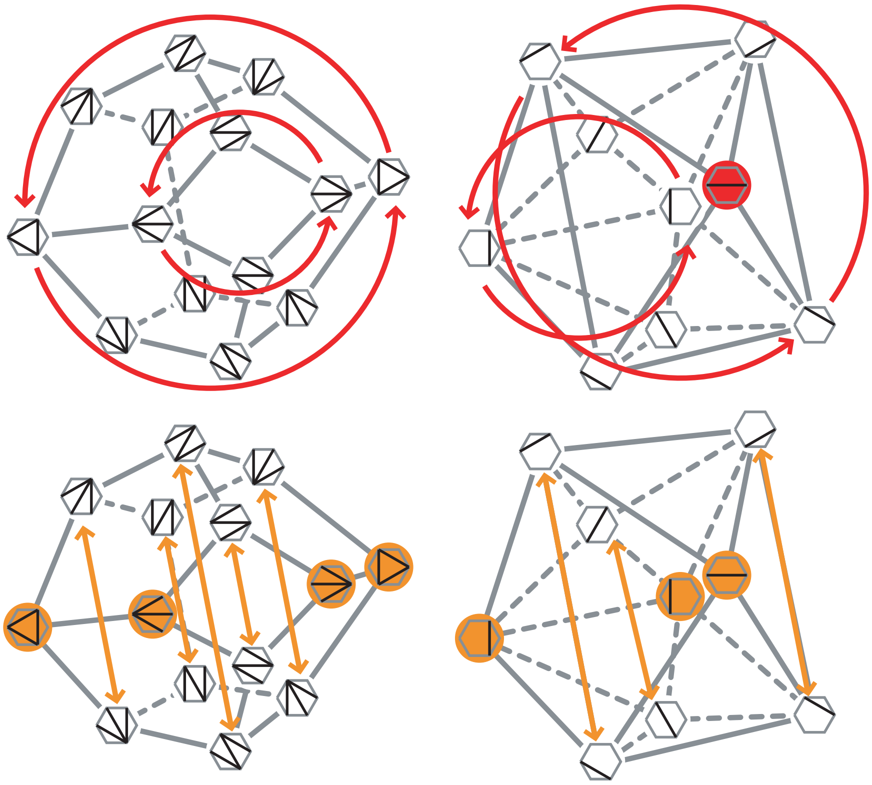

Figure 4.15: Two symmetries on the 3-dimensional associahedron.

both indirect on the hexagon (they are both reflections), the corresponding isometries on the secondary polytope can be direct or indirect.

Observe that our two reflections generate the complete dihedral group $\mathbb{D}_6$ of the regular hexagon. Thus, the action of any isometry of the hexagon on the secondary polytope can be deduced from Figure 4.15. It is however not always easy to see: imagine for example the action on Σ_6 of the rotation of angle $\pi/3$ of the hexagon.

Remark 4.35. This construction of the secondary polytope is not restricted to the very special situation of convex point configurations in the plane. If P is an arbitrary point set in $\mathbb{R}^d$, the secondary polytope of P is defined as the convex hull of the volume vectors of all triangulations of P — where the volume vector of a triangulation T of P is the vector of $\mathbb{R}^{|P|}$ whose pth coordinate (for $p \in P$) is the sum of the volumes of the simplices of T adjacent to the vertex p. Then the face lattice of the secondary polytope is isomorphic to the refinement lattice on regular subdivisions of P. It has dimension $|P| - d - 1$, and its vertices (resp. edges) correspond to regular triangulations of P (resp. flips between them). We refer to [BFS90, GKZ94, dLRS10] for further details, and restrict to convex configurations in the plane.

4.3.1.2 Loday's construction of the associahedron

The second construction of the associahedron that we try to generalize is due to Jean-Louis Loday [Lod04]. The resulting polytope is a bit less symmetric, but has other advantages: in particular, it has integer coordinates, and its facets have simple equations. Here, we follow the original presentation [Lod04] which first defines a polytope associated to binary trees. We will see later in Section 4.3.3 an equivalent definition in terms of beam arrangements and its generalization to multitriangulations.

We call DFS-*labeling* of a rooted binary tree the labeling obtained by a depth-first search of the tree: we start from the root, and for each internal node, we first completely search its left child, then label our node with the smallest free label, and finally visit its right child. In other words, the DFS-labeling is the unique labeling of the tree with the property that the label of any node is bigger than any label in its left child and smaller than any label in its right child.

The construction associates a vector to each binary tree as follows:

Definition 4.36 ([Lod04])**.** *The* DFS-vector *of a rooted binary tree τ on m nodes is the vector $\psi(\tau) \in \mathbb{R}^m$ whose ith coordinate (for $i \in [m]$) is the product of the number of leaves in the left child by the number of leaves in the right child of the node labeled by i in the* DFS*-labeling of τ. The* DFS-polytope Ω_m *is the convex hull of the* DFS*-vectors of all rooted binary trees on m nodes.*

Remember that triangulations of the n-gon and binary trees on $n-2$ nodes are in bijective correspondence (see Section 1.1). Thus, we define by extension the DFS-*vector* of a triangulation of the n-gon to be the DFS-vector of its dual binary tree on $n-2$ nodes.

Theorem 4.37 ([Lod04])**.** *The boundary complex of the polar $\Omega_{n-2}^\diamond$ of the* DFS*-polytope is isomorphic to the simplicial complex $\Delta_{n,1}$ of crossing-free sets of diagonals of the n-gon. Indeed,*

(i) Ω_{n-2} is included in the affine hyperplane $\left\{x \in \mathbb{R}^{n-2} \,\middle|\, \langle \mathbb{1} \,|\, x\rangle = \binom{n-1}{2}\right\}$; and

(ii) for any $0 \le u < v \le n-1$, the equation $\sum_{p=u+1}^{v-1} x_p = \binom{v-u}{2}$ defines a facet of Ω_{n-2} which contains all the DFS*-vectors of the triangulations of the n-gon containing the edge $[u, v]$, and only these ones.* □

We do not repeat here the proof of [Lod04] since our interpretation of this construction in Section 4.3.3 in terms of beam arrangements will provide a visual and simple proof.

Example 4.38. Figure 4.16 shows the 3-dimensional associahedron as realized by Loday's construction.

Observe that since this polytope is defined on binary trees, its symmetry group is automatically not the full dihedral group of isometries of the regular n-gon. However, the construction conserves the symmetry of the trees:

Lemma 4.39. *The polytope Ω_m is symmetric under reversing coordinates.*

Proof. Reversing the coordinates of the DFS-vector corresponds to inverting left and right in the depth-first search. □

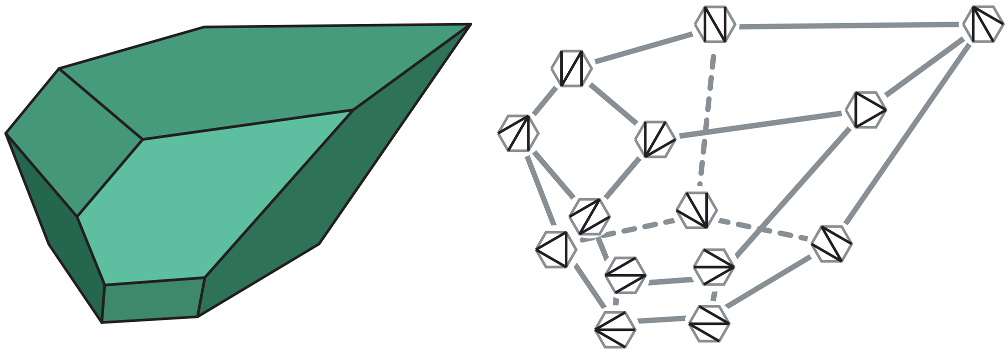

Figure 4.16: Loday's construction of the 3-dimensional associahedron.

This symmetry corresponds to the reflection of the n-gon with respect to the diameter passing through the middle of the edge $[0, n-1]$. In Figure 4.16, it is a rotation around an axis passing through the center of the preserved square and the center of the preserved edge.

4.3.2 The space of symmetric realizations of $\Delta_{8,2}$

In this section, we focus on symmetric realizations of the simplicial complex $\Delta_{n,k}$, in the following sense:

Definition 4.40. *A polytope $P \subset \mathbb{R}^d$ is a realization of a simplicial complex Δ if its boundary complex ∂P is isomorphic to Δ, i.e. if there is a bijection $\gamma : \Delta \to \partial P$ which respects inclusion: $S \subset T \Leftrightarrow \gamma(S) \subset \gamma(T)$, for all $S, T \in \Delta$. We say that P is a symmetric realization under a group G acting on Δ if for any $g \in G$, the action $\partial P \to \partial P : y \mapsto gy := \gamma(g\gamma^{-1}(y))$ of g on ∂P is an isometry.*

When G is the complete symmetry group of the simplicial complex Δ, we sometimes do not mention G explicitely, and we just say that P is a symmetric realization of Δ. As far as the simplicial complex $\Delta_{n,k}$ is concerned, we already know examples of symmetric realizations:

$\boxed{k=1}$ The associahedron Σ_n constructed as the secondary polytope of the regular n-gon is a symmetric realization of $\Delta_{n,1}$ under the dihedral group $\mathbb{D}_n$.

$\boxed{n=2k+1}$ A point is a symmetric realization of $\Delta_{2k+1,k}$.

$\boxed{n=2k+2}$ The regular k-simplex is symmetric under any permutation of its vertices, and thus, is a symmetric realization of $\Delta_{2k+2,k}$ under $\mathfrak{S}_{k+1}$.

$\boxed{n=2k+3}$ Define the $2k$-dimensional cyclic polytope with $2k+3$ vertices embedded on the *Caratheodory curve* $\nu_{2k} : \theta \mapsto (\cos(\ell\theta), \sin(\ell\theta))_{\ell\in[k]}$ as

$$C_{2k}(2k+3) := \operatorname{conv}\left\{\nu_{2k}\left(e^{\frac{2i\pi m}{2k+3}}\right) \,\middle|\, m \in \mathbb{Z}_{2k+3}\right\} \subset \mathbb{R}^{2k}.$$

Then $C_{2k}(2k+3)$ is a symmetric realization of $\Delta_{2k+3,k}$ under the dihedral group $\mathbb{D}_{2k+3}$ (see for example [KW10]).

The main result of this section concerns the first non-trivial case: we study symmetric realizations of the simplicial complex $\Delta_{8,2}$ of 3-crossing-free sets of 2-relevant edges of the octagon. We use computer enumeration to obtain a complete description of the space of symmetric realizations of $\Delta_{8,2}$. This enumeration works in two steps:

(i) We first enumerate all possible "combinatorial" configurations (matroid polytopes) which could realize the simplicial complex $\Delta_{8,2}$.

(ii) Then, from the knowledge of these combinatorial configurations, we deduce all "geometric" polytopes realizing $\Delta_{8,2}$ and symmetric under the dihedral group.

Before presenting this result, we briefly remind the notions we need in the world of oriented matroids (which will make precise what we mean by "combinatorial configurations"), and we expose the method on the basic example of $\Delta_{6,1}$.

4.3.2.1 Chirotopes and symmetric matroid realizations

For our purpose, *oriented matroids* are combinatorial abstractions of point configurations: they keep track of the arrangement in a point set, by encoding relative positions of its points. For example, we have already met pseudoline arrangements in Chapter 3, which correspond to point configurations in a (topological) plane. We refer to [BVS+99, Bok06, RGZ97] for expositions on the different aspects of oriented matroids, and we focus here on a short overview of what we will really use in the next sections.

Among other possible definitions of oriented matroids, we use the concept of chirotopes:

Definition 4.41. *The chirotope of a point set $P := \{p_i \,|\, i \in I\} \subset \mathbb{R}^d$ indexed by a set I is the application $\chi_P : I^{d+1} \to \{-1, 0, 1\}$ which associates to each $(d+1)$-tuple $(i_0, \dots, i_d)$ of elements of I the orientation of the simplex formed by the points of P indexed by $i_0, \dots, i_d$, that is:*

$$\chi_P(i_0, \dots, i_d) := \operatorname{sign}\det\begin{pmatrix} 1 & 1 & \dots & 1 \\ p_{i_0} & p_{i_1} & \dots & p_{i_d} \end{pmatrix}.$$

Two points configurations P and Q indexed by the same set I have the same *order type* if there exists a bijection $\alpha : I \to I$ which makes coincide the chirotopes of P and Q, *i.e.* such that $\chi_P(i_0, \dots, i_d) = \chi_Q(\alpha(i_0), \dots, \alpha(i_d))$ for any $(d+1)$-tuple $(i_0, \dots, i_d) \in I^{d+1}$. For example, there are only four different order types of configurations of four points in the plane, represented in Figure 4.17.

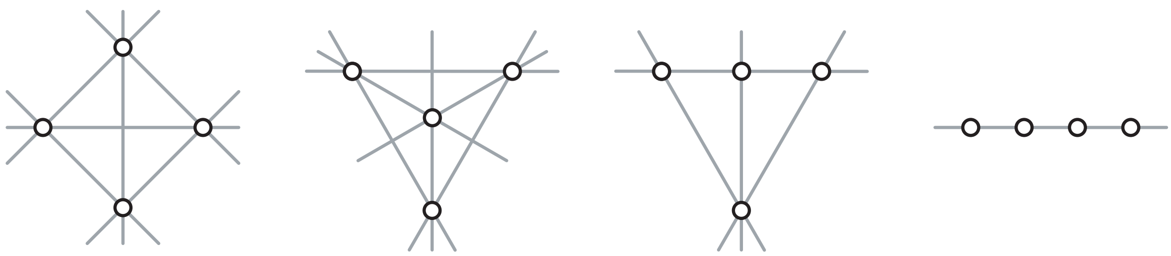

Figure 4.17: The four possible order types on configurations of four (distinct) points.

From the geometry of point configurations, we derive the following combinatorial properties of chirotopes:

Lemma 4.42. *The chirotope $\chi : I^{d+1} \to \{-1, 0, 1\}$ of a d-dimensional point configuration indexed by I satisfies the following relations:*

(i) Alternating relations*: for any $(d+1)$-tuple $(i_0, \dots, i_d) \in I^{d+1}$ and any permutation π of $\{0, \dots, d\}$ of signature σ,*

$$\chi(i_{\pi(0)}, \dots, i_{\pi(d)}) = \sigma\chi(i_0, \dots, i_d).$$

(ii) Matroid property*: the set $\chi^{-1}(\{-1, 1\})$ of non-degenerate $(d+1)$-tuples of I satisfies the* Steinitz exchange axiom*: for any non-degenerate $(d+1)$-tuples $X, Y \in \chi^{-1}(\{-1, 1\})$ and any element $x \in X \smallsetminus Y$, there exists $y \in Y \smallsetminus X$ such that $X \triangle \{x, y\} \in \chi^{-1}(\{-1, 1\})$.*

(iii) Grassmann-Plücker relations*: for any $i_0, \dots, i_{d-2}, j_1, j_2, j_3, j_4 \in I$, the set*

$$\begin{aligned}\{ \quad & \chi(i_0, \dots, i_{d-2}, j_1, j_2)\, \chi(i_0, \dots, i_{d-2}, j_3, j_4), \\ & -\chi(i_0, \dots, i_{d-2}, j_1, j_3)\, \chi(i_0, \dots, i_{d-2}, j_2, j_4), \\ & \chi(i_0, \dots, i_{d-2}, j_1, j_4)\, \chi(i_0, \dots, i_{d-2}, j_2, j_3) \quad \}\end{aligned}$$

either contains $\{-1, 1\}$ or is contained in $\{0\}$.

Proof. Alternating relations come from alternating properties of the determinant. The set of non-degenerate $(d+1)$-tuples corresponds to the set of bases of our point set, and thus satisfies the matroid property. The Grassmann-Plücker relations are derived from the 3-terms Grassmann-Plücker equality on determinants: for any matrix M with $d+1$ rows and $d+3$ columns,

$$\det(M_{\hat{1}\hat{2}}) \det(M_{\hat{3}\hat{4}}) - \det(M_{\hat{1}\hat{3}}) \det(M_{\hat{2}\hat{4}}) + \det(M_{\hat{1}\hat{4}}) \det(M_{\hat{2}\hat{3}}) = 0,$$

where $M_{\hat{p}\hat{q}}$ denotes the submatrix of M obtained by deleting its pth and qth columns. In turn, this equality is a simple calculation when multiplying M by the inverse of the bottom square submatrix $M_{\hat{1}\hat{2}}$. □

These properties are the basement of the combinatorial definition of chirotopes: we now completely forget point configurations and define chirotopes as follows.

Definition 4.43. *A* chirotope *of rank r on a set I is any application $\chi : I^r \to \{-1, 0, 1\}$ which is not identically zero and satisfies the three properties of Lemma 4.42.*

By definition, the chirotope of a (non-degenerate) d-dimensional point configuration is a chirotope of rank $d+1$. However, for the same reason that some pseudoline arrangements are not realizable, there exist chirotopes which do not arise as chirotopes of point configurations. These two sentences together give a method as well as its limits to look for a (small) point configuration satisfying certain combinatorial properties: we can first enumerate all chirotopes which satisfy the constraints, and then try to realize these chirotopes as euclidean point configurations.

We will apply this method to obtain all symmetric realizations of a simplicial complex.We first express the combinatorial constraints we are focussing on:

Lemma 4.44. *Let $\Delta \subset 2^I$ be a simplicial complex (whose vertices are indexed by I), and G be a group acting on Δ. Let $P := \{p_i \mid i \in I\} \subset \mathbb{R}^d$ be a d-dimensional point configuration (indexed by I) whose convex hull is a symmetric realization of Δ under G. Then the chirotope χ_P of P satisfies the following properties:*

(i) Alternating relations.

(ii) Matroid property.

(iii) Grassmann-Plücker relations.

(iv) Necessary Simplex Orientations*: if $i_0, \ldots, i_d \in I$ are such that both $\{i_0, \ldots, i_{d-2}, i_{d-1}\}$ and $\{i_0, \ldots, i_{d-2}, i_d\}$ are facets of Δ, then for any $j \in I \smallsetminus \{i_0, \ldots, i_d\}$,*

$$\chi_P(i_0, \ldots, i_{d-2}, i_{d-1}, i_d) = \chi_P(i_0, \ldots, i_{d-2}, i_{d-1}, j) = \chi_P(i_0, \ldots, i_{d-2}, j, i_d).$$

(v) Symmetry*: there exists a morphism $\tau : G \to \{\pm 1\}$ such that for any $i_0, \ldots, i_d \in I$, and any $g \in G$,*

$$\chi_P(gi_0, \ldots, gi_d) = \tau(g)\chi_P(i_0, \ldots, i_d).$$

□

As before, these properties lead to the following combinatorial abstraction:

Definition 4.45. *A* symmetric matroid realization *of Δ under G is any application which associates to a $(d+1)$-tuple of I a sign in $\{-1, 0, 1\}$ and satisfies the five properties of Lemma 4.44.*

In the following paragraphs, we investigate symmetric matroid realizations of $\Delta_{n,k}$ as the first step to understand its symmetric geometric realizations. This enables us to describe the space of symmetric realizations of little cases such as the first non-trivial case $\Delta_{8,2}$. To expose the method, we start with a simpler example.

4.3.2.2 A basic example: the space of symmetric realizations of $\Delta_{6,1}$

As our first example of the use of oriented matroids, we study symmetric realizations of the polar of the 3-dimensional associahedron. It is convenient to use letters a, b, c, d, e, f, G, H and I to denote the edges $[0,2]$, $[1,3]$, $[2,4]$, $[3,5]$, $[4,0]$, $[5,1]$, $[0,3]$, $[1,4]$ and $[2,5]$ of the hexagon respectively (the three capital letters correspond to the long diagonals). We use these letters to index the vertices of $\Delta_{6,1}$.

Since the polar $\Sigma_6^\diamond$ of the secondary polytope of the regular hexagon is a symmetric realization of $\Delta_{6,1}$, its chirotope $\chi_{\Sigma_6^\diamond}$ provides a symmetric matroid realization. To describe this chirotope, instead of listing the signs of all possible 4-tuples of $\{\mathrm{a}, \mathrm{b}, \ldots, \mathrm{I}\}$, we give the sign of one representative for each orbit under permutation of the coordinates and under the action of $\mathbb{D}_6$:

$\lvert\mathrm{abcd}\rvert = 1$	$\lvert\mathrm{abce}\rvert = -1$	$\lvert\mathrm{abcG}\rvert = -1$	$\lvert\mathrm{abcI}\rvert = 1$	$\lvert\mathrm{abde}\rvert = 0$	$\lvert\mathrm{abdG}\rvert = 1$
$\lvert\mathrm{abdH}\rvert = -1$	$\lvert\mathrm{abdI}\rvert = -1$	$\lvert\mathrm{abGH}\rvert = 1$	$\lvert\mathrm{abHI}\rvert = 1$	$\lvert\mathrm{aceG}\rvert = -1$	$\lvert\mathrm{acGH}\rvert = 0$
$\lvert\mathrm{acGI}\rvert = -1$	$\lvert\mathrm{adGH}\rvert = 1$	$\lvert\mathrm{adGI}\rvert = 1$	$\lvert\mathrm{aGHI}\rvert = 1$		

where $|\mathrm{xyzt}|$ is an abbreviation for $\chi_{\Sigma_6^\diamond}(\mathrm{x}, \mathrm{y}, \mathrm{z}, \mathrm{t})$. You can recover all the chirotope $\chi_{\Sigma_6^\diamond}$ by remembering that the reflection ρ_v (resp. ρ_h) of the hexagon, with respect to the vertical (resp. horizontal) axis, corresponds to a direct (resp. indirect) isometry of $\Sigma_6^\diamond$. In other words, $\tau(\rho_v) = 1$ and $\tau(\rho_h) = -1$.

Using our computer enumeration (see Appendix A.2 for a presentation of the HASKELL implementation), we obtain that the chirotope given by the secondary polytope is in fact the unique solution:

Proposition 4.46. *The chirotope $\chi_{\Sigma_6^\diamond}$ is the unique symmetric matroid realization of $\Delta_{6,1}$ (up to the inversion of all the signs).* $\square$

It remains to understand all possible symmetric geometric realizations of this chirotope (for the moment, we know only one such realization: the polar of the secondary polytope itself). Given such a realization, consider the matrix M with 4 rows and 9 columns formed by the homogeneous coordinates of its vertices. Let N be the square submatrix of M formed by the columns a, G, H and I. Since $|\mathrm{aGHI}| = 1$, we know that N is invertible, and we denote

$$M' := N^{-1}M := \begin{pmatrix} 1 & b_0 & c_0 & d_0 & e_0 & f_0 & 0 & 0 & 0 \\ 0 & b_1 & c_1 & d_1 & e_1 & f_1 & 1 & 0 & 0 \\ 0 & b_2 & c_2 & d_2 & e_2 & f_2 & 0 & 1 & 0 \\ 0 & b_3 & c_3 & d_3 & e_3 & f_3 & 0 & 0 & 1 \end{pmatrix}.$$

We determine the unknown coefficients of this matrix, using the fact that not only the signs of the determinants of the (4×4)-submatrices of M' (*i.e.* the chirotope) are symmetric under the action of $\mathbb{D}_6$, but also the determinants themselves. For example, applying the rotation of the hexagon of angle $\pi/3$ (which acts as an indirect isometry on the chirotope), we know that

$$[\mathrm{aGHI}] = -[\mathrm{bGHI}] = [\mathrm{cGHI}] = -[\mathrm{dGHI}] = [\mathrm{eGHI}] = -[\mathrm{fGHI}],$$

(where $[\mathrm{xyzt}]$ denotes the determinant of the square submatrix of M' formed by the columns x, y, z and t). Thus, we derive that $1 = -b_0 = c_0 = -d_0 = e_0 = -f_0$. Similarly, we obtain the following relations between the coefficients of the matrix M':

$$\begin{aligned} [\mathrm{abHI}] = [\mathrm{afGH}] \quad &\Longrightarrow \quad b_1 = f_3; \\ [\mathrm{abGH}] = -[\mathrm{abGI}] = [\mathrm{afGI}] = -[\mathrm{afHI}] = -[\mathrm{bcHI}] \quad &\Longrightarrow \quad b_3 = b_2 = f_2 = f_1 = b_1 + c_1; \\ [\mathrm{acGI}] = [\mathrm{acHI}] = [\mathrm{afGH}] = [\mathrm{afGI}] \quad &\Longrightarrow \quad -c_2 = c_1 = e_3 = -e_2; \\ [\mathrm{acGH}] = [\mathrm{aeHI}] = [\mathrm{bdHI}] = 0 \quad &\Longrightarrow \quad c_3 = e_1 = b_1 - d_1 = 0; \\ \text{and} \qquad [\mathrm{adGH}] = [\mathrm{adHI}] \quad &\Longrightarrow \quad d_3 = d_1. \end{aligned}$$

Furthermore, in each column of M', the coordinates sum to 1 (since we have homogeneous coordinates when multipling by the matrix N). This implies that $b_1 = 2 - 2b_2$ and $d_2 = 2 - 2d_1$. Thus, the matrix M' can be written

$$M' = \begin{pmatrix} 1 & -1 & 1 & -1 & 1 & -1 & 0 & 0 & 0 \\ 0 & -2t+2 & 3t-2 & -2t+2 & 0 & t & 1 & 0 & 0 \\ 0 & t & -3t+2 & 4t-2 & -3t+2 & t & 0 & 1 & 0 \\ 0 & t & 0 & -2t+2 & 3t-2 & -2t+2 & 0 & 0 & 1 \end{pmatrix}.$$

Finally, from our knowledge on the chirotope, we know that $|\mathrm{abGH}| = |\mathrm{aGHI}| = 1$ and that $|\mathrm{adGI}| = |\mathrm{aGHI}| = -1$, which implies that $0 < t < 1/2$.

In order to complete our understanding of the space of symmetric realizations of $\Delta_{6,1}$, it only remains to study the possible values of the matrix N. By symmetry, the triangle formed by the vertices labeled by G, H and I is equilateral. Thus, since a dilation (the composition of an homothecy by an isometry) does not destruct the symmetry, we can assume without loss of generality that this triangle is formed by the vectors of the canonical basis in $\mathbb{R}^3$, *i.e.* that the matrix N is of the form

$$N := \begin{pmatrix} 1 & 1 & 1 & 1 \\ x & 1 & 0 & 0 \\ y & 0 & 1 & 0 \\ z & 0 & 0 & 1 \end{pmatrix}.$$

Since a is equidistant from G and I, we have $x = z$, and since b is equidistant from G and H, we have $y = x + 3t - 2$. Finally, since N is invertible, its determinant $\det N = 3 - 3x - 3t$ does not vanish, and $x \neq 1 - t$.

Knowing the matrices M' and N, we have a complete description of the matrix M:

Proposition 4.47. *Any symmetric realization of the simplicial complex $\Delta_{6,1}$ is a dilation of the set of column vectors of the matrix*

$$\begin{pmatrix} x & -x-2t+2 & x+3t-2 & -x-2t+2 & x & -x+t & 1 & 0 & 0 \\ x+3t-2 & -x-2t+2 & x & -x+t & x & -x-2t+2 & 0 & 1 & 0 \\ x & -x+t & x & -x-2t+2 & x+3t-2 & -x-2t+2 & 0 & 0 & 1 \end{pmatrix}$$

for a couple $(t, x) \in \mathbb{R}^2$, with $0 < t < 1/2$ and $x \neq 1 - t$. Reciprocally, any such dilation is a symmetric realization of $\Delta_{6,1}$. $\square$

The reciprocal part of this proposition is easy to check (for example with a computer algebra system): we only have to verify that for any admissible values of t and x:

(i) The boundary complex of the convex hull of the column vectors of M is indeed isomorphic to $\Delta_{6,1}$. For this, we check that the chirotope of the column vectors of M' coincides with the chirotope $\chi_{\Sigma_6^\diamond}$ (and we only have to check equality for one representative of each of the 16 orbits under $\mathbb{D}_6$).

(ii) The dihedral group $\mathbb{D}_6$ indeed acts by isometry on the columns vectors of M (and we only have to check the action of the two reflections ρ_v and ρ_h, since they generate $\mathbb{D}_6$).

Corollary 4.48. *Up to dilation, the space of symmetric realizations of the simplicial complex $\Delta_{6,1}$ has dimension 2.* $\square$

To illustrate this result, Figure 4.18 shows the convex hull of the column vectors of M for different values of t and x. The two dimensions of the space of symmetric realizations are apparent in this picture: if you see the associahedron as three egyptian pyramids stacked on the square facets of a triangular prism, you can variate the height of the prism and the height of the pyramids. The bounds on the possible values of t correspond to the moment when the pyramids disappear ($t = 0$) and when they merge ($t = 1/2$). See Figure 4.18.

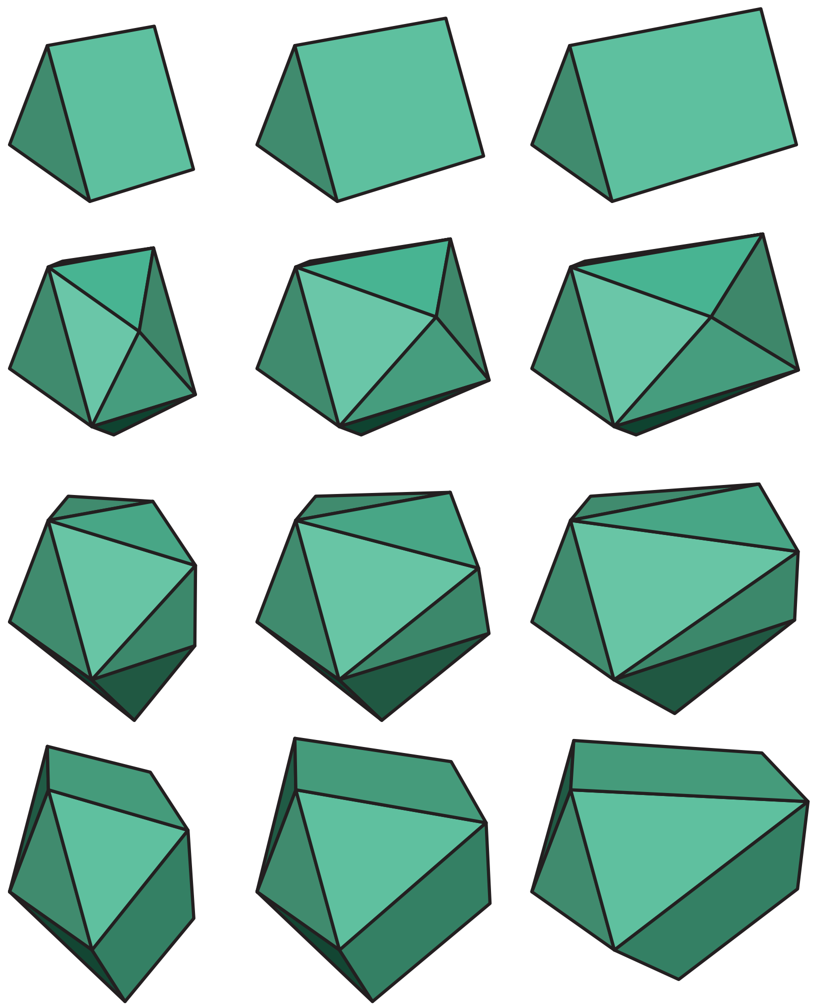

Figure 4.18: The space of symmetric realizations of $\Delta_{6,1}$.

4.3.2.3 The first non-trivial case: the space of symmetric realizations of $\Delta_{8,2}$

Using the same method, we now study the symmetric realizations of the simplicial complex $\Delta_{8,2}$ of 3-crossing-free sets of 2-relevant edges of the octagon. The polytope we want to construct would be a 6-polytope, with 12 vertices (the 2-relevant edges of the octagon), 66 edges (because $\Delta_{8,2}$ is 2-neighborly), 192 2-faces, 306 3-faces, 252 ridges, and 84 facets (the 2-triangulations of the octagon). As before, it is convenient to label the 2-relevant edges of the octagon with letters: let $\mathrm{a} := [0,3]$, $\mathrm{b} := [1,4]$, $\mathrm{c} := [2,5]$, $\mathrm{d} := [3,6]$, $\mathrm{e} := [4,7]$, $\mathrm{f} := [5,0]$, $\mathrm{g} := [6,1]$, $\mathrm{h} := [7,2]$, $\mathrm{I} := [0,4]$, $\mathrm{J} := [1,5]$, $\mathrm{K} := [2,6]$, and $\mathrm{L} := [3,7]$ (the capital letters denote the long diagonals).

As before, a computer enumeration (see Appendix A.2) provides the complete list of all possible symmetric matroid realizations of our simplicial complex:

Proposition 4.49. *There are 15 symmetric matroid realizations of $\Delta_{8,2}$ (up to the inversion of all the signs).* □

To present these solutions, we only give the sign of one representative for each of the 62 orbits of $\{\mathrm{a}, \mathrm{b}, \dots, \mathrm{L}\}^7$ under permutation and symmetry. First, all solutions have the following 59 common signs:

$$
\begin{array}{lllll}
|\mathrm{abcdefg}| = 0 & |\mathrm{abcdefI}| = -1 & |\mathrm{abcdefJ}| = 1 & |\mathrm{abcdefK}| = -1 & |\mathrm{abcdegI}| = 1 \\
|\mathrm{abcdegJ}| = -1 & |\mathrm{abcdeIK}| = -1 & |\mathrm{abcdeIL}| = 1 & |\mathrm{abcdeJK}| = 1 & |\mathrm{abcdfgI}| = -1 \\
|\mathrm{abcdfgJ}| = 1 & |\mathrm{abcdfgL}| = 1 & |\mathrm{abcdfIJ}| = 1 & |\mathrm{abcdfIK}| = 1 & |\mathrm{abcdfIL}| = -1 \\
|\mathrm{abcdfJK}| = -1 & |\mathrm{abcdfJL}| = 1 & |\mathrm{abcdfKL}| = -1 & |\mathrm{abcdIJK}| = -1 & |\mathrm{abcdIJL}| = 1 \\
|\mathrm{abcdIKL}| = -1 & |\mathrm{abcefgI}| = 0 & |\mathrm{abcefgK}| = 0 & |\mathrm{abcefIJ}| = -1 & |\mathrm{abcefIK}| = 1 \\
|\mathrm{abcefIL}| = 1 & |\mathrm{abcefJK}| = -1 & |\mathrm{abcefJL}| = -1 & |\mathrm{abcefKL}| = 1 & |\mathrm{abcegIJ}| = 1 \\
|\mathrm{abcegIK}| = -1 & |\mathrm{abcegIL}| = -1 & |\mathrm{abcegKL}| = -1 & |\mathrm{abceIJL}| = -1 & |\mathrm{abceIKL}| = 1 \\
|\mathrm{abceJKL}| = -1 & |\mathrm{abcfIJK}| = -1 & |\mathrm{abcfIKL}| = -1 & |\mathrm{abcIJKL}| = 1 & |\mathrm{abdegIJ}| = 1 \\
|\mathrm{abdegIK}| = 1 & |\mathrm{abdegIL}| = 1 & |\mathrm{abdegJK}| = -1 & |\mathrm{abdeIJK}| = 1 & |\mathrm{abdeIJL}| = -1 \\
|\mathrm{abdfIJL}| = 1 & |\mathrm{abdfIKL}| = 1 & |\mathrm{abdfJKL}| = -1 & |\mathrm{abdgIJK}| = -1 & |\mathrm{abdgIJL}| = -1 \\
|\mathrm{abdgJKL}| = 1 & |\mathrm{abdIJKL}| = -1 & |\mathrm{abefIJK}| = -1 & |\mathrm{abefIJL}| = -1 & |\mathrm{abefJKL}| = 1 \\
|\mathrm{abeIJKL}| = 1 & |\mathrm{acegIJK}| = -1 & |\mathrm{aceIJKL}| = -1 & |\mathrm{acfIJKL}| = 1 &
\end{array}
$$

The three remaining orbits are those of the tuples $(\mathrm{a}, \mathrm{b}, \mathrm{c}, \mathrm{d}, \mathrm{e}, \mathrm{I}, \mathrm{J})$, $(\mathrm{a}, \mathrm{b}, \mathrm{c}, \mathrm{e}, \mathrm{I}, \mathrm{J}, \mathrm{K})$ and $(\mathrm{a}, \mathrm{b}, \mathrm{d}, \mathrm{f}, \mathrm{I}, \mathrm{J}, \mathrm{K})$. The following table summarizes the possible signs for these three orbits (only 15 of the 27 possibilities are admissible):

	A	B	C	D	E	F	G	H	I	J	K	L	M	N	O
$\lvert\mathrm{abcdeIJ}\rvert$	-1	-1	-1	0	0	0	1	1	1	1	1	1	1	1	1
$\lvert\mathrm{abceIJK}\rvert$	1	1	1	1	1	1	-1	-1	-1	0	0	0	1	1	1
$\lvert\mathrm{abdfIJK}\rvert$	-1	0	1	-1	0	1	-1	0	1	-1	0	1	-1	0	1

The second step is to realize geometrically these matroid polytopes. Given such a realization, we define again the matrix M with 7 rows and 12 columns formed by the homogeneous coordinates of its vertices. Let N be the square submatrix of M formed by the columns $\mathrm{a}, \mathrm{b}, \mathrm{c}, \mathrm{I}, \mathrm{J}, \mathrm{K}$ and L. Since $|\mathrm{abcIJKL}| = 1$, we know that N is invertible, and we denote

$$
M' := N^{-1}M := \begin{pmatrix}
1 & 0 & 0 & d_0 & e_0 & f_0 & g_0 & h_0 & 0 & 0 & 0 & 0 \\
0 & 1 & 0 & d_1 & e_1 & f_1 & g_1 & h_1 & 0 & 0 & 0 & 0 \\
0 & 0 & 1 & d_2 & e_2 & f_2 & g_2 & h_2 & 0 & 0 & 0 & 0 \\
0 & 0 & 0 & d_3 & e_3 & f_3 & g_3 & h_3 & 1 & 0 & 0 & 0 \\
0 & 0 & 0 & d_4 & e_4 & f_4 & g_4 & h_4 & 0 & 1 & 0 & 0 \\
0 & 0 & 0 & d_5 & e_5 & f_5 & g_5 & h_5 & 0 & 0 & 1 & 0 \\
0 & 0 & 0 & d_6 & e_6 & f_6 & g_6 & h_6 & 0 & 0 & 0 & 1
\end{pmatrix} := \begin{pmatrix} I_3 & T & 0_{3\times 4} \\ 0_{4\times 3} & B & I_4 \end{pmatrix},
$$

where $T \in \mathbb{R}^{3\times 5}$ and $B \in \mathbb{R}^{4\times 5}$ denote respectively the “top” and “bottom” unknown submatrices. We use the symmetry of the determinants of the (7×7)-submatrices of M' under the action of the dihedral group to determine the unknown coefficients in the matrices T and B.

Lemma 4.50. *The matrix T equals*

$$\begin{pmatrix} -1 & 1+\sqrt{2} & -2-\sqrt{2} & 2+\sqrt{2} & -1-\sqrt{2} \\ -1-\sqrt{2} & 2+2\sqrt{2} & -3-2\sqrt{2} & 2+2\sqrt{2} & -1-\sqrt{2} \\ -1-\sqrt{2} & 2+\sqrt{2} & -2-\sqrt{2} & 1+\sqrt{2} & -1 \end{pmatrix}.$$

Proof. From symmetry, we derive the following equalities between the determinants of the submatrices of M':

$$\begin{aligned}
&[\mathrm{abcIJKL}] = -[\mathrm{bcdIJKL}] = -[\mathrm{abhIJKL}] \quad \Longrightarrow \quad 1 = -d_0 = -h_2;\\
&[\mathrm{abdIJKL}] = -[\mathrm{abgIJKL}] = -[\mathrm{acdIJKL}] = -[\mathrm{achIJKL}] = -[\mathrm{bceIJKL}] = [\mathrm{bchIJKL}]\\
&\qquad \Longrightarrow \quad d_2 = -\,g_2 = d_1 = h_1 = -e_0 = h_0 =: \alpha;\\
&[\mathrm{abeIJKL}] = -[\mathrm{abfIJKL}] = -[\mathrm{bcfIJKL}] = [\mathrm{bcgIJKL}] \quad \Longrightarrow \quad e_2 = -f_2 = -f_0 = g_0 =: \beta;\\
&\text{and} \quad [\mathrm{aceIJKL}] = [\mathrm{acgIJKL}] \quad \Longrightarrow \quad -e_1 = -g_1 =: -\,\gamma.
\end{aligned}$$

Thus, we can already write the matrix T as follows:

$$T = \begin{pmatrix} -1 & -\alpha & -\beta & \beta & \alpha \\ \alpha & \gamma & \delta & \gamma & \alpha \\ \alpha & \beta & -\beta & -\alpha & -1 \end{pmatrix}.$$

Furthermore,

$$\begin{aligned}
&[\mathrm{bdhIJKL}] = -[\mathrm{aceIJKL}] \quad \Longrightarrow \quad \alpha^2 - 1 = \gamma;\\
\text{and} \quad &[\mathrm{adhIJKL}] = -[\mathrm{abeIJKL}] \quad \Longrightarrow \quad -\alpha^2 - \alpha = -\beta.
\end{aligned}$$

Thus, the matrix T can be written:

$$T = \begin{pmatrix} -1 & -\alpha & -\alpha^2-\alpha & \alpha^2+\alpha & \alpha \\ \alpha & \alpha^2-1 & \delta & \alpha^2-1 & \alpha \\ \alpha & \alpha^2+\alpha & -\alpha^2-\alpha & -\alpha & -1 \end{pmatrix}.$$

Finally,

$$\begin{aligned}
&[\mathrm{defIJKL}] = -[\mathrm{abcIJKL}] \quad \Longrightarrow \quad -\alpha^4 - 2\alpha^3 - 2\alpha^2 - \alpha + \delta\alpha = -1\\
&\qquad \Longrightarrow \quad \delta = \frac{1}{\alpha}(\alpha^4 + 2\alpha^3 + 2\alpha^2 + \alpha - 1);\\
\text{and} \quad &[\mathrm{dehIJKL}] = -[\mathrm{abeIJKL}] \quad \Longrightarrow \quad \alpha^3 + 2\alpha^2 - 1 = -\alpha^2 - \alpha\\
&\qquad \Longrightarrow \quad \alpha \in \{-1, -1+\sqrt{2}, -1-\sqrt{2}\}.
\end{aligned}$$

According to our description of all symmetric matroid realizations, we have $|\mathrm{adgIJKL}| \neq 0$ and $|\mathrm{abdIJKL}| < 0$. Thus, $\alpha \neq -1$ and $\alpha < 0$. Consequently, $\alpha = -1 - \sqrt{2}$, which completes the proof of the lemma. $\square$

Lemma 4.51. *There exists* $u \in (-1-2\sqrt{2}, -1-3\sqrt{2}/2)$ *such that the matrix* B *equals*

$$\begin{pmatrix} 1+\frac{\sqrt{2}}{2} & u & -(1+\sqrt{2})(1+u) & (1+\sqrt{2})(1+u)+1 & -\frac{\sqrt{2}}{2}-u \\ -\frac{\sqrt{2}}{2}-u & (1+\sqrt{2})(1+u)+1 & -(1+\sqrt{2})(1+u) & u & 1+\frac{\sqrt{2}}{2} \\ 1+\frac{\sqrt{2}}{2} & -2-2\sqrt{2}-u & (1+\sqrt{2})(3+u)+2 & -(1+\sqrt{2})(3+u)-1 & 2+\frac{3\sqrt{2}}{2}+u \\ 2+\frac{3\sqrt{2}}{2}+u & -(1+\sqrt{2})(3+u)-1 & (1+\sqrt{2})(3+u)+2 & -2-2\sqrt{2}-u & 1+\frac{\sqrt{2}}{2} \end{pmatrix}.$$

Proof. From the symmetry, we derive the following relations:

$$\begin{aligned} [\text{abcdIJK}] = -[\text{abchIJL}] &\implies -d_6 = -h_5; \\ [\text{abcdIJL}] = [\text{abcdJKL}] = -[\text{abchIJK}] = -[\text{abchIKL}] &\implies d_5 = d_3 = h_6 = h_4; \\ [\text{abcdIKL}] = -[\text{abchJKL}] &\implies -d_4 = -h_3; \\ [\text{abceIJK}] = -[\text{abcgIJL}] &\implies -e_6 = -g_5; \\ [\text{abceIJL}] = -[\text{abcgIJK}] &\implies e_5 = g_6; \\ [\text{abceIKL}] = -[\text{abcgJKL}] &\implies -e_4 = -g_3; \\ [\text{abceJKL}] = -[\text{abcgIKL}] &\implies e_3 = g_4; \\ [\text{abcfIJK}] = -[\text{abcfIJL}] &\implies -f_6 = -f_5; \\ [\text{abcfIKL}] = -[\text{abcfJKL}] &\implies -f_4 = -f_3. \end{aligned}$$

With these equalities, the matrix B can be written:

$$B = \begin{pmatrix} d_3 & e_3 & f_3 & e_4 & d_4 \\ d_4 & e_4 & f_3 & e_3 & d_3 \\ d_3 & e_5 & f_5 & e_6 & d_6 \\ d_6 & e_6 & f_5 & e_5 & d_3 \end{pmatrix}.$$

Furthermore, for any symmetric matroid realization, $d_3 = |\text{abcdJKL}| \neq 0$. Thus:

$$\begin{aligned} [\text{abcdeKL}] = -[\text{abcdhIL}] &\implies d_3e_4 - d_4e_3 = d_3^2 - d_4d_6 \implies e_4 = \frac{1}{d_3}(d_3^2 - d_4d_6 + d_4e_3); \\ [\text{abcdeJL}] = [\text{abcdhIK}] &\implies d_3(e_3-e_5) = d_3(d_6-d_4) \implies e_5 = e_3 + d_4 - d_6; \\ [\text{abcdeJK}] = [\text{abcdhIJ}] &\implies d_3e_6 - d_6e_3 = d_3^2 - d_6^2 \implies e_6 = \frac{1}{d_3}(d_3^2 - d_6^2 + d_6e_3). \end{aligned}$$

We also know that $|\text{abcdhKL}| \neq 0$ and $|\text{abcdhIJ}| \neq 0$. Thus, $d_3 \neq d_4$ and $d_3 \neq d_6$, and

$$\begin{aligned} [\text{abcdfKL}] = -[\text{abcdgIL}] &\implies f_3(d_3-d_4) = d_3e_3 - d_4e_6 \\ &\implies f_3 = \frac{1}{d_3(d_3-d_4)}(d_3^2e_3 - d_4d_3^2 + d_4d_6^2 - d_4d_6e_3); \\ [\text{abcdfIJ}] = [\text{abcdgJK}] &\implies f_5(d_3-d_6) = d_3e_5 - d_6e_4 \\ &\implies f_5 = \frac{1}{d_3(d_3-d_6)}(d_3^2e_3 + d_3^2d_4 - 2d_3^2d_6 + d_4d_6^2 - d_4d_6e_3). \end{aligned}$$

From our knowledge of the symmetric matroid realizations, we derive that

$$0 = [\text{abcdegh}] = (d_4 - d_6)^2(2d_3 + d_4 + d_6)(2d_3 - d_4 - d_6).$$

Since $d_4 \neq d_6$, this implies that $d_4 = \pm 2d_3 - d_6$. Assume first that $d_4 = -2d_3 - d_6$. Then

$$0 = [\text{abcdefg}] = \frac{32(d_3 + d_6)^4(d_3 + d_6 - e_3)^2}{(3d_3 + d_6)(d_3 - d_6)},$$

and we obtain $d_6 = -d_3 + e_3$ or $d_6 = -d_3$. But this is impossible since $d_3 = [\text{abcdJKL}] > 0$, $e_3 = [\text{abceJKL}] < 0$ and $d_6 = -[\text{abcdIJK}] > 0$. Consequently, $d_4 = 2d_3 - d_6$.

Similarly, the knowledge of the chirotope ensures that

$$0 = [\text{abcefgI}] = \frac{4}{d_3^2}(d_3 - d_6)^2(d_6 - e_3 - d_3)(d_6 - (1 + \sqrt{2})d_3 - e_3)(d_6 - (1 - \sqrt{2})d_3 - e_3).$$

Since $d_3 \neq d_6$, this implies that $d_6 = d_3 + e_3$ or $d_6 = (1 \pm \sqrt{2})d_3 + e_3$. The solution $d_6 = d_3 + e_3$ is eliminated since $0 \neq [\text{abcdegJ}] = (d3 - d6)^2(e3 + d3 - d6)$. The solution $d_6 = (1 - \sqrt{2})d_3 + e_3$ is eliminated since $d_3 > 0$, $e_3 < 0$ and $d_6 > 0$. Consequently, we are sure that $d_6 = (1 + \sqrt{2})d_3 + e_3$.

Furthermore, in each column of the matrix M', the coordinates sum to 1 (since we have homogeneous coordinates when multipling by the matrix N). This implies that $d_3 = 1 + \sqrt{2}/2$ and the matrix B can be written as stated in the lemma. Finally, the bounds on the possible value of u are derived from the signs of the chirotope: we have $|\text{abcdfIK}| = 1$, $|\text{abcdfIJ}| = 1$ and $|\text{abefIJL}| = -1$, which implies that $u + 1 + \sqrt{2} < 0$, $(u + 1 + \sqrt{2})(u + 1 + 2\sqrt{2}) < 0$ and $2u + 2 + 3\sqrt{2} < 0$ respectively. Thus, we have $-1 - 2\sqrt{2} < u < -1 - \frac{3\sqrt{2}}{2}$. □

These lemmas imply that only three of the 15 symmetric matroid realizations of $\Delta_{8,2}$ are realizable geometrically by a polytope with symmetric determinants: if $u < -2 - \sqrt{2}$ we obtain the chirotope G, if $u = -2 - \sqrt{2}$ we obtain K, and if $-2 - \sqrt{2} < u$ we obtain O.

In order to complete our understanding of the space of symmetric realizations of $\Delta_{8,2}$, it only remains to study the possible values of the matrix N. To determine N, we again use symmetry, but this time on the length of the edges of P. For example, we know that the vertices I, J, K, and L span a 3-simplex with $|\text{IJ}| = |\text{JK}| = |\text{KL}| = |\text{IL}|$ and $|\text{IK}| = |\text{JL}|$ (where $|\text{xy}|$ denotes the euclidean distance from x to y). Thus, since a dilation does not destruct the symmetry, we can assume that the matrix N is of the form:

$$N := \begin{pmatrix} 1 & 1 & 1 & 1 & 1 & 1 & 1 \\ x_1 & 0 & 0 & 0 & 0 & 0 & 0 \\ x_2 & y_2 & 0 & 0 & 0 & 0 & 0 \\ x_3 & y_3 & z_3 & 0 & 0 & 0 & 0 \\ x_4 & y_4 & z_4 & 1 & -1 & 1 & -1 \\ x_5 & y_5 & z_5 & v & 0 & -v & 0 \\ x_6 & y_6 & z_6 & 0 & v & 0 & -v \end{pmatrix},$$

with $x_1 > 0$, $y_2 > 0$, $z_3 > 0$, and $v > 0$.

Using the remaining equations given by the symmetries, we obtain (with the help of a computer algebra system) the following constraints:

Lemma 4.52. *The coefficients of the matrix N satisfy:*

$$x_1 = \sqrt{\frac{(2+\sqrt{2})(2y_3+z_3\sqrt{2})(y_3+z_3)z_3}{y_3-z_3}}, \qquad x_2 = \frac{y_3(2+\sqrt{2})(y_3+z_3)}{\sqrt{z_3^2-y_3^2}},$$

$$y_2 = \sqrt{z_3^2-y_3^2}, \qquad x_3 = -(2+\sqrt{2})(y_3+z_3\frac{\sqrt{2}}{2}), \qquad x_4 = y_4 = z_4 = 0,$$

$$x_5 = -x_6 = y_5 = y_6 = -z_5 = z_6 = -\frac{1}{2}\sqrt{2}v(1+\sqrt{2}+u),$$

with $-z_3 < y_3 < -\frac{z_3}{\sqrt{2}}$. □

Reciprocally, it is easy to check (again with a computer algebra system) that under these conditions, the convex hull of the column vectors of $M = NM'$ is a symmetric realization of $\Delta_{8,2}$: we only have to verify that for any admissible values of u, v, y_3 and z_3:

(i) The boundary complex of the convex hull of the column vectors of M is indeed isomorphic to $\Delta_{6,1}$. This is encoded in the chirotope (and we only have to check the signs for one representative of each orbit under the dihedral group $\mathbb{D}_8$).

(ii) The dihedral group $\mathbb{D}_8$ indeed acts by isometry on the columns vectors of M (and we only have to check it on two generators of $\mathbb{D}_8$).

Thus, we obtain the main result of this section:

Proposition 4.53. *Up to dilation, the space of symmetric realizations of the simplicial complex $\Delta_{8,2}$ has dimension* 4. □

4.3.2.4 A general construction?

Even if our study of symmetric realizations of the simplicial complex $\Delta_{8,2}$ cannot be extended to general n and k, we consider that it provides new evidence and motivation for the general investigation. In particular, it seems reasonable to attempt to construct symmetric realizations of the multiassociahedron, in much the same way the secondary polytope of the n-gon is constructed:

(i) First, associate to each k-triangulation T of the n-gon a vector $\phi(T) \in \mathbb{R}^{nk}$, with k coordinates for each vertex v of the n-gon. These coordinates would be computed according to the k-stars of T which contain v.

(ii) Then, consider the convex hull of the vectors $\phi(T)$ of all k-triangulations of the n-gon, which should be of codimension $k(2k+1)$.

We don't have a full candidate for the vector $\phi(T)$, but it seems at least natural to choose, for the first coordinate of $\phi(T)$ associated to a vertex v of the n-gon, the sum of the areas of the k-stars of T containing v. (Remember that the area of a k-star S of the n-gon is the integral over $\mathbb{R}^2$ of the winding number of S; that is to say, a point of the plane is counted with multiplicity

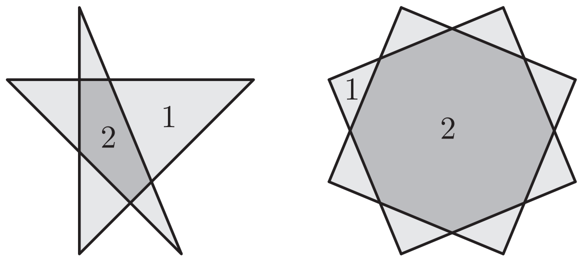

Figure 4.19: The area of a 2-star (each region is counted with multiplicity equal to the winding number of the 2-star around it) and the 2-depth of the octagon.

equal to the number of revolutions of S around it). However, it turns out that the only relation between these coordinates comes from the total area covered by the k-stars of T:

$$\mathcal{A}_k(V_n) = \sum_{S \in T} \mathcal{A}(S) = \frac{1}{2k+1} \sum_{v \in V_n} \sum_{v \in S \in T} \mathcal{A}(S),$$

where $\mathcal{A}_k(V_n)$ is the integral over $\mathbb{R}^2$ of the k-depth with respect to V_n (in other words, the sum of the winding numbers of the k-boundary components of the n-gon). See Figure 4.19. In particular, there is no more relations between the centers of mass of the k-stars of a k-triangulation. For example, the 84 area vectors of $\mathbb{R}^8$ corresponding to the 2-triangulations of the octagon (the vth coordinate of the vector associated to T is the sum of the areas of the 2-stars of T containing v) span an affine space of dimension 7 which is already to big to be completed into a 6-polytope.

4.3.3 A generalization of Loday's associahedron

In this section, we present another attempt to construct a multiassociahedron. We reinterpret Loday's construction 4.36 of the associahedron in terms of beam arrangements. This interpretation has two main advantages: on the one hand, the construction becomes much more visual, which leads to a simple proof of Theorem 4.37; on the other hand our definition naturally extends to multitriangulations and gives rise to a polytope with nice combinatorial properties. We start with a short reminder on the properties of the vector configuration formed by the columns of the incidence matrix of a directed graph.

4.3.3.1 The incidence cone of a directed graph

Let G be a directed (multi)graph on p vertices, whose underlying undirected graph is connected. An oriented edge with origin i and endpoint j is denoted (i,j). Let $(e_1, \dots, e_p)$ be the canonical basis of $\mathbb{R}^p$.

Definition 4.54. *The incidence configuration of the directed (multi)graph G is the vector configuration $I(G) := \{e_i - e_j \mid (i,j) \in G\}$. The incidence cone of G is the cone $C(G)$ generated by $I(G)$, i.e. its positive span.*

In other words, the incidence configuration of a graph consists of the column vectors of its incidence matrix. We will use the following relations between the graph properties of G and the orientation properties of $I(G)$. We refer to [BVS+99, Section 1.1] for details.

Observation 4.55. Consider a subgraph H of G. Then the vectors of $I(H)$:

(i) are independent if and only if H has no (non-necessarily oriented) cycle;

(ii) form a basis of the hyperplane $\sum x_i = 0$ if and only if H is a spanning tree;

(iii) form a circuit if and only if H is a (non-necessarily oriented) cycle; the positive and negative parts of the circuit correspond to the subsets of edges oriented in one or the other direction along the cycle; in particular, $I(H)$ is a positive circuit if and only if H is an oriented cycle;

(iv) form a cocircuit if and only if H is a minimal (non-necessarily oriented) cut; the positive and negative parts of the cocircuit correspond to the edges in one or the other direction in this cut; in particular, $I(H)$ is a positive cocircuit if and only if H is an oriented cut.

Observation 4.56. (i) The incidence cone $C(G)$ is pointed if and only if G is an acyclic directed graph. That is, if it induces a partial order on its set of nodes.

(ii) In this case, the rays of $C(G)$ correspond to the edges of the Hasse diagram of G. In particular, the cone is simplicial if and only if the Hasse diagram of G is a tree.

(iii) The facets of $C(G)$ correspond to the complement of the minimal directed cuts of G.

With this tool in mind, we can tackle serenely the topic of this section.

4.3.3.2 Loday's construction revisited

Let T be a triangulation of the n-gon. Consider its beam arrangement (*i.e.* its dual pseudoline arrangement drawn on the integer grid) — remember if necessary Section 4.1.4 and see Figure 4.20. As stated in Proposition 4.12, the ith beam B_i is an x- and y-monotone lattice path, coming from $(-\infty, i)$ and going to $(i, +\infty)$, which reflects in exactly three mirrors. For such a beam B_i, we define its *area* $\mathcal{A}_i$ to be the area inside the box $[0, i] \times [i, n-1]$ and below B_i.

Lemma 4.57. *Loday's* DFS*-vector* $\psi(T)$ *coincides with the* beam vector $(\mathcal{A}_1, \ldots, \mathcal{A}_{n-2})$.

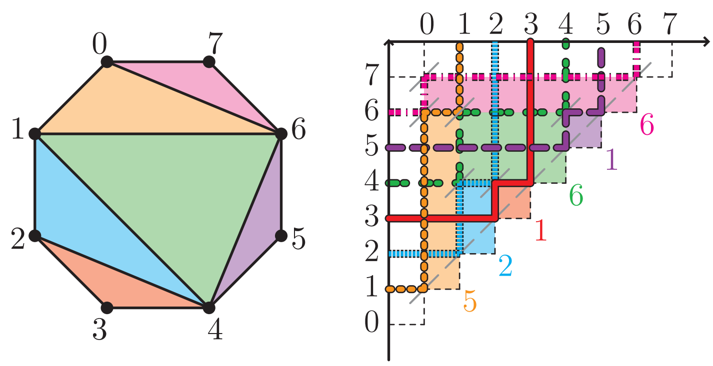

Figure 4.20: Loday's DFS-vector of a triangulation interpreted on its beam arrangement.

Proof. Let T be a triangulation of the n-gon and τ denote its dual binary tree on $n-2$ nodes (rooted at the triangle of T containing the edge $[0, n-1]$). The node x_i labeled by i in the DFS-labeling of τ corresponds to the triangle whose second vertex is i, that is, to the ith beam. Furthermore, if this triangle has vertices $h < i < j$, then the number of leaves in the left (resp. right) child of x_i is exactly $i - h$ (resp. $j - i$). Thus, the ith coordinate of $\psi(T)$, which is by definition the product of the numbers of leaves in both children of x_i, equals the area $\mathcal{A}_i = (i-h)(j-i)$ of the square located between the beam B_i and the lines $x = i$ and $y = i$. $\square$

Consequently, we see the DFS-polytope Ω_{n-2} as the convex hull of the beam vectors of all triangulations of the n-gon. With this interpretation, we present a simple proof of Loday's Theorem 4.37, based on the behavior of the beam vectors with respect to flips:

Lemma 4.58. *Let T and T' be two triangulations of the n-gon related by a flip which exchanges the diagonals in the quadrangle formed by gluing their ith and jth triangles. Then the difference $\psi(T) - \psi(T')$ of their beam vectors is parallel to $e_i - e_j$.*

Proof. Only the beams B_i and B_j are perturbed, and the area lost by B_i is transferred to B_j. $\square$

Corollary 4.59. *Ω_{n-2} is contained in the affine hyperplane $\left\{x \in \mathbb{R}^{n-2} \,\middle|\, \langle \mathbb{1} \,|\, x\rangle = \binom{n-1}{2}\right\}$.*

Proof. The beam vector of the minimal triangulation $T_{n,1}^{\min}$ belongs to this hyperplane. Since the difference between the beam vectors of two triangulations related by a flip is orthogonal to the vector $\mathbb{1}$, the result follows from the connectedness of the flip graph. $\square$

Let $\square_{u,v}$ denote the unit grid square $\{(u,v),(u-1,v),(u,v+1),(u-1,v+1)\}$ whose bottom right vertex is (u,v). Another way to prove the previous lemma is to observe that, for any triangulation T of the n-gon and any $1 \le u \le v \le n-2$, the square $\square_{u,v}$ is covered exactly once by the beam arrangement of T, meaning that there exists a unique $1 \le i \le n-2$ such that $\square_{u,v}$ lies between the beam B_i and the lines $x = i$ and $y = i$. We refer to Figure 4.20 for an illustration of this property.

Proposition 4.60. *For any internal edge $[u,v]$ of the n-gon, the equation $\sum_{p=u+1}^{v-1} x_p = \binom{v-u}{2}$ defines a facet $F_{u,v}$ of Ω_{n-2}. This facet contains precisely the beam vectors of all triangulations of the n-gon containing the edge $[u,v]$.*

Proof. Any square $\square_{x,y}$ is covered by a beam B_i which satisfies $x \le i \le y$. Consequently, the beams $\{B_i \,|\, u < i < v\}$ cover at least the zone $Z_{u,v}$ located to the right of the line $x = u$ and below the line $y = v$. This zone has area $\binom{v-u}{2}$ which proves that the inequality is valid.

Consider now a triangulation T of the n-gon containing the edge $[u,v]$. For any i,j such that $u < i < v < j$, the edge $[i,j]$ cannot be in T. Consequently, B_i is straight from (i,v) to $(i,+\infty)$. Similarly, B_i is straight from $(-\infty,i)$ to (u,i). Thus, the beams $\{B_i \,|\, u < i < v\}$ are the only beams passing in the region $Z_{u,v}$, and all their crossing points are located in $Z_{u,v}$. Consequently, we can interpret them as a beam arrangement of the $(v-u+1)$-gon, which implies (by the previous lemma) that $\sum_{p=u+1}^{v-1} x_p = \binom{v-u}{2}$.

Reciprocally, if the edge $[u, v]$ is not in T, then by maximality there is another edge $[x, y]$ preventing it to be in T. Assuming that $0 \leq x < y \leq n-1$, we have either $u < x < v < y$, or $x < u < y < v$. In the first (resp. second) case, the beam B_x (resp. B_y) cannot be straight from (x, v) to $(x, +\infty)$ (resp. from $(-\infty, y)$ to (u, y)), and thus, B_x (resp. B_y) covers at least one square outside $Z_{u,v}$. Consequently, the beams $\{B_i \mid u < i < v\}$ cover at least the zone $Z_{u,v}$ plus one square, which proves that the inequality is strict if $[u, v]$ is not is T.

Finally, we shall prove that $F_{u,v}$ is indeed a facet, and not a face of smaller dimension. Given a triangulation T containing $[u, v]$, we stay in $F_{u,v}$ when we flip any edge different from $[u, v]$. This gives rise to $n-4$ linearly independent directions in $F_{u,v}$. According to Corollary 4.59, this ensures that $F_{u,v}$ is a facet and that the polytope Ω_{n-2} has dimension $n-3$. $\square$

Proposition 4.61. *Let T be a triangulation of the n-gon, and τ denote its dual binary tree, where the edges are oriented towards the root. Then the cone $C(T)$ of Ω_{n-2} at $\psi(T)$ equals the incidence cone $C(\tau)$.*

Proof. The cone $C(T)$ certainly contains the incidence cone $C(\tau)$: for any $(i, j) \in \tau$, the ray $\mathbb{R}^+(e_i - e_j)$ of $C(\tau)$ is obtained in Ω_{n-2} by flipping the edge common to the ith and jth triangles of T. Reciprocally, the facet of $C(\tau)$ obtained as the convex hull of all rays except that of the edge $(i, j) \in \tau$ corresponds to the facet $F_{i,j}$ of Ω_{n-2}. $\square$

Corollary 4.62. *Every facet of Ω_{n-2} is of the form $F_{u,v}$ for some relevant edge $[u, v]$ of the n-gon.*

Proof. For any triangulation T, all the facets of the cone at $\psi(T)$ are of this form. $\square$

These results prove that $\Omega^{\diamond}_{n-2}$ realizes $\Delta_{n,1}$: the boundary complex of $\Omega^{\diamond}_{n-2}$ and the simplicial complex $\Delta_{n,1}$ have exactly the same vertex-facet incidences, and these incidences characterize the complete complex. To summarize our results, we have shown that:

1. All beam vectors lie in a hyperplane orthogonal to $\mathbb{1}$, and Ω_{n-2} has dimension $n-3$.
2. For each relevant edge $[u, v]$ of the n-gon, the vector $\sum_{p=u+1}^{v-1} e_i$ is the normal vector of a facet of Ω_{n-2}, whose vertices are precisely the beam vectors of all triangulations containing $[u, v]$. Furthermore all facets of Ω_{n-2} are of this form.
3. For each triangulation T, the cone of Ω_{n-2} at the beam vector $\psi(T)$ equals the incidence cone of the dual tree of T.
4. $\Omega^{\diamond}_{n-2}$ realizes the simplicial complex $\Delta_{n,1}$.

4.3.3.3 The beam polytope

The main advantage of our interpretation of Loday's construction via the beam arrangement is its natural extension to multitriangulations. Remember that a k-triangulation of the n-gon can also be seen by duality as a beam arrangement (*i.e.* a pseudoline arrangement drawn on the integer grid) — see Figure 4.21. The ith beam B_i is an x- and y-monotone lattice path, coming from $(-\infty, k-1+i)$ and going to $(k-1+i, +\infty)$, which reflects in exactly $2k+1$ mirrors.

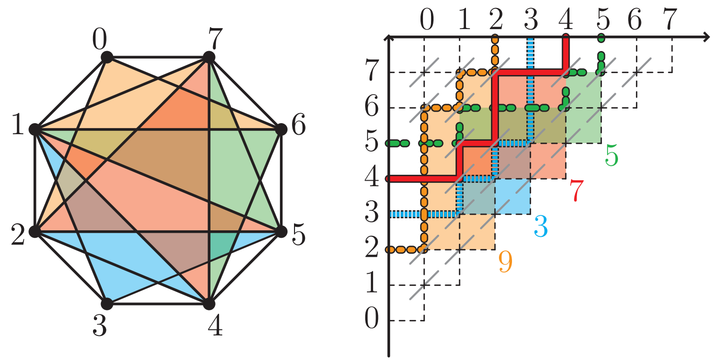

Figure 4.21: The beam vector of the 2-triangulation of Figure 1.4.

Definition 4.63. *The* beam vector *of a k-triangulation T of the n-gon is the vector $\psi(T) \in \mathbb{R}^{n-2k}$ whose ith coordinate is the area $\mathcal{A}_i$ of the region located below the beam B_i and inside the box $[0, k-1+i] \times [k-1+i, n-1]$. The* beam polytope *$\Omega_{n,k}$ is the convex hull of the beam vectors of all k-triangulations of the n-gon.*

Remark 4.64. We could have defined directly the beam vector $\psi(T)$ of a k-triangulation T with a formula: its ith coordinate is given by

$$\psi(T)_i := \sum_{j=1}^{k} (s_{j+1} - s_j)(s_{k+1+j} - s_{k+1}),$$

where $0 \preccurlyeq s_1 \prec \ldots \prec s_{2k+1} \preccurlyeq n-1$ are the vertices of the k-star of T whose $(k+1)$th vertex s_{k+1} is the vertex $k-1+i$.

As for triangulations, the interesting property of the beam vectors is their behavior with respect to flips:

Lemma 4.65. *Let T and T' be two k-triangulations of the n-gon related by a flip which involves their ith and jth k-stars. Then the difference $\psi(T) - \psi(T')$ of their beam vectors is parallel to $e_i - e_j$.*

Proof. Only the beams B_i and B_j are perturbed, and the area lost by B_i is transferred to B_j. $\square$

Corollary 4.66. *The polytope $\Omega_{n,k}$ is contained in the affine hyperplane defined by*

$$\left\{ x \in \mathbb{R}^{n-2k} \;\middle|\; \langle \mathbb{1} \,|\, x \rangle = \frac{k(n-2k)(n-k)}{2} \right\}.$$

Proof. The proof is similar to that of Corollary 4.59: the lemma is derived from the connectedness of the flip graph and from the calculation:

$$\langle \mathbb{1} \,|\, \psi(T_{n,k}^{\min}) \rangle = \sum_{i=1}^{n-2k} \left(\frac{k(k+1)}{2} + k(n-2k-i) \right) = \frac{k(n-2k)(n-k)}{2}. \qquad \square$$

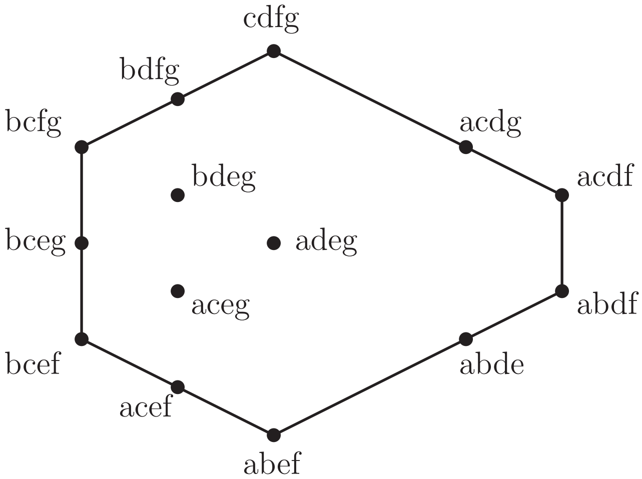

Figure 4.22: The 2-polytope $\Omega_{7,2}$.

Example 4.67. The beam vectors of the 2-triangulations of the heptagon are:

$$\begin{bmatrix}3\\5\\7\end{bmatrix}, \begin{bmatrix}7\\3\\5\end{bmatrix}, \begin{bmatrix}5\\7\\3\end{bmatrix}, \begin{bmatrix}3\\7\\5\end{bmatrix}, \begin{bmatrix}5\\3\\7\end{bmatrix}, \begin{bmatrix}7\\5\\3\end{bmatrix}, \begin{bmatrix}5\\5\\5\end{bmatrix}, \begin{bmatrix}5\\4\\6\end{bmatrix}, \begin{bmatrix}3\\8\\4\end{bmatrix}, \begin{bmatrix}6\\3\\6\end{bmatrix}, \begin{bmatrix}4\\8\\3\end{bmatrix}, \begin{bmatrix}6\\4\\5\end{bmatrix}, \begin{bmatrix}4\\4\\7\end{bmatrix}, \begin{bmatrix}7\\4\\4\end{bmatrix}.$$

The sum of their coordinates always equals 15. Projecting on the hyperplane $\langle(1,1,1)\,|\,x\rangle = 15$, we obtain the point set in Figure 4.22. Observe that we have chosen the projection in such a way that the symmetry of this point set (obtained by reversing the coordinates of the beam vectors in $\mathbb{R}^3$) is the orthogonal reflection with respect to the horizontal axis. For convenience, we have labeled the 2-relevant edges by letters ($\mathrm{a} := [0,3]$, $\mathrm{b} := [1,4]$, etc.), and the 2-triangulations by their set of 2-relevant edges. For example, abef is the 2-triangulation whose set of 2-relevant edges is $\{[0,3],[1,4],[0,4],[1,5]\}$.

The f-vectors of the polytopes $\Omega_{8,2}$, $\Omega_{9,2}$ and $\Omega_{10,2}$ are $(22,33,13)$, $(92,185,118,25)$ and $(420,1062,945,346,45)$ respectively. We have represented $\Omega_{8,2}$ and $\Omega_{9,2}$ in Figures 4.23 and 4.24. The polytope $\Omega_{8,2}$ is simple while the polytope $\Omega_{9,2}$ has two non-simple vertices (which are contained in the projection facet of the Schlegel diagram on the right of Figure 4.24) and the polytope $\Omega_{10,2}$ has 24 non-simple vertices. We will characterize later non-simple vertices in the beam polytope.

The dimension of the beam polytope $\Omega_{n,k}$ is $n-2k-1$, and thus differs from the dimension $k(n-2k-1)$ of the k-associahedron we would like to construct. However, it is reasonable to think that the beam polytope $\Omega_{n,k}$ could be a projection of a k-associahedron. In this case, we could use the beam polytope $\Omega_{n,k}$ as a starting point to construct this k-associahedron, splitting each of the coordinates of $\Omega_{n,k}$ into k coordinates. With this motivation, we study in the next section the facets of the beam polytope and check that they are compatible with $\Delta_{n,k}$: we prove that the k-triangulations whose beam vector belongs to a given facet of the beam polytope form a face of $\Delta_{n,k}$.

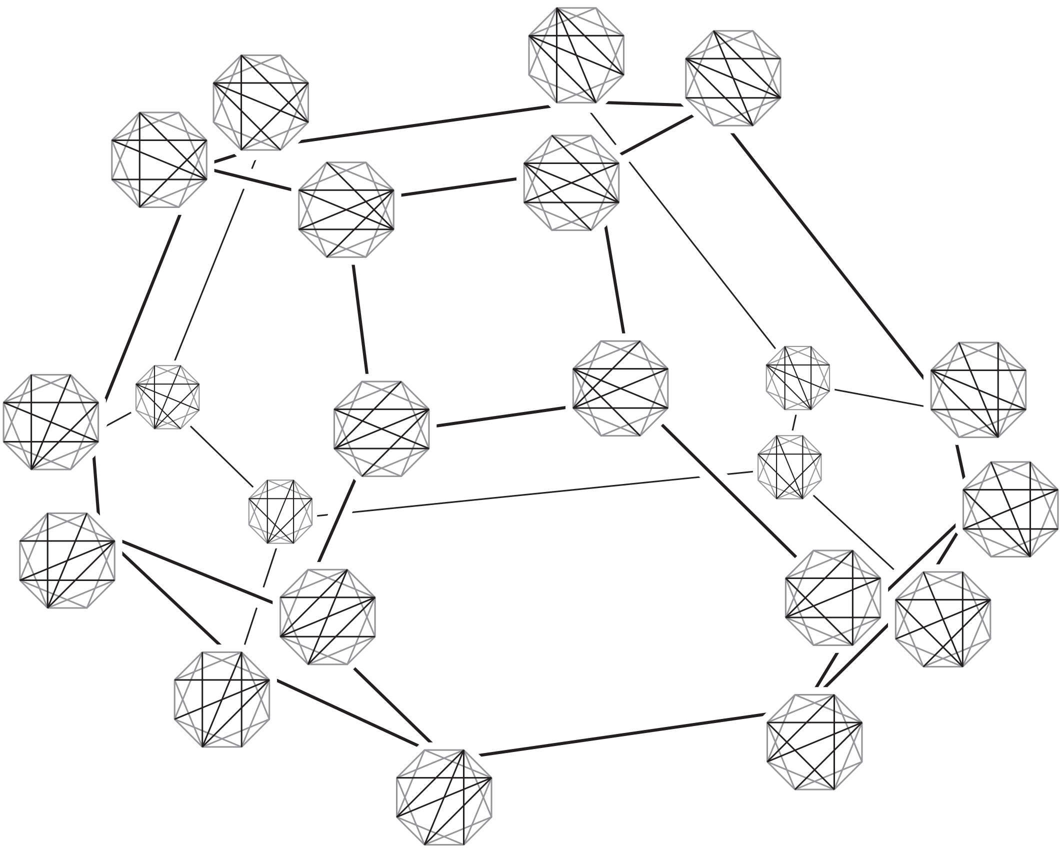

Figure 4.23: The 3-polytope $\Omega_{8,2}$.

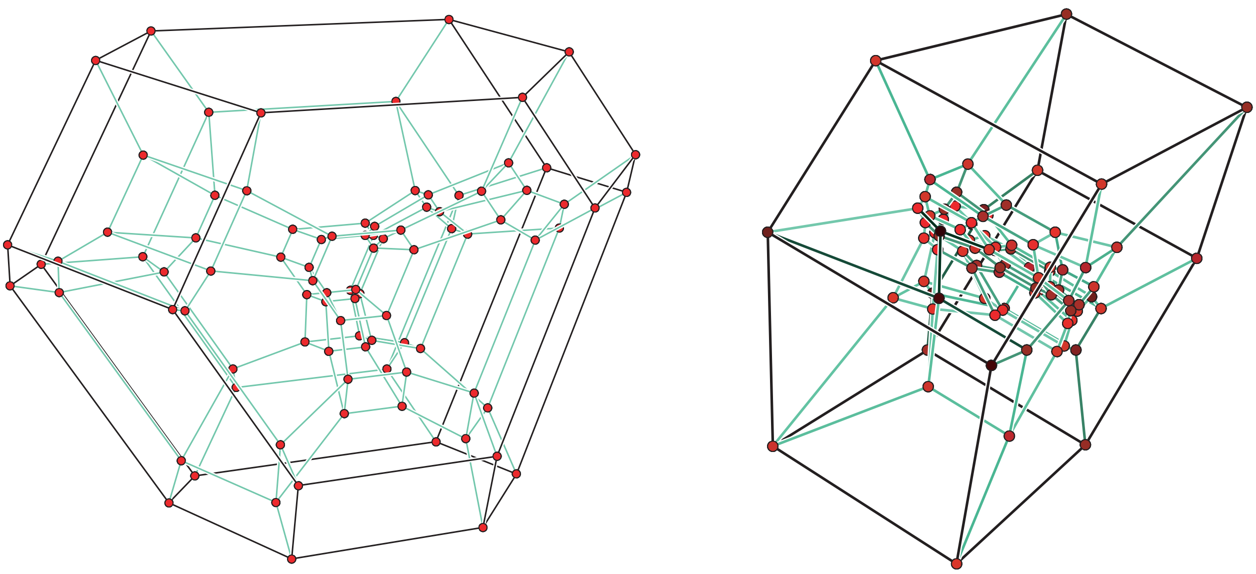

Figure 4.24: Two Schlegel diagrams of the 4-polytope $\Omega_{9,2}$. On the second one, the two leftmost vertices of the projection facet are non-simple vertices.

4.3.3.4 k-valid $0/1$-sequences and facet description

To emphasize the rich combinatorial structure of our beam polytope $\Omega_{n,k}$, we give a simple description of its facet-defining equations and of its vertex-facet incidences, which generalizes Proposition 4.60. The main characters of this description are the following sequences:

Definition 4.68. *We call* p-valid $0/1$-sequence *of size* q *any sequence of* $\{0,1\}^q$ *which is neither* $(0,0,\ldots,0)$*, nor* $(1,1,\ldots,1)$ *and does not contain a subsequence* 10^r1 *for* $r \geq p$*. In other words, all subsequences of* p *consecutive zeros appear before the first one or after the last one.*

Example 4.69. 1-valid $0/1$-sequences are sequences whose only zeros are located at the beginning or at the end, *i.e.* sequences of the form $0^x1^y0^z$ with $x+y+z=q$ and $y \neq 0 \neq x+z$. Observe that these sequences are exactly the normal vectors of Loday's DFS-polytope Ω_q (see Proposition 4.60).

Remark 4.70. Let $\mathrm{VS}_{p,q}$ denote the number of p-valid $0/1$-sequences of size q. It is easy to see that $\mathrm{VS}_{1,q} = \frac{1}{2}(q-1)(q+2)$ (the number of internal diagonals of a $(q+2)$-gon!) and that $\mathrm{VS}_{2,q} = F_{q+4} - (q+4)$, where F_n denotes the nth Fibonacci number (indeed, if u_q denotes the number of $0/1$-sequences of length q which start with a 1 and do not contain a subsequence 00 before their last 1, then $u_q = u_{q-1} + u_{q-2} + 1$ and $\mathrm{VS}_{2,q} = \mathrm{VS}_{2,q-1} + u_q$). To compute $\mathrm{VS}_{p,q}$ in general, consider the non-ambiguous rational expression $0^*(1,10,100,\ldots,10^{p-1})^*10^*$. The corresponding rational language consists of all p-valid $0/1$-sequences plus all non-empty sequences of 1. Thus, the generating function of p-valid $0/1$-sequences is:

$$\sum_{q\in\mathbb{N}} \mathrm{VS}_{p,q} x^q = \frac{1}{1-x}\,\frac{1}{1-\sum_{i=1}^p x^i}\,x\,\frac{1}{1-x} - \frac{x}{1-x} = \frac{x^2(2-x^p)}{(1-2x+x^{p+1})(1-x)}.$$

We use these sequences to describe the facets of the beam polytope. For this, we need one more definition. Let σ be a $0/1$-sequence of length $n-2k$. Let $|\sigma|_0$ denote the number of zeros in σ. For all $i \leq |\sigma|_0 + 2k$, we denote by $\zeta_i(\sigma)$ the position of the ith zero in the $0/1$-sequence $0^k\sigma 0^k$, obtained from σ by appending a prefix and a suffix of k consecutive zeros. We associate to σ the set of edges:

$$D(\sigma) := \{[\zeta_i(\sigma), \zeta_{i+k}(\sigma)] \mid i \in [|\sigma|_0 + k]\}.$$

Observe that $D(\sigma)$ can contain some k-boundary edges of the n-gon.

Theorem 4.71. *Each* k*-valid* $0/1$*-sequence* σ *of size* $n-2k$ *is the normal vector of a facet* F_σ *of the beam polytope* $\Omega_{n,k}$*, which contains precisely the beam vectors of the* k*-triangulations of the* n*-gon containing* $D(\sigma)$*.*

Proof. We denote by $Z(\sigma) := \{(x,y) \in \mathbb{R}^2 \mid \exists\,[u,v] \in D(\sigma), x \geq u \text{ and } y \leq v\}$ the zone of all points of the plane which see $D(\sigma)$ in their north-west quadran.

We first prove that the value of $\langle \sigma \mid \psi(T)\rangle$ is the same for all k-triangulations of the n-gon which contain $D(\sigma)$. Let T be such a k-triangulation. For any integer i with $\sigma_i = 1$, any mirror located out of the zone $Z(\sigma)$ and on one of the lines $x = i$ or $y = i$ creates a $(k+1)$-crossing with $D(\sigma)$. Thus, the beam B_i arrives straight from $(-\infty, i+k-1)$ until it enters $Z(\sigma)$, and goes straight to $(i+k-1, +\infty)$ as soon as it goes out of $Z(\sigma)$. In other words, the beams B_i with $\sigma_i = 1$ are the only beams passing through a vertex in $Z(\sigma)$ not in $D(\sigma)$. Consequently, the only contact points between a beam B_i with $\sigma_i = 1$ and a beam B_j with $\sigma_j = 0$ are those of $D(\sigma)$. Thus, the flip of any edge not in $D(\sigma)$ does not change the value of $\langle \sigma \,|\, \psi(T) \rangle$. This value is constant on all k-triangulations of the n-gon which contain $D(\sigma)$ by connectedness of the flip graph.

Consider now a k-triangulation T of the n-gon which does not contain the set $D(\sigma)$. For any $u \le i+k-1 \le v$, the beam B_i covers the square $\square_{u,v}$ except if it passes in a level between the points (u,v) and $(i+k-1, i+k-1)$. Consequently, each square of $Z(\sigma)$ is covered by the beams $(B_i)_{\sigma_i=1}$ of T at least as many times as it is covered by those of any k-triangulation containing $D(\sigma)$. Furthermore, if $[u,v]$ is an edge of $D(\sigma)$ which is not in T, then at least one beam B_i of T with $u \le i+k-1 \le v$ and $\sigma_i = 1$ covers a square out of $Z(\sigma)$. This ensures that $\langle \sigma \,|\, . \rangle$ is strictly bigger on $\psi(T)$ than on the beam vector of a k-triangulation containing $D(\sigma)$.

We still have to prove that F_σ is indeed a facet, and not a face of smaller dimension. This is a direct consequence of the study of the vertex cones of $\Omega_{n,k}$ to come next. $\square$

In the next section, we prove furthermore that all the facets of the beam polytope are derived from k-valid $0/1$-sequences as those of Theorem 4.71.

4.3.3.5 Directed dual multigraphs, cones, and vertex characterization

We consider the dual multigraph $T^\#$ of T. Remember (see the definition in Section 2.6.2) that $T^\#$ has one vertex for each k-star of T and one edge between its two vertices corresponding to the k-stars R and S of T for each common k-relevant edge of R and S. We label by i the vertex of $T^\#$ which corresponds to the ith k-star of T, that is, to the ith beam B_i. For the edges, we need two notations: on the one hand, we denote by $e^\#$ the edge of $T^\#$ which is dual to the k-relevant edge e of T; on the other hand, we write (i,j) for an edge of $T^\#$ which relates its vertices i and j (we can have more than one edge (i,j)). Observe that $T^\#$ comes naturally with its edges oriented: each edge (i,j) of $T^\#$, corresponding to a mirror separating the two beams B_i and B_j of the beam arrangement of T, is oriented from i to j if B_i lies above B_j at this mirror, and in the other direction otherwise.

We first need to understand the directed cuts of this oriented multigraph:

Lemma 4.72. *Let T be a k-triangulation of the n-gon. Consider a set of k-relevant edges $E \subset T$ and its dual set $E^\# := \left\{ e^\# \,\middle|\, e \in E \right\} \subset T^\#$. Assume that $E^\#$ is a directed cut of $T^\#$: there is a partition $U \sqcup V = [n-2k]$ of the vertices of $T^\#$ such that $E^\# = T^\# \cap \{(u,v) \,|\, u \in U, v \in V\}$ and $T^\# \cap \{(v,u) \,|\, u \in U, v \in V\} = \emptyset$. Let σ be the caracteristic $0/1$-sequence of V, i.e. the sequence of length $n-2k$ with $\sigma_i = 1$ if $i \in V$ and 0 otherwise. Then:*

(i) E is precisely the set of k-relevant edges in $D(\sigma)$.

(ii) If the directed cut $E^\#$ is minimal, then σ is k-valid.

Proof. We define again the zone $Z(\sigma) := \{(x,y) \in \mathbb{R}^2 \,|\, \exists\, [u,v] \in D(\sigma), x \geq u \text{ and } y \leq v\}$ of all points of the plane which see $D(\sigma)$ in their north-west quadran.

We claim that all the beams B_i with $i \in V$ are straight out of $Z(\sigma)$: otherwise, we would have in $T^{\#}$ an edge from V to U. Consequently, the beams B_i with $i \in V$ precisely cover the zone $Z(\sigma)$ plus all the vertical an horizontal straight lines $x = i$ and $y = i$ for $i \in V$. This implies that the contact points between a beam B_i with $i \in V$ and a beam B_j with $j \in U$ are precisely the k-relevant edges in $D(\sigma)$.

For the second point, assume that σ is not k-valid. Then there exists a sequence of at least k zeros between two ones. Let V_1 (resp. V_2) denote the set of all positions of ones before (resp. after) this sequence of zeros. Then the beams B_i with $i \in V_1$ have no contact points with the beams B_j with $j \in V_2$. Consequently, the sets V_1 and $U \cup V_2$ are separated by a directed cut of $T^{\#}$ which is strictly contained in $E^{\#}$. This proves that $E^{\#}$ was not minimal. □

Theorem 4.73. *Let T be a k-triangulation of the n-gon and $T^{\#}$ denote its oriented dual multigraph. The cone $C(T)$ of $\Omega_{n,k}$ at $\psi(T)$ equals the incidence cone $C(T^{\#})$.*

Proof. The proof is similar to that of Proposition 4.61. Observe first that the cone $C(T)$ certainly contains the incidence cone $C(T^{\#})$: for any $(i,j) \in T^{\#}$, the ray $\mathbb{R}^+(e_i - e_j)$ of $C(T^{\#})$ is obtained in $C(T)$ by flipping an edge common to the ith and jth stars of T.

To prove the reciprocal inclusion, we show that each facet of $C(T^{\#})$ is also a facet of $C(T)$. Let F be a facet of $C(T^{\#})$. According to Observation 4.56(iii), there is a minimal directed cut $E^{\#}$ of $T^{\#}$ such that F is the cone over $\{e_i - e_j \,\big|\, (i,j) \in T^{\#} \smallsetminus E^{\#}\}$. The previous lemma then ensures that $E^{\#}$ is the dual of the set of k-relevant edges in $D(\sigma)$, where σ is a k-valid $0/1$-sequence. Consequently, the facet F of $C(T^{\#})$ is also a facet F_σ of $C(T)$. □

Observe that this proof also finishes the proof of Theorem 4.71: any F_σ is indeed a facet of the cones at its vertices. It ensures moreover that:

Corollary 4.74. *Any facet of $\Omega_{n,k}$ is of the form F_σ for a k-valid $0/1$-sequence σ of length $n-2k$.*

Proof. All the facets of the cone at any vertex of $\Omega_{n,k}$ are of this form. □

Example 4.75. For example, the numbers of facets of the beam polytopes $\Omega_{7,2}$, $\Omega_{8,2}$, $\Omega_{9,2}$ and $\Omega_{10,2}$ are respectively 6, 13, 25 and 45. They equal the numbers $\mathrm{vs}_{2,n-4} = F_n - n$ of 2-valid $0/1$-sequences of length $n-4$ (where F_n denotes the nth Fibonacci number).

Furthermore, Theorem 4.73 together with Observation 4.56(i) provide a criterion to characterize the vertices of the beam polytope:

Corollary 4.76. *Let T be a k-triangulation of the n-gon.*

(i) The beam vector $\psi(T)$ is a vertex of the beam polytope $\Omega_{n,k}$ if and only if the oriented dual multigraph $T^{\#}$ of T is acyclic.

(ii) When $T^{\#}$ is acyclic, it defines a partially ordered set on its vertices, and the vertex $\psi(T)$ is simple if and only if the Hasse diagram of this poset is a tree.

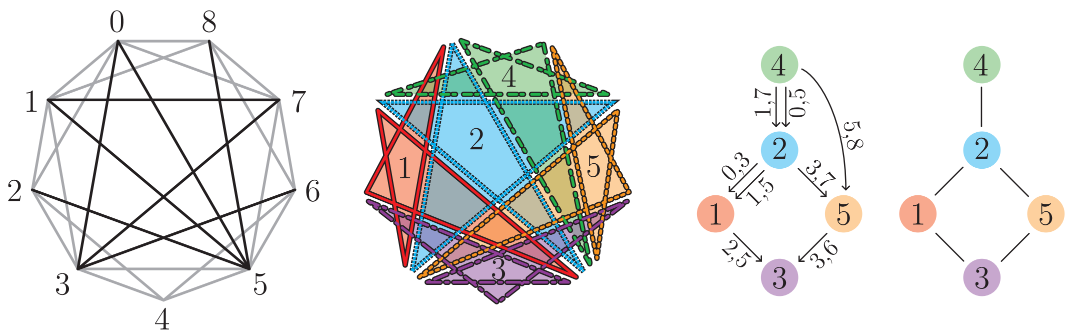

Figure 4.25: A 2-triangulation T of the 9-gon whose oriented dual multigraph $T^\#$ is acyclic, but whose Hasse diagram is not a tree. Its beam vector $\psi(T)$ is a non-simple vertex of the beam polytope $\Omega_{9,2}$. We have represented the 2-triangulation T, its decomposition into 2-stars, its oriented dual multigraph $T^\#$ and the associated Hasse diagram. We have labeled by i the node of $T^\#$ corresponding to the ith 2-star of T, and by u, v the dual edge of $[u, v] \in T$.

Example 4.77. The beam polytope $\Omega_{9,2}$ has 92 vertices, two of which are not simple. For one of them, we have represented in Figure 4.25 the corresponding 2-triangulation of the 9-gon, its dual multigraph, and its Hasse diagram.

Let us summarize our combinatorial description of the beam polytope:

1. All beam vectors lie in a common hyperplane orthogonal to $\mathbb{1}$, and the beam polytope has dimension $n - 2k - 1$.
2. Each k-valid 0/1-sequence σ of length $n-2k$ is the normal vector of a facet F_σ of $\Omega_{n,k}$, and the set of k-triangulations whose beam vector is contained in F_σ is a face of the simplicial complex $\Delta_{n,k}$. Furthermore, all facets of $\Omega_{n,k}$ are of this form.
3. The cone of $\Omega_{n,k}$ at the beam vector $\psi(T)$ of a k-triangulation T of the n-gon is the cone $C(T^\#)$ of the oriented dual multigraph $T^\#$ of T.
4. The vertices of the beam polytope $\Omega_{n,k}$ are the beam vectors of the k-triangulations whose oriented dual multigraph is acyclic. A vertex $\psi(T)$ is simple if and only if the Hasse diagram of $T^\#$ is a tree.

4.3.3.6 Projection obstruction

Despite these encouraging properties, it turns out that the beam polytope can in fact not be the projection of a realization of $\Delta_{n,k}$. We finish this section with a proof that $\Omega_{7,2}$ is not the projection of a realization of $\Delta_{7,2}$.

Proposition 4.78. *Let P be a 4-polytope with 14 vertices labeled by the 14 2-triangulations of the heptagon such that the faces of P are faces of $\Delta_{7,2}$. Then it is not possible to project P down to the plane such that, for each 2-triangulation of the heptagon, the vertex of P labeled by T is sent to $\psi(T)$.*

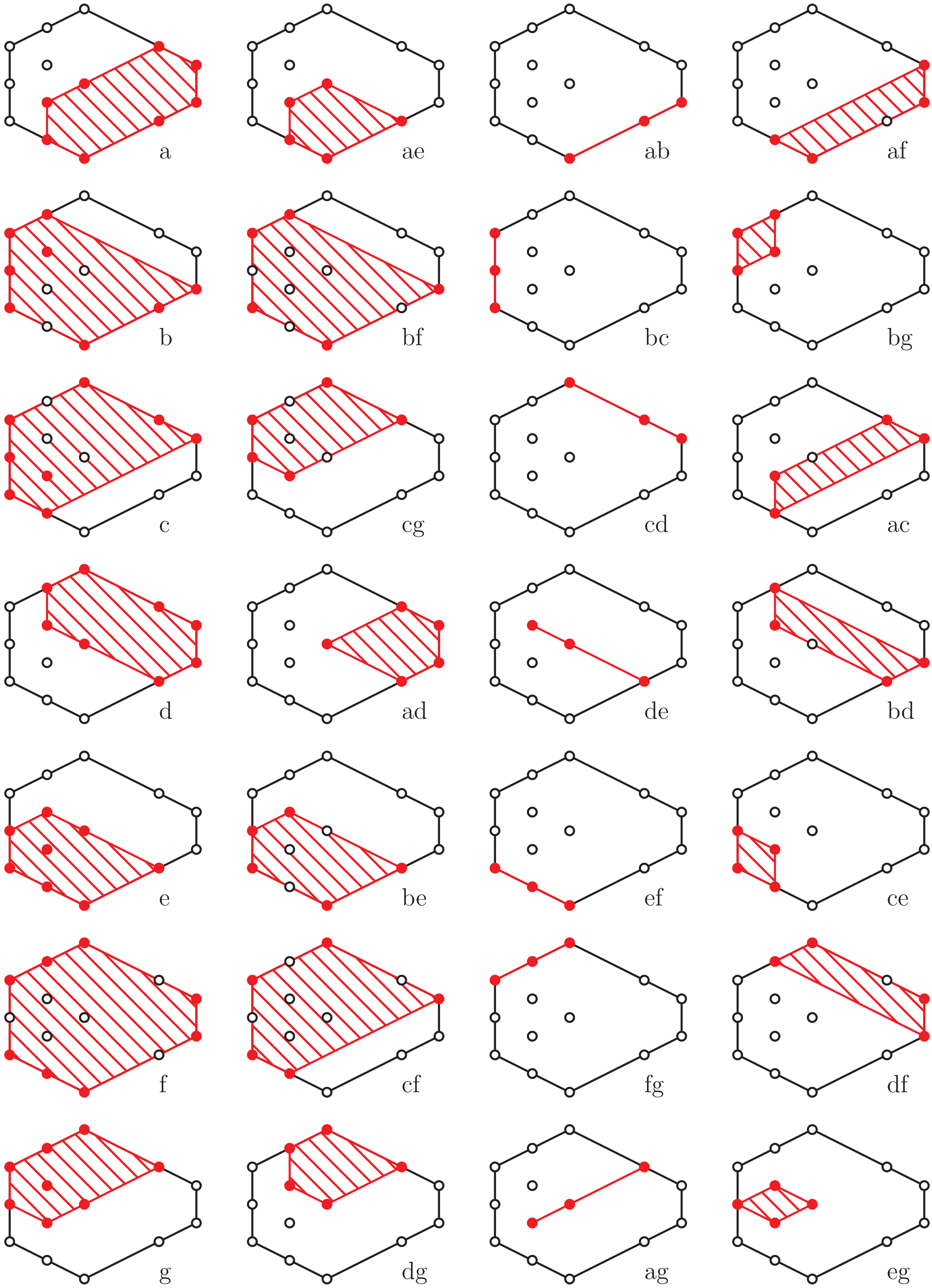

Figure 4.26: Projections of the 1- and 2-codimensional faces of $\Delta^{\diamond}_{7,2}$.

Proof. We prove the result by contradiction. Assume that there exists a 4-dimensional point set $V := \{v_T \,|\, T \text{ 2-triangulation of the heptagon}\} \subset \mathbb{R}^4$ labeled by the 2-triangulations of the heptagon such that:

(i) the faces of $\mathrm{conv}(V)$ are faces of $\Delta_{n,k}$; and

(ii) the orthogonal projection on the plane $\mathbb{R}x + \mathbb{R}y$ sends v_T to $\psi(T)$.

Then, projecting the point set V only partially on $\mathbb{R}x + \mathbb{R}y + \mathbb{R}z$ yields a 3-dimensional point set $W := \{w_T \,|\, T \text{ 2-triangulation of the heptagon}\} \subset \mathbb{R}^3$ with the same properties (i) and (ii). We prove that such a point configuration W cannot exist.

The argument is based on a careful study of the projections of the faces of $\Delta^{\diamond}_{7,2}$. For any face F of $\Delta^{\diamond}_{7,2}$ we denote by $\psi(F) := \{\psi(T) \,|\, T \in F\}$ its projection on the plane. For example, we have represented in Figure 4.26 the projections of all 1- and 2-codimensional faces of $\Delta^{\diamond}_{7,2}$: the left column represents, for each 2-relevant edge e of the heptagon, the set of 2-triangulations which contain e; the other three columns represent, for each pair of 2-relevant edges $\{e, f\}$ of the heptagon, the set of 2-triangulations which contain $\{e, f\}$.

We denote by $\mathcal{F}^+$ the set of faces F of $\Delta^{\diamond}_{7,2}$ such that $\mathrm{conv}\,\{w_T \,|\, T \in F\}$ is an upper facet of $\mathrm{conv}\, W$ (with respect ot the last coordinate z). Similarly, let $\mathcal{F}^-$ denote the set of faces of $\Delta^{\diamond}_{7,2}$ corresponding to lower facets of $\mathrm{conv}\, W$. The projections of the upper facets of $\mathrm{conv}\, W$ define a tiling of the polytope $\Omega_{7,2}$, *i.e.* they satisfy:

(i) *covering property*: $\Omega_{7,2} = \bigcup_{F \in \mathcal{F}^+} \mathrm{conv}\,\psi(F)$; and

(ii) *intersection property*: for all $F, F' \in \mathcal{F}^+$, the intersection $\mathrm{conv}\,\psi(F) \cap \mathrm{conv}\,\psi(F')$ is either empty, or an edge or a vertex of both $\mathrm{conv}\,\psi(F)$ and $\mathrm{conv}\,\psi(F')$, and F and F' coincide on this interesection:

$$\mathrm{conv}\,\psi(F) \cap \mathrm{conv}\,\psi(F') \cap \psi(F) = \mathrm{conv}\,\psi(F) \cap \mathrm{conv}\,\psi(F') \cap \psi(F').$$

A case analysis proves that we have only ten solutions for this tiling, represented in Figure 4.27. Thus, we already know all possibilities for the upper and lower parts $\mathcal{F}^+$ and $\mathcal{F}^-$.

Now, the upper and lower hulls of W have to be glued together, using if necessary some vertical facets. We have five possible vertical facets, which appear in the third column of Figure 4.26: any triple of points of W which projects to an edge of $\Omega_{7,2}$ either is colinear in W, or forms a vertical triangular facet of $\mathrm{conv}\, W$. If it is colinear, this triple belongs to one facet of $\mathcal{F}^+$ and to one facet of $\mathcal{F}^-$. If we have a vertical facet, then the two endpoints belong to two different facets in $\mathcal{F}^+$ (both containing the middle point), and to one facet in $\mathcal{F}^-$ which does not contain the middle point, or *vice versa*. For example, the rightmost edge separates the ten possible tilings of Figure 4.27 into three groups: call type A the tilings f, $\mathrm{bf} + \mathrm{df}$ and $\mathrm{cf} + \mathrm{af}$ in which the rightmost edge contains only two vertices; call type B the tilings $\mathrm{b} + \mathrm{df}$ and $\mathrm{c} + \mathrm{af}$ in which the rightmost edge contains three vertices and is contained in a face; and call type C the five remaining tilings, in which the rightmost edge contains three vertices and is subdivided between two faces. Then either both $\mathcal{F}^+$ and $\mathcal{F}^-$ are of type B, or $\mathcal{F}^+$ is of type A and $\mathcal{F}^-$ is of type C (or *vice versa*). It is easy to check that in fact there exists no pair of tilings in Figure 4.27 which are compatible for all the boundary edges. This implies that W cannot exist, and thus, finishes the proof of the proposition. $\square$

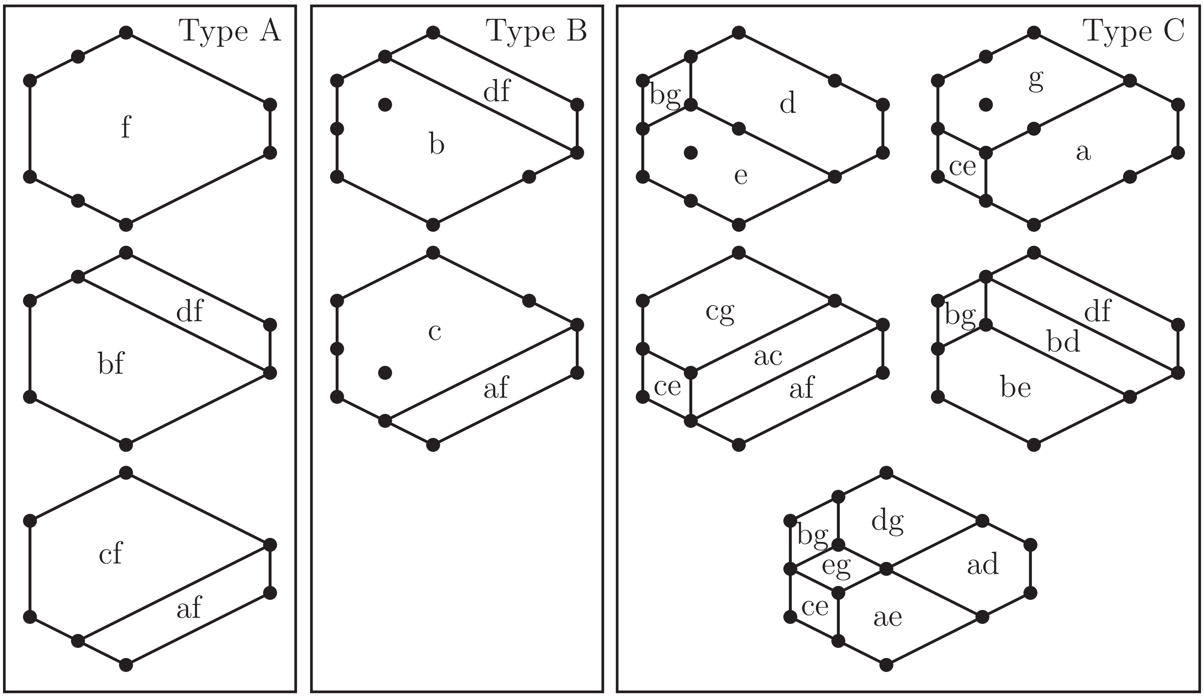

Figure 4.27: The ten possible solutions for the upper and lower hull of W.

4.3.4 Pseudoline arrangements with the same support

To finish this section, we discuss the extension of the polytopality question to a more general family of simplicial complexes arising from the framework developed in Chapter 3:

Definition 4.79. *Given the support $\mathcal{S}$ of a pseudoline arrangement, let $\Delta(\mathcal{S})$ denote the simplicial complex whose maximal simplices are the sets of contact points of pseudoline arrangements supported by $\mathcal{S}$.*

For any integers n and k, the simplicial complex $\Delta_{n,k}$ is isomorphic to $\Delta(V_n^{*k})$, where V_n^{*k} denotes the k-kernel of the dual pseudoline arrangement of V_n. We present in the next section the other motivating example, whose graph is the flip graph on pseudotriangulations of a point set.

4.3.4.1 The polytope of pseudotriangulations via rigidity properties

Let P be a point set in general position in the plane and P^{*1} denote the first kernel of the dual arrangement of P. According to the results of Chapter 3, the complex $\Delta(P^{*1})$ is isomorphic to the simplicial complex of all non-crossing and pointed sets of internal edges of E. The maximal elements of this complex are in bijection with the pseudotriangulations of P, and its ridge graph is the graph of flips $G(P)$. We have seen in Chapter 3 that this graph is connected and regular (of degree $2|P| - 3 - h$, where h denotes the number of points of P on its convex hull).

In [RSS03], Günter Rote, Francisco Santos and Ileana Streinu proved that when P is an Euclidean point set, the simplicial complex $\Delta(P^{*1})$ is in fact polytopal (see Figure 4.28):

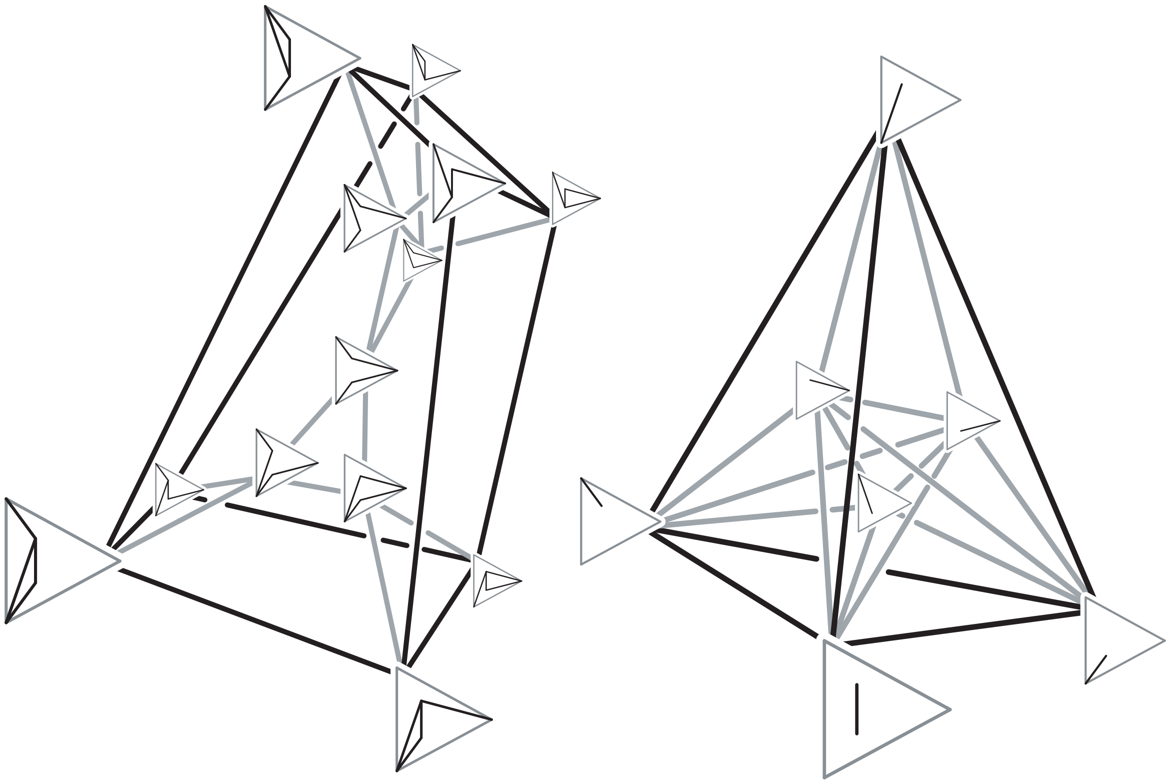

Figure 4.28: The polytope of (pointed) pseudotriangulations of a configuration P of five points (left). Its dual polytope (right) realizes the simplicial complex $\Delta(P^{*1})$. The only missing edge in $\Delta(P^{*1})$ corresponds to the only pair of crossing edges in P.

Theorem 4.80 ([RSS03])**.** *Let P be a point set in general position in the Euclidean plane, with h points on the convex hull. Then the simplicial complex $\Delta(P^{*1})$ is the boundary complex of a simplicial $(2|P| - 3 - h)$-polytope.* □

Remark 4.81. The proof in [RSS03] relies on rigidity properties of pseudotriangulations [Str05]:

(i) As a consequence of Lemma 3.16 and Theorem 4.13, all pseudotriangulations are generically minimally rigid in the plane. In fact, every planar minimally generically rigid graph can be embedded as a pseudotriangulation [HOR$^+$05].

(ii) The framework obtained by removing one boundary edge from a pseudotriangulation is an expansive mechanism[1].

[1] An *infinitesimal motion* of a framework (P, E) is an assignement $v : P \to \mathbb{R}^2$ of a velocity to each point such that $\langle p - q \mid v(p) - v(q) \rangle = 0$ for any edge $(p, q) \in E$ of the framework. Infinitesimal motions correspond to the first derivatives of the motions of (P, E). We quotient the space of infinitesimal motions by the subspace of rigid ones, that is, by the first derivatives of rigid motions of the whole plane.

An infinitesimal motion is said to be *expansive* if all distances increase: $\langle p - q \mid v(p) - v(q) \rangle \geq 0$ for all $p, q \in P$. A *mechanism* is a framework whose space of infinitesimal motions is 1-dimensional. A mechanism is *expansive* if its (unique up to a scalar) infinitesimal motion is expansive.

The polytope of pseudotriangulations is obtained as a perturbation of the cone

$$\mathcal{E}(P) := \left\{ v : P \to \mathbb{R}^2 \,\middle|\, \langle p - q \,|\, v(p) - v(q) \rangle \geq 0 \text{ for all } p, q \in P \right\}$$

of infinitesimal expansive motions of P. An extreme ray of the *expansion cone* $\mathcal{E}(P)$ corresponds to an expansive mechanism, and thus, to many "pseudotriangulations minus one boundary edge" (which have the same rigid components). A suitable choice of perturbation of the inequalities of the expansion cone $\mathcal{E}(P)$ is used to "separate" all pseudotriangulations which correspond to the same expansive mechanism. The vertices of the resulting polyhedron are in bijection with the pseudotriangulations of P and are all contained in a bounded face, whose boundary complex is the dual complex of $\Delta(P^{*1})$.

Remark 4.82. In much the same way as for pseudotriangulations, rigidity properties of multitriangulations would provide insight to the question of the polytopality of $\Delta_{n,k}$. We shortly present the ideas of the possible construction via the rigidity matrix (see [Gra01, Fel04] for rigidity notions and [RSS03] for the construction).

Consider a generic embedding $P : [n] \to \mathbb{R}^d$ of n points in a d-dimensional space. We associate to each pair $\{u, v\} \in \binom{[n]}{2}$ its *rigidity vector* $\phi_{u,v} := (f_1, f_2, \ldots, f_n) \in (\mathbb{R}^d)^n = \mathbb{R}^{dn}$ defined by $f_u := P(u) - P(v)$, $f_v := P(v) - P(u)$ and $f_i := 0 \in \mathbb{R}^d$ for all $i \in [n] \smallsetminus \{u, v\}$. This vector configuration naturally lives in the orthogonal complement X (of dimension $dn - \binom{d+1}{2}$) of the space of rigid infinitesimal motions. The rigidity properties of a graph G on n vertices can be read on its *rigidity configuration* $\phi(G) := \{\phi_{u,v} \,|\, \{u, v\} \in G\}$:

(i) G is infinitesimally rigid if and only if $\phi(G)$ spans X; and

(ii) G is *stress-free* (*i.e.* no edge of G can be removed preserving the same rigid components) if and only if $\phi(G)$ is independent.

Consequently, the minimally generically rigid graphs on n vertices in dimension d are precisely the graphs whose rigidity configuration $\phi(G)$ forms a basis of X.

Assume now that we can prove that every k-triangulation of the n-gon is generically rigid in dimension $2k$. Then the cone hull $C(T)$ of the rigidity configuration $\phi(T)$ of each k-triangulation T of the n-gon is a full-dimensional simplicial cone in the vector space X. Since each edge in a k-triangulation can be uniquely flipped, the complex $\Theta_{n,k}$ formed by all cones $C(T)$ associated to all k-triangulations of the n-gon is a pure pseudo-manifold (every facet of every full-dimensional simplicial cone is a facet of precisely two cones).

Assume furthermore that there exists a generic embedding $P : [n] \to \mathbb{R}^{2kn}$ such that for every k-triangulations T and T' of the n-gon related by a flip, in the expansive mechanism $(P, T \cap T')$, the edge of $T \smallsetminus T'$ expands when the edge of $T' \smallsetminus T$ contracts. Then in the complex $\Theta_{n,k}$, two cones which share a facet are separated by this facet. This would imply that the simplicial complex $\Delta_{n,k}$ is a complete simplicial fan. And this simplicial fan would hopefully be regular, so that it would be the face fan of a simplicial polytope.

This was our initial motivation to study rigidity properties of multitriangulations.

4.3.4.2 The polytope of pseudoline arrangements with acyclic dual graphs

In this section, we observe that our construction of the beam polytope of Section 4.3.3 can be extended to the framework developed in Chapter 3. We skip the proofs of this extension (because they are essentially the same as those of Section 4.3.3, but also because we prove in the next section that multitriangulations are sufficiently universal to cover the general setting).

Let $\mathcal{S}$ be the support of a pseudoline arrangement in the Möbius strip, and χ be a cut of $\mathcal{S}$. When we cut the Möbius strip along χ, we obtain a representation of $\mathcal{S}$ on the band $[0, \pi) \times \mathbb{R}$. Consider now a pseudoline arrangement Λ supported by $\mathcal{S}$, and denote by $\lambda_1, \dots, \lambda_n$ the pseudolines of Λ, such that their points on the vertical axis are ordered from top to bottom. We associate to Λ the vector $\psi(\Lambda) \in \mathbb{R}^n$ whose ith coordinate is the number of faces of the arrangement located below the pseudoline λ_i. Finally, we define the polytope $\Omega(\mathcal{S}, \chi)$ as the convex hull of the vectors $\psi(\Lambda)$ associated to all pseudoline arrangements Λ supported by $\mathcal{S}$.

The crucial property of the beam polytope remains valid in this setting: if Λ and Λ' are two pseudoline arrangements with the same support related by a flip which involve their ith and jth pseudolines, then the difference $\psi(\Lambda) - \psi(\Lambda')$ is parallel to $e_i - e_j$. This implies in particular that $\Omega(\mathcal{S}, \chi)$ is contained in an hyperplane orthogonal to $\mathbb{1}$.

To describe the vertices of $\Omega(\mathcal{S}, \chi)$, we need to consider the oriented dual multigraph $\Lambda^\#$ of a pseudoline arrangement Λ supported by $\mathcal{S}$. This graph has one vertex for each pseudoline of Λ and an edge between two vertices for each contact point between the corresponding pseudolines of Λ. Each edge is oriented from the pseudoline passing above the contact point to the pseudoline passing below it. With this definition, the cone of $\Omega(\mathcal{S}, \chi)$ at the vertex $\psi(\Lambda)$ equals the incidence cone $C(\Lambda^\#)$ of the oriented dual multigraph $\Lambda^\#$. In particular, the vector $\psi(\Lambda)$ is a vertex of $\Omega(\mathcal{S}, \chi)$ if and only if the oriented graph $\Lambda^\#$ is acyclic. Moreover, this vertex is simple when the Hasse diagram of $\Lambda^\#$ is a tree.

Finally, the normal vectors of the facets of $\Omega(\mathcal{S}, \chi)$ are precisely the normal vectors of all the cones $C(\Lambda^\#)$, that is, all the characteristic vectors of the sink sets of the minimal directed cuts of the oriented dual graphs $\Lambda^\#$.

4.3.4.3 Universality of the multiassociahedron

We finish our discussion concerning the multiassociahedron with the proof of a universality result. The goal of this section is to observe that the family of multiassociahedra $(\Delta_{n,k})_{n \geq 2k+1}$ together with all their faces already contains full generality: any simplicial complex of the form $\Delta(\mathcal{S})$ is a coface of a multiassociahedron $\Delta_{n,k}$ for some $n, k \in \mathbb{N}$. More precisely:

Theorem 4.83 (Universality of the multiassociahedron)**.** *If $\mathcal{S}$ is the support of an arrangement of n pseudolines with m intersection points (crossing or contact points), then the simplicial complex $\Delta(\mathcal{S})$ is isomorphic to a coface of $\Delta_{n+2m-2,m-1}$.*

Proof. We choose an arbitrary sweep of the support $\mathcal{S}$ and order the vertices of $\mathcal{S}$ according to it. We represent the result as a *wiring diagram* of $\mathcal{S}$ (see [Fel04, Chapter 6] for the definition and Figure 4.29): a vertex of $\mathcal{S}$ is represented by a (vertical) comparator between two consecutive (horizontal) supporting lines. Index the supporting lines with $[n]$ from top to bottom, and for any $i \in [m]$, let $i^\square$ be such that the ith comparator join the horizontal lines $i^\square$ and $i^\square + 1$. Define the set $W := \big\{[i-1, i+i^\square+m-2] \,\big|\, i \in [m]\big\}$.

We claim that the simplicial complex $\Delta(\mathcal{S})$ is isomorphic to the simplicial complex of all m-crossing-free subsets of $(m-1)$-relevant edges of the $(n+2m-2)$-gon which contain

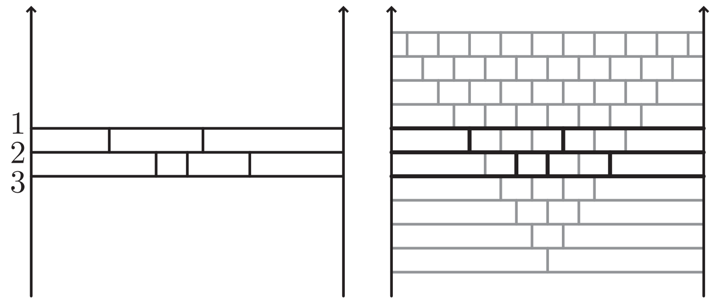

Figure 4.29: Universality of multitriangulations: the wiring diagram of the left pseudoline arrangement is a subdiagram of the wiring diagram in convex position.

the complement of W. Indeed, by duality, the $(m-1)$-triangulations of this complex correspond to the pseudoline arrangements supported by $V^{*(m-1)}_{n+2m-2}$ (*i.e.* the $(m-1)$-kernel of the arrangement of $n+2m-2$ pseudolines in convex position) whose sets of contact points contain $\{u^* \wedge v^* \,|\, [u,v] \notin W\}$. Thus, our claim follows from the observation that, by construction, the remaining contact points $\{u^* \wedge v^* \,|\, [u,v] \in W\}$ are positioned exactly as those of $\mathcal{S}$ (see Figure 4.29). □

Corollary 4.84. *Any pseudoline arrangement is (isomorphic to) the dual pseudoline arrangement of a multitriangulation.* □

Remark 4.85. Theorem 4.83 ensures that an arrangement of n pseudolines with no contact point is a multitriangulation of an N-gon, with $N \leq n^2+2n-2$. The family of pseudoline arrangements suggested by Figure 4.30 is an example for which N is necessarily quadratic in n.

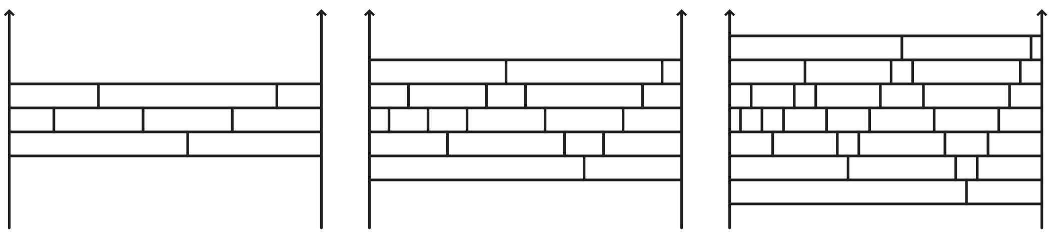

Figure 4.30: A family of pseudoline arrangements whose representing multitriangulation is necessarily quadratic.

By universality, all the results and the conjectures on "multitriangulations of a convex polygon" translate to *equivalent* results and conjectures on "pseudoline arrangements with a given support". Let us give three examples to close our discussion:

Corollary 4.86. *The simplicial complex $\Delta(\mathcal{S})$ associated to the support $\mathcal{S}$ of a pseudoline arrangement is a combinatorial sphere.* □

Conjecture 4.87. *The shortest path in the flip graph $G(\mathcal{S})$ between two pseudoline arrangements Λ and Λ' supported by $\mathcal{S}$ never flips a common contact point of Λ and Λ'.*

Conjecture 4.88. *Given any support $\mathcal{S}$ of a pseudoline arrangement, the simplicial complex $\Delta(\mathcal{S})$ is the boundary complex of a polytope.*

Appendix One

TWO ENUMERATION ALGORITHMS

This appendix is devoted to the presentation of the implementation of two enumeration algorithms that we mentioned in Chapters 3 and 4: the first one enumerates arrangements of pseudolines and double pseudolines, and the second one deals with symmetric matroid polytopes realizing the simplicial complex of $(k+1)$-crossing-free sets of k-relevant edges of the n-gon.

A.1 DOUBLE PSEUDOLINE ARRANGEMENTS

Pseudoline arrangements (or in higher dimension, pseudohyperplane arrangements) have been extensively studied in the last decades as a useful combinatorial abstraction of configurations of points [BVS+99, Bok06, Knu92, Goo97]. Recently, Luc Habert and Michel Pocchiola [HP09], motivated by the question of efficient visibility graph algorithms for convex shapes, introduced double pseudoline arrangements as a combinatorial abstraction of configurations of disjoint convex bodies. The main structural properties of pseudoline arrangements — connectedness of their mutation graph, embedability in projective or affine geometries, axiomatic characterization in terms of chirotopes — extend to double pseudoline arrangements. Definitions and results of [HP09] are recalled in Section A.1.1.

To help our understanding of double pseudoline arrangements, and in order to carry out computer experiments, it is interesting to develop algorithms to enumerate arrangements with few double pseudolines. For pseudoline arrangements, or more generally for pseudohyperplane arrangements, different enumeration algorithms have been proposed and implemented [BdO00, FF02, AAK02]. The number p_n of isomorphism classes of simple pseudoline arrangements in the projective plane is given by the following the table:

n	1	2	3	4	5	6	7	8	9	10	11
p_n	1	1	1	1	1	4	11	135	4 382	312 356	41 848 591

For example, Figure A.1 gives one representative for each of the four isomorphism classes of simple projective arrangements of six pseudolines.

In this section, we present the implementation of an incremental algorithm to enumerate simple projective arrangements of double pseudolines. Before the description of the algorithm in Section A.1.3, we shortly recall some preliminaries on arrangements in Section A.1.1, and prove in Section A.1.2 the connectedness property on which our incremental algorithm relies.

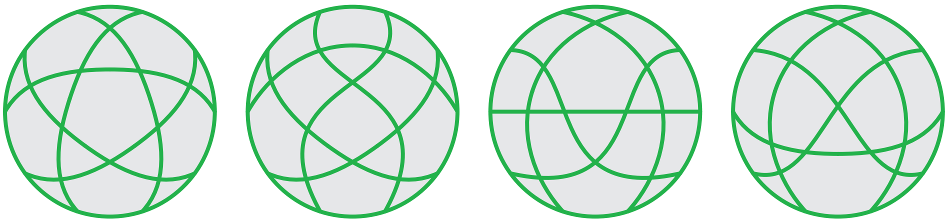

Figure A.1: The four isomorphism classes of simple projective arrangements of six pseudolines.

Finally in Section A.1.5, we briefly discuss three possible variations of this algorithm: to mixed arrangements (with both pseudolines and double pseudolines), to arrangements in the Möbius strip, and to non-simple arrangements (where three pseudolines can meet at the same vertex).

A.1.1 Preliminaries

A.1.1.1 Pseudoline and double pseudoline arrangements

We denote the *projective plane* by $\mathcal{P}$ and represent it as a disk with antipodal boundary points identified.

A simple closed curve in $\mathcal{P}$ is a *pseudoline* if it is non-separating (or equivalently, non-contractible), and a *double pseudoline* otherwise (see Figure A.2). The complement of a pseudoline is a topological disk. The complement of a double pseudoline ℓ has two connected components: a Möbius strip M_ℓ and a topological disk D_ℓ.

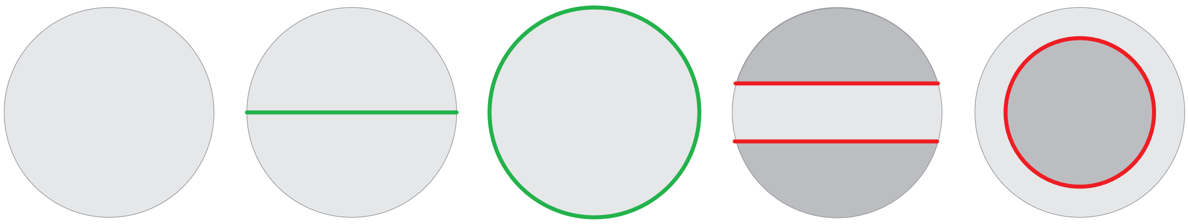

Figure A.2: A projective plane, two pseudolines, and two double pseudolines (their enclosed topological disk is represented darker).

A *pseudoline arrangement* is a finite set of pseudolines such that any two of them intersect exactly once (see Figure A.1). A *double pseudoline arrangement* is a finite set of double pseudolines such that any two of them have exactly four intersection points, cross transversally at these points, and induce a cell decomposition of $\mathcal{P}$ (see Figure A.3). To simplify the presentation, we first focus only on *simple* arrangements, that is, where no three curves meet at the same point. Non-simple arrangements will be discussed in Section A.1.5.

Two arrangements L and L' are *isomorphic* if there is an homeomorphism of the projective plane that sends L on L' (or equivalently, if there is an isotopy joining L to L'). For example, the arrangements (c) and (d) in Figure A.3 are isomorphic while (e) is not isomorphic to

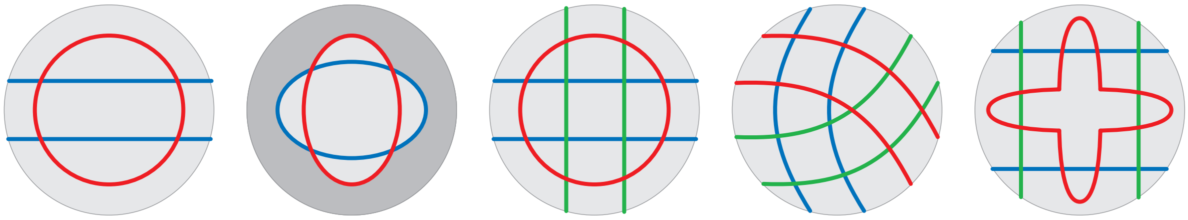

Figure A.3: (a) An arrangement of 2 double pseudolines; (b) Two double pseudolines which do not form an arrangement; (c-d-e) Arrangements of 3 double pseudolines.

them. As mentioned previously, different algorithms have been implemented to enumerate isomorphism classes of pseudoline arrangements, and their number is know up to 11 pseudolines. In this section, we develop an algorithm to enumerate isomorphism classes of double pseudolines arrangements.

A.1.1.2 Mutations

A *mutation* is a local transformation of an arrangement L that only inverts a triangular face of L (see Figure A.4). More precisely, it is a homotopy of arrangements in which only one curve ℓ moves, sweeping a single vertex of the remaining arrangement $L \smallsetminus \{\ell\}$. Iterating this elementary transformation is in fact sufficient to obtain all possible arrangements:

Theorem A.1 ([HP09]). *The graph of mutations on arrangements is connected: any two arrangements with the same numbers of (double) pseudolines are homotopic via a finite sequence of mutations followed by an isotopy.*

This result is known as Ringel's Homotopy Theorem for arrangements of pseudolines. For double pseudolines, it is proved in [HP09] by reduction to the case of pseudoline arrangements. The argument consists in mutating each double pseudoline of the arrangement until it becomes *thin* (that is, until there remains no point inside its enclosed Möbius strip), and to observe that arrangements of thin double pseudolines behave exactly as pseudoline arrangements. The fact that an arrangement can be mutated until all its double pseudolines become thin is ensured by the following crucial lemma (see Figure A.4):

Lemma A.2 (Pumping Lemma [HP09]). *In an arrangement L, if a double pseudoline ℓ encloses at least one vertex of L in its enclosed Möbius strip M_ℓ, then there is a triangular face of L included in M_ℓ and supported by ℓ.*

From Theorem A.1, we may derive a simple enumeration algorithm which consists in traversing the graph of mutations starting from any given arrangement. This naive algorithm is sufficient for the enumeration of small cases but already fails (because of RAM memory limitations) for arrangements of five double pseudolines. In order to go a little bit further (and particularly, to enumerate arrangements of five double pseudolines), we use an incremental version of this algorithm — still based on mutations — presented in Sections A.1.2 and A.1.3.

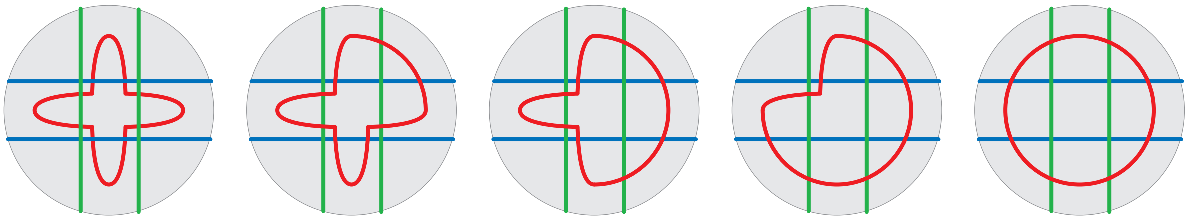

Figure A.4: A sequence of mutations from the double pseudoline arrangement of Figure A.3(e) to the double pseudoline arrangement of Figure A.3(c). All the vertices in the enclosed Möbius strip of the "flower" double pseudoline of the left arrangement are pumped out.

A.1.1.3 Geometric Representation Theorem

A *projective geometry* is a couple $(\mathbb{P}, \mathbb{L})$, where $\mathbb{P}$ is a projective plane and $\mathbb{L}$ is a set of pseudolines of $\mathbb{P}$, such that any two pseudolines of $\mathbb{L}$ have exactly one intersection point (which depends continuously on the two lines) and through any pair of points of $\mathbb{P}$ passes a unique pseudoline of $\mathbb{L}$ (which depends continuously on the two points). In a projective geometry, the *dual* of a point p (of $\mathbb{P}$) is its set p^* of incident pseudolines (of $\mathbb{L}$), and the *dual* of a point set P is the set $P^* := \{p^* \,|\, p \in P\}$ of duals of points of P. Similarly, the *dual* of a convex body C (of $\mathbb{P}$) is its set C^* of tangent pseudolines (of $\mathbb{L}$), and the *dual* of a set S of convex bodies is the set $S^* := \{C^* \,|\, C \in S\}$ of duals of bodies of S. It is known that:

(i) The line space $\mathbb{L}$ is a projective plane.

(ii) The dual of a finite point set is a pseudoline arrangement (which is simple if the point set is in general position).

(iii) The dual of a finite set of pairwise disjoint convex bodies is a double pseudoline arrangement (which is simple if no three convex share a common tangent).

The *Geometric Representation Theorem* asserts that the converse is also true:

Theorem A.3 (Geometric Representation Theorem)**.** *Any arrangement of pseudolines (resp. of double pseudolines) is isomorphic to the dual arrangement of a finite point set (resp. of a finite set of pairwise disjoint convex bodies) of a projective geometry.*

For pseudoline arrangements, this theorem is a consequence of duality in projective geometries combined with the embedabbility of any pseudoline arrangement in the line space of a projective geometry [GPWZ94]. It was extended in [HP09] for double pseudoline arrangements. From this result, it is easy to derive the following extension of the Pumping Lemma A.2, which will be useful in our algorithm:

Lemma A.4 (Improved Pumping Lemma)**.** *Let L be an arrangement, ℓ be a double pseudoline of L and x be a point on ℓ. If the Möbius strip M_ℓ enclosed by ℓ contains at least one vertex of L, then there is a triangular face of L included in M_ℓ, supported by ℓ, and avoiding the point x.*

A.1.1.4 Chirotopes

An *indexed oriented arrangement* is an arrangement whose curves are oriented and one-to-one indexed with an indexing set. The *chirotope* of an indexed oriented arrangement is the application that assigns to each triple τ of indices the isomorphism class of the subarrangement indexed by τ. Since there are only two indexed and oriented simple arrangements of three pseudolines, it is convenient to call them $+$ and $-$ and to define a chirotope as an application from triples of indices to $\{+, -\}$ (this relates to the other definition of chirotopes given in the context of oriented matroids in Chapter 4 and used in Appendix A.2). For double pseudoline arrangements, there are much more indexed and oriented simple arrangements of three double pseudolines. However, appart from the number, chirotopes of pseudoline arrangements and double pseudoline arrangements behave exactly the same. On the one hand, the chirotope of an arrangement characterizes its isomorphism class:

Theorem A.5 ([HP09]). *The isomorphism class of an indexed oriented arrangement only depends on its chirotope.*

On the other hand, chirotopes are characterized by their restrictions to subconfigurations of size at most five:

Theorem A.6 ([HP09]). *Given an application χ that assigns to each triple τ of indices an isomorphism class of an oriented arrangement indexed by τ, the following properties are equivalent:*
(i) χ is the chirotope of an indexed oriented arrangement; and
(ii) the restriction of χ to the set of triples of any subset of at most five indices is the chirotope of an indexed oriented arrangement.

This result provides a strong motivation for enumerating arrangements of at most five simple and double pseudolines: the complete list of these arrangements gives an axiomatization of the chirotopes of all arrangements.

A.1.2 Connectedness of the one-extension space

Our enumeration algorithm is incremental, and relies on the following objects:

Definition A.7. *A one-extension of an arrangement L of n double pseudolines is an arrangement of $n+1$ double pseudolines of which L is a subarrangement. The added double pseudoline is called the one-extension curve.*

A mutation of a one-extension of L is certainly still a one-extension of L when the moving curve is the one-extension curve. We call such a mutation a *one-extension mutation*. It is crucial for our algorithm that these restricted mutations still generate the complete one-extension space:

Theorem A.8. *The graph of one-extension mutations is connected: any two one-extensions of an arrangement are homotopic via a finite sequence of mutations (followed by an isotopy) during which the only moving curve is the one-extension curve.*

Proof. Let L be an arrangement, λ be a distinguished double pseudoline of L, and $M := L \cup \{\mu\}$ and $N := L \cup \{\nu\}$ be two one-extensions of L. Using continuous motions — thanks to the duality principle — we can assume the following facts on μ:

(i) μ is a *thin* double pseudoline in M (*i.e.* its enclosed Möbius strip contains no vertex of M);

(ii) λ and μ are *touching*: a cell σ of size two of the subarrangement $\{\lambda, \mu\}$ is also a cell of the whole arrangement M;

(iii) the Möbius strip M_μ enclosed by μ is a tubular neighborhood of a pseudoline μ_* which intersects any double pseudoline of L in exactly two points, the intersection being transversal.

Similarly, we can assume that ν is a thin double pseudoline, which touches λ, and whose enclosed Möbius strip defines a tubular neighborhood of a pseudoline ν_* which intersects (transversally) any double pseudoline of L in two points. Furthermore, we can restrict the analysis to the following case:

(iv) μ and ν coincide in the topological disk D_λ;

(v) μ_* and ν_* coincide in D_λ, have finitely many intersections in M_λ, and intersect transversally at these points;

(vi) $M_\mu \cup M_\nu$ forms a tubular neighborhood of $\mu_* \cup \nu_*$.

We consider the arrangements $M_* := L \cup \{\mu_*\}$ and $N_* := L \cup \{\nu_*\}$. As in the proof of Theorem A.1, the proof of this theorem boils down to show that the mixed arrangements M_* and N_* are homotopic via a finite sequence of mutations during which the only moving curves are the pseudolines μ_* and ν_*. We prove this by induction on the number of vertices in the Möbius strip M_λ enclosed by λ:

- if λ is a thin double pseudoline, then we are done up to an isotopy;
- otherwise, the Improved Pumping Lemma A.4 ensures that there exists a triangular face Δ of the arrangement supported by λ and not adjacent to the "touching cell" σ. We can assume that μ_* and ν_* do not intersect Δ, modulo a finite sequence of mutations in M_* and N_*, during which the only moving curves are the pseudolines μ_* and ν_* (these mutations are possible since for each connected component X of the trace of a double pseudoline of L on M_λ, both μ_* and ν_* intersect X at most once). We can then perform the mutation of Δ: let $\tilde{M}_*$ and $\tilde{N}_*$ denote the mutated arrangements. By induction hypothesis, there is a finite sequence of mutations which transforms $\tilde{M}_*$ to $\tilde{N}_*$ only moving the pseudolines μ_* and ν_*. But this sequence also transforms M_* to N_*, which finishes the proof. $\square$

A.1.3 The incremental algorithm

A.1.3.1 Description

Let $\mathcal{A}_n$ be the set of isomorphism classes of arrangements of n double pseudolines and $q_n := |\mathcal{A}_n|$. Our algorithm enumerates $\mathcal{A}_n$ from $\mathcal{A}_{n-1}$ by mutating an added distinguished double pseudoline.

A *pointed* arrangement is an arrangement with a distinguished double pseudoline. For any integer n, let $\mathcal{A}_n^\bullet$ denote the set of isomorphism classes of pointed arrangements of n double pseudolines (two pointed arrangements are isomorphic if there is an isomorphism of the projective plane which sends one arrangement to the other, respecting their distinguished double pseudoline). We always use the notation $A^\bullet$ for a pointed arrangement and A for its non-pointed version (and similarly for sets of pointed arrangements). We also use the notation $\mathrm{sub}(A)$ for the set of subarrangements of an arrangement A.

For each $i \in \{1, \dots, q_{n-1}\}$, the algorithm enumerates the set $S_i^\bullet$ of arrangements of $\mathcal{A}_n^\bullet$ containing the ith arrangement a_i of $\mathcal{A}_{n-1}$ as a subarrangement, by mutations of a distinguished added double pseudoline. From the set S_i, it selects the subset R_i of arrangements with no subarrangements in $\{a_1, \dots, a_{i-1}\}$. In other words, R_i is the set of arrangements of $\mathcal{A}_n$ whose first subarrangement, among the set $\mathcal{A}_{n-1} := \{a_1, \dots, a_{q_{n-1}}\}$, is the ith arrangement a_i. Thus, $\mathcal{A}_n$ is the disjoint union of the sets R_i.

INCREMENTAL ENUMERATION

Require: $\mathcal{A}_{n-1} = \{a_1, \dots, a_{q_{n-1}}\}$.
Ensure: $\mathcal{A}_n$.

```
for i from 1 to q_{n-1} do
  A• ← add a pointed double pseudoline to a_i.
  Q• ← [A•]. S• ← {A•}. R ← {}.
  if sub(A) ∩ {a_1, ..., a_{i-1}} = ∅ then
    write A. R ← {A}.
  end if
  while Q• ≠ ∅ do
    A• ← pop Q•.
    T ← list the triangles of A• adjacent to its pointed double pseudoline.
    for t ∈ T do
      B• ← mutate the triangle t in A•.
      if B• ∉ S• then
        if sub(B) ∩ {a_1, ..., a_{i-1}} = ∅ and B ∉ R then
          write B. R ← R ∪ {B}.
        end if
        push(B•, Q•). S• ← S• ∪ {B•}.
      end if
    end for
  end while
end for
```

An alternative approach[1] for counting arrangements is to enumerate the subsets $S_i^\bullet$ and to compute, for each arrangement $A^\bullet$ of $S_i^\bullet$, the number $\sigma(A^\bullet)$ of double pseudolines α of A such that A pointed at α is isomorphic to $A^\bullet$. Then:

$$q_n = \frac{1}{n} \sum_{i=1}^{q_{n-1}} \sum_{A^\bullet \in S_i^\bullet} \sigma(A^\bullet).$$

The disadvantage of this version is that it only counts q_n and cannot provide a data base for $\mathcal{A}_n$.

[1] We thank Luc Habert for this suggestion.

A.1.3.2 Encoding an arrangement

In order to manipulate arrangements, one can represent them in several different ways. We use two different encodings:

1. *Flag representation*: An arrangement defines a map on a surface (the projective plane), and thus can be manipulated with the corresponding tools. A *flag* of an arrangement L is any triple (v, e, f) consisting of one vertex v, one edge e and one face f (of the cell complex defined by L), such that $v \in e \subset f$. The geometric information of the arrangement is contained in the three involutions σ_0, σ_1 and σ_2 which respectively change the vertex, the edge and the face of a flag (see Figure A.5). This representation is convenient to perform all the necessary elementary operations we need to apply on arrangements (such as mutations, extensions, etc.).

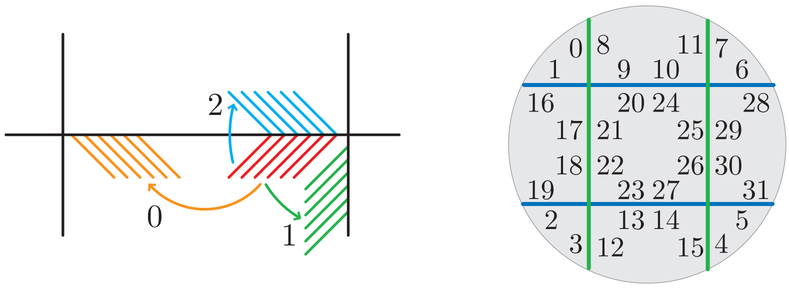

Figure A.5: The three involutions σ_0, σ_1 and σ_2 (left). An example of flag representation (right).

2. *Encoding*: In the enumeration process, once we have finished to manipulate an arrangement L, we still have to remember it and to test whether the new arrangements we find afterwards are or not isomorphic to L. For this, we compute another representation of L, which is shorter than the flag representation, and which allows a quick isomorphism test. We first associate to each flag $\phi = (v, e, f)$ of the arrangement L a word w_ϕ constructed as follows. Let ℓ_1 be the simple or double pseudoline containing e, and, for all $2 \leq p \leq n$, let ℓ_p be the pth double pseudoline crossed by ℓ_1 on a walk starting at ϕ and oriented by $\sigma_0\sigma_1\sigma_2\sigma_1$. This walk also defines a starting flag ϕ_i for each ℓ_i. We then walk successively on $\ell_1, \dots, \ell_n$, starting from ϕ_i and in the direction given by $\sigma_0\sigma_1\sigma_2\sigma_1$, and index the vertices by $1, 2, \dots, V$ in the order of appearance. For all i, let w_i denote the word formed by reading the indices of the vertices of ℓ_i starting from ϕ_i. The word w_ϕ is the concatenation of $w_1, w_2, \dots, w_n$. Finally, we associate to the arrangement L the lexicographically smallest word among all the w_ϕ where ϕ ranges over all the flags of L. It is easy to check that two arrangements are isomorphic if and only if they get the same encoding.

A.1.3.3 Adding a double pseudoline

One of the important steps of the incremental method is to add a double pseudoline to an initial arrangement. It is easy to achieve when the initial arrangement contains at least one pseudoline, but it is more involved when we have only double pseudolines. Our method uses three steps (see Figure A.6):

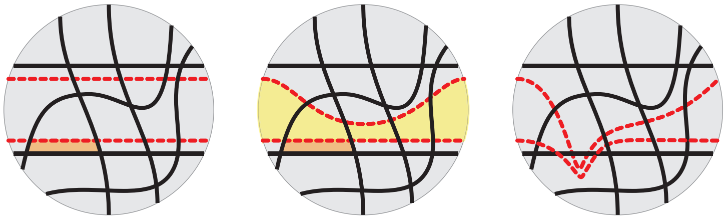

Figure A.6: Three steps to insert a double pseudoline in an arrangement: duplicate a double pseudoline (left), flatten it (middle) and add four crossings (right).

(a) *Duplicate a double pseudoline*: We choose one arbitrary double pseudoline ℓ and duplicate it, drawing a new double pseudoline ℓ' completely included in the Möbius strip M_ℓ enclosed by ℓ. We choose an arbitrary rectangle R delimited by ℓ and ℓ'.

(b) *Flatten*: We pump the double pseudoline ℓ' (using Lemma A.4) such that no vertex of the arrangement lies in the Möbius strip $M_{\ell'}$. During the process, we do not touch the rectangle R.

(c) *Add four crossings*: We replace the rectangle R by four crossings between ℓ and ℓ'.

If we think of our double pseudoline arrangement as the dual of a configuration of convex bodies, this method corresponds to: (a) choosing one convex C and drawing a new convex C' inside C; (b) flattening the convex C' until it becomes almost a single point, maintaining it almost in contact with the boundary of C; and (c) moving C' outside C.

A.1.4 Results

We have implemented this algorithm in C++ programming language. The documentation (as well as the source code) of this implementation is available upon request by email.

This implementation provided us with the following values of the number q_n of isomorphism classes of simple arrangements of n double pseudolines:

n	1	2	3	4	5
q_n	1	1	13	6570	181 403 533

For example, Figure A.7 gives one representative for each of the thirteen isomorphism classes of simple projective arrangements of three double pseudolines.

Let us briefly comment on running time and working space. Observe first that our algorithm can be parallelized very easily (separating each enumeration of S_i and R_i, for $i \in \{1, \dots, q_{n-1}\}$). In order to obtain the number q_5 of simple arrangements of five double pseudolines, we used four 2GHz processors for almost three weeks. The working space is bounded by $\max |S_i^\bullet| = 279\,882$ (times the space of the encoding of a single configuration, *i.e.* about 80 characters).

Figure A.8 shows the evolution of the ratio between the sizes of the sets R_i and $S_i^\bullet$, during the enumeration of arrangements of five double pseudolines. It is also interesting to observed that $\sum |S_i^\bullet| / \sum |R_i| \simeq 5$, which confirms that hardly any configurations of five convex bodies have symmetries.

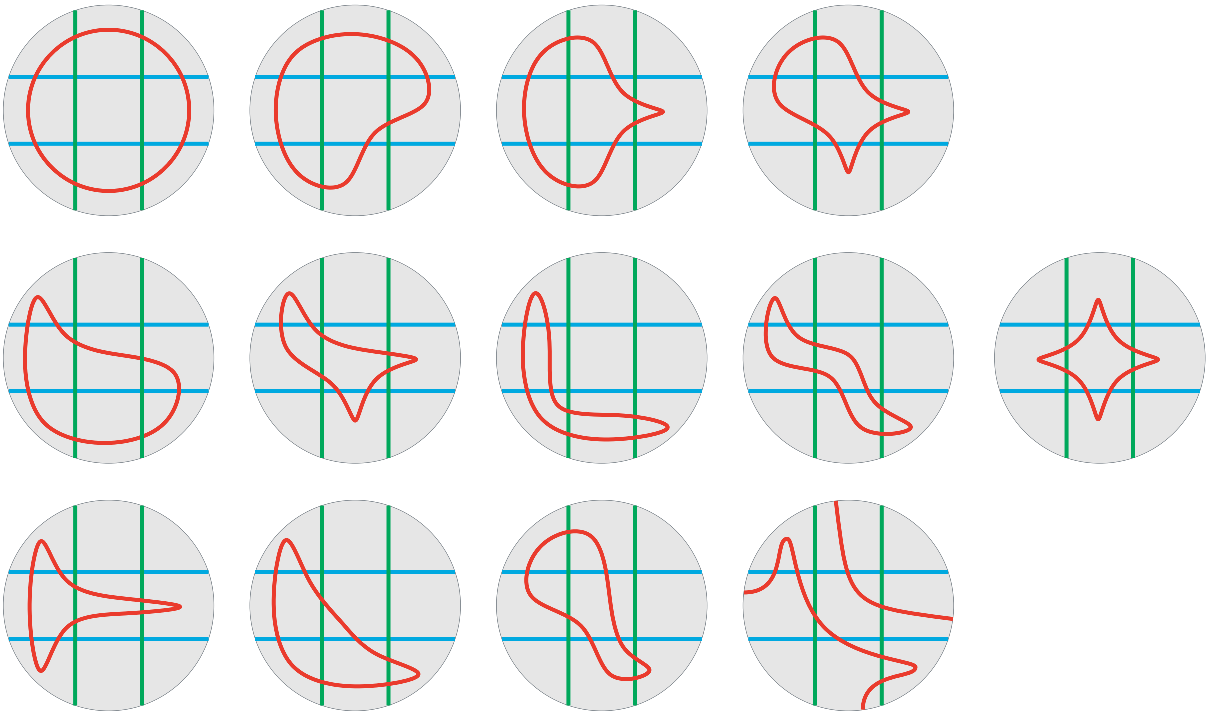

Figure A.7: The thirteen isomorphism classes of simple projective arrangements of three double pseudolines.

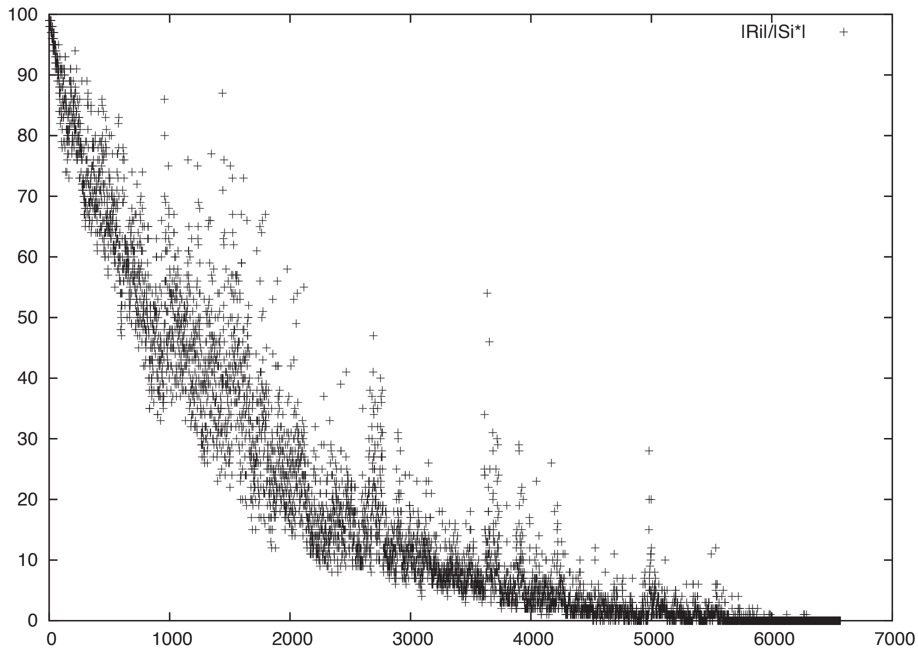

Figure A.8: Percentage $|R_i|/|S_i^\bullet|$ of new configurations among all generated configurations during the recursive enumeration of arrangements of five double pseudolines.

A.1.5 Three variations

A.1.5.1 Mixed arrangements

An *arrangement of simple and double pseudolines* (or *mixed arrangement*) is a finite set of pseudolines and double pseudolines such that:

(i) any two pseudolines have a unique intersection point;

(ii) a pseudoline and a double pseudoline have exactly two intersection points and cross transversally at these points; and

(iii) any two double pseudolines have exactly four intersection points, cross transversally at these points, and induce a cell decomposition of $\mathcal{P}$.

Figure A.9 shows these three conditions, *i.e.* the three admissible mixed arrangements of size 2.

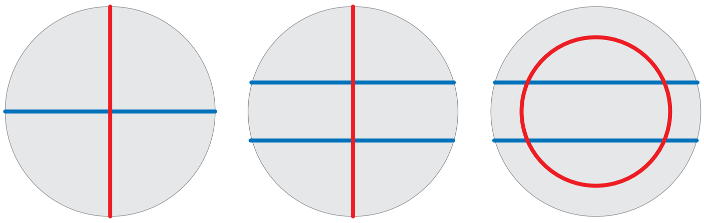

Figure A.9: The three mixed arrangements of size 2.

All the properties of arrangements — connectedness of their mutation graph, embedability in projective geometries, axiomatic characterization in terms of chirotopes — remain valid in this context.

As already used in the proofs, there is a correspondence between the isomorphism classes of arrangements with n pseudolines and m double pseudolines, and isomorphism classes of arrangements of $n+m$ double pseudolines, n of which are thin (*i.e.* do not contain any vertex of the arrangement in there enclosed Möbius strip).

Mixed arrangements can be enumerated by the same algorithm as before. The numbers of mixed (simple projective) arrangements with n pseudolines and m double pseudolines are given by the following table:

$n \diagdown m$	0	1	2	3	4	5
0			1	13	6 570	181 403 533
1		1	4	626	4 822 394	
2	1	2	48	86 715		
3	1	5	1 329			
4	1	25	80 253			
5	1	302				
6	4	9 194				
7	11	556 298				
8	135					
9	4 382					
10	312 356					

A.1.5.2 Möbius arrangements

If we consider configurations of points and convex bodies in a plane (rather than projective) geometry, then we need to enumerate mixed arrangements in the Möbius strip (rather than the projective plane). Since a Möbius strip is a projective plane minus one point (at infinity), we enumerate mixed arrangements in the Möbius strip with essentially the same method. The only difference is that we have to maintain one additional information: we mark the external face, which contains the point at infinity. This information is used to deal with the two following constraints: first, the external face can never be mutated; second, two Möbius arrangements are isomorphic if there is an isomorphism sending one to the other, and conserving the external face. The numbers of mixed simple Möbius arrangements with n pseudolines and m double pseudolines are given by the following table:

$n \setminus m$	0	1	2	3	4	5
0			1	16	11 502	238 834 187
1		1	7	1 499	9 186 477	
2	1	3	140	245 222		
3	1	13	5 589			
4	2	122	416 569			
5	3	2 445				
6	16	102 413				
7	135	7 862 130				
8	3 315					
9	158 830					

A.1.5.3 Non-simple arrangements

Finally, our algorithm and our implementation can easily be extended to non-simple arrangements (*i.e.* arrangements in which more than two curves can cross at a given vertex. The main difference lies in the possibility of the two following inverse *half mutations* (see Figure A.10):

1. *Leaving half mutation*: A curve ℓ passing through a non-simple vertex v is pushed out of v and creates a fan with apex v and based on ℓ.
2. *Reaching half mutation*: A fan with apex v based on a curve ℓ is destroyed, the curve ℓ being pushed to be incident to the vertex v.

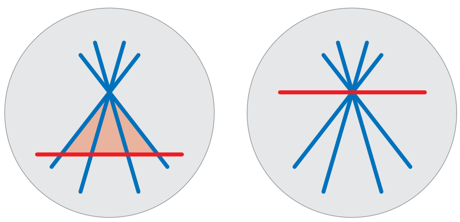

Figure A.10: Half mutations in a non-simple arrangement.

The numbers of mixed (non-necessary simple) arrangements with n pseudolines and m double pseudolines are given by the following table:

$n \backslash m$	0	1	2	3	4
0			1	46	153 528
1		1	9	6 998	
2	1	3	265		
3	1	16	18 532		
4	2	159			
5	4	4 671			
6	17	342 294			
7	143				
8	4 890				
9	461 053				

A.1.6 Further developments

To close this section, we mention three possible further developments related to this algorithm:

1. *Drawing an arrangement*: We have seen a method to add a pseudoline in a mixed arrangement. Combined with a planar-graph-drawing algorithm, this provides an algorithm to draw an arrangement in the unit disk. For example, the number of isomorphism classes of mixed arrangements with 1 pseudoline and n double pseudolines can be interpreted as the number of drawings of the arrangements of $\mathcal{A}_n$. As an illustration, we have represented in Figure A.11 the four isomorphism classes of arrangements with 1 pseudoline and 3 double pseudolines, together with the corresponding planar drawings.

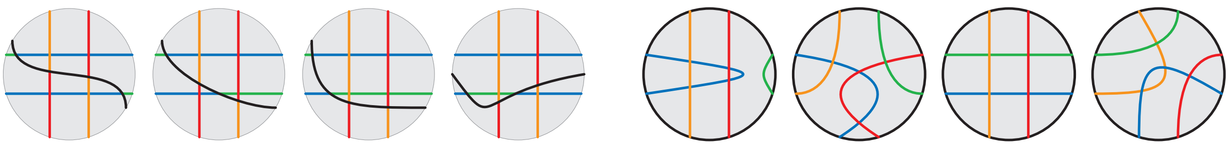

Figure A.11: Drawings of arrangement: the four isomorphism classes of arrangements with 1 pseudoline and 3 double pseudolines (left) and the corresponding planar drawings obtained by cutting the projective plane along the pseudoline of each arrangement (right).

2. *Axiomatization*: Pseudoline arrangements admit simple axiomatizations [BVS+99, Knu92], with few axioms dealing with configurations of at most five pseudolines. Theorem A.6 affirms that the complete list of arrangements of at most five simple and double pseudolines is an axiomatization of mixed arrangements. Is there any simpler axiomatization? Is it possible to algorithmically reduce this axiomatization?
3. *Realizability*: It is well-known that certain pseudoline arrangements are not realizable in the Euclidean plane. Inflating pseudolines into thin double pseudolines in such an arrangement gives rise to non-realizable double pseudoline arrangements. Are there smaller examples? Are all arrangements of at most five curves realizable?

A.2 SYMMETRIC MATROID POLYTOPES

Our second algorithm [BP09] enumerates the symmetric matroid realizations of the simplicial complex $\Delta_{n,k}$ of $(k+1)$-crossing-free sets of k-relevant edges of the n-gon. The matroid realizations it provides when $n = 8$ and $k = 2$ (Proposition 4.49) are the starting point of our study of symmetric geometric realizations of $\Delta_{8,2}$ (Section 4.3.2.3). Since it was written with the functional language HASKELL, the code is sufficiently concise and simple to be presented in this document. We start with a very brief presentation of the language features of HASKELL.

A.2.1 About Haskell

The programming language HASKELL, officially born in 1987, is named in honor of the mathematician and logician Haskell B. Curry[2]. Its particularities are the following:

$\boxed{\textit{functions}}$ HASKELL is a *purely functional programming language*, which means that its basic method of computation is the evaluation of functions on arguments. Contrarily to imperative languages, a functional language avoids state and mutable data. For example, to compute the factorial of an integer n, when an imperative language multiplies iteratively the n first integers, HASKELL defines *recursively*:

factorial 0 = 1 and factorial (n+1) = (n+1)*factorial n.

$\boxed{\textit{types}}$ All functions and arguments in HASKELL have a type (Int, Bool, Int -> Bool, etc.), which can be explicitly mentioned by the user after the symbol ::. If no type is mentioned, HASKELL will anyway deduce automatically the type, checking that types are coherent. It also provides *polymorphic type* (a type that can be parametrized by another type, *e.g.* the type [a] of a list containing elements of type a), and *type classes* (types that share common operations, *e.g.* the Eq class of all types supporting the operations == and /=).

$\boxed{\textit{list comprehension}}$ One of the main tools that make HASKELL code readable for a non-programmer reader is the possibility to create lists based on existing lists, exactly in the same way we construct sets from other sets in mathematics. For example, given a function f :: a -> b, a condition cond :: a -> Bool and a list[3] L :: [a], we can construct a new list

[f x | x <- L, cond x] :: [b]

which contains the images under f of all elements of L which satisfy the condition cond. The list L is the generator, and the condition cond is a guard. We can furthermore have multiple generators and/or guards. An interesting example is the map function (whose type is (a -> b) -> [a] -> [b]) which applies a function f to all elements of a list L and can be defined as map f L = [f x | x <- L].

$\boxed{\textit{lazy evaluation}}$ HASKELL is a lazy programming language in the sense that it delays the evaluation of an expression until the result is required. It avoids unnecessary computation,

[2] Haskell B. Curry worked on the theory of formal languages and processes. His name is in particular associated with the interpretation of a function with multiple arguments as a chain of functions with a single argument. For example, for a two-arguments function, $f : (a, b) \mapsto c \;\simeq\; \mathrm{curry}(f) : a \mapsto (b \mapsto c)$.

[3] In HASKELL, capital letters are reserved for constructors. For the sake of readability, we have decided however to use capital letters in our presentation, in particular for lists.

but also enables the user to perform constructions that would not be possible otherwise, such as infinite structures. For example, finding the first integer which satisfies a condition cond :: Int -> Bool can be achieved by evaluating head [n | n <- [1..], cond n].

guarded equations & pattern matching The result of a function often depends on a condition. In HASKELL, instead of writing a conditional control structure with if – then – else like in many other programming languages, we can simply use guarded equations indicated by a | symbol. For example, the code:

```
f args | cond1  = out1
       | cond2  = out2
       | otherwise  = out3
```

means that the function f, applied on the arguments args, returns out1 if cond1 is fulfilled, otherwise out2 if cond2 is fulfilled, and finally, out3 otherwise.
Finally, as many functional languages, HASKELL also provides the possibility of matching the arguments of a function with a given pattern. This was the case for example when we wrote HASKELL's definition of the factorial: we match its argument either with 0 or with n+1. It is also useful when we program with lists.

Lists in HASKELL are managed by the ListPrelude and List modules. The functions we use on a list L are the usual functions:

head L	first element of L	take p L	takes p elements from the front of L
tail L	all but the first element of L	drop p L	drops p elements from the front of L
length L	length of the list	L!!p	pth element of L ($0 \leq p <$ length L)
L++M	concatenation of L and M	L\\M	L setminus M
x:L	adds x to the front of L	delete x L	deletes x from L
elem x L	is x an element of L?	elemIndices x L	lists positions where x occurs in L
sort L	sorts L in increasing order	nub L	eliminates repetitions in L
and L	conjonction of booleans	or L	disjonction of booleans

To illustrate certain of these functions, and to give a first example of HASKELL code, we describe in detail the function tuples which, for a given integer p and a list L, lists all ordered p-tuples of L (*i.e.* all tuples which appear sorted as in the list):

```
-- tuples p L = all ordered p-tuples of the list L
tuples :: Int -> [a] -> [[a]]
tuples 0 _ = [[]]
tuples _ [] = []
tuples p (h:t) = [ h:tu | tu <- tuples (p-1) t ] ++ tuples p t
```

Let us briefly comment this code since all our functions follow the same pattern. In the first line of all our functions (starting with --), we give a brief description of the function. The second line declares the type of the function. The other lines define the function.

Here, the function tuples is recursive and should be read as follows: an ordered p-tuple of L either starts with the first element of L, followed by an ordered (p-1)-tuple of the remaining list, or is an ordered p-tuple of the tail of L. Observe the use of pattern matching for initializations.

This function, applied on the arguments 3 [1,4,2,5,3] returns the following list:

```
> tuples 3 [1,4,2,5,3]
[[1,4,2], [1,4,5], [1,4,3], [1,2,5], [1,2,3], [1,5,3], [4,2,5], [4,2,3], [4,5,3], [2,5,3]]
```

We believe that this short introduction is sufficient to understand our enumeration algorithm, and we refer to [Hut07, Bok06] for further reading on HASKELL programming language.

A.2.2 Enumeration of all k-triangulations of the n-gon

We first need to generate all facets of $\Delta_{n,k}$, that is, all k-triangulations of the n-gon (remember that we only consider the k-relevant edges of E_n since any k-triangulation contains all non-k-relevant edges). According to Corollary 2.21, one possibility for this is to enumerate all $k(n-2k-1)$-tuples of k-relevant edges of E_n and to keep only $(k+1)$-crossing-free such tuples. The corresponding HASKELL code is very concise using list comprehension:

```
-- Fix the parameters n and k
n, k :: Int
n = 8; k = 2

-- kRelevantEdges = all k-relevant edges of the n-gon
kRelevantEdges :: [[Int]]
kRelevantEdges = nub [ sort [i, mod (i+j) n] | j <- [k+1..n-k-1], i <- [0..n-1] ]

-- crossing e f = do e and f cross each other?
crossing :: [Int] -> [Int] -> Bool
crossing [a,b] [c,d] = and [a<c, c<b, b<d] || and [c<a, a<d, d<b]

-- kCrossingFree E = is the set of edges E (k+1)-crossing-free?
kCrossingFree :: [[Int]] -> Bool
kCrossingFree E = and [ or [ not (crossing e f) | [e,f] <- tuples 2 F ] | F <- tuples (k+1) E ]

-- kTriangulations = all k-triangulations of the n-gon
kTriangulations :: [[[Int]]]
kTriangulations = [ T | T <- tuples (k*(n-2*k-1)) kRelevantEdges, kCrossingFree T ]
```

Even if this method is really naïve, it is sufficient for our purpose (after all, we only have to enumerate the 2-triangulations of the octagon). However, for completeness, and to demonstrate the use of flips as local transformations, we present another way to enumerate k-triangulations, based on the graph of flips.

The first step is to compute the two k-stars adjacent to a given k-relevant edge of a k-triangulation. According to Lemma 2.11, a k-star can be traced following its angles in the k-triangulation:

```
-- angle T [b,c] = the vertex a such that (a,b,c)={[a,b],[b,c]} is an angle of T
angle :: [[Int]] -> [Int] -> Int
angle T [b,c] = head [ a | a <- map (\i -> mod (c+i) n) [1..], mod (a+k) n == b || elem (sort [a,b]) T ]

-- completeStar T e = the k-star of T adjacent to the (k-relevant) edge e
completeStar :: [[Int]] -> [Int] -> [Int]
completeStar T L
   | length L == 2*k+1  = L
   | otherwise  = completeStar T ((angle T (take 2 L)):L)
```

Observe the use of lazy evaluation in the definition of our function angle: HASKELL will only compute the first vertex a after c such that the edge [a,b] is an edge of the k-triangulation (which might be a k-boundary edge).

The next step is the definition of the flip operation. Remember that this operation is local: given a k-relevant edge e of a k-triangulation T, the flip of e in T consists in exchanging in T the edge e with the common bisector f of the two k-stars R and S of T containing e. The previous function completeStar computes the vertices of the k-stars $R := \{r_0, \ldots, r_{2k}\}$ and $S := \{s_0, \ldots, r_{2k}\}$ in star order (and with $e = [r_{2k-1}, r_{2k}] = [s_{2k}, s_{2k-1}]$), and we just have to find their common bisector f. One way to compute it would be to try, for any $p, q \in \mathbb{Z}_{2k+1}$, whether $[r_p, s_q]$ bisects both R and S, *i.e.* whether $r_{p+1} \prec s_q \prec r_{p-1}$ and $s_{q+1} \prec r_p \prec s_{q-1}$. But according to Lemma 2.26, we even have to consider only the edges $[r_p, s_p]$ (*i.e.* the case $p = q$).

```
-- edgeFlip T e = flips the (k-relevant) edge e in the k-triangulation T
edgeFlip :: [[Int]] -> [Int] -> [[Int]]
edgeFlip T e = sort (f:(delete e T))
 where R = completeStar T e
         S = completeStar T (reverse e)
         cyclic :: [Int] -> Bool
         cyclic [a,b,c] = elem (sort (nub [a,b,c])) [[a,b,c], [b,c,a], [c,a,b]]
         f = head [ sort [R!!p, S!!p] | p <- [0..],
                                         cyclic [R!!(mod (p+1) (2*k+1)), S!!p, R!!(mod (p-1) (2*k+1))]
                                      && cyclic [S!!(mod (p+1) (2*k+1)), R!!p, S!!(mod (p-1) (2*k+1))] ]
```

Inside the code of a function, HASKELL allows to locally define expressions and functions, either with the syntax let – in (expression style), or with the word where (declaration style). For example, if g :: a -> Int, the three following declarations of f :: a -> Int are equivalent:

f x = (g x)^2 + g x   f x = let y = g x in y^2 + y   f x = y^2 + y where y = g x

The advantage of the two last formulations is that g x is written and computed only once.

Concerning the code of the function edgeFlip, let us also mention that the function reverse changes the orientation of the edge e: we compute one star on each side of e.

We are now ready to traverse the graph of flips to enumerate all k-triangulations of the n-gon. According to Lemma 2.30, we can start from the minimal k-triangulation $T_{n,k}^{\min}$ (called initial in the following code) and flip only k-relevant edges incident to one of the first k vertices of the n-gon:

```
-- kTriangulations = all k-triangulations of the n-gon
kTriangulations :: [[[Int]]]
kTriangulations = searchFlipGraph [initial] [ (initial, e) | e <- initial ]
 where initial = [ [i, mod (i+j) n] | i <- [0..k-1], j <- [k+1..n-k-1] ]
          searchFlipGraph :: [[[Int]]] -> [([[Int]],[Int])] -> [[[Int]]]
          searchFlipGraph L [] = L
          searchFlipGraph L (h:t)
             | elem T L   = searchFlipGraph L t
             | otherwise   = searchFlipGraph (T:L) (t ++ [ (T,e) | e <- T, head e < k ])
           where T = edgeFlip (fst h) (snd h)
```

Let us now simplify notations: we index the k-relevant edges of E_n by numbers (their position in the list kRelevantEdges) and we transform any k-triangulation in kTriangulations into a list of indices:

```
-- edgeIndex e = the index of the edge e in the list of k-relevant edges of the n-gon
edgeIndex :: [Int] -> Int
edgeIndex e = head (elemIndices e kRelevantEdges)

-- facets = all facets of Delta_nk
facets :: [[Int]]
facets = map (\T -> sort (map edgeIndex T)) kTriangulations
```

We finish this section by checking that we obtain the expected number of 2-triangulations of the octagon:

```
> length facets
84
```

A.2.3 Necessary simplex orientations

Let $m := \binom{n}{2} - kn$ denote the number of k-relevant edges of E_n, let $I := \{0, \dots, m-1\}$, and let $d := k(n-2k-1)$ be the number of k-relevant edges in a k-triangulation of the n-gon (which is the dimension of the polytopes we want to construct). We first fix these parameters in the code (d is denoted dim to avoid collision later):

```
-- Fix the parameters m and dim
m, dim :: Int
m = div (n*(n-2*k-1)) 2; dim = k*(n-2*k-1)
```

We now start computing all symmetric matroid realizations of $\Delta_{n,k}$. Remember that each solution is a function $\chi : I^{d+1} \to \{-1,0,1\}$ which satisfies the five properties of Lemma 4.44:

(i) *Alternating relations*: for any $(d+1)$-tuple $(i_0,\dots,i_d) \in I^{d+1}$ and any permutation π of $\{0,\dots,d\}$ of signature σ,

$$\chi(i_{\pi(0)},\dots,i_{\pi(d)}) = \sigma\chi(i_0,\dots,i_d).$$

(ii) *Matroid property*: the set $\chi^{-1}(\{-1,1\})$ of non-degenerate $(d+1)$-tuples of I satisfies the *Steinitz exchange axiom*: for any non-degenerate $(d+1)$-tuples $X, Y \in \chi^{-1}(\{-1,1\})$ and any element $x \in X \smallsetminus Y$, there exists $y \in Y \smallsetminus X$ such that $X \triangle \{x,y\} \in \chi^{-1}(\{-1,1\})$.

(iii) *Grassmann-Plücker relations*: for any $i_0,\dots,i_{d-2},j_1,j_2,j_3,j_4 \in I$, the set

$$\begin{aligned}\{ \quad &\chi(i_0,\dots,i_{d-2},j_1,j_2)\,\chi(i_0,\dots,i_{d-2},j_3,j_4),\\ -&\chi(i_0,\dots,i_{d-2},j_1,j_3)\,\chi(i_0,\dots,i_{d-2},j_2,j_4),\\ &\chi(i_0,\dots,i_{d-2},j_1,j_4)\,\chi(i_0,\dots,i_{d-2},j_2,j_3) \quad \}\end{aligned}$$

either contains $\{-1,1\}$ or is contained in $\{0\}$.

(iv) *Necessary Simplex Orientations*: if $i_0,\dots,i_d \in I$ are such that both $\{i_0,\dots,i_{d-2},i_{d-1}\}$ and $\{i_0,\dots,i_{d-2},i_d\}$ are facets of Δ, then for any $j \in I \smallsetminus \{i_0,\dots,i_d\}$,

$$\chi_P(i_0,\dots,i_{d-2},i_{d-1},i_d) = \chi_P(i_0,\dots,i_{d-2},i_{d-1},j) = \chi_P(i_0,\dots,i_{d-2},j,i_d).$$

(v) *Symmetry*: there exists a morphism $\tau : G \to \{\pm 1\}$ such that for any $i_0,\dots,i_d \in I$, and any $g \in G$,

$$\chi_P(gi_0,\dots,gi_d) = \tau(g)\chi_P(i_0,\dots,i_d).$$

We see such a function as a set of pairs (tu, s), that we call *oriented bases*, where tu is a $(d+1)$-tuple of elements of I, and $s = \chi(tu) \in \{-1,0,1\}$. To limit the number of oriented bases we are considering, we only remember those corresponding to ordered $(d+1)$-tuples of I, which we also call *normalized oriented base*. Of course, we need a function to normalize an arbitrary oriented base:

```
-- norm ob = normalizes the oriented base ob
norm :: ([Int],Int) -> ([Int],Int)
norm ([],s) = ([],s)
norm (h:t, s) = (take i tu ++ [h] ++ drop i tu, r*(-1)^(mod i 2))
 where (tu,r) = norm (t,s)
        i = length [ x | x <- tu, h > x ]
```

Thus, a symmetric matroid realization is collection of $\binom{m}{d+1}$ normalized oriented bases which satisfies the four properties (ii), (iii), (iv) and (v). To construct such a collection of signs, we start with the necessary simplex orientations, and try to deduce from these initial informations the signs of all normalized oriented bases.

To obtain the necessary simplex orientations, we first need to compute all pairs $\{sf, \{x,y\}\}$ (where sf is a subfacet of $\Delta_{n,k}$ and x and y are two vertices disjoint from sf) such that both $sf \cup \{x\}$ and $sf \cup \{y\}$ are facets of $\Delta_{n,k}$. We name such pairs *subfacet bounds*.

```
-- subfacets = all subfacets of Delta_nk
subfacets :: [[Int]]
subfacets = nub (concat (map (\f -> [ delete j f | j <- f ]) facets))

-- subfacetBounds = all subfacet bounds of Delta_nk
subfacetBounds :: [([Int],[Int])]
subfacetBounds = [ (sf, [x,y]) | sf <- subfacets, [x,y] <- tuples 2 ([0..m-1]\\sf),
                                 elem (sort (x:sf)) facets, elem (sort (y:sf)) facets ]
```

Now that we have all subfacet bounds, we arbitrarily fix the orientation of an arbitrary subfacet bound (say the first subfacet bound in the list subfacetBounds gets oriented positively), and deduce from this initial oriented base all necessary simplex orientations. For this, we have a function fan which deduces, from the orientation of a subfacet bound, all implied orientations (see Property (iv) of all symmetric matroid realizations):

```
-- fan sfbd s = all orientations implied by the orientation of a subfacet bound sfbd
fan :: ([Int],[Int]) -> Int -> [([Int],Int)]
fan (sf, [x,y]) s = [ norm (sf ++ [x,z], s) | z <- vertices ] ++ [ norm (sf ++ [z,y], s) | z <- vertices ]
 where vertices = [0..m-1]\\(sf ++ [x,y])

-- necessarySimplexOrientations = necessary simplex orientations of Delta_nk
necessarySimplexOrientations :: [([Int],Int)]
necessarySimplexOrientations = generateNSO subfacetBounds [norm (sf0 ++ p0, 1)]
 where (sf0,p0) = head subfacetBounds
         generateNSO :: [([Int],[Int])] -> [([Int],Int)] -> [([Int],Int)]
         generateNSO [] OM = OM
         generateNSO (sfbd@(sf,p):t) OM
            | elem (norm (sf ++ p, 1)) OM  = generateNSO t (nub (OM ++ fan sfbd 1))
            | elem (norm (sf ++ p, -1)) OM  = generateNSO t (nub (OM ++ fan sfbd (-1)))
            | otherwise  = generateNSO (t ++ [sfbd]) OM
```

By construction, at the end of this process, we have all necessary simplex orientations (and in particular, all subfacet bounds have been oriented). It is interesting to observe that we already know 304 orientations of the $\binom{12}{7} = 792$ normalized oriented bases:

```
> length necessarySimplexOrientations
304
```

In order to get more information, we need to use properties (iii) and (v) of the symmetric matroid realizations of $\Delta_{n,k}$.

A.2.4 Grassmann-Plücker relations

We have now an embryo of oriented matroid, that we want to complete into a full oriented matroid (with all signs of the $\binom{m}{d+1}$ normalized oriented bases). For this, we will use extensively Grassmann-Plücker relations.

First of all, we need to manipulate signs of our oriented bases. Given a $(d+1)$-tuple of I, the following function tells us its sign (-1, 0, or 1) in our embryo of oriented matroid. For this, it normalizes this tuple and looks for its normalized version in our set of normalized oriented bases. If our embryo has still no orientation for this tuple, the function will answer ± 2.

```
-- sign tu OM = what is the sign of the tuple tu in the oriented matroid OM
sign :: [Int] -> [([Int],Int)] -> Int
sign tu OM = ns*signNormalized ntu OM
 where (ntu, ns) = norm (tu, 1)
         signNormalized :: [Int] -> [([Int],Int)] -> Int
         signNormalized _ [] = 2
         signNormalized tu1 ((tu2,s):t)
            | tu1 == tu2  = s
            | otherwise  = sign tu1 t
```

Concerning Grassmann-Plücker relations, we need two different functions: given a set OM of oriented bases, we need:

(i) a *verification* function contrGP which tells whether the set of oriented bases OM contradicts Grassmann-Plücker relations; and

(ii) a *deduction* function consGP which computes all consequences of Grassmann-Plücker relations from the signs in OM.

For the verificiation function, we check that for any $w, x, y, z \in I$, and for any hyperline hl disjoint from $\{w, x, y, z\}$, the set

$$\{\chi(hl,w,x)\chi(hl,y,z), -\chi(hl,w,y)\chi(hl,x,z), \chi(hl,w,z)\chi(hl,x,y)\}$$

either contains $\{-1, 1\}$ or is contained in $\{0\}$:

```
-- contradiction hl [w,x,y,z] OM = does (hl,[w,x,y,z]) contradict Grassmann-Plücker relations?
contradiction :: [Int] -> [Int] -> [([Int],Int)] -> Bool
contradiction hl [w,x,y,z] OM = elem (sort (nub ([a*b, -c*d, e*f]))) [[1], [-1], [0,1], [-1,0]]
 where a = sign (hl ++ [w,x]) OM; b = sign (hl ++ [y,z]) OM
         c = sign (hl ++ [w,y]) OM; d = sign (hl ++ [x,z]) OM
         e = sign (hl ++ [w,z]) OM; f = sign (hl ++ [x,y]) OM

-- contrGP OM = does OM contradict Grassmann-Plücker relations?
contrGP :: [([Int],Int)] -> Bool
contrGP OM = or [ contradiction hl q OM | q <- tuples 4 [0..m-1], hl <- tuples (dim-1) ([0..m-1]\\q) ]
```

The deduction function, is very similar. For example, given a 4-tuple $(w, x, y, z) \in I^4$ and a hyperline hl disjoint form $\{w, x, y, z\}$:

(i) if $-\chi(hl, w, y)\chi(hl, x, z) = \chi(hl, w, z)\chi(hl, x, y) = 0$ and $\chi(hl, y, z) \neq 0$, then $\chi(hl, w, x)$ necessarily equals 0;

(ii) if $\{-\chi(hl, w, y)\chi(hl, x, z), \chi(hl, w, z)\chi(hl, x, y)\} \cap \{-1, 1\} = \{\varepsilon\}$, with $\varepsilon \in \{-1, 1\}$, then $\chi(hl, w, x)$ necessarily equals $-\varepsilon\chi(hl, y, z)$;

Similarly, we have equations relating $\chi(hl, w, y)$ with $\chi(hl, x, z)$ and $\chi(hl, w, z)$ with $\chi(hl, x, y)$. These equations can be translated into HASKELL as follows:

```
-- consequence hl [w,x,y,z] OM = consequence of the Grassmann-Plücker relations
consequence :: [Int] -> [Int] -> [([Int],Int)] -> [([Int],Int)]
consequence hl [w,x,y,z] OM
   | abs a == 2 && abs b == 1 && elem [-c*d, e*f] set  = [norm (hl ++ [w,x], b*signum (c*d-e*f))]
   | abs b == 2 && abs a == 1 && elem [-c*d, e*f] set  = [norm (hl ++ [y,z], a*signum (c*d-e*f))]
   | abs c == 2 && abs d == 1 && elem [a*b, e*f] set  = [norm (hl ++ [w,y], d*signum (a*b+e*f))]
   | abs d == 2 && abs c == 1 && elem [a*b, e*f] set  = [norm (hl ++ [x,z], c*signum (a*b+e*f))]
   | abs e == 2 && abs f == 1 && elem [a*b, -c*d] set  = [norm (hl ++ [w,z], f*signum (-a*b+c*d))]
   | abs f == 2 && abs e == 1 && elem [a*b, -c*d] set  = [norm (hl ++ [x,y], e*signum (-a*b+c*d))]
   | otherwise  = []
 where a = sign (hl ++ [w,x]) OM; b = sign (hl ++ [y,z]) OM
         c = sign (hl ++ [w,y]) OM; d = sign (hl ++ [x,z]) OM
         e = sign (hl ++ [w,z]) OM; f = sign (hl ++ [x,y]) OM
         set = [[-1,-1], [0,0], [1,1], [0,-1], [-1,0], [0,1], [1,0]]
```

In the previous function, the function signum :: Int -> Int gives the sign (-1, 0, or 1) of an integer, and should not be confused with the function sign (which gives the sign of a tuple in a set of oriented bases). The reader can also observe that for a given 4-tuple and a given disjoint hyperline, we can have either no or one consequence of the Grassmann-Plücker relations. This is the reason why we return a list of consequences (which can either be empty or have a single element).

We can finally write the function consGP which iteratively deduces all consequences of Grassmann-Plücker relations in a set OM of oriented bases. At each step, it first computes all immediate consequences of Grassmann-Plücker relations, applying the function consequence to all 4-tuples and disjoint hyperlines. If we have no new consequence, we return OM. If we have new consequences, but if they are not coherent (*i.e.* if two consequences contradict themself), then we return the empty set: no oriented matroid can be constructed from the set OM of oriented bases. Finally, if we have new coherent consequences, then we add them to the set of oriented bases and we run consGP again.

```
-- coherent OM = is OM coherent?
coherent :: [([Int],Int)] -> Bool
coherent OM = and [ fst (sortedOM!!(i-1)) /= fst (sortedOM!!i) | i<-[1..(length sortedOM)-1] ]
 where sortedOM = sort OM
```

```
-- consGP OM = consequences of Grassmann-Plücker relations in OM
consGP :: [([Int],Int)] -> [[([Int],Int)]]
consGP OM
   | newSigns == []  = [OM]
   | coherent newSigns  = consGP (nub (OM ++ newSigns))
   | otherwise  = []
 where newSigns = nub (concat [ consequence hl q OM | q <- tuples 4 [0..m-1],
                                                  hl <- tuples (dim-1) ([0..m-1]\\q) ])
```

A.2.5 Symmetry under the dihedral group

We now focus on the action of the dihedral group on our oriented matroids. We first define the action on the oriented matroid of the rotation $\rho : v \mapsto v + 1$ and the reflection $\sigma : v \mapsto -v$:

```
-- rotation i = the rotation v -> v + i
rotation :: Int -> [Int] -> [Int]
rotation i T = map (\e -> edgeIndex (sort (map (\v -> mod (v+i) n) (kRelevantEdges!!e)))) T

-- reflection = the reflexion v -> -v
reflection :: [Int] -> [Int]
reflection T = map (\e -> edgeIndex (sort (map (\v -> mod (-v) n) (kRelevantEdges!!e)))) T
```

These transformations generate the complete dihedral group:

$$\mathbb{D}_n = \left\{ \rho^i \,\middle|\, i \in [n] \right\} \cup \left\{ \rho^i \circ \sigma \,\middle|\, i \in [n] \right\}.$$

In order to deduce from the action of the dihedral group the signs of new oriented bases, we need to know the signs of the action of ρ and σ (*i.e.* the signs $\tau(\rho)$ and $\tau(\sigma)$). Since the dihedral group already acts on the necessary simplex orientations, these signs are already determined:

```
-- signRot = the sign of the action of the rotation v -> v + 1 on the oriented matroid
signRot :: Int
signRot = s*(sign (rotation 1 tu) necessarySimplexOrientations)
 where (tu,s) = head necessarySimplexOrientations

-- signRef = the sign of the action of the reflectino v -> -v on the oriented matroid
signRef :: Int
signRef = s*(sign (reflection tu) necessarySimplexOrientations)
 where (tu,s) = head necessarySimplexOrientations
```

Now, given a set of oriented bases, we can compute the orbit of these signs under the action of the dihedral group:

```
-- orbitDG OM = the orbit under the dihedral group of the set of oriented bases OM
orbitDG :: [([Int],Int)] -> [([Int],Int)]
orbitDG OM = sort (nub (concat (map (\(tu,s) -> ([ norm (rotation i tu, (signRot^i)*s) | i <- [0..n-1] ]
                ++ [ norm (rotation i (reflection tu), (signRot ^i)*signRef*s) | i <- [0..n-1] ])) OM)))
```

Applying the function orbitDG to a set of oriented bases yields a set of oriented bases closed under the action of $\mathbb{D}_n$. It is convenient to present such a set of oriented bases keeping only one representative per orbit under $\mathbb{D}_n$:

```
-- reduceOrbitDG OM = one representative by orbit under the dihedral group
reduceOrbitDG :: [([Int],Int)] -> [([Int],Int)]
reduceOrbitDG [] = []
reduceOrbitDG (h:t) = h:(reduceOrbitDG (t\\orbit))
 where orbit = orbitDG [h]
```

Using this function, we can count the number of orbits in our necessary simplex orientations (observe that we are sure that they are closed under the action of $\mathbb{D}_n$ since they were deduced from a symmetric set of facets):

```
> length (reduceOrbitDG necessarySimplexOrientations)
25
```

To finish this section on the dihedral group, we want to observe that imposing a realization of a simplicial complex to be symmetric sometimes forces the determinant of certain tuples to vanish. Indeed, if $\chi : I^{d+1} \to \{-1, 0, 1\}$ is a symmetric matroid realization of a simplicial complex Δ under a group G, then for any $i_0, \dots, i_d \in I$, and any $g \in G$,

$$\chi(i_0, \dots, i_d) = \tau(g)\chi(gi_0, \dots, gi_d) = \tau(g)\chi(i_{\pi(0)}, \dots, i_{\pi(d)}) = \varepsilon\tau(g)\chi(i_0, \dots, i_d),$$

where π is the permutation of $\{0, \dots, d\}$ defined by $i_{\pi(j)} = gi_j$, and ε is the signature of π. In particular, if $\varepsilon = -\tau(g)$, then it forces $\chi(i_0, \dots, i_d)$ to vanish. We say that $\chi(i_0, \dots, i_d)$ is a *necessary zero*. These necessary zeros are easy to compute: they are the $(d+1)$-tuples of I whose orbit under the dihedral group is not coherent:

```
-- necessaryZeros = tuples whose determinant is forced to vanish by the dihedral action
necessaryZeros :: [([Int],Int)]
necessaryZeros = [ (b,0) | b <- tuples (dim+1) [0..m-1], not (coherent (orbitDG [(b,1)])) ]
```

Observe that when we add these necessary zeros to our necessary simplex orientations, we obtain new Grassmann-Plücker consequences:

```
> length necessaryZeros
16
> length (consGP (sort (necessarySimplexOrientations ++ necessaryZeros)))
456
```

Thus, we already now 456 normalized oriented bases (of the 792 in total). In order to complete this embryo of oriented matroid, we need to start "guessing signs".

A.2.6 Guessing signs

We now have to guess new signs to complete our current set of oriented bases into a full oriented matroid. The method consists in picking one $(d+1)$-tuple of I whose sign remains unknown, and to try the three possibilities -1, 0 and 1. Applying symmetry and Grassmann-Plücker relations, we may obtain:

(1) either a contradiction, and we eliminate this choice of sign for this $(d+1)$-tuple;

(2) or a complete symmetric matroid realization of $\Delta_{8,2}$;

(3) or a certain number of additional signs, but not all, and we have to iterate the guessing process until we arrive at situation (1) or (2).

The point of this section is to make a good choice for the $(d+1)$-tuple for which we would like to guess the sign, that is, a choice which will provide as much information as possible.

Let hl be an hyperline and w, x, y, z be four indices not in hl. Consider the six $(d+1)$-tuples $hl \cup \{w, x\}$, $hl \cup \{y, z\}$, $hl \cup \{w, y\}$, $hl \cup \{x, z\}$, $hl \cup \{w, z\}$, and $hl \cup \{x, y\}$ which appear in the Grassmann-Plücker relation $\{hl, [w, x, y, z]\}$. In our current set of oriented bases, the signs of some of these six $(d+1)$-tuples are known, while the others remain unknown. Assume for example that both $\chi(hl, w, x)\chi(hl, y, z)$ and $-\chi(hl, w, y)\chi(hl, x, z)$ are known and equal, while both $\chi(hl, w, z)$ and $\chi(hl, x, y)$ remain unknown. Then finding $\chi(hl, w, z)$ would automatically provide $\chi(hl, x, y)$ and *vice versa*. We call *key base* (of $\{hl, [w, x, y, z]\}$) any such base, *i.e.* any base whose sign, if known, would allow us to derive the sign of another base. The function keyBases lists all key bases of a given Grassmann-Plücker relation:

```
-- keyBases OM GPrelation = key bases of the Grassmann-Plücker relation
keyBases :: [([Int],Int)] -> ([Int],[Int]) -> [[([Int],Int)]]
keyBases OM (hl,q) = [ [(b,s)] | b <- map (\p -> sort (hl ++ p)) (tuples 2 q), s <- [-1,1],
                                  sign b OM == 2, consequence hl q ((b,s):OM) /= [] ]
```

A good choice for the $(d+1)$-tuple for which we would like to guess the sign should be, as well as its images under the dihedral group, a key base of many Grassmann-Plücker relations. The following function bestTuple computes our best possible choice: it enumerates the key bases of all Grassmann-Plücker relations, and chooses the $(d+1)$-tuple whose orbit under $\mathbb{D}_n$ is the most represented among all these key bases. (The routine mostRep chooses in a list the most represented element: for example, mostRep [1,4,2,1,2,2] returns [2].)

```
-- mostRep L = the most represented element in L
mostRep :: Ord a => [a] -> [a]
mostRep L
   | L == []  = []
   | otherwise  = [head (head (sortBy (\x y -> compare (length y) (length x)) (group (sort L))))]

-- bestTuple OM = the best choice for the tuple for which we would like to guess the sign
bestTuple :: [([Int],Int)] -> [Int]
bestTuple OM
   | b == []  = head ((tuples (dim+1) [0..m-1])\\(map fst OM))
   | otherwise  = fst (head (head b))
 where GPrels = [ (hl,q) | hl <- tuples (dim-1) [0..m-1], q <- tuples 4 ([0..m-1]\\hl) ]
         b = mostRep (map orbitDG (concat (map (keyBases  OM) GPrels)))
```

With this rule for choosing the best possible tuple, we can now write the run function, which starts from a set of oriented bases and iteratively guess new signs, until it founds a full oriented matroid:

```
-- run = the iterative guessing process
run :: [[([Int],Int)]] -> [[([Int],Int)]]
run [] = []
run (OM:t)
   | length OM == length (tuples (dim+1) [0..m-1])  = OM:(run t)
   | otherwise  = run ([ [newOM] | newOM <- newOMs, not (contrGP newOM) ] ++ t)
 where b = bestTuple OM
         newOMs = concat [ consGP ((orbitDG [(b,s)]) ++ OM) | s <- [1,0,-1] ]
```

A.2.7 Results

We finally obtain our symmetric realizations of $\Delta_{8,2}$:

```
-- symmetricMatroidRealizations = the list of symmetric matroid realizations of Delta_nk
symmetricMatroidRealizations :: [[([Int],Int)]]
symmetricMatroidRealizations = run [necessarySimplexOrientations ++ necessaryZeros]

-- reducedSMR = the list of symmetric matroid realizations, with one representative per orbit
reducedSMR :: [[([Int],Int)]]
reducedSMR = map reduceOrbitDG symmetricMatroidRealizations
```

We obtain Proposition 4.49 with the following command:

```
> length symmetricMatroidRealizations
15
```

In order to describe these 15 symmetric matroid realizations, we reduce each of them, keeping only one representative for each of the 62 orbits under the dihedral group: we obtain the list reducedSMR. These 15 realizations share the following 59 orbits:

```
> simplify (sort (interesection reducedSMR))
(abcdefg, 0), (abcdefI, 1), (abcdefJ, -1), (abcdefK, 1), (abcdegI, -1), (abcdegJ, 1), (abcdeIK, 1),
(abcdeIL, -1), (abcdeJK, -1), (abcdfgI, 1), (abcdfgJ, -1), (abcdfgL, -1), (abcdfIJ, -1), (abcdfIK, -1),
(abcdfIL, 1), (abcdfJK, 1), (abcdfJL, -1), (abcdfKL, 1), (abcdIJK, 1), (abcdIJL, -1), (abcdIKL, 1),
(abcefgI, 0), (abcefgK, 0), (abcefIJ, 1), (abcefIK, -1), (abcefIL, -1), (abcefJK, 1), (abcefJL, 1),
(abcefKL, -1), (abcegIJ, -1), (abcegIK, 1), (abcegIL, 1), (abcegKL, 1), (abceIJL, 1), (abceIKL, -1),
(abceJKL, 1), (abcfIJK, 1), (abcfIKL, 1), (abcIJKL, -1), (abdegIJ, -1), (abdegIK, -1), (abdegIL, -1),
(abdegJK, 1), (abdeIJK, -1), (abdeIJL, 1), (abdfIJL, -1), (abdfIKL, -1), (abdfJKL, 1), (abdgIJK, 1),
(abdgIJL, 1), (abdgJKL, -1), (abdIJKL, 1), (abefIJK, 1), (abefIJL, 1), (abefJKL, -1), (abeIJKL, -1),
(acegIJK, 1), (aceIJKL, 1), (acfIJKL, -1)
```

Here, the function intersection intersects all realizations, and the function simplify transforms the tuple [0,1,2,3,4,5,6] into the word abcdefg. Finally, the three remaining orbits are those of abcdeIJ, abceIJK and abdfIJK. The following command list their respective signs in the 15 realizations:

```
> map (map snd) (map (\x -> sort (x\\(intersection reducedSMR))) reducedSMR)
[[1,-1,1], [1,-1,0], [1,-1,-1], [0,-1,1], [0,-1,0], [0,-1,-1], [-1,1,1], [-1,1,0], [-1,1,-1], [-1,0,1], [-1,0,0],
[-1,0,-1], [-1,-1,1], [-1,-1,0], [-1,-1,-1]]
```

We finish by a short remark. To obtain all possible symmetric matroid realizations of $\Delta_{8,2}$, we started from the necessary simplex orientations (and the necessary zeros), and we iteratively guessed signs, applying at each step symmetry and Grassmann-Plücker relations. Thus, by construction, the sets of oriented bases we obtain satisfy points (i), (iii), (iv) and (v) of the definition of symmetric matroid realization. To conclude, we still have to check point (ii), namely that the set of non-degenerate $(d+1)$-tuples forms a matroid. This is easily done by the following function:

```
-- matroid M = checks that the set of (sorted) bases M forms a matroid
matroid :: [[Int]] -> Bool
matroid M = and [ or [ elem (sort (y:(delete x X))) M | y <- Y\\X ] | (X,Y) <- tuples 2 M, x <- X\\Y ]
```

```
> and [ map (\OM -> matroid [ tu | (tu,s) <- OM, s /= 0 ]) symmetricMatroidRealizations ]
True
```

II

Part Two

Polytopality of products

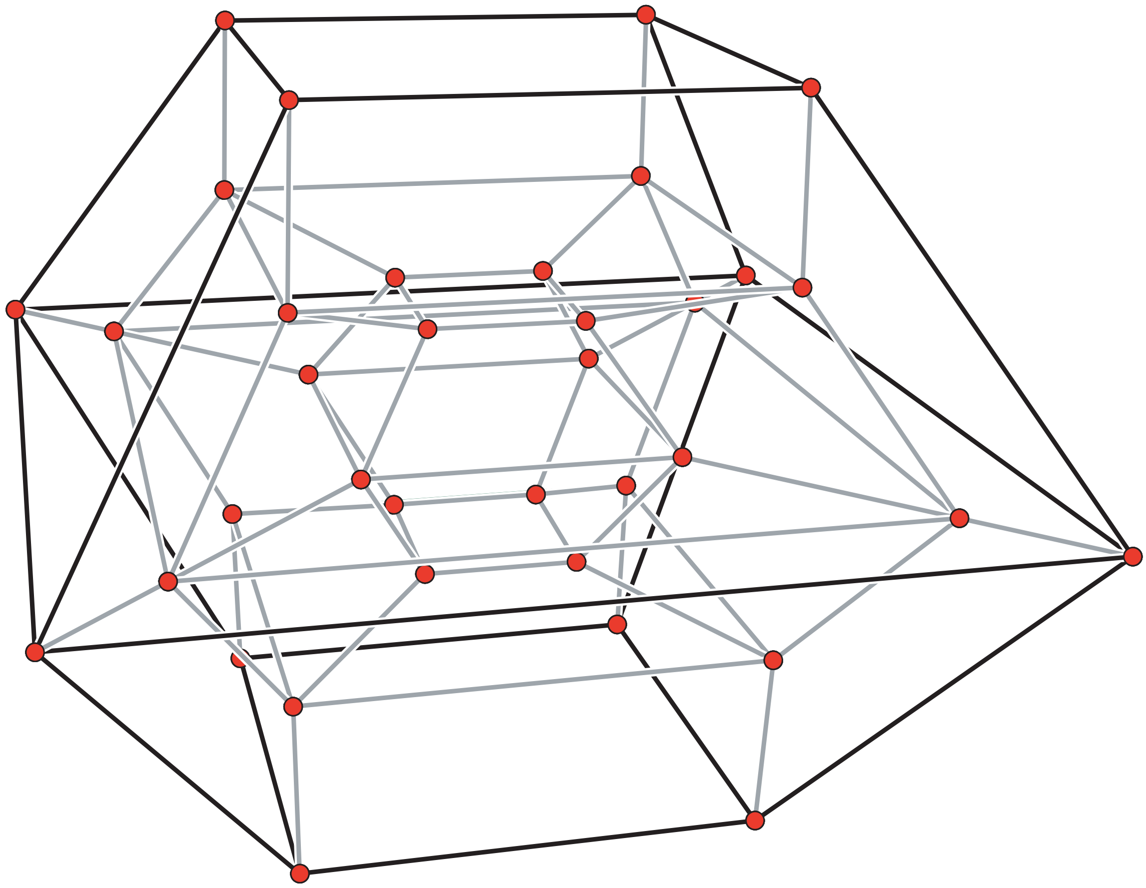

Chapter Five 5

INTRODUCTION

The second part of this dissertation focusses on *polytopality* questions: given an abstract polytopal k-complex, we ask *"whether it is the k-skeleton of a polytope?"*, *"what dimension can a realizing polytope have?"* and *"how does a realizing polytope look like?"*. This kind of questions can be studied for complexes:

(i) either derived from combinatorial structures: for example, the simplicial complex of all non-crossing diagonals of a convex polygon, or the graph of flips on multitriangulations of a point set (remember our discussion in Section 4.3), or the graph whose vertices are permutations of $[n]$ and where two permutations are related by an edge if they differ by a single adjacent transposition, etc. See [Zie95, Lecture 9] for more examples.

(ii) or obtained by certain operations on other complexes: for example, the next two chapters deal with complexes obtained as products of other complexes.

The most prominent result on realizability problems is Steinitz' Theorem (see Theorem 6.2) which characterizes graphs of 3-polytopes and describes their realization space. No similar statement can be expected in higher dimensions, where realizability is a difficult question in general. In fact, even 4-polytopes can have arbitrarily wild and complicated realization spaces (this is known as the *Universality Theorems* for polytopes [RG96]).

In the second part of this thesis, we consider a specific realizability question: it concerns k-complexes obtained as products of smaller complexes. More precisely:

- In Chapter 6, we explore polytopality questions on *Cartesian products of graphs*. This product is defined in such a way that the graph of a product of polytopes is the product of their graphs; in particular, products of polytopal graphs are automatically polytopal. Our question addresses the reciprocal statement: are the two factors of a polytopal product necessarily polytopal?
- In Chapter 7, we study *prodsimplicial-neighborly polytopes*, whose k-skeleton is combinatorially equivalent to that of a given product of simplices. The goal is to construct PSN polytopes which minimize the possible dimension among all PSN polytopes.

Before summarizing our results in Section 5.2, we fix in the next section some notation and terminology. Since we will use them extensively in the coming chapters, we also recall the definition and elementary properties of the famous cyclic polytopes as an illustration of dimensional ambiguous polytopes. The reader familiar with polytope theory is invited to jump directly to Section 5.2.

5.1 GENERALITIES ON POLYTOPES

5.1.1 Notation and terminology

A *polytope* is the convex hull of a finite point set of $\mathbb{R}^n$, or equivalently a bounded intersection of finitely many half-spaces in $\mathbb{R}^n$. We write $P := \mathrm{conv}(X) := \{x \in \mathbb{R}^n \mid Ax \leq b\}$, where $X \subset \mathbb{R}^n$ is finite, $A \in \mathbb{R}^{n \times f}$ and $b \in \mathbb{R}^f$. The *dimension* of a polytope is the dimension of its affine span (we abbreviate "d-dimensional polytope" into "d-polytope").

Dating back to antiquity, the study of polytopes was initially limited to dimensions 2 and 3, and focussed on their (sym)metric properties: famous examples are regular polygons and Platonic solids. During the last centuries, the study of polytopes was extended to higher dimensions, and the interest on polytopes shifted from their geometric properties to more combinatorial aspects. We now pay particular attention to their face structure.

A *face* of a polytope P is an intersection $F := P \cap H$ of P with a supporting hyperplane H of P (the empty set is also considered as a face of P). If $H = \{x \in \mathbb{R}^n \mid \langle h \mid x \rangle = c\}$ and $\langle h \mid x \rangle < c$ for all $x \in P$, then we say that h is an (outer) *normal vector* of the face F. A 0-face (resp. 1-face, resp. $(d-1)$-face) of a d-polytope is called a *vertex* (resp. an *edge*, resp. a *facet*). The *f-vector* of a d-polytope P is the vector $f(P) := (f_{-1}(P), f_0(P), \ldots, f_{d-1}(P))$, where $f_k(P)$ denotes the number of k-faces of P (by convention, the empty face has dimension -1). For $k \in \mathbb{N}$, the *k-skeleton* of a polytope is the polytopal k-complex formed by all its faces of dimension at most k. In particular, the 1-skeleton of a polytope is its *graph* and the $(d-1)$-skeleton of a d-polytope is its *boundary complex*.

As mentioned previously, we are interested in combinatorial properties of polytopes: two polytopes are considered as equivalent if the incidence relations between their faces behave similarly in both polytopes. More precisely, two complexes $\mathcal{C}$ and $\mathcal{C}'$ are *combinatorially equivalent* if there is an inclusion-preserving bijection from one to the other: $\phi : \mathcal{C} \to \mathcal{C}'$ with $A \subset B \Leftrightarrow \phi(A) \subset \phi(B)$.

Example 5.1. A d-simplex is the convex hull of $d+1$ affinely independent points: for example, $\triangle_d := \mathrm{conv}\,\{e_k \mid k \in [d+1]\}$, where $(e_1, \ldots, e_{d+1})$ denotes the canonical orthogonal basis of $\mathbb{R}^{d+1}$. The convex hull of any subset of its vertices forms a face of the simplex. In particular, its graph is the complete graph, its f-vector is given by $f_k(\triangle_d) = \binom{d+1}{k+1}$, and all simplices are combinatorially equivalent.

To finish, let us recall that a polytope is *simplicial* if all its facets are simplices, and *simple* if all its vertex figures are simplices (the vertex figure of a vertex v in a polytope P is the intersection of P with an hyperplane that only cuts off vertex v). In other words, the vertices of a simplicial polytope are in general position (no $d+1$ of them lie in an hyperplane) while the facet-defining inequalities of a simple polytope are in general position. For example, a simplex is both simple and simplicial.

All along the text of the next two chapters, we will recall classical results of polytope theory when we need them. For a detailed presentation on polytopes, we refer to the excellent books of Branko Grünbaum [Grü03] and Günter Ziegler [Zie95], as well as the expository chapters [Mat02, Chapter 5] and [HRGZ97, BB97, Kal97].

5.1.2 Polytopality and ambiguity

The main property we will be interested in (in particular for graphs) is the following:

Definition 5.2. *A k-complex $\mathcal{C}$ is* polytopal *if it is combinatorially equivalent to the k-skeleton of some polytope P. If P is d-dimensional, we say that $\mathcal{C}$ is* d-polytopal.

As soon as a k-complex is polytopal, we want to know which (combinatorial types of) polytopes realize it. Certain complexes determine the combinatorial type of their possible realizations (for example, graphs of 3-polytopes — see Theorem 6.2); some others are far from that: even the dimension of the realization is sometimes not fixed by the k-complex.

Definition 5.3. *A k-complex is* dimensionally ambiguous *if there exist two polytopes realizing it in two different dimensions. We define the* polytopality range *of a k-complex $\mathcal{C}$ to be the set of integers d for which $\mathcal{C}$ is d-polytopal, and the* polytopality dimension *to be the minimal dimension of a realizing polytope.*

As an illustration, we recall the definition and basic properties of cyclic polytopes, which are fundamental examples in polytope theory because of their extremal properties:

Definition 5.4. *Let $t \mapsto \mu_d(t) := (t, t^2, \dots, t^d)^T$ denote the* moment curve *in $\mathbb{R}^d$, and choose n arbitrary distinct real numbers $t_1 < t_2 < \dots < t_n$. We denote by $C_d(n) := \operatorname{conv}\{\mu_d(t_i) \,|\, i \in [n]\}$ "the"* cyclic polytope *of dimension d with n vertices (the convex hull of any n distinct points on the moment curve always leads to the same combinatorial polytope).*

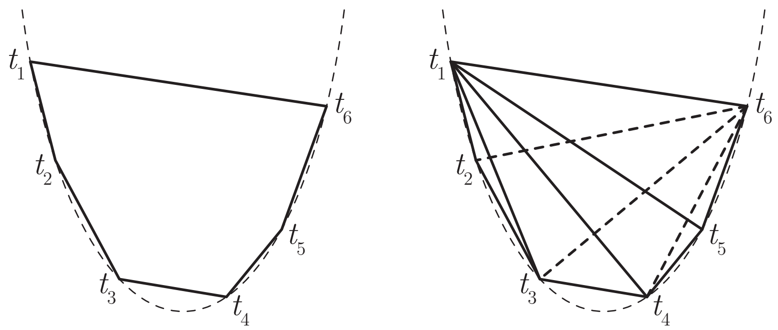

Figure 5.1: The cyclic polytopes $C_2(6)$ (with a unique upper facet $\{1, 6\}$) and $C_3(6)$ (with its upper facets $\{i, i+1, 6\}$, $i \in [4]$).

Proposition 5.5. *The cyclic polytope $C_d(n)$ is* $\lfloor \frac{d}{2} \rfloor$-neighborly*: any subset of at most $\lfloor \frac{d}{2} \rfloor$ vertices forms a face of $C_d(n)$.*

In particular, for any $4 \le d < n$, the graph of the cyclic polytope $C_d(n)$ is the complete graph. In other words, for $n \ge 5$, the polytopality range of the complete graph K_n contains, and in fact equals $\{4, \dots, n-1\}$.

The proof of Proposition 5.5 is classic but we recall it since we will use similar ideas in Section 7.1. We naturally identify a face $\operatorname{conv}\{\mu(t_i) \,|\, i \in F\}$ of $C_d(n)$ with the subset F of $[n]$.

Gale's evenness criterion (Proposition 5.6) characterizes which subsets of $[n]$ are facets of $C_d(n)$. To state it, define the ***blocks*** of a subset F of $[n]$ to be the maximal subsets of consecutive elements of F. The ***initial*** (resp. ***final***) block is the block containing 1 (resp. n) — when it exists. Other blocks are called ***inner*** blocks. For example, $\{1,2,3,6,7,9,10,11\} \subset [11]$ has 3 blocks: $\{1,2,3\}$ (initial), $\{6,7\}$ (inner) and $\{9,10,11\}$ (final).

Proposition 5.6 (Gale's evenness criterion [Gal63])**.** *A subset F of $[n]$ is a facet of $C_d(n)$ if and only if $|F| = d$ and all inner blocks of F have even size. Furthermore, such a facet F is supported by the hyperplane $H_F := \left\{ z \in \mathbb{R}^d \,\middle|\, \langle (\gamma_i(F))_{i\in[d]} \,|\, z\rangle = -\gamma_0(F) \right\}$, where $\gamma_0(F), \dots, \gamma_d(F)$ are defined as the coefficients of $t^0, \dots, t^d$ in the polynomial:*

$$\Pi_F(t) := \prod_{i\in F}(t - t_i) := \sum_{i=0}^{d} \gamma_i(F) t^i.$$

Finally, according to the parity of the size ℓ of the final block of F:

(i) If ℓ is odd, then the whole cyclic polytope lies below H_F (with respect to the last coordinate). We say that F is an upper facet*. Its normal vector is $(\gamma_i(F))_{i\in[d]}$.*

(ii) If ℓ is even, then the whole cyclic polytope lies above H_F. We say that F is a lower facet*. Its normal vector is $(-\gamma_i(F))_{i\in[d]}$.*

Proof. Observe first that:

(i) Vandermonde determinant

$$\det\begin{pmatrix} 1 & 1 & \dots & 1 \\ \mu(x_0) & \mu(x_1) & \dots & \mu(x_d) \end{pmatrix} = \prod_{0\le i<j\le d} (x_j - x_i)$$

ensures that any $d+1$ points on the d-dimensional moment curve are affinely independent, and thus, that the cyclic polytope is simplicial.

(ii) For any $t \in \mathbb{R}$,

$$\langle (\gamma_i(F))_{i\in[d]} \,|\, \mu_d(t)\rangle + \gamma_0(F) = \sum_{i=0}^{d} \gamma_i(F) t^i = \Pi_F(t).$$

(iii) the coefficient $\gamma_d(F)$ is always 1, and thus, the vector $(\gamma_i(F))_{i\in[d]}$ points upwards (with respect to the last coordinate).

Let F be a subset of $[n]$ of size d. Then:

(i) for all $j \in F$, $\Pi_F(t_j) = 0$; thus, H_F is the affine hyperplane spanned by F;

(ii) for all $j \notin F$, the sign of $\Pi_F(t_j)$ is $(-1)^{|F\cap\{j+1,\dots,n\}|}$.

In particular, if F has an odd inner block $\{a, a+1, \dots, b\}$, then $\Pi_F(t_{a-1})$ and $\Pi_F(t_{b+1})$ have different signs, and F is not a facet. Reciprocally, if all inner blocks have even size, then the sign of all $\Pi_F(t_j)$ is $(-1)^\ell$, where ℓ is the size of the final block. Thus, F is an upper facet when ℓ is odd, and a lower facet when ℓ is even. $\square$

5.2 Polytopality of products: our results

The *Cartesian product* of two polytopes P, Q is the polytope $P \times Q := \{(p,q) \,|\, p \in P, q \in Q\}$. The combinatorial structure of the product is completely understood from the structure of its factors:

(i) The dimension of $P \times Q$ is the sum of the dimensions of P and Q.

(ii) The non-empty faces of $P \times Q$ are precisely the products of non-empty faces of P by non-empty faces of Q.

(iii) The f-vector of $P \times Q$ is given by $f_k(P \times Q) = \sum_{i+j=k} f_i(P) f_j(Q)$.

Example 5.7. Let $\underline{n} := (n_1 \ldots, n_r)$ be a tuple of positive integers. The product of simplices $\triangle_{\underline{n}} := \triangle_{n_1} \times \cdots \times \triangle_{n_r}$ has dimension $\sum n_i$ and its f-vector is given by

$$f_k(\triangle_{\underline{n}}) = \sum_{\substack{0 \le k_i \le n_i \\ k_1 + \cdots + k_r = k}} \prod_{i \in [r]} \binom{n_i + 1}{k_i + 1}.$$

In particular, $f_0(\triangle_{\underline{n}}) = \prod n_i$ and $f_1(\triangle_{\underline{n}}) = \sum_{i \in [r]} \binom{n_i+1}{2} \prod_{j \ne i}(n_j + 1)$. The graphs of $\triangle_{(i,6)}$ $(i \in [3])$ are represented in Figure 5.2.

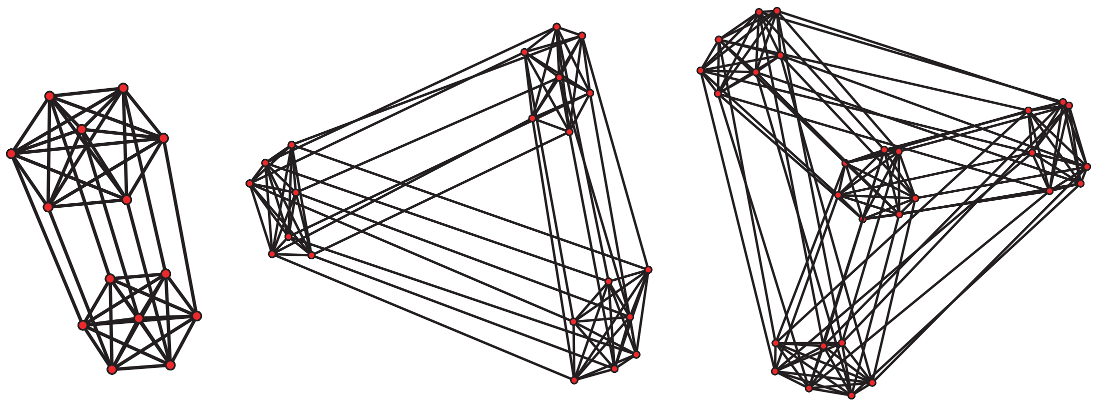

Figure 5.2: The graphs of the products $\triangle_{(i,6)} := \triangle_i \times \triangle_6$, for $i \in [3]$.

5.2.1 Polytopality of products of non-polytopal graphs

In Chapter 6, we set out to study the polytopality of products of graphs. The *Cartesian product* of two graphs G and H is the graph $G \times H$ with vertex set $V(G \times H) := V(G) \times V(H)$ and edge set $E(G \times H) := \big(V(G) \times E(H)\big) \cup \big(E(G) \times V(H)\big)$. In other words, for $a, c \in V(G)$ and $b, d \in V(H)$, the vertices (a, b) and (c, d) of $G \times H$ are adjacent if either $a = c$ and $\{b, d\} \in E(H)$, or $b = d$ and $\{a, c\} \in E(G)$. This product is consistent with the product of polytopes: the graph of a product of two polytopes is the product of their graphs. In particular, the product of two polytopal graphs is automatically polytopal. In this chapter, we consider the reciprocal question: given two graphs G and H, does the polytopality of the product $G \times H$ imply the polytopality of the factors G and H?

The product of a triangle by a path of length 2 is a simple counter-example to this question: although the path is not polytopal, the resulting graph is the graph of a 3-polytope obtained by gluing two triangular prisms along a triangular face. We neutralize such simple examples by requiring furthermore both factors to be regular graphs. Let d and e denote the regularity degree of G and H respectively. In this case, the product $G \times H$ is $(d+e)$-regular and it is natural to wonder whether it is the graph of a simple $(d+e)$-polytope. The answer is given by the following theorem:

Theorem 5.8. *The product $G \times H$ is the graph of a simple polytope if and only if both G and H are graphs of simple polytopes. In this case, there is a unique (combinatorial type of) simple polytope whose graph is $G \times H$: it is precisely the product of the unique (combinatorial types of) simple polytopes whose graphs are G and H respectively.* □

In this theorem, the uniqueness of the simple polytope realizing $G \times H$ is a direct application of the fact that a simple polytope is uniquely determined by its graph [BML87, Kal88]. These results rely on the following basic property of simple polytopes: any $k+1$ edges adjacent to a vertex of a simple polytope P define a k-face of P.

As an application of Theorem 5.8 we obtain a large family of non-polytopal 4-regular graphs: the product of a non-polytopal 3-regular graph by a segment is non-polytopal and 4-regular.

We then wonder whether the product of two non-polytopal regular graphs can be polytopal in a dimension smaller than its degree. The following examples partially answer this question:

Theorem 5.9. *(i) For $n \geq 3$, the product $K_{n,n} \times K_2$ of a complete bipartite graph by a segment is not polytopal.*

(ii) The product of a d-polytopal graph by the graph of a regular subdivision of an e-polytope is $(d+e)$-polytopal. This provides polytopal products of non-polytopal regular graphs (see for example Figure 5.3). □

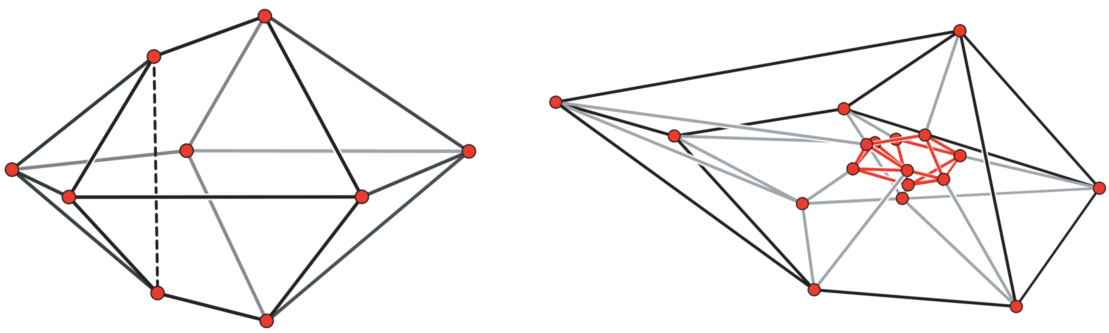

Figure 5.3: A non-polytopal 4-regular graph H which is the graph of a regular subdivision of a 3-polytope (left) and the Schlegel diagram of a 4-polytope whose graph is the product of H by a segment (right).

5.2.2 Prodsimplicial-neighborly polytopes

In Chapter 7, we consider polytopes whose skeletons are that of a product of simplices:

Definition 5.10. *Let $k \geq 0$ and $\underline{n} := (n_1, \dots, n_r)$, with $r \geq 1$ and $n_i \geq 1$ for all i. A polytope is $(k, \underline{n})$-prodsimplicial-neighborly — or $(k, \underline{n})$-PSN for short — if its k-skeleton is combinatorially equivalent to that of the product of simplices $\triangle_{\underline{n}} := \triangle_{n_1} \times \cdots \times \triangle_{n_r}$.*

This definition is essentially motivated by two particular classes of PSN polytopes:
(i) *neighborly* polytopes arise when $r = 1$;
(ii) *neighborly cubical* polytopes [JZ00, JR07, SZ10] arise when $\underline{n} = (1, 1, \dots, 1)$.

Remark 5.11. In the literature, a polytope is *k-neighborly* if any subset of at most k of its vertices forms a face. Observe that such a polytope is $(k-1, n)$-PSN with our notation.

Obviously, the product $\triangle_{\underline{n}}$ itself is a $(k, \underline{n})$-PSN polytope of dimension $\sum n_i$. We are naturally interested in finding $(k, \underline{n})$-PSN polytopes in smaller dimensions. For example, the cyclic polytope $C_{2k+2}(n+1)$ is a (k, n)-PSN polytope in dimension $2k+2$. We denote by $\delta(k, \underline{n})$ the smallest possible dimension that a $(k, \underline{n})$-PSN polytope can have.

PSN polytopes can be obtained by projecting the product $\triangle_{\underline{n}}$, or a combinatorially equivalent polytope, onto a smaller subspace. For example, the cyclic polytope $C_{2k+2}(n+1)$ (just like any polytope with $n+1$ vertices) can be seen as a projection of the simplex $\triangle_n$ to $\mathbb{R}^{2k+2}$.

Definition 5.12. *We say that a $(k, \underline{n})$-PSN polytope is $(k, \underline{n})$-projected-prodsimplicial-neighborly — or $(k, \underline{n})$-PPSN for short — if it is a projection of a polytope combinatorially equivalent to $\triangle_{\underline{n}}$.*

We denote by $\delta_{pr}(k, \underline{n})$ the smallest possible dimension of a $(k, \underline{n})$-PPSN polytope.

Chapter 7 may be naturally divided into two parts. In the first part (Sections 7.1 and 7.2), we present three methods for constructing low-dimensional PPSN polytopes:
(i) Reflections of cyclic polytopes;
(ii) Minkowski sums of cyclic polytopes;
(iii) Deformed product constructions in the spirit of Raman Sanyal and Günter Ziegler [Zie04, SZ10].

The second part (Section 7.3) derives topological obstructions for the existence of such objects, using techniques developed by Raman Sanyal in [San09] to bound the number of vertices of Minkowski sums. In view of these obstructions, our constructions in the first part turn out to be optimal for a wide range of parameters.

Constructions. Our first non-trivial example is a $(k, (1, n))$-PSN polytope in dimension $2k+2$, obtained in Section 7.1.1 by reflecting the cyclic polytope $C_{2k+2}(n+1)$ in a well-chosen hyperplane:

Proposition 5.13. *For any $k \geq 0$, $n \geq 2k+2$ and $\lambda \in \mathbb{R}$ sufficiently large, the polytope*

$$\operatorname{conv}\left(\left\{(t_i, \dots, t_i^{2k+2})^T \,\middle|\, i \in [n+1]\right\} \cup \left\{(t_i, \dots, t_i^{2k+1}, \lambda - t_i^{2k+2})^T \,\middle|\, i \in [n+1]\right\}\right)$$

is a $(k, (1, n))$-PSN polytope of dimension $2k+2$. □

For example, this provides us with a 4-polytope whose graph is $K_2 \times K_n$, for any $n \geq 3$.

Next, we form in Section 7.1.2 well-chosen Minkowski sums of cyclic polytopes to obtain explicit coordinates for $(k, \underline{n})$-PPSN polytopes:

Theorem 5.14. *Let $k \geq 0$ and $\underline{n} := (n_1, \ldots, n_r)$ with $r \geq 1$ and $n_i \geq 1$ for all i. There exist index sets $I_1, \ldots, I_r \subset \mathbb{R}$, with $|I_i| = n_i$ for all i, such that the polytope*

$$\operatorname{conv}\left\{w_{a_1,\ldots,a_r} \mid (a_1, \ldots, a_r) \in I_1 \times \cdots \times I_r\right\} \subset \mathbb{R}^{2k+r+1}$$

is $(k, \underline{n})$-PPSN, where $w_{a_1,\ldots,a_r} := \left(a_1, \ldots, a_r, \sum_{i\in[r]} a_i^2, \ldots, \sum_{i\in[r]} a_i^{2k+2}\right)^T$. Consequently:

$$\delta(k, \underline{n}) \leq \delta_{pr}(k, \underline{n}) \leq 2k + r + 1. \qquad \square$$

For $r = 1$ we recover neighborly polytopes.

Finally, we extend in Section 7.2 Raman Sanyal and Günter Ziegler's technique of "projecting deformed products of polygons" [Zie04, SZ10] to products of arbitrary simple polytopes: we suitably project a suitable polytope combinatorially equivalent to a given product of simple polytopes in such a way as to preserve its complete k-skeleton. More concretely, we describe how to use colorings of the graphs of the polar polytopes of the factors in the product to raise the dimension of the preserved skeleton. The basic version of this technique yields the following result:

Proposition 5.15. *Let $P_1, \ldots, P_r$ be simple polytopes. For each polytope P_i, denote by n_i its dimension, by m_i its number of facets, and by $\chi_i := \chi(\mathrm{gr}(P_i^\diamond))$ the chromatic number of the graph of its polar polytope $P_i^\diamond$. For a fixed integer $d \leq n$, let t be maximal such that $\sum_{i=1}^t n_i \leq d$. Then there exists a d-polytope whose k-skeleton is combinatorially equivalent to that of the product $P_1 \times \cdots \times P_r$ as soon as*

$$0 \leq k \leq \sum_{i=1}^{r}(n_i - m_i) + \sum_{i=1}^{t}(m_i - \chi_i) + \left\lfloor \frac{1}{2}\left(d - 1 + \sum_{i=1}^{t}(\chi_i - n_i)\right)\right\rfloor. \qquad \square$$

Among polytopes that minimize the last summand are products of *even polytopes* (all 2-faces have an even number of vertices). See Example 7.16 for the details, and the end of Section 7.2.1 for extensions of this technique.

Specializing the factors to simplices provides another construction of PPSN polytopes. When some of these simplices are small compared to k, this technique in fact yields our best examples of PPSN polytopes:

Theorem 5.16. *For any $k \geq 0$ and $\underline{n} := (n_1, \ldots, n_r)$ with $1 = n_1 = \cdots = n_s < n_{s+1} \leq \cdots \leq n_r$,*

$$\delta_{pr}(k, \underline{n}) \leq \begin{cases} 2(k + r) - s - t & \text{if } 3s \leq 2k + 2r, \\ 2(k + r - s) + 1 & \text{if } 3s = 2k + 2r + 1, \\ 2(k + r - s + 1) & \text{if } 3s \geq 2k + 2r + 2, \end{cases}$$

where $t \in \{s, \ldots, r\}$ is maximal such that $3s + \sum_{i=s+1}^{t}(n_i + 1) \leq 2k + 2r$. $\square$

If $n_i = 1$ for all i, we recover the neighborly cubical polytopes of [SZ10].

Obstructions. In order to derive lower bounds on the minimal dimension $\delta_{pr}(k, \underline{n})$ that a $(k, \underline{n})$-PPSN polytope can have, we apply in Section 7.3 a method due to Raman Sanyal [San09]. For any projection which preserves the k-skeleton of $\triangle_{\underline{n}}$, we construct via Gale duality a simplicial complex guaranted to be embeddable in a space of a certain dimension. The argument is then a topological obstruction based on Sarkaria's criterion for the embeddability of a simplicial complex in terms of colorings of Kneser graphs [Mat03]. We obtain the following result:

Theorem 5.17. *Let* $\underline{n} := (n_1, \dots, n_r)$ *with* $1 = n_1 = \dots = n_s < n_{s+1} \leq \dots \leq n_r$. *Then:*

1. *If*
$$0 \leq k \leq \sum_{i=s+1}^{r} \left\lfloor \frac{n_i - 2}{2} \right\rfloor + \max \left\{ 0, \left\lfloor \frac{s-1}{2} \right\rfloor \right\},$$
then $\delta_{pr}(k, \underline{n}) \geq 2k + r - s + 1$.
2. *If* $k \geq \left\lfloor \frac{1}{2} \sum_i n_i \right\rfloor$ *then* $\delta_{pr}(k, \underline{n}) \geq \sum_i n_i$. □

In particular, the upper and lower bounds provided by Theorems 5.14 and 5.17 match over a wide range of parameters:

Theorem 5.18. *For any* $\underline{n} := (n_1, \dots, n_r)$ *with* $r \geq 1$ *and* $n_i \geq 2$ *for all* i, *and for any* k *such that* $0 \leq k \leq \sum_{i \in [r]} \left\lfloor \frac{n_i - 2}{2} \right\rfloor$, *the smallest* $(k, \underline{n})$-PPSN *polytope has dimension exactly* $2k + r + 1$. *In other words:*

$$\delta_{pr}(k, \underline{n}) = 2k + r + 1.$$
□

Remark 5.19. The last two sections of Chapter 7 consist in applying (and partially extending) methods and results on projections of polytopes developed by Raman Sanyal and Günter Ziegler [Zie04, SZ10, San09]. We have decided to develop them in this dissertation since their application to products of simplices yields new results which complete our study on polytopality of products. Moreover, after the completion of our work on obstructions for projections of products of simplices, we learned that Thilo Rörig and Raman Sanyal obtained similar results in a recent work [RS09] (see also [Rör08, San08]).

5.3 Sources of material

The work presented in the second part of this thesis was initiated during my stay at the *Centre de Recerca Matemàtica* in Barcelona for the *i-MATH Winter School DocCourse Combinatorics and Geometry 2009: Discrete and Computational Geometry* [CRM09], under the tutoring of Julian Pfeifle. The results presented in the coming chapters have been submitted in two papers in collaboration with participants of this event:

1. The motivation for studying polytopality of products of graphs came from the course of Günter Ziegler [CRM09] who presented the prototype example of this question: "is the product of two Petersen graphs polytopal?" The (partial) answers that we propose to this question are developed in a preprint written in collaboration with Julian Pfeifle and Francisco Santos [PPS10].

2. The study of PSN polytopes was proposed by Julian Pfeifle as a research project during this DocCourse [CRM09]. Our results are exposed in a preprint in collaboration with Benjamin Matschke and Julian Pfeifle [MPP09].

Chapter Six

CARTESIAN PRODUCTS OF NON-POLYTOPAL GRAPHS

This chapter is devoted to a discussion on polytopality of graphs. In Section 6.1, we shortly review and discuss the current knowledge concerning polytopality of general graphs. We attach a particular attention to a variety of examples (some of which are well-known while some others are originals), which we will use afterwards. In Section 6.2, we focus on Cartesian products of graphs. This product is defined in such a way that the graph of a product of polytopes is the product of their graphs; in particular, products of polytopal graphs are automatically polytopal. This Chapter concerns the reciprocal statement: are the two factors of a polytopal product necessarily polytopal?

6.1 POLYTOPALITY OF GRAPHS

Definition 6.1. *A graph G is polytopal if it is isomorphic to the 1-skeleton of some polytope P. If P is d-dimensional, we say that G is d-polytopal.*

In small dimension, polytopality is easy to deal with. For example, 2-polytopal graphs are exactly cycles. The first interesting question is 3-polytopality, which is characterized by Steinitz' "fundamental theorem of convex types":

Theorem 6.2 (Steinitz [Ste22])**.** *A graph G is the graph of a 3-polytope P if and only if G is planar and 3-connected. Moreover, the combinatorial type of P is uniquely determined by G.* □

We refer to [Grü03, Zie95] for a discussion on three possible approaches for the proof of this fundamental theorem.

Throughout this chapter, we will notice that a first step to realize a graph G is to understand the possible face lattice of a polytope realizing G. For example, it is often difficult to decide what cycles of G can be the graphs of 2-faces of a d-polytope realizing G. In dimension 3, graphs of 2-faces are characterized by the following separation condition:

Theorem 6.3 (Whitney [Whi32])**.** *Let G be the graph of a 3-polytope P. The graphs of the faces of P are precisely the induced cycles in G that do not separate G.* □

In contrast to the easy 2- and 3-dimensional worlds, d-polytopality becomes much more involved as soon as $d \geq 4$. As an illustration, the existence of neighborly polytopes (see the cyclic polytopes in Proposition 5.5) proves that all possible edges can be present in the graph of a 4-polytope. Starting from a neighborly polytope, and stacking vertices on undesired edges, one can even observe the following:

Observation 6.4 (Perles)**.** Every graph is an induced subgraph of the graph of a 4-polytope.

It is a long-standing question of polytope theory how to determine whether a graph is d-polytopal or not. In the next section, we recall some general necessary conditions and apply them to discuss polytopality of small examples.

6.1.1 Necessary conditions for polytopality

Proposition 6.5. *A d-polytopal graph G satisfies the following properties:*

1. Balinski's Theorem*: G is d-connected [Bal61].*
2. Principal Subdivision Property *(d-PSP): Every vertex of G is the principal vertex of a principal subdivision of K_{d+1}. Here, a* subdivision *of K_{d+1} is obtained by replacing edges by paths, and a* principal subdivision *of K_{d+1} is a subdivision in which all edges incident to a distinguished* principal vertex *are not subdivided [Bar67].*
3. Separation Property*: The maximal number of components into which G may be separated by removing $n > d$ vertices equals $f_{d-1}\big(C_d(n)\big)$, the maximum number of facets of a d-polytope with n vertices [Kle64].* □

Remark 6.6. The principal subdivision property together with Steinitz' Theorem ensure that no graph of a 3-polytope is d-polytopal for $d \neq 3$. In other words, any 3-polytope is the unique polytopal realization of its graph. This property is also obviously true in dimension 0, 1 or 2. In contrast, it is strongly wrong in dimension 4 and higher.

Before providing examples of application of Proposition 6.5, let us insist on the fact that these necessary conditions are not sufficient (see also Examples 6.15 and 6.22):

Example 6.7 (Non-polytopality of the complete bipartite graph [Bar67])**.** For any two integers $m, n \geq 3$, the complete bipartite graph $K_{m,n}$ is not polytopal, although $K_{n,n}$ satisfies all properties of Proposition 6.5 to be 4-polytopal as soon as $n \geq 7$.

Indeed, assume that $K_{n,m}$ is the graph of a d-polytope P. Then $d \geq 4$ because $K_{n,m}$ is non-planar. Consider the induced subgraph H of $K_{n,m}$ corresponding to some 3-face F of P. Because H is induced and has minimum degree at least 3, it contains a $K_{3,3}$ minor, so F was not a 3-face after all.

Example 6.8 (Circulant graphs)**.** Let n be an integer and S be a subset of $\big\{1, \dots, \lfloor \frac{n}{2} \rfloor\big\}$. The *circulant* graph $\Gamma_n(S)$ is the graph whose vertex set is $\mathbb{Z}_n$ and whose edge set is the set of pairs of vertices whose difference lies in $S \cup (-S)$. Observe that the degree of $\Gamma_n(S)$ is precisely $|S \cup (-S)|$ (in particular, the degree is odd only if n is even and S contains $n/2$) and that $\Gamma_n(S)$ is connected if and only if $S \cup \{n\}$ is relatively prime. For example, Figure 6.1 represents all connected circulant graphs on at most 8 vertices.

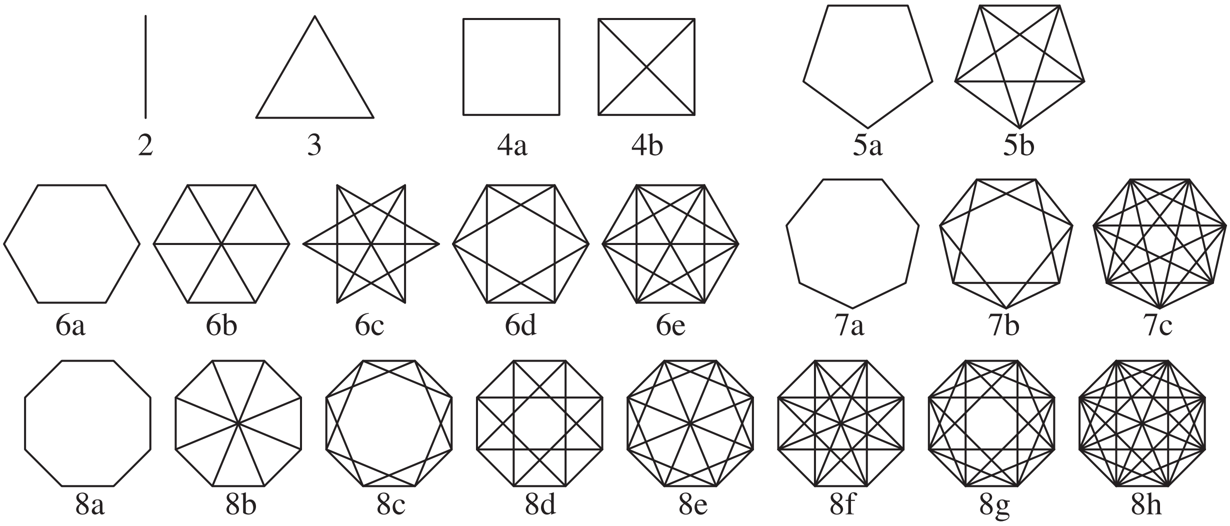

Figure 6.1: Connected circulant graphs with at most 8 vertices.

Using Proposition 6.5 we can determine the polytopality of various circulant graphs:

$\boxed{\text{Degree } 2}$ A connected graph of degree 2 is a cycle, and thus the graph of a polygon.

$\boxed{\text{Degree } 3}$ Up to isomorphism, the only connected circulant graphs of degree 3 are $\Gamma_{2m}(1, m)$ and $\Gamma_{4m+2}(2, 2m+1)$. When $m \geq 3$, the first one is not planar, and thus not polytopal. The second one is the graph of a prism over a $(2m+1)$-gon.

$\boxed{\text{Degree } 4}$ As soon as we reach degree 4, we cannot provide a complete description of polytopal circulant graphs, but we can discuss special cases, namely the circulant graphs $\Gamma_n(1, s)$ for $s \in \{2, 3, 4\}$:

(a) $s = 2$: For any $m \geq 2$, the graph $\Gamma_{2m}(1, 2)$ is the graph of an antiprism over an m-gon. In contrast, for any $m \geq 3$, the graph $\Gamma_{2m+1}(1, 2)$ is not polytopal: it is not planar and does not satisfy the principal subdivision property for dimension 4.

(b) $s \in \{3, 4\}$: For any $n \geq 7$, the graph $\Gamma_n(1, 3)$ is not polytopal. Indeed, the 4-cycles induced by the vertices $\{1, 2, 3, 4\}$ and $\{2, 3, 4, 5\}$ should define 2-faces of any realization (because of Theorem 6.3 in dimension 3 and of Proposition 6.12 in dimension 4), but they intersect improperly. Similarly, for any $n \geq 9$, the graph $\Gamma_n(1, 4)$ is not polytopal.

$\boxed{\text{Degree } n-2}$ The graph $\Gamma_{2m}(1, 2, \ldots, m-1)$ is the only circulant graph with two vertices more than its degree. It is not planar when $m \geq 4$ and it is not $(2m-2)$-polytopal since it does not satisfy the principal subdivision property in this dimension. However, it is always the graph of the m-dimensional cross-polytope, and when m is even, it is also the graph of the join of two $(m/2)$-dimensional cross-polytopes.

$\boxed{\text{Degree } n-1}$ The complete graph on n vertices is the graph of any neighborly polytope, and its polytopality range is $\{4, \ldots, n-1\}$ (as soon as $n \geq 5$).

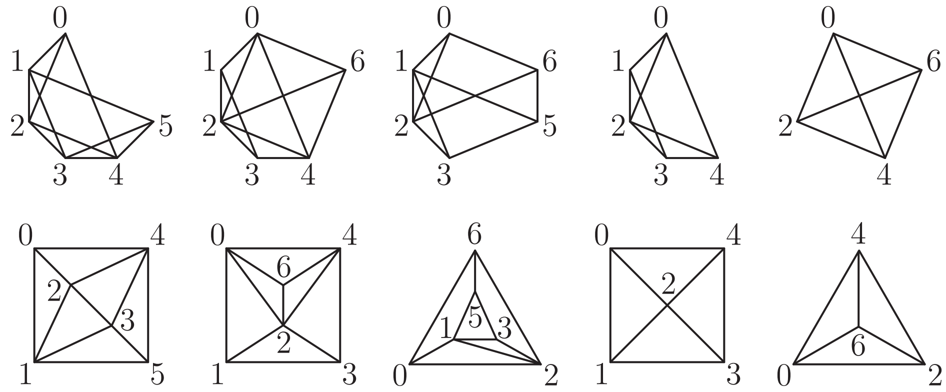

Figure 6.2: The 3-polytopal induced subgraphs of the circulant graph $\Gamma_8(1,2,4)$. The faces of the planar drawing below each of these subgraphs are the 2-faces of the corresponding 3-polytope.

The sporadic cases developed above are sufficient to determine the polytopality range of all circulant graphs on at most 8 vertices, except the graphs 8e and 8f of Figure 6.1 that we treat separately now. None of them can be 3-polytopal since they are not planar. We prove that they are not 4-polytopal by discussing what could be the 3-faces of a possible realization:

- We start with the graph $\Gamma_8(1,3,4)$ represented in Figure 6.1(8f). Consider any subgraph of $\Gamma_8(1,3,4)$ induced by 6 vertices. If the distance between the two missing vertices is odd (resp. even), then the subgraph is not planar (resp. not 3-connected). Consequently, any subgraph of $\Gamma_8(1,3,4)$ induced by 7 vertices is not planar, while any subgraph of $\Gamma_8(1,3,4)$ induced by 5 vertices is not 3-connected. Thus, the only possible 3-faces are tetrahedra, but $\Gamma_8(1,3,4)$ contains only 4 induced K_4. Thus, $\Gamma_8(1,3,4)$ is not polytopal.
- The case of $\Gamma_8(1,2,4)$ is more involved. Up to rotation, its only 3-polytopal induced subgraphs are represented in Figure 6.2. Assume that the subgraph induced by $\{0,1,2,3,4,5\}$ defines a 3-face F in a realization P of $\Gamma_8(1,2,4)$. Then the triangle 123 is a 2-face of P and thus should be contained in another 3-face of P. But any 3-face which contains 123 also contains either 0 or 4, and thus intersects improperly with F. Consequently, the subgraph induced by $\{0,1,2,3,4,5,6\}$ cannot define a 3-face of a realization of $\Gamma_8(1,2,4)$. For the same reason, the subgraphs induced by $\{0,1,2,3,4,6\}$ and $\{0,1,2,3,4\}$ cannot define 3-faces. Assume now that the subgraph induced by $\{0,1,2,3,5,6\}$ forms a 3-face in a realization P of $\Gamma_8(1,2,4)$. Then the triangle 123 is a 2-face of P and should be contained in another 3-face of P. The only possibility is the subgraph induced by $\{1,2,3,4,6,7\}$ which intersects improperly F. Finally, the only possible 3-faces are the two tetrahedra induced respectively by the odd and the even vertices, and thus, $\Gamma_8(1,2,4)$ is not polytopal.

The following table summarizes the polytopality range of all the graphs of Figure 6.1:

2	3	4a	4b	5a	5b	6a	6b	6c	6d	6e
$\{1\}$	$\{2\}$	$\{2\}$	$\{3\}$	$\{2\}$	$\{4\}$	$\{2\}$	$\emptyset$	$\{3\}$	$\{3\}$	$\{4,5\}$

7a	7b	7c	8a	8b	8c	8d	8e	8f	8g	8h
$\{2\}$	$\emptyset$	$\{4,5,6\}$	$\{2\}$	$\emptyset$	$\{3\}$	$\emptyset$	$\emptyset$	$\emptyset$	$\{4,5\}$	$\{4,5,6,7\}$

Example 6.9 (A graph whose polytopality range is $\{d\}$ [Kle64]). An interesting application of the separation property of Proposition 6.5 is the possibility to construct, for any integer d, a polytope whose polytopality range is exactly the singleton $\{d\}$. The construction, proposed by Victor Klee [Kle64], consists in stacking a vertex on all facets of the cyclic polytope $C_d(n)$ (for example on all facets of a simplex). The graph of the resulting polytope can be separated in $f_{d-1}(C_d(n))$ isolated points by removing the n initial vertices, and thus is not d'-polytopal for $d' < d$, by the separation property. It can not be d'-polytopal for $d' > d$ either, since the stacked vertices have degree d (because the cyclic polytope is simplicial). Thus, the dimension of the resulting graph is not ambiguous.

6.1.2 Simple polytopes

A d-polytope is *simple* if its vertex figures are simplices. In other words, its facet-defining hyperplanes are in general position, so that a vertex is contained in exactly d facets, and also in exactly d edges (and thus the graph of a simple d-polytope is d-regular). Surprisingly, a d-regular graph can be realized by at most one simple polytope:

Theorem 6.10 ([BML87, Kal88]). *Two simple polytopes are combinatorially equivalent if and only if they have the same graph.* □

This property, conjectured by Micha Perles, was first proved by Roswitha Blind and Peter Mani [BML87]. Gil Kalai [Kal88] then gave a very simple way of reconstructing the face lattice from the graph, and Eric Friedman [Fri09] showed that this can even be done in polynomial time.

As mentioned previously, the first step to find a polytopal realization of a graph is often to understand how can the face lattice of this realization look like. Theorem 6.10 ensures that if the realization is simple, there is only one choice. This motivates to temporarily restrict the study of realization of regular graphs only to simple polytopes:

Definition 6.11. *A graph is* simply d-polytopal *if it is the graph of a simple d-polytope.*

We can exploit properties of simple polytopes to obtain results on the simple polytopality of graphs. For us, the key property turns out to be that any k-tuple of edges incident to a vertex of a simple polytope is contained in a k-face. For example, this implies the following result:

Proposition 6.12. *All induced cycles of length 3, 4 and 5 in the graph of a simple d-polytope P are graphs of 2-faces of P.*

Proof. For 3-cycles, the result is immediate: any two adjacent edges of a 3-cycle induce a 2-face, which must be a triangle because the graph is induced.

Next, let $\{a, b, c, d\}$ be consecutive vertices of a 4-cycle in the graph of a simple polytope P. Any pair of edges emanating from a vertex lies in a 2-face of P. Let C_a be the 2-face of P that contains the edges $\operatorname{conv}\{a, b\}$ and $\operatorname{conv}\{a, d\}$. Similarly, let C_c be the 2-face of P that contains $\operatorname{conv}\{b, c\}$ and $\operatorname{conv}\{c, d\}$. If C_a and C_c were distinct, they would intersect improperly, at least in the two vertices b and d. Thus, $C_a = C_c = \operatorname{conv}\{a, b, c, d\}$ is a 2-face of P.

The case of 5-cycles is a little more involved. We first show it for 3-polytopes. If a 5-cycle C in the graph G of a simple 3-polytope does not define a 2-face, it separates G into two nonempty subgraphs A and B (Theorem 6.3). Since G is 3-connected, both A and B are connected to C by at least three edges. But the endpoints of these six edges must be distributed among the five vertices of C, so one vertex of C receives two additional edges, and this contradicts simplicity.

For the general case, we show that any 5-cycle C in a simple polytope is contained in some 3-face, and apply the previous argument (a face of a simple polytope is simple). First observe that any three consecutive edges in the graph of a simple polytope lie in a common 3-face. This is true because any two adjacent edges define a 2-face, and a 2-face together with another adjacent edge defines a 3-face. Thus, four of the vertices of C are already contained in a 3-face F. If the fifth vertex w of C lies outside F, then the 2-face defined by the two edges of C incident to w intersects improperly with F. $\square$

Remark 6.13. Observe that there is an induced 6-cycle in the graph of the cube (resp. an induced p-cycle in the graph of a double pyramid over a p-cycle, for $p \geq 3$) which is not the graph of a 2-face. It is also interesting to notice that contrarily to dimension 3 (Theorem 6.3), the 2-faces of a 4-polytope are not characterized by a separation property: a pyramid over a cube has a non-separating induced 6-cycle which does not define a 2-face.

Corollary 6.14. *A simply polytopal graph cannot:*

(i) be separated by an induced cycle of length 3, 4 *or* 5.

(ii) contain two induced cycles of length 4 *or* 5 *which share* 3 *vertices.* $\square$

Example 6.15 (An infinite family of non-polytopal graphs for non-trivial reasons [NdO09]). Consider the family of graphs suggested in Figure 6.3. The nth graph of this family is the graph G_n whose vertex set is $\mathbb{Z}_{2n+3} \times \mathbb{Z}_2$ and where the vertex (x, y) is related with the vertices $(x+y+1, y)$, $(x+y, y+1)$, $(x-y-1, y)$ and $(x+y-1, y+1)$.

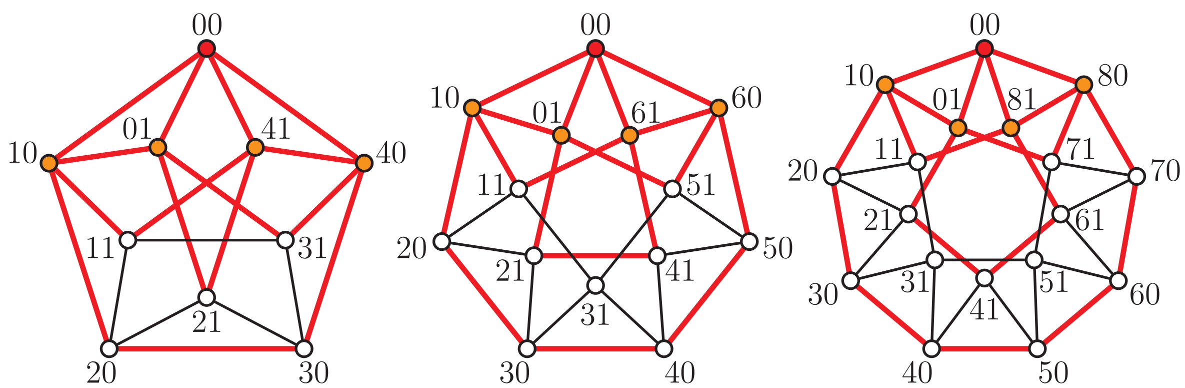

Figure 6.3: An infinite family of non-polytopal graphs (for non-trivial reasons). The vertex 00 is the principal vertex of a principal subdivision of K_5 whose edges are colored in red.

Observe first that the graphs of this family satisfy all necessary conditions of Proposition 6.5:

1. They are 4-connected: when we remove 3 vertices, either the external cycle $\{i0 \mid i \in \mathbb{Z}_{2n+1}\}$ or the internal cycle $\{i1 \mid i \in \mathbb{Z}_{2n+1}\}$ remains a path, to which all the vertices are connected.

2. They satisfy the principal subdivision property for dimension 4: the edges of a principal subdivision of K_5 with principal vertex 00 are colored in Figure 6.3.
3. They satisfy the separation property: the cyclic 4-polytope on m vertices has $\frac{m(m-3)}{2}$ facets while removing m vertices from G_n cannot create more than m connected components.

Consider the first graph G_1 of this family (on the left in Figure 6.3). Since the 5-cycles induced by $\{00, 10, 20, 30, 40\}$ and $\{00, 10, 20, 21, 41\}$ share two edges, G_1 is not polytopal (because of Theorem 6.3 in dimension 3 and of Proposition 6.12 in dimension 4). In fact, Proposition 6.12 even excludes all graphs of the family:

Lemma 6.16. *None of the graphs of the infinite family suggested in Figure 6.3 is polytopal.*

Proof. Since they contain a subdivision of K_5, they are not 3-polytopal.

Denote by e_i the edge of the external cycle from vertex $i0$ to vertex $(i+1)0$. If the graph G_n were 4-polytopal, then all 3- and 4-cycles would define 2-faces. Now consider two consecutive angles e_1e_2 and e_2e_3 of the external cycle. Each of them defines a 2-face by simplicity. These two 2-faces must in fact coincide, since e_2 is already contained in a square and a triangular 2-face, none of which contain the angles e_1e_2 and e_2e_3. By iterating this argument, we obtain that the entire external cycle forms a 2-face.

Consider a 3-face F containing the external cycle. The edge e_1 must also be contained in either the adjacent square or the adjacent triangle; without loss of generality, let it be the square. Then the triangle adjacent to the next edge e_2 must also be in F (because F already contains two of its edges). By the same reasoning, the square adjacent to e_3 is also contained in F, and iterating this argument (and using that n is odd) shows that in fact F contains all the squares and triangles of G_n, contradiction. □

6.1.3 Truncation and star-clique operation

We consider the polytope $\tau_v(P)$ obtained by cutting off a single vertex v in a polytope P: the set of inequalities defining $\tau_v(P)$ is that of P together with a new inequality satisfied by all the vertices of P except v. The faces of $\tau_v(P)$ are: (i) all the faces of P which do not contain v; (ii) the truncations $\tau_v(F)$ of all faces F of P containing v; and (iii) the vertex figure of v in P together with all its faces. In particular, if v is a simple vertex in P, then the truncation of v in P replaces v by a simplex. On the graph of P, it translates into the following transformation:

Definition 6.17. *Let G be a graph and v be a vertex of degree d of G. The star-clique operation (at v) replaces vertex v by a d-clique K, and assigns one edge incident to v to each vertex of K. The resulting graph $\sigma_v(G)$ has $d-1$ more vertices and $\binom{d}{2}$ more edges.*

Example 6.18. The truncation of a vertex in a d-simplex creates (combinatorially) a prism over a $(d-1)$-simplex. Its graph is the product $K_2 \times K_d$ and thus can be realized as the product of a segment by any neighborly polytope P on d vertices. The next chapter will furthermore prove that it is also 4-polytopal. Observe that the complete graph is also realized by any neighborly polytope but that the result of the truncation of a vertex in such a polytope is not always a star-clique operation on the graph (it is the case only when the vertex figure of the cutted vertex in the realization is neighborly).

Proposition 6.19. *Let v be a vertex of degree d in a graph G. Then $\sigma_v(G)$ is d-polytopal if and only if G is d-polytopal.*

Proof. If a d-polytope P realizes G, then the truncation $\tau_v(P)$ realizes $\sigma_v(G)$. For the other direction, consider a d-polytope Q which realizes $\sigma_v(G)$. We use simplicity to assert that the d-clique replacing v forms a facet F of Q. Up to a projective transformation, we can assume that the d facets of Q adjacent to F intersect behind F. Then, removing the inequality defining F from the facet description of Q creates a polytope which realizes G. □

Remark 6.20. In degree 3, star-clique operations, usually called ΔY-transformations, are used to prove Steinitz' Theorem 6.2. The argument is that any 3-connected and planar graph can be reduce to the complete graph K_4 by a sequence of such transformations (see [Zie95] for details).

We can exploit Proposition 6.19 to construct several families of non-polytopal graphs:

Corollary 6.21. *Any graph obtained from the graph of a 4-regular 3-polytope by a finite nonempty sequence of star-clique operations is non-polytopal.*

Proof. No such graph can be 3-polytopal since it is not planar. If the resulting graph were 4-polytopal, Proposition 6.19 would assert that the original graph was also 4-polytopal, which would contradict Remark 6.6. □

Example 6.22. For $n \geq 3$, consider the family of graphs suggested by Figure 6.4. They are constructed as follows: place a regular $2n$-gon C_{2n} into the plane, centered at the origin. Draw a copy C'_{2n} of C_{2n} scaled by $\frac{1}{2}$ and rotated by $\frac{\pi}{2n}$, and lift the vertices of C'_{2n} alternately to heights 1 and -1 into the third dimension. The graph $\diamond_n$ is the graph of the convex hull of the result.

Let $\diamond_n^\star$ be the result of successively applying the star-clique operation to all vertices on the external cycle C_{2n}. Corollary 6.21 ensures that $\diamond_n^\star$ is not polytopal, although it satisfies all necessary conditions to be 4-polytopal (we skip this discussion which is similar to that in Example 6.15).

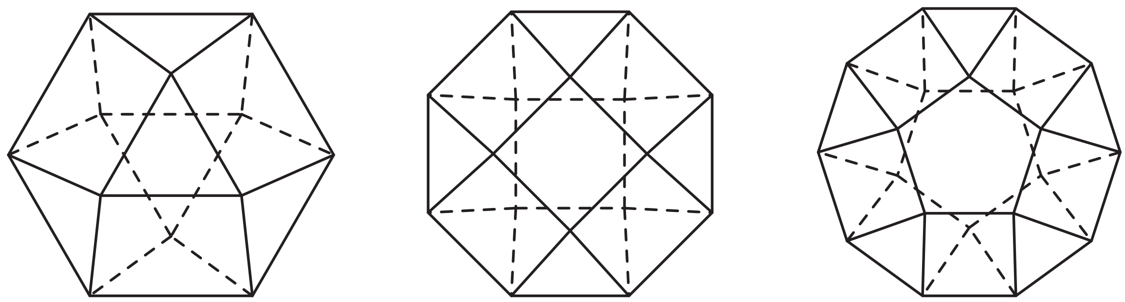

Figure 6.4: The graphs $\diamond_n$ for $n \in \{3, 4, 5\}$.

6.2 Polytopality of products of graphs

Define the *Cartesian product* $G \times H$ of two graphs G and H to be the graph with vertex set $V(G \times H) := V(G) \times V(H)$, and edge set $E(G \times H) := \big(V(G) \times E(H)\big) \cup \big(E(G) \times V(H)\big)$. In other words, for $a, c \in V(G)$ and $b, d \in V(H)$, the vertices (a, b) and (c, d) of $G \times H$ are adjacent if either $a = c$ and $\{b, d\} \in E(H)$, or $b = d$ and $\{a, c\} \in E(G)$. Notice that this product is usually denoted by $G \square H$ in graph theory. We choose to use the notation $G \times H$ to be consistent with the Cartesian product of polytopes: if G and H are the graphs of the polytopes P and Q respectively, then the product $G \times H$ is the graph of the product $P \times Q$. In this section, we focus on the polytopality of products of non-polytopal graphs.

As already mentioned, the factors of a polytopal product are not necessarily polytopal: consider for example the product of a triangle by a path, or the product of a segment by two glued triangles (see Figure 6.5 and more generally Proposition 6.30). We neutralize these elementary examples by further requiring the product $G \times H$, or equivalently the factors G and H, to be regular (the degree of a vertex (v, w) of $G \times H$ is the sum of the degrees of the vertices v of G and w of H). In this case, it is natural to investigate when such regular products can be simply polytopal. The answer is given by Theorem 6.24.

Our study of polytopality of products of graphs was inspired by Günter Ziegler's prototype question: "is the Cartesian product of two Petersen graphs polytopal?" In fact, observe that we incidentally already answered this question in the case of dimension 6 in Corollary 6.14: the product of two Petersen graphs cannot be simply polytopal since it contains two induced 5-cycles which share three vertices (more generally, Theorem 6.24 characterizes simple polytopality of products). However, we have no answer for dimensions 4 and 5: the combinatorial approach we use is not sufficient to prove non-polytopality since there exists a pseudo-manifold whose graph is the product of two Petersen graphs (see Proposition 6.40).

Before starting, let us observe that the necessary conditions of Proposition 6.5 are preserved under Cartesian products in the following sense:

Proposition 6.23. *If two graphs G and H are respectively d- and e-connected, and respectively satisfy d- and e-PSP, then their product $G \times H$ is $(d+e)$-connected and satisfies $(d+e)$-PSP.*

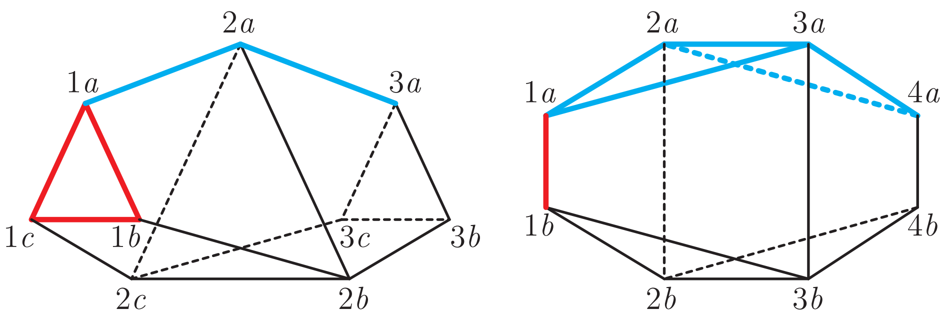

Figure 6.5: Polytopal products of non-polytopal graphs: the product of a triangle abc by a path 123 (left) and the product of a segment ab by two glued triangles 123 and 234 (right).

Proof. The connectivity of a Cartesian product of graphs was studied in [CS99]. In fact, it is even proved in [Špa08] that $\kappa(G \times H) = \min(\kappa(G)|H|, \kappa(H)|G|, \delta(G) + \delta(H)) \geq \kappa(G) + \kappa(H)$, where $\kappa(G)$ and $\delta(G)$ respectively denote the connectivity and the minimum degree of a graph G.

For the principal subdivision property, consider a vertex (v, w) of $G \times H$. Choose a principal subdivision of K_{d+1} in G with principal vertex v and neighbors N_v, and a principal subdivision of K_{e+1} in H with principal vertex w and neighbors N_w. This gives rise to a principal subdivision of K_{d+e+1} in $G \times H$ with principal vertex (v, w) and neighbors $(N_v \times \{w\}) \cup (\{v\} \times N_w)$. Indeed, for $x, x' \in N_v$, the vertices (x, w) and (x', w) are connected by a path in $G \times w$ by construction; similarly, for $y, y' \in N_w$, the vertices (v, y) and (v, y') are connected by a path in $v \times H$. Finally, for each $x \in N_v$ and $y \in N_w$, connect (x, w) to (v, y) via the path of length 2 that passes through (x, y). All these paths are disjoint by construction. □

6.2.1 Simply polytopal products

A product of simply polytopal graphs is automatically simply polytopal. We prove that the reciprocal statement is also true:

Theorem 6.24. *A product of graphs is simply polytopal if and only if its factors are.*

Applying Theorem 6.10, we obtain a strong characterization of the simply polytopal products:

Corollary 6.25. *Products of simple polytopes are the only simple polytopes whose graph is a product.* □

Let G and H be two connected regular graphs of degree d and e respectively, and assume that the graph $G \times H$ is the graph of a simple $(d + e)$-polytope P. By Proposition 6.12, for all edges a of G and b of H, the 4-cycle $a \times b$ is the graph of a 2-face of P.

Observation 6.26. Let F be any facet of P, let v be a vertex of G, and let $\{x, y\}$ be an edge of H such that $(v, x) \in F$ and $(v, y) \notin F$. Then $G \times \{x\} \subset F$ and $G \times \{y\} \cap F = \emptyset$.

Proof. Since the polytope is simple, all neighbors of (v, x) except (v, y) are connected to (v, x) by an edge of F. Let v' be a neighbor of v in G, and let C be the 2-face $\mathrm{conv}\{v, v'\} \times \mathrm{conv}\{x, y\}$ of P. If (v', y) were a vertex of F, the intersection $C \cap F$ would consist of exactly three vertices (because $(v, y) \notin F$), a contradiction. In summary, $(v', x) \in F$ and $(v', y) \notin F$, for all neighbors v' of v. Repeating this argument and using the fact that G is connected yields $G \times \{x\} \subset F$ and $G \times \{y\} \cap F = \emptyset$. □

Lemma 6.27. *The graph of any facet of P is either of the form $G' \times H$ for a $(d-1)$-regular induced subgraph G' of G, or of the form $G \times H'$ for an $(e-1)$-regular induced subgraph H' of H.*

Proof. Assume that the graph of a facet F is not of the form $G' \times H$. Then there exists a vertex v of G and an edge $\{x, y\}$ of H such that $(v, x) \in F$ and $(v, y) \notin F$. By Observation 6.26, the subgraph H' of H induced by the vertices $y \in H$ such that $G \times \{y\} \subset F$ is nonempty. We now prove that the graph $\mathrm{gr}(F)$ of F is exactly $G \times H'$.

The inclusion $G \times H' \subset \mathrm{gr}(F)$ is clear: by definition, $G \times \{y\}$ is a subgraph of $\mathrm{gr}(F)$ for any vertex $y \in H'$. For any edge $\{x, y\}$ of H' and any vertex $v \in G$, the two vertices (v, x) and (v, y) are contained in F, so the edge between them is an edge of F; if not, we would have an improper intersection between F and this edge.

For the other inclusion, let $H'' := \{y \in H \mid G \times \{y\} \cap F = \emptyset\}$ and $H''' := H \setminus (H' \cup H'')$. If $H''' \neq \emptyset$, the fact that H is connected ensures that there is an edge between some vertex of H''' and either a vertex of H' or H''. This contradicts Observation 6.26.

We have proved that $G \times H' = \mathrm{gr}(F)$. The fact that F is a simple $(d + e - 1)$-polytope and the d-regularity of G together ensure that H' is $(e - 1)$-regular. □

Proof of Theorem 6.24. One direction is clear. For the other direction, proceed by induction on $d+e$, the cases $d = 0$ and $e = 0$ being trivial. Now assume that $d, e \geq 1$, that $G \times H = \mathrm{gr}(P)$, and that G is not the graph of a d-polytope. By Lemma 6.27, all facets of P are of the form $G' \times H$ or $G \times H'$, where G' (resp. H') is an induced $(d - 1)$-regular (resp. $(e - 1)$-regular) subgraph of G (resp. H). By induction, the second case does not arise. We fix a vertex w of H. Then induction tell us that $F_w := G' \times \{w\}$ is a face of P, and $G' \times H$ is the only facet of P that contains F_w by Lemma 6.27. This cannot occur unless F_w is a facet, but this only happens in the base case $H = \{w\}$. □

Corollary 6.28. *Consider a graph G d-regular, d-connected, satisfying d-PSP, but not simply d-polytopal. Then, any product of G by a simply e-polytopal graph is $(d + e)$-regular, $(d + e)$-connected, satisfies $(d + e)$-PSP, but is not simply $(d + e)$-polytopal.*

Example 6.29. The product of the circulant graph $C_8(1, 4)$ by the graph of the d-dimensional cube is a non simply polytopal graph for non-trivial reasons. For any $m \geq 4$, the product of the circulant graph $C_{2m}(1, m)$ by a segment is non-polytopal for non-trivial reasons.

6.2.2 Polytopal products of non-polytopal graphs

In this section, we give a general construction to obtain polytopal products starting from a polytopal graph G and a non-polytopal one H. We need the graph H to be the graph of a *regular subdivision* of a polytope Q, that is, the graph of the upper[1] envelope (the set of all upper facets with respect to the last coordinate) of the convex hull of the point set $\{(q, \omega(q)) \mid q \in V(Q)\} \subset \mathbb{R}^{e+1}$ obtained by lifting the vertices of $Q \subset \mathbb{R}^e$ according to a *lifting function* $\omega : V(Q) \to \mathbb{R}$.

Proposition 6.30. *If G is the graph of a d-polytope P, and H is the graph of a regular subdivision of an e-polytope Q, then $G \times H$ is $(d + e)$-polytopal. In the case $d > 1$, the regular subdivision of Q can even have internal vertices.*

Proof. Let $\omega : V(Q) \to \mathbb{R}_{>0}$ be a lifting function that induces a regular subdivision of Q with graph H. Assume without loss of generality that the origin of $\mathbb{R}^d$ lies in the interior of P. For

[1]The unusual convention to define a subdivision as the projection of the upper facets of the lifting simplifies the presentation of the construction.

each $p \in V(P)$ and $q \in V(Q)$, we define the point $\rho(p,q) := (\omega(q)p, q) \in \mathbb{R}^{d+e}$. Consider

$$R := \operatorname{conv}\{\rho(p,q) \mid p \in V(P), q \in V(Q)\}.$$

Let g be a facet of Q defined by the linear inequality $\langle \psi \mid y \rangle \leq 1$. Then $\langle (0,\psi) \mid (x,y) \rangle \leq 1$ defines a facet of R, with vertex set $\{\rho(p,q) \mid p \in P, q \in g\}$, and isomorphic to $P \times g$.

Let f be a facet of P defined by the linear inequality $\langle \phi \mid x \rangle \leq 1$. Let c be a cell of the subdivision of Q, and let $\psi_0 h + \langle \psi \mid y \rangle \leq 1$ be the linear inequality that defines the upper facet corresponding to c in the lifting. Then we claim that the linear inequality

$$\chi(x,y) = \psi_0 \langle \phi \mid x \rangle + \langle \psi \mid y \rangle \leq 1$$

selects a facet of R with vertex set $\{\rho(p,q) \mid p \in f, q \in c\}$ that is isomorphic to $f \times c$. Indeed,

$$\chi\big(\rho(p,q)\big) = \chi(\omega(q)p, q) = \psi_0 \omega(q) \langle \phi \mid p \rangle + \langle \psi \mid q \rangle \leq 1,$$

where equality holds if and only if $\langle \phi \mid p \rangle = 1$ and $\psi_0 \omega(q) + \langle \psi \mid q \rangle = 1$, so that $p \in f$ and $q \in c$.

The above set $\mathcal{F}$ of facets of R in fact contains all facets: indeed, any $(d+e-2)$-face of a facet in $\mathcal{F}$ is contained in precisely two facets in $\mathcal{F}$. Since the union of the edge sets of the facets in $\mathcal{F}$ is precisely $G \times H$, it follows that the graph of R equals $G \times H$.

A similar argument proves the same statement in the case when $d > 1$ and H is a regular subdivision of Q with internal vertices (meaning that not only the vertices of Q are lifted, but also a finite number of interior points). $\square$

We already mentioned two examples obtained by such a construction in the beginning of this section (see Figure 6.5): the product of a polytopal graph by a path and the product of a segment by a subdivision of an n-gon with no internal vertex. Proposition 6.30 even produces examples of regular polytopal products which are not simply polytopal:

Example 6.31. Let H be the graph obtained by a star-clique operation from the graph of an octahedron. It is non-polytopal (Corollary 6.21), but it is the graph of a regular subdivision of a 3-polytope (see Figure 6.6). Consequently, the product of H by any regular polytopal graph is polytopal. Thus, there exist regular polytopal products which are not simply polytopal.

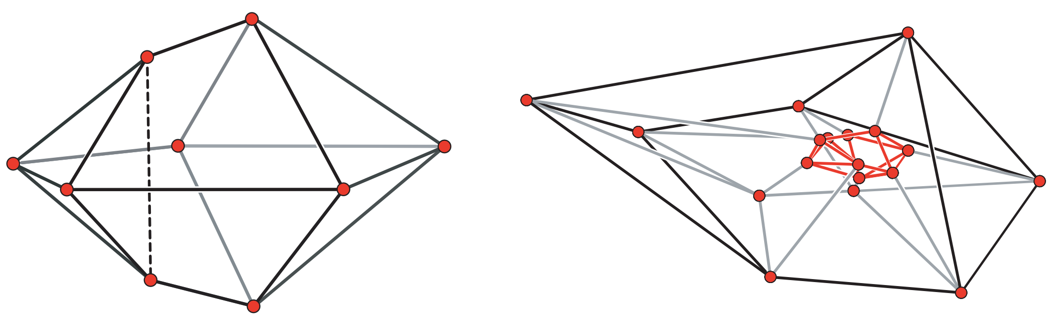

Figure 6.6: A non-polytopal 4-regular graph H which is the graph of a regular subdivision of a 3-polytope (left) and the Schlegel diagram of a 4-polytope whose graph is the product of H by a segment (right).

Finally, Proposition 6.30 also produces polytopal products of two non-polytopal graphs:

Example 6.32 (Product of dominos)**.** Define the *p-domino graph* D_p to be the product of a path P_p of length p by a segment. Let $p, q \geq 2$. Observe that D_p and D_q are not polytopal and that $D_p \times P_q$ is a regular subdivision of a 3-polytope. Consequently, the product of dominos $D_p \times D_q$ is a 4-polytopal product of two non-polytopal graphs (see Figure 6.7).

Finally, let us observe that the product $D_p \times D_q = P_p \times P_q \times (K_2)^2$ can be decomposed in different ways into a product of two graphs. However, in any such decomposition, at least one of the factors is non-polytopal.

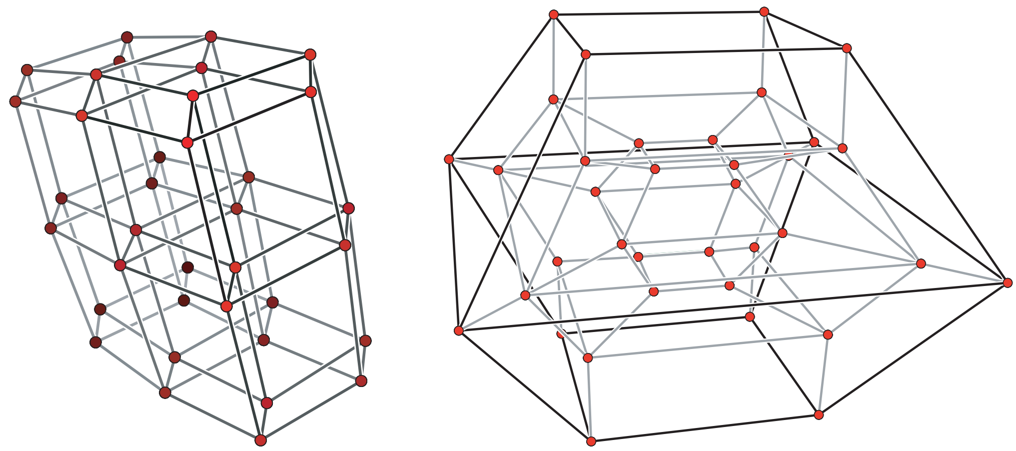

Figure 6.7: The graph of the product of two 2-dominos (left) and the Schlegel diagram of a realizing 4-polytope (right).

6.2.3 Product with a segment

In this section, we complete our list of examples of products of a segment by a regular graph H. The goal is to illustrate all possible behaviors of such a product regarding polytopality:

1. If H is polytopal, then $K_2 \times H$ is polytopal. However, some ambiguities can appear:
   a) either the dimension is ambiguous. For example, $K_2 \times K_n$ is realized by the product of a segment by any neighborly polytope. See Chapter 7 for a discussion on dimensional ambiguity of products of complete graphs.
   b) or the dimension is unambiguous, but there exist realizations in the same dimension which are not combinatorially equivalent. In this case, H is not simply polytopal (Theorem 6.10). In Proposition 6.36, we determine all possible realizations of the graph of a prism over an octahedron.
   c) or there is no ambiguity at all. It is the case for example if H is simply 3-polytopal.
2. If H is not polytopal, then $K_2 \times H$ is not simply polytopal (Theorem 6.24). However:
   a) either $K_2 \times H$ is polytopal in smaller dimension (Example 6.31).
   b) or $K_2 \times H$ is not polytopal at all. It is the case when H is the complete graph $K_{n,n}$ (Proposition 6.33) or when H is non-polytopal and 3-regular (Proposition 6.35).

Proposition 6.33. *For $n \geq 3$, the graph $K_2 \times K_{n,n}$ is not polytopal.*

To prove this proposition, we will need the following well known lemma:

Lemma 6.34. *A 3-polytope with no triangular facet has at least 8 vertices.*

Proof. Let P be a 3-polytope. For $k \geq 3$, denote by v_k the number of vertices of degree k and by p_k the number of 2-faces with k vertices. By double counting and Euler's Formula (see [Grü03, Chapter 13] for details),

$$v_3 + p_3 = 8 + \sum_{k \geq 5} (k-4)(v_k + p_k).$$

The lemma immediately follows. □

Proof of Proposition 6.33. Observe that $K_2 \times K_{n,n}$ is not d-polytopal for $d \leq 3$ because it contains a $K_{3,3}$-minor, and for $d = n+1$ by Theorem 6.24.

The proof proceeds by contradiction. Suppose that $K_2 \times K_{n,n}$ is the graph of a d-polytope P, for some d with $3 \leq d \leq n$, and consider a 3-face F of P. Since $K_2 \times K_{n,n}$ contains no triangle, Lemma 6.34 says that F has at least 8 vertices. Denote by A and B the two maximal independent sets in $K_{n,n}$, and by A_0, B_0, A_1, B_1 their corresponding copies in the cartesian product $K_2 \times K_{n,n}$. We discuss the possible repartition of the vertices of F in these sets.

Assume first that F has at least three vertices in A_0; let x, y, z be three of them. Then it cannot have more than two vertices in B_0, because otherwise its graph would contain a copy of $K_{3,3}$. In fact, there must be exactly two vertices u, v in B_0: since any vertex of F has degree at least 3, and each vertex in A_0 can only be connected to vertices in B_0 or to its corresponding neighbor in A_1, each vertex of F in A_0 must have at least, and thus exactly, two neighbors in B_0 and one in A_1. Thus, F also has at least three vertices in A_1, and by the same reasoning, there must be exactly two vertices in B_1; call one of them w. But now $\{x, y, z\}$ and $\{u, v, w\}$ are the two maximal independent sets of a subdivision of $K_{3,3}$ included in F.

By symmetry and Lemma 6.34, F has exactly two vertices in each of the sets A_0, B_0, A_1, B_1. Since all these vertices have degree 3, we have proved that P's only 3-faces are combinatorial cubes whose graphs are cartesian products of K_2 with 4-cycle in $A_0 \cup B_0 = K_{n,n}$. However, this 4-cycle is not contained in any other 3-face, which is an obstruction to the existence of P. □

Proposition 6.35. *If H is a non-polytopal and 3-regular graph, then $K_2 \times H$ is non-polytopal.*

Proof. We distinguish two cases:

(i) If H contains a K_4-minor, then $K_2 \times H$ is not 3-polytopal because it contains a K_5-minor, and it is not 4-polytopal by Theorem 6.24. Since $K_2 \times H$ is 4-regular, these are the only possibilities.

(ii) Otherwise, H is a series-parallel graph. Thus, it can be obtained from K_2 by a sequence of *series* and *parallel* extensions, *i.e.* subdividing or duplicating an edge. Since duplicating an edge creates a double edge, and subdividing an edge yields a vertex of degree two, H is either not simple or not 3-regular. □

To complete our collection of examples of products with a segment, we examine the possible realizations of the graph of the prism over the octahedron:

Proposition 6.36. *The graph of the prism over the octahedron is realized by exactly four combinatorially different polytopes.*

In order to exhibit four different realizations, we need to remember the context and the proof of Proposition 6.30. Given the graph G of a d-polytope P and the graph H of a regular subdivision of an e-polytope Q defined by a lifting function $\omega : V(Q) \to \mathbb{R}$, we construct a $(d+e)$-polytope with graph $G \times H$ as follows: we start from the product $P \times Q$ and we deform each face $\{p\} \times Q$ according to the lifting function ω. This subdivides the face $\{p\} \times Q$ and makes appear the subgraph $\{p\} \times H$ of the product $G \times H$. We want to observe now that the deformation can be different at each vertex of P: we can use at each vertex of P a different lifting function, which will produce combinatorially different polytopes.

To illustrate this, we come back to the prism over the octahedron. Denote by H the graph of the octahedron. Observe that the octahedron has four regular subdivisions with no additional edges: the octahedron itself (for a constant lifting function) and the three subdivisions of the octahedron into two egyptian pyramids glued along their square face (for a lifting function positive on one vertex, negative on the opposite one, and vanishing on the other four vertices). This leads to four combinatorially different realizations of $K_2 \times H$: in our previous construction, we can choose either the octahedron at both ends of the segment (thus obtaining the prism over the octahedron), or the octahedron at one end and the glued square pyramid at the other, or the glued square pyramids for both ends of the segment (and this leads to two possibilities according on whether we choose the same square or two orthogonal squares to subdivide the octahedron).

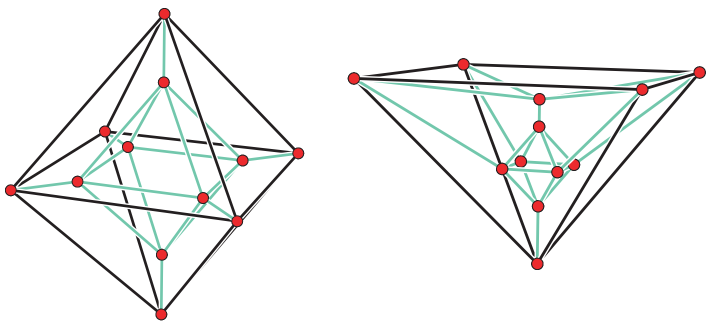

Figure 6.8: The prism over the octahedron (left) and a combinatorially different polytope with the same graph (right).

In fact, by the same argument, we can even slightly improve Proposition 6.30:

Observation 6.37. Let G be the graph of a d-polytope P and H be the graph of an e-polytope Q. For all $v \in G$, choose a lifting function $\omega_v : V(Q) \to \mathbb{R}$, and denote by H_v the graph of the corresponding regular subdivision of Q. Then the graph obtained by replacing in $G \times H$ the subgraph $\{v\} \times H$ by $\{v\} \times H_v$ is polytopal.

The result remains true if $d > 1$ and all subdivisions of Q have the same interior points.

It remains to prove that any realization of $K_2 \times H$ is combinatorially equivalent to one of the four described above. First, the dimension is unambiguous: $K_2 \times H$ can only be 4-polytopal (by Remark 6.6 and Theorem 6.24). In particular, any realization has the following property:

Definition 6.38. *A d-polytope is* almost simple *if its graph is $(d+1)$-regular.*

The vertex figures of a simple polytope are all simplices, which implies that any two incident edges in a simple polytope lie in a common 2-face. For almost simple polytopes, the vertex figures are almost as restricted: they are *$(d-1)$-circuits*, that is, $(d-1)$-polytopes with $d+1$ vertices. This implies the following property:

Proposition 6.39. *Let $\{v, w\}$ be an edge of an almost simple d-polytope P. Then:*
(a) either $\{v, w\}$ together with any other edge incident to v forms a 2-face;
(b) or there exists exactly one more edge incident to v which does not form a 2-face with $\{v, w\}$, but any two 2-faces both incident to $\{v, w\}$ lie in a 3-face.

Proof. Consider the vertex figure F_v of v. It is a $(d-1)$-polytope with $d+1$ vertices, one of which, say $\overline{w}$, corresponds to the edge $\{v, w\}$. This vertex $\overline{w}$ can be adjacent to either d or $d-1$ vertices of F_v. The first case corresponds to statement (a). In the second case, $\overline{w}$ has exactly one missing edge in F_v (corresponding to a missing 2-face in P), but the edge figure of $\{v, w\}$ is a $(d-2)$-simplex. This implies statement (b). ☐

With this in mind, we can finally prove Proposition 6.36:

Proof of Proposition 6.36. We first introduce some notations: let $V := \{1, \bar{1}, 2, \bar{2}, 3, \bar{3}\}$ denote the 6 vertices of the octahedron such that $\{1, \bar{1}\}$, $\{2, \bar{2}\}$ and $\{3, \bar{3}\}$ are the three missing edges, and let a and b denote the two endpoints of the segment factor. We denote the vertices of $K_2 \times H$ by $\{1a, 1b, \bar{1}a, \dots, \bar{3}b\}$. We call *horizontal edges* the edges of the form $\{ia, ib\}$, for $i \in V$, and *vertical edges* the edges of the form $\{ix, jx\}$, for $i \in V$, $j \in V \setminus \{i, \bar{i}\}$ and $x \in \{a, b\}$.

We first use "almost simplicity" to study the possible 2-faces of a realization P of $K_2 \times H$. Assume that there exists a 2-face F which is neither a triangle nor a square. It has to contain an angle between a horizontal edge and a vertical edge, say without loss of generality $\{1a, 1b\}$ and $\{1a, 2a\}$. By inducedness, the next edges of F are necessarily $\{2a, \bar{1}a\}$ and $\{\bar{1}a, \bar{1}b\}$. Since the edges $\{1a, 1b\}$ and $\{1a, 2a\}$ form an angle of F, the two edges $\{2a, 2b\}$ and $\{1b, 2b\}$ cannot form an angle: otherwise the 4-cycle $(1a, 1b, 2b, 2a)$ would form a square face which improperly intersects F. Similarly, since the edges $\{2a, \bar{1}a\}$ and $\{\bar{1}a, \bar{1}b\}$ form an angle, the edges $\{2a, 2b\}$ and $\{2b, \bar{1}b\}$ cannot form an angle. Thus, $\{2a, 2b\}$ is adjacent to two missing angles, which is impossible by Proposition 6.39. We conclude that the 2-faces of any realization of $K_2 \times H$ can only be squares and triangles.

We now use this information on the 2-faces to understand the possible 3-faces of P. Assume first that none of the angles of the 4-cycles $(1a, 2a, \bar{1}a, \bar{2}a)$, $(1a, 3a, \bar{1}a, \bar{3}a)$, and $(2a, 3a, \bar{2}a, \bar{3}a)$ forms a 2-face. Then for each $i \in V$, the vertex ia has already two missing angles. Consequently, the remaining angles necessarily form a 2-face of P by Proposition 6.39. By inducedness, we obtain all the triangles of the a-copy of H, and any two adjacent of these triangles are contained in a common 3-face. This 3-face is necessarily an octahedron.

Assume now that one of the angles of the 4-cycles $(1a, 2a, \bar{1}a, \bar{2}a)$, $(1a, 3a, \bar{1}a, \bar{3}a)$, and $(2a, 3a, \bar{2}a, \bar{3}a)$ forms a 2-face. By symmetry, we can suppose that it is the angle defined by the edges $\{1a, 2a\}$ and $\{2a, \bar{1}a\}$. Let F denote the corresponding 2-face of P. By inducedness, the last vertex of F cannot be either $3a$ or $\bar{3}a$, and F is necessarily the square $(1a, 2a, \bar{1}a, \bar{2}a)$. It is now easy to see that none of the angles of the 4-cycle $(1a, 3a, \bar{1}a, \bar{3}a)$ (resp. $(2a, 3a, \bar{2}a, \bar{3}a)$) can be an angle of a 2-face of P: otherwise, this 4-cycle would be a 2-face of P (by a symmetric argument), which would intersect improperly with F. All together, this implies that the vertices $3a$ and $\bar{3}a$ both have already two missing angles, and thus, that all the other angles form 2-faces by Proposition 6.39. Furthermore, any two 2-faces adjacent to an edge $\{3a, ia\}$, with $i \in \{1, \bar{1}, 2, \bar{2}\}$, form a 3-face. This implies that all angles adjacent to a vertex ia, except the angles of the 4-cycles $(1a, 3a, \bar{1}a, \bar{3}a)$ and $(2a, 3a, \bar{2}a, \bar{3}a)$ form a 2-face.

Since the two above cases can occur independently at both ends of the segment (a, b), we obtain the claimed result. □

6.2.4 Topological products

To finish, we come back to Günter Ziegler's motivating question: "is the product of two Petersen graphs polytopal?" We proved in Theorem 6.24 that it is not 6 polytopal, but the question remains open in dimension 4 and 5.

Proposition 6.40. *The product of two Petersen graphs is the graph of a* 4*-dimensional pseudo-manifold of Euler characteristic* 1.

Proof. The Petersen graph is the graph of a cellular decomposition of the projective plane $\mathcal{P}$ with 6 pentagons (see Figure 6.9). Consequently, the product of two Petersen graphs is the graph of a cellular decomposition of $\mathcal{P} \times \mathcal{P}$, whose Euler characteristic is 1 (the Euler characteristic of a product is the product of the Euler characteristics of the factors). The maximal cells of this decomposition are 36 products of two pentagons. □

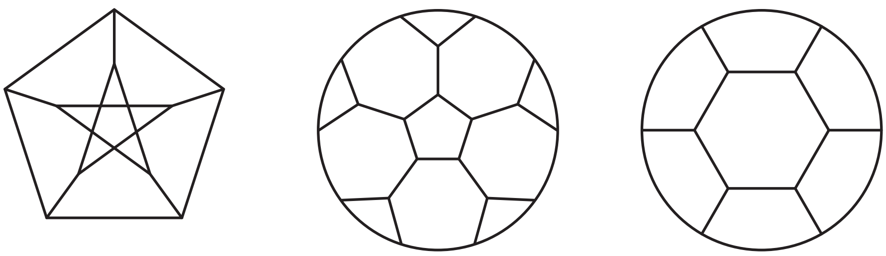

Figure 6.9: The Petersen graph (left), its embedding on the projective plane (middle) and the embedding of $K_{3,3}$ on the projective plane (right). Antipodal points on the circle are identified.

This proposition tells that understanding the possible 4-faces of a realization, and their possible incidence relations (as we did for example in Proposition 6.33) is not enough to disprove the polytopality of the product of two Petersen graphs. Observe that the same remark holds for the product of any graphs of cellular decompositions of manifolds: for example, the product of a triangle by the Petersen graph is the graph of a 3-dimensional pseudo-manifold of Euler characteristic 0.

Another interesting example is the product of $K_{3,3}$ by a triangle. Indeed, in contrast with $K_{3,3} \times K_2$, the graph $K_{3,3} \times K_3$ is the graph of a 3-dimensional pseudo-manifold of Euler characteristic 0. To see this, embed $K_{3,3}$ in the projective plane $\mathcal{P}$ as in Figure 6.9, and multiply this embedding by a triangle. The only difference with Proposition 6.40 is that the central hexagon in the embedding of Figure 6.9 intersects improperly the three external squares. Consequently, in the product with the triangle, each of the three hexagonal prisms intersects improperly three cubes. This can be solved by replacing the chain of three hexagonal prisms by a chain of six triangular prisms with the same boundary. We leave the details to the reader.

Chapter Seven

7

PRODSIMPLICIAL NEIGHBORLY POLYTOPES

In this dissertation, we focus on polytopal realizations of Cartesian products of graphs (or more generally of complexes). In Chapter 6, we mainly studied the existence of a realization. In this chapter, we investigate the possible dimension of a realization of a product. For this purpose, the simplest products are already interesting (and challenging) enough:

Definition 7.1. *Let $k \geq 0$ and $\underline{n} := (n_1, \dots, n_r)$, with $r \geq 1$ and $n_i \geq 1$ for all i. A polytope is* $(k, \underline{n})$-prodsimplicial-neighborly *— or* $(k, \underline{n})$-PSN *for short — if its k-skeleton is combinatorially equivalent to that of the product of simplices $\triangle_{\underline{n}} := \triangle_{n_1} \times \cdots \times \triangle_{n_r}$.*

Remark 7.2. This definition is essentially motivated by two particular classes of PSN polytopes:

(i) *neighborly* polytopes arise when $r = 1$. In the literature, a polytope is *k-neighborly* if any subset of at most k of its vertices forms a face. Note that such a polytope is $(k-1, n)$-PSN with our notation.

(ii) *neighborly cubical* polytopes [JZ00, JR07, SZ10] arise when $\underline{n} = (1, 1, \dots, 1)$.

In this chapter, we investigate the possible dimension of a $(k, \underline{n})$-PSN polytope. Since the product $\triangle_{\underline{n}}$ itself is $(k, \underline{n})$-PSN, the highest dimension is obviously $\sum n_i$. On the other side, we denote by $\delta(k, \underline{n})$ the smallest possible dimension that a $(k, \underline{n})$-PSN polytope can have.

In order to construct $(k, \underline{n})$-PSN polytopes, a natural approach is to project the product $\triangle_{\underline{n}}$ (or a combinatorially equivalent polytope) onto a smaller subspace in such a way to conserve the k-skeleton. This yields the following fundamental subclass of PSN polytopes:

Definition 7.3. *We say that a $(k, \underline{n})$-PSN polytope is* $(k, \underline{n})$-projected-prodsimplicial-neighborly *— or* $(k, \underline{n})$-PPSN *for short — if it is a projection of a polytope combinatorially equivalent to $\triangle_{\underline{n}}$.*

We denote by $\delta_{pr}(k, \underline{n})$ the smallest possible dimension of a $(k, \underline{n})$-PPSN polytope.

In this chapter, we present upper and lower bounds on this minimal possible dimension. For the upper bounds, we present two methods to construct PSN polytopes:

1. In Section 7.1, we give *explicit* constructions based on Minkowski sums of cyclic polytopes.
2. In Section 7.2, we extend Raman Sanyal and Günter Ziegler's technique of *projecting deformed products of polygons* [Zie04, SZ10] to products of arbitrary simple polytopes, and apply it to products of simplices.

To obtain lower bounds, we apply in Section 7.3 the *topological obstruction method* developed by Raman Sanyal to bound the number of vertices in a Minkowski sum. In view of these obstructions, our constructions in the first part turn out to be optimal for a wide range of parameters.

7.1 Constructions from cyclic polytopes

Remember that $C_d(n) := \operatorname{conv}\left\{(t_i, t_i^2, \dots, t_i^d)^T \,\middle|\, i \in [n]\right\}$ denotes the cyclic d-polytope with n vertices. Cyclic polytopes and their products yield our first examples of PSN polytopes:

Example 7.4. For any integers $k \geq 0$ and $n \geq 2k+2$, the cyclic polytope $C_{2k+2}(n+1)$ is (k,n)-PPSN: it is PSN by Proposition 5.5, and PPSN because any polytope with $n+1$ vertices is a projection of the n-simplex.

Example 7.5. For any $k \geq 0$ and $\underline{n} := (n_1, \dots, n_r)$ with $r \geq 1$ and $n_i \geq 1$ for all i, define $I := \{i \in [r] \,|\, n_i \geq 2k+3\}$. Then the product

$$\prod_{i \in I} C_{2k+2}(n_i+1) \times \prod_{i \notin I} \triangle_{n_i}$$

is a $(k, \underline{n})$-PPSN polytope of dimension $(2k+2)|I| + \sum_{i \notin I} n_i$ (which is smaller than $\sum_{i \in [r]} n_i$ when I is not empty). Consequently:

$$\delta(k, \underline{n}) \leq \delta_{pr}(k, \underline{n}) \leq (2k+2)|I| + \sum_{i \notin I} n_i.$$

7.1.1 Reflections of cyclic polytopes

Our next example deals with the special case of the product $\triangle_1 \times \triangle_n$ of a segment by a simplex. Using products of cyclic polytopes as in Example 7.5, we can realize the k-skeleton of this polytope in dimension $2k+3$. We can lower this dimension by 1 by reflecting the cyclic polytope $C_{2k+2}(n+1)$ in a well-chosen hyperplane:

Proposition 7.6. *For any $k \geq 0$, $n \geq 2k+2$ and $\lambda \in \mathbb{R}$ sufficiently large, the polytope*

$$P := \operatorname{conv}\left(\left\{(t_i, \dots, t_i^{2k+2})^T \,\middle|\, i \in [n+1]\right\} \cup \left\{(t_i, \dots, t_i^{2k+1}, \lambda - t_i^{2k+2})^T \,\middle|\, i \in [n+1]\right\}\right)$$

is a $(k,(1,n))$-PSN polytope of dimension $2k+2$.

Proof. The polytope P is obtained as the convex hull of two copies of the cyclic polytope $C_{2k+2}(n+1)$. The first one $Q := \operatorname{conv}\{\mu_{2k+2}(t_i) \,|\, i \in [n+1]\}$ lies on the moment curve μ_{2k+2}, while the second one is obtained as a reflection of Q with respect to a hyperplane that is orthogonal to the last coordinate vector e_{2k+2} and sufficiently far away. During this process:

(i) We destroy all the faces of Q only contained in upper facets of Q.

(ii) We create prisms over faces of Q that lie in at least one upper and one lower facet of Q. In other words (see Definition 7.12), we create prisms over the faces of Q strictly preserved under the orthogonal projection $\pi : \mathbb{R}^{2k+2} \to \mathbb{R}^{2k+1}$ with kernel $\mathbb{R}e_{2k+2}$.

The projected polytope $\pi(Q)$ is nothing but the cyclic polytope $C_{2k+1}(n+1)$. Since this polytope is k-neighborly, any $(\leq k-1)$-face of Q is strictly preserved by π, and thus, we take a prism over all $(\leq k-1)$-faces of Q.

Thus, in order to complete the proof that the k-skeleton of P is that of $\triangle_1 \times \triangle_n$, it is enough to show that any k-face of Q remains in P. This is obviously the case if this k-face is also a k-face of $C_{2k+1}(n+1)$, and follows from the next combinatorial lemma otherwise. $\square$

Lemma 7.7. *A k-face of $C_{2k+2}(n+1)$ which is not a k-face of $C_{2k+1}(n+1)$ is only contained in lower facets of $C_{2k+2}(n+1)$.*

Proof. Let $F \subset [n+1]$ be a k-face of $C_{2k+2}(n+1)$ that is contained in at least one upper facet $G \subset [n+1]$ of $C_{2k+2}(n+1)$. By Proposition 5.6, we have $n+1 \in G$. Thus:

(i) If $n+1 \notin F$, then $G \smallsetminus \{n+1\}$ is a facet of $C_{2k+1}(n+1)$ containing F.

(ii) If $n+1 \in F$, and $F' := F \smallsetminus \{n+1\}$ has only k elements. Thus, F' is a face of $C_{2k}(n)$, and can be completed to a facet of $C_{2k}(n)$. Adding the index $n+1$ back to this facet, we obtain a facet of $C_{2k+1}(n+1)$ containing F.

In both cases, we have shown that F is a k-face of $C_{2k+1}(n+1)$. $\square$

Remark 7.8. Observe that the previous construction is similar to our construction of polytopal products of non-polytopal graphs of Proposition 6.30, except that we now care not only about the graph, but about a bigger skeleton. The crucial property (presented in the previous lemma) is that there exists a regular subdivision of the cyclic polytope $C_{2k+1}(n+1)$ whose k-skeleton is combinatorially equivalent to that of the n-simplex. In particular, this method can be used to construct $(k, \underline{n})$-PSN polytopes in dimension $(2k+1)|I| + \max\left(1, \sum_{i \notin I} n_i\right)$ where $I := \{i \in [r] \,|\, n_i \geq 2k+3\}$. We do not explicitly present the construction here since our next section provides even better results as soon as $\underline{n} \neq (1, n)$.

7.1.2 Minkowski sums of cyclic polytopes

Our next examples are Minkowski sums of cyclic polytopes. We first describe an easy construction that avoids all technicalities, but only yields $(k, \underline{n})$-PPSN polytopes in dimension $2k+2r$. After that, we show how to reduce the dimension to $2k+r+1$, which according to Corollary 7.33 is best possible for large n_i's.

Proposition 7.9. *Let $k \geq 0$ and $\underline{n} := (n_1, \dots, n_r)$ with $r \geq 1$ and $n_i \geq 1$ for all i. For any pairwise disjoint index sets $I_1, \dots, I_r \subset \mathbb{R}$, with $|I_i| = n_i$ for all i, the polytope*

$$P := \operatorname{conv}\left\{v_{a_1,\dots,a_r} \,|\, (a_1, \dots, a_r) \in I_1 \times \dots \times I_r\right\} \subset \mathbb{R}^{2k+2r}$$

is $(k, \underline{n})$-PPSN, where $v_{a_1,\dots,a_r} := \left(\sum_{i\in[r]} a_i, \sum_{i\in[r]} a_i^2, \dots, \sum_{i\in[r]} a_i^{2k+2r}\right)^T \in \mathbb{R}^{2k+2r}$.

Proof. The vertex set of $\triangle_{\underline{n}}$ is indexed by $I_1 \times \cdots \times I_r$. Let $A := A_1 \times \cdots \times A_r \subset I_1 \times \cdots \times I_r$ define a k-face of $\triangle_{\underline{n}}$. Consider the polynomial

$$f(t) := \prod_{i\in[r]} \prod_{a\in A_i} (t-a)^2 := \sum_{j=0}^{2k+2r} c_j t^j.$$

Since A indexes a k-face of $\triangle_{\underline{n}}$, we know that $\sum |A_i| = k + r$, so that the degree of $f(t)$ is indeed $2k + 2r$. Since $f(t) \geq 0$, and equality holds if and only if $t \in \bigcup_{i\in[r]} A_i$, the inner product $\langle (c_1, \ldots, c_{2k+2r}) \,|\, v_{a_1,\ldots,a_r} \rangle$ equals

$$(c_1, \ldots, c_{2k+2r}) \begin{pmatrix} \sum_{i\in[r]} a_i \\ \vdots \\ \sum_{i\in[r]} a_i^{2k+2r} \end{pmatrix} = \sum_{i\in[r]} \sum_{j=1}^{2k+2r} c_j a_i^j = \sum_{i\in[r]} \big(f(a_i) - c_0\big) \geq -rc_0,$$

with equality if and only if $(a_1, \ldots, a_r) \in A$. Thus, A indexes a face of P defined by the linear inequality $\sum_{i\in[r]} c_i x_i \geq -rc_0$. $\square$

To realize the k-skeleton of $\triangle_{n_1} \times \cdots \times \triangle_{n_r}$ even in dimension $2k+r+1$, we slightly modify this construction in the following way:

Theorem 7.10. *Let $k \geq 0$ and $\underline{n} := (n_1, \ldots, n_r)$ with $r \geq 1$ and $n_i \geq 1$ for all i. There exist index sets $I_1, \ldots, I_r \subset \mathbb{R}$, with $|I_i| = n_i$ for all i, such that the polytope*

$$P := \operatorname{conv}\{w_{a_1,\ldots,a_r} \,|\, (a_1, \ldots, a_r) \in I_1 \times \cdots \times I_r\} \subset \mathbb{R}^{2k+r+1}$$

is $(k, \underline{n})$-PPSN, where $w_{a_1,\ldots,a_r} := \Big(a_1, \ldots, a_r, \sum_{i\in[r]} a_i^2, \ldots, \sum_{i\in[r]} a_i^{2k+2}\Big)^T \in \mathbb{R}^{2k+r+1}$.

Proof. We will choose the index sets I_i to be sufficiently separated in a sense that will be made explicit later in the proof. This choice will enable us, for each k-face F of $\triangle_{\underline{n}}$ indexed by $A_1 \times \cdots \times A_r \subset I_1 \times \cdots \times I_r$, to construct a *monic* polynomial (*i.e.* a polynomial with leading coefficient equal to 1)

$$f_F(t) := \sum_{j=0}^{2k+2} c_j t^j$$

that has, for all $i \in [r]$, the form

$$f_F(t) = Q_i(t) \prod_{a\in A_i} (t-a)^2 + s_i t + r_i,$$

with polynomials $Q_i(t)$ everywhere positive and certain reals r_i and s_i. From the coefficients of this polynomial, we build the vector

$$n_F := (s_1 - c_1, \ldots, s_r - c_1, -c_2, -c_3, \ldots, -c_{2k+2}) \in \mathbb{R}^{2k+r+1}.$$

To prove that n_F is a face-defining normal vector for F, take an arbitrary r-tuple $(a_1, \ldots, a_r)$ in $I_1 \times \cdots \times I_r$, and consider the following inequality for the inner product:

$$\begin{aligned} \langle n_F \mid w_{a_1,\ldots,a_r} \rangle &= \sum_{i\in[r]} \left(s_i a_i - \sum_{j=1}^{2k+2} c_j a_i^j \right) = \sum_{i\in[r]} (s_i a_i + c_0 - f_F(a_i)) \\ &= \sum_{i\in[r]} \left(c_0 - Q_i(a_i) \prod_{a\in A_i} (a_i - a)^2 - r_i \right) \le r c_0 - \sum_{i\in[r]} r_i. \end{aligned}$$

Equality holds if and only if $(a_1, \ldots, a_r) \in A_1 \times \cdots \times A_r$. Given the existence of a polynomial f_F with the claimed properties, this proves that $A_1 \times \cdots \times A_r$ indexes all $w_{a_1,\ldots,a_r}$'s that lie on a face F' in P, and they of course span F' by definition of P. To prove that F' is combinatorially equivalent to F it suffices to show that each $w_{a_1,\ldots,a_r} \in F'$ is in fact a vertex of P, since P is a projection of $\triangle_{\underline{n}}$. This can be shown with the normal vector $(2a_1, \ldots, 2a_r, -1, 0, \ldots, 0)$, using the same calculation as before.

Before showing how to choose the index sets I_i that enable us to construct the polynomials f_F in general, we would like to make a brief aside to show the smallest example. $\square$

Example 7.11. For $k = 1$ and $r = 2$, choose the index sets $I_1, I_2 \subset \mathbb{R}$ arbitrarily, but separated in the sense that the largest element of I_1 be smaller than the smallest element of I_2. For any 1-face F of P indexed by $\{a, b\} \times \{c\} \subset I_1 \times I_2$, consider the polynomial f_F of degree $2k+2 = 4$:

$$f_F(t) := (t - a)^2(t - b)^2 = (t^2 + \alpha t + \beta)(t - c)^2 + s_2 t + r_2,$$

where $\alpha := 2(-a - b + c)$, $\beta := a^2 + b^2 + 3c^2 + 4ab - 4ac - 4bc$,
$r_2 := a^2b^2 - \beta c^2$, $s_2 := -2a^2b - 2ab^2 - \alpha c^2 + 2\beta c$.

Since the index sets I_1, I_2 are separated, the discriminant $\alpha^2 - 4\beta = -8(c-a)(c-b)$ is negative, which implies that the polynomial $Q_2(t) = t^2 + \alpha t + \beta$ is positive for all values of t.

Proof of Theorem 7.10, continued. We still need to show how to choose the index sets I_i that enable us to construct the polynomials f_F in general. Once we have chosen these index sets, finding f_F is equivalent to the task of finding polynomials $Q_i(t)$ such that:

(i) $Q_i(t)$ is monic of degree $2k + 2 - 2|A_i|$.
(ii) The r polynomials $f_i(t) := Q_i(t) \prod_{a\in A_i} (t - a)^2$ are equal up to possibly the coefficients in front of t^0 and t^1.
(iii) $Q_i(t) > 0$ for all $t \in \mathbb{R}$.

The first two items form a linear equation system on the coefficients of the $Q_i(t)$'s which has the same number of equations as variables. We will show that it has a unique solution if one chooses the right index sets I_i (the third item will be dealt with at the end). To do this, choose pairwise distinct reals $\bar{a}_1, \ldots, \bar{a}_r \in \mathbb{R}$ and look at the similar equation system:

(i) $\bar{Q}_i(t)$ are monic polynomials of degree $2k + 2 - 2|A_i|$.
(ii) The r polynomials $\bar{f}_i(t) := \bar{Q}_i(t)(t - \bar{a}_i)^{2|A_i|}$ are equal up to possibly the coefficients in front of t^0 and t^1.

The first equation system moves into the second when we deform the points of the sets A_i continuously to $\bar{a}_i$, respectively. If we show that the second equation system has a unique solution then so has the first equation system as long as we have chosen the sets I_i close enough to the $\bar{a}_i$'s, by continuity of the determinant (note that in the end, we can fulfill all these closeness conditions required for all k-faces of $\triangle_{\underline{n}}$ since there are only finitely many k-faces).

Note that a polynomial $\bar{f}_i(t)$ of degree $2k+2$ has the form

$$\bar{Q}_i(t)(t-\bar{a}_i)^{2|A_i|} + s_i t + r_i \tag{7.1}$$

for a monic polynomial $\bar{Q}_i$ and some reals s_i and r_i, if and only if $\bar{f}_i''(t)$ has the form

$$R_i(t)(t-\bar{a}_i)^{2(|A_i|-1)} \tag{7.2}$$

for a polynomial $R_i(t)$ with leading coefficient $(2k+2)(2k+1)$. The backward direction can be settled by assuming without loss of generality $\bar{a}_i = 0$ (otherwise just make a variable shift $(t-\bar{a}_i) \mapsto t$) and then integrating (7.2) twice with integration constants zero to obtain (7.1).

Therefore the second equation system is equivalent to the following third one:

(i) $R_i(t)$ are polynomials of degree $2k-2(|A_i|-1)$ with leading coefficient $(2k+2)(2k+1)$.
(ii) The r polynomials $g_i(t) := R_i(t)(t-\bar{a}_i)^{2(|A_i|-1)}$ all equal the same polynomial, say $g(t)$.

Since $\sum_i 2(|A_i|-1) = 2k$, it has the unique solution

$$R_i(t) = (2k+2)(2k+1)\prod_{j\neq i}(t-\bar{a}_j)^{2(|A_j|-1)},$$

with

$$g(t) = (2k+2)(2k+1)\prod_{j\in[r]}(t-\bar{a}_j)^{2(|A_j|-1)}.$$

Therefore the second system also has a unique solution, where the $\bar{f}_i(t)$ are obtained by integrating $g_i(t)$ twice with some specific integration constants. For a fixed i we can again assume $\bar{a}_i = 0$. Then both integration constants have been zero for this i, hence $\bar{f}_i(0) = 0$ and $\bar{f}_i'(0) = 0$. Since g_i is non-negative and zero only at isolated points, $\bar{f}_i$ is strictly convex, hence non-negative and zero only at $t = 0$. Therefore $\bar{Q}_i(t)$ is positive for $t \neq 0$. Since we chose $\bar{a}_i = 0$, we can quickly compute the correspondence between the coefficients of $\bar{Q}_i(t) = \sum_j \bar{q}_{i,j}t^j$ and of $R_i(t) = \sum_j r_{i,j}t^j$:

$$r_{i,j} = \big(2|A_i|(2|A_i|-1) + 4j|A_i| + j(j-1)\big)\bar{q}_{i,j}.$$

In particular

$$\bar{Q}_i(0) = \bar{q}_{i,0} = \frac{r_{i,0}}{2|A_i|(2|A_i|-1)} = \frac{R_i(0)}{2|A_i|(2|A_i|-1)} > 0,$$

therefore $\bar{Q}_i(t)$ is everywhere positive, hence so is $Q_i(t)$ if one chooses I_i possibly even closer to $\bar{a}_i$, since the solutions of linear equation systems move continuously when one deforms the entries of the equation system by a homotopy (as long as the determinant stays non-zero), since the determinant and taking the adjoint matrix are continuous maps. The positivity of $Q_i(t)$ finishes the proof. □

7.2 PROJECTIONS OF DEFORMED PRODUCTS

In the previous section, we saw an explicit construction of polytopes whose k-skeleton is equivalent to that of a product of simplices. In this section, we provide another construction of $(k, \underline{n})$-PPSN polytopes, using Raman Sanyal and Günter Ziegler's technique of *projecting deformed products of polygons* [Zie04, SZ10] and generalizing it to products of arbitrary simple polytopes. This generalized technique consists in suitably projecting suitable polytopes combinatorially equivalent to a given product of simple polytopes in such a way as to preserve its complete k-skeleton. The case of products of simplices then yields $(k, \underline{n})$-PPSN polytopes.

7.2.1 Projection of deformed product of simple polytopes

We first discuss the general setting: for any given product $P := P_1 \times \cdots \times P_r$ of simple polytopes, we construct a polytope $P^{\sim}$ combinatorially equivalent to P and whose k-skeleton is preserved under the projection on the first d coordinates.

Deformed products of simple polytopes. Let $P_1, \dots, P_r$ be *simple* polytopes of respective dimensions $n_1, \dots, n_r$ and facet descriptions $P_i = \{x \in \mathbb{R}^{n_i} \mid A_i x \le b_i\}$, where each real matrix $A_i \in \mathbb{R}^{m_i \times n_i}$ has one row for each of the m_i facets of P_i and $n_i = \dim P_i$ many columns, and b_i is a right-hand side vector in $\mathbb{R}^{m_i}$. The product $P := P_1 \times \cdots \times P_r$ then has dimension $n := \sum_{i \in [r]} n_i$, and is given by the $m := \sum_{i \in [r]} m_i$ inequalities:

$$\begin{pmatrix} A_1 & & \\ & \ddots & \\ & & A_r \end{pmatrix} x \le \begin{pmatrix} b_1 \\ \vdots \\ b_r \end{pmatrix}.$$

The left hand $m \times n$ matrix shall be denoted by A. It is proved in [AZ99] that for any matrix $A^{\sim}$ obtained from A by *arbitrarily* changing the zero entries above the diagonal blocks, there exists a right-hand side $b^{\sim}$ such that the deformed polytope $P^{\sim}$ defined by the inequality system $A^{\sim} x \le b^{\sim}$ is combinatorially equivalent to P. The equivalence is the obvious one: it maps the facet defined by the ith row of A to the one given by the ith row of $A^{\sim}$, for all i. Following the ideas of [SZ10], we will use this "deformed product" construction in such a way that the projection of $P^{\sim}$ to the first d coordinates preserves its k-skeleton in the following sense.

Preserved faces and the Projection Lemma. For integers $n > d$, let $\pi : \mathbb{R}^n \to \mathbb{R}^d$ denote the orthogonal projection to the first d coordinates, and $\tau : \mathbb{R}^n \to \mathbb{R}^{n-d}$ denote the dual orthogonal projection to the last $n - d$ coordinates. Let P be a full-dimensional simple polytope in $\mathbb{R}^n$, with 0 in its interior. We consider the following notion of preserved faces (see Figure 7.1):

Definition 7.12 ([Zie04]). *A proper face F of a polytope P is* strictly preserved *under π if:*

(i) $\pi(F)$ is a face of $\pi(P)$,

(ii) F and $\pi(F)$ are combinatorially isomorphic, and

(iii) $\pi^{-1}(\pi(F))$ equals F.

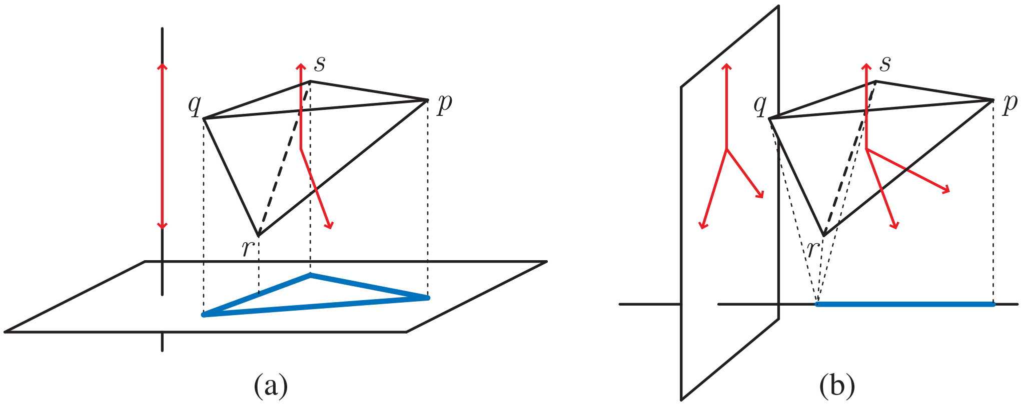

Figure 7.1: (a) Projection of a tetrahedron onto $\mathbb{R}^2$: the edge pq is strictly preserved, while neither the edge qr, nor the face qrs, nor the edge qs are (because of conditions (i), (ii) and (iii) respectively). (b) Projection of a tetrahedron to $\mathbb{R}$: only the vertex p is strictly preserved.

The characterization of strictly preserved faces of P uses the normal vectors of the facets of P. Let $F_1, \dots, F_m$ denote the facets of P and for all $i \in [m]$, let f_i denote the normal vector of F_i, and $g_i := \tau(f_i)$. For any face F of P, let $\varphi(F)$ denote the set of indices of the facets of P containing F, *i.e.* such that $F = \bigcap_{i \in \varphi(F)} F_i$.

Lemma 7.13 (Projection Lemma [AZ99, Zie04]). *A face F of the polytope P is strictly preserved under the projection π if and only if $\{g_i \mid i \in \varphi(F)\}$ is positively spanning.* □

A first construction. Let $t \in \{0, 1, \dots, r\}$ be maximal such that the matrices $A_1, \dots, A_t$ are entirely contained in the first d columns of A. Let $\overline{m} := \sum_{i=1}^t m_i$ and $\overline{n} := \sum_{i=1}^t n_i$. By changing bases appropriately, we can assume that the bottom $n_i \times n_i$ block of A_i is the identity matrix, for each $i \geq t+1$. In order to simplify the exposition, we also assume first that $\overline{n} = d$, *i.e.* that the projection on the first d coordinates separates the first t block matrices from the last $r - t$. See Figure 7.2(a).

Let $\{g_1, \dots, g_{\overline{m}}\} \subset \mathbb{R}^{n-d}$ be a set of vectors such that $G := \{e_1, \dots, e_{n-d}\} \cup \{g_1, \dots, g_{\overline{m}}\}$ is the Gale transform of a full-dimensional simplicial neighborly polytope Q — see [Zie95, Mat02] for definition and properties of Gale duality. By elementary properties of the Gale transform, Q has $\overline{m} + n - d$ vertices, and $\dim Q = (\overline{m} + n - d) - (n - d) - 1 = \overline{m} - 1$. In particular, every subset of $\left\lfloor \frac{\overline{m}-1}{2} \right\rfloor$ vertices spans a face of Q, so every subset of $\overline{m} + n - d - \left\lfloor \frac{\overline{m}-1}{2} \right\rfloor =: \alpha$ elements of G is positively spanning.

We deform the matrix A into the matrix $A^{\sim}$ of Figure 7.2(a), using the vectors $g_1, \dots, g_{\overline{m}}$ to deform the top $\overline{m}$ rows. We denote by $P^{\sim}$ the corresponding deformed product. We say that a facet of $P^{\sim}$ is *good* if the right part of the corresponding row of $A^{\sim}$ is covered by a vector of G, and *bad* otherwise. Bad facets are hatched in Figure 7.2(a). Observe that there are $\beta := m - \overline{m} - n + d$ bad facets in total.

Let F be a k-face of $P^{\sim}$. Since $P^{\sim}$ is a simple n-polytope, F is the intersection of $n-k$ facets, among which at least $\gamma := n - k - \beta$ are good facets. If the corresponding elements of G are

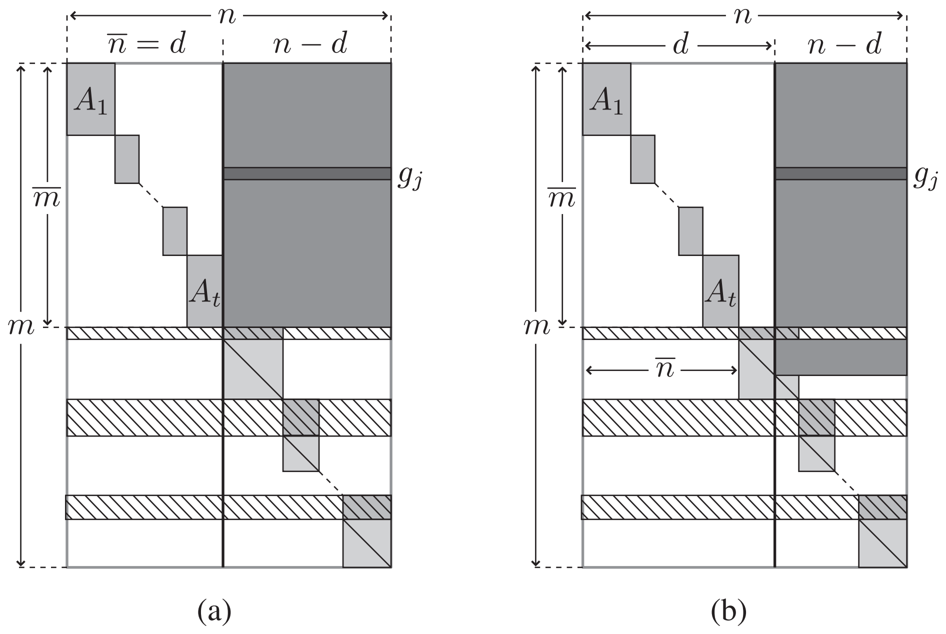

Figure 7.2: The deformed matrix $A^{\sim}$ (a) when the projection does not slice any block ($\overline{n} = d$), and (b) when the block A_{t+1} is sliced ($\overline{n} < d$). Horizontal hatched boxes denote bad row vectors. The top right solid block is formed by the vectors $g_1, \dots, g_{\overline{m}}$.

positively spanning, then F is strictly preserved under projection on the first d coordinates. Since we have seen that any subset of α vectors of G is positively spanning, F will surely be preserved if $\alpha \leq \gamma$, which is equivalent to:

$$k \leq n - m + \left\lfloor \frac{\overline{m} - 1}{2} \right\rfloor .$$

Thus, under this assumption, we obtain a d-polytope whose k-skeleton is combinatorially equivalent to the one of $P = P_1 \times \cdots \times P_r$.

When the projection slices a block. We now discuss the case when $\overline{n} < d$, for which the method is very similar. We consider $\overline{m}+d-\overline{n}$ vectors $g_1, \dots, g_{\overline{m}+d-\overline{n}}$ such that the set of vectors $G := \{e_1, \dots, e_{n-d}\} \cup \{g_1, \dots, g_{\overline{m}+d-\overline{n}}\}$ is the Gale dual of a neighborly polytope. We deform the matrix A into the matrix $A^{\sim}$ shown in Figure 7.2(b), using again the vectors $g_1, \dots, g_{\overline{m}}$ to deform the top $\overline{m}$ rows and the vectors $g_{\overline{m}+1} \dots, g_{\overline{m}+d-\overline{n}}$ to deform the top $d - \overline{n}$ rows of the $n_{t+1} \times n_{t+1}$ bottom identity submatrix of A_{t+1}. This is indeed a valid deformation since we can prescribe the $n_{t+1} \times n_{t+1}$ bottom submatrix of A_{t+1} to be any upper triangular matrix, up to changing the basis appropriately. For the same reasons as before:

(i) any subset of at least $\alpha := \overline{m} + n - \overline{n} - \left\lfloor \frac{\overline{m}+d-\overline{n}-1}{2} \right\rfloor$ elements of G is positively spanning;

(ii) the number of bad facets is $\beta := m - \overline{m} - n + \overline{n}$, and thus any k-face of $P^{\sim}$ is contained in at least $\gamma := n - k - \beta$ good facets.

Thus, the condition $\alpha \leq \gamma$ translates to:

$$k \leq n - m + \left\lfloor \frac{\overline{m} + d - \overline{n} - 1}{2} \right\rfloor,$$

and we obtain the following proposition:

Proposition 7.14. *Let $P_1, \dots, P_r$ be simple polytopes of respective dimension n_i, and with m_i many facets. For a fixed integer $d \leq n$, let t be maximal such that $\sum_{i=1}^{t} n_i \leq d$. Then there exists a d-polytope whose k-skeleton is combinatorially equivalent to that of the product $P_1 \times \cdots \times P_r$ as soon as*

$$0 \leq k \leq \sum_{i=1}^{r}(n_i - m_i) + \left\lfloor \frac{1}{2}\left(d - 1 + \sum_{i=1}^{t}(m_i - n_i)\right)\right\rfloor. \qquad \square$$

In the next two paragraphs, we present two improvements on the bound of this proposition. Both use colorings of the graphs of the polar polytopes $P_i^\diamond$, in order to weaken the condition $\alpha \leq \gamma$, in two different directions:

(i) the first improvement decreases the number of required vectors in the Gale transform G, which in turn, decreases the value of α;

(ii) the second one decreases the number of bad facets, and thus, increases the value of γ.

Multiple vectors. In order to raise our bound on k, we can save vectors of G by repeating some of them several times. Namely, any two facets that have no k-face in common can share the same vector g_j. Since any two facets of a simple polytope containing a common k-face share a ridge, this condition can be expressed in terms of incidences in the graph of the polar polytope: facets not connected by an edge in this graph can use the same vector g_j. For a graph H, we denote as usual its chromatic number by $\chi(H)$. Then, each P_i with $i \leq t$ only contributes $\chi_i := \chi(\mathrm{gr}(P_i^\diamond))$ different vectors in G, instead of m_i of them. Thus, we only need in total $\overline{\chi} := \sum_{i=1}^{t} \chi_i$ different vectors g_j. This improvement replaces $\overline{m}$ by $\overline{\chi}$ in the formula of α, while β and γ do not change, and the condition $\alpha \leq \gamma$ is equivalent to

$$k \leq n - m + \overline{m} - \overline{\chi} + \left\lfloor \frac{\overline{\chi} - d - \overline{n} - 1}{2} \right\rfloor.$$

Thus, we obtain the following improved proposition:

Proposition 7.15. *Let $P_1, \dots, P_r$ be simple polytopes. For each polytope P_i, denote by n_i its dimension, by m_i its number of facets, and by $\chi_i := \chi(\mathrm{gr}(P_i^\diamond))$ the chromatic number of the graph of its polar polytope $P_i^\diamond$. For a fixed integer $d \leq n$, let t be maximal such that $\sum_{i=1}^{t} n_i \leq d$. Then there exists a d-polytope whose k-skeleton is combinatorially equivalent to that of the product $P_1 \times \cdots \times P_r$ as soon as*

$$0 \leq k \leq \sum_{i=1}^{r}(n_i - m_i) + \sum_{i=1}^{t}(m_i - \chi_i) + \left\lfloor \frac{1}{2}\left(d - 1 + \sum_{i=1}^{t}(\chi_i - n_i)\right)\right\rfloor. \qquad \square$$

Example 7.16. Since polars of simple polytopes are simplicial, $\chi_i \geq n_i$ is an obvious lower bound for the chromatic number of the dual graph of P_i. Polytopes that attain this lower bound with equality are characterized by the property that all their 2-faces have an even number of vertices, and are called *even* polytopes.

If all P_i are even polytopes, then $\overline{n} = \overline{\chi}$, and we obtain a d-polytope with the same k-skeleton as $P_1 \times \cdots \times P_r$ as soon as

$$k \leq n - m + \overline{m} - \overline{n} + \left\lfloor \frac{d-1}{2} \right\rfloor.$$

In order to maximize k, we should maximize $\overline{m} - \overline{n}$, subject to the condition $\overline{n} \leq d$. For example, if all n_i are equal, this amounts to ordering the P_i by decreasing number of facets.

Scaling blocks. We can also apply colorings to the blocks A_i with $i \geq t+1$, by filling in the area below G and above the diagonal blocks. To explain this, assume for the moment that $\chi_i \leq n_{i+1}$ for a certain fixed $i \geq t+2$. Assume that the rows of A_i are colored with χ_i colors using a valid coloring $c : [m_i] \to [\chi_i]$ of the graph of the polar polytope $P_i^\diamond$. Let Γ be the incidence matrix of c, defined by $\Gamma_{j,k} = 1$ if $c(j) = k$, and $\Gamma_{j,k} = 0$ otherwise. Thus, Γ is a matrix of size $m_i \times \chi_i$. We put this matrix to the right of A_i and above A_{i+1} as in Figure 7.3(b), so that we append the same unit vector to each row of A_i in the same color class. Moreover, we scale all entries of the block A_i by a sufficiently small constant $\varepsilon > 0$.

In this setting, the situation is slightly different:

(i) In the Gale dual G, we do not need anymore the n_i basis vectors of $\mathbb{R}^{n-d}$ hatched in Figure 7.3(b). Let $a := \sum_{j<i} n_j$ denote the index of the last column vector of A_{i-1} and $b := 1 + \sum_{j \leq i} n_j$ denote the index of the first column vector of A_{i+1}. We define the vector set $G := \{e_1, \dots, e_{a-d}, e_{b-d}, \dots, e_{n-d}\} \cup \{g_1, \dots, g_{\overline{m}}\}$ to be the Gale transform of a simplicial neighborly polytope Q of dimension $\overline{m} - 1 - n_i$. As before, any subset of at least $\alpha := \overline{m} + n - \overline{n} - n_i - \left\lfloor \frac{\overline{m}+d-\overline{n}-n_i-1}{2} \right\rfloor$ vectors of G positively spans $\mathbb{R}^{n-d}$.

(ii) *Bad* facets are defined as before, except that the top $m_i - n_i$ rows of A_i are not bad anymore, but all of the first $m_{i+1} - n_{i+1} + \chi_i$ rows of A_{i+1} are now bad. Thus, the net change in the number of bad rows is $\chi_i - m_i + n_i$, so that any k-face is contained in at least $\gamma := 2n - k - m + \overline{m} - \overline{n} + m_i - n_i - \chi_i$ good rows. Up to ε-entry elements, the last $n - d$ coordinates of these rows correspond to pairwise distinct elements of G.

Applying the same reasoning as above, the k-skeleton of $P^\sim$ is strictly preserved under projection to the first d coordinates as soon as $\alpha \leq \gamma$, which is equivalent to:

$$k \leq n - m + m_i - \chi_i + \left\lfloor \frac{\overline{m} + d - \overline{n} - n_i - 1}{2} \right\rfloor.$$

Thus, we improve our bound on k as soon as

$$\Delta := m_i - \chi_i + \left\lfloor \frac{\overline{m} + d - \overline{n} - n_i - 1}{2} \right\rfloor - \left\lfloor \frac{\overline{m} + d - \overline{n} - 1}{2} \right\rfloor > 0.$$

For example, this difference Δ is big for polytopes whose polars have many vertices but a small chromatic number.

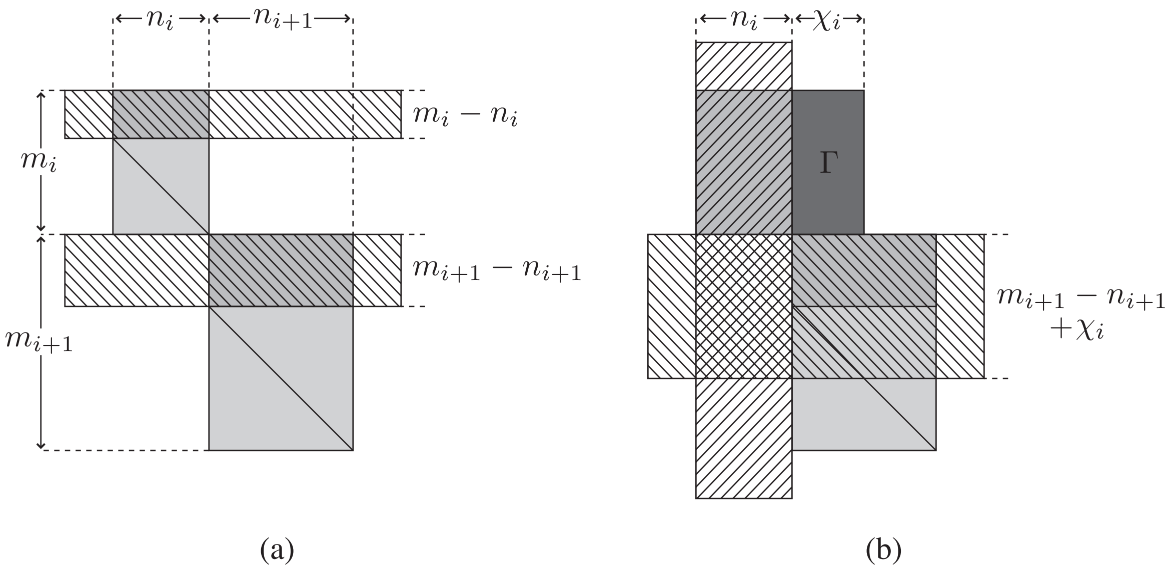

Figure 7.3: How to raise the dimension of the preserved skeleton by inserting the incidence matrix Γ of a coloring of the graph of the polar polytope $P_i^\diamond$. Part (a) shows the situation before the insertion of Γ, and Part (b) the changes that have occurred. Bad row vectors and unnecessary columns are hatched. The entries in the matrix to the left of Γ must be rescaled to retain a valid inequality description of P.

Finally, observe that one can apply this "scaling" improvement even if $\chi_i > n_{i+1}$ (except that it will perturb more than the two blocks A_i and A_{i+1}) and to more than one matrix A_i. See the example in Figure 7.4. In this picture, the Γ blocks are incidence matrices of colorings of the graphs of the polar polytopes. Call "diagonal entries" all entries on the diagonal of the $n_i \times n_i$ bottom submatrix of a factor A_i. A column is unnecessary (hatched in the picture) if its diagonal entry has a Γ block on the right and no Γ block above. Good rows are those covered by a vector g_j or a Γ block, together with the basis vectors whose diagonal entry has no Γ block above (bad rows are hatched in the picture).

Example 7.17. 1. If P_i is a segment, then $n_i = 1$, $m_i = 2$ and $\chi_i = 1$, so that $\Delta = 1$ if $\overline{m}$ is even and 0 otherwise. Iterating this, if P_i is an s-cube, then $\Delta \simeq \frac{s}{2}$. This yields *neighborly cubical polytopes* — see [JZ00, JR07, SZ10].

2. If P_i is an even cycle, then $n_i = 2$, $m_i = 2p$ and $\chi_i = 2$, so that $\Delta = 2p - 3$. This yields *projected products of polygons* — see [Zie04, SZ10].

In general, it is difficult to give the explicit ordering of the factors and choice of deformation that will yield the largest possible value of k attainable by a concrete product $P_1 \times \cdots \times P_r$ of simple polytopes, and consequently to summarize this improvement by a precise proposition as we did for our first improvement. However, this best value can clearly be found by optimizing over the finite set of all possible orderings and types of deformation. Furthermore, we can be much more explicit for products of simplices, as we detail in the next section.

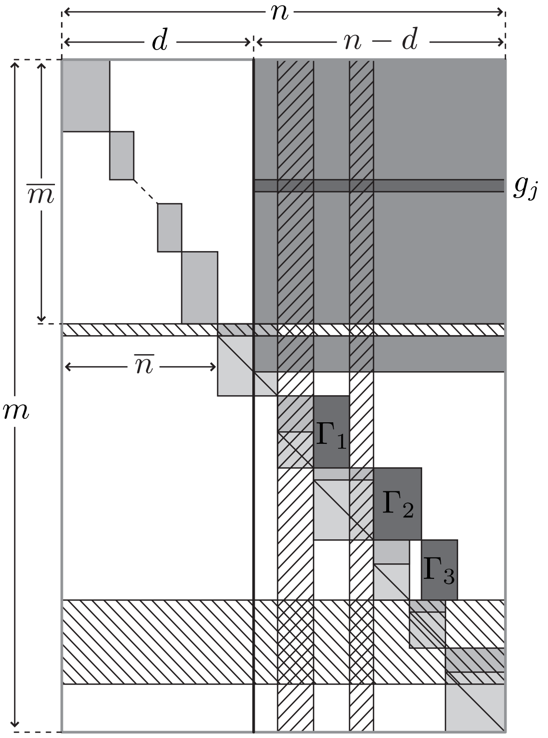

Figure 7.4: How to reduce the number of vectors in the Gale transform using various coloring matrices of polar polytopes. Situations where $\chi_i > n_{i+1}$ can be accommodated for as illustrated by the matrix Γ_2 in the picture.

7.2.2 Projection of deformed product of simplices

We are now ready to apply this general construction to the particular case of products of simplices. For this, we represent the simplex $\triangle_{n_i}$ by the inequality system $A_i x \leq b_i$, where

$$A_i := \begin{pmatrix} -1 & \dots & -1 \\ 1 & & \\ & \ddots & \\ & & 1 \end{pmatrix}$$

and b_i is a suitable right-hand side. We express the results of the construction with a case distinction according to the number $s := |\{i \in [r] \mid n_i = 1\}|$ of segments in the product $\triangle_{\underline{n}}$.

Proposition 7.18. *Let* $\underline{n} := (n_1, \dots, n_r)$ *with* $1 = n_1 = \dots = n_s < n_{s+1} \leq \dots \leq n_r$. *Then*
(1) for any $0 \leq d \leq s-1$, *there exists a* d*-dimensional* $(k, \underline{n})$-PPSN *polytope as soon as*

$$k \leq \left\lfloor \frac{d}{2} \right\rfloor - r + s - 1.$$

(2) for any $s \le d \le n$, there exists a d-dimensional $(k, \underline{n})$-PPSN polytope as soon as

$$k \le \left\lfloor \frac{d+t-s}{2} \right\rfloor - r + s,$$

where $t \in \{s, \dots, r\}$ denotes the maximal integer such that $\sum_{i=1}^{t} n_i \le d$.

Proof of (1). This is a special case of the results obtainable with the methods of Section 7.2.1. The best construction is obtained using the matrix in Figure 7.5, from which we read off that:

(i) any subset of at least $\alpha := n - \left\lfloor \frac{d}{2} \right\rfloor$ vectors in G is positively spanning;

(ii) the number of bad facets is $\beta := r - s + 1$, and therefore any k-face of $P^{\sim}$ is contained in at least $\gamma := n - k - r + s - 1$ good facets.

From this, the claim follows. □

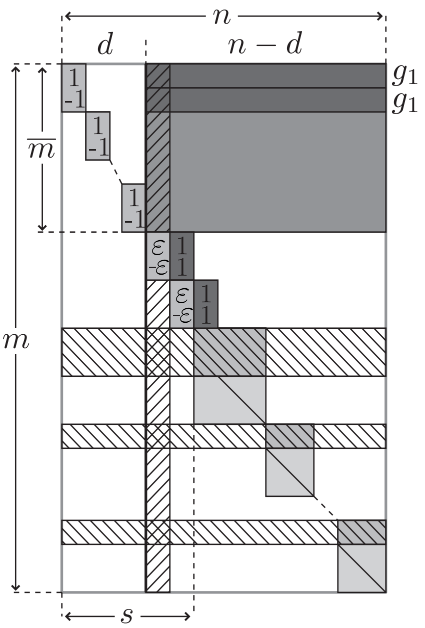

Figure 7.5: How to obtain PPSN polytopes from a deformed product construction, when the number s of segment factors exceeds the target dimension d of the projection.

Proof of (2). Consider the deformed product of Figure 7.6(a). Using similar calculations as before, we deduce that:

(i) any subset of at least $\alpha := t - s + n - \left\lfloor \frac{d+t-s-1}{2} \right\rfloor$ vectors in G is positively spanning;

(ii) the number of bad facets is $\beta := r - t$, and therefore any k-face of $P^{\sim}$ is contained in at least $\gamma := n - k - r + t$ good facets.

This yields a bound of

$$k \le \left\lfloor \frac{d+t-s-1}{2} \right\rfloor - r + s.$$

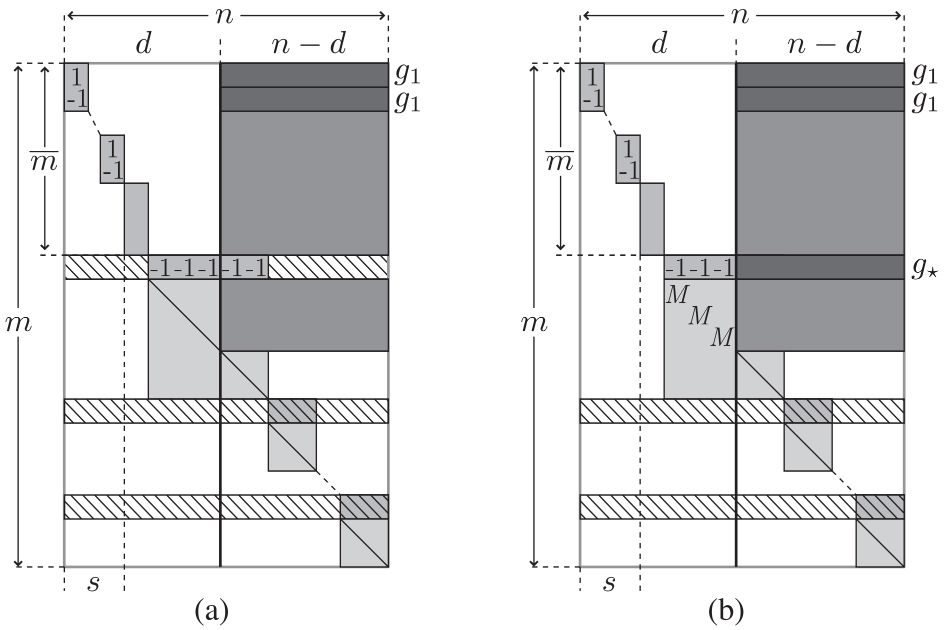

Figure 7.6: Obtaining PPSN polytopes from a deformed product construction, when few of the factors are segments. Part (a) shows the technique used so far, and Part (b) an additional optimization that exchanges a bad facet for a new vector in the Gale transform.

We optimize the final '-1' away by suitably deforming the matrix A_{t+1} as in Figure 7.6(b). This amounts to adding one more vector $g_\star$ to the Gale diagram, so that the first row of A_{t+1} ceases to be a bad facet. This deformation is valid because:

(i) the matrix

$$\begin{pmatrix} -1 & \dots & -1 & \star & \dots & \star \\ M & & & & & \\ & \ddots & & & & \\ & & M & & & \\ & & & 1 & & \\ & & & & \ddots & \\ & & & & & 1 \end{pmatrix}$$

still defines a simplex, as long as the '$\star$' entries are negative and $M \gg 0$ is chosen sufficiently large.

(ii) we can in fact choose the new vector $g_\star$ to have only negative entries, by imposing an additional restriction on the Gale diagram $G = \{e_1, \dots, e_{n-d}, g_1, \dots, g_{d+t}, g_\star\}$ of Q. Namely, we require the vertices of the simplicial $(d+t)$-polytope Q that correspond to the Gale vectors $g_1, \dots, g_{d+t}$ to lie on a facet. This forces the remaining vectors $e_1, \dots, e_{n-d}, g_\star$ to be positively spanning, so that $g_\star$ has only negative entries. $\square$

Finally, we reformulate Proposition 7.18 to express, in terms of k and $\underline{n} := (n_1, \dots, n_r)$, what dimensions a $(k, \underline{n})$-PPSN polytope can have. This yields upper bounds on $\delta_{pr}(k, \underline{n})$.

Theorem 7.19. *For any $k \geq 0$ and $\underline{n} := (n_1, \dots, n_r)$ with $1 = n_1 = \cdots = n_s < n_{s+1} \leq \cdots \leq n_r$,*

$$\delta_{pr}(k, \underline{n}) \leq \begin{cases} 2(k+r) - s - t & \text{if } 3s \leq 2k + 2r, \\ 2(k+r-s) + 1 & \text{if } 3s = 2k + 2r + 1, \\ 2(k+r-s+1) & \text{if } 3s \geq 2k + 2r + 2, \end{cases}$$

where $t \in \{s, \dots, r\}$ is maximal such that

$$3s + \sum_{i=s+1}^{t} (n_i + 1) \leq 2k + 2r.$$

Proof. Apply Part (1) of Proposition 7.18 when $3s \geq 2k + 2r + 2$ and Part (2) otherwise. □

Remark 7.20. When all the n_i's are large compared to k, the dimension of the $(k, \underline{n})$-PPSN polytope provided by this theorem is bigger than the dimension $2k + r + 1$ of the $(k, \underline{n})$-PPSN polytope obtained by the Minkowski sum of cyclic polytopes of Theorem 7.10. However, if we have many segments (neighborly cubical polytopes), or more generally if many n_i's are small compared to k, this construction provides our best examples of PPSN polytopes.

7.3 Topological obstructions

In this section, we give lower bounds on the minimal dimension $\delta_{pr}(k, \underline{n})$ of a $(k, \underline{n})$-PPSN polytope, applying a method developed by Raman Sanyal [San09] to bound the number of vertices of Minkowski sums of polytopes. This method provides lower bounds on the target dimension of any linear projection that preserves a given set of faces of a polytope. It uses Gale duality to associate a certain simplicial complex $\mathcal{K}$ to the set of faces that are preserved under the projection. Then lower bounds on the embeddability dimension of $\mathcal{K}$ transfer to lower bounds on the target dimension of the projection. In turn, the embeddability dimension is bounded via colorings of the Kneser graph of the system of minimal non-faces of $\mathcal{K}$, via Sarkaria's Embeddability Theorem.

After the completion of this work, we learned that Thilo Rörig and Raman Sanyal [RS09, Rör08, San08] also applied Sanyal's topological obstruction method to derive lower bounds on the target dimension of a projection preserving skeleta of different kind of products (products of polygons, products of simplices, and wedge products of polytopes). In particular, for a product $\triangle_n \times \cdots \times \triangle_n$ of r identical simplices, $r \geq 2$, they obtain our Theorem 7.29 and a result [RS09, Theorem 4.5] that is only slightly weaker than Theorem 7.32 in this setting. We decided to present this part in this dissertation since it completes our study on products of polytopes.

For the convenience of the reader, we first quickly recall Sarkaria's embeddability criterion. We then provide a brief overview of Raman Sanyal's method before applying it to obtain lower bounds on the dimension of $(k, \underline{n})$-PPSN polytopes. As mentioned in the introduction, these bounds match the upper bounds obtained from our different constructions for a wide range of parameters, and thus give the exact value of the minimal dimension of a PPSN polytope.

7.3.1 Sarkaria's embeddability criterion

7.3.1.1 Kneser graphs

Recall that a *k-coloring* of a graph $G := (V, E)$ is a map $c : V \to [k]$ such that $c(u) \neq c(v)$ for $(u, v) \in E$. As usual, we denote $\chi(G)$ the *chromatic number* of G (*i.e.* the minimal k such that G admits a k-coloring). We are interested in the chromatic number of Kneser graphs.

Let $\mathcal{Z}$ be a subset of the power set $2^{[n]}$ of $[n]$. The *Kneser graph* on $\mathcal{Z}$, denoted $\mathrm{KG}(\mathcal{Z})$, is the graph with vertex set $\mathcal{Z}$, where two vertices $X, Y \in \mathcal{Z}$ are related if and only if $X \cap Y = \emptyset$:

$$\mathrm{KG}(\mathcal{Z}) := \big(\mathcal{Z}, \big\{(X, Y) \in \mathcal{Z}^2 \,\big|\, X \cap Y = \emptyset\big\}\big).$$

Let $\mathrm{KG}_n^k := \mathrm{KG}\big(\binom{[n]}{k}\big)$ denote the Kneser graph on the set of k-tuples of $[n]$. For example, the graph KG_n^1 is the complete graph K_n (of chromatic number n) and the graph KG_5^2 is the Petersen graph (of chromatic number 3).

Remark 7.21. (i) If $n \leq 2k - 1$, then any two k-tuples of $[n]$ intersect and the Kneser graph KG_n^k is independent (*i.e.* it has no edge). Thus its chromatic number is $\chi(\mathrm{KG}_n^k) = 1$.

(ii) If $n \geq 2k-1$, then $\chi(\mathrm{KG}_n^k) \leq n-2k+2$. Indeed, the map $c : \binom{[n]}{k} \to [n-2k+2]$ defined by $c(F) := \min(F \cup \{n-2k+2\})$ is a $(n-2k+2)$-coloring of KG_n^k.

In fact, it turns out that this upper bound is the exact chromatic number of the Kneser graph: $\chi(\mathrm{KG}_n^k) = \max\{1, n-2k+2\}$. This result has been conjectured by Martin Kneser and proved by László Lovász applying the Borsuk-Ulam Theorem — see [Mat03] for more details. However, we will only need the upper bound for the topological obstruction.

7.3.1.2 Sarkaria's Theorem

Our lower bounds on the dimension of $(k, \underline{n})$-PPSN polytopes rely on lower bounds for the dimension in which certain simplicial complexes can be embedded. Among other possible methods (see [Mat03]), we use Sarkaria's Coloring and Embedding Theorem.

We associate to any simplicial complex $\mathcal{K}$ the set system $\mathcal{Z}$ of *minimal non-faces* of $\mathcal{K}$, that is, the inclusion-minimal sets of $2^{V(\mathcal{K})} \smallsetminus \mathcal{K}$. For example, the system of minimal non-faces of the k-skeleton of the n-simplex is $\binom{[n+1]}{k+2}$. Sarkaria's Theorem provides a lower bound on the dimension into which $\mathcal{K}$ can be embedded, in terms of the chromatic number of the Kneser graph of $\mathcal{Z}$.

Theorem 7.22 (Sarkaria's Theorem)**.** *Let $\mathcal{K}$ be a simplicial complex embeddable in $\mathbb{R}^d$, $\mathcal{Z}$ be the system of minimal non-faces of $\mathcal{K}$, and $\mathrm{KG}(\mathcal{Z})$ be the Kneser graph on $\mathcal{Z}$. Then*

$$d \geq |V(\mathcal{K})| - \chi(\mathrm{KG}(\mathcal{Z})) - 1. \qquad \square$$

In other words, we get large lower bounds on the possible embedding dimension of $\mathcal{K}$ when we obtain colorings with few colors of the Kneser graph on the system of minimal non-faces of $\mathcal{K}$. We refer to the excellent treatment in [Mat03] for further details.

7.3.2 Sanyal's topological obstruction method

For given integers $n > d$, we consider the orthogonal projection $\pi : \mathbb{R}^n \to \mathbb{R}^d$ to the first d coordinates, and its dual projection $\tau : \mathbb{R}^n \to \mathbb{R}^{n-d}$ to the last $n-d$ coordinates. Let P be a full-dimensional simple polytope in $\mathbb{R}^n$, with 0 in its interior, and assume that its vertices are strictly preserved under π. Let $F_1, \dots, F_m$ denote the facets of P, and for all $i \in [m]$, let f_i denote the normal vector of F_i, and $g_i := \tau(f_i)$. For any face F of P, let $\varphi(F)$ denote the set of indices of the facets of P containing F, *i.e.* such that $F = \bigcap_{i \in \varphi(F)} F_i$.

Lemma 7.23 (Sanyal [San09]). *The vector configuration $G := \{g_i \,|\, i \in [m]\} \subset \mathbb{R}^{n-d}$ is the Gale transform of the vertex set of a (full-dimensional) polytope Q of $\mathbb{R}^{m-n+d-1}$. Up to a slight perturbation of the facets of P, we can even assume Q to be simplicial.* □

We will refer to the polytope Q as *Sanyal's projection polytope*. We denote its vertices by $a_1, \dots, a_m$ such that a_i is transformed into g_i by Gale duality. The faces of this polytope capture the key notion of strictly preserved faces of P — remember Definition 7.12. Indeed, the Projection Lemma 7.13 ensures that for any face F of P strictly preserved by the projection π, the set $\{g_i \,|\, i \in \varphi(F)\}$ is positively spanning, which implies by Gale duality that the set of vertices $\{a_i \,|\, i \in [m] \smallsetminus \varphi(F)\}$ forms a face of Q.

Example 7.24. Let P be a triangular prism in 3-space that projects to a hexagon as in Figure 7.7(a), so that $n = 3$, $d = 2$ and $m = 5$. The vector configuration $G \subset \mathbb{R}^1$ obtained by projecting P's normal vectors consists of three vectors pointing up and two pointing down, so that Sanyal's projection polytope Q is a bipyramid over a triangle. An edge $F_i \cap F_j$ of P that is preserved under projection corresponds to the face $[5] \smallsetminus \{i, j\}$ of Q. Notice that the six faces of Q corresponding to the six edges of P that are preserved under projection (in bold in Figure 7.7(a)) make up the entire boundary complex of the bipyramid Q.

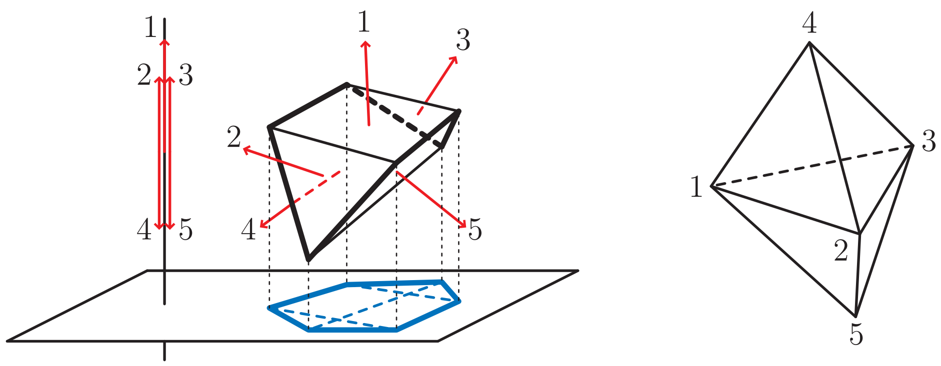

(a) (b)

Figure 7.7: (a) A projection of a triangular prism and (b) its associated projection polytope Q. The six faces of Q corresponding to the six edges of P preserved under projection (bold) make up the entire boundary complex of Q.

Let $\mathcal{F}$ be a subset of the set of all strictly preserved faces of P under π. Define $\mathcal{K}$ to be the simplicial complex induced by $\{[m] \smallsetminus \varphi(F) \mid F \in \mathcal{F}\}$.

Remark 7.25. Notice that not all non-empty faces of $\mathcal{K}$ correspond to non-empty faces in $\mathcal{F}$: in Example 7.24, if $\mathcal{F}$ consists of all strictly preserved edges, then $\mathcal{K}$ is the entire boundary complex of Sanyal's projection polytope Q, so that it contains the edge $\{2, 3\}$. But then the complementary intersection of facets, $F_1 \cap F_4 \cap F_5$, does not correspond to any non-empty face of P (and *a fortiori* of $\mathcal{F}$).

Since the set of vertices $\{a_i \mid i \in [m] \smallsetminus \varphi(F)\}$ forms a face of Q for any face $F \in \mathcal{F}$, and since Q is simplicial, $\mathcal{K}$ is a subcomplex of the face complex of $Q \subset \mathbb{R}^{m-n+d-1}$. In particular, when $\mathcal{K}$ is not the entire boundary complex of Q, it embeds into $\mathbb{R}^{m-n+d-2}$ by stereographic projection (otherwise, it only embeds into $\mathbb{R}^{m-n+d-1}$, as happens in Example 7.24).

Thus, given the simple polytope $P \subset \mathbb{R}^n$, and a set $\mathcal{F}$ of faces of P that we want to preserve under projection, the study of the embeddability of the corresponding abstract simplicial complex $\mathcal{K}$ provides lower bounds on the dimension d in which we can project P. We proceed in the following way:

1. we first choose our subset $\mathcal{F}$ of strictly preserved faces sufficiently simple to be understandable, and sufficiently large to provide an obstruction;
2. we then understand the system $\mathcal{Z}$ of minimal non-faces of the simplicial complex $\mathcal{K}$;
3. finally, we find a suitable coloring of the Kneser graph on $\mathcal{Z}$ and apply Sarkaria's Theorem 7.22 to bound the dimension in which $\mathcal{K}$ can be embedded: a t-coloring of $\mathrm{KG}(\mathcal{Z})$ ensures that $\mathcal{K}$ is not embeddable into $|V(\mathcal{K})| - t - 2 = m - t - 2$, which by the previous paragraph bounds the dimension d from below as follows:

Theorem 7.26 (Sanyal [San09])**.** *Let P be a simple polytope in $\mathbb{R}^n$ whose facets are in general position, and let $\pi : \mathbb{R}^n \to \mathbb{R}^d$ be a projection. Let $\mathcal{F}$ be a subset of the set of all strictly preserved faces of P under π, let $\mathcal{K}$ be the simplicial complex induced by $\{[m] \smallsetminus \varphi(F) \mid F \in \mathcal{F}\}$, and let $\mathcal{Z}$ be its system of minimal non-faces. If the Kneser graph $\mathrm{KG}(\mathcal{Z})$ is t-colorable, then:*
(1) if $\mathcal{K}$ is not the entire boundary complex of the Sanyal polytope Q, then $d \geq n - t + 1$;
(2) otherwise, $d \geq n - t$. □

In the remainder of this section, we apply Sanyal's topological obstruction to our problem. The hope was initially to extend it to bound the target dimension of a projection preserving the k-skeleton of an arbitrary product of simple polytopes. However, the combinatorics involved to deal with this general question turn out to be too complicated and we restrict our attention to products of simplices. We obtain in this manner bounds on the minimal dimension $\delta_{pr}(k, \underline{n})$ of a $(k, \underline{n})$-PPSN polytope.

7.3.3 Preserving the k-skeleton of a product of simplices

In this section, we understand the abstract simplicial complex $\mathcal{K}$ corresponding to our problem, and describe its system of minimal non-faces.

The facets of $\triangle_{\underline{n}}$ are exactly the products

$$\psi_{i,j} := \triangle_{n_1} \times \cdots \times \triangle_{n_{i-1}} \times (\triangle_{n_i} \smallsetminus \{j\}) \times \triangle_{n_{i+1}} \times \cdots \times \triangle_{n_r},$$

for $i \in [r]$ and $j \in [n_i+1]$. We identify the facet $\psi_{i,j}$ with the element $j \in [n_i+1]$ of the disjoint union $[n_1+1] \uplus [n_2+1] \uplus \cdots \uplus [n_r+1]$.

Let $F := F_1 \times \cdots \times F_r$ be a k-face of $\triangle_{\underline{n}}$. Then F is contained in a facet $\psi_{i,j}$ of $\triangle_{\underline{n}}$ if and only if $j \notin F_i$. Thus, the set of facets of $\triangle_{\underline{n}}$ that do not contain F is exactly $F_1 \uplus \cdots \uplus F_r$. Consequently, if we want to preserve the k-skeleton of $\triangle_{\underline{n}}$, then the abstract simplicial complex $\mathcal{K}$ we are interested in is induced by

$$\left\{ F_1 \uplus \cdots \uplus F_r \;\middle|\; \emptyset \neq F_i \subset [n_i+1] \text{ for all } i \in [r], \text{ and } \sum_{i\in[r]} (|F_i|-1) = k \right\}. \tag{7.3}$$

Remark 7.27. In contrast to the general case, when we want to preserve the *complete* k-skeleton of a product of simplices, the complex $\mathcal{K}$ cannot be the entire boundary complex of the Sanyal polytope Q. In consequence, the better lower bound from Part (1) of Sanyal's Theorem 7.26 always holds, and we always use it from now on without further notice.

To prove that $\mathcal{K}$ cannot cover the entire boundary complex of Q, observe that

$$\dim Q = m - n + d - 1 = \sum (n_i+1) - \sum n_i + d - 1 = r + d - 1,$$

while $\dim \mathcal{K} = r+k-1$ by (7.3). A necessary condition for $\mathcal{K}$ to be the entire boundary complex of Q is that $\dim \mathcal{K} = \dim Q - 1$, which translates to $d = k+1$. Now suppose that the entire k-skeleton of $\triangle_{\underline{n}}$ is preserved under projection to dimension $k+1$. Then the projections of those k-faces are facets of $\pi(\triangle_{\underline{n}})$. Since any ridge of the projected polytope is contained in exactly two facets, and the *entire* k-skeleton of $\triangle_{\underline{n}}$ is preserved, we know that any $(k-1)$-face of $\triangle_{\underline{n}}$ is also contained in exactly two k-faces. But this can only happen if $k = n-1$, which means $n = d$.

Observe again that $\mathcal{K}$ can be the entire boundary complex of Q if we do not preserve *all* k-faces of $\triangle_{\underline{n}}$ — see Example 7.24.

The following lemma gives a description of the minimal non-faces of $\mathcal{K}$:

Lemma 7.28. *The system of minimal non-faces of $\mathcal{K}$ is*

$$\mathcal{Z} = \left\{ G_1 \uplus \cdots \uplus G_r \;\middle|\; |G_i| \neq 1 \textit{ for all } i \in [r], \textit{ and } \sum_{i \,|\, G_i \neq \emptyset} (|G_i|-1) = k+1 \right\}.$$

Proof. A subset $G := G_1 \uplus \cdots \uplus G_r$ of $[n_1+1] \uplus [n_2+1] \uplus \cdots \uplus [n_r+1]$ is a face of $\mathcal{K}$ when it can be extended to a subset $F_1 \uplus \cdots \uplus F_r$ with $\sum(|F_i|-1) = k$ and $\emptyset \neq F_i \subset [n_i+1]$ for all $i \in [r]$, that is, when

$$k \geq |\{i \in [r] \,|\, G_i = \emptyset\}| + \sum_{i\in[r]} (|G_i|-1) = \sum_{i \,|\, G_i \neq \emptyset} (|G_i|-1).$$

Thus, G is a non-face if and only if

$$\sum_{i \,|\, G_i \neq \emptyset} (|G_i|-1) \geq k+1.$$

If $\sum_{i \,|\, G_i \neq \emptyset}(|G_i| - 1) > k + 1$, then removing any element provides a smaller non-face. If there is an i such that $|G_i| = 1$, then removing the unique element of G_i provides a smaller non-face. Thus, if G is a minimal non-face, then $\sum_{i \,|\, G_i \neq \emptyset}(|G_i| - 1) = k + 1$, and $|G_i| \neq 1$ for all $i \in [r]$.

Reciprocally, if G is a non-minimal non-face, then it is possible to remove one element keeping a non-face. Let $i \in [r]$ be such that we can remove one element from G_i, keeping a non-face. Then, either $|G_i| = 1$, or

$$\sum_{j \,|\, G_j \neq \emptyset} (|G_j| - 1) \geq 1 + (|G_i| - 2) + \sum_{j \neq i \,|\, G_j \neq \emptyset} (|G_j| - 1) \geq k + 2,$$

since we keep a non-face. □

7.3.4 Colorings of $\mathrm{KG}(\mathcal{Z})$

The next step consists in providing a suitable coloring for the Kneser graph on the system $\mathcal{Z}$ of minimal non-faces of $\mathcal{K}$. Let $S := \{i \in [r] \,|\, n_i = 1\}$ denote the set of indices corresponding to the segments, and $R := \{i \in [r] \,|\, n_i \geq 2\}$ the set of indices corresponding to the non-segments in the product $\triangle_{\underline{n}}$. We first provide a coloring for two extremal situations.

Theorem 7.29 (Topological obstruction for low-dimensional skeleta)**.** *If $k \leq \sum_{i \in R} \left\lfloor \frac{n_i - 2}{2} \right\rfloor$, then the dimension of any $(k, \underline{n})$-PPSN polytope cannot be smaller than $2k + |R| + 1$:*

$$\delta_{pr}(k, \underline{n}) \geq 2k + |R| + 1.$$

Proof. Let $k_1, \ldots, k_r \in \mathbb{N}$ be such that

$$\sum_{i \in [r]} k_i = k \quad \text{and} \quad \begin{cases} k_i = 0 & \text{for } i \in S; \\ 0 \leq k_i \leq \frac{n_i - 2}{2} & \text{for } i \in R. \end{cases}$$

Observe that:

1. Such a tuple exists since $k \leq \sum_{i \in R} \left\lfloor \frac{n_i - 2}{2} \right\rfloor$.
2. For any minimal non-face $G := G_1 \uplus \cdots \uplus G_r$ of $\mathcal{Z}$, there exists $i \in [r]$ such that $|G_i| \geq k_i + 2$. Indeed, if $|G_i| \leq k_i + 1$ for all $i \in [r]$, then

$$k + 1 = \sum_{i \,|\, G_i \neq \emptyset} (|G_i| - 1) \leq \sum_{i \,|\, G_i \neq \emptyset} k_i \leq \sum_{i \in [r]} k_i = k,$$

which is impossible.

For all $i \in [r]$, we fix a proper coloring $\gamma_i : \binom{[n_i+1]}{[k_i+2]} \to [\chi_i]$ of the Kneser graph $\mathrm{KG}^{k_i+2}_{n_i+1}$, with $\chi_i = 1$ color if $i \in S$ and $\chi_i = n_i - 2k_i - 1$ colors if $i \in R$ — see Section 7.3.1.1. Then, we define a coloring $\gamma : \mathcal{Z} \to [\chi_1] \uplus \cdots \uplus [\chi_r]$ of the Kneser graph on $\mathcal{Z}$ as follows. Let $G := G_1 \uplus \cdots \uplus G_r$ be a given minimal non-face of $\mathcal{Z}$. We choose arbitrarily an $i \in [r]$ such that $|G_i| \geq k_i + 2$, and again arbitrarily a subset g of G_i with $k_i + 2$ elements. We color G with the color of g in $\mathrm{KG}^{k_i+2}_{n_i+1}$, that is, we define $\gamma(G) := \gamma_i(g)$.

The coloring γ is a proper coloring of the Kneser graph $\mathrm{KG}(\mathcal{Z})$. Indeed, let $G := G_1 \uplus \cdots \uplus G_r$ and $H := H_1 \uplus \cdots \uplus H_r$ be two minimal non-faces of $\mathcal{Z}$ related by an edge in $\mathrm{KG}(\mathcal{Z})$, which means that they do not intersect. Let $i \in [r]$ and $g \subset G_i$ be such that we have colored G with $\gamma_i(g)$, and similarly $j \in [r]$ and $h \subset G_j$ be such that we have colored H with $\gamma_j(h)$. Since the color sets of $\gamma_1, \dots, \gamma_r$ are disjoint, the non-faces G and H can receive the same color $\gamma_i(G) = \gamma_j(H)$ only if $i = j$ and g and h are not related by an edge in $\mathrm{KG}^{k_i+2}_{n_i+1}$, which implies that $g \cap h \neq \emptyset$. But this cannot happen, because $g \cap h \subset G_i \cap H_i$, which is empty by assumption. Thus, G and H get different colors.

This provides a proper coloring of $\mathrm{KG}(\mathcal{Z})$ with $\sum \chi_i$ colors. According to Theorem 7.26 and Remark 7.27, we know that the dimension d of the projection is at least

$$\sum_{i\in[r]} n_i - \sum_{i\in[r]} \chi_i + 1 = 2k + |R| + 1. \qquad \square$$

Theorem 7.30 (Topological obstruction for high-dimensional skeleta). *If $k \geq \left\lfloor \frac{1}{2} \sum_i n_i \right\rfloor$, then any $(k, \underline{n})$-PPSN polytope is combinatorially equivalent to $\triangle_{\underline{n}}$:*

$$\delta_{pr}(k, \underline{n}) \geq \sum n_i.$$

Proof. Let $G := G_1 \uplus \cdots \uplus G_r$ and $H := H_1 \uplus \cdots \uplus H_r$ be two minimal non-faces of $\mathcal{Z}$. Let $A := \{i \in [r] \mid G_i \neq \emptyset \text{ or } H_i \neq \emptyset\}$. Then

$$\begin{aligned} \sum_{i\in A}(|G_i| + |H_i|) &\geq \sum_{G_i\neq\emptyset}(|G_i| - 1) + \sum_{H_i\neq\emptyset}(|H_i| - 1) + |A| \\ &= 2k + 2 + |A| > \sum_{i\in[r]} n_i + |A| \geq \sum_{i\in A}(n_i + 1). \end{aligned}$$

Thus, there exists $i \in A$ such that $|G_i| + |H_i| > n_i + 1$, which implies that $G_i \cap H_i \neq \emptyset$, and proves that $G \cap H \neq \emptyset$.

Consequently, the Kneser graph $\mathrm{KG}(\mathcal{Z})$ is independent (and we can color it with only one color). We obtain that the dimension d of the projection is at least $\sum n_i$. In other words, in this extremal case, there is no better $(k, \underline{n})$-PSN polytope than the product $\triangle_{\underline{n}}$ itself. $\square$

Remark 7.31. Theorem 7.30 can sometimes be strengthened a little: if $k = \frac{1}{2} \sum n_i - 1$, and $k+1$ is not representable as a sum of a subset of $\{n_1, \dots, n_r\}$, then $\delta_{pr}(k, \underline{n}) = \sum n_i$.

Proof. As in the previous theorem, we prove that the Kneser graph $\mathrm{KG}(\mathcal{Z})$ is independent. Indeed, assume that $G := G_1 \uplus \cdots \uplus G_r$ and $H := H_1 \uplus \cdots \uplus H_r$ are two minimal non-faces of $\mathcal{Z}$ related by an edge in $\mathrm{KG}(\mathcal{Z})$. Then, $G \cap H$ is empty, which implies that for all $i \in [r]$,

$$|G_i| + |H_i| \leq n_i + 1. \tag{7.4}$$

Let $U := \{i \mid G_i \neq \emptyset\}$ and $V := \{i \mid H_i \neq \emptyset\}$. Then,

$$\begin{aligned}\sum_{i\in U\cup V}(|G_i|+|H_i|) &= \sum_{i\in U}(|G_i|-1)+\sum_{i\in V}(|H_i|-1)+|U|+|V| = 2k+2+|U|+|V|\\ &= \sum_{i\in[r]} n_i+|U|+|V| \overset{(\star)}{\geq} \sum_{i\in U\cup V} n_i+|U\cup V| = \sum_{i\in U\cup V}(n_i+1).\end{aligned}$$

Summing (7.4) over $i \in U \cup V$ implies that both the inequality $(\star)$ and (7.4) for $i \in U \cup V$ are in fact equalities. The tightness of $(\star)$ implies furthermore that $|U| + |V| = |U \cup V|$, so that $U \cap V = \emptyset$; in other words, H_i is empty whenever G_i is not. The equality in (7.4) then asserts that $|G_i| = n_i + 1$ for all $i \in U$, and therefore

$$k+1 = \sum_{i\in U}(|G_i|-1) = \sum_{i\in U} n_i$$

is representable as a sum of a subset of the n_i, which contradicts the assumption. $\square$

Finally, to fill the gap in the ranges of k covered by Theorems 7.29 and 7.30, we merge both coloring ideas as follows.

We partition $[r] = A \uplus B$ and choose $k_i \geq 0$ for all $i \in A$ and $k_B \geq 0$ such that

$$\left(\sum_{i\in A} k_i\right) + k_B \leq k. \tag{7.5}$$

We will see later what the best choice for A, B, k_B and the k_i's is. Let $n_B := \sum_{i\in B} n_i$. Color the Kneser graphs $\mathrm{KG}^{k_i+2}_{n_i+1}$ for $i \in A$ and $\mathrm{KG}^{k_B+1}_{n_B}$ with pairwise disjoint color sets with

$$\chi_i = \begin{cases} n_i - 2k_i - 1 & \text{if } 2k_i \leq n_i - 2,\\ 1 & \text{if } 2k_i \geq n_i - 2,\end{cases} \qquad \text{and} \qquad \chi_B = \begin{cases} 0 & \text{if } n_B = 0,\\ n_B - 2k_B & \text{if } 2k_B \leq n_B - 1,\\ 1 & \text{if } 2k_B \geq n_B - 1,\end{cases}$$

colors respectively.

Observe now that for all minimal non-faces $G := G_1 \uplus \cdots \uplus G_r$,

- either there is an $i \in A$ such that $|G_i| \geq k_i + 2$,
- or $\sum_{i\in B \mid G_i\neq\emptyset}(|G_i| - 1) \geq k_B + 1$.

Indeed, otherwise

$$k+1 = \sum_{i \mid G_i\neq\emptyset}(|G_i|-1) \leq \left(\sum_{i\in A} k_i\right) + k_B \leq k.$$

This permits us to define a coloring of $\mathrm{KG}(\mathcal{Z})$ in the following way. For each minimal non-face $G = G_1 \uplus \cdots \uplus G_r$, we arbitrarily choose one of the following strategies:

1. If we can find an $i \in A$ such that $|G_i| \geq k_i + 2$, we choose an arbitrary subset g of G_i with $k_i + 2$ elements, and color G with the color of g in $\mathrm{KG}^{k_i+2}_{n_i+1}$;

2. Otherwise, $\sum_{i\in B\,|\,G_i\neq\emptyset}(|G_i|-1)\geq k_B+1$, and we choose an arbitrary subset g of

$$\biguplus_{i\in B}(G_i\smallsetminus\{n_i+1\})\subset\biguplus_{i\in B}[n_i]$$

with k_B+1 elements and color G with the color of g in $\mathrm{KG}_{n_B}^{k_B+1}$.

By exactly the same argument as in the proof of Theorem 7.29, one can verify that this provides a valid coloring of the Kneser graph $KG(\mathcal{Z})$ with

$$\chi:=\chi(A,B,\underline{k_i},k_B):=\sum_{i\in A}\chi_i+\chi_B$$

many colors. Therefore Sanyal's Theorem 7.26 and Remark 7.27 yield the following lower bound on the dimension d of any $(k,\underline{n})$-PPSN polytope:

$$d\geq d_k:=d_k(A,B,\underline{k_i},k_B):=\sum_i n_i+1-\chi\geq\delta_{pr}(k,\underline{n}).$$

It remains to choose parameters A, B, and $\{k_i\,|\,i\in A\}$ and k_B that maximize this bound. We proceed algorithmically, by first fixing A and B, and choosing the k_i's and k_B to maximize the bound on the dimension d_k. For this, we first start with $k_i=0$ for all i and $k_B=0$, and observe the variation of d_k as we increase individual k_i's or k_B. By (7.5), we are only allowed a total of k such increases. During this process, we will always maintain the conditions $2k_i\leq n_i-1$ for all $i\in A_i$ and $2k_B\leq n_B$ (which makes sense by the formulas for χ_i and χ_B).

We start with $k_i=0$ for all i and $k_B=0$. Then

$$\begin{aligned}\chi(A,B,\underline{0},0) &= \sum_{i\in A}(n_i-1)+|S\cap A|+n_B\\ &= \sum_{i\in A}n_i-|A|+|S\cap A|+\sum_{i\in B}n_i=\sum_{i\in[r]}n_i-r+|B\cup S|,\end{aligned}$$

and

$$d_k(A,B,\underline{0},0)=1+r-|B\cup S|,$$

where $S:=\{i\in[r]\,|\,n_i=1\}$ denotes the set of segments.

We now study the variation of d_k as we increase each of the k_i's and k_B by one. For $i\in A$, increasing k_i by one decreases χ_i by

$$\begin{cases}2, & \text{if } 2k_i\leq n_i-4,\\ 1, & \text{if } 2k_i=n_i-3,\\ 0, & \text{if } 2k_i\geq n_i-2,\end{cases}$$

and hence increases d_k by the same amount. Observe in particular that d_k remains invariant if we increase k_i for some segment $i\in S$ (because $n_i=1$ for segments). Thus, it makes sense to choose B to contain all segments. Similarly, increasing k_B by one decreases χ_B by

$$\begin{cases} 2, & \text{if } 2k_B \le n_B - 3, \\ 1, & \text{if } 2k_B = n_B - 2, \\ 0, & \text{if } 2k_B \ge n_B - 1, \end{cases}$$

and increases d_k by the same amount.

Recall that we are allowed at most k increases of k_i's or k_B by (7.5). Heuristically, it seems reasonable to first increase the k_i's or k_B that increase d_k by two, and then these that increase d_k by one. Hence we get a case distinction on k, which also depends on A and B:

Theorem 7.32 (Topological obstruction, general case)**.** *Let $k \ge 0$ and $\underline{n} := (n_1, \dots, n_r)$ with $r \ge 1$ and $n_i \ge 1$ for all i. Let $[r] = A \uplus B$ be a partition of $[r]$ with $B \supset S := \{i \in [r] \mid n_i = 1\}$. Define*

$$K_1 := K_1(A,B) := \sum_{i \in A} \left\lfloor \frac{n_i - 2}{2} \right\rfloor + \max\left\{0, \left\lfloor \frac{n_B - 1}{2} \right\rfloor\right\},$$

$$K_2 := K_2(A,B) := |\{i \in A \mid n_i \textit{ is odd}\}| + \begin{cases} 1 & \textit{if } n_B \textit{ is even and non-zero}, \\ 0 & \textit{otherwise}. \end{cases}$$

Then the following lower bounds hold for the dimension of a $(k, \underline{n})$-PPSN polytope:

(1) If $0 \le k \le K_1$, then $\delta_{pr}(k, \underline{n}) \ge r + 1 - |B| + 2k$;

(2) If $K_1 \le k \le K_1 + K_2$, then $\delta_{pr}(k, \underline{n}) \ge r + 1 - |B| + K_1 + k$;

(3) If $K_1 + K_2 \le k$, then $\delta_{pr}(k, \underline{n}) \ge r + 1 - |B| + 2K_1 + K_2$.

This theorem enables us to recover Theorem 7.29 and Theorem 7.30:

Corollary 7.33. *Let $k \ge 0$ and $\underline{n} := (n_1, \dots, n_r)$ with $r \ge 1$ and $n_i \ge 1$ for all i, and define $S := \{i \in [r] \mid n_i = 1\}$ and $R := \{i \in [r] \mid n_i \ge 2\}$. Then:*

1. *If*
$$0 \le k \le \sum_{i \in R} \left\lfloor \frac{n_i - 2}{2} \right\rfloor + \max\left\{0, \left\lfloor \frac{|S| - 1}{2} \right\rfloor\right\},$$
then $\delta_{pr}(k, \underline{n}) \ge 2k + |R| + 1$.
2. *If $k \ge \left\lfloor \frac{1}{2} \sum n_i \right\rfloor$ then* $\delta_{pr}(k, \underline{n}) \ge \sum_i n_i$.

Proof. Take $A = R$ and $B = S$ for (1), and $A = \emptyset$ and $B = [r]$ for (2). □

To conclude, observe that the upper bounds on $\delta_{pr}(k, \underline{n})$ provided by the constructions of Section 7.1 and 7.2 match the lower bound of Corollary 7.33 for a wide range of parameters. In particular:

Theorem 7.34. *For any* $\underline{n} := (n_1, \dots, n_r)$ *with* $r \geq 1$ *and* $n_i \geq 2$ *for all* i, *and for any* k *such that* $0 \leq k \leq \sum_{i\in[r]} \left\lfloor \frac{n_i-2}{2} \right\rfloor$, *the smallest* $(k, \underline{n})$-PPSN *polytope has dimension exactly* $2k + r + 1$. *In other words:*

$$\delta_{pr}(k, \underline{n}) = 2k + r + 1.$$

BIBLIOGRAPHY

[AAK02] Oswin Aichholzer, Franz Aurenhammer, and Hannes Krasser. Enumerating order types for small point sets with applications. *Order*, 19(3):265–281, 2002.

[AAKS04] Oswin Aichholzer, Franz Aurenhammer, Hannes Krasser, and Bettina Speckmann. Convexity minimizes pseudo-triangulations. *Comput. Geom.*, 28(1):3–10, 2004.

[AOSS08] Oswin Aichholzer, David Orden, Francisco Santos, and Bettina Speckmann. On the number of pseudo-triangulations of certain point sets. *J. Combin. Theory Ser. A*, 115(2):254–278, 2008.

[AZ99] Nina Amenta and Günter M. Ziegler. Deformed products and maximal shadows of polytopes. In *Advances in discrete and computational geometry (South Hadley, MA, 1996)*, volume 223 of *Contemp. Math.*, pages 57–90. Amer. Math. Soc., Providence, RI, 1999.

[Bal61] Michel L. Balinski. On the graph structure of convex polyhedra in n-space. *Pacific J. Math.*, 11:431–434, 1961.

[Bar67] David Barnette. A necessary condition for d-polyhedrality. *Pacific J. Math.*, 23:435–440, 1967.

[BB97] Louis J. Billera and Anders Björner. Face numbers of polytopes and complexes. In *Handbook of discrete and computational geometry*, CRC Press Ser. Discrete Math. Appl., pages 291–310. CRC, Boca Raton, FL, 1997.

[BdO00] Jürgen Bokowski and Antonio Guedes de Oliveira. On the generation of oriented matroids. *Discrete Comput. Geom.*, 24(2-3):197–208, 2000. The Branko Grünbaum birthday issue.

[Ber05] Sergey Bereg. Enumerating pseudo-triangulations in the plane. *Comput. Geom.*, 30(3):207–222, 2005.

[BFS90] Louis J. Billera, Paul Filliman, and Bernd Sturmfels. Constructions and complexity of secondary polytopes. *Adv. Math.*, 83(2):155–179, 1990.

[Bir74] Joan S. Birman. *Braids, links, and mapping class groups*, volume 82 of *Annals of Mathematics Studies*. Princeton University Press, Princeton, N.J., 1974.

[BKPS06] Hervé Brönnimann, Lutz Kettner, Michel Pocchiola, and Jack Snoeyink. Counting and enumerating pointed pseudotriangulations with the greedy flip algorithm. *SIAM J. Comput.*, 36(3):721–739 (electronic), 2006.

[BML87] Roswitha Blind and Peter Mani-Levitska. Puzzles and polytope isomorphisms. *Aequationes Math.*, 34(2-3):287–297, 1987.

[Bok06] Jürgen G. Bokowski. *Computational oriented matroids*. Cambridge University Press, Cambridge, 2006.

[BP09] Jürgen G. Bokowski and Vincent Pilaud. On symmetric realizations of the simplicial complex of 3-crossing-free sets of diagonals of the octagon. In *21st Canadian Conference on Comput. Geom. (Vancouver)*. 2009.

[BS97] Ulrich Brehm and Egon Schulte. Polyhedral maps. In *Handbook of discrete and computational geometry*, CRC Press Ser. Discrete Math. Appl., pages 345–358. CRC, Boca Raton, FL, 1997.

[BVS+99] Anders Björner, Michel Las Vergnas, Bernd Sturmfels, Neil White, and Günter M. Ziegler. *Oriented matroids*, volume 46 of *Encyclopedia of Mathematics and its Applications*. Cambridge University Press, Cambridge, second edition, 1999.

[CDD+07] William Y. C. Chen, Eva Y. P. Deng, Rosena R. X. Du, Richard P. Stanley, and Catherine H. Yan. Crossings and nestings of matchings and partitions. *Trans. Amer. Math. Soc.*, 359(4):1555–1575 (electronic), 2007.

[Cox69] Harold S. M. Coxeter. *Introduction to geometry*. John Wiley & Sons Inc., New York, Second edition, 1969.

[Cox73] Harold S. M. Coxeter. *Regular polytopes*. Dover Publications Inc., New York, Third edition, 1973.

[CP92] Vasilis Capoyleas and János Pach. A Turán-type theorem on chords of a convex polygon. *J. Combin. Theory Ser. B*, 56(1):9–15, 1992.

[CRM09] CRM. Report of the *i-MATH Winter School DocCourse Combinatorics and Geometry 2009: Discrete and Computational Geometry*. 2009.

[CS99] Wen-Sz Chiue and Bih-Sheue Shieh. On connectivity of the Cartesian product of two graphs. *Appl. Math. Comput.*, 102(2-3):129–137, 1999.

[dB74] Nicolaas G. de Bruijn. Sorting by means of swappings. *Discrete Math.*, 9:333–339, 1974.

[DKKM01] Andreas W. M. Dress, Michael Klucznik, Jacobus H. Koolen, and Vincent Moulton. $2kn - \binom{2k+1}{2}$: note on extremal combinatorics of cyclic split systems. *Sém. Lothar. Combin.*, 47:Article B47b, 17 pp. (electronic), 2001.

[DKM02] Andreas W. M. Dress, Jacobus H. Koolen, and Vincent Moulton. On line arrangements in the hyperbolic plane. *European J. Combin.*, 23(5):549–557, 2002.

[DKM04] Andreas W. M. Dress, Jacobus H. Koolen, and Vincent Moulton. $4n - 10$. *Ann. Comb.*, 8(4):463–471, 2004.

[dLRS10] Jesus A. de Loera, Jörg Rambau, and Francisco Santos. Triangulations: Structures and algorithms. To appear, 2010.

[dSCV86] Myriam de Sainte-Catherine and Xavier Gérard Viennot. Enumeration of certain Young tableaux with bounded height. In *Combinatoire énumérative (Montreal,* *Quebec)*, volume 1234 of *Lecture Notes in Math.*, pages 58–67. Springer, Berlin, 1986.

[Eli07] Sergi Elizalde. A bijection between 2-triangulations and pairs of non-crossing Dyck paths. *J. Combin. Theory Ser. A*, 114(8):1481–1503, 2007.

[Fel04] Stefan Felsner. *Geometric graphs and arrangements*. Advanced Lectures in Mathematics. Friedr. Vieweg & Sohn, Wiesbaden, 2004. Some chapters from combinatorial geometry.

[FF02] Lukas Finschi and Komei Fukuda. Generation of oriented matroids — a graph theoretical approach. *Discrete Comput. Geom.*, 27(1):117–136, 2002. *Geometric combinatorics (San Francisco, 2000).*

[FPP08] Julien Ferté, Vincent Pilaud, and Michel Pocchiola. On the number of simple arrangements of five double pseudolines. In *18th Fall Workshop on Comput. Geom. (Troy)*. 2008.

[Fri09] Eric J. Friedman. Finding a simple polytope from its graph in polynomial time. *Discrete Comput. Geom.*, 41(2):249–256, 2009.

[Gal63] David Gale. Neighborly and cyclic polytopes. In *Proc. Sympos. Pure Math., Vol. VII*, pages 225–232. Amer. Math. Soc., Providence, R.I., 1963.

[GKZ94] Israel M. Gel′fand, Mikhail M. Kapranov, and Andrei V. Zelevinsky. *Discriminants, resultants, and multidimensional determinants*. Mathematics: Theory & Applications. Birkhäuser Boston Inc., Boston, MA, 1994.

[GO04] Jacob E. Goodman and Joseph O'Rourke, editors. *Handbook of discrete and computational geometry*. Discrete Mathematics and its Applications (Boca Raton). Chapman & Hall/CRC, Boca Raton, FL, second edition, 2004.

[Goo97] Jacob E. Goodman. Pseudoline arrangements. In *Handbook of discrete and computational geometry*, CRC Press Ser. Discrete Math. Appl., pages 83–109. CRC, Boca Raton, FL, 1997.

[GPWZ94] Jacob E. Goodman, Richard Pollack, Rephael Wenger, and Tudor Zamfirescu. Arrangements and topological planes. *Amer. Math. Monthly*, 101(9):866–878, 1994.

[Gra01] Jack E. Graver. *Counting on frameworks*, volume 25 of *The Dolciani Mathematical Expositions*. Mathematical Association of America, Washington, DC, 2001. Mathematics to aid the design of rigid structures.

[Grü72] Branko Grünbaum. *Arrangements and spreads*. American Mathematical Society Providence, R.I., 1972. *Conference Board of the Mathematical Sciences Regional Conference Series in Mathematics, No. 10*.

[Grü03] Branko Grünbaum. *Convex polytopes*, volume 221 of *Graduate Texts in Mathematics*. Springer-Verlag, New York, second edition, 2003. Prepared and with a preface by Volker Kaibel, Victor Klee and Günter M. Ziegler.

[GSS93] Jack E. Graver, Brigitte Servatius, and Herman Servatius. *Combinatorial rigidity*, volume 2 of *Graduate Studies in Mathematics*. American Mathematical Society, Providence, RI, 1993.

[GV85] Ira Gessel and Xavier Gérard Viennot. Binomial determinants, paths, and hook length formulae. *Adv. in Math.*, 58(3):300–321, 1985.

[Haa02] Ruth Haas. Characterizations of arboricity of graphs. *Ars Combin.*, 63:129–137, 2002.

[Hen11] L. Henneberg. Die graphische statik der starren systeme. *Leipzig*, 1911.

[HL07] Christophe Hohlweg and Carsten E. M. C. Lange. Realizations of the associahedron and cyclohedron. *Discrete Comput. Geom.*, 37(4):517–543, 2007.

[HOR+05] Ruth Haas, David Orden, Günter Rote, Francisco Santos, Brigitte Servatius, Herman Servatius, Diane Souvaine, Ileana Streinu, and Walter Whiteley. Planar minimally rigid graphs and pseudo-triangulations. *Comput. Geom.*, 31(1-2):31–61, 2005.

[HP] Luc Habert and Michel Pocchiola. Computing pseudotriangulations and constrained pseudotriangulations via branched coverings. Submitted to *Discrete Comput. Geom.* Abbreviated partial version in *20th European Workshop on Comput. Geom. (Seville, 2004)*, pages 111–114.

[HP09] Luc Habert and Michel Pocchiola. Arrangements of double pseudolines. Submitted to *Discrete Comput. Geom.* Abbreviated version in *25th Annual ACM Symposium on Comput. Geom. (Aahrus, 2009)*, pages 314–323. Preliminary version in *12th European Workshop on Comput. Geom. (Delphes, 2006)*, pages 211–214. Poster version at the *Workshop on Geometric and Topological Combinatorics (Alcala de Henares, 2006)*, 2009.

[HRGZ97] Martin Henk, Jürgen Richter-Gebert, and Günter M. Ziegler. Basic properties of convex polytopes. In *Handbook of discrete and computational geometry*, CRC Press Ser. Discrete Math. Appl., pages 243–270. CRC, Boca Raton, FL, 1997.

[HT92] Jürgen Herzog and Ngô Viêt Trung. Gröbner bases and multiplicity of determinantal and Pfaffian ideals. *Adv. Math.*, 96(1):1–37, 1992.

[Hut07] Graham Hutton. *Programming in Haskell*. Cambridge University Press, Cambridge, 2007.

[Iva02] Nikolai V. Ivanov. Mapping class groups. In *Handbook of geometric topology*, pages 523–633. North-Holland, Amsterdam, 2002.

[Jon03] Jakob Jonsson. Generalized triangulations of the n-gon. Unpublished manuscript. An abstract was included in *"Topological and Geometric Combinatorics, April 2003"*, Mathematisches Forschungsinstitut Oberwolfach, Report No. 16, 2003.
`http://www.mfo.de/programme/schedule/2003/15/Report16_2003.pdf`

[Jon05] Jakob Jonsson. Generalized triangulations and diagonal-free subsets of stack polyominoes. *J. Combin. Theory Ser. A*, 112(1):117–142, 2005.

[JR07] Michael Joswig and Thilo Rörig. Neighborly cubical polytopes and spheres. *Israel J. Math.*, 159:221–242, 2007.

[JZ00] Michael Joswig and Günter M. Ziegler. Neighborly cubical polytopes. *Discrete Comput. Geom.*, 24(2-3):325–344, 2000. The Branko Grünbaum birthday issue.

[Kal88] Gil Kalai. A simple way to tell a simple polytope from its graph. *J. Combin. Theory Ser. A*, 49(2):381–383, 1988.

[Kal97] Gil Kalai. Polytope skeletons and paths. In *Handbook of discrete and computational geometry*, CRC Press Ser. Discrete Math. Appl., pages 331–344. CRC, Boca Raton, FL, 1997.

[Kle64] Victor Klee. A property of d-polyhedral graphs. *J. Math. Mech.*, 13:1039–1042, 1964.

[Knu73] Donald E. Knuth. *The art of computer programming. Volume 3*. Addison-Wesley Publishing Co., Reading, Mass.-London-Don Mills, Ont., 1973. Sorting and searching, Addison-Wesley Series in Computer Science and Information Processing.

[Knu92] Donald E. Knuth. *Axioms and hulls*, volume 606 of *Lecture Notes in Computer Science*. Springer-Verlag, Berlin, 1992.

[Kra06] Christian Krattenthaler. Growth diagrams, and increasing and decreasing chains in fillings of Ferrers shapes. *Adv. in Appl. Math.*, 37(3):404–431, 2006.

[KW10] Volker Kaibel and Arnold Waßmer. Automorphism groups of cyclic polytopes. In F. H. Lutz*, Triangulated Manifolds*. 2010. To appear.

[Lam70] Gerard Laman. On graphs and rigidity of plane skeletal structures. *J. Engrg. Math.*, 4:331–340, 1970.

[Lee89] Carl W. Lee. The associahedron and triangulations of the n-gon. *European J. Combin.*, 10(6):551–560, 1989.

[Lin73] Bernt Lindström. On the vector representations of induced matroids. *Bull. London Math. Soc.*, 5:85–90, 1973.

[Lod04] Jean-Louis Loday. Realization of the Stasheff polytope. *Arch. Math. (Basel)*, 83(3):267–278, 2004.

[LS08] Audrey Lee and Ileana Streinu. Pebble game algorithms and sparse graphs. *Discrete Math.*, 308(8):1425–1437, 2008.

[Mak09] A. N. Maksimenko. The diameter of the ridge-graph of a cyclic polytope. *Discrete Mathematics and Applications*, 19(1):47–53, 2009.

[Mat02] Jiří Matoušek. *Lectures on discrete geometry*, volume 212 of *Graduate Texts in Mathematics*. Springer-Verlag, New York, 2002.

[Mat03] Jiří Matoušek. *Using the Borsuk-Ulam theorem.* Universitext. Springer-Verlag, Berlin, 2003. Lectures on topological methods in combinatorics and geometry, Written in cooperation with Anders Björner and Günter M. Ziegler.

[McM70] Peter McMullen. The maximum numbers of faces of a convex polytope. *Mathematika*, 17:179–184, 1970.

[MPP09] Benjamin Matschke, Julian Pfeifle, and Vincent Pilaud. Prodsimplicial neighborly polytopes. Available at `arXiv:0908.4177`, 2009.

[MT01] Bojan Mohar and Carsten Thomassen. *Graphs on surfaces.* Johns Hopkins Studies in the Mathematical Sciences. Johns Hopkins University Press, Baltimore, MD, 2001.

[Nak00] Tomoki Nakamigawa. A generalization of diagonal flips in a convex polygon. *Theoret. Comput. Sci.*, 235(2):271–282, 2000. *Combinatorics and optimization (Okinawa, 1996).*

[NdO09] Marc Noy and António Guedes de Oliveira. Personal communication. 2009.

[Nic08] Carlos M. Nicolas. *Structural and enumerative properties of k-triangulations of the n-gon.* PhD thesis, University of Kentucky, 2008.

[Nic09] Carlos M. Nicolas. Another bijection between 2-triangulations and pairs of non-crossing dyck paths. In *21th International Conference on Formal Power Series and Algebraic Combinatorics (Hagenberg), Discrete Mathematics and Theoretical Computer Science, DMTCS*, pages 699–710. 2009.

[PA95] János Pach and Pankaj K. Agarwal. *Combinatorial geometry.* Wiley-Interscience Series in Discrete Mathematics and Optimization. John Wiley & Sons Inc., New York, 1995. A Wiley-Interscience Publication.

[Poc97] Michel Pocchiola. Horizon trees versus pseudo-triangulations. In *13th European Workshop on Comput. Geom. (Würzburg)*. 1997.

[PP09] Vincent Pilaud and Michel Pocchiola. Multipseudotriangulations. In preparation. Extended abstract in *25th European Workshop on Comput. Geom. (Bruxelles)*, 2009.

[PPS10] Julian Pfeifle, Vincent Pilaud, and Francisco Santos. On polytopality of Cartesian products of graphs. In preparation, 2010.

[PS09] Vincent Pilaud and Francisco Santos. Multitriangulations as complexes of star polygons. *Discrete Comput. Geom.*, 41(2):284–317, 2009. *20th International Conference on Formal Power Series and Algebraic Combinatorics (Valparaiso, 2008).*

[PS10] Vincent Pilaud and Francisco Santos. A generalization of Loday's associahedron. In preparation, 2010.

[PV94] Michel Pocchiola and Gert Vegter. Order types and visibility types of configurations of disjoint convex plane sets. Technical report, LIENS, Paris, 1994.

[PV96a] Michel Pocchiola and Gert Vegter. Pseudo-triangulations: theory and applications. In *12th Annual ACM Symposium on Comput. Geom. (Philadelphia)*, pages 291–300. 1996.

[PV96b] Michel Pocchiola and Gert Vegter. Topologically sweeping visibility complexes via pseudotriangulations. *Discrete Comput. Geom.*, 16(4):419–453, 1996. *11th Annual ACM Symposium on Comput. Geom. (Vancouver, 1995)*.

[PV96c] Michel Pocchiola and Gert Vegter. The visibility complex. *Internat. J. Comput. Geom. Appl.*, 6(3):279–308, 1996. *9th Annual ACM Symposium on Comput. Geom. (San Diego, 1993)*.

[Rec84] András Recski. A network theory approach to the rigidity of skeletal structures. I. Modelling and interconnection. *Discrete Appl. Math.*, 7(3):313–324, 1984.

[RG96] Jürgen Richter-Gebert. *Realization spaces of polytopes*, volume 1643 of *Lecture Notes in Mathematics*. Springer-Verlag, Berlin, 1996.

[RGZ97] Jürgen Richter-Gebert and Günter M. Ziegler. Oriented matroids. In *Handbook of discrete and computational geometry*, CRC Press Ser. Discrete Math. Appl., pages 111–132. CRC, Boca Raton, FL, 1997.

[Rör08] Thilo Rörig. *Polyhedral Surfaces, Polytopes, and Projections*. PhD thesis, Technische Universität Berlin, 2008.

[RS09] Thilo Rörig and Raman Sanyal. Non-projectability of polytope skeleta. Available at `arXiv:0908.0845`, 2009.

[RSS03] Günter Rote, Francisco Santos, and Ileana Streinu. Expansive motions and the polytope of pointed pseudo-triangulations. In *Discrete and computational geometry*, volume 25 of *Algorithms Combin.*, pages 699–736. Springer, Berlin, 2003.

[RSS08] Günter Rote, Francisco Santos, and Ileana Streinu. Pseudo-triangulations — a survey. In *Surveys on discrete and computational geometry*, volume 453 of *Contemp. Math.*, pages 343–410. Amer. Math. Soc., Providence, RI, 2008.

[Rub07] Martin Rubey. Increasing and decreasing sequences in fillings of moon polyominoes. In *19th International Conference on Formal power series and algebraic combinatorics (Tianjin)*. 2007. Available at `arXiv:math.CO/0604140`.

[San08] Raman Sanyal. *Constructions and obstructions for extremal polytopes*. PhD thesis, Technische Universität Berlin, 2008.

[San09] Raman Sanyal. Topological obstructions for vertex numbers of Minkowski sums. *J. Combin. Theory Ser. A*, 116(1):168–179, 2009.

[SBG$^+$95] Helmut Salzmann, Dieter Betten, Theo Grundhöfer, Hermann Hähl, Rainer Löwen, and Markus Stroppel. *Compact projective planes*, volume 21 of *de Gruyter Expositions in Mathematics*. Walter de Gruyter & Co., Berlin, 1995.

[Špa08] Simon Špacapan. Connectivity of Cartesian products of graphs. *Appl. Math. Lett.*, 21(7):682–685, 2008.

[Sta99] Richard P. Stanley. *Enumerative combinatorics. Vol. 2*, volume 62 of *Cambridge Studies in Advanced Mathematics*. Cambridge University Press, Cambridge, 1999.

[Sta09] Richard P. Stanley. Catalan addendum. Version of 11 August 2009. Available at `http://www-math.mit.edu/ rstan/ec/catadd.pdf`, 2009.

[Ste22] Ernst Steinitz. Polyeder und raumeinteilungen. In *Encyclopädie der mathematischen Wissenschaften, Band 3 (Geometrie), Teil 3AB12*, pages 1–139. 1922.

[Str05] Ileana Streinu. Pseudo-triangulations, rigidity and motion planning. *Discrete Comput. Geom.*, 34(4):587–635, 2005.

[STT88] Daniel D. Sleator, Robert E. Tarjan, and William P. Thurston. Rotation distance, triangulations, and hyperbolic geometry. *J. Amer. Math. Soc.*, 1(3):647–681, 1988.

[SZ10] Raman Sanyal and Günter M. Ziegler. Construction and analysis of projected deformed products. *Discrete Comput. Geom.*, 43(2):412–435, 2010.

[Tur54] Paul Turán. On the theory of graphs. *Colloquium Math.*, 3:19–30, 1954.

[Vie00] Xavier Gérard Viennot. A combinatorial interpretation of the quotient-difference algorithm. In *12th International Conference on Formal power series and algebraic combinatorics (Moscow)*, pages 379–390. Springer, Berlin, 2000.

[Whi32] Hassler Whitney. Non-separable and planar graphs. *Trans. Amer. Math. Soc.*, 34(2):339–362, 1932.

[Whi90] Walter Whiteley. Vertex splitting in isostatic frameworks — la division de sommet dans les charpentes isostatiques. *Structural Topology*, (16):23–30, 1990. Dual French-English text.

[Zie95] Günter M. Ziegler. *Lectures on polytopes*, volume 152 of *Graduate Texts in Mathematics*. Springer-Verlag, New York, 1995.

[Zie04] Günter M. Ziegler. Projected products of polygons. *Electron. Res. Announc. Amer. Math. Soc.*, 10:122–134 (electronic), 2004.

Index

Cette thèse aborde deux sujets particuliers de géométrie discrète, les *multitriangulations* et les *réalisations polytopales de produits*, dont la problématique commune est la recherche de réalisations polytopales de structures combinatoires.

Une k-triangulation est un ensemble maximal de cordes du n-gone convexe ne contenant pas de sous-ensemble de $k+1$ cordes qui se croisent deux à deux. Nous proposons une étude combinatoire et géométrique des multitriangulations basée sur leurs étoiles, qui jouent ici le même rôle que les triangles des triangulations. Cette étude nous amène à interpréter les multitriangulations par dualité comme des *arrangements de pseudodroites avec points de contact* de support donné. Nous exploitons finalement ces résultats pour discuter quelques problèmes ouverts sur les multitriangulations, en particulier la question de la réalisation polytopale de leurs graphes de flip.

Nous étudions dans un deuxième temps la polytopalité des produits cartésiens. Nous nous interrogeons d'abord sur l'existence de réalisations polytopales d'un produit cartesien de graphes, puis nous recherchons la dimension minimale que peut avoir un polytope dont le k-squelette est celui d'un produit de simplexes.

Mots-clés : triangulation, multitriangulation, pseudotriangulation, graphe de flip, associahèdre, nombre de Catalan, arrangement de pseudodroites, rigidité, polytope, produit cartésien.

Esta memoria versa sobre dos temas particulares de geometría discreta, las *multitriangulaciones* y las *realizaciones politopales de productos*, cuya problemática común es la búsqueda de realizaciones politopales de estructuras combinatorias.

Una k-triangulación es un conjunto maximal de cuerdas del n-gono convexo que no contiene ningún subconjunto de $k+1$ cuerdas que se cruzan dos a dos. Proponemos un estudio combinatorio y geométrico de las multitriangulaciones basado en sus estrellas, que desempeñan el mismo papel que los triángulos de los triangulaciones. Este estudio nos lleva a interpretar las multitriangulaciones por dualidad como *arreglos de pseudorectas con puntos de contacto* de soporte dado. Explotamos finalmente estos resultados para discutir algunos problemas abiertos sobre multitriangulaciones, en particular la pregunta de la realización politopal de sus grafos de flip.

Estudiamos en segundo lugar la politopalidad de productos cartesianos. Nos preguntamos primero sobre la existencia de realizaciones politopales de un producto cartesiano de grafos, y buscamos después la dimensión mínima que puede tener un politopo cuyo k-esqueleto es el de un producto de símplices.

Palabras-clave: triangulación, multitriangulación, pseudotriangulación, grafo de flip, associaedro, número de Catalan, arreglo de pseudorectas, rigidez, politopo, producto cartesiano.

This thesis explores two specific topics of discrete geometry, the *multitriangulations* and the *polytopal realizations of products*, whose connection is the problem of finding polytopal realizations of a given combinatorial structure.

A k-triangulation is a maximal set of chords of the convex n-gon such that no $k+1$ of them mutually cross. We propose a combinatorial and geometric study of multitriangulations based on their stars, which play the same role as triangles of triangulations. This study leads to interpret multitriangulations by duality as *pseudoline arrangements with contact points* covering a given support. We exploit finally these results to discuss some open problems on multitriangulations, in particular the question of the polytopal realization of their flip graphs.

We study secondly the polytopality of Cartesian products. We investigate the existence of polytopal realizations of cartesian products of graphs, and we study the minimal dimension that can have a polytope whose k-skeleton is that of a product of simplices.

Keywords: triangulation, multitriangulation, pseudotriangulation, graph of flip, associahedron, Catalan number, pseudoline arrangement, rigidity, polytope, Cartesian product.